Therya

Volumen 17 Número 2 Mayo 2026

AMMAC

www.mastozoologiamexicana.org

La portada

El murciélago orejón de León Paniagua (*Corynorhinus leonpaniaguae*) es una especie endémica de México cuya distribución se extiende a lo largo del norte de la Sierra Madre Oriental, incluyendo los estados de Coahuila, Nuevo León y Tamaulipas. Este ejemplar es una hembra fotografiada en el municipio de Arteaga, Coahuila, México. Fotografía de Issachar L. López Cuamatzi.

Issue cover

The León Paniagua's big-eared bat (*Corynorhinus leonpaniaguae*) is an endemic Mexican species whose distribution extends across the northern Sierra Madre Oriental, including the states of Coahuila, Nuevo León, and Tamaulipas. This individual is a female photographed in the municipality of Arteaga, Coahuila, Mexico. Photograph by Issachar L. López Cuamatzi.

Nuestro logo "Ozomatli"

El nombre de "Ozomatli" proviene del náhuatl se refiere al símbolo astrológico del mono en el calendario azteca, así como al dios de la danza y del fuego. Se relaciona con la alegría, la danza, el canto y las habilidades. Al signo decimoprimero en la cosmogonía mexica. "Ozomatli" es una representación pictórica del mono araña (*Ateles geoffroyi*). La especie de primate de más amplia distribución en México. Es habitante de los bosques, sobre todo de los que están por donde sale el sol en Anáhuac. Tiene el dorso pequeño, es barrigudo y su cola, que a veces se enrosca, es larga. Sus manos y sus pies parecen de hombre; también sus uñas. Los Ozomatin gritan y silban y hacen visajes a la gente. Arrojan piedras y palos. Su cara es casi como la de una persona, pero tienen mucho pelo.

Therya

Volumen 17, número 2 Mayo 2026

Contenido

fascículo 50 https://mastozoologiamexicana.com/therya/index.php/THERYA/issue/view/50

Therya

THERYA
Lilia Ruiz Ruiz. Editora de formato. Centro de Investigaciones Tropicales, Universidad Veracruzana. E-mail: correo.therya@gmail.com
Malinalli Cortés Marcial. Tesorera de la Revista THERYA. Universidad Autónoma Metropolitana Unidad Xochimilco. E-mail: therya.tesoreria@gmail.com
Alina Gabriela Monroy Gamboa. Difusión. Centro de Investigaciones Biológicas del Noroeste. Av. Instituto Politécnico Nacional 195. La Paz 23096, Baja California Sur. México. E-mail: beu_ribetzin@hotmail.com
Maria Elena Sánchez Salazar. Traducción.

El objetivo y la intención de THERYA es ser una revista científica para la publicación de artículos sobre los mamíferos. Estudios de investigación original, editoriales y artículos de revisión son bienvenidos.

Jesús Alonso Panti May. Centro de Investigaciones Regionales "Dr. Hideyo Noguchi", Universidad Autónoma de Yucatán, Mérida, Yucatán, México. E-mail: pantialonso@gmail.com
Rafael Reyna Hurtado. El Colegio de la Frontera Sur, Unidad Campeche. Avenida Rancho s/n, Lerma Campeche, 24500. México. E-mail: rafaelcalakmul@gmail.com
Cintya Segura Trujillo. Universidad de Guadalajara, Jalisco, México. E-mail: c.a.biolsegura@gmail.com
Sergio Solari. Editor asociado. Instituto de Biología. Universidad de Antioquia. Calle 67 No53-108 / AA 1226. Medellín, Colombia. E-mail: solari.udea@gmail.com
Ella Vázquez Domínguez. Laboratorio de genética y ecología, Instituto de Ecología, Universidad Nacional Autónoma de México. C.U., Coyoacán, 04510 Ciudad de México, México. E-mail: evazquez@ecologia.unam.mx

THERYA, 2026, Vol. 17(2):125-130

DOI: 10.12933/therya.2026.6322 ISSN 2007-3364

Editorial

Honoring Dr. Livia León-Paniagua: a life dedicated to Mexican Mammalogy

On September 25th, 2024, Dr. Livia León-Paniagua received the "José Ticul Álvarez Solorzano Award" (Figure 1), presented by the Asociación Mexicana de Mastozoología A. C. (AMMAC) to recognize outstanding academic achievement and exceptional contributions to the study of mammals in Mexico. Nearly two years later, with deep gratitude and admiration, we dedicate this special issue to Livia in recognition of her distinguished career, her unwavering commitment to Mexican and Mesoamerican mammalogy, and her lasting influence as a scientist, mentor, colleague, friend, and human being.

Since childhood in the early 1960's, Livia has been deeply fascinated by nature. Inspired by documentaries and influential teachers, she decided to study Biology at the Universidad Nacional Autónoma de México. It is important to emphasize that she began building her academic career during the 1980's, a period when opportunities for women in science were far from as equitable as they are today. As an undergraduate student, she joined the Museo de Zoología–Facultad de Ciencias (MZFC), initially through her university social service program and later in a part–time position (Figure 2A). Her dedication and talent were quickly recognized by the museum staff, who gradually increased her responsibilities, later supported her appointment as a research technician, and eventually helped her to attain a full professor position years later.

Step by step, Livia built her career through perseverance, discipline, and sustained academic excellence, while simultaneously balancing the demands of being a mother, wife, field biologist, teacher, and researcher. Remarkably, many of her influential scientific and mentoring contributions were achieved long before she formally attained the rank of full professor. Her trajectory, therefore, represents not only a story of scientific achievement but also one of resilience and determination in overcoming the structural gender inequalities that shaped academia throughout much of her career.

During her time at the MZFC, Livia forged a renowned career exploring mammalian diversity, particularly faunistics, systematics, and biogeography, with emphasis on rodents and bats. She contributed to mammal inventories across several Mexican states, and used those data to examine biogeographic patterns at multiple spatial scales (e.g., León-Paniagua and Morrone 2009; Rodríguez-Macedo *et al.* 2014). Her work also helped to clarify the taxonomy of numerous mammalian groups, producing pivotal work on the Rodentia and Chiroptera genera *Baiomys*, *Glossophaga*, *Habromys*, *Neotoma*, and *Peromyscus* (e.g., Ávila-Valle *et al.* 2012; Calahorra-Oliart *et al.* 2021), as well as lagomorphs and brocket deer (Cano-Sánchez *et al.* 2022; Escobedo-Morales *et al.* 2025). In addition, her research contributed to the description of *Habromys schmidlyi* Romo-Vázquez *et al.* 2005, *Cryptotis lacandonensis* Guevara *et al.* 2014, and *Vampyressa villai* Garbino *et al.* 2014.

Livia has also explored the genetic diversity and evolutionary history of rodents, including some species of the genera *Habromys*, *Osgoodomys*, *Peromyscus*, and *Reithrodontomys* (e.g., León-Paniagua *et al.* 2007; Castañeda-Rico *et al.* 2014), as well as from bat genera such as *Desmodus*, *Leptonycteris*, *Noctilio*, and *Sturnira* (e.g., Hernández-Canchola and León-Paniagua 2017; Ospina-Garcés and Léon-Paniagua 2022). Beyond taxonomy and evolution, her research has also contributed to ecology (e.g., Guevara *et al.* 2018; Marines-Macías *et al.* 2018), conservation (e.g., Peterson *et al.* 1993), and emerging topics including biomonitoring (Redón-Lugo *et al.* 2017), viral diseases and bacteria associated with bats and rodents (e.g., Colunga-Salas *et al.* 2021), and supporting the development of taxonomy of ecto– and endoparasites (e.g., Guzmán-Cornejo *et al.* 2012). Her academic legacy includes more than 120 scientific publications and over 50 outreach, communication, and teaching works. In recognition of her contributions to Mexican mammalogy, the species *Corynorhinus leonpaniaguae* López-Cuamatzi *et al.* 2024 was named in her honor.

A defining aspect of Livia's career has been her commitment to teaching and mentorship. Throughout her scientific career, she simultaneously trained students, conducted research, and built institutional projects. She has taught more than 120 undergraduate and

Figure 1. Dr. Livia León-Paniagua at the "José Ticul Álvarez Solorzano Award" ceremony during the XVI National Conference of Mammalogy in Pachuca, Hidalgo, Mexico. From left to right: Dr. Gerardo Sánchez-Rojas, Dr. Livia León-Paniagua, Dr. Cristina Mac Swiney-González, Dr. Jorge Ortega, and Dr. Celia Sélem-Salas. Photo credit: Dr. Giovani Hernández-Canchola.

graduate courses and supervised 43 university social service students, 34 undergraduates, 15 graduates, and 6 postdoctoral researchers. In addition, she has participated in the evaluation of more than 270 students through examinations, candidacy reviews, and thesis committees.

For many of us, her mentorship has been extended far beyond scientific training. Livia consistently encouraged critical thinking, intellectual curiosity, and innovation, but she also reminds us that scientific accomplishment should never come at the expense of kindness, integrity, or personal well-being. One of her most enduring lessons has been that, before being scientists, we should strive to be good people.

Today, Livia remains an active and deeply committed scientist, widely admired for her ability to communicate ideas with clarity and enthusiasm. She continues conducting fieldwork (Figure 3A), mentoring students from undergraduate to postdoctoral levels, leading research projects, participating in institutional committees, and fostering national and international collaborations. Across 43 years, she has earned the respect and affection of generations of students and colleagues through her professionalism, ethics, generosity, and warmth. Her influence endures in the scientists she has trained, the collaborative networks she has strengthened, and the academic community she has helped to build.

As curator of the MZFC mammal collection, Livia transformed a small reference collection of only a few hundred specimens (Figure 2A) into a resource of national and international importance, now housing approximately 20,000 specimens and 10,000 tissue samples (Figure 2B). Notably, she expanded the collection while serving as the sole staff mammalogist at the MZFC. This legacy underpins diverse research projects in several fields, serving past, present, and future generations of students and researchers in Mexico and beyond. In sum, Dr. Livia León-Paniagua has shaped modern Mexican mammalogy through her research, the cultivation of new generations

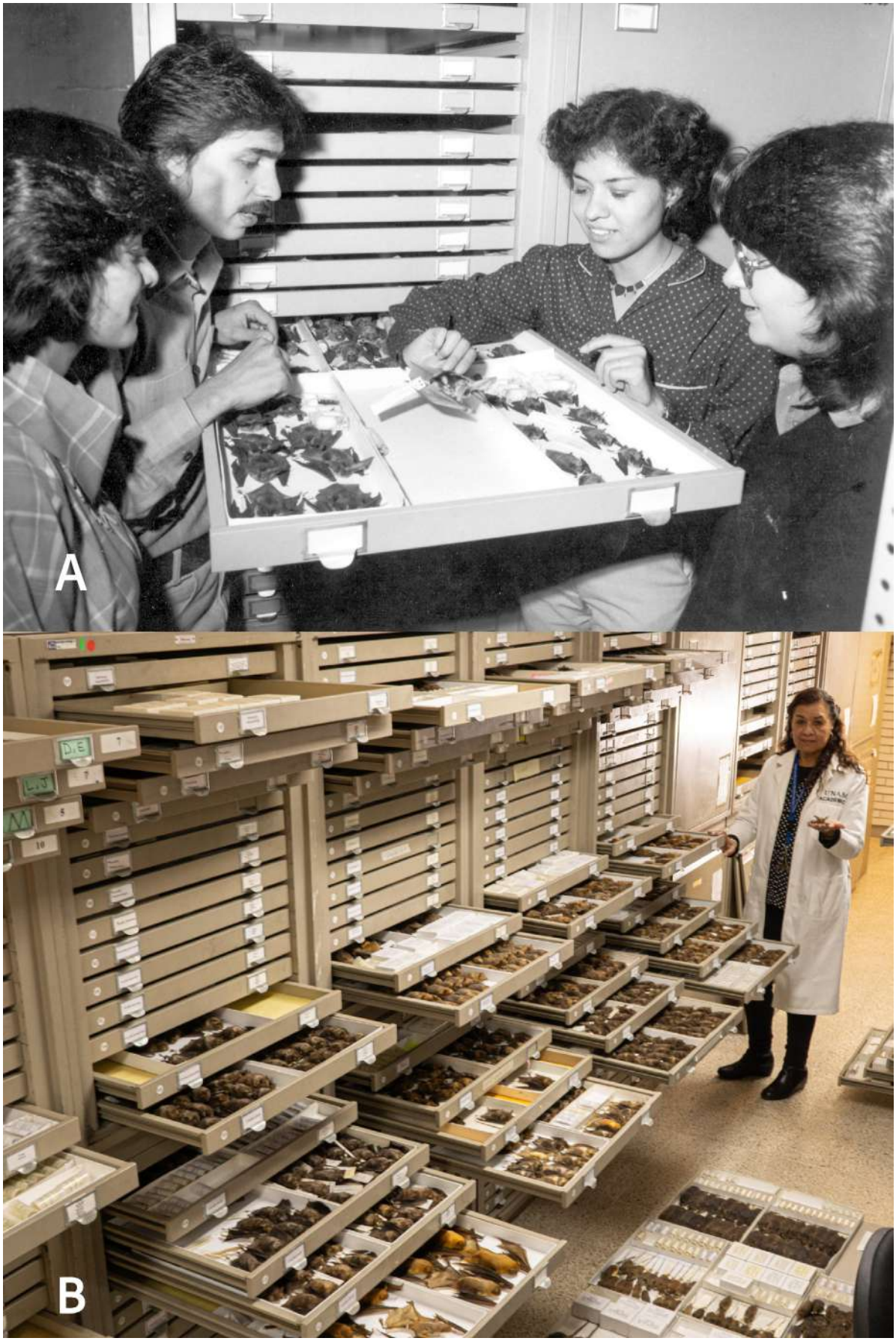

Figure 2. Livia León Paniagua, in the mammal collection at the MZFC, underscores the significant growth of the collection under her leadership. (A) Early in her career (1980's), Livia displays her favorite specimen, *Euderma maculatum* –one of the few collected specimens in Mexico– when the entire collection fit into just two cabinets (at back). From left to right: Teresa Jiménez, Julio Juárez, Livia León, and Esther Romo. (B) More recently, Dr. León-Paniagua stands in a current section of the MZFC, highlighting her key role as curator in transforming a modest set into one of the most important collections in Mexico. Photo credits: (A) MSc. Alejandro Martínez Mena and Dr. Jorge Llorente-Bousquets; (B) Luis Armando Navarro Zarco.

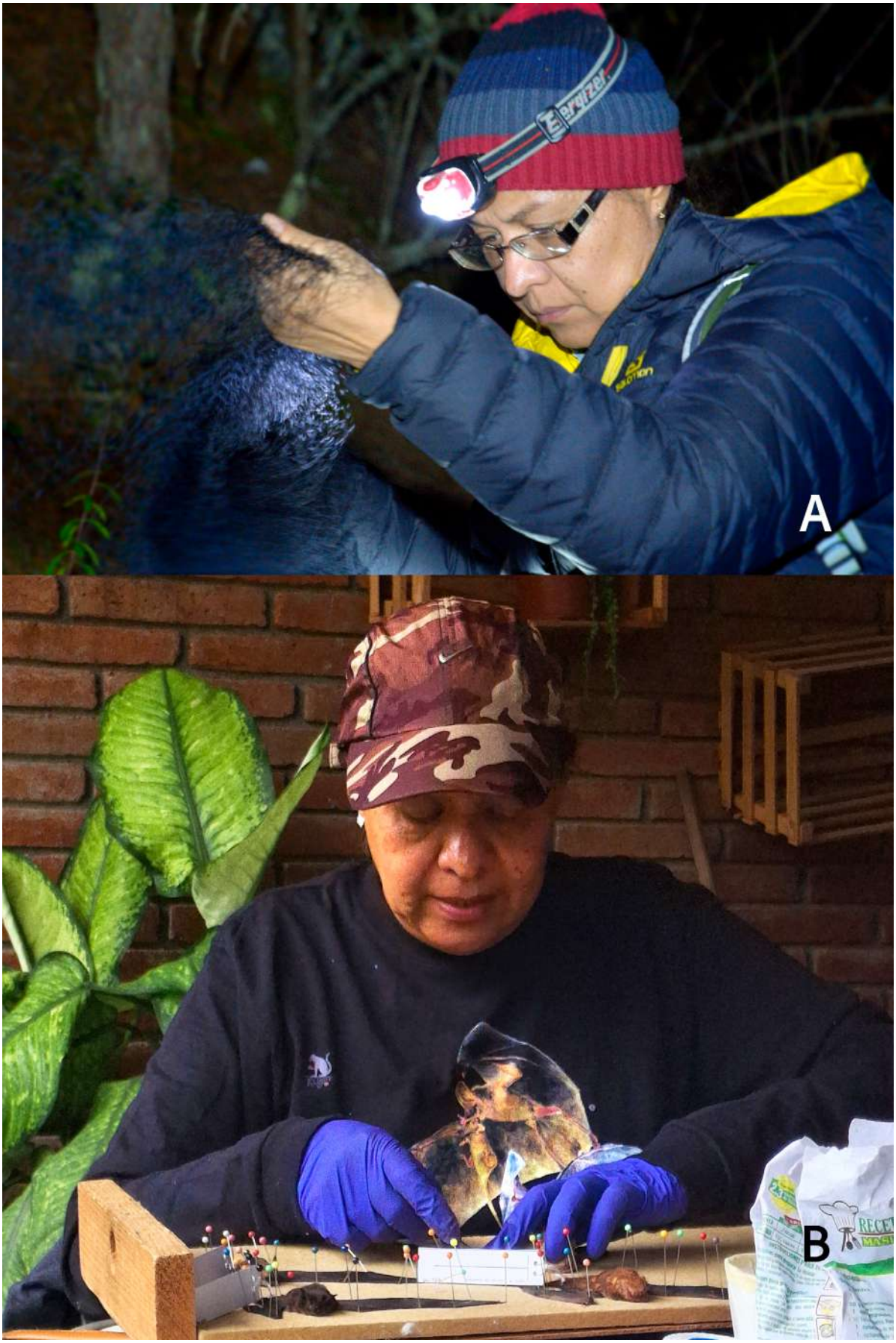

Figure 3. Livia León Paniagua exemplifies her deep commitment to mentoring students and her passion for field biology, demonstrating how she has combined scientific rigor with mentorship to nurture both academic and personal growth. (A) Livia sets a mist net during fieldwork in Perote, Veracruz, Mexico, illustrating her hands-on approach to teaching by example. (B) Livia prepares specimens during a mammal inventory in San Ildefonso Villa Alta, Oaxaca, Mexico. These moments not only provided scientific training but also fostered reflection, learning, and lasting bonds among Livia, students, and colleagues. Photo credits: (A) Dr. Rafael de Villa Magallón; (B) Rodrigo Pilar-Ruiz.

of mammalogists, and the advancement of biological collections. Livia was one of the 14 enthusiastic students – one of the six women– who founded AMMAC in 1984; as a mentor, educator, and collaborator, she set the groundwork for mammalogy in Mexico and has been an example and inspiration for women in science.

The contributions in this special issue reflect the breadth of scientific influence that Livia has explored throughout her career, with studies spanning North, Central, and South America. This issue brings together 56 authors from 31 institutions across seven countries from the Americas, including many of her former students and collaborators. Their contributions address contemporary questions in mammalogy, including the effectiveness of protected areas under climate change, the adaptive potential of threatened species, species delimitation, genomic and morphological variation, host–parasite interactions, and the role of mammals in understanding pathogen evolution. Other studies highlight the use of metadata and genomic resources for conservation and examine ecological and biogeographic patterns across spatial gradients. Together, these contributions demonstrate not only the diversity of topics inspired by Livia's work in the Neotropics and Nearctic regions but also the lasting influence of her scientific visions on contemporary mammalogy.

We would also like to express our heartfelt gratitude for the profound impact Livia has had on generations of students, collaborators, and colleagues. As two of her former students, and on behalf of her alumni, colleagues, and friends, we deeply value not only her extraordinary mentorship and unwavering support for the professional development of everyone who has passed through her laboratory, but also the generosity, trust, warmth, and humanity with which she has accompanied our personal and academic lives, as well as those of our "masto familia". Through her guidance, Livia has created far more than a research group; she has fostered a close and supportive community grounded in friendship, respect, collaboration, and genuine care for one another.

Beyond her role as mentor and colleague, many of us treasure the privilege of her friendship and the countless moments shared alongside her. Conversations with Livia are always thoughtful, engaging, and insightful, unfolding in an atmosphere of openness and mutual respect. During long days of work both indoors and outdoors, shared meals, and late–night conversations, she taught us lessons that extended far beyond science (Figure 3B). Through her example, she showed us the importance of curiosity, resilience, humility, empathy, kindness, and camaraderie, transforming demanding days of work into opportunities for personal growth and human connection. Despite her vast experience and accomplishments, she has always remained approachable, humble, and willing to learn from others, including younger students. Her sincere concern for the well-being and development of her students has left a profound and lasting mark on all of us fortunate enough to know and work alongside her and remains an essential part of the legacy she continues to build.

Finally, we hope that the contributions gathered in this special issue reflect, even if only partially, the admiration, gratitude, and affection felt by many people whose lives and careers have been shaped by Livia's science, mentorship, and humanity. Her influence endures not only in Mexican mammalogy but also among generations of students, colleagues, and friends who continue to learn from her example.

Acknowledgements

Firstly, we would like to thank the Editors–in–Chief for their trust in us to coordinate and edit this special issue. Secondly, we sincerely thank all the alumni, colleagues, and collaborators who graciously contributed high–quality manuscripts to honor Livia's academic career. We are also deeply grateful to all reviewers, whose work was always carried out in anonymity and whose careful evaluations were essential to the success of this project: Alejandro Flores-Manzanero, Ángel León-Tapia, Austin Chipps, Berenit Mendoza, Claudia Moreno, Daily Martínez-Borrego, Darwin Morales-Martínez, Fabricio Villalobos, Gabriela Borja-Martínez, Gabriela Monroy-Gamboa, Gerardo Soria-Ortiz, Guilherme Garbino, Héctor Ramírez-Chaves, Jesús Alonso Panti-May, Jesús A. Fernández, Jocelyn Gutiérrez-Guerrero, Jorge Brito, Jorge Galindo-González, Jorge Gómez-Díaz, Juan J. Morrone, Juan Pech-Canché, Julieta Vargas-Cuenca, Lucas Carneiro, Luis A. Sánchez-González, Luis Verde Arregoitia, Marco Ortiz-Ramírez, Omar Hernández-Dávila, Rosario Mata-López, Tania Garrido-Garduño, Thomas Giarla, and Yolocalli Cisneros-Bernal for their valuable support. In the final stages, we would like to express our sincere gratitude to Isabel Vargas Fernández, Rodrigo Pilar-Ruiz, Mariana Hernández Canchola, and the entire Therya editorial team, whose assistance and dedication made this project possible.

Giovani Hernández-Canchola[1], and Pablo Colunga-Salas[2]

[1]Laboratorio de Mastozoología Evolutiva y Colecciones Científicas, Museo de Zoología "Alfonso L. Herrera", Departamento de Biología Evolutiva, Facultad de Ciencias, Universidad Nacional Autónoma de México, 04510, Mexico City, Mexico. Email: giovani@ciencias.unam.mx

[2]Laboratorio de Mamíferos y Parásitos, Instituto de Biotecnología y Ecología Aplicada, Universidad Veracruzana, 91090, Xalapa-Enríquez, Veracruz, Mexico. Email: pcolunga@uv.mx

Literature Cited

Ávila-Valle ZA, Castro-Campillo A, León-Paniagua L, Salgado-Ugalde IH, Navarro-Sigüenza AG, Hernández-Baños BE, *et al*. 2019. Geographic variation and molecular evidence of the Blackish Deer Mouse complex (*Peromyscus furvus*,

Rodentia: Muridae). *Mammalian Biology* 77: 166–177. https://doi.org/10.1016/j.mambio.2011.09.008

Calahorra-Oliart A, Ospina-Garcés S, and León-Paniagua L. 2021. Cryptic species in *Glossophaga soricina* (Chiroptera: Phyllostomidae): Do morphological data support molecular evidence? *Journal of Mammalogy* 102: 54–68. https://doi.org/10.1093/jmammal/gyaa116

Cano-Sánchez E, Rodríguez-Gómez F, Ruedas LA, Oyama K, León-Paniagua L, Mastretta-Yanes A, *et al.* 2022. Using ultraconserved elements to unravel lagomorph phylogenetic relationships. *Journal of Mammalian Evolution* 29:395–411. https://doi.org/10.1007/s10914-021-09595-0

Castañeda-Rico S, León-Paniagua L, Vázquez-Domínguez E, and Navarro-Sigüenza AG. 2014. Evolutionary diversification and speciation in rodents of the Mexican lowlands: *The Peromyscus melanophrys* species group. *Molecular Phylogenetics and Evolution* 70: 454–463. https://doi.org/10.1016/j.ympev.2013.10.004

Colunga-Salas P, Sánchez-Montes S, León-Paniagua L, and Becker I. 2021. *Borrelia* in neotropical bats: Detection of two new phylogenetic lineages. *Ticks and Tick-borne Diseases* 12: 101642. https://doi.org/10.1016/j.ttbdis.2020.101642

Escobedo-Morales LA, Castañeda-Rico S, Mandujano S, León-Paniagua L, Martínez-Meyer E, and Maldonado JE. 2025. Mitochondrial genome and ultraconserved elements reveal a species complex within the Central American brocket deer *Mazama temama* (Artiodactyla: Cervidae). *Molecular Phylogenetics and Evolution* 211:108400. https://doi.org/10.1016/j.ympev.2025.108400

Garbino GST, Hernández-Canchola G, León-Paniagua L, and Tavares VDC. 2024. A new Mexican endemic species of yellow-eared bat in the genus *Vampyressa* (Phyllostomidae, Stenodermatinae). *Journal of Mammalogy* 105:563–576. https://doi.org/10.1093/jmammal/gyae001

Guevara L, Morrone JJ, and León-Paniagua L. 2018. Spatial variability in species' potential distributions during the Last Glacial Maximum under different global circulation models: Relevance in evolutionary biology. *Journal of Zoological Systematics and Evolutionary Research* 57:113–126. https://doi.org/10.1111/jzs.12238

Guevara L, Sánchez-Cordero V, León-Paniagua L, and Woodman N. 2014. A new species of small-eared shrew (Mammalia, Eulipotyphla, *Cryptotis*) from the Lacandona rain forest, Mexico. *Journal of Mammalogy* 95:739–753. https://doi.org/10.1644/14-MAMM-A-018

Guzmán-Cornejo C, García-Prieto L, Acosta-Gutiérrez R, Falcón-Ordaz J, and León-Paniagua L. 2012. Metazoarios parásitos de *Tlacuatzin canescens* y *Marmosa mexicana* (Mammalia: Didelphimorphia) de México. *Revista Mexicana de Biodiversidad* 83:557–561. https://doi.org/10.22201/ib.20078706e.2012.2.951

Hernández-Canchola G, and León-Paniagua L. 2017. Genetic and ecological processes promoting early diversification in the lowland Mesoamerican bat *Sturnira parvidens* (Chiroptera: Phyllostomidae). *Molecular Phylogenetics and Evolution* 114:334–345. https://doi.org/10.1016/j.ympev.2017.06.015

León-Paniagua L, and Morrone JJ. 2009. Do the Oaxacan highlands represent a natural biotic unit? A cladistic biogeographical test based on vertebrate taxa. *Journal of Biogeography* 36:1939–1944. https://doi.org/10.1111/j.1365-2699.2009.02134.x

León-Paniagua L, Navarro-Sigüenza AG, Hernández-Baños BE, and Morales JC. 2007. Diversification of the arboreal mice of the genus *Habromys* (Rodentia: Cricetidae: Neotominae) in the Mesoamerican highlands. *Molecular Phylogenetics and Evolution* 42:653–664. https://doi.org/10.1016/j.ympev.2006.08.019

López-Cuamatzi IL, Ortega J, Ospina-Garcés SM, Zuñiga G, and MacSwiney MC. 2024. Molecular and morphological data suggest a new species of big-eared bat (Vespertilionidae: *Corynorhinus*) endemic to northeastern Mexico. *PLoS ONE* 19:e0296275. https://doi.org/10.1371/journal.pone.0296275

Marines-Macías T, Colunga-Salas P, Verde-Arregoitia LD, Narjando EJ, and León-Paniagua L. 2018. Space use by two arboreal rodent species in a Neotropical cloud forest. *Journal of Natural History* 52:1417–1431. https://doi.org/10.1080/00222933.2018.1459921

Ospina-Garcés SM, and León-Paniagua L. 2022. The influence of geography in the cranial diversification of the bulldog bats of the genus *Noctilio* (Noctilionidae: Chiroptera). *Organisms Diversity & Evolution* 22:1099–1121. https://doi.org/10.1007/s13127-022-00567-7

Peterson AT, Flores-Villela OA, León-Paniagua L, Llorente-Bousquets JE, Luis-Martínez MA, Navarro-Sigüenza AG, *et al.* 1993. Conservation priorities in Mexico: Moving up in the world. *Biodiversity Letters* 1:33–38. https://doi.org/10.2307/2999648

Rendón-Lugo AN, Puente-Lee I, and León-Paniagua L. 2017. Permeability of hair to cadmium, copper and lead in five species of terrestrial mammals and implications in biomonitoring. *Environmental Monitoring and Assessment* 189:640. https://doi.org/10.1007/s10661-017-6338-z

Rodríguez-Macedo M, González-Christen A, and León-Paniagua L. 2014. Diversidad de los mamíferos silvestres de Misantla, Veracruz, México. *Revista Mexicana de Biodiversidad* 85:262–275. https://doi.org/10.7550/rmb.36143

Romo-Vázquez E, León-Paniagua L, and Sánchez O. 2005. A new species of *Habromys* (Rodentia: Neotominae) from México. *Proceedings of the Biological Society of Washington* 118:605–618. https://doi.org/10.2988/0006-324X(2005)118[605:ANSOHR]2.0.CO;2

THERYA, 2026, Vol. 17(2):131-142 DOI: 10.12933/therya.2026.6248 ISSN 2007-3364

Reopening the case of the enigmatic record hitherto referred to as the Mayan shrew, *Cryptotis mayensis* (Mammalia, Soricidae)

Lázaro Guevara[1,*], Reinhard E. Matadamas[2,3], Stephanye Mata-González[1,3], Paola Zeferino[1], and Joaquín Arroyo-Cabrales[4]

[1]Colección Nacional de Mamíferos, Departamento de Zoología, Instituto de Biología, Universidad Nacional Autónoma de México, Apartado Postal 70-153, CP 04510 Mexico City, Mexico. E-mail: matags_bio@ciencias.unam.mx (SMG); E-mail: paola-zeferino@ciencias.unam.mx (PZ)
[2]Museo de Zoología Alfonso L. Herrera, Facultad de Ciencias, Universidad Nacional Autónoma de México, Apartado Postal 70-153, CP 04510 Mexico City, Mexico. reinhardmata@ciencias.unam.mx (REM).
[3]Posgrado en Ciencias Biológicas, Universidad Nacional Autónoma de México.
[4]Instituto Nacional de Antropología e Historia, Subdirección de laboratorio y Apoyo Académico, Laboratorio de Arqueozoología "M. en C. Ticul Álvarez Solórzano", Moneda Núm. 16, Col. Centro, 06060 Ciudad de México, México. E-mail: arromatu@hotmail.com (JAC)
[*]Corresponding author: llg@ib.unam.mx

The Mayan small-eared shrew, *Cryptotis mayensis*, is endemic to the Yucatán Peninsula, with records from México, Belize, and Guatemala. For half a century, skull fragments from dozens of individuals found in pellets of the barn owl (*Tyto furcata*) in Guerrero, Mexico, previously identified as the Mayan shrew, have intrigued taxonomists and biogeographers. A previous robust analysis of current and fossil *C. mayensis* dentary samples, including those from Guerrero, showed a high morphometric similarity between them. Given that these owl pellet remains are located 1,000 km from the known distribution of *C. mayensis* in the Yucatán Peninsula, this has raised the hypothesis that they are not an isolated population of *C. mayensis* but rather an as-yet-undescribed species. By integrating new specimens of *C. mayensis* from the Yucatán Península and Guerrero, as well as *Cryptotis lacandonensis*, the sister species of *C. mayensis*, we reanalyzed the morphological attributes. In addition, we used paleodistribution estimates to investigate the possible isolation of the records previously referred to as *C. mayensis* in Guerrero, Mexico. Multivariate analyses of morphological data from the cranium and dentary revealed high similarity in size among the three samples analyzed, especially between *C. mayensis sensu stricto* and *Cryptotis* from Guerrero. Paleodistribution models suggest that the population of Guerrero has remained in long-term isolation from the populations of the Yucatan Peninsula due to a very large area with unsuitable conditions for the connectivity of the shrew population during the last glacial-interglacial cycle. It is possible that the Guerrero population is an independent lineage, despite its morphological similarity to *C. mayensis sensu stricto*; however, genetic evidence to confirm this is essential.

Keywords: Eulipotyphla, morphometrics, Neotropics, niche modelling, taxonomy

La musaraña maya de orejas cortas, *Cryptotis mayensis*, es endémica de la Península de Yucatán, con registros en México, Belice y Guatemala. Durante medio siglo, fragmentos de cráneo de docenas de individuos, encontrados en egagrópilas de lechuza común (*Tyto furcata*) en Guerrero, México, que anteriormente se identificaron como la musaraña maya, han intrigado a taxónomos y biogeógrafos. Un exhaustivo análisis previo de muestras dentales actuales y fósiles de *C. mayensis*, incluidas las de Guerrero, mostró una alta similitud morfométrica entre ellas. Dado que estos restos de egagrópilas se encuentran a 1000 km de la distribución conocida de *C. mayensis* en la Península de Yucatán, esto ha planteado la hipótesis de que no se trata de una población aislada de *C. mayensis*, sino de una especie aún no descrita. Al integrar nuevos especímenes de *C. mayensis* de la Península de Yucatán y de Guerrero, así como de *C. lacandonensis*, especie hermana de *C. mayensis*, reanalizamos los atributos morfológicos. Además, utilizamos estimaciones de paleodistribución para investigar el posible aislamiento de los registros previamente atribuidos a *C. mayensis* en Guerrero, México. Los análisis multivariados de datos morfológicos del cráneo y del dentario revelaron una alta similitud en tamaño entre las tres muestras analizadas, especialmente entre *C. mayensis sensu stricto* y *Cryptotis* de Guerrero. Los modelos de paleodistribución sugieren que la población de Guerrero ha permanecido aislada durante largo tiempo de las poblaciones de la Península de Yucatán debido a una extensa área con condiciones desfavorables para la conectividad poblacional durante el último ciclo glacial-interglacial. Es posible que la población de Guerrero sea un linaje independiente, a pesar de su similitud morfológica con *C. mayensis sensu stricto*; sin embargo, es indispensable contar con evidencia genética que lo confirme.

Palabras clave: Eulipotyphla, modelado de nicho, morfometría, Neotrópico, taxonomía

Shrews of the genus *Cryptotis* are small mammals found from southern Canada to northern South America. So far this century, the number of species within this genus has doubled due to intensive taxonomic research, making it the third most diverse genus among the 29 genera of shrews, with 55 species (Mammal Diversity Database 2025). Advances in taxonomic studies have refined previous proposals regarding the evolutionary relationships among several species and established species groups within the genus that may represent monophyletic groups (Guevara and Cervantes 2014; He *et al.* 2015; 2021). One such group is the *Cryptotis nigrescens* group, which includes eight species found from southern Mexico to northern Colombia (Woodman and Timm 2023): *C. mayensis*, *C. merriami*, *C.*

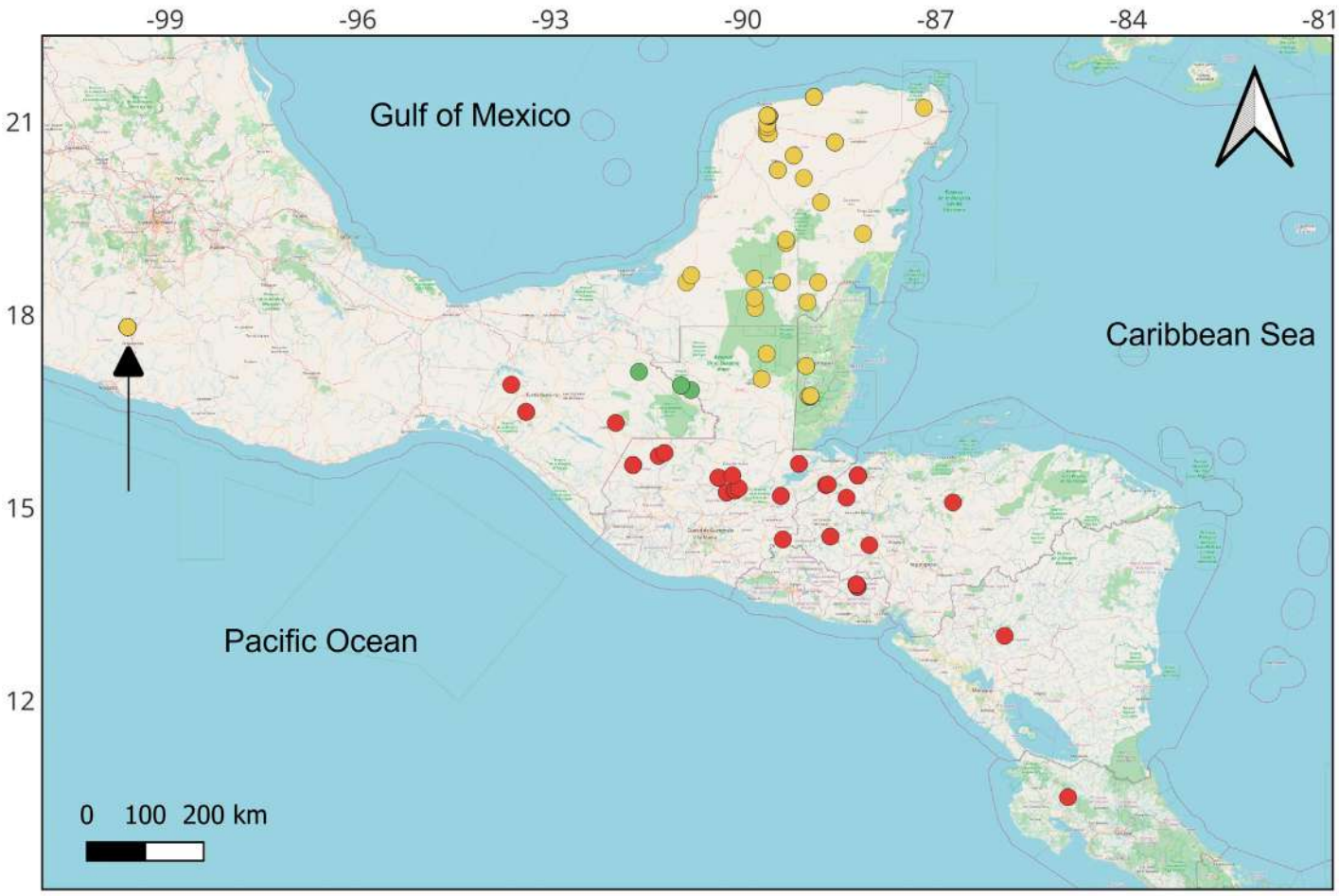

Figure 1. Occurrence records of small-eared shrews of the *Cryptotis nigrescens* group north of Mesoamerica (Guevara *et al.* 2015): Mayan shrew, *Cryptotis mayensis* (yellow dots); Lacandona shrew, *C. lacandonensis* (green dots), and Merriam's shrew, *C. merriami* (red dots). The arrow indicates the approximate location of owl pellet records obtained in 1969.

lacandonensis, *C. nigrescens*, *C. hondurensis*, *C. merus*, *C. brachyonyx*, and *C. colombianus*.

Within the *Cryptotis nigrescens* group, *C. mayensis* (the Mayan shrew) is the most boreal in distribution and endemic to the Yucatán Peninsula, with records from Mexico, Belize, and Guatemala (Lorenzo *et al.* 2019; Woodman 2019). *Cryptotis mayensis* was described based on one specimen "from a Maya ruin at Chichén Itzá, Yucatan", collected on February 5, 1901, by E. W. Nelson and E. A. Goldman (Merriam 1901; Woodman and Timm 1993), and its specific epithet "*mayensis*" refers to the predominant Mayan culture in the region (Carraway 2007; Guevara and Ramírez-Chaves 2025). It remained a little-known species until more specimens were collected decades later (Choate 1970). Nowadays, *C. mayensis* is distributed in lowland areas, usually at <100 m elevation, although a noteworthy record is from the Chiquibul Forest Reserve, Belize, at about 600 m elevation (Engilis *et al.* 2012). It inhabits lowland tropical forests, characterized by dry scrub, deciduous, and seasonally dry forests (Carraway 2007). *Cryptotis mayensis* has also been reported from Pleistocene fossils in the Loltún and Actun Spukil caves, Yucatán (Hatt 1953). The species most closely related to *C. mayensis* is *C. lacandonensis* (the Lacandona shrew), whose distribution is restricted to the Selva Maya on the border between Mexico and Guatemala, in humid tropical forests and seasonally flooded areas at elevations below 200 m (Guevara *et al.* 2014; Pérez *et al.* 2019).

For half a century, mandibles and incomplete skulls from almost 40 individuals found in pellets of the barn owl (*Tyto furcata;* previously *T. alba*) in Guerrero have intrigued taxonomists and biogeographers (López-Forment and Urbano 1977). The pellets were collected by William López-Forment in September 1969, within a stony and arid area surrounding the Cueva del Zopilote, located 13 km south of the Mezcala Bridge (Figure 1; Ramírez-Pulido and Sánchez-Hernández 1972). Based on the similarity of dental features and cranial and dental size, the preliminary assignment of the owl pellet was made to *C. mayensis* (Choate 1970; Woodman and Timm 1993). Their anatomical characteristics allowed these remains to be classified as belonging to the *C. nigrescens* group and not to the *C. goldmani* or *C. parvus* groups, which may also inhabit that region of Guerrero (Guevara *et al.* 2015). For example, the shape of the dentary, the location of the zygomatic plate, and the cusps on the lower and upper third molars are typical of what is observed in *C. mayensis* (Woodman and Timm 1993). Woodman (1995) analyzed current and fossil *C. mayensis* dentary samples, including those from Guerrero, to test the hypothesis that phenotypic changes may be a possible response to Quaternary climatic factors.

He found a high degree of morphometric similarity between the modern samples from Yucatán and Guerrero, which differ slightly from the fossil samples. Given that these remains from owl pellets are located about 1,000 km from the known distribution of *C. mayensis* in the Yucatán Peninsula, this has raised the hypothesis that they are not from an isolated population of *C. mayensis*, but rather from an as-yet-undescribed species (Woodman and Timm 1993; Monroy-Gamboa 2021). The reason for this remarkable geographic isolation has been intuitively attributed to Quaternary environmental changes that have eliminated suitable habitat for this group of shrews between Guerrero and the Yucatán Peninsula, leaving a small population in Guerrero completely isolated (Choate 1970; Woodman and Timm 1993).

To our knowledge, no additional samples or complete specimens of these shrews have been obtained in Guerrero so far, and conducting fieldwork is currently unfeasible due to the high and growing insecurity in that region of the country (Carpio-Domínguez 2021), which has hindered the resolution of the enigma of *C. mayensis* records in Guerrero. In addition, genetic data remain limited for Neotropical *Cryptotis*, which complicates progress in resolving complex taxonomic questions. Over the last two decades, our team and collaborators have consulted with several natural history museums to refine databases for the genus *Cryptotis*, thereby obtaining high-quality morphological and geographic data (Guevara *et al.* 2024). This raises the possibility of reopening old taxonomic and biogeographical questions and addressing them with consideration of new evidence.

Hence, by integrating morphological and distributional analyses, we aim to reexamine the origin of the records referred to as *Cryptotis mayensis* in Guerrero, Mexico, in a more in-depth manner. To do so, (1) we collected more morphological information on populations of interest to assess morphological variation, and (2) we modeled the environmental requirements for *C. mayensis* in the Yucatán Peninsula to estimate its distributional pattern across the Late Quaternary. We predict that including more data will reveal significant differences between samples from the Yucatán Peninsula and Guerrero, suggesting long-term geographic isolation and divergence at a specific level.

Materials and methods

Specimens examined. All specimens examined in the present study are housed in the following collections: Colección Nacional de Mamíferos, Instituto de Biología, Universidad Nacional Autónoma de México, México City (CNMA); Colección Zoológica Regional Mammalia, Instituto de Historia Natural y Ecología (CZRMA); Colección Mastozoológica, El Colegio de la Frontera Sur, San Cristóbal de las Casas (ECO-SC-M); The University of Kansas Natural History Museum, Lawrence (KU); Museo de Zoología "Alfonso L. Herrera", Facultad de Ciencias, Universidad Nacional Autónoma de México, México City (MZFC), Colección de Mamíferos de la Universidad, Autónoma de Yucatán, Mérida (UADY), the National Museum of Natural History, Smithsonian Institution, Washington (USNM), and Colección de Mamíferos, Universidad Veracruzana, Xalapa (UV).

We examined 25 *Cryptotis mayensis sensu stricto* specimens from the Yucatan Peninsula (CNMA 23796-23801; ECO-SC-M 2354-2356, 2358; KU 91463, 143892; UADY 833-840; USNM 170862, 108087, 173000; UV 3535, 3758), 37 skull remains recovered from the owl pellets in Guerrero (CNMA 11031-11043, 12666-12688, 12690), and two specimens of its sister species, *C. lacandonensis* (MZFC 7107, 7168) to gain a better understanding of the possible morphological variation within this clade. It is important to highlight that the material available for *C. lacandonensis* and *C. merriami* in Mexico is extremely scarce (Lorenzo *et al.* 2019; Guevara *et al.* 2024).

Morphometric analyses. Given the fragmentary nature of owl pellets and the difficulty of recovering complete material from all individuals, we performed separate morphometric analyses of the skull and mandibles. We obtained measurements of 20 skulls from the Yucatan Peninsula, 34 from Guerrero, and two from *C. lacandonensis*. For mandibles, we measured 20 right dentaries from the Yucatan Peninsula, seven right dentaries from Guerrero, and two right dentaries from *C. lacandonensis*.

We recorded four measurements of the cranium and five of the mandible (Figure 2) using a Mitutoyo electronic caliper, 500-171-20 model, at 0.1 mm precision under a stereomicroscope: interorbital breadth (IO), breadth of palate across second molars (M2B), breadth of zygomatic plate (ZP); length of molariform toothrow (MTR), height of coronoid process (HCP), the height of articular condyle (HAC), height of coronoid valley (HCV), lower toothrow length (TRD), distance from the upper border of the articular condyle to the posterior edge of the m3 (LAM). Tabular univariate statistics include mean ± SD and total range for each variable (Table 1).

To characterize and evaluate overall size variation across all specimens, we performed principal component analyses (PCA). To explore the cohesion of known species and samples from Guerrero and identify variables that distinguish them, we used discriminant function analyses (DFA). We performed multivariate analyses on correlation matrices of log10-transformed variables for the cranium and mandible separately, using Statistica software (StatSoft Inc. 2005).

Potential distribution over time. To investigate the possible long-term geographic isolation of *Cryptotis* from Guerrero, we modeled the climatic niche of *C. mayensis sensu stricto*. Based on the hypothesis of niche conservatism, we assume that the environmental requirements of the samples from Guerrero are similar to those of *C. mayensis s.s.*, which will allow us to predict its distribution and, therefore, understand the possible dynamics in distribution during the last glacial-interglacial cycle. Hence, we estimated the potential distribution of *C. mayensis s.s.* through time, using the

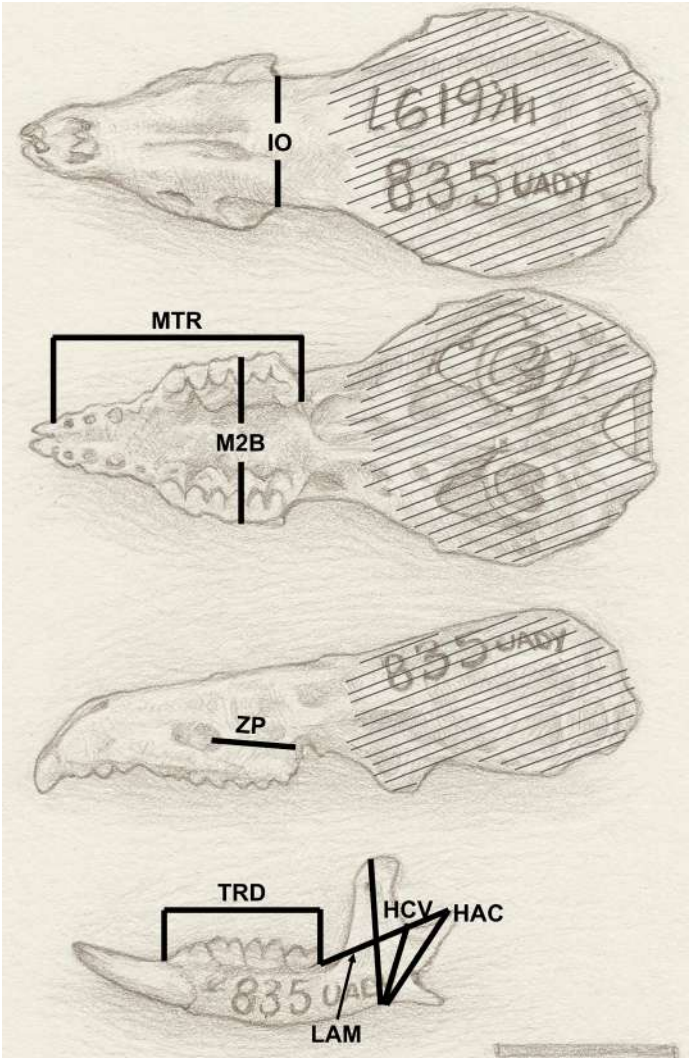

Figure 2. AI-generated image from scientific photographs of a *Cryptotis mayensis* specimen to illustrate the nine qualitative characters measured in the skull and mandible. The lines represent the region of the skull that is generally destroyed or severely damaged in specimens from the owl pellets collected in Guerrero. Scale bar: 5 mm.

Table 1. Cranial and mandibular measurements of three samples of small-eared shrews (Mammalia, *Cryptotis*) from the *Cryptotis nigrescens* group. Statistics are mean ± SD and range, and the number of samples examined by variable.

	C. mayensis s.s.	Guerrero	*C. lacandonensis*
IO	4.51 ± 0.19	4.42 ± 0.19	4.75 ± 0.01
	4.88 - 4.22	4.77 - 4.14	4.76 - 4.74
	n = 20	n = 27	n = 2
ZP	2.33 ± 0.23	2.35 ± 0.14	2.53 ± 0.23
	2.67 – 1.68	2.60 – 2.05	2.69 – 2.36
	n = 23	n = 28	n = 2
MTR	4.90 ± 0.16	4.99 ± 0.14	5.28 ± 0.07
	5.17 – 4.57	5.30 – 4.45	5.33 – 5.23
	n = 23	n = 25	n = 2
M2B	5.11 ± 0.22	5.21 ± 0.14	5.21 ± 0.14
	5.63 - 4.49	5.50 – 5.02	5.50 – 5.02
	n = 23	n = 21	n = 2
HCP	5.19 ± 0.26	5.34 ± 0.23	5.43 ± 0.11
	5.54 - 4.7	5.83 – 5.18	5.50 – 5.35
	n = 22	n = 7	n = 2
HAC	3.73 ± 0.18	3.73 ± 0.15	3.61 ± 0.09
	4.07 – 3.4	3.94 – 3.53	3.67 – 3.54
	n = 22	n = 7	n = 2
HCV	2.82 ± 0.19	2.86 ± 0.14	2.75 ± 0.07
	3.13 – 2.3	3.03 – 2.59	2.80 – 2.70
	n = 22	n = 7	n = 2
LAM	4.77 ± 0.21	4.69 ± 0.29	5.00 ± 0.01
	5.08 - 4.24	4.97 – 5.54	5.00 – 4.99
	n = 22	n = 7	n = 2
TRD	5.37 ± 0.19	5.36 ± 0.27	5.73 ± 0.16
	5.68 – 5.02	5.54 - 4.9	5.84 – 5.62
	n = 22	n = 5	n = 2

present conditions, the Mid-Holocene, and the Last Glacial Maximum (LGM), as climatic extremes during the Quaternary. Ecological niche models (ENMs) and cross-time projections were optimized using the 'kuenm' package (Cobos *et al.* 2019) and the Maxent modeling algorithm (Phillips *et al.* 2017) in R software version 4.4.2 (R Core Team, 2025).

Our initial database was obtained from Guevara *et al*. (2024), which contains 118 unique localities and represents the most up-to-date and refined database available for *C. mayensis*. To reduce bias introduced by field sampling strategies, we spatially filtered the full set of species occurrence records using the spThin package (Aiello-Lammens *et al.* 2015). We retained only records that were at least 5 km apart, resulting in a final data set of 22 unique locations for calibrating and evaluating niche models. For further analysis, we spatially partitioned our data (i.e, checkerboard) into 70% for model calibration and 30% for model evaluation.

As environmental predictors, we initially selected 19 bioclimatic variables from the WorldClim v2.1 portal (Fick and Hijmans 2017). These variables describe various aspects of temperature and precipitation and were downloaded at a 30-second resolution for the period from 1970 to 2000. All bioclimatic layers were downloaded from the terra package using WorldClim version 2.1 climate data for the period 1970-2000 at a 30-second resolution. Then, we computed Pearson's correlation coefficient for each pairwise comparison to assess whether the variables are highly correlated and to decide which, if any, should be removed. Thus, we retained the variables BIO4 (temperature seasonality (standard deviation ×100)), BIO6 (minimum temperature of coldest month), BIO11 (mean temperature of coldest quarter), and BIO16 (precipitation of wettest quarter) because they showed lower correlations with the other variables in the calibration area ($r \leq 0.8$).

For model calibration, we delimited an area by combining ecoregions (Dinerstein *et al.* 2017) and biogeographic provinces (Morrone 2014) that encompass our unique locations, excluding areas unlikely to be accessible to the species given their dispersal abilities (Barve *et al.* 2011). To obtain a high representation of the environments available in the study area, we randomly sampled ~195,000 pixels

within the delimited area (50% of the total area; Guevara *et al.* 2018). To identify model settings approximating optimal levels of complexity, we constructed niche models with a wide variety of combinations of feature classes (Linear; Linear and Quadratic; Linear, Quadratic, and Product; Linear, Quadratic, Product, and Threshold; Linear, Quadratic, Product, Threshold, and Hinge) and regularization multipliers (0.4 – 6 at 0.25 intervals). This process yielded 115 unique FC-RM combinations. To select the optimal settings for building a final Maxent model, we examined the omission rate (OR5) at a 5% training omission rate threshold and the area under the curve (AUC) for testing points. These two metrics help evaluate performance with respect to overfitting and discrimination, respectively.

We transferred the final model onto the present, Mid-Holocene, and LGM climatic conditions to estimate potential distributions over the last interglacial–glacial cycle across Central America (i.e., from Mexico to Panama). We used unconstrained extrapolation for model projection, disabling the default 'clamping' option in Maxent (Guevara *et al.* 2018). To consider the variability in past climatic reconstructions (Guevara *et al.* 2019), we used three different General Circulation Models (GCMs): the Community Climate System Model (CCSM4), the Model for Interdisciplinary Research on Climate (MIROC-ESM), and the Max-Planck-Institute für Meteorologie (MPI). We downloaded past bioclimatic layers from the WorldClim database at a resolution of 2.5 arc-min. To identify uncertainty due to model extrapolation, we created a Multivariate Environmental Similarity Surface (MESS) map, which helps detect areas where non-analog conditions occur.

Finally, to display the final maps for the present and the paleoclimatic scenarios, we classified the continuous model output into suitable and unsuitable conditions using the 10th percentile training presence threshold. This threshold excludes the lowest 10% of suitability scores from locations where the species is known to occur (Merow *et al*. 2013). We retained the suitability values in the original continuous format above this threshold to show the suitability gradient, and we also converted the original model output into a binary prediction of suitable-unsuitable areas. Using binary maps (0 = unsuitable; 1 = suitable), we summed the present and past potential distribution maps (for each of the three GCMs) to identify regions that have remained climatically suitable for *C. mayensis*.

Results

Considering the fragmentary origin of the owl pellet remains from Guerrero and the limitations this entails, they are very similar to *Cryptotis mayensis sensu stricto*. The zygomatic plate is quite broad (ZP = 2.35 ± 0.14 mm); the anterior border of the zygomatic plate runs from the parastyle-mesostyle valley to the mesostyle of M1, and the posterior border runs from the metastyle of M2 to the middle of M3. The mandible is moderately long (LAM = 4.69 ± 0.29 mm), and the coronoid process of the mandible is high (HCP = 5.34 ± 0.23 mm); the anterior border of the mandible joins the horizontal ramus at approximately a right angle.

Principal component analysis. For the analysis of the skulls, the principal components 1 and 2 explained 78.6% of the variation in the data (PC 1 = 60.6% and PC 2 = 18.0%) and were primarily correlated with the length of molariform toothrow (MTR) and the breadth of zygomatic plate (ZP), respectively. In the plot of 1st PCs from the PCA, the specimens of Lacandona shrew tended to plot among the largest in the sample (Figure 3a). Regarding the analysis of the dentary, the principal components 1 and 2 explained 70.6% of the variation in the data (PC 1 = 55.6% and PC 2 = 15.0%) and were primarily correlated with the height of articular condyle (HAC) and distance from the upper border of the articular condyle to the posterior edge of the m3 (LAM), respectively. A plot of the 1st PCs from the PCA highlights again the difference in size of *C. lacandonensis* with respect to *C. mayensis sensu stricto* and the samples from Guerrero, which tend to show a very similar pattern of variation in size (Figure 3). In general, the PCA analyses indicate that the specimens of *C. mayensis sensu stricto* and *Cryptotis* from Guerrero exhibit a similar pattern of morphometric variation and differ from *C. lacandonensis*.

Discriminant function analysis. For the analysis of the crania, the 1st function accounts for over 80.7% of the explained variance (Table 2), which is weighted most heavily by the length of molariform toothrow (MTR), contrasted with the interorbital breadth (IO). A plot of the two canonical axes failed to show a clear separation of the samples in multivariate space. The DFA based on the four cranial variables did not efficiently discriminate the Guerrero specimens from the other species (Wilks' Lambda = 0.652; F8,66 = 1.9626; P < 0.0651). In addition, the DFA of the four cranial variables produced moderate to null correct classification rates of 75%, 53%, and 0% for *C. mayensis sensu stricto* (n = 20), *Cryptotis* from Guerrero (n = 17), and *C. lacandonensis* (n = 2), respectively, demonstrating the high morphometric similarity between the samples. In general, the length of molariform toothrow (MTR) is the measure that most helps distinguish samples, but only between the Lacandona shrew from the other two groups.

Table 2. Standardized coefficients of canonical variables based on four and five log-transformed cranial and mandibular variables, respectively, of three samples of small-eared shrews (Mammalia, *Cryptotis*) from the *Cryptotis nigrescens* group.

	Cranial			Mandibular	
	Root 1	**Root 2**		**Root 1**	**Root 2**
IO	-0.324328	-1.03949	**HCP**	0.527026	-0.675966
PZ	-0.368533	-0.43909	**HAC**	0.531030	0.912683
MTR	0.959846	0.05730	**HCV**	0.559793	-0.500879
M2B	0.530850	0.51862	**LAM**	-0.776315	0.529173
-	-	-	**TRD**	-0.948245	-0.673339
Eigenval	0.399078	0.09528		1.000187	0.180837
Explained variance (%)	80.7%	19.2%		84.7%	15.3%

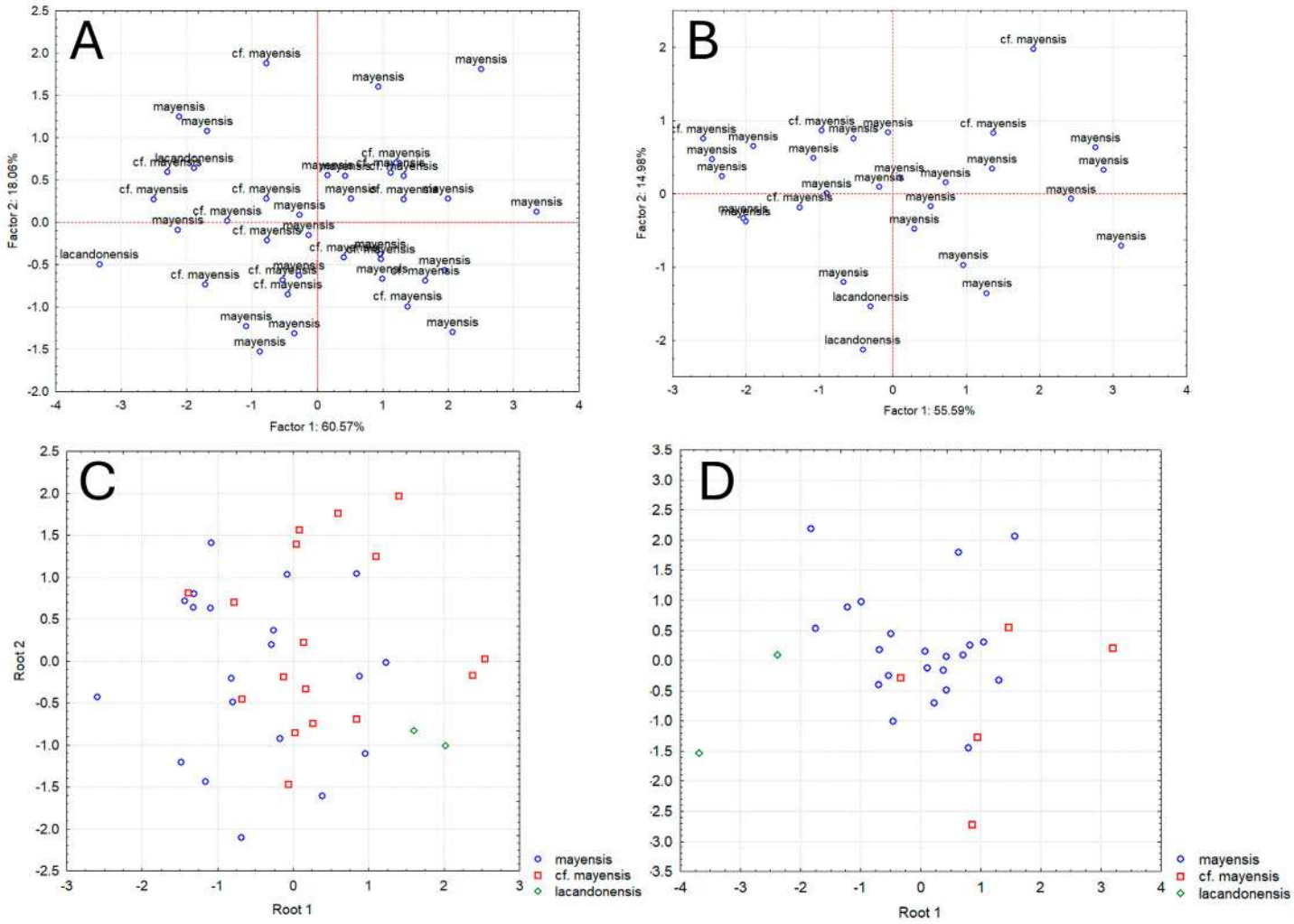

Figure 3. Plot of scores on first two axes from principal components (PCA) and discriminant function (DFA) analyses of the cranium and mandibles of specimens from *Cryptotis mayensis* s.s., *C. lacandonensis,* and samples from Guerrero, México. A, PCA for cranium; B, PCA for mandibles; C, DFA for cranium; D, DFA for mandibles.

On the other hand, for the analysis of the mandibles, the 1st function accounts for over 85% of the explained variance (Table 2), which is weighted most heavily by the lower toothrow length (TRD), contrasted with the height of the articular condyle (HAC). A plot of the two canonical axes shows that the specimens of the Lacandona shrew are slightly separated on the first axis due to their larger size. In contrast, the second axis does not allow a clear separation between the three samples (Figure 3d). The DFA based on the five variables showed better performance than the one based only on the skull for distinguishing the a priori groups (Wilks' Lambda = 0.423; F10,44 = 2.3621, P < 0.0246). In addition, the DFA produced correct classification rates of 100%, 40%, and 50% for *C. mayensis sensu stricto* (n = 22), *Cryptotis* from Guerrero (n = 5), and *C. lacandonensis* (n = 2), respectively, suggesting that this structure may have a greater contribution to distinguishing between taxa. In general, lower tooth length (TRD) in isolation is the measure that most helps distinguish samples, but again, only between the Lacandona shrew and the other two taxa (*C. lacandonensis*: 5.73 ± 0.16 mm; *C. mayensis s.s.*: 5.37 ± 0.19 mm; Guerrero: 5.36 ± 0.27 mm).

In sum, considering the small sample size of *C. lacandonensis*, multivariate analyses of the cranium and dentary indicate high similarity in size across the three samples analyzed, especially between *C. mayensis sensu stricto* and *Cryptotis* from Guerrero. *Cryptotis lacandonensis* is distinguishable from the other two by its larger size, which can be more easily detected by measuring both the upper and lower tooth rows (Table 1).

Biogeographic analyses. Of the 115 niche models generated for *C. mayensis sensu stricto*, four stood out for their better performance based on significance, omission rate, and AICc. Although these four models did not show significant differences, we present the output of the model that performed slightly better. This model was implemented using the following feature classes and regularization multiplier: Linear and Quadratic, with a value of 1.2 (AUC: 0.829; mean AUC ratio: 1.8392; omission rate at 5%: <0%). Of the four variables used to build the final model, precipitation of the wettest quarter (BIO 16) was the most important, indicating a steep decline in climatic suitability when precipitation exceeds 400 mm. Accordingly, the model suggests a current potential distribution that is closely linked to the distribution of warm-humid and warm-dry forests of the Yucatan Peninsula and the Pacific slope, including the area surrounding the Cueva del Zopilote,

Guerrero, where the owl pellets were collected. Between the estimated suitable conditions for *C. mayensis s.s.* on the Yucatan Peninsula and those towards the Pacific slope, there are more than 500 km of areas with unsuitable habitat for this shrew, where more humid and temperate climates predominate across several mountain ranges (Figure 4).

When the model was transferred to Mid-Holocene and LGM conditions, the predictions showed an apparent reduction in suitable areas across the three GCMs, with the reduction even more pronounced during the LGM (Figure 4). During the Mid-Holocene, approximately 6,000 years ago, suitable conditions for *C. mayensis* appear to have persisted across much of the Yucatan Peninsula; however, this is less extensive if we consider only the continental crust at the surface or currently exposed. On the Pacific slope, conditions may have occurred in a more restricted area and farther from the area surrounding Cueva del Zopilote. During the LGM, around 20,000 years ago, suitable conditions for *C. mayensis* declined considerably on the Yucatán Peninsula and the Pacific coast, although less drastically in the latter region. As in the Mid-Holocene, favorable climatic conditions for *Cryptotis mayensis* may have been restricted to a smaller area, farther from Cueva del Zopilote.

The MESS analysis indicates that the climatic conditions of the various paleoclimatic scenarios closely resemble those of the calibration area, particularly in the Yucatan Peninsula and along the Pacific slope. This similarity in climatic conditions is consistent across the three analyzed Global Climate Models (GCMs), with positive values observed in these regions. In contrast, areas indicating non-analogous climatic conditions are primarily located in northern Mexico. Specific scenarios, such as the MIROC model during the mid-Holocene, also reveal regions with non-analogous climates that seem to correspond with mountainous areas in Chiapas and central Mexico. However, these areas of high uncertainty do not impact the predicted distribution of *C. mayensis*. Overall, the MESS analysis reinforces our model projections, showing that climatic conditions in the Pacific region remained within the range used to train the model.

In sum, none of the three-time-slice analyses support the hypothesis of a corridor of suitable conditions for the connectivity of shrew populations with requirements similar to those of *C. mayensis* during the last glacial-interglacial cycle or in analogous climatic phases.

Discussion

Owl pellets and an old biogeographical dilemma. We are still in the discovery stage on the diversity and distribution of Neotropical shrews (Woodman 2019; Guevara *et al.* 2024). For example, the environmental requirements and geographical distribution of most species remain poorly delimited and contain much information gaps due to the difficulty of collecting specimens in the field and the lack of more taxonomists specializing in this group. Pellet analyses have been a beneficial source for complementing these knowledge gaps, as they can provide records of rare or difficult-to-collect species (Avenant 2005; Biedma *et al.* 2019). However, due to the fragmentary nature of the specimens and the difficulty in unequivocally assigning the geographical origin of individuals consumed by raptors, the taxonomic identification of samples can be a significant challenge.

The claim that pellets recovered in Cueva del Zopilote, Guerrero, come from the Barn owl, *Tyto furcata*, was based on the identification by the renowned ornithologist Allan R. Phillips, who conducted numerous expeditions in Mexico (López-Forment and Urbano 1977). This bird of prey is very common in both natural and altered ecosystems, feeding on small mammals, including shrews (Biedma *et al.* 2019). The area surrounding the Cueva del Zopilote was described by the original collector as stony and arid, with plant species of the genera *Bursera*, *Ceiba*, *Cephalocereus, Erythrina*, *Ficus*, and *Ipomoea*. In addition to this species of shrews, records of common mammal species on the Pacific slope were also found, including *Heteromys irroratus*, *Osgoodomys banderanus*, *Tlacuatzin canescens*, *Megasorex gigas*, *Spilogale pygmaea*, and several bat species (Ramírez-Pulido and Sánchez-Hernández 1972; López-Forment and Urbano 1977). Interestingly, the record of two skulls of the climbing rat, *Ototylomys phyllotis*, is noteworthy, as its species' distribution ranges from the Yucatan Peninsula to Central America (Lawlor 1982; Espinosa-Martínez *et al.* 2017). The fact that at least these two terrestrial mammal species exhibit the same remarkable disjunct geographic distribution pattern further calls for clarifying the taxonomic status of the Guerrero individuals with additional sources of evidence and analytical methods.

New answers and new questions. The taxonomic uncertainty about the identity of the specimens from Guerrero has been addressed on several occasions using morphological comparisons with both current and Pleistocene samples of *Cryptotis mayensis s.s.* from the Yucatan Peninsula (Choate 1970; Woodman and Timm 1993; Woodman 1995). These analyses did not reveal significant and sufficient differences to distinguish a different species, so the Guerrero samples continue to be referred to as *C. mayensis* (Monroy-Gamboa 2021). Our new analysis, which includes a larger number of samples than previous studies, including *C. lacandonensis*, the sister species of *C. mayensis*, also did not allow a clear qualitative and quantitative distinction. However, we found that the Guerrero samples are morphologically more like *C. mayensis s.s.* than *C. lacandonensis*, a species found in wetter conditions at the base of the Yucatán Peninsula (Guevara *et al.* 2014). We cannot rule out that, if complete skulls and skeletons become available in the future, it may be possible to find differences that allow for discrimination, as has been the case when analyzing other structures such as the humeri or claws in shrews of this genus (Woodman and Morgan 2005; Woodman and Gaffney 2014). Future field studies, including proper methods for sampling shrews such as pitfall traps (Lorenzo *et al.* 2019), and increased sampling in the area

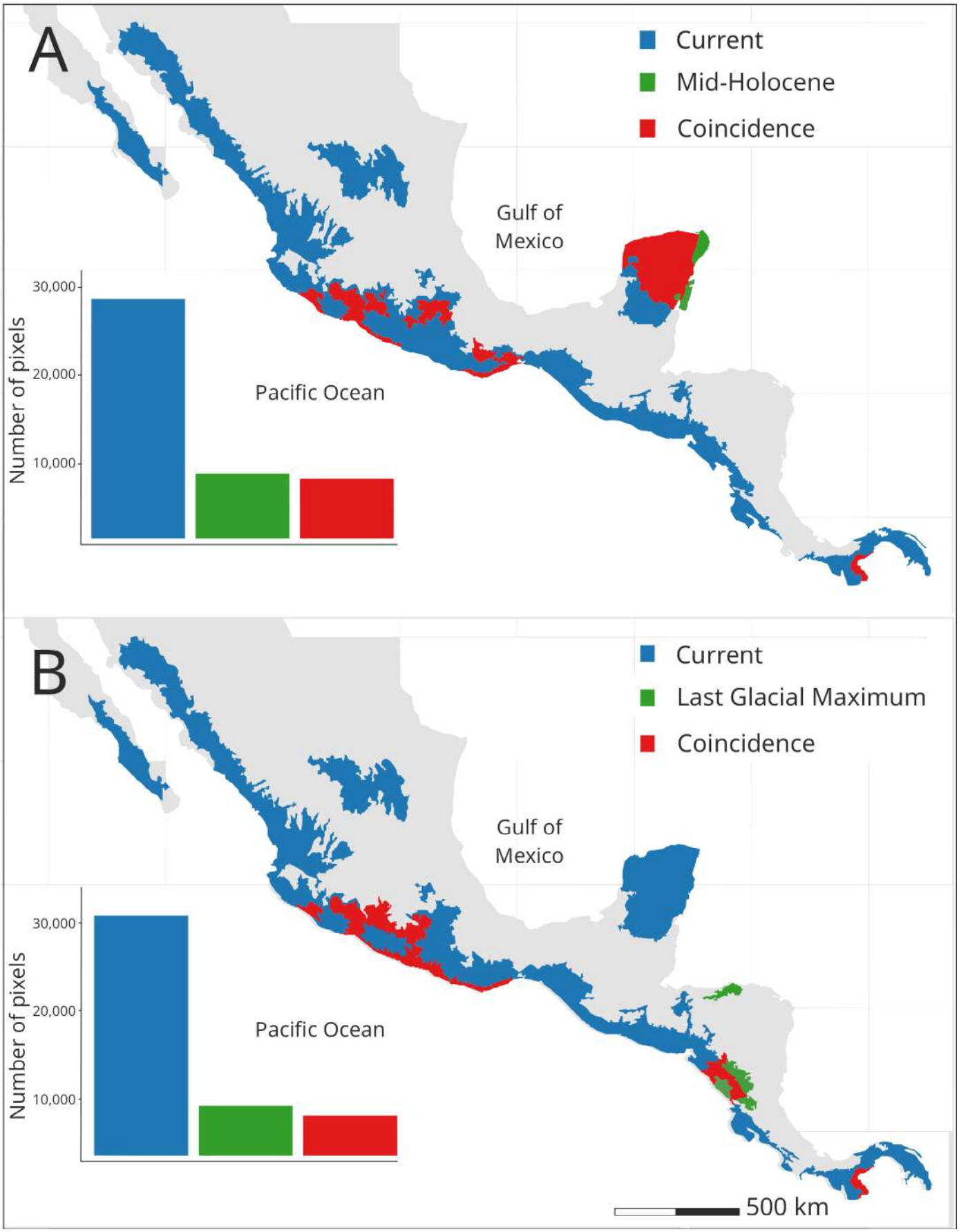

Figure 4. Potential distribution of the Mayan shrew, *Cryptotis mayensis*, estimated for the present, the Mid-Holocene, and the Last Glacial Maximum using ecological niche models. The estimation of Mid-Holocene (A), and Last Glacial Maximum (B) is based on the consensus of three general circulation models, CCSM4, MIROC-ESM, and MPI-ESM-P. The colors on the map indicate the three temporal scenarios considered: Present (blue), mid-Holocene or Last Glacial Maximum (green), and overlap zones between them (red). The bar chart shows the number of pixels estimated to contain suitable conditions for *C. mayensis* in each period.

near Cueva del Zopilote Cave, could be highly beneficial to searching for complete specimens of this shrew; however, as we mentioned earlier, the current public safety situation in this country could complicate this urgent action.

In any case, morphological differences are not the only source of evidence for recognizing differentiated lineages at a specific level in mammals (Baker and Bradley 2006; Bonilla-Sánchez *et al.* 2024). In recent years, improvements in sequencing technologies have made it possible to obtain genomic-scale data from old museum specimens by extracting DNA, including bones (Guimaraes *et al.* 2016). Therefore, the next step is to conduct a destructive analysis of the samples to extract DNA and analyze it in a phylogenetic context. Meanwhile, other methodological approaches can help solve the current puzzle. In this case, it is well recognized that correlative ecological niche modeling can help identify possible geographic barriers and isolated populations, thereby leading to the discovery of heretofore unknown populations or species (Raxworthy *et al.* 2003; Peterson *et al.* 2011).

With paleodistribution estimates, niche models allow inference of the possible long-term isolation in which populations have been maintained, assisting in decision-making on taxonomic status (Guevara *et al.* 2019). In the case of Neotropics, the Late Quaternary is a crucial period for understanding the current diversity of shrews (Barnosky 2005). The constant climatic fluctuations that have occurred over the last thousands of years have altered geographic distributions, causing expansion-contraction and fragmentation-connectivity events across populations (Choate 1970; Woodman and Timm 1999; Woodman 2005; Guevara and Sánchez-Cordero 2018). Some shrew populations may have remained isolated due to the complex topography of the region; consequently, long-term isolation could have promoted lineage divergence (Guevara and Sánchez-Cordero 2018).

Diversification within the *Cryptotis nigrescens* group may have been accentuated by Pleistocene climatic changes (Ceballos *et al.* 2010). Based on the hypotheses derived from the paleodistributions, we suggest that differentiation may have begun before or at the onset of the Quaternary. Still, glacial-interglacial cycles could have helped reinforce differentiation among taxa within the *C. nigrescens* group, which needs to be tested as environmental reconstructions in the region progress further (León-Carreño *et al.* 2025).

In summary, based on the morphological and biogeographic analyses presented here, along with previously published morphological studies (Choate 1970; Woodman 1995), it is possible that the Guerrero population is an independent lineage; however, genetic evidence to support this hypothesis is essential. The absence of records for any species from the *Cryptotis nigrescens* group on the Pacific slope, combined with a relatively high number of records for shrews from other groups or genera (Guevara *et al.* 2015; 2024), suggests that this lineage may have a very restricted distribution or even be extinct.

Acknowledgments

We dedicate this work to Dr. Livia León Paniagua, whose distinguished career and inspiring leadership have significantly advanced Mexican mammalogy. Her dedication, integrity, mentorship, and passion for science and education have shaped generations of new scientists.

We thank the following curators and collection managers for the facilities they provided for the examination of specimens in their collections: F. A. Cervantes, J. Vargas, and Y. Hortelano-Moncada (CNMA); A. Riechers (CZRMA); C. Lorenzo and J. Bolaños Citalán (ECO-SC-M); Robert M. Timm (KU); L. León Paniagua (MZFC), S. Hernández Betancourt (UADY), Neal Woodman and S. Peurach (USNM), and C. A. Delfín Alfonso and N. V. Rodríguez Santiago (UV). This work was supported by UNAM-PAPIIT (IN218125).

Declaration of Artificial Intelligence use

ChatGPT Plus was used to generate Figure 2, with a scientific photograph of a museum specimen as input. Grammarly Pro, an AI writing assistant, was used to review the spelling and structure of English.

Author contributions

Lazaro Guevara: Conceptualization (lead); Data curation (supporting); Formal analysis (lead); Writing – review and editing (lead). Reinhard E. Matadamas: Data curation (lead); Formal analysis (lead); Writing – review and editing (supporting). Stephanye Mata-González: Formal analysis (lead); Writing – review and editing (supporting). Paola Zeferino: Conceptualization (supporting); Data curation (supporting); Joaquín Arroyo-Cabrales: Conceptualization (supporting); Writing – review and editing (supporting).

Literature cited

Aiello-Lammens ME, Boria RA, Radosavljevic A, Vilela B, and Anderson RP. 2015. spThin: an R package for spatial thinning of species occurrence records for use in ecological niche models. *Ecography* 38:541–545. https://doi.org/10.1111/ecog.01132

Avenant N. 2005. Barn owl pellets: a useful tool for monitoring small mammal communities. *Belgian Journal of Zoology* 135:39–43.

Baker RJ, and Bradley RD. 2006. Speciation in mammals and the genetic species concept. *Journal of Mammalogy* 87:643–662. https://doi.org/10.1644/06-MAMM-F-038R2.1

Barnosky AD. 2005. Effects of Quaternary climatic change on speciation in mammals. *Journal of Mammalian Evolution* 12:247–264. https://doi.org/10.1007/s10914-005-4858-8

Barve N, Barve V, Jiménez-Valverde A, Lira-Noriega A, Maher SP, Peterson AT, *et al.* 2011. The crucial role of the accessible area in ecological niche modeling and species distribution modeling. *Ecological Modelling* 222:1810–1819. https://doi.org/10.1016/j.ecolmodel.2011.02.011

Biedma L, Román J, Godoy JA, and Calzada J. 2019. Using owl pellets to infer habitat associations and clarify

the regional distribution of a cryptic shrew. *Journal of Zoology* 308:139–148. https://doi.org/10.1111/jzo.12660

Bonilla-Sánchez A, Sartor CC, Fox-Rosales LA, Feijó A, Ramírez-Fernández JD, Brenes-Mora E, *et al*. 2024. Ecological niche modeling of the *Leopardus tigrinus* complex sheds light on its elusive evolutionary history. *Journal of Mammalogy* 105:953–964. https://doi.org/10.1093/jmammal/gyae074

Carpio-Domínguez JL. 2021. Crimen organizado (narcotráfico) y conservación ambiental: el tema pendiente de la seguridad pública en México. *CS* 33:237–274. https://doi.org/10.18046/recs.i33.4076

Carraway LN. 2007. Shrews (Eulypotyphla: Soricidae) of México. *Monographs of the Western North American Naturalist* 3:1–91.

Ceballos G, Arroyo-Cabrales J, and Ponce E. 2010. Effects of Pleistocene environmental changes on the distribution and community structure of the mammalian fauna of Mexico. *Quaternary Research* 73:464–473. https://doi.org/10.1016/j.yqres.2010.02.006

Choate J. 1970. Systematics and Zoogeography of Middle American shrews of the genus *Cryptotis*. *University of Kansas Publications, Museum of Natural History* 19:195–317. https://doi.org/10.5962/bhl.part.15450

Cobos ME, Peterson AT, Barve N, and Osorio-Olvera L. 2019. kuenm: an R package for detailed development of ecological niche models using Maxent. *PeerJ* 7:e6281. https://doi.org/10.7717/peerj.6281

Dinerstein E, Olson D, Joshi A, Vynne C, Burgess ND, Wikramanayake E, *et al*. 2017. An ecoregion-based approach to protecting half the terrestrial realm. *BioScience* 67:534–545. https://doi.org/10.1093/biosci/bix014

Engilis A, Cole RE, and Caro TM, editors. 2012. Small mammal survey of Chiquibul forest reserve, Maya mountains, Belize, 2001. Lubbock, TX (EEUU): Museum of Texas Tech University.

Espinosa-Martínez DV, Ríos-Muñoz CA, Rosales Nanduca H, Arroyo-Cabrales J, and León-Paniagua L. 2017. Mamíferos de Guerrero. *Revista Mexicana de Mastozoología* 7:38–67. https://doi.org/10.22201/ie.20074484e.2017.1.2.247

Fick SE, and Hijmans RJ. 2017. WorldClim 2: new 1km spatial resolution climate surfaces for global land areas. *International Journal of Climatology* 37:4302–4315. https://doi.org/10.1002/joc.5086

Guevara L, and Cervantes FA. 2014. Molecular systematics of small-eared shrews (Soricomorpha, Mammalia) within *Cryptotis mexicanus* species group from Mesoamérica. *Acta theriologica* 59:233–242. https://doi.org/10.1007/s13364-013-0165-6

Guevara L, Cervantes FA, and Sánchez-Cordero V. 2015. Riqueza, distribución y conservación de los topos y las musarañas (Mammalia, Eulipotyphla) de México. *Therya* 6:43–68. https://doi.org/10.12933/therya-15-211

Guevara L, Gerstner BE, Kass JM, and Anderson RP. 2018. Toward ecologically realistic predictions of species distributions: A cross-time example from tropical montane cloud forests. *Global Change Biology* 24:1511–1522. https://doi.org/10.1111/gcb.13992

Guevara L, Morrone JJ, and León-Paniagua L. 2019. Spatial variability in species' potential distributions during the last glacial maximum under different global circulation models: Relevance in evolutionary biology. *Journal of Zoological Systematics and Evolutionary Research* 57:113–126. https://doi.org/10.1111/jzs.12238

Guevara L, and Ramírez-Chaves HE. 2025. *Cryptotis nigrescens* Species Group (*C. brachyonyx*, *C. colombianus*, *C. hondurensis*, *C. lacandonensis*, *C. mayensis*, *C. merriami*, *C. merus*, and *C. nigrescens*). In Guevara L, and León-Tapia MA, editors. *Mammals of Middle and South America: Eulipotyphla*. Cham: Springer Nature Switzerland; p. 1–4. https://doi.org/10.1007/978-3-031-24765-1

Guevara L, and Sánchez-Cordero V. 2018. Patterns of morphological and ecological similarities of small-eared shrews (Soricidae, *Cryptotis*) in tropical montane cloud forests from Mesoamerica. *Systematics and Biodiversity* 16:551–564. https://doi.org/10.1080/14772000.2018.1470582

Guevara L, Sánchez-Cordero V, León-Paniagua L, and Woodman N. 2014. A new species of small-eared shrew (Mammalia, Eulipotyphla, *Cryptotis*) from the Lacandona rain forest, Mexico. *Journal of Mammalogy* 95:739–753. https://doi.org/10.1644/14-MAMM-A-018

Guevara L, Vargas-Cuenca J, Hortelano-Moncada Y, and Cervantes FA. 2024. A specimen-based database of small-eared shrews (Mammalia, Eulipotyphla, *Cryptotis*) in the Neotropical Region. *Biodiversity Data Journal* 12:e135180. https://doi.org/10.3897/BDJ.12.e135180

Guimaraes S, Fernandez-Jalvo Y, Stoetzel E, Gorgé O, Bennett EA, Denys C, *et al*. (2016). Owl pellets: a wise DNA source for small mammal genetics. *Journal of Zoology* 298:64–74. https://doi.org/10.1111/jzo.12285

Hatt RT. 1953. The mammals. In: R.T. Hatt, H.I. Fisher, D.A. Langebartel, and G.W. Brainerd, editors. *Faunal and archeological researches in Yucatan Caves*. Cranbrook Institute of Science Bulletin; p. 45–77. https://doi.org/10.1093/aibsbulletin/3.3.12-f

He K, Chen X, Qiu YB, Liu Z, Wang WZ, Woodman N, Maldonado JE, and Pan X. 2021. Mitogenome and phylogenetic analyses support rapid diversification among species groups of small-eared shrews genus *Cryptotis* (Mammalia: Eulipotyphla: Soricidae). *Zoological Research* 42:739–745. https://doi.org/10.24272/j.issn.2095-8137.2021.199

He K, Woodman N, Boaglio S, Roberts M, Supekar S, and Maldonado JE. 2015. Molecular phylogeny supports repeated adaptation to burrowing within small-eared shrews genus of *Cryptotis* (Eulipotyphla, Soricidae). *PloS One* 10:e0140280. https://doi.org/10.1371/journal.pone.0140280

Lawlor TE. 1982. *Ototylomys phyllotis*. *Mammalian Species* 181:1–3. https://doi.org/10.2307/3503849

León-Carreño M, Correa-Metrio A, Ramos-Fabiel MA, Escobar J, Curtis JH, Franco-Gaviria F., *et al*. 2025. The environmental signal of lake sediments in Mesoamerica: Modern pollen and geochemical composition. *The Holocene* 35:600–615. https://doi.org/10.1177/09596836251320342

López-Forment W, and Urbano G. 1977. Restos de pequeños mamíferos recuperados en regurgitaciones de lechuza, *Tyto alba* en México. *Anales del Instituto de Biología, Universidad Nacional Autónoma de México, Serie Zoología* 48:231–242.

Lorenzo C, Bolaños-Citalán J, Navarrete-Gutiérrez D, Pérez-López JA, and Guevara L. 2019. In search of shrews of Chiapas: analysis of their distribution and conservation. *Therya* 10:121–129. https://doi.org/10.12933/therya-19-717

Mammal Diversity Database. 2025. Mammal Diversity Database (Version 2.3) [Soricidae]. Zenodo. https://doi.org/10.5281/zenodo.17033774

Merow C, Smith MJ, and Silander Jr JA. 2013. A practical guide to MaxEnt for modeling species' distributions: what it does, and why inputs and settings matter. *Ecography* 36:1058–1069. https://doi.org/10.1111/j.1600-0587.2013.07872.x

Merriam CH. 1901. Seven new mammals from Mexico, including a new genus of rodents. *Proceedings of the Washington Academy of Sciences* 3:559–563.

Monroy-Gamboa AG. 2021. The ghost mammals from Mexico and their implications. *Therya* 12:477–486. https://doi.org/10.12933/therya-21-1186

Morrone JJ. 2014. Biogeographical regionalisation of the Neotropical region. *Zootaxa* 3782:1–110. https://doi.org/10.11646/zootaxa.3782.1.1

Pérez SG, Jolón MR, Mérida JE, and Andino-Madrid AJ. 2019. First record of the shrew *Cryptotis lacandonensis* (Eulipotyphla: Soricidae) for Guatemala. *Therya* 10:187–193. https://doi.org/10.12933/therya-19-766

Peterson AT, Soberón J, Pearson RG, Anderson RP, Martínez-Meyer E, Nakamura M, *et al*. 2011. Ecological niches and geographic distributions. Princeton (EEUU): Princeton University Press. https://doi.org/10.1515/9781400840670

Phillips SJ, Anderson RP, Dudík M, Schapire RE, and Blair ME. 2017. Opening the black box: An open-source release of Maxent. *Ecography* 40:887–893. https://doi.org/10.1111/ecog.03049

R Core Team. 2025. *R: A Language and Environment for Statistical Computing*. R Foundation for Statistical Computing, Vienna, Austria. https://www.R-project.org/

Ramírez-Pulido J, and Sánchez-Hernández C. 1972. Regurgitaciones de lechuza, procedentes de la cueva del Cañón del Zopilote, Guerrero, México. *Revista de la Sociedad Mexicana de Historia Natural* 33:107–112.

Raxworthy CJ, Martinez-Meyer E, Horning N, Nussbaum RA, Schneider GE, Ortega-Huerta MA, *et al*. 2003. Predicting distributions of known and unknown reptile species in Madagascar. *Nature* 426:837–841. https://doi.org/10.1038/nature02205

StatSoft Inc. 2005. STATISTICA (data analysis software system). Version 7.1. www.statsoft.com.

Woodman N. 1995. Morphological variation between Pleistocene and recent samples of *Cryptotis* (Insectivora: Soricidae) from the Yucatan Peninsula, Mexico. *Journal of Mammalogy* 76:223–231. https://doi.org/10.2307/1382330

Woodman N. 2005. Size evolution in Goodwin's small-eared shrew, *Cryptotis goodwini* (Mammalia: Soricomorpha: Soricidae). *Special Publication of the International Society of Shrew Biologists*. 125–138.

Woodman N. 2019. Three new species of small-eared shrews, genus *Cryptotis*, from El Salvador, Guatemala, and Honduras (Mammalia: Eulipotyphla: Soricidae). *Special Publications of the Museum of Texas Tech University*.

Woodman N, and Gaffney SA. 2014. Can they dig it? Functional morphology and semifossoriality among small-eared shrews, genus *Cryptotis* (Mammalia, Soricidae). *Journal of Morphology* 275:745–759. https://doi.org/10.1002/jmor.20254

Woodman N, and Morgan J.J. 2005. Skeletal morphology of the forefoot in shrews (Mammalia: Soricidae) of the genus *Cryptotis*, as revealed by digital X-rays. *Journal of Morphology* 266:60–73. https://doi.org/10.1002/jmor.10367

Woodman N, and Timm RM. 1993. Intraspecific and interspecific variation in the *Cryptotis nigrescens* species complex of small-eared shrews (Insectivora: Soricidae), with the description of a new species from Colombia. *Fieldiana Zoology* 74:1–30. https://doi.org/10.5962/bhl.title.3574

Woodman N, and Timm RM. 1999. Geographic variation and evolutionary relationships among broad-clawed shrews of the *Cryptotis goldmani*-group (Mammalia: Insectivora: Soricidae). *Fieldiana Zoology* 91:1–35. https://doi.org/10.5962/bhl.title.2669

Woodman N, and Timm RM. 2023. *Cryptotis nigrescens* (Eulipotyphla: Soricidae). *Mammalian Species* 55(1035):1–11. https://doi.org/10.1093/mspecies/sead011

Associated editors: Giovani Hernández Canchola and Pablo Colunga Salas
Submitted: October 31, 2025; Reviewed: December 12, 2025
Accepted: March 4, 2026; Published online: May 29, 2026

THERYA, 2026, Vol. 17(2):143-162 DOI: 10.12933/therya.2026.6245 ISSN 2007-3364

Evolutionary and environmental influences on cranial shape and forearm length variation in *Corynorhinus mexicanus*

Issachar L. López-Cuamatzi[1,4], Jorge Ortega[2], Sandra M. Ospina-Garcés[3], and M. Cristina MacSwiney G.[4*]

[1]Red de Biología y Conservación de Vertebrados, Instituto de Ecología A.C., Xalapa-Enríquez, Veracruz, Mexico. E-mail: isachar26@hotmail.com (ILL-C)
[2]Departamento de Zoología, Instituto Politécnico Nacional, Escuela Nacional de Ciencias Biológicas, Mexico City, Mexico. E-mail: artibeus2@aol.com (JO)
[3]Centro de Investigación en Biodiversidad y Conservación, Universidad Autónoma del Estado de Morelos, Cuernavaca, Morelos, Mexico. E-mail: ospinagarcess@gmail.com (SMO-G)
[4]Centro de Investigaciones Tropicales, Universidad Veracruzana, Xalapa-Enríquez, Veracruz, Mexico.
[*]Corresponding author: cmacswiney@uv.mx

Phenotypic variation in bats reflects the combined influence of environmental and evolutionary factors. Body size often responds to thermal gradients (Bergmann's rule), whereas cranial and mandibular morphology are often associated with evolutionary history and diet, which are further shaped by resource seasonality. *Corynorhinus mexicanus*, an endemic bat of Mexico's temperate forests, was analyzed to assess if environmental factors, evolutionary history, and their interaction influence forearm size and cranial and mandibular shape. Linear mixed models were fitted using forearm measurements and principal components derived from environmental variables, incorporating previously documented intraspecific lineages. Models were compared under annual and monthly temperature variation, accounting for reproductive timing and sex-specific energetic investment. Cranial and mandibular variation were examined using a two-dimensional geometric morphometric protocol to assess the influence of lineage and environmental seasonality as a proxy for dietary composition. Forearm length did not differ between lineages in females but did in males, with those from the Sierra Madre Occidental lineage being smaller. In both sexes, body size followed Bergmann's rule. Cranial differences between lineages were restricted to the lateral view of the braincase and the ventral view of the rostrum. Overall, cranial variation appeared to be primarily driven by evolutionary history, whereas forearm size reflected a combined influence of evolutionary and environmental factors. Maximum temperatures during the reproductive period influenced forearm length in males, while minimum temperatures affected females. Finally, we highlighted the importance of considering temporal extent and environmental resolution in eco-evolutionary studies.

Key words: Bergmann's rule, body size, diet, heat conservation, heat dissipation, Vespertilionidae

La variación fenotípica en murciélagos refleja la influencia conjunta de factores ambientales y evolutivos. El tamaño corporal suele responder a gradientes térmicos (regla de Bergmann), mientras que la morfología craneal y mandibular suele relacionarse con la historia evolutiva y la dieta, modulada por la estacionalidad. *Corynorhinus mexicanus*, un murciélago endémico de los bosques templados de México, fue analizado para evaluar si factores ambientales, la historia evolutiva y su interacción influyen en el tamaño del antebrazo y en la forma y tamaño del cráneo y la mandíbula. Se ajustaron modelos lineales mixtos con medidas de antebrazo y componentes principales de variables ambientales, incorporando los linajes intraespecíficos conocidos. Los modelos se compararon considerando la variación anual y mensual de la temperatura, en relación con los periodos reproductivos y la asincronía energética entre sexos. La variación craneal y mandibular se evaluó mediante un protocolo de morfometría geométrica en dos dimensiones, analizando el efecto del linaje y la estacionalidad como un proxy de la dieta. La longitud del antebrazo no difirió entre linajes en hembras, pero sí en machos, siendo los del linaje de la Sierra Madre Occidental más pequeños. El tamaño corporal de ambos sexos siguió el patrón de la regla de Bergmann. Las diferencias craneales entre linajes se restringieron a la vista lateral de la caja craneal y a la ventral del rostro. En conjunto, los resultados indican que la variación craneal está determinada principalmente por la historia evolutiva, mientras que el tamaño del antebrazo responde de forma combinada a factores evolutivos y ambientales. Las temperaturas máximas durante el periodo reproductivo influyeron principalmente en la longitud del antebrazo en machos, mientras que las mínimas lo hicieron en las hembras. Finalmente, se destaca la importancia de considerar la escala temporal y la resolución ambiental en los estudios eco-evolutivos.

Palabras clave: Conservación del calor, dieta, disipación del calor, regla de Bergmann, tamaño corporal, Vespertilionidae

Variation in phenotypic traits within species is a common phenomenon with important ecological consequences (e.g., community structure and demographic patterns; Bolnick *et al.* 2003; 2011). Such variation can arise from several factors, including adaptation to environmental conditions (e.g., Stevens *et al.* 2016; Maluleke *et al.* 2017), exploitation of specific resources (e.g., Encarnação *et al.* 2005; Hedrick 2021), interspecific competition (Salinas-Ramos *et al.* 2020), sex (e.g., Myers 1978; Camargo and de Oliveira 2012; Ulpian and Rossi 2017), genetic characteristics of individuals (e.g., Majerus and Mundy 2003), and the evolutionary history of populations (e.g., Uvizl and Benda 2021; Gorobeyko *et al.* 2025). Exploring how phenotypic traits relate to intrinsic and extrinsic factors can yield valuable insights into species' responses to environmental change, such as global climate shifts (Paltrinieri *et al.* 2025), and can support biodiversity conservation by serving as potential indicators of metapopulation persistence (Gibert 2016).

Intraspecific phenotypic variation in bats has been widely documented, particularly in body size (e.g., Myers 1978; Williams and Findley 1979; Ulpian and Rossi 2017; Russo *et al.* 2024) and cranial and mandibular morphology (e.g., Marchan-Rivadeneira *et al.* 2012; Morales *et al.* 2018; Hedrick 2021), both of which exhibit diverse responses associated with evolutionary history and environmental conditions.

Body size variation within species has traditionally been attributed to adaptive responses to environmental clines (Ashton 2002; Clauset and Erwin 2008; Meiri 2008; Chown and Gaston 2010). In bats, the association between body size and environmental factors has been explained through several mechanisms, often linked to physiological constraints (Safi *et al.* 2013; Castillo-Figueroa 2022; Alston *et al.* 2023). In a physiological context, variation in bats' body size has been negatively correlated with the environmental temperature where the organism lives (Bergmann 1848; Safi *et al.* 2013). This pattern referred to as Bergmann's rule, although originally proposed to describe interspecific patterns, has also been applied at the intraspecific level, predicting larger individuals in colder regions as a result of enhanced heat conservation (Ashton *et al.* 2000; Watt *et al.* 2010). Despite the main reason behind body size variation according to the Bergmann's rule is the heat conservation (Bergmann 1848), other reasons have been proposed to produce the same pattern. One particularly is relating to heat stress, where larger individuals have lower critical thermal maxima, favoring smaller body sizes in warmer environments (Smith *et al.* 1995; Peralta-Maraver and Rezende 2021). Both mechanisms (heat conservation and heat dissipation) may produce the same pattern of body size variation, but the environmental constraints are different, and they obey opposite boundaries of thermal tolerance of individuals. Another phenomenon behind body size variation is related to trophic resource availability, suggesting that individuals tend to be larger in more productive environments (McNab 2010), where higher primary productivity, temperature, and precipitation provide greater energy and resource inputs (Chu *et al.* 2016). As noted, the pattern exhibited here is opposite to Bergmann's rule.

Regarding intraspecific variation in cranial and mandibular morphology, both structures are often influenced by several interacting factors, including evolutionary history and dietary adaptations (e.g., Marchan-Rivadeneira *et al.* 2012; Morales *et al.* 2018; Hedrick 2021), with the former reflecting evolutionary history effects and the latter shaped by diet influence.

In insectivorous bats, diet composition may depend, among other factors, on prey availability, which is strongly influenced by environmental conditions, as insect diversity and abundance fluctuate with seasonal changes in temperature and precipitation, as well as primary productivity (e.g., Borer *et al.* 2012; Moosman *et al.* 2012; Lind *et al.* 2017; Zhu *et al.* 2024). These fluctuations are most evident along latitudinal and altitudinal gradients (Alston *et al.* 2023), where seasonal variations in primary productivity may alter insect abundance and diversity, potentially forcing bats to broaden their prey spectrum (e.g., Moosman *et al.* 2012) and driving local cranial and mandibular morphological adaptations (e.g., Mendes *et al.* 2024).

Corynorhinus mexicanus G.M. Allen, 1916, is an insectivorous bat endemic to temperate forests located on the slopes of the Sierra Madre Occidental (SMOc) and the Trans-Mexican Volcanic Belt (TMVB) in Mexico (López-Cuamatzi *et al.* 2024). Previous study suggested this species comprises two mitochondrial lineages, each restricted to each mountain range, showing low genetic divergence (López-Cuamatzi *et al.* 2024). Variations in body size (measured as forearm length) and cranial morphology have been documented and attributed to evolutionary history (mitochondrial lineages) (López-Cuamatzi *et al.* 2024), although the influence of environmental factors has not been formally tested.

Recognizing environmental conditions and evolutionary history as primary drivers of intraspecific phenotypic variation, this study aims to elucidate the relationship between forearm length and cranial and mandibular shape variation in *C. mexicanus* with thermal and precipitation variables, mitochondrial linages, as well as the interaction between these components.

Specifically, for body size (measured as forearm length), we tested the following non-mutually exclusive hypotheses and predictions (Figure 1):

- Lineage–Driven Hypothesis (LD): Variation in forearm length in *C. mexicanus* is structured by mitochondrial lineages, Sierra Madre Occidental and Trans-Mexican Volcanic Belt (see López-Cuamatzi *et al.* 2024), such that individuals assigned to one lineage are expected to differ in forearm length from those assigned to the other lineage.
- General Environmental–Driven Hypothesis (GED): Variation in forearm length is structured by thermal conditions consistent with heat conservation and heat dissipation dynamics, with shorter forearms expected in warmer environments and longer forearms in cooler environments. The Bergman's Rule pattern.
- Resource Availability–Driven Hypothesis (RAD): Variation in forearm length in *C. mexicanus* is linked to resource availability, such that individuals inhabiting more productive environments are predicted to have greater forearm length. The opposite Bergmann's rule pattern.

However, a methodological limitation in studies testing the heat conservation and heat-stress mechanisms of Bergmann's rule is the assumption that environmental pressures –commonly represented by monthly, quarterly, or annual temperature extremes (e.g., Castillo-Figueroa 2022; Alston *et al.* 2023; Paltrinieri *et al.* 2025)– affect all individuals uniformly and continuously, regardless of their phenological stage. This simplification could bias interpretations of temperature–body size relationships.

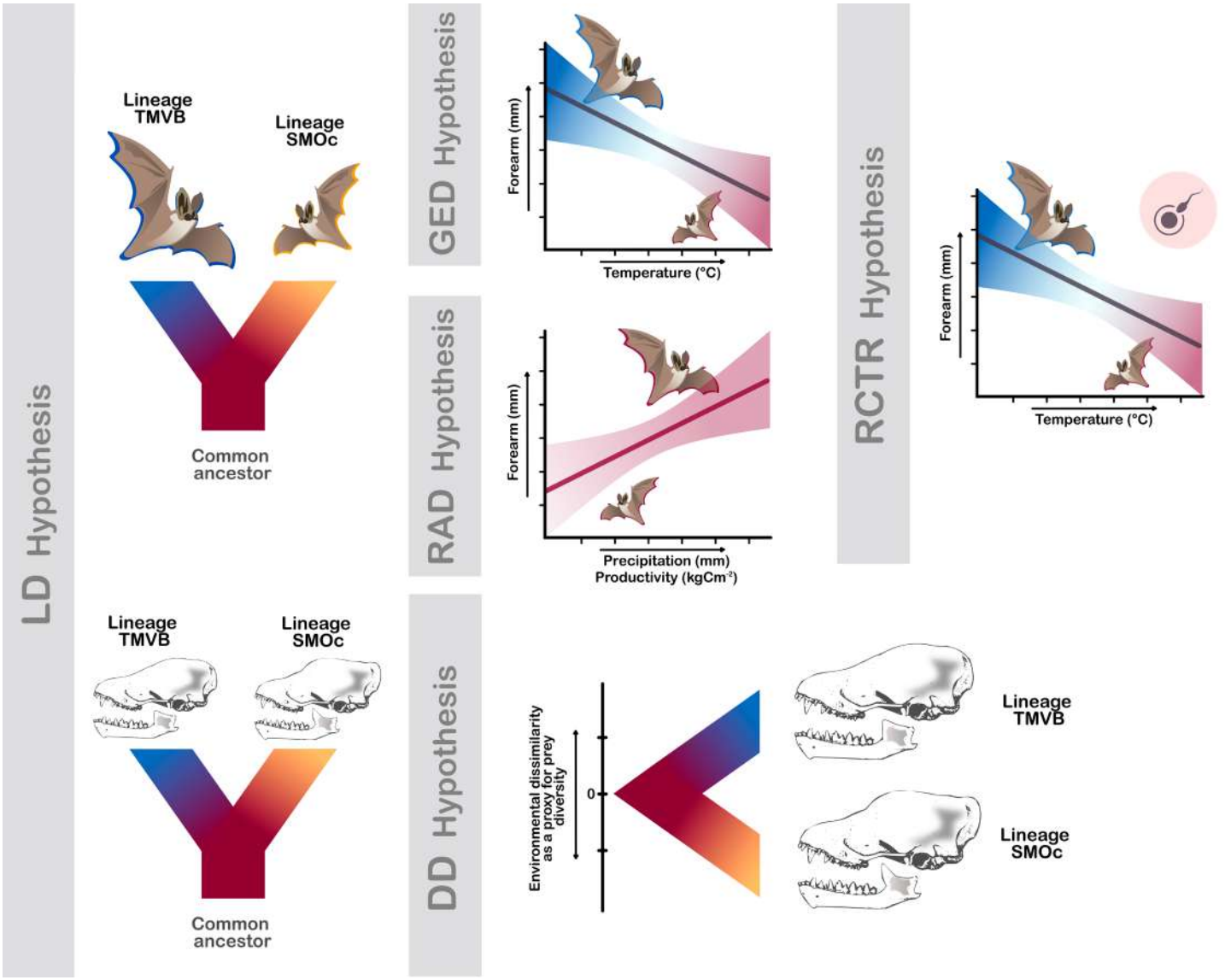

Figure 1. Schematic representation of the hypotheses tested for forearm, cranial, and mandibular shape variation.

In temperate zones, maximum and minimum values of temperatures and precipitation occur in specific seasons that may not coincide with critical periods such as reproduction, when the energy demands of Holarctic bats are highest (Kurta and Kunz 1987; McLean and Speakman 1999). This complexity is further amplified by sex-specific phenological patterns, as males and females of some Nearctic species often reach peak reproductive energy demands at different times of the year (Gustafson 1979; Oxberry 1979). Considering this, we test a modification of GED hypothesis but considering the phenological demands of individuals:

- Reproductive-Cost by Thermal Regulation Hypothesis (RCTR): Analogous to the heat conservation and heat-stress mechanisms under GED, but focusing on the temporal window when energetic demands are highest, particularly during reproductive activity.
- Regarding to cranial and mandible shape and size variation, we tested the two following non–mutually exclusive hypotheses:
- Lineage-Driven Hypothesis (LD): Cranial and mandibular shape and size variation in *C. mexicanus* are associated with previously identified mitochondrial lineages. This hypothesis predicts that cranial and mandibular morphological traits differ between individuals belonging to distinct lineages.
- Dietary–Driven Hypothesis (DD): Cranial and mandibular shape variation is associated with diet composition, particularly with prey availability indirectly estimated through seasonal precipitation patterns and primary productivity. It is predicted that cranial and mandibular shape changes will follow gradients of precipitation and primary productivity.

Materials and methods

Collection of forearm data. We compiled forearm measurements of individuals from various localities representing the two genetic groups identified in *C. mexicanus* (Figure S1 of Supplementary Data SD1). These data were obtained from the specimen database

of taxidermy-preserved individuals reviewed in López-Cuamatzi *et al.* (2024). Individuals catalogued as juvenile were excluded from the analyses.

Collection of cranial and mandible shape data. To characterize the cranial and mandibular shape variation, we photographed the mandible and dorsal, ventral and lateral views of the cranium using a Nikon D3000 reflex camera (Nikon Corporation, Tokyo, Japan) and a Nikkor 2.8F 60 mm macro lens (Nikon Corporation, Tokyo, Japan). Two-dimensional landmark and semi-landmark configurations were digitized on the cranial and mandibular images using the software tpsUtil and tpsDig2 (Rohlf 2017, 2019). The number of landmarks and semi-landmarks varied between views (see López-Cuamatzi *et al.* 2024 for details).

Landmark configurations were aligned using Generalized Procrustes Analysis to remove non-shape variation by standardizing origin, scale, and rotation (Rohlf 1990). Bone contours were digitized as semi-landmarks and aligned by minimizing Procrustes distances to the consensus curve (Pérez *et al.* 2006; Gunz and Mitteroecker 2013). Because skull views are bilaterally symmetrical, shapes were averaged across sides using bilateral symmetry analysis (Klingenberg 2015). Shape variables were represented as Procrustes coordinates, and size was estimated as centroid size (CS), calculated as the square root of the summed distances from landmarks to the centroid (Bookstein 1997). Analyses were performed in the "R-package" *geomorph* v.4.0.1 (Adams *et al.* 2025) on R v.4.4.2 (R Core Team 2024).

To reduce sample size requirements, each cranial view was divided into two developmentally and functionally recognized modules (rostral and basicranial), commonly described in mammals, including bats (Marroig *et al.* 2009; Porto *et al.* 2009). Although cranial modularity has previously been reported in *C. mexicanus* (López-Cuamatzi *et al.* 2024), modularity was re-evaluated because the current analysis excludes observations from Sierra Madre Oriental (formally *C. leonpaniaguae*) included in the previous study. Modularity was evaluated using the covariance ratio (CR) with 1,000 permutations, implemented in the *geomorph* R-package v.4.0.1 (Adams *et al.* 2025). When the CR indicated a lack of modularity, the entire structure was analyzed as a single unit. To compare shape independently of size, we fitted linear models between shape and centroid size for each view or module and used the residuals as size-free shape coordinates for subsequent analysis, using Procrutes ANOVA models.

Collection of environmental data. We used the geographic coordinates of each voucher specimen to extract environmental data from climatic raster files. To test the General Environmental–Driven Hypothesis (GED), we compiled a dataset with values from WordClim's bioclimatic variables (Fick and Hijmans 2017): Bio5 (Max Temperature of Warmest Month) and Bio10 (Mean Temperature of Warmest Quarter) as proxies for heat dissipation and Bio6 (Min Temperature of Coldest Month) and Bio11 (Mean Temperature of Coldest Quarter) as proxies for heat conservation. We used minimum and maximum temperature data instead of mean temperature because our objective was to assess the thermal stress experienced by individuals, and mean temperature does not capture the minimum and maximum thermal exposures that may generate such stress. Additionally, thermal variability also influences physiological tolerance, affecting individual fitness (see Bozinovic *et al.* 2011) and spatial distribution (i.e., Zimmermann *et al.* 2009).

Environmental data were extracted at three spatial resolutions, 30-arcseconds (~1 km), 2.5-arcminute (~4.5 km), and 5-arcminute (~9.25 km), to account for resolution-related uncertainty. The 5-arcminute resolution approximates the dispersal capacity reported for *Corynorhinus* species (Fellers and Pierson 2002) but may introduce environmental error due to its coarse resolution. In contrast, 30-arcsecond raster offer finer environmental detail but may not adequately capture broader gradients relevant to *Corynorhinus* movements and habitat use.

Following (Alston *et al.* 2023), to evaluate the Resource Availability–Driven Hypothesis (RAD), we used the MODIS monthly Net Primary Productivity (NPP) dataset (NASA Earth Observatory 2025) at a 0.1° spatial resolution (~10 km) as a proxy for insect abundance. Primary productivity is strongly associated with insect biomass (Lind *et al.* 2017) and has previously shown a moderate positive correlation (r = 0.66; Borer *et al.* 2012). For each specimen locality, we extracted 24 years of data (2001–2024) and calculated the median NPP value. Additionally, we used Bio18 (Precipitation of the Warmest Quarter) at 30-arcsecond and 5-arcminute resolutions as a proxy for trophic resource availability for bats, reflecting insect abundance during summer (see Frick *et al.* 2010).

To evaluate the Reproductive-Cost by Thermal Regulation (RCTR) hypothesis, we compiled historical monthly climate data from WorldClim (Fick and Hijmans 2017) for each individual. This dataset consists of raster files at 5-arcminute resolution, including average minimum and maximum temperature (°C) from 1950 to 2024. We extracted monthly data for each of the 75 years available and calculated the median for each month, resulting in 75-year monthly medians. Median values were used to minimize the influence of outliers, which are common in environmental datasets. Two sex-specific datasets were generated to reflect periods of peak energetic demand: August–November for males, when *C. mexicanus* invests in spermatogenesis and sperm maturation (León-Galván *et al.* 2005), and March–July for females, corresponding to gestation and lactation (López-Wilchis 1989).

To test the Dietary–Driven Hypothesis (DD), we generated a dataset including WorldClim's variables Bio4 (Temperature Seasonality), Bio15 (Precipitation Seasonality) (Fick and Hijmans 2017), together with Bio 18 and NPP, as proxies for insect richness and abundance. We used Bio4 and Bio15 because insect diversity can be influenced by thermal and humidity seasonality along

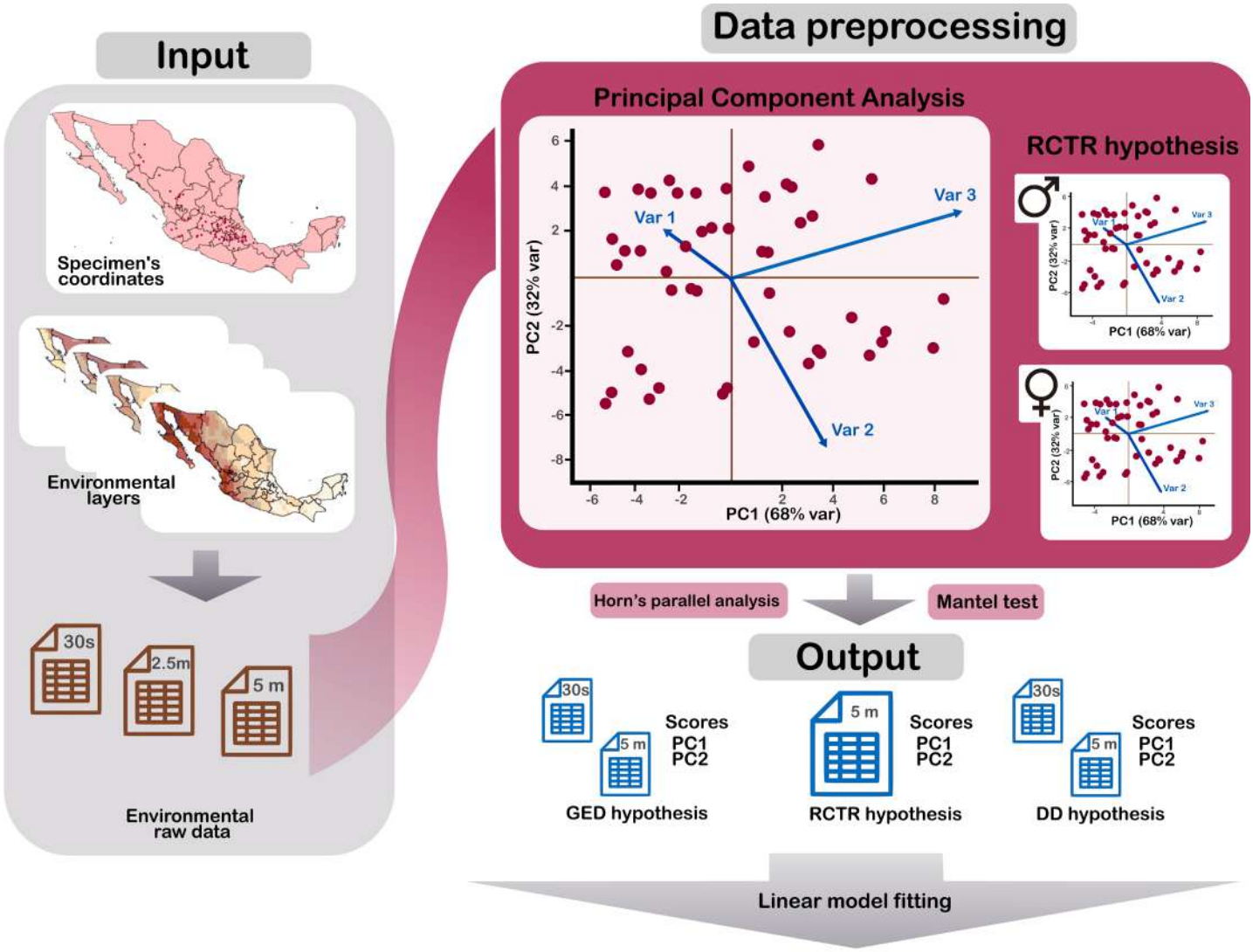

Figure 2. Workflow for processing environmental data. The diagram depicts the steps from initial input data (coordinates and environmental layers) to the final datasets used for linear model fitting. During preprocessing for the RCTR hypothesis, PCA was performed separately by sex. Final datasets (Outputs) were selected based on Mantel test results.

altitudinal gradients, such as in mountainous environments (i.e., Wilson *et al.* 2007; Montañez-Reyna *et al.* 2022). As with the GDE, RAD and RCTR datasets, environmental data for DD were extracted at resolutions of 30-arcseconds and 5-arcminute.

Treatment of environmental variables. For the GED dataset, we compared environmental variable values (Bio5, Bio6, Bio10, and Bio11) across three spatial resolutions (30-arcseconds, 2.5-arcminute, and 5-arcminute) using Mantel tests based on Spearman's rank correlation to reduce sensitivity to outliers and non-linear relationships. Euclidean distances were used to construct distance matrices for each environmental variable, and Mantel tests were performed with 9,999 permutations using the "vegan" R-package in R (Oksanen *et al.* 2025). This analysis evaluated whether datasets of differing resolutions produced consistent results and whether resolution influenced model outcomes. We then performed a Principal Component Analysis (PCA) on each dataset of bioclimatic variables to reduce dimensionality and summarize environmental information. The number of components to retain was determined using Horn's parallel analysis (Dinno 2009), as implemented in the *fa.parallel* function of the R-package *psych* (Revelle and Revelle 2015). Retained components were subsequently used in further analyses. For the RCTR and DD datasets, PCAs were conducted as described above. In the RCTR dataset, PCAs were performed separately by sex due to differences in the number of monthly climatic variables considered (Figure 2). For the RAD hypothesis, Bio18 and NPP were used directly without dimensionality reduction through PCA; however, both variables were standardized to a mean of zero and unit variance. Additionally, we assessed their correlation using a Spearman correlation test to avoid collinearity in subsequent modeling.

Sexual dimorphism in forearm, and cranial and mandible shape. Because the RCTR hypothesis implies sex-specific associations with climatic variables, we tested for sexual dimorphism. Forearm length was analyzed using Welch's t-test, appropriate for unbalanced designs, after confirming normality (Shapiro-test, $P > 0.05$) and homoscedasticity (Levene's test, $P > 0.05$). For each cranial and mandibular view or module, we evaluated the effect of sex on size-free

shape using Procrustes ANOVA in Geomorph, and analyzed centroid size using linear models with random permutations in the "RRPP" R-package (Collyer and Adams 2018). Both analyses were conducted with 1,000 permutations.

Modeling unit. For the forearm analysis, multiple specimens were collected from some localities (i.e., identical geographic coordinates). Therefore, each individual was treated as the unit of analysis, while acknowledging that some individuals were spatially clustered. To account for this structure, we fitted linear mixed models (LMMs) (Korner-Nievergelt *et al.* 2015), including locality as a random effect, with individuals grouped according to shared geographic coordinates.

Because several localities were represented by a single individual, the dataset contained a substantial proportion of singleton groups (i.e., clusters with only one observation). Such imbalance can lead to random-effect variance estimates approaching zero. Nevertheless, simulation studies indicate that LMMs are generally robust to high proportions of singleton clusters, even under moderate sample sizes (Bruyndonckx *et al.* 2018). Although some approaches recommend removing random effects when variance estimates are negligible, we retained the hierarchical structure given the inherent spatial grouping of the data. We therefore report the LMM results while acknowledging that, in some cases, the estimated random-effect variance was close to zero.

In contrast, for the morphometric analyses we used the mean cranial and mandibular shape per locality as the modeling unit. Although individual-level variation provides valuable insight into intraspecific morphological patterns, incorporating individuals directly into the models could bias inference regarding environmental or lineage effects. By aggregating shape data at the locality level, we reduced pseudo-replication and ensured that the modeling unit matched the scale at which environmental variables were measured.

Statistical analyses: forearm. We fitted linear mixed-effects models (LMMs) using the *lmer* function from the "lme4" R-package (Bates *et al.* 2015) to test the proposed hypotheses. We used forearm length as the response variable, locality as a random effect, and the LD, GED, RAD, and RCTR datasets as predictors. Because the LD hypothesis is not mutually exclusive with the rest of the hypotheses, we also fitted models including both additive (e.g., LD + GED) and interaction terms (e.g., LD * GED) to evaluate their combined and interactive effects. Model assumptions, including dispersion, residual uniformity, and outlier detection, were evaluated using the *simulateResiduals* function from the "performance" R-package (Lüdecke *et al.* 2021).

Model comparison was conducted using AIC, AICc, and ΔAICc, with selection based on the lowest AIC and AICc values (Korner-Nievergelt *et al.* 2015). The significance of each term of the model was assessed considering ($P < 0.05$). An intercept-only null mixed-effects model was fitted as a baseline to assess whether the observed patterns differed from those expected under random variation (Gotelli and Graves 1996). When multiple models showed comparable support (ΔAICc < 2) and were not nested, all top-ranked models were considered. However, when competing models were nested, we used likelihood ratio tests (through the *anova* function in the "stats" R-package [R Core Team 2024]) to evaluate whether the more complex model provided a significantly better fit. If the null hypothesis was not rejected, the simpler model was retained.

The intraclass correlation coefficient (ICC) and marginal and conditional R^2 values of models selected were computed using the *icc* and *r2* functions in the "performance" R-package (Lüdecke *et al.* 2021). In instances where variance components of the random effects could not be reliably estimated, conditional R^2 was not computed; instead, marginal R^2 and variance components are presented. Additionally, when interaction terms in the model selected were statistically supported, simple slopes of continuous predictors within each factor level were estimated using the *emtrends* function from the "emmeans" R-package (Lenth and Piaskowski 2025).

Statistical analyses: cranial and mandible shape. The LD and DD hypotheses for cranial and mandibular shape were tested using Procrustes ANOVA in the Geomorph. Linear models were fitted on size-free shape coordinates derived from the residuals of the allometric regression between centroid size and shape. Predictors variables included the DD dataset and mitochondrial linage (LD hypothesis). As the two hypotheses are not mutually exclusive, we also tested models with interaction terms between lineage and environmental variables.

Models were compared using ANOVA, and the significance of each term was evaluated ($P < 0.05$). Model selection followed a nested structure, for example, LD, LD+DD, and LD*DD formed one set, while DD, LD+DD, and LD*DD formed another. However, the simple LD and DD models are not nested within each other. When the best-fitting models were simple, both were discussed. If a more complex model was supported in one set but not the other, the simpler nested model was preferred. A null model was also included for baseline comparison. Finally, centroid size was analyzed with linear models implemented in "RRPP" R-package (Collyer and Adams 2018), following the same logic as using 1,000 permutations.

After identifying significant predictors, we conducted individual tests to assess the association with size-free shape and centroid size. When lineage had a significant effect on size-free shape, we performed paired comparisons between the group means, and their significance was tested by permutation testing (10,000 permutations) and Bonferroni's correction, comparing the observed Procrustes distance (procD) with that obtained from the random assignment of observation to groups in the R-package "Morpho" v. 2.7 (Schlager 2017). Differences in mean shape configurations among lineages were assessed

using a Discriminant Function Analysis (DFA) based on the first ten principal components (PCs) obtained from a prior Principal Components Analysis. For views and modules exhibiting significant differences between lineages, Mahalanobis distances and corresponding P-values were calculated using permutation tests of the original data matrix with 1,000 replicates. Classification accuracy was evaluated using cross-validation, where each specimen was sequentially excluded from the training dataset and classified using discriminant functions built from the remaining individuals. For environmental variables we applied two-block Partial Least Squares (PLS) analyses with 999 iterations. For centroid size, significant lineage effects were evaluated using pairwise-distance tests with 999 iterations, while environmental variables were tested using Pearson or Spearman correlations depending on the normality of centroid size residuals.

Results

Environmental data summary. Regarding the environmental variable datasets used for GED hypothesis, Mantel tests revealed a strong correlation between the 2.5-arcminute and 5-arcminute environmental datasets ($r = 0.95$, $P < 0.05$), whereas the correlation between the 30-arcsecond and 5-arcminute datasets was notably lower ($r = 0.67$, $p < 0.05$). Based on these results, subsequent analyses were conducted using the 30-arcsecond and 5-arcminute datasets. Monthly climatic data for testing the RCTR hypothesis were analyzed at 5-arcminute resolution, while data for the DD hypothesis were analyzed at both resolutions to ensure comparability across analyses. Under the RAD hypothesis, Bio18 and NPP were only weakly correlated (NPP-Bio18 at 30-arcseconds, *rho* = -0.3, $P < 0.001$; NPP-Bio18 at 5-arcminute, *rho* = -0.29, $P = 0.001$), allowing both variables to be included as predictors in subsequent analyses.

Sexual dimorphism and modularity in cranial shape. The forearm dataset used to test sexual dimorphism consisted of 131 observations (63 females and 68 males). Welch's t-test revealed significant sexual dimorphism, with females exhibiting greater forearm length than males ($t_{125.35}$ = -7.059, $P < 0.05$; Figure S2 of Supplementary Data SD1). Consequently, all subsequent models were performed separately for each sex.

The number of observations for cranial and mandibular shape analyses varied among datasets (Table S1, Supplementary Data SD1). The modularity test supported the division into rostral and basicranial modules in the lateral (CR = 0.7578, $P = 0.001$) and ventral (CR = 0.7665, $P = 0.001$) views, whereas the dorsal view lacks statistically significant modularity (CR = 0.964, $P = 0.44$). Procrustes ANOVA detected sexual dimorphism in size-free shape only in the dorsal cranial view and lateral basicranial view (Table S1, Supplementary Data SD1). *Post hoc* tests indicated that in the dorsal view, females and males differed (procD = 0.003, $P = 0.049$), primarily in nasal bone width and maxilla length, while in the lateral basicranial view (procD = 0.008, $P = 0.013$), differences were concentrated at the base of the braincase (Figure S3, Supplementary Data SD1). Centroid size also exhibited sexual dimorphism in lateral rostral, ventral basicranial, and mandibular views (Table S2, Supplementary Data SD1). The trend of dimorphism varied across structures: females were larger than males in the lateral rostrum and mandible, whereas the opposite pattern occurred in the ventral braincase (Figure S4, Supplementary Data SD1).

PCA environmental variables. For the GED hypothesis, the first two principal components (PCs) explained 99.1% (PC1 = 59.87%; PC2 = 39.23%) of the total variance at the 30-arcsecond resolution and 98.83% (PC1 = 64.67%; PC2 = 34.16) at the 5-arcminute resolution. Horn's parallel analysis suggested retaining two components in each dataset.

At the 30-arcsecond resolution, PC1 represented a general temperature gradient, with all bioclimatic variables loading positively, and Bio10 and Bio11 showed the strongest contributions to this component. PC2 differentiated variables associated with lower temperature contrast (lower maximum temperatures; positive loadings) from those linked to higher temperature contrast (higher maximum temperatures; negative loadings) between maximum and minimum temperature conditions, with Bio5 and Bio6 contributing most strongly to this axis. At the 5-arcminute resolution, we observed a similar arrangement of components to that obtained from the 30-arcsecond resolution PCA. The only difference was the opposite sign of the PC1 loadings (negative loadings), which reflects the arbitrary orientation of principal component axes and does not indicate structural differences between analyses.

For the RCTR hypothesis, the first two principal components explained 96.42% of the total variance in males (PC1 = 79.8%; PC2 = 16.5%) and 94.39% in females (PC1 = 65.0%; PC2 = 29.2%). Although Horn's parallel analysis indicated that one component should be retained in males and two in females, the first two components were retained in both sexes to maintain comparability. In males, PC1 represented a general thermal gradient across months, with all maximum and minimum temperature variables loading positively, indicating that this axis captured overall temperature conditions during the August–November period. Maximum temperatures across months, together with minimum temperatures of August and September, showed strong contributions to this component. PC2 distinguished maximum temperatures (positive loadings) from minimum temperatures (negative loadings), with November and October minimum temperatures exhibiting the strongest negative contributions. This pattern reflects a contrast between daytime and nighttime thermal conditions, particularly emphasizing the influence of late-season minimum temperatures, and therefore represents a gradient of increasing dominance of nocturnal cooling toward the end of the period.

In females, PC1 represented a general thermal gradient across months, with all maximum and minimum temperature variables loading positively. The strongest contributions to

this component were observed for minimum temperatures, particularly May and June, together with maximum temperatures from early spring months (April and March), indicating that this axis captured overall thermal conditions during the March–July period. PC2 contrasted high summer maximum temperatures (June and July, which showed the strongest positive loadings, followed by May) with lower minimum temperatures of early spring months (especially March and April, which exhibited the strongest negative loadings). This pattern reflects a seasonal contrast between peak summer heat and cooler spring nights, representing the degree of thermal intensification from early spring to midsummer. In simple terms, PC2 indicates how midsummer and early spring temperatures were similar.

For the DD hypothesis, the first two principal components (PCs) at 30-arcsecond resolution explained 83.9% of the total variance (PC1 = 68.3%; PC2 = 15.6%), whereas the first three PCs at 5-arcminute resolution accounted for 84.7% (PC1 = 70%; PC2 = 14.7%) of the variance. At 30-arcsecond resolution, PC1 was primarily associated positively with Bio4 and negatively with NPP, while PC2 was negatively associated with Bio15 and Bio18. This pattern reflects a dominant environmental gradient in which increasing seasonality is associated with decreasing productivity. Similar patterns of variable contribution were observed at the 5-arcminute resolution.

Testing hypotheses: forearm. The forearm dataset used for modeling included 131 individuals grouped into 65 localities, which were treated as a random effect in the LMMs. When separated by sex, the female dataset comprised 63 individuals (31 from TMVB and 32 from SMOc), whereas the male dataset included 68 individuals (48 from TMVB and 20 from SMOc).

Based on AICc and ΔAICc criteria, the best-supported model for males corresponded to the LD hypothesis in the 30-arcsecond dataset and to the GED hypothesis in the 5-arcminute dataset. However, in both cases, alternative models also showed comparable support (ΔAICc < 2), specifically the model representing the RCTR hypothesis in the 30-arcsecond dataset, and the LD and RCTR hypotheses in the 5-arcminute dataset (Table 1). Because the models retained under the ΔAICc criterion were not nested, all of them were considered in subsequent interpretations.

For females, the best-supported model included the GED effect in the 30-arcseconds dataset and the LD × RCTR interaction in the 5-arcminute dataset. However, in the 30-arcseconds dataset, alternative models also showed comparable support (ΔAICc < 2), particularly LD + GED, LD * GED, and LD * RCTR. Because GED, LD + GED, and LD * GED are nested models, likelihood ratio tests were performed. These tests indicated that the more complex models did not provide a significantly better fit than the simpler ones (GED vs. LD + GED: $X^2_1 = 0.48$, $P = 0.48$; GED vs. LD * GED: $X^2_3 = 5.74$, $P = 0.12$). Therefore, only the GED and LD * RCTR models were retained for subsequent interpretation. All fitted models for both sexes and datasets, including those not selected, met the assumptions of dispersion, uniformity, and absence of outliers.

In males, the LD model revealed a significant effect of lineage, with SMOc individuals showing lower values of forearm than TMVB (β = -0.71, SE = 0.25, CI95% = -1.23 – -0.22, $t^{14.71}$ = -2.84, P = 0.013) (Figure 3A). For this model, random-effect variance was negligible (σ^2 = 0.001, SD = 0.04), with ICC = 0 and marginal R^2 = 0.11. In the GED model (5-arcminute dataset) for males, PC2 had a significant positive effect (β = 0.25, SE = 0.11, CI95% = 0.03 – 0.47, $t^{30.25}$ = 2.19, P = 0.035) (Figure 3B), whereas PC1 was not significant (β = 0.14, SE = 0.08, CI95% = -0.02 – 0.3, $t^{24.19}$ = 1.74, P = 0.09). Since positive values of PC2 indicate localities with greater influence of cold conditions and less dominance of extreme heat, these results indicates that males tend to be larger in colder locations and smaller in locations dominated by extreme heat. For this model, random-effect variance was low (σ^2 = 0.06, SD = 0.26; ICC = 0.036), with marginal and conditional R^2 values of 0.15 and 0.18, respectively.

Under the RCTR model, PC1 had a significant negative effect on forearm length (β = -0.13, SE = 0.048, CI95% = -0.23 – -0.03, $t^{17.5}$ = -2.79, P = 0.012) (Figure 3C), whereas PC2 was not significant (β = -0.13, SE = 0.1, CI95% = -0.33 – 0.06, $t^{33.05}$ = -1.29, P = 0.2). This result indicate that males inhabiting warmer environments, particularly during August–September, tend to exhibit shorter forearm length. For this model, random-effect variance was low (σ^2 = 0.06, SD = 0.24; ICC = 0.014), with marginal and conditional R^2 of 0.13 and 0.14, respectively.

In females, the GED model showed a significant negative effect of PC1 on forearm length (β = -0.30, SE = 0.09, CI95% = -0.48 – -0.11, t^{60} = -3.24, P = 0.001) (Figure 3D), while PC2 was not significant (β = 0.04, SE = 0.1, CI95% = -0.15 – 0.25, t^{60} = 0.48, P = 0.63). These findings suggest that females inhabiting colder environments tend to exhibit greater forearm length, while individuals from warmer environments show reduced forearm size. For this model, the random-effect variance was zero, resulting in ICC = 0 and a marginal R^2 of 0.15.

The LD × RCTR model for females revealed significant effects of lineage, PC1, and PC2, as well as significant interactions between lineage and both principal components (Figure 3E-F). The SMOc lineage exhibited lower forearm values than the reference lineage (TMVB) (β = -2.39, SE = 1.02, CI95% = -4.25 – -0.50, $t^{36.22}$ = -2.34, P = 0.025). PC1 was negatively associated with the forearm length (β = -0.76, SE = 0.22, CI95% = -1.16 – -0.35, $t^{26.76}$ = -3.40, P = 0.002), whereas PC2 showed a positive association (β = 1.28, SE = 0.50, CI95% = 0.36 – 2.16, $t^{28.9}$ = 2.58, P = 0.015). Significant interactions were detected between lineage and PC1 (β = 0.76, SE = 0.24, CI95% = 0.32 – 1.18, $t^{27.2}$ = 3.18, P = 0.004) and between lineage and PC2 (β = -1.33, SE = 0.57, CI95% = -2.32 – -0.26, $t^{28.49}$ = -2.35, P = 0.026), indicating lineage-specific relationships between principal components and the forearm length (Figure 3G). Random-effect variance was small (σ^2 = 0.11, SD = 0.34), with ICC = 0.012 and marginal

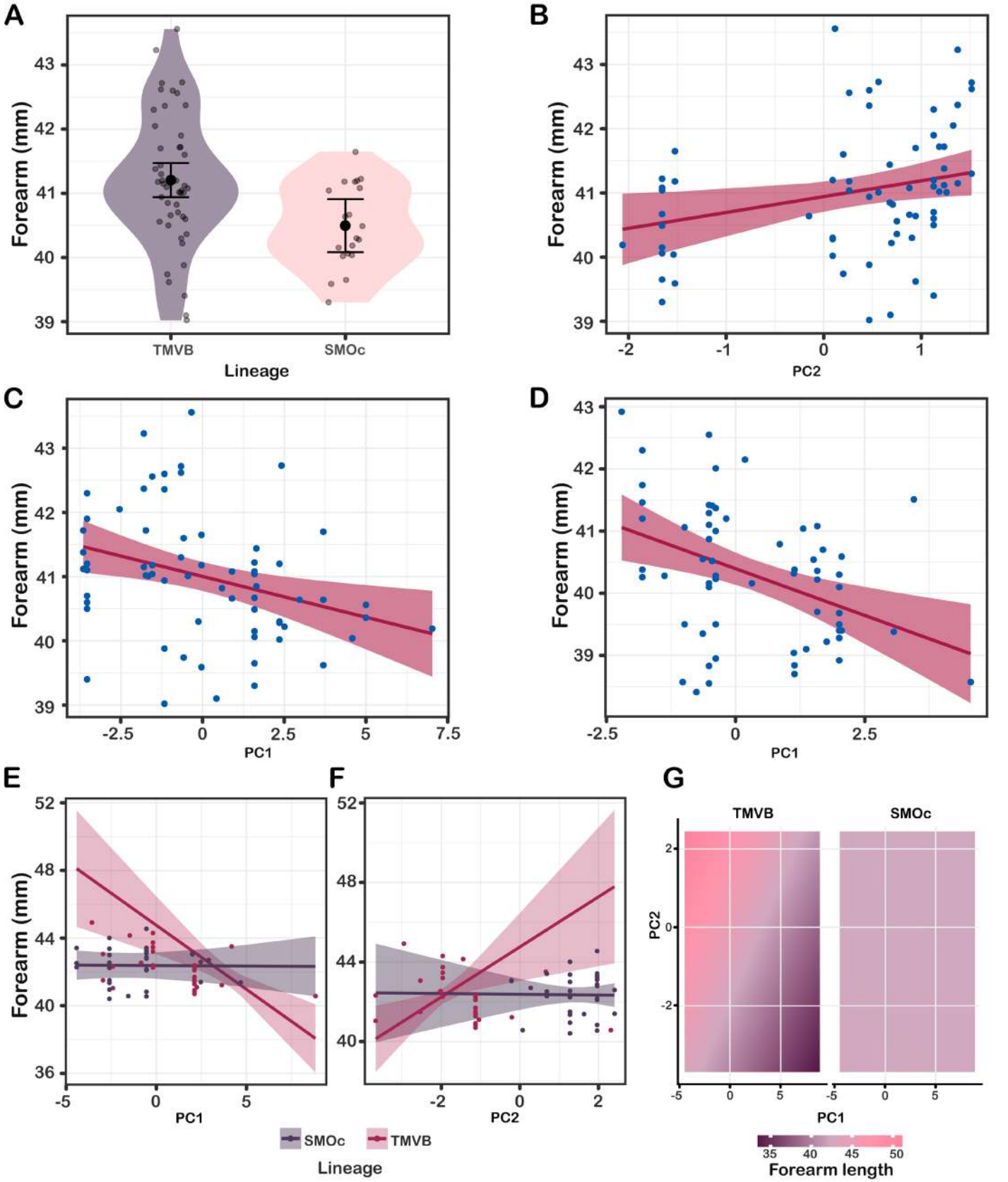

Figure 3. (A) Differences in forearm length between lineages in male *C. mexicanus*. (B) Positive association between forearm length and PC2 of the GED (5-arc-minute) dataset in males; positive PC2 values indicate lower temperature contrast (lower maximum temperatures), whereas negative values indicate higher contrast (higher maximum temperatures). (C) Negative association between forearm length and PC1 of the RCTR dataset in males; positive PC1 values correspond to higher temperatures and negative values to lower temperatures. (D) In females, forearm length was negatively associated with PC1 of the GED (30-arc-second) dataset, where positive values represent higher temperatures and negative values represent lower temperatures. (E–F) In the LD+RCTR dataset, forearm length in females showed significant interactions with lineage for both PC1 and PC2. For PC1, positive values indicate higher temperatures and negative values lower temperatures; for PC2, positive values reflect greater temperature contrast between early spring and midsummer, whereas negative values indicate more similar seasonal temperatures. SMOc individuals showed no detectable relationship between temperature and forearm length (G), displaying a homogeneous response to climatic PCs (uniform color), whereas TMVB individuals exhibited forearm variation associated with both PC1 and PC2 (color gradient).

and conditional R^2 values of 0.24 and 0.25, respectively.

Simple slope analyses showed that PC1 was negatively associated with the forearm length in TMVB (β = -0.75, CI95% = -1.21 – -0.30) but not in SMOc (β = -0.005, CI95% = -0.18 – 0.16) (Figure 3E). Similarly, PC2 had a positive effect in TMVB (= 1.25, CI95% = 0.25 – 2.26) (Figure 3F) but no significant association in SMOc (β = -0.018, CI95% = -0.57 – 0.54). Because PC1 represents a general thermal gradient during March–July, the negative association indicates that females inhabiting generally warmer localities exhibited shorter forearms. In contrast, PC2, which captures seasonal changes from early spring to midsummer, suggests that females from localities with a more pronounced seasonal transition between these periods had longer forearms.

Testing hypotheses: cranial and mandible shape and size. For most cranial views, fitted shape models using either the 30-arcsecond or 5-arcminute datasets did not outperform the null models. Only the lateral-view modules and ventral rostrum view showed better fit than the null models. None of the centroid size models outperformed the null models.

In the lateral braincase module, for females, the best-fitting model in both datasets (30-arcseconds and 5-arcminute) was the LD*DD interaction. None of the individual terms were significant, but PC1 ($F^{1, 18}$ = 1.85, P = 0.053) and PC2 ($F^{1, 18}$ = 1.91, P = 0.058) approached significance. In males, no model outperformed the null model in the 30-arcsecond resolution, but at 5-arcminute resolution, the best-fitting model was also LD*DD, with lineage ($F^{1, 26}$ = 2.46, P = 0.017) and lineage*PC2 ($F^{1, 26}$ = 2.35, P = 0.024). Pairwise analyses showed differences between TMVB and SMOc males in the frontal and basal regions of the braincase (procD = 0.013, P = 0.017) (Figure 4A). Discriminant Function Analysis (DFA) based on the first 10 PCs supported these differences (Mahalanobis D = 2.06, p < 0.001), with cross-validation correctly classifying 84% of TMVB and 50% of SMOc individuals (Figure 4B). PLS analyses revealed a positive, though non-significant, trend between shape and PC2 within lineages (Table 2).

In the lateral rostrum module, models using the 30-arcsecond dataset did not outperform the null model. In contrast, for the 5-arcminute dataset, the best-fitting model included LD*DD interactions, with significant lineage*PC1 ($F^{1, 41}$ = 2.96, P = 0.023) and lineage*PC2 ($F^{1, 41}$ = 4.13, P = 0.007) effects. PLS analyses within lineages indicated positive but non-significant relationships for both interactions (Table 2).

In ventral rostrum view, the best fitting model included only the lineage term ($F^{1, 43}$ = 2.36, P = 0.022), which was significant. Pairwise analyses showed that TMVB and SMOc individuals differed in nasal bone size and length (procD = 0.012, P = 0.012) (Figure 4C). DFA based on the first 10 PCs confirmed these differences (Mahalanobis D = 1.26, P = 0.003), with cross-validation correctly classifying 75% of TMVB and 37.5% of SMOc individuals (Table 2, Figure 4D).

Discussion

In our study, models associated with the LD and RTCR hypotheses provided the most consistent explanation for fore-

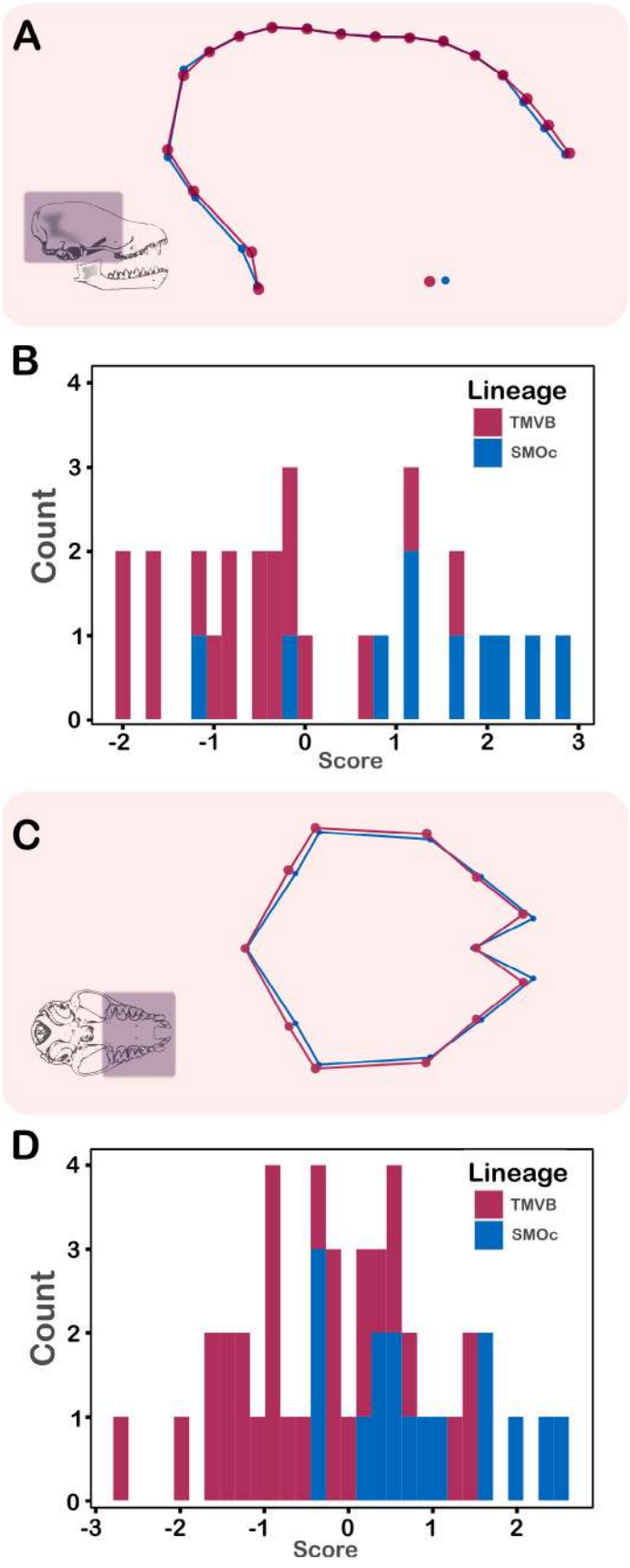

Figure 4. (A) Lateral braincase shape variation in males of *C. mexicanus*, amplified using "mag = 3" for clearer visualization. (B) Linear Discriminant Function (LDF) scores for males from TMVB and SMOc based on lateral braincase shape. (C) Ventral rostrum shape variation, amplified using "mag = 3". (D) LDF scores for individuals from TMVB and SMOc based on ventral rostrum shape.

Table 2. Summary of the best Procrustes ANOVA models fitted for cranial and mandibular shape. Sex and resolution categories are indicated below each view, along with sample size (n).

View	n	Factor	d.f.	SS	MS	R^2	F	Z	P
Lateral braincase	24	Lineage	1	0.0005849	0.00058489	0.04811	1.3176	0.69787	0.249
Females		PC1	1	0.0008224	0.00082245	0.06765	1.8528	1.62565	0.053
30 sec		PC2	1	0.0008496	0.00084957	0.06988	1.9138	1.56436	0.058
		Lineage*PC1	1	0.0007242	0.00072415	0.05956	1.6313	1.29356	0.111
		Lineage*PC2	1	0.0005303	0.00053025	0.04362	1.1945	0.55129	0.295
		Residuals	18	0.0079903	0.0004439	0.67523			
		Total	23	0.0121575					
Lateral braincase	24	Lineage	1	0.0008136	0.00081358	0.06692	1.7084	1.18269	0.119
Females		PC1	1	0.0005085	0.00050846	0.04182	1.0677	0.36244	0.362
5 min		PC2	1	0.0005309	0.00053088	0.04367	1.1148	0.46211	0.32
		Lineage*PC1	1	0.0004954	0.00049538	0.04075	1.0402	0.27462	0.395
		Lineage*PC2	1	0.0009379	0.00093788	0.07714	1.9694	1.52011	0.06
		Residuals	18	0.008572	0.00047622	0.70508			
		Total	23	0.0121575					
Lateral braincase	32	Lineage	1	0.0010894	0.00108942	0.07129	2.4677	2.12624	0.017
Males		PC1	1	0.0004505	0.00045047	0.02948	1.0204	0.12911	0.452
5 min		PC2	1	0.000559	0.00055896	0.03658	1.2661	0.5972	0.28
		Lineage*PC1	1	0.0007205	0.00072055	0.04715	1.6322	1.25127	0.113
		Lineage*PC2	1	0.0010416	0.00104155	0.06816	2.3593	2.04082	0.024
		Residuals	26	0.0114781	0.00044147	0.75115			
		Total	31	0.0152807					
Lateral rostrum	47	Lineage	1	0.001616	0.0016159	0.03872	1.9171	1.29774	0.102
Both sexes		PC1	1	0.001298	0.0012977	0.0311	1.5395	0.98793	0.168
5 min		PC2	1	0.000408	0.0004083	0.00978	0.4844	-0.78256	0.764
		Lineage*PC1	1	0.002497	0.0024966	0.05983	2.9619	2.0349	0.023
		Lineage*PC2	1	0.003489	0.0034887	0.0836	4.1389	2.43528	0.007
		Residuals	41	0.034559	0.0008429	0.82818			
		Total	46	0.041729					
Ventral rostrum	45	Lineage	1	0.0014626	0.00146264	0.05208	2.3627	1.9463	0.022
Both sexes		Residuals	43	0.0266191	0.00061905	0.94792			
30 sec		Total	44	0.0280817					

arm variation in *C. mexicanus*. Although the GD hypothesis was similarly supported in both sexes, its performance varied depending on the spatial resolution of the environmental dataset. Given that hypothesis support contingent upon predictor resolution may reflect scale-dependent effects rather than clear biological mechanisms, we limit further discussion of the GED hypothesis. Nonetheless, we acknowledge that when GD hypothesis was supported, the relationship between forearm length and environmental variables followed the pattern predicted by Bergmann's rule.

By the other hand, despite the comparative suitability of forearm length and body mass as proxies of intraspecific body size in bats is beyond the scope of this study, we provide the follow rationale to clarify our decision to use forearm length as a structural measure of body size in *C. mexicanus* in the present discussion.

Since size refers to the spatial extent occupied by an object in a three-dimensional space, size is fundamentally the volume, which depends on linear dimensions (height, length, and width). Although mass is often correlated with volume, it represents the amount of matter rather than the space occupied; therefore, mass and size are related but conceptually distinct properties. In bats, both body mass and forearm length have been widely used as proxies of body size at the interspecific level, as they generally scale in the same direction (Safi *et al.* 2013). However, at the intraspecific level, forearm length has been questioned as a proxy because it does not necessarily scale proportionally with body mass (McGuire *et al.* 2018; Mellado *et al.* 2024). We argue that dismissing forearm length on the basis that body mass represents a "truer" measure of size reflects a conceptual conflation between mass and volume. While body mass is appropriate for interspecific comparisons, its use at the intraspecific level often reflects variation in body condition or nutritional state rather than structural size.

In this context, we highlight two considerations of our study. First, the absence of support for the RAD hypothesis may be related to the use of forearm length rather than

body mass as the response variable, given that resource availability is more directly associated with body condition and nutritional state. Second, because Bergmann's rule is grounded in surface-to-volume dynamics (Bergmann 1848), we consider forearm length an appropriate structural proxy of size, even at the intraspecific level, as changes in linear dimensions necessarily affect volume. In other words, affect the amount of space that individuals occupied, which by definition is their size.

Variation of forearm. Our results indicate a sex-specific pattern of forearm length variation: in females, forearm seems to be more strongly constrained by environmental selective pressures than by the species' evolutionary history, whereas in males, although environmental factors also play a role, evolutionary history also has an influence on forearm length. Previously, López-Cuamatzi *et al.* (2024) reported forearm differentiation between the SMOc and TMVB lineages in males but not in females, suggesting that the "Big Mother Hypothesis" (Stevens *et al.* 2013) could explain the absence of differentiation in females. According to this hypothesis, sexual dimorphism in forearm length in vespertilionid bats, characterized by a bias toward larger sizes in females, is the result of a positive selection favoring females due to the cost-benefit balance of energy expenditure during reproduction and lactation (Stevens *et al.* 2013). Our findings support this interpretation, indicating that environmental conditions during the reproductive period may select for specific body sizes (measured here as forearm length), leading to phenotypic convergence among females regardless of lineage.

Nevertheless, the lack of differences in forearm size among females' lineage does not necessarily imply an absence of influence from evolutionary history. Our results for females for both resolution datasets reveal a significant interaction between lineage and environment during reproductive period: in the TMVB lineage, female forearm size is influenced by environmental variables, whereas in the SMOc lineage it is not. This could be interpreted as a reduced or negligible effect of temperature in SMOc, either due to an unknown biological factor or because temperatures in that region may be more homogeneous and span a narrower range. However, our data do not allow us to discern which of these hypotheses is more plausible, indicating that the lineage-dependent nature of this response requires further investigation.

Regarding specific environmental effects, in TMVB females, PC1 was negatively related to forearm size, exhibiting the classic Bergmann's rule pattern. This component was mainly associated with minimum temperatures during the reproductive months, but also with maximum temperatures in March and April, the latter corresponding to the highest values of the maximum temperature set (Figure 5A). This pattern suggests that forearm size variation in females may be mainly shaped by selection for heat conservation, underscoring the role of efficient thermoregulation during gestation (March-

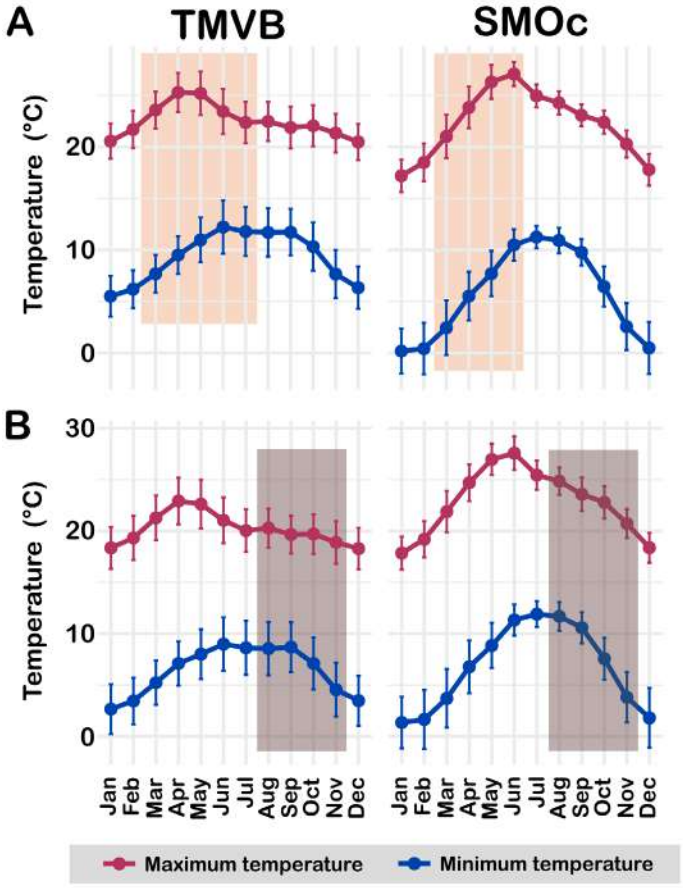

Figure 5. Trends of maximum and minimum temperatures by sex and lineage. The reproductive period (colored rectangle) used to test the RCTR hypothesis is shown for females (A) and males (B), with mean values (circles) and standard deviations (intervals) calculated from historical monthly records spanning 1950-2024.

April) (López-Wilchis 1989), when energy resources are partitioned between maternal maintenance and fetal development. But also, the high temperatures of March and April may also indicate selective pressure for heat dissipation during the early stages of gestation. Elevated thermoregulatory demands during this period –whether conserving or dissipating heat– could impose fitness costs on *C. mexicanus* females at TMVB.

Heat dissipation and conservation patterns in TMVB females are also reflected in the relationship between PC2 and forearm length. In localities where early spring (early gestation) and midsummer (lactation) temperatures are similar, forearm length tends to be shorter, likely due to relatively homogeneous and warmer conditions where avoiding overheating is important. Conversely, where early spring is cooler and the seasonal contrast is stronger, females exhibit longer forearms, possibly reflecting greater selective pressure for heat conservation during early gestation (Wolf *et al.* 2025).

In males, differentiation between lineages, also reported by López-Cuamatzi *et al.* (2024), underscores the relevance of evolutionary factors in forearm variation. However, our analyses indicate that environmental conditions during the reproduction (RCTR hypothesis) also play an important role. It is important to note that the

hypotheses tested in this study (lineage and environment) are not mutually exclusive. Therefore, interpretation should not focus on determining which hypothesis better explains forearm size variation in males, but rather on recognizing that such variation reflects environmental effects acting in both lineages within their respective morphological ranges.

The PC1 of RCTR model was negatively related to forearm length and exhibited the classic Bergmann pattern. This component was associated with maximum temperatures during the reproductive period and with minimum temperatures in August and September, the warmest months in the analyzed series (Figure 5B). This suggests that, unlike in females, forearm variation in males may be influenced by thermal stress due to overheating under higher temperatures. Komar *et al.* (2022) have demonstrated that male bats tend to reduce the maturation speed and production of sperm at high temperatures, reducing the chances of mating. Since August and September coincide with key reproductive processes in males of *C. mexicanus* –epididymal development, recrudescence of testes, and accessory sexual glands (Léon-Galván *et al.* 2005)– additional energy expenditure for heat dissipation could affect sperm quality and, consequently, reproductive success.

Paltrinieri *et al.* (2025) previously demonstrated a sex-specific response of forearm length to environmental temperature, with females of European bats exhibiting adaptations toward heat conservation and males showing evidence of both heat conservation and dissipation. However, unlike their conclusion that both mechanisms are equally plausible for males, our results suggest a stronger selective pressure for heat dissipation.

Variation in the shape and size of the cranium and mandible. Our results indicate that the skull and mandible are relatively conserved structures in *C. mexicanus*, with morphological differences so subtle that, in most analyzed modules, they did not deviate from a random pattern. López-Cuamatzi *et al.* (2024) previously attributed this morphological conservatism to low genetic differentiation and the recent divergence between lineages, a pattern also observed in *Myotis velifer peninsularis* (Nájera-Cortazar *et al.* 2015). Our data support this conclusion and further show that environmental variables –considered as proxies for insect abundance and diversity– play a minimal or negligible role in the morphological variation of these structures.

The only significant differences observed in some skull modules were primarily associated with mitochondrial lineage. Although López-Cuamatzi *et al.* (2024) previously reported differentiation in the lateral view of the cranial vault in females, our analysis unexpectedly detected this differentiation in males, while it was absent in females. This discrepancy may be explained by the analytical approach: López-Cuamatzi *et al. (2024)* used the individual as the sampling unit, whereas in our study we used the locality as the unit, averaging the cranial shape of multiple individuals from the same population. This procedure led to a loss of variability that our analysis could not recover. Nonetheless, we considered a locality-based approach more suitable for assessing ecological patterns at a spatial scale, as individual-level variation in our dataset could obscure the effects of environmental factors.

Similar to the lateral cranial view, the ventral view of the rostrum showed differences associated with mitochondrial lineage. Although this differentiation had not been previously reported, its subtlety and cross-validation values suggest an emerging signal that should be re-evaluated in the future with a larger sample size. While lineage appears as a factor associated with variation in both modules (cranial vault and rostrum), this does not necessarily imply causality. Therefore, if this variation reflects the species' evolutionary history, its interpretation must be approached cautiously.

Regarding the lateral view of the rostrum, López-Cuamatzi *et al.* (2024) previously reported a trend toward differentiation between the SMOc and TMVB lineages, although it was not statistically significant. Our results suggest that this variation may be associated with lineage or its interaction with environmental variables; however, regression analyses conducted separately for each lineage did not recover statistical significance. This is consistent with statistical reasoning, as a term may be significant in a global model but not in separate analyses, especially when effects are weak (Pike 2011). Furthermore, this result was obtained only using environmental data at 5-arcminute resolution and was not consistent across both datasets (30-arcseconds and 5-arcminute), indicating that the finding should be interpreted cautiously, as it may be an artifact of the data.

Consideration of temporal extent and spatial resolution of the database. The performance and predictive capacity of a geospatial model are affected by three types of uncertainty across spatial and temporal dimensions: uncertainty in estimating the response variable, uncertainty in estimating predictor variables, and uncertainty arising from model formulation and structure (Svensson *et al.* 2013). At both dimensions, two factors are particularly relevant for predictor variable uncertainty: resolution and extent (Svensson *et al.* 2013).

Although high-resolution predictor variables often improve predictive performance of geospatial models (e.g., Franklin *et al.* 2013; Chauvier *et al.* 2022; Cohen and Jetz 2025; but see Lowen *et al.* 2016), they may not be the most biologically appropriate. Because bats exhibit considerable interspecific variation in dispersal abilities and home-range sizes (Wood *et al.* 2024), using environmental data at a spatial resolution finer than a species' dispersal capacity may underestimate the influence of environmental features across its effective area of movement. Conversely, coarser resolutions, although potentially more representative of the environmental conditions across an individual's movement area, may overestimate environmental characteristics by incorporating suboptimal habitats into the averaged

values. Thus, selecting the appropriate resolution in spatial analyses constitutes a trade-off that should fundamentally depend on species-specific biological knowledge.

In our study, information provided by the 30-arcsecond resolution was particularly suitable, as the distribution of *C. mexicanus* in montane ecosystems exhibits climatic variation determined by altitudinal gradients (see Oke and Thompson 2015; Scherrer *et al.* 2019). Fine resolution allows these altitudinal gradients to be captured more accurately. However, although useful in the case of *C. mexicanus*, it should not be considered ideal for all species.

Results on lateral rostrum shape indicate that model term significance, particularly for lineage, depended on the resolution of environmental data used. This demonstrates that methodological decisions can influence conclusions and lead to interpretations that may or may not accurately reflect species biology. Therefore, we recommend that studies analyzing ecological phenomena using spatial data include analyses at multiple resolutions to minimize methodological bias in biological interpretations. This recommendation is especially relevant for research on highly mobile species, such as bats.

Regarding the temporal extent of environmental variables, studies testing Bergmann's rule have commonly relied on monthly, quarterly, or annual temperature ranges to evaluate the relationship between temperature and body size (e.g., Barros *et al.* 2014; Castillo-Figueroa 2022; Alston *et al.* 2023; but see Paltrinieri *et al.* 2025). This approach implicitly assumes that the influence of thermal conditions on body size operates equally throughout the year. Under this assumption, thermoregulatory and energetic demands are considered temporally uniform, thereby justifying the use of annual or temporally aggregated variables. However, thermoregulatory and energetic demands are not constant over time and often peak during specific periods depending on sex and life-history stage (Gustafson 1979; Oxberry 1979; Kurta and Kunz 1987; McLean and Speakman 1999). This is especially evident during the reproductive season, when energetic requirements increase (Kurta and Kunz 1987; McLean and Speakman 1999). Males allocate energy to spermatogenesis and gonadal maturation, whereas females invest in fetal development and lactation (Kurta and Kunz 1987, León-Galván *et al.* 2005). If individuals must simultaneously allocate additional energy to thermoregulation during these periods, this energy is diverted from reproduction. Because thermoregulatory efficiency is influenced by body size, thermal conditions experienced during reproduction are likely to impose stronger selective pressures on body size than conditions encountered during periods of lower energetic demand.

For example, two hypothetical females of different body sizes inhabiting the same colony would experience similar overall thermal conditions. However, if temperatures during lactation are relatively cool, the larger female would conserve heat more efficiently due to a lower surface-area-to-volume ratio. In contrast, the smaller female would lose heat more rapidly and would need to allocate additional energy to thermoregulation, thereby reducing the energy available for milk production. A similar rationale applies to males: under warm autumn conditions, larger males may need to invest more energy in heat dissipation, potentially decreasing the energy available for gonadal development and sperm maturation. Because these energetic trade-offs directly affect reproductive performance, they may have fitness consequences and thus be subject to natural selection.

Therefore, we argue that the influence of environmental conditions on body size is likely strongest during reproductive periods. Assessing temperature effects at an annual scale using mean yearly values may obscure these relationships, as such measures incorporate thermal conditions from periods of lower energetic demand. Consequently, this approach may introduce thermal noise and mask biologically meaningful patterns. Our results indicate that models based on environmental variables restricted to the reproductive period had greater explanatory power than those using annual variables, supporting the idea that the strength of environmental influence on body size is not uniform throughout the year. In this context, our study provides a framework for future research exploring this pattern in bats more broadly, particularly among Holarctic species that exhibit asynchronous reproductive energy investment.

Conclusions

Our study examined phenotypic variation in forearm length as a proxy of body size, as well as cranial and mandibular morphology, in *C. mexicanus*, exploring their associations with evolutionary history and environmental factors. Phenotypic variation in *C. mexicanus* displays sex-biased patterns, with distinct factors driving variation in each sex. Forearm length aligns with the LD and RCTR hypotheses in males and the LD*RCTR hypothesis in females. However, the temperatures associated with forearm variation in the RCTR hypothesis suggest different underlying mechanisms such as conservation in females and heat dissipation in males. In contrast to forearm length, cranial and mandibular shape and size exhibit morphological conservatism, with only slight differences in certain views among lineages, consistent with the LD hypothesis.

Our findings also contribute to ongoing discussions about the appropriate temporal scale of temperature data used to test Bergmann's rule and geographic patterns of body size variation, particularly at the intraspecific level. We propose that, within species, environmental thermal conditions exert their strongest influence on body size during the reproductive season, when energetic investment is highest. During this period, physiological pressures related to heat conservation or dissipation may intensify, allowing environmental conditions to play a critical role due to their direct effects on individual fitness.

Nevertheless, these conclusions require further evaluation through additional studies to determine whether

this pattern is universal or broadly applicable. Moreover, the spatial resolution of environmental data should be carefully considered, as uncertainty in predictor estimates may influence model performance and, consequently, the interpretation of results.

Acknowledgments

All the authors wish to honor, through this text, the tireless work of Dr. Livia León Paniagua. Each of us has had the privilege of collaborating closely with her on projects, shared advisorships, and conjoined publications, and on every occasion, we have witnessed her exceptional qualities as both an academic and a human being, as well as her ability to inspire students and young researchers close to her.

We are grateful to the following curators and museums for providing access to their collections: Dr. Celia López González from the Colección de Mamíferos, CIIDIR-Durango, Instituto Politécnico Nacional; Dr. Livia León Paniagua from the Colección de Mamíferos, Museo de Zoología "Alfonso L. Herrera", FC-UNAM; Dr. Fernando A. Cervantes and Yolanda Hortelano-Moncada from the Colección Nacional de Mamíferos, IB-UNAM; Dr. Cynthia Elizalde Arellano from the Colección Mastozoológica, ENCB-IPN; Dr. Rogelio Rosas Valdez from the Laboratorio de Colecciones Biológicas y Sistemática Molecular de la UACB, UAZ; Dr. Santiago Espinosa Andrade from the Colección de Vertebrados, Facultad de Ciencias-UASLP; Dr. Christian A. Delfín and MSc. Nallely Verónica Rodríguez Santiago from the Colección de Mamíferos, IIB-UV; Dr. José Ramírez Pulido and Noé González Ruiz from the Colección de Mamíferos de la Sierra Volcánica Transversal de México, UAM-Iztapalapa, as well as the Colección de Mamíferos de UAEH. We are also grateful for the assistance of Dr. Pedro A. Aguilar-Rodríguez, MSc. Melany Aguilar López and Dr. Melina del Real Monroy during specimens' revisions. The first author gratefully acknowledges the Secretaría de Ciencia, Humanidades, Tecnología e Innovación (SECIHTI) for the Master's and SNI-III Research Assistant fellowships (No. 1018336), and the Centro de Investigaciones Tropicales, UV, for support through a fieldwork grant.

Declaration of Artificial Intelligence use

The authors declare that AI was used to assist with style suggestions, textual clarity, and revision of grammar and syntax in English.

Author contributions

Issachar L. López-Cuamatzi: Conceptualization, Formal analysis, Investigation, Methodology, Visualization, Writing – Original Draft Preparation. Jorge Ortega: Conceptualization, Funding Acquisition, Methodology, Project administration, Resources, Writing- Reviewing and Editing. Sandra M. Ospina-Garcés: Conceptualization, Methodology, Writing- Reviewing and Editing. M. Cristina MacSwiney G.: Conceptualization, Funding acquisition, Methodology, Project administration, Resources, Supervision, Writing- Reviewing and Editing.

Supplementary data

SD1. Results of sexual dimorphism analysis for forearm length and cranial and mandibular shapes.

Literature cited

Adams D, Collyer M, Kaliontzopoulou A, and Baken E. 2025. *"Geomorph: Software for geometric morphometric analyses*. R-package version 4.0.10." https://cran.r–project.org/R-package=geomorph.

Alston JM, Keinath DA, Willis CK, Lausen CL, O'Keefe JM, Tyburec JD, *et al*. 2023. Environmental drivers of body size in North American bats. *Functional Ecology* 37:1020–1032. https://doi.org/10.1111/1365-2435.14287

Ashton KG. 2002. Patterns of within-species body size variation of birds: strong evidence for Bergmann's rule. *Global Ecology and Biogeography* 11:505–523. https://doi.org/10.1046/j.1466-822X.2002.00313.x

Ashton KG, Tracy MC, and Queiroz AD. 2000. Is Bergmann's rule valid for mammals? *The American Naturalist* 156:390–415. https://doi.org/10.1086/303400

Barros LAVD, Fortes RDR, and Lorini ML. 2014. The Application of Bergmann´ s Rule to *Carollia perspicillata* (Mammalia, Chiroptera). *Chiroptera Neotropical* 20:1243–1251.

Bates D, Mächler M, Bolker B, and Walker S. 2015. Fitting Linear Mixed-Effects Models Using lme4. *Journal of Statistical Software* 67:1–48. https://doi.org/10.48550/arXiv.1406.5823

Bergmann C. 1848. Über die Verhältnisse der Wärmeökonomie der Thiere zu ihrer Grösse. Göttingen (GER): Vandenhoeck und Ruprecht.

Bolnick DI, Amarasekare P, Araújo MS, Bürger R, Levine JM, Novak M, *et al*. 2011. Why intraspecific trait variation matters in community ecology. *Trends in Ecology and Evolution* 26:183–192. https://doi.org/10.1016/j.tree.2011.01.009

Bolnick DI, Svanbäck R, Fordyce JA, Yang LH, Davis JM, Hulsey CD, *et al*. 2003. The ecology of individuals: incidence and implications of individual specialization. *The American Naturalist* 161:1–28. https://doi.org/10.1086/343878

Bookstein FL. 1997. Morphometric tools for landmark data: Geometry and biology. Cambridge (UK): Cambridge University Press.

Borer ET, Seabloom EW, and Tilman D. 2012. Plant diversity controls arthropod biomass and temporal stability. *Ecology Letters* 15:1457–1464. https://doi.org/10.1111/ele.12006

Bozinovic F, Bastías DA, Boher F, Clavijo-Baquet S, Estay SA, and Angilletta Jr. MJ. 2011. The mean and variance of environmental temperature interact to determine physiological tolerance and fitness. *Physiological and Biochemical Zoology* 846:543–552. https://doi.org/10.1086/662551

Bruyndonckx R, Hens N, and Aerts M. 2018. Simulation-based evaluation of the linear-mixed model in the presence of an increasing proportion of singletons.

Biometrical Journal 601:49–65. https://doi.org/10.1002/bimj.201700025

Camargo NFD, and de Oliveira, HF. 2012. Sexual dimorphism in *Sturnira lilium* (Chiroptera, Phyllostomidae): can pregnancy and pup carrying be responsible for differences in wing shape? *PLoS One* 7:e49734. https://doi.org/10.1371/journal.pone.0049734

Castillo–Figueroa D. 2022. Does Bergmann's rule apply in bats? Evidence from two neotropical species. *Neotropical Biodiversity* 8:200–221. https://doi.org/10.1080/23766808.2022.2075530

Chauvier Y, Descombes P, Guéguen M, Boulangeat L, Thuiller W, and Zimmermann NE. 2022. Resolution in species distribution models shapes spatial patterns of plant multifaceted diversity. *Ecography* 2022:e05973. https://doi.org/10.1111/ecog.05973

Chown SL, and Gaston KJ. 2010. Body size variation in insects: a macroecological perspective. *Biological Reviews* 85:139–169. https://doi.org/10.1111/j.1469-185X.2009.00097.x

Chu C, Bartlett M, Wang Y, He F, Weiner J, Chave J, and Sack L. 2016. Does climate directly influence NPP globally? *Global Change Biology* 22:12–24. https://doi.org/10.1111/gcb.13079

Clauset A, and Erwin DH. 2008. The evolution and distribution of species body size. *Science* 321:399–401. https://doi.org/10.1126/science.1157534

Cohen JM, and Jetz W. 2025. Fine-Grain Predictions Are Key to Accurately Represent Continental-Scale Biodiversity Patterns. *Global Ecology and Biogeography* 34:e13934. https://doi.org/10.1111/geb.13934

Collyer ML, and Adams DC. 2018. RRPP: An package for fitting linear models to high-dimensional data using residual randomization. *Methods in Ecology and Evolution* 9:1772–1779. https://doi.org/10.1111/2041-210X.13029

Dinno A. 2009. Exploring the sensitivity of Horn's parallel analysis to the distributional form of random data. *Multivariate Behavioral Research* 443: 362–388. https://doi.org/10.1080/00273170902938969

Encarnação JA, Kierdorf U, Holweg D, Jasnoch U, and Wolters V. 2005. Sex-related differences in roost-site selection by Daubenton's bats *Myotis daubentonii* during the nursery period. *Mammal Review* 35:285–294. https://doi.org/10.1111/j.1365-2907.2005.00066.x

Fellers GM, and Pierson ED. 2002. Habitat use and foraging behavior of Townsend's big–eared bat (*Corynorhinus townsendii*) in coastal California. *Journal of Mammalogy* 83:167–177. https://doi.org/10.1644/1545-1542(2002)083%3C0167:HUAFBO%3E2.0.CO;2

Fick SE, and Hijmans RJ. 2017. WorldClim 2: new 1km spatial resolution climate surfaces for global land areas. *International Journal of Climatology* 37:4302–4315. https://doi.org/10.1002/joc.5086

Franklin J, Davis FW, Ikegami M, Syphard AD, Flint LE, Flint AL, *et al*. 2013. Modeling plant species distributions under future climates: how fine scale do climate projections need to be? *Global Change Biology* 19:473–483. https://doi.org/10.1111/gcb.12051

Frick WF, Reynolds DS, and Kunz TH. 2010. Influence of climate and reproductive timing on demography of little brown myotis *Myotis lucifugus*. *Journal of Animal Ecology* 79:128–136. https://doi.org/10.1111/j.1365-2656.2009.01615.x

Gibert JP. 2016. The effect of phenotypic variation on metapopulation persistence. *Population Ecology* 58:345–355. https://doi.org/10.1007/s10144-016-0548-z

Gorobeyko UV, Kazakov DV, Kadetova AA, Sheremetyeva IN, Guskov VY, Kartavtseva IV, *et al*. 2025. Intraspecific structure of *Myotis petax* Hollister, 1912 (Chiroptera: Vespertilionidae) based on mitochondrial DNA and morphological data. *Vertebrate Zoology* 75:87–106. https://doi.org/10.3897/vz.75.e134683

Gotelli NJ, and Graves GR. 1996. *Null models in ecology*. Washington D.C. (EEUU): Smithsonian Institution Press.

Gunz P, and Mitteroecker P. 2013. Semi landmarks: a method for quantifying curves and surfaces. *Hystrix* 24:103–109. https://doi.org/10.4404/hystrix–24.1–6292

Gustafson AW. 1979. Male reproductive patterns in hibernating bats. *Reproduction* 56:317–331. https://doi.org/10.1530/jrf.0.0560317

Hedrick BP. 2021. Inter–and intraspecific variation in the *Artibeus* species complex demonstrates size and shape partitioning among species. *PeerJ 9*:e11777. https://doi.org/10.7717/peerj.11777

Klingenberg CP. 2015. Analyzing fluctuating asymmetry with geometric morphometrics: concepts, methods, and applications. *Symmetry* 7:843–934. https://doi.org/10.3390/sym7020843

Komar E, Fasel NJ, Szafrańska PA, Dechmann DK, Zegarek M, and Ruczyński I. 2022. Energy allocation shifts from sperm production to self–maintenance at low temperatures in male bats. *Scientific Reports* 12:1–11. https://doi.org/10.1038/s41598-022-05896-3

Korner-Nievergelt F, Roth T, Von Felten S, Guélat J, Almasi B, and Korner-Nievergelt P. 2015. Bayesian data analysis in ecology using linear models with R BUGS and Stan. Massachusetts (EEUU): Academic Press. https://doi.org/10.1016/C2013-0-23227-X

Kurta A, and Kunz TH. 1987. Size of bats at birth and maternal investment during pregnancy. *Symposia of the Zoological Society of London* 57:79–106.

Lenth R, and Piaskowski J. 2025. emmeans: Estimated Marginal Means aka Least-Squares Means R package version 201. https://githubcom/rvlenth/emmeans

León-Galván MA, López-Wilchis R, Hernández-Pérez O, Arenas-Ríos E, and Rosado A. 2005. Male reproductive cycle of Mexican big–eared bats, *Corynorhinus mexicanus* (Chiroptera: Vespertilionidae). *The Southwestern Naturalist* 50:453–460.

Lind EM, Pierre KJL, Seabloom EW, Alberti J, Iribarne O, Firn J, *et al*. 2017. Increased grassland arthropod production with mammalian herbivory and eutrophication: A test of

mediation pathways. *Ecology* 98:3022–3033. https://doi.org/10.1002/ecy.2029

López-Cuamatzi IL, Ortega J, Ospina-Garcés SM, Zúñiga G, and MacSwiney G MC. 2024. Molecular and morphological data suggest a new species of big-eared bat (Vespertilionidae: *Corynorhinus*) endemic to northeastern Mexico. *PLoS One* 19:e0296275. https://doi.org/10.1371/journal.pone.0296275

López–Wilchis R. 1989. *Biología de Plecotus mexicanus (Chiroptera: Vespertilionidae) en el estado de Tlaxcala, México*. [PhD thesis]. [Ciudad de México (MEX)]: Universidad Nacional Autónoma de México.

Lowen JB, McKindsey CW, Therriault TW, and DiBacco C. 2016. Effects of spatial resolution on predicting the distribution of aquatic invasive species in nearshore marine environments. *Marine Ecology Progress Series* 556:17–30. https://doi.org/10.3354/meps11765

Lüdecke D, Ben-Shachar MS, Patil I, Waggoner P, and Makowski D. 2021. performance: An R package for assessment comparison and testing of statistical models. *Journal of Open Source Software* 660: 1–8. https://doi.org/10.21105/joss.03139

Majerus ME, and Mundy NI. 2003. Mammalian melanism: natural selection in black and white. *Trends in Genetics* 19:585–588. https://doi.org/10.1016/j.tig.2003.09.003

Maluleke T, Jacobs DS, and Winker H. 2017. Environmental correlates of geographic divergence in a phenotypic trait: A case study using bat echolocation. *Ecology and Evolution* 7:7347–7361. https://doi.org/10.1002/ece3.3251

Marchan-Rivadeneira MR, Larsen PA, Phillips CJ, Strauss RE, and Baker RJ 2012. On the association between environmental gradients and skull size variation in the great fruit–eating bat, *Artibeus lituratus* (Chiroptera: Phyllostomidae). *Biological Journal of the Linnean Society* 105:623–634. https://doi.org/10.1111/j.1095-8312.2011.01804.x

Marroig G, Shirai LT, Porto A, de Oliveira FB, and De Conto V. 2009. The evolution of modularity in the mammalian skull II: evolutionary consequences. *Evolutionary Biology* 36:136–148. https://doi.org/10.1007/s11692-009-9051-1

McGuire LP, Kelly LA, Baloun DE, Boyle WA, Cheng TL, Clerc J, *et al.* 2018. Common condition indices are no more effective than body mass for estimating fat stores in insectivorous bats. *Journal of Mammalogy* 995:1065–1071. https://doi.org/10.1093/jmammal/gyy103

McLean JA, and Speakman JR. 1999. Energy budgets of lactating and non-reproductive brown long-eared bats (*Plecotus auritus*) suggest females use compensation in lactation. *Functional Ecology* 13:360–372. https://doi.org/10.1046/j.1365-2435.1999.00321.x

McNab BK. 2010. Geographic and temporal correlations of mammalian size reconsidered: a resource rule. *Oecologia* 164:13–23. https://doi.org/10.1007/s00442-010-1621-5

Meiri S. 2008. Evolution and ecology of lizard body sizes. *Global Ecology and Biogeography* 17:724–734. https://doi.org/10.1111/j.1466-8238.2008.00414.x

Mellado B, de Oliveira Carneiro L, Nogueira MR, and Monteiro LR. 2024. Not all size measures are created equal: Different body size proxies are not equivalent fitness predictors in the bat *Carollia perspicillata*. *Journal of Mammalian Evolution* 311:1–12. https://doi.org/10.1007/s10914-024-09702-x

Mendes SB, Stefanello F, Costa CLDS, Lima ACDS, Olímpio APM, Pires W MDM, *et al*. 2024. Morphological and molecular data combined reveal inter–and intraspecific cranial shape variations in bats of *Artibeus* Leach, 1821 (Chiroptera: Phyllostomidae). *Biological Journal of the Linnean Society* 143:blae031. https://doi.org/10.1093/biolinnean/blae031

Montañez-Reyna M, León-Cortés JL, Infante F, Naranjo EJ, and Gómez-Velasco A. 2022. Diversity and climatic distribution of moths in the tribe Arctiini Lepidoptera: Erebidae: Arctiinae in Mexico. *Annals of the Entomological Society of America* 1153:253–266. https://doi.org/10.1093/aesa/saac002

Moosman Jr PR, Thomas HH, and Veilleux JP. 2012. Diet of the widespread insectivorous bats *Eptesicus fuscus* and *Myotis lucifugus* relative to climate and richness of bat communities. *Journal of Mammalogy* 93:491–496. https://doi.org/10.1007/s13364-023-00678-2

Morales AE, De la Mora M, and Piñero D. 2018. Spatial and environmental factors predict skull variation and genetic structure in the cosmopolitan bat *Tadarida brasiliensis*. *Journal of Biogeography* 45:1529–1540. https://doi.org/10.1111/jbi.13243

Myers P. 1978. Sexual dimorphism in size of vespertilionid bats. *The American Naturalist* 112:701–711.

Nájera-Cortazar LA, Álvarez-Castañeda ST, and De Luna E. 2015. An analysis of *Myotis peninsularis* (Vespertilionidae) blending morphometric and genetic datasets. *Acta Chiropterologica* 17:37–47. https://doi.org/10.3161/15081109ACC2015.17.1.003

NASA Earth Observatory. 2025. *Net primary productivity (1 month – Terra/MODIS)*. Washington D.C. (EEUU): National Aeronautics and Space Administration; July, 2025. [Accessed July 21th, 2025]. https://neo.gsfc.nasa.gov/view.php?datasetId=MOD17A3H_Y_NPP

Oke OA, and Thompson KA. 2015. Distribution models for mountain plant species: the value of elevation. *Ecological Modelling* 301:72–77. https://doi.org/10.1016/j.ecolmodel.2015.01.019

Oksanen J, Simpson G, Blanchet F, Kindt R, Legendre P, Minchin P, *et al*. 2025. vegan: Community Ecology R-package. R-package version 2.8-0, https://vegandevs.github.io/vegan/.

Oxberry BA. 1979. Female reproductive patterns in hibernating bats. *Reproduction* 56:359–367. https://doi.org/10.1530/jrf.0.0560359

Paltrinieri L, Razgour O, Santini L, Russo D, Aihartza J, Aizpurua O, *et al*. 2025. The effects of climate on

bat morphology across space and time. *Ecography* 2025:e07663. https://doi.org/10.1002/ecog.07663

Peralta–Maraver I, and Rezende EL. 2021. Heat tolerance in ectotherms scales predictably with body size. *Nature Climate Change* 11:58–63. https://doi.org/10.1038/s41558-020-00938-y

Pérez SI, Bernal V, and González PN. 2006. Differences between sliding semi–landmark methods in geometric morphometrics with an application to human craniofacial and dental variation. *Journal of Anatomy* 208:769–784. https://doi.org/10.1111/j.1469–7580.2006.00576.x

Pike N. 2011. Using false discovery rates for multiple comparisons in ecology and evolution. *Methods in Ecology and Evolution* 2:278–282. https://doi.org/10.1111/j.2041-210X.2010.00061.x

Porto A, de Oliveira FB, Shirai LT, De Conto V, and Marroig G. 2009. The evolution of modularity in the mammalian skull I: morphological integration patterns and magnitudes. *Evolutionary Biology* 36:118–135. https://doi.org/10.1007/s11692-008-9038-3

R Core Team. 2024. R: A language and environment for statistical computing R Foundation for Statistical Computing Vienna Austria https://wwwR-projectorg/

Revelle W, and Revelle MW. 2015. Package 'psych'. *The comprehensive R archive network*. https://personality-project.org/r/psych/

Rohlf FJ. 1990. Rotational fit Procrustes methods. In: Rohlf FJ, Bookstein FL, editors. *Proceedings of the Michigan morphometrics workshop*. Ann Arbor (EEUU): University of Michigan Museum of Zoology Special Publication 2; p. 227–236.

Rohlf FJ. 2017. TpsDig2 v.2.3.6. Department of Ecology and Evolution, State University of New York. New York.

Rohlf FJ. 2019. TpsUtil ver. 1.7.8. Department of Ecology and Evolution, State University of New York. New York.

Russo D, Jones G, Martinoli A, Preatoni DG, Spada M, Pereswiet-Soltan A, and Cistrone L. 2024. Climate is changing, are European bats too? A multispecies analysis of trends in body size. *Ecology and Evolution* 14:e10872. https://doi.org/10.1002/ece3.10872

Safi K, Meiri S, Jones KE, Smith FA, and Lyons K. 2013. Evolution of body size in bats. In: Smith FA, and Lyons SK, editors. *Animal body size: Linking pattern and process across space, time, and taxonomic group*. Chicago (EEUU): The University of Chicago Press; p. 95–151.

Salinas-Ramos VB, Ancillotto L, Bosso L, Sánchez-Cordero V, and Russo, D. 2020. Interspecific competition in bats: state of knowledge and research challenges. *Mammal Review* 50:68–81. https://doi.org/10.1111/mam.12180

Scherrer D, Christe P, and Guisan A. 2019. Modelling bat distributions and diversity in a mountain landscape using focal predictors in ensemble of small models. *Diversity and Distributions* 25:770–782. https://doi.org/10.1111/ddi.12893

Schlager S. 2017. Morpho and Rvcg–Shape Analysis in R: R-packages for geometric morphometrics shape analysis and surface manipulations. In: Zheng G, Li S, Szekely G, editors. *Statistical shape and deformation analysis: methods, implementation and applications*. London (UK): Academic Press p. 217–256. https://doi.org/10.1016/B978-0-12-810493-4.00011-0

Smith FA, Betancourt JL, and Brown JH. 1995. Evolution of body size in the woodrat over the past 25,000 years of climate change. *Science* 270:2012–2014. https://doi.org/10.1126/science.270.5244.2012

Stevens RD, Johnson ME, and McCulloch ES. 2016. Geographic variation of wing morphology of great fruit–eating bats (*Artibeus lituratus*): environmental, genetic and spatial correlates of phenotypic differences. *Biological Journal of the Linnean Society* 118:734–744. https://doi.org/10.1111/bij.12787

Svensson JR, Jonsson L, and Lindegarth M. 2013. Excessive spatial resolution decreases performance of quantitative models, contrary to expectations from error analyses. *Marine Ecology Progress Series* 485:57–73. https://doi.org/10.3354/meps10307

Ulpian CM, and Rossi MN. 2017. Intraspecific variation in body size and sexual size dimorphism, and a test of Rensch's rule in bats. *Acta Zoologica*, 98:377–386. https://doi.org/10.1111/azo.12183

Uvizl M, and Benda P. 2021. Intraspecific variation of *Myotis emarginatus* (Chiroptera: Vespertilionidae) inferred from mitochondrial and nuclear genetic markers. *Acta Chiropterologica* 23:285–300. https://doi.org/10.3161/15081109ACC2021.23.2.002

Watt C, Mitchell S, and Salewski V. 2010. Bergmann's rule; a concept cluster? *Oikos* 119:89–100. https://doi.org/10.1111/j.1600-0706.2009.17959.x

Williams DF, and Findley JS. 1979. Sexual size dimorphism in vespertilionid bats. *American Midland Naturalist* 113–126. https://doi.org/10.2307/2425072

Wilson RJ, Gutierrez D, Gutierrez J, and Monserrat VJ. 2007. An elevational shift in butterfly species richness and composition accompanying recent climate change. *Global Change Biology* 139:1873–1887. https://doi.org/10.1111/j.1365-2486.2007.01418.x

Wolf JM, Lehmann P, and Kerth G. 2025. Field respirometry in a wild maternity colony of Bechstein's bats *Myotis bechsteinii* indicates high metabolic costs above but not below the thermoneutral zone. *Journal of Experimental Biology*. 228:JEB249975. https://doi.org/10.1242/jeb.249975

Wood MR, de Vries JL, Monadjem A, and Markotter W. 2024. Review and meta-analysis of correlates of home range size in bats. *Journal of Mammalogy* 105:1044–1056. https://doi.org/10.1093/jmammal/gyae036

Zhu D, Liu Y, Gong L, Si M, Wang Q, Feng J, and Jiang T. 2024. The consumption and diversity variation responses of agricultural pests and their dietary niche differentiation in insectivorous bats. *Animals* 14:1–22. https://doi.org/10.3390/ani14050815

Zimmermann NE, Yoccoz NG, Edwards Jr. TC, Meier ES, Thuiller W, Guisan A, and Pearman PB. 2009. Climatic

extremes improve predictions of spatial patterns of tree species. *Proceedings of the National Academy of Sciences* 106:19723–19728. https://doi.org/10.1073/pnas.0901643106

Associated editors: Giovani Hernández Canchola and Pablo Colunga Salas
Submitted: October 30, 2025; Reviewed: January 8, 2026
Accepted: March 9, 2026; Published online: May 29, 2026

THERYA, 2026, Vol. 17(2):163-170 DOI: 10.12933/therya.2026.6247 ISSN 2007-3364

Parasitic metazoans of wild rodents (Mammalia) from Mexico. Geographic distribution and host spectrum

Carmen Guzmán-Cornejo[1], Angel Herrera-Mares[1,2], Roxana Acosta[3], Ricardo Paredes-León[4], Rosario Mata-López[5], and Luis García Prieto[6*]

[1]Laboratorio de Acarología, Departamento de Biología Comparada, Facultad de Ciencias, Universidad Nacional Autónoma de México, C.P. 04510, Ciudad de México, México. E-mail: carguzmancornejo@gmail.com (CG-C)
[2]Laboratorio de Ecología de Enfermedades y Una Salud, Departamento de Etología, Fauna Silvestre y Animales de Laboratorio, Facultad de Medicina Veterinaria y Zootecnia, Universidad Nacional Autónoma de México, C.P. 04510, Ciudad de México, México. E-mail: angelmares@ciencias.unam.mx (AH-M)
[3]Museo de Zoología "Alfonso L. Herrera", Departamento de Biología Evolutiva, Facultad de Ciencias, Universidad Nacional Autónoma de México, C.P. 04510, Ciudad de México, México E-mail: roxana_a2003@ciencias.unam.mx (RA-G)
[4]Colección Nacional de Ácaros, Instituto de Biología, Universidad Nacional Autónoma de México, Ciudad de México, México. E-mail: rparedes@ib.unam.mx (RP-L)
[5]Laboratorio de Sistemática y Evolución de Helmintos de Vertebrados Silvestres, Departamento de Biología Evolutiva, Facultad de Ciencias, Universidad Nacional Autónoma de México, C.P. 04510, Ciudad de México, México. E-mail: rmatalopez@ciencias.unam.mx (RM-L)
[6]Colección Nacional de Helmintos, Instituto de Biología, Universidad Nacional Autónoma de México, C.P. 04510, Ciudad de México, México.
[*]Corresponding author: luis.garcia@ib.unam.mx

Among the most common animal lifestyles, parasitism stands out, often occurring in groups that also include free-living organisms. Among metazoans, helminths and arthropods include a large number of parasitic species. The objective of the present study was to compile, update and list for the first time all nominal species of metazoans that infect and infest wild rodents, analyzing their geographic distribution, defining the state of the art, and suggesting possible avenues of research that will allow us to complete the knowledge of the group. A total of 3,909 records of metazoan parasites of 204 rodent species were obtained from the 32 states of Mexico. Estado de México (Mexico) and Oaxaca were the states with the greatest parasite richness. At a national level, this richness is composed of 70 nominal species of helminths, 204 of mites, 40 of anoplurans, 67 of chewing lice, and 136 species of fleas.

Keywords: ectoparasites, endoparasites, helminths, parasitic arthropods, wild rodents

Entre los estilos de vida animal más comunes, destaca el parasitismo, que a menudo se presenta en grupos que también incluyen organismos de vida libre. Entre los metazoarios, los helmintos y los artrópodos contienen gran cantidad de especies parásitas. El objetivo del presente estudio fue recopilar, actualizar y listar por primera vez todas las especies nominales de metazoos que infectan e infestan roedores silvestres, analizando su distribución geográfica, definiendo el estado del arte y las posibles líneas de investigación que permitan completar el conocimiento del grupo. Se obtuvieron un total de 3,909 registros de parásitos metazoarios de 204 especies de roedores de los 32 estados de la República Mexicana. El Estado de México y Oaxaca fueron los estados con la mayor riqueza parasitaria. A nivel nacional, la riqueza está conformada por 70 especies nominales de helmintos, 204 de ácaros, 40 de anopluros, 67 de piojos masticadores y 136 especies de pulgas.

Palabras clave: artrópodos parásitos, ectoparásitos, endoparásitos, helmintos, roedores silvestres

Among the most common animal lifestyles, parasitism stands out, often occurring in groups that also include free-living organisms. Among metazoans, helminths and arthropods include a large number of parasitic species (Goater *et al.* 2014). Helminths, which constitute a non-natural grouping, comprise organisms belonging to four phyla that are characterized by being worm-like and parasitic: Platyhelminthes (dorsoventrally flattened worms), Rotifera-Acanthocephala (worms with the proboscis armed with hooks), Nematoda (roundworms) and Annelida-Hirudinea (ringed worms). On the other hand, Arthropoda is the phylum that includes the largest number of animals on Earth; they are characterized by the presence of articulated legs, segments fused into tagmas and appendages formed by segments (Brusca *et al.* 2022).

The systematic study of parasites from both groups in Mexico began asynchronously; the first helminth recorded in the country was the nematode *Litomosoides sigmodontis*, a parasite of the Hispid Cotton Rat *Sigmodon hispidus* Say and Ord, 1825 in Jalisco and Michoacán (Ochoterena and Caballero y Caballero 1932). Regarding arthropods, the chewing louse *Eutrichophilus mexicanus* was reported by Rudow (1866) on the Mexican Hairy Porcupine (*Coendou mexicanus* (Kerr, 1972)) from an undetermined locality in Mexico. Since then, both lines of research have been addressed by national and international researchers from

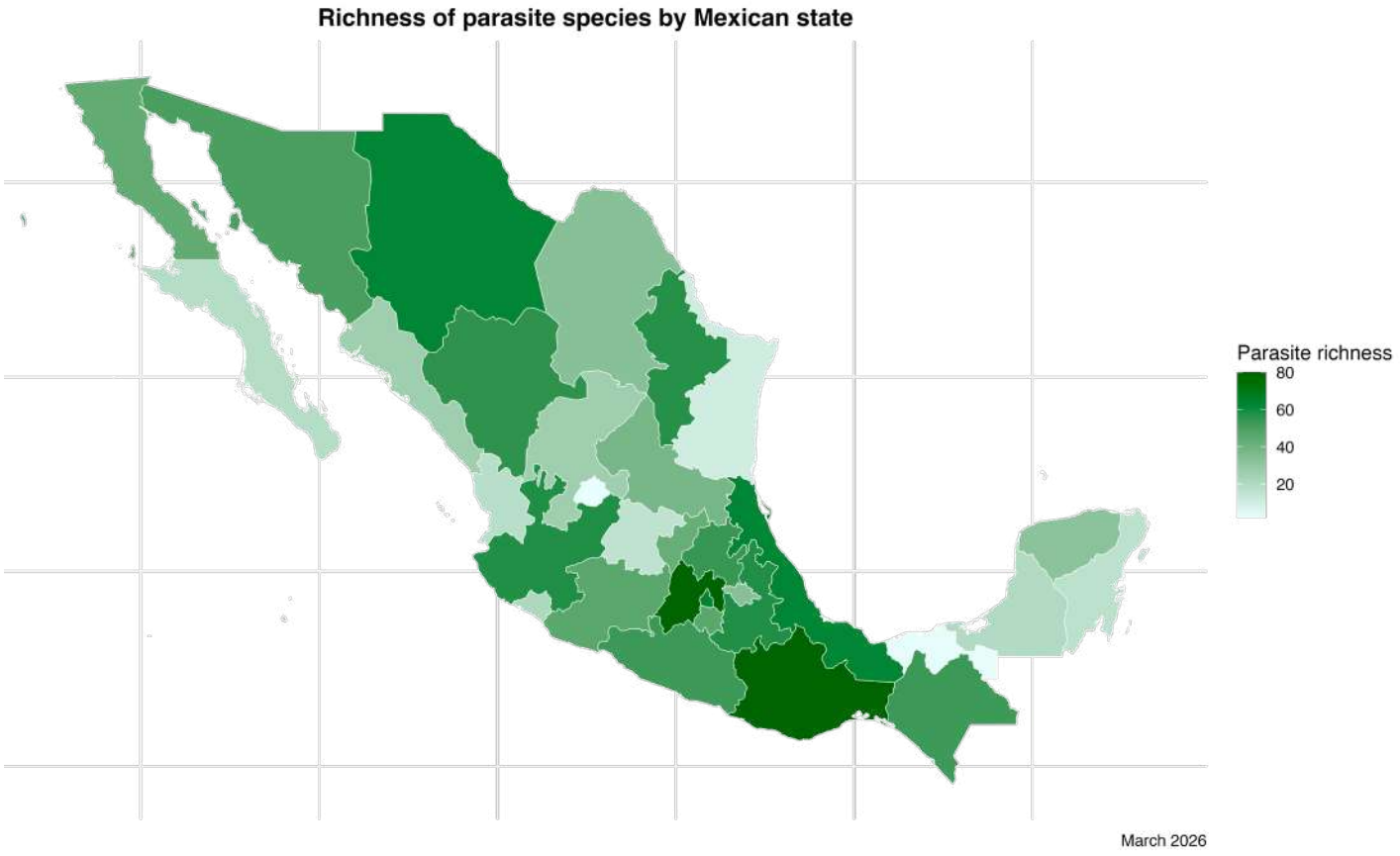

Figure 1. Richness of parasitic metazoan associated with wild rodents by Mexican state.

various institutions, with the most notable being the Instituto de Biología, Universidad Nacional Autónoma de México (UNAM), in Mexico, for both groups (helminths and arthropods), and Facultad de Ciencias, UNAM, and Instituto Politécnico Nacional for arthropods.

The first attempt to quantify the richness of helminths associated with rodents in Mexico was made by García-Prieto *et al.* (2012); however, these authors considered both wild and synanthropic rodents. In the case of arthropods, Whitaker and Morales-Malacara (2005) gathered published information related to ectosymbionts of wild rodents in a single study. Based on the above, the objective of the present study was to compile, update and list for the first time all nominal species of metazoans that infect and infest wild rodents and analyze their geographic distribution, defining the state of the art and suggesting possible lines of research that will allow us to complete the knowledge of the group.

Materials and methods

Systematic searches were carried out in electronic databases such as BioOne (https://bioone-org), CAB Abstracts (https://www.cabidigitallibrary.org), Clarivate Analytics (https://www.webofscience.com) and Google Scholar (https://scholar.google.com) between 1913 and 2025. In addition, some faunal lists were consulted, such as: Whitaker and Morales-Malacara (2005); García-Prieto *et al.* (2012); Sánchez-Montes *et al.* (2013; 2018); Light *et al.* (2020); Herrera-Mares *et al.* (2022).

The keywords for the searches were combined in Spanish and English: helminths, flatworms, Platyhelminthes, nematodes, Nematoda, acanthocephalans, Acanthocephala, leeches, Hirudinea, parasitic arthropods, ectoparasites, mites, Acari, fleas, Siphonaptera, ticks, Argasidae, Ixodidae, lice, chiggers, Trombiculidae, Phthiraptera, rodents, Rodentia, Mexico. The classification and nomenclature of parasitic metazoans was updated based on keys and specialized literature. For the nomenclature of rodents we follow The Mammal Diversity Database (2025) V.2.0 (MDD2).

All metazoan records were entered into an Excel spreadsheet, including the following fields for both groups, parasites and hosts: family, genus, and species. The state, bibliographic reference and full citation were included for each record. For the total count of parasitic and host species, only nominal species (identified at the species level) were used. The numbers of metazoan parasites were represented in a choropleth map. The present study is a bibliographic compilation; therefore, it was not required to follow the guidelines of the American Society of Mammalogists or the approval of the Committee for the Care and Use of Animals in Research-Experimentation.

Results

The knowledge of metazoan parasites of rodents in Mexico consists of 3,909 records obtained from all the 32 states; these records correspond to 518 species, from 155 genera and 50 families (Table 1; Figure 1), associated with 204

rodent species classified into 58 genera and eight families. The states with the greatest parasite richness are Estado de México and Oaxaca, with 80 species, associated with 31 and 36 host species, respectively. The most complete record of metazoan parasites was achieved in the states of Jalisco, Nuevo León, and Hidalgo, with seven of the eight groups of metazoans considered in this study associated with rodents. On the other hand, in the state of Aguascalientes, only two species of Ischnocera have been reported. The highest number of studied hosts has been recorded in the states of Chihuahua (38) and Oaxaca (36), whereas in Aguascalientes and Tabasco, only one and two species of rodents have been sampled, respectively. Asymmetric knowledge among metazoan parasitic groups is also evident, with helminths being the most neglected (Table 2).

Table 1. Number of species, genera and families of parasites by metazoan parasitic group.

Parasite taxa	Number of families	Number of genera	Number of species
Trematoda	3	4	5
Cestoda	5	7	11
Acanthocephala	1	1	1
Nematoda	13	29	53
Acari	16	58	204
Anoplura	2	6	40
Ischnocera	1	3	67
Siphonaptera	9	49	136

The eight families of wild rodents examined have at least one species of parasitic metazoan, highlighting that Cricetidae and Heteromyidae are parasitized by six groups of metazoans except for Ischnocera, which only infests Geomyidae and Erethizontidae (Figure 2).

The most widely distributed parasitic metazoan species in the country are the flea *Jellisonia breviloba breviloba* Traub, 1950 and the chewing louse *Geomydoecus* (*Geomydoecus*) *welleri* Price and Hellenthal, 1981 in 15 states each, followed by the mesostigmate mite *Steptolaelaps liomydis* in 13 states.

Table 2. Richness of parasitic metazoans in rodent species by Mexican state. Tre = Trematoda; Ces= Cestoda; Acn = Acantocefala; Nem = Nematoda; Aca = Acari; Ano = Anoplura; Isc= Ischnocera; Sip = Siphonaptera.

State	Tre	Ces	Acn	Nem	Aca	Ano	Isc	Sip	Total parasite richness	Richness of hosts studied
Aguascalientes	0	0	0	0	0	0	2	0	2	1
Baja California	0	0	0	0	27	2	5	10	44	27
Baja California Sur	0	0	0	0	15	2	2	0	19	13
Campeche	0	1	0	4	11	0	2	2	20	12
Chiapas	1	0	0	2	26	5	1	18	53	31
Chihuahua	0	0	0	6	5	8	11	31	61	38
Ciudad de México	0	0	0	0	19	4	5	36	64	23
Coahuila	0	0	0	3	8	4	14	4	33	15
Colima	0	1	0	1	14	2	3	0	21	15
Durango	0	0	0	1	27	3	10	15	56	31
Estado de México	0	2	0	5	20	5	11	37	80	31
Guanajuato	0	0	0	8	0	1	4	3	16	10
Guerrero	0	0	0	0	17	5	0	31	53	26
Hidalgo	1	4	0	13	7	2	6	21	54	30
Jalisco	2	0	1	3	19	8	13	12	58	20
Michoacán	0	0	0	3	14	1	6	22	46	25
Morelos	0	0	0	7	10	4	2	23	46	18
Nayarit	0	0	0	1	7	5	4	1	18	9
Nuevo León	1	2	0	2	10	6	5	31	57	30
Oaxaca	0	0	0	1	35	9	3	32	80	36
Puebla	1	0	0	2	18	3	11	23	58	29
Querétaro	0	0	0	0	0	1	2	40	43	30
Quintana Roo	0	0	0	4	11	0	1	1	17	11
San Luis Potosí	0	0	0	7	19	2	7	3	38	24
Sinaloa	0	0	0	0	13	5	5	3	26	20
Sonora	0	0	0	1	32	2	6	9	50	30
Tabasco	0	0	0	0	0	2	1	0	3	2
Tamaulipas	0	0	0	0	2	3	6	0	11	9
Tlaxcala	1	0	0	2	0	0	8	22	33	24
Veracruz	0	1	0	9	20	8	10	15	63	31
Yucatán	0	2	0	6	16	3	2	3	32	13
Zacatecas	0	0	0	6	6	4	9	1	26	16

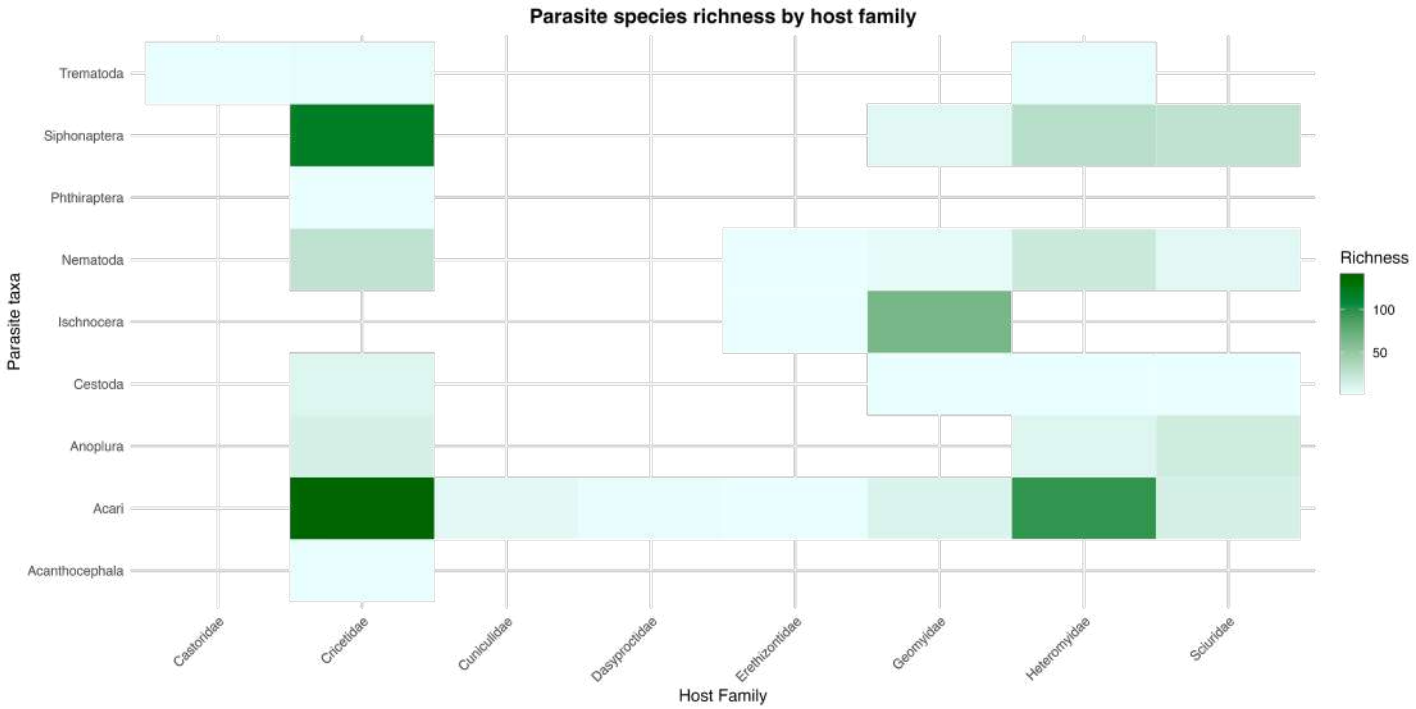

Figure 2. Graphical representation of the richness of parasitic metazoan by rodent family.

The hosts with the greatest parasite richness correspond to species of the Cricetidae family: *Peromyscus difficilis* (J. A. Allen, 1891) (73 species), *Peromyscus maniculatus* (J. A. Wagner, 1844) (60), *Microtus mexicanus* (de Saussure, 1861) (49) and *Peromyscus melanotis* J. A. Allen and F. M. Chapman, 1897 (47), followed by the heteromyid (Heteromyidae) *Heteromys pictus* O. Thomas, 1893 (41 species).

To date, the helminthological record for wild rodents in Mexico consists of 70 nominal species, which parasitize 49 host species belonging to five families, among which Cricetidae and Heteromyidae stand out for hosting the largest number of helminth species (38 and 21, respectively). These hosts have been collected in 23 states. Individually, the phylum Nematoda is the most represented (53 species), followed by Platyhelminthes (with 16) and Acanthocephala with one, with no species of Annelida having been recorded to date associated with this group of mammals (Figure 3).

The first helminth described for a Mexican wild rodent is *Micropleura sigmodontis* Ochoterena and Caballero y Caballero, 1932 (currently *Litomosoides sigmodontis* (Chandler, 1931)), in the cricetid *S. hispidus* from Jalisco and Michoacán. The nematode *Vexillata vexillata* (Hall, 1916) represents the helminth with the widest geographic distribution, having been collected in six states, followed by the nematodes *Heteromyoxyuris longejector* Quentin, 1973 and *Vexillata liomyos* Falcón-Ordaz, Gardner and Pérez-Ponce de León, 2001, each in five states. The most extensive helminthological record is harbored by the cricetid *P. difficilis*, which comprises 13 helminth species.

Mites (Parasitiformes and Acariformes) that are parasitic on rodents in Mexico are represented by 204 species classified in 58 genera from 16 families. These species are widely distributed among rodents throughout Mexico,

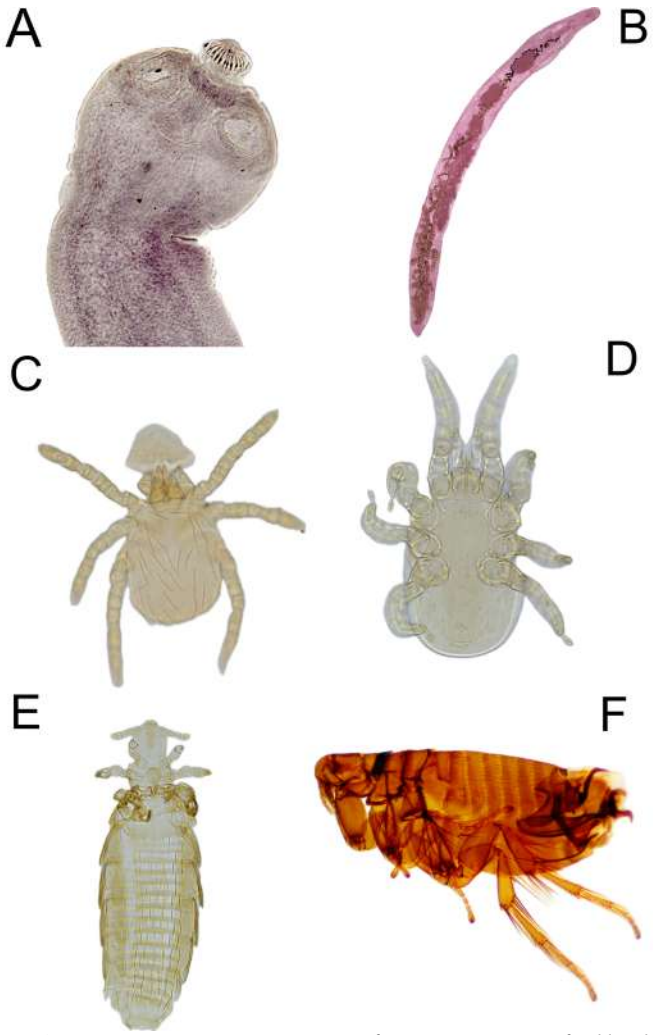

Figure 3. Some representative species of metazoan parasites of wild rodents in Mexico. A) *Rodentolepis nana* (Cestode). B) *Caballerolecythus ibunami* (Trematode). C) *Hoffmannina* sp. (Acari: Acariformes). D) *Echinonyssu liomys* (Acari: Parasitiformes). E) *Hoplopleura reithrodontomydis* (Phthiraptera). F) *Dactylospylla samalayucae* (Siphonaptera).

except for the states of Aguascalientes, Guanajuato, Querétaro, Tabasco, and Tlaxcala. The first records of rodent mites in Mexico correspond to *Ornithodoros nicollei* (Parasitiformes: Argasidae) in the nests of rats of the genus *Hodomys* (Brumpt *et al.* 1939) and *Eutrombicula alfreddugesi* (Oudemans, 1910) (Acariformes: Trombiculidae) in the ground squirrel *Otospermophilus variegatus* (Erxleben, 1777) (Islas 1943). The most widely distributed mite species are *Steptolaelaps liomydis* (Grant, 1947), *Androlaelaps fahrenholzi* (Berlese, 1911), and *E. alfreddugesi*, found in rodents from 13, 12, and 10 states, respectively.

These mite species parasitize 132 rodent species from 37 genera and seven families (Cricetidae, Cuniculidae, Dasyproctidae, Erethizontidae, Geomyidae, Heteromyidae, and Sciuridae). The host with the greatest richness is *Heteromys pictus* (Cricetidae) with 29 associated mite species, followed by *Peromyscus difficilis* with 19 and *H. irroratus* with 18. The most studied host, that is, the one with the greatest number of records, is also *H. pictus*.

Among insects, anoplurans are represented by 40 species belonging to six genera and two families, distributed across 28 states in Mexico. Among the first records of anoplurans in the country are those of *Enderleinellus extremus* Ferris, 1919 and *Enderleinellus suturalis* (Osborn, 1891), in squirrels of the genera *Sciurus* (Chiapas, Oaxaca, Tamaulipas, and Veracruz) and *Callospermophilus* (Chihuahua), respectively. The most widespread species of sucking lice are *Polyplax auricularis* Kellogg and Ferris, 1915 and *Neohaematopinus sciurinus* (Mjöberg, 1910) in eight Mexican states, followed by *Fahrenholzia ehrlichi* Johnson, 1962 in seven, and *Fahrenholzia pinnata* Kellogg and Ferris, 1915, and *Hoplopleura hirsuta* Ferris, 1916 in six states. These lice species are associated with 65 rodent species from 26 genera and three families (Cricetidae, Heteromyidae, and Sciuridae).

The host with the greatest richness is *Sciurus aureogaster* F. Cuvier in É. Geoffroy Saint-Hilaire and F. Cuvier, 1829 with four associated species (*Enderleinellus deppei* Kim, 1966, *E. extremus, Enderleinellus mexicanus* Werneck, 1948 and *N. sciurinus*); the most studied host is *Heteromys irroratus* J. E. Gray, 1868 with records in nine states of Mexico.

Regarding chewing lice, the national record includes 67 species and 21 subspecies (Ischnocera), belonging to three genera and one family (Trichodectidae); the oldest record for this group is *Eutrichophilus mexicanus* (Rudow 1866) associated with *C. mexicanus*. The most widely distributed species in the country is *G.* (*Geomydoecus*) *welleri* in 15 states, followed by *Thomomydoecus* (*Thomomydoecus*) *zacatecae* (Price and Hellenthal, 1980) in seven.

Chewing lice are associated with 21 rodent species from eight genera and two families. The host with the greatest number of associated species is *Megascapheus umbrinus* (J. Richardson, 1829) (=*Thomomys umbrinus*, which included several subspecies), with 22 species and three subspecies. It is also the most studied host in 18 states of Mexico.

Finally, Siphonaptera (fleas) is represented by 136 species belonging to 49 genera and nine families, distributed in 27 states. The first record of flea species (*Pleochaetis mundus* Jordan and Rothschild, 1922) in wild rodents of Mexico was made in two species of rodents: *Reithrodontomys megalotis* (S. F. Baird, 1857) and *P. difficilis*. The most widely distributed species of fleas are *J. breviloba breviloba* and *Plusetis mathesoni* in 15 and 12 states of Mexico respectively, followed by *Jellisonia weismani* Eads, 1951 and *Plusaetis sibynus* (Jordan, 1925), in 11 states. Flea species are associated with 101 species of rodents from 32 genera and four families (Sciuridae, Cricetidae, Heteromyidae and Geomyidae). The host with the greatest richness is *P. maniculatus* with 45 flea species, while the most studied is *P. difficilis* with 166 records.

Discussion

This work represents the first approach towards a comprehensive understanding of the richness of metazoan parasites (helminths and arthropods) in wild rodents in Mexico. The results of this study reveal a significant asymmetry in knowledge between the two groups. An important explanation for these differences can be found in the greater adaptive radiation shown by arthropods compared to any other animal group, since we are dealing with the most diverse group on the planet (Brusca *et al.* 2022). Another possible reason for this is the different start dates for the study of each group, with the study of helminths in rodents beginning in 1932 (Ochoterena and Caballero y Caballero 1932) and that of arthropods in 1866 (Rudow 1866).

However, this pattern may also be explained by other factors, such as the requirement to euthanize hosts to obtain helminths, in contrast to arthropod collection, which does not require euthanasia and thus facilitates their capture in larger numbers. Additionally, there is a bias toward the study of helminths infecting synanthropic rodents (Panti-May *et al.* 2018), as well as challenges related to the morphological complexity of some parasite groups, particularly trichostrongylid nematodes, which frequently infect these hosts. Furthermore, some helminth groups, such as Acanthocephala, exhibit relatively low richness, reducing the likelihood of their detection in wild rodents. Supporting this, our electronic literature search conducted to compile the information analyzed in this study yielded eight records of acanthocephalans, of which only one was associated with wild rodents (Lynggaard *et al.* 2021).

From a biological point of view, the differences in intra-group (metazoan groups) and inter-group (helminths vs. arthropods) richness could be attributed to the intrinsic nature of each one, that is, its particular richness and abundance, as well as the geographical distribution and host specificity they exhibit, their ability to evade the immune response, and the characteristic overdispersed distribution exhibited by the parasites.

Additionally, the process for the study of arthropods is relatively easier, so it requires less time. The processing of helminths applies particular techniques for each group, such as heat fixation, staining of specimens, clearing and

mounting in Canada balsam (turpentine) or, in the case of nematodes, cross-sections of the body and clearing with Amman lactophenol (Guzmán-Cornejo *et al.* 2012).

Another issue we identified is that some records of ectoparasitic arthropods were attributed to Mexico by Guzmán-Torres and Cano-Santana (2021) (e.g., *Enderleinellus suturalis* from Chihuahua). However, this record was originally cited by Ritzi (2014) in a study on ectoparasites of mammals from the northern extent of the Chihuahuan Desert in the United States. Therefore, such records were excluded from this manuscript.

On the other hand, in the initial stage of knowledge about Mexican arthropods, the contribution of foreign researchers was notable (Grant 1947; Furman 1955; Fain 1973; Loomis 1969; Genoways 1973; Werneck 1948, among others), while for helminths this has been developed mainly by national researchers in a punctual manner, and recently in a more systematic aproach: Pulido-Flores *et al.* (2005); Preisser and Falcón-Ordaz (2019); Panti-May *et al.* (2023); Falcón-Ordaz *et al.* (2024).

The nomenclatural revision of both parasites and hosts aimed to achieve the greatest possible accuracy in the records we present. However, some were problematic, such as *Peromyscus maniculatus*, since according to the database we followed (The Mammal Diversity Database 2025) this species is not distributed in Mexico. Notwithstanding, a recent study (Boria and Blois 2023) based on populations of this species in the USA found that *P. maniculatus* split into two regionally distinct subspecies: *P. m. gambelii* and *P. m. sonorensis,* both distributed in Northwestern Mexico. The inclusion of records of "*P. maniculatus*" in our study needs to be confirmed with a similar analysis to that referred to previously. Likewise, in accordance with Rose (2025), *S. hispidus* is distributed exclusively in northern Mexico; however, we found several records of parasites in the central and southern part of Mexico, which do not correspond to the current reported distribution of this rodent species. Unfortunately, the preservation of symbiotypes (*sensu* Frey *et al.* 1992) was not a common practice among parasitologists, so the identity of the specimens cannot be clarified. Some studies refer to this same problem (Light *et al.* 2020). To address this limitation, some efforts have included the collection of host tissue for subsequent DNA-based identification or the deposition of specimens in mammal collections.

Regarding the distribution of these groups of parasites, we can point out that they are distributed throughout all 32 states of Mexico; however, we also observed a significant asymmetry in sampling effort, with more than 220 records in states such as Estado de México, Querétaro, and Oaxaca, while only four have been recorded in other states such as Aguascalientes and Tabasco. Furthermore, it highlights that although sampling effort has been similar in Querétaro (where 30 rodent species have been analyzed), in Estado de México and Oaxaca, the richness of metazoans is practically half of what is reported in these last two states (80 species each). This can be explained by a probable lower regional richness of parasites in Querétaro than in the two states mentioned above, particularly in Oaxaca, which is in the Neotropical portion of the country, and occupies the first place in number of mammal species in Mexico (Briones-Salas *et al.* 2015). To establish the true current distribution of metazoans associated with wild Mexican rodents, a detailed study mapping the collection sites would be necessary; however, many of the older records are difficult to locate on maps due to their imprecise descriptions. Fortunately, many recent works include the precise geographic coordinates [e.g., Herrera-Mares *et al.* (2022); Panti-May *et al.* 2023)] of the sites where the material was obtained among their collection data.

On the other hand, as Herrera-Mares *et al.* (2022) highlighted, some regions still remain unexplored or poorly investigated because they face problems related to violence associated with drug cartels which can limit sampling in these particular areas.

According to the results obtained from the list presented, we found that the eight families of wild rodents have records of parasitic metazoans. However, the two families with the greatest parasite richness are Cricetidae (110 species) and Heteromyidae (40), which is likely related to the high diversity of both groups: 150 species of Cricetidae and 40 of Heteromyidae (Light *et al.* 2020), and to the extensive sampling of species belonging to both families.

In accordance with The Mammal Diversity Database (2025) V.2.0 (MDD2) the number of wild rodent species distributed in Mexico is 270; as result of our study, 204 have been reported as hosts of metazoans, representing 75.5% of the total. This could indicate that the knowledge of parasitic metazoans in this group of hosts is quite advanced in Mexico; notwithstanding, analyzing the individual host records, we can see that the number of metazoan species associated with these mammals varies widely, ranging from one species in *Dipodomys ornatus* (Falcón-Ordaz *et al.* 2024) to 73 in *P. difficilis*.

Parasites and rodents are crucial components of biodiversity and the ecosystems they inhabit. Furthermore, several of these parasitic species are of medical and veterinary importance, either as disease-causing agents by feeding on hosts infected with worms (e.g., *Rodentolepis nana*) or as potential vectors of disease-causing pathogens, since some rodent species are reservoirs of microorganisms (Keesing and Ostfeld 2024). Therefore, we consider it essential to continue monitoring the population dynamics of these parasites in their hosts, not only in relatively well-studied areas, but especially in less explored ones. This task is urgent considering the accelerating impact of human activities and global climate change, which in certain circumstances favor the survival of some species of public health importance.

Acknowledgments

This work is dedicated to Dr. Livia León-Paniagua for her career over 38 years studying Mexican mammalogy,

in which she has made important contributions to its knowledge, and for the great support she has given us in the field collections that we have carried out together. We thank Georgina Ortega-Leite for providing important bibliographic references and to Lázaro Gervara López for their comments abouth the species of Peromyscus. RP-L thanks to program UNAM-PAPIIT IA204525.

Declaration of Artificial Intelligence use

Google translator was used to correct the grammar of the writing.

Author contributions

Carmen Guzmán-Cornejo conceptualization, investigation, data curation, methodology, writing-original draft; Angel Herrera-Mares conceptualization, investigation, data curation, methodology, draft revision; Roxana Acosta-Gutiérrez conceptualization, investigation, data curation, methodology, draft revision; Ricardo Paredes-León conceptualization, investigation, data curation, methodology, draft revision; Rosario Mata-López conceptualization, investigation, data curation, methodology, draft revision; Luis García-Prieto conceptualization, investigation, data curation, methodology, writing-original draft.

Supplementary data

SD1. Records of parasitic metazoans associated with wild rodents in Mexico.

SD2. Literature of parasitic metazoans associated with wild rodents of Mexico.

Literature cited

Boria RA, and Blois J. 2023. Phylogeography within the *Peromyscus maniculatus* species group. *Molecular Phylogenetics and Evolution* 180:107701. https://doi.org/10.1016/j.ympev.2023.107701

Briones-Salas M, Lavariega NMC, Cortes-Marcial M, Monroy-Gamboa AG, and Mases-García CA. 2015. In: Briones-Salas M, Hortelano MY, Magaña CG, Sánchez RG, and Sosa EJE, editors. *Riqueza y conservación de los mamíferos en México a nivel estatal*: Vol. I. Ciudad de México (MEX): Asociación Mexicana de Mastozoología A.C., p. 329–366.

Brumpt EL, Mazzotti L, and Brumpt LC. 1939. Étude épidemiologique de la fiévre récurrente endémique des hauts plateau Mexicains. *Annales de Parasitologie Humaine et Comparée* 17:275–286.

Brusca RC, Giribet G, and Moore W. 2022. *Invertebrates (4th ed. Edition)*. Oxford (UK): Oxford University Press.

Fain A. 1973. Diagnoses d'acariens nouveaux (Listrophoroidea et Myobiidae). *Revue de Zoologie et de Botanique Africaine* 87:330–332.

Falcón-Ordáz J, Aquino-Camacho M, Guevara-Barcenas K, and Fernández J. 2024. Helminths parasites of heteromyid rodents from semiarid regions of Mexico. *Therya notes* 5:157–161. https://doi.org/10.12933/therya_notes-24-164

Frey JK, Yates TL, Duszynski DW, Gannon WL, and Gardner SL. 1992. Designation and curatorial management of type host specimens (symbiotypes) for new parasite species. *Journal of Parasitology* 78:930-932. https://doi.org/10.2307/3283335

Furman DP. 1955. *Steptolaelaps* (Acarina: Laelaptidae) a new genus of mites parasitic on neotropical rodents. *Journal of Parasitology* 41:519–525. https://doi.org/10.2307/3273813

García-Prieto L, Falcón-Ordaz J, and Guzmán-Cornejo C. 2012. Helminth parasites of wild Mexican mammals: list of species, hosts and geographical distribution. *Zootaxa* 3290:1–92. https://doi.org/10.11646/zootaxa.3290.1.1

Genoways HH. 1973. Systematics and evolutionary relationships of spiny pocket mice, genus *Liomys*. *Special Publication Museum Texas Tech University* 5:1–368.

Goater TM, Goater CP, and Esch GW. 2014. *Parasitism: the diversity and ecology of animal parasites*. Nueva York (EEUU): Cambridge University Press.

Grant CD. 1947. North American species of the genus *Laelaps* (Arachnida: Acarina: Parasitidae). *Microentomology* 12:2–21.

Guzmán-Cornejo C, García-Prieto L, Rivas G, Mendoza-Garfías B, Osorio-Sarabia D, and Montiel-Parra G. 2012. *Manual de prácticas de metazoarios parásitos de vertebrados*. Ciudad de México (MEX): Las Presas de Ciencias, Facultad de Ciencias, Universidad Nacional Autónoma de México.

Guzmán-Torres M, and Cano-Santana Z. 2021. Actualización del listado de piojos (Insecta: Phthiraptera) de México: distribución, riqueza, grado de especificidad y pediculosis humana. *Revista Mexicana de Biodiversidad* 92:e923800 https://doi.org/10.22201/ib.20078706e.2021.92.3800

Herrera-Mares A, Guzmán-Cornejo C, García-Prieto L, Rebollo-Hernández A, León-Paniagua L, Del Castillo-Martínez L, Montiel-Parra G, and Ríos-Sais G. 2022. Acari (Parasitiformes and Acariformes) From Mexico: Analysis of Their Geographical and Host Distribution in Rodentia (Cricetidae). *Journal of Medical Entomology* 59:1880–1890. https://doi.org/10.1093/jme/tjac135

Islas F. 1943. Observaciones sobre el tlazahuate de Izúcar de Matamoros y Acatlán, Puebla (Acarina: Trombiididae). Anales del Instituto de Biología, Universidad Nacional Autónoma de México 14: 439–450.

Keesing F, and Ostfeld RS. 2024. Emerging patterns in rodent-borne zoonotic diseases. *Science* 385:1305–1310. https://doi.org/10.1126/science.adq7993

Light JE, Durden LA, Oconnor BM, Preisser WC, Acosta R, and Eckerlin RP. 2020. Checklist of ectoparasites of cricetid and heteromyid rodents in Mexico. *Therya* 11:79–136. https://doi.org/10.12933/therya-20-785

Lynggaard C, García-Prieto L, Guzmán-Cornejo C, and García-Varela M. 2021. Description of a new species of *Moniliformis* (Acanthocephala: Moniliformidae) from *Peromyscus hylocetes* (Rodentia: Cricetidae) in Mexico. *Parasitology International* 83:102315. https://doi.org/10.1016/j.parint.2021.102315

Loomis RB. 1969. Chiggers (Acarina, Trombiculidae) from vertebrates of the Yucatan Peninsula, Mexico. Miscellaneous *Publications, University of Kansas Museum of Natural History* 50:1–22.

Mammal Diversity Database. 2025. *Mammal Diversity Database* (Version 2.3) [Data set]. Zenodo. [Accessed September-October, 2025]. https://doi.org/10.5281/zenodo.17033774

Ochoterena I, and Caballero y Caballero E. 1932. Filaria parásita de las ratas de campo *Micropleura sigmodoni* spec., nov. *Anales del Instituto de Biología, Universidad Nacional Autónoma de México* 3:123–125.

Panti-May JA, Digiani MC, Palomo-Arjona EE, Gurubel-González YM, Navone GT, Williams CM, *et al*. 2018. A checklist of the helminth parasites of sympatric rodents from two Mayan villages in Yucatán, México. *Zootaxa* 4403:495–512. https://doi.org/10.11646/zootaxa.4403.3.4

Panti-May JA, Moguel CWI, Hernández MDI, Cárdenas VMH, Torres CM, García-Prieto L, *et al*. 2023. Helminths of small rodents (Heteromyidae and Cricetidae) in the Yucatan Peninsula, Mexico: an integrative taxonomic approach to their inventory. *Zootaxa* 5357:205–240. https://doi.org/10.11646/zootaxa.5357.2.3

Preisser W, and Falcón-Ordaz J. 2019. A checklist of the parasitic helminths of cricetid and heteromyid rodents in Mexico. *Therya* 10:329–341. https://10.12933/therya-19-787.

Pulido-Flores G, Moreno-Flores S, and Monks S. 2005. Helminths of rodents (Rodentia: Muridae) from Metztitlán, San Cristóbal, and Rancho Santa Elena, Hidalgo, Mexico. *Comparative Parasitology* 72:186–92.

Ritzi CM. 2014. A review of mammalian ectoparasites from the Northern Chihuahuan Desert. In: Hoyt CA, and Karges J, editors. *Proceedings of the Sixth Symposium on the Natural Resources of the Chihuahuan Desert Region*. October 14–17. Fort Davis, Texas (EEUU): Chihuahuan Desert Research Institute; p. 151–184.

Rose RK. 2025. *Sigmodon hispidus* Rodentia: Cricetidae). *Mammalian Species* 57:1–26 https://doi.org/10.1093/mspecies/seae007

Rudow F. 1866. Sechs neue Haarlinge. *Zeitschrift für die gesammten Naturwissenschaften* 27:109–112.

Sánchez-Montes S, Guzmán-Cornejo C, León-Paniagua L, and Rivas G. 2013. A checklist of sucking lice (Insecta: Phthiraptera: Anoplura) associated with Mexican wild mammals, including geographical records and a host-parasite list. *Zootaxa* 3722:183–203. https://doi.org/10.11646/zootaxa.3722.2.4

Sánchez-Montes S, Colunga-Salas P, Álvarez-Castillo L, Guzmán-Cornejo C, and Montiel-Parra G. 2018. Chewing lice (Insecta: Phthiraptera) associated with vertebrates in Mexico. *Zootaxa* 4372:1–109. https://doi.org/10.11646/zootaxa.4372.1.1

Werneck FL. 1948 Notas sôbre o gênero *Enderleinellus* (Anoplura). *Memórias do Instituto Oswaldo Cruz* 45:281–306. http://dx.doi.org/10.1590/s0074-02761947000200001

Whitaker JO Jr, and Morales-Malacara JB. 2005. Ectoparasites and other associates (Ectodytes) of mammals of Mexico. In: Sánchez-Cordero V, and Medellín RA, editors. *Contribuciones mastozoológicas en homenaje a Bernardo Villa*. Distrito Federal (MEX): Instituto de Biología e Instituto de Ecología, Universidad Nacional Autónoma de México and CONABIO; p. 535–666.

Associated editors: Giovani Hernández Canchola and Pablo Colunga Salas
Submitted: October 31, 2025 ; Reviewed: December 12, 2025
Accepted: March 19, 2026; Published online: May 29, 2026

THERYA, 2026, Vol. 17(2):171-190 DOI: 10.12933/therya.2026.6251 ISSN 2007-3364

Genomic approximations for the study and conservation of mammals

Gabriela Castellanos-Morales[1*], Jorge Ortega[2], Anahí Canedo-Téxon[1], Carlos A. Barrera[2], Jesús Antonio Rocamontes-Morales[1], and Katia Hernández-Bolaños[1]

[1]Departamento de Conservación de la Biodiversidad, El Colegio de la Frontera Sur, Unidad Villahermosa. Carretera Villahermosa-Reforma km 15.5, Ranchería Guineo 2a sección, C.P. 86280. Villahermosa, Tabasco, México. E-mail: anahi.canedo@ecosur.mx (AC-T), jesus.rocamontes@posgrado.ecosu.mx (JAR-M); katia.hernandez@posgrado.ecosur.mx (KH-B)
[2]Laboratorio de Bioconservación y Manejo, Posgrado en Ciencias Quimicobiológicas, Departamento de Zoología, Escuela Nacional de Ciencias Biológicas, Instituto Politécnico Nacional, Ciudad de México, México. E-mail: artibeus2@aol.com (JO), carlosalbbarrera98@gmail.com (CAB)
[*]Corresponding author: gcastellanos@ecousr.mx

Genomics is the study of the genome's structure, function, evolution and mapping, including gene interactions with each other and with the environment. Genomics is a tool that allows studying fine evolutionary processes in non-model mammals. These approximations provide valuable information regarding levels and distribution patterns of neutral and adaptive genetic variation. Additionally, genomics allows studying organisms responses to environmental changes and anthropogenic activities. This information has high potential applications in the development of management and conservation plans for threatened mammalian populations and species. The present work provides information so that the reader can understand and outline a mammal conservation genomics project. This is an introductory guide for the use of genomics in the study of mammals, with emphasis in the link between genomics and conservation biology. This guide explains some general aspects of the genomics approximation that allow studying mammals such as sequencing methodologies, reduced representation sequencing, mitogenomes, whole genome sequencing, low coverage whole genome sequencing, metagenomics and transcriptomics; including some examples of their applications in conservation. We conclude this document with some challenges and perspectives for the application of mammal conservation genomics.

Keywords: Conservation genomics, mammals, mitogenomes, next generation sequencing, pangenome, reduced representation sequencing, transcriptomics, whole genome sequencing.

La genómica es el estudio de la estructura, función, evolución y mapeo de genomas, incluyendo la interacción de los genes entre sí y con el ambiente. La genómica es una herramienta que permite el estudio de procesos evolutivos finos en mamíferos no-modelo, aportando información muy valiosa respecto a niveles y patrones de distribución de la variabilidad genética neutral y adaptativa, así como sobre la respuesta de los organismos a los cambios ambientales y a las presiones antropogénicas. Por lo anterior, esta información tiene alto potencial para el desarrollo de planes de manejo y conservación de especies y poblaciones de mamíferos en riesgo. El presente trabajo provee la información necesaria para comprender y delimitar un proyecto de genómica para la conservación. Presentamos una guía introductoria a la genómica aplicada en el estudio de mamíferos con énfasis en la conexión de la genómica con la conservación. La guía aborda distintas aproximaciones genómicas que permiten el estudio de mamíferos, como las plataformas de secuenciación, representación reducida de genomas, mitogenomas, secuenciación de genomas completos, secuenciación de genomas completos a baja resolución, metagenómica y transcriptómica; incluyendo algunos ejemplos de su aplicación en la conservación. Concluimos con algunos retos y perspectivas respecto a la aplicación de la genómica para la conservación de mamíferos.

Palabras clave: Genómica de la conservación, mamíferos, mitogenomas, secuenciación de nueva generación, pangeno, secuenciación de representación reducida, transcriptómica, secuenciación del genoma completo.

Conservation genetics and genomics

Conservation genetics refers to the application of population genetics, evolutionary theory and molecular tools in combination with ecological data for the conservation of wildlife (Frankham 2003; Allendorf *et al.* 2010; Ouborg *et al.* 2010). Traditional conservation genetics approaches have been useful to solve phylogenetic uncertainty, to understand the levels and distribution of genetic diversity, and its correlation to extinction risk.

Conservation genetics aims at better understanding the extent of the impact of human activities, such as habitat fragmentation and habitat loss, on the loss of genetic diversity and the disruption of population structure. Also, conservation genetics has been applied to infer biological aspects of inconspicuous or understudied species, to assess the levels of inbreeding and the risk of inbreeding depression to propose genetic rescue, and in wildlife forensics (Frankham 2003; 2005; 2010; Allendorf *et al.* 2010; Ouborg *et al.* 2010; Shafer *et al.* 2015; Whiteley *et al.* 2015; Hedrick and Garcia-Dorado 2016).

Initially, conservation genetics relied on data obtained from isozymes. Then, with the technical advances of molecular biology and Sanger Sequencing, studies focused more on mitochondrial DNA (mtDNA; see Supplementary Materials S1 for a list of abbreviations), which is maternally inherited and provides a window into evolutionary processes that occur over geological time, such as lineage divergence, speciation, adaptive radiations, and extinctions. The design of species-specific nuclear microsatellite loci allowed the analysis of biparentally inherited loci, which provides information about historical processes on an ecological scale such as connectivity between populations or gene flow, inbreeding and kinship, genetic drift, effective population size and human-mediated bottlenecks, and natural selection (Sunnucks 2000; Schlötterer 2004; Selkoe and Tonnen 2006; Allendorf *et al.* 2010).

The combined use of mtDNA and nuclear microsatellite loci allowed making inferences regarding breeding strategies, sex proportions, and evolutionary vs. historical processes. Today, with the advent of next-generation sequencing and the genomic era, we have the potential to unlock the information contained in whole genomes from non-model species, mitogenomes, reduced representation of genomes, metagenomics, transcriptomics, and other omics approaches (Schlötterer 2004; Allendorf *et al.* 2010; Ouborg *et al.* 2010; Shafer *et al.* 2015; Allendorf 2017).

This review will provide a concise guide for applying genomics and transcriptomics in the conservation of mammals. We expect that this information is useful to uncover the potential of genomic tools for the study and conservation of mammals, and we will provide basic information and concepts (Supplementary Materials S2) for mammalogists who are getting started in the field of conservation genomics.

Next- Generation Sequencing platforms

The introduction of Next Generation Sequencing (NGS) made it possible to obtain the genetic information of a species in a relatively short time. Initially, this approach was very expensive, but with technologic advancement and increases in the demand for this methodology, sequencing costs have gradually decreased, making it accessible to laboratories with modest budgets. NGS conforms to a group of advanced sequencing technologies that allow for the rapid sequencing of DNA and RNA. The advantages of NGS lie in technological advancements, speed, cost-effectiveness, and data output capabilities (Goodwin *et al.* 2016). Moreover, NGS allows incrementing the quantity of loci from few loci to thousands of loci, thus providing higher statistical power to analyses; also, it allows sequencing multiple fragments simultaneously. NGS data can be used in adaptive genomics, to study loci involved in adaptation to environmental changes, to assess levels of neutral and genetic variation and to understand resilience to climate change and habitat fragmentation (Li *et al.* 2020).

NGS uses massively parallel sequencing where millions of DNA fragments are sequenced simultaneously. NGS varied platforms use different technologies, such as sequencing by synthesis (Illumina), nanopore sequencing (Oxford Nanopore), or real-time sequencing (PacBio), allowing to obtain millions of sequences in a short time (Hu *et al.* 2021). The Illumina platform (i.e. HiSeq, NovaSeq; www.illumina.com) produces short reads that are typically 50-300 bp long, offer high accuracy, low cost per base, and high throughput. Short-reads are suitable for applications, such as re-sequencing, population genomics, and metagenomics (Simon *et al.* 2009). In particular, for monitoring genetic diversity, detecting inbreeding in populations, identifying candidate loci under selection and determining population connectivity. It is also useful in resolving phylogenomic relationships among populations and species, especially with conservation concerns. Lastly, it can be used to detect the presence of species in environmental samples, which helps monitor elusive or endangered species (Fuentes-Pardo and Ruzzante 2017). However, short-reads often struggle to resolve repetitive regions, structural variants, and complex genomes due to their limited length.

On the other hand, technologies like PacBio (www.pacb.com) and Oxford Nanopore (nanoporetech.com/es) produce long-reads that are several kilobases long (thousands of bases long). Long reads allow sequencing and assembling the repetitive regions in the genome, thus producing highly contiguous genomes. Long-read technologies have the caveat of higher error rates than short-read sequencing (but this has been improving in recent years) and are generally more expensive compared to short-read technologies (Cuber *et al.* 2023). Using long-reads for *de novo* genomic assemblies produces high-quality reference genomes for species without existing data, that are assembled to the chromosome level. Thanks to long reads spanning large regions of the genome, it is possible to identify structural variants in the genome, such as large insertions, deletions, or rearrangements that might be linked to adaptation or disease susceptibility (Lu *et al.* 2016).

Each sequencing approach offers unique strengths: short-reads provide high accuracy and depth, while long-reads offer extended sequencing that can span complex genomic regions. Both types can be integrated and offer the possibility of hybrid sequencing approaches that can achieve superior genome assemblies and variant detection (Whibley *et al.* 2021). In conjunction, this hybrid approach allows for an understanding of the genetic makeup of endangered species. Current technologies, such as high-throughput chromosome conformation capture (Hi-C) and PacBio high fidelity (HiFi), produce highly accurate long reads, provide uniform coverage and allow us to assemble genomes to the chromosome level (www.pacb.com).

NGS technologies have revolutionized conservation genomics by enabling the collection of detailed genetic data, previously limited by traditional sequencing. This information can be used to understand the biological and

ecological factors that affect species' survival, adaptation, and resilience, informing more effective conservation strategies. NGS allows for the comprehensive assessment of genetic diversity at the whole-genome level. This allows detecting single nucleotide polymorphisms (SNPs), microsatellites, and other types of genetic variation such as transposable elements and structural variants across entire populations, offering a detailed picture of genetic variability to identify adaptive traits, make informed management strategies, detect hybridization and monitor genetic health (Supple and Shapiro 2018).

For example, in the Mountain Gorillas (*Gorilla beringei beringei*), a species critically endangered due to habitat loss, poaching, and disease, a high-quality reference genome was obtained through the combination of short-reads (Illumina) and long-reads (PacBio), overcoming the challenges posed by its complex repetitive genome structure. This high-quality genome assembly revealed regions of the genome susceptible to inbreeding depression and identified genetic variants linked to immune function, helping inform breeding programs to maintain the genetic diversity of the Mountain Gorilla (Xue *et al.* 2015).

Massive parallel sequencing offers a wide range of possibilities for the study of wildlife which are detailed in the following sections and compared in Table 1.

Reduced Representation Sequencing (RRS)

There are several genotyping-by-sequencing (GBS) methodologies to obtain SNPs based on Reduced Representation Sequencing (RRS). These methods are based on the use of restriction enzymes for library preparation, followed by fragment size selection, adaptor ligation, PCR amplification and multiplexing (see review in Andrews *et al.* 2016). Sequencing is performed with a short-read platform. The most used methods for the study of mammals are restriction site-associated DNA sequencing (RADseq) and double digest restriction site-associated DNA sequencing (ddRADseq), which use one or two restriction enzymes, respectively, to cut DNA (Miller *et al.* 2007; Baird *et al.* 2008; Peterson *et al.* 2012).

RRS refers to sequencing a small fraction of the genome to obtain SNPs; typically, between 1 and 10 % of the genome is covered (Peterson *et al.* 2012; Andrews *et al.* 2016, Figure 1). This approach allows obtaining genomic data from hundreds of individuals, and it is usual to obtain thousands to tens of thousands of SNPs (Davey *et al.* 2011; 2013; Andrews *et al.* 2016). The number of SNPs or coverage required will depend on the study's objective, for example, higher coverage will be needed if we want to search for signals of selection (Andrews *et al.* 2016; Ahrens *et al.* 2018).

To implement this type of study, several aspects should be considered, such as the restriction enzymes to be used to digest the DNA, as the type and number of enzymes will have an impact on the number of SNPs obtained depending on the genome size of the studied species, and the number of SNPs required (Davey *et al.* 2011; 2013; Peterson *et al.* 2012; Andrews *et al.* 2016; Fu *et al.* 2016).

Other methodological aspects to consider are biases and errors that could be introduced during library preparation (Mastretta-Yanes *et al.* 2014; O'Leary *et al.* 2018). The number of reads per sample (coverage and depth of coverage) will also impact the number of SNPs discovered; this will depend on the objective of the study, the number of SNPs to uncover, and the genome size of the species (O'Leary *et al.* 2018). As previously mentioned, to discover candidate loci under selection, a higher number of SNPs is required. Previous studies conducted on the same or on closely related species may serve as a guide; also, if this information is not available for our study species, we could conduct pilot studies to test different enzyme combinations and different sequencing depths (Davey *et al.* 2013; O'Leary *et al.* 2018).

SNPs discovery based on RRS can be performed with and without a reference genome (see O'Leary *et al.* 2018;

Table 1. Comparison of Whole Genome Sequencing (WGS), Low-coverage WGS (lcWGS), and Reduced Representation Sequencing (RRS) in evolutionary and conservation studies.

Feature / Application	WGS	lcWGS	RRS
Genome coverage	High (>20× recommended for SMC). Complete breadth.	Low (<5× typical). Random but complete breadth.	Very low (<10% of genome). Sparse/ fragmented breadth.
Primary variant type	SNPs, Indels, and Structural Variants (SVs).	Primarily SNPs via genotype likelihoods.	Primarily SNPs at targeted restriction sites.
Genetic load & inbreeding	Excellent; gold standard for Runs of Homozygosity (ROH)	Reliable for population-level inbreeding coefficients.	Limited; misses rare variants and many ROH due to data gaps.
Selection (adaptation)	High; identifies narrow genomic islands of divergence	High; enables genome-wide selection scans and genotype-environment association.	Lower; likely to miss localized adaptive signals.
Demographic Inference	High resolution for deep and recent history (MSMC/PSMC).	Robust for recent history; accurate Site Frequency Spectrum models.	Reliable for broad signals, but may miss specific parameters
Reference requirement	Essential; requires high-quality assembly.	High; requires a species-specific or related reference	Low; can be used *de novo* without a reference genome.
Main advantage	Capture of all variation types, including complex SVs.	Cost-effective population screening while retaining individual info.	Low cost; high individual sample sizes possible.
Main limitation	High sequencing and computational costs.	Requires specialized probabilistic tools (e.g., ANGSD).	Biased by "null alleles" and lack of functional genome context.

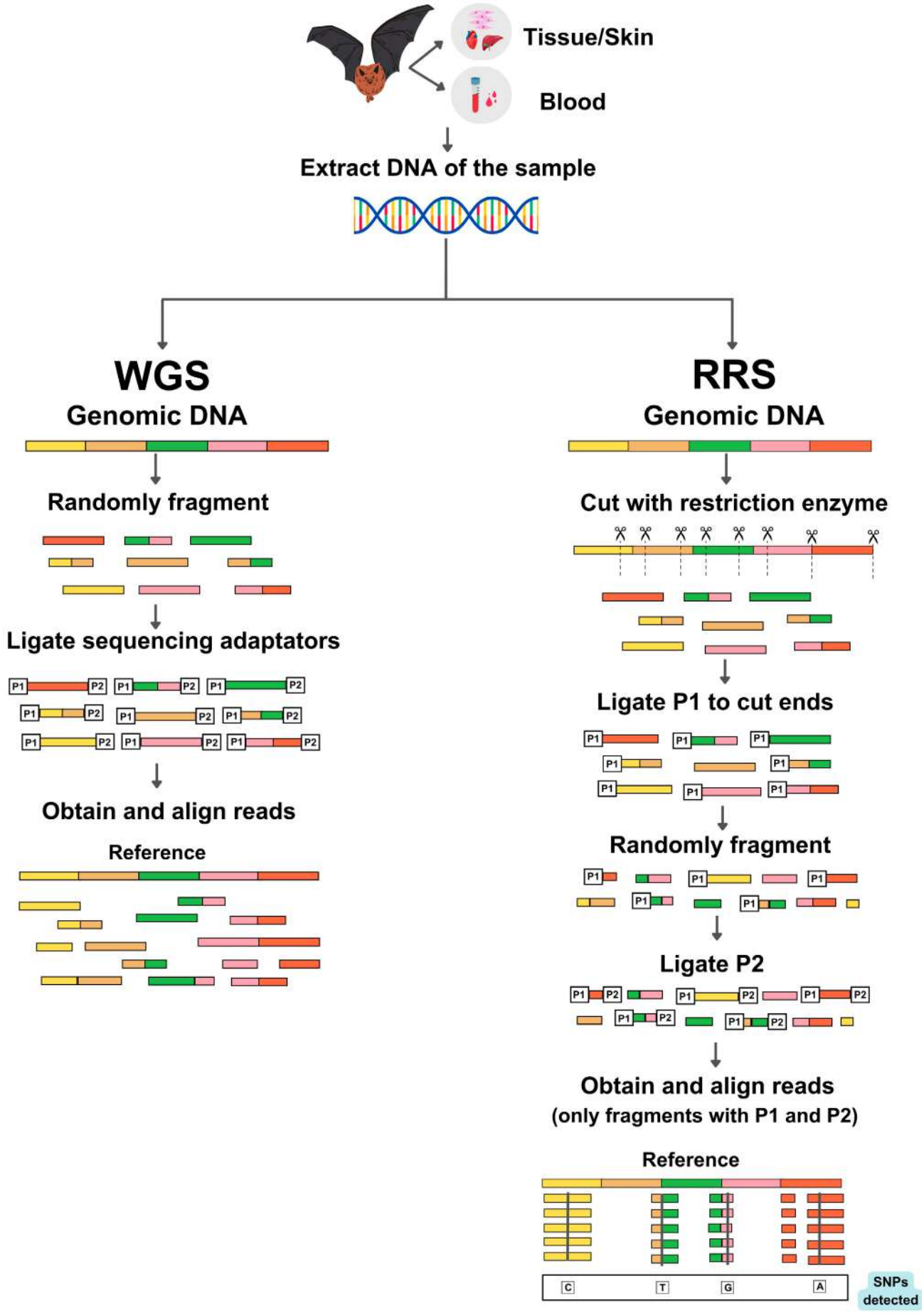

Figure 1. Overview of library preparation for whole genome sequencing (WGS) and reduced representation sequencing (RRS) for the study of mammals.

Bohling 2020). The selection of a reference genome will impact variant calling pipelines: the closer the species, the better the results (Bohling 2020). When a reference genome is not available (*de novo* variant calling), it is recommended to implement optimization protocols to define parameter values to identify SNPs (Paris *et al.* 2017).

RRS is useful for estimating levels of genetic diversity and genetic structure that allows us to propose conservation actions such as defining management units and assessing connectivity between populations. This approach was used to assess the impact of urbanization on genetic variation and genetic differentiation in the eastern grey squirrel (*Sciurus carolinensis*) (Fusco *et al.* 2023). The authors used a landscape genomics approximation to assess connectivity in rural and urban areas within the species' native range. Accordingly, connectivity was higher than expected in urban areas, whilst connectivity was lower than expected in areas impacted by agriculture.

Also, RRS provides accurate measures of inbreeding and allows performing robust kinship and relatedness analyses (Luikart *et al.* 2019). For example, relatedness analyses were used to assess if kinship influences home range overlap in an urban population of bobcats (*Lynx rufus*) (Payne *et al.* 2025). These analyses were performed by combining positioning data, to estimate individual home range and home range overlap, with SNPs data, to estimate relatedness between pairs of individuals. Accordingly, there was higher relatedness between female pairs than between male pairs and male-female pairs; also, mother-daughter pairs showed higher home-range overlap than unrelated individuals. Results suggest that urbanization doesn't seem to have a negative effect on genetic variation in this population yet, but expansion of the urban matrix will likely have major impacts on population fragmentation, isolation, and inbreeding, as has been reported in other urban bobcat populations. Moreover, this study shows that these felines are not as solitary as previously thought.

One of the advantages of genomics data is the implementation of genotype-environmental association studies and other methods to search for candidate loci under selection in non-model organisms and without a reference genome, such as *FST* outlier tests (Davey *et al.* 2011; Andrews *et al.* 2016; Ahrens *et al.* 2018). The latter permits uncovering processes of local adaptation and identifying putatively adaptive genetic variation that could be considered in conservation actions (Luikart *et al.* 2019). This approach was used to uncover candidate loci, associated with local adaptation, resulting from habitat specialization, in two species of *Dromiciops*, a marsupial endemic to the Valdivian Forest in Chile and Argentina (Quintero-Galvis *et al.* 2024). These authors also assessed the potential changes in allele frequencies as a response to future environmental change. This study helped identify vulnerable areas for the preservation of both species (*D. bozinovici* and *D. gliroides*), and to prioritize populations for conservation taking future environmental change into consideration.

RRS, in combination with fecundity and survival data, is useful to assess inbreeding depression. For example, a study used ddRADseq data to assess inbreeding depression in North Atlantic right whales (*Eubalaena glacialis*), a highly endangered marine mammal (Crossman *et al.* 2024). Even though these authors found low correlation between inbreeding and fecundity, they identified a few SNPs with potential involvement in reproduction that may be associated with fecundity. They suggest that several factors, such as body size and anthropogenic stressors, may affect fitness.

RRS is a promising genomic approximation for the conservation of mammals given that its lower costs allow sequencing a higher number of individuals than whole genome sequencing (WGS) and low coverage whole genome sequencing (lcWGS). Moreover, this approach provides higher resolution than other types of molecular markers (i.e. mtDNA and microsatellite loci) for the estimation of key population parameters such as effective population sizes and kinship, as previously mentioned. Finally, the possibility of differentiating and measuring neutral and adaptive genetic variation offers a great opportunity for the study and preservation of species and their potential to respond to environmental change.

Mitogenomics

The mitochondrion is an organelle with its own genetic material (the mitogenome), present in nearly all eukaryotic cells, whose origin dates to ancient bacterial endosymbiosis (Jin *et al.* 2020). The mitogenome is a circular, double-stranded molecule, approximately 16 to 18 kb in length in animals (Nicholls and Minczuk 2014). This molecule contains 13 protein-coding genes (PCGs) involved in oxidative phosphorylation (aerobic respiration), 2 ribosomal RNA genes, 22 transfer RNA genes, and a non-coding control region (CR) which is approximately 1 kb in length (Gibson *et al.* 2004; Ladoukakis and Zouros 2017). The synteny of the mitogenome in mammals is highly conserved and the array does not change between taxonomic units (Meganathan *et al.* 2012). Each of the two strands of the mitogenome contains an origin of replication and is labeled as "heavy" (OH) and "light" (OL) origins (Nicholls and Minczuk 2014).

The mitogenome is characterized by maternal inheritance and a compact synteny, meaning that coding sequences are separated by only a few bases, lacking introns, or even exhibiting small overlaps (Fernández-Silva *et al.* 2004). Many of the protein-coding genes can have incomplete stop codons (such as TA or T), for which stop codons are generated through the process of polyadenylation (addition of a repetitive adenine nucleotide sequence) after transcription (Donath *et al.* 2019). Although the primary function of mitochondria is to participate in the process of oxidative phosphorylation, they are also related to a wide variety of cellular processes such as apoptosis, aging, signaling, metabolic homeostasis, and the biosynthesis of macromolecules

such as pyrimidines, amino acids, phospholipids, folate coenzymes, heme and urea (Attardi and Schatz 1988; Ladoukakis and Zouros 2017).

The mitogenome has an estimated average of 9.04×10^{-9} substitutions per nucleotide per year in mammals (Soares *et al.* 2013). Synonymous mutations are more common than non-synonymous mutations (Konrad *et al.* 2017). Asymmetric replication is the main explanation for the high mutation rate of the mitogenome (Hassanin *et al.* 2005; Nicholls and Minczuk 2014). Most mutations occur in the non-coding region, making the presence of a conserved (coding) and a less conserved (non-coding) region sources of genetic diversity among species, or even among individuals within the same population (Gibson *et al.* 2004; Ladoukakis and Zouros 2017). Studies on molecular evolution of the mitochondrial genome in mammals have shown that the protein coding regions (PCGs) are mainly subject to purifying selection, but substitution rates, as well as the strength and patterns of selection, are heterogeneous (da Fonseca *et al.* 2008; Shen *et al.* 2010; Botero-Castro *et al.* 2018; Rocamontes-Morales *et al.* 2025). Such variation has been related to metabolic demands or other life history attributes (da Fonseca *et al.* 2008). For example, changes in selection regimes along the mitochondrial genome have been associated with the evolution of sanguivory and nectarivory in bats (Botero-Castro *et al.* 2018; Rocamontes-Morales *et al.* 2025).

The study and characterization of the mitogenome and mitochondrial markers have served as the foundation for molecular analyses of phylogeny, phylogeography, and population connectivity in a wide range of mammal species (Avise and Ellis 1986; Jin *et al.* 2020). Intra- and inter-population genetic diversity is also addressed using mitochondrial markers. This is often studied to propose new conservation strategies based on connectivity, gene flow, and the preservation of diversity. Recently, there has been a suggestion that the widespread influence of both direct and indirect selection on mitochondrial markers makes any conclusions drawn from it unclear or open to interpretation. In mammals, indirect selection on mtDNA can result from linkage disequilibrium with maternally inherited traits (Hurst and Jiggins 2005; Mohammadi *et al.* 2019). The combined use of mitochondrial markers with nuclear markers provides better resolution for integrative systematic studies of a taxonomic group, enabling the ability to differentiate between species, individuals, or populations. This approach allows researchers to gain a more comprehensive understanding of evolutionary relationships and genetic diversity within and among species or populations. Combining both types of markers facilitated the identification of mitochondrial-like sequences within the nuclear genomes of numerous animals known as nuclear-mitochondrial DNA segments (NUMTs), which are common in mammalian genomes and have the potential to be used for phylogenetic inference (Calabrese *et al.* 2017; Uvizl *et al.* 2023). NUMTs themselves can be useful molecular tools for phylogenetic and population genetic studies, because of their fast evolution (Zhang and Hewitt 1996; Toews and Brelsford 2012; Calabrese *et al.* 2017; Uvizl *et al.* 2023).

Recently, the complete assembly of mitogenomes has been achieved through the implementation of NGS. This allows for comparative inferences and evolutionary phylogenetics. Despite the abundance of mitogenome reconstructions made possible by different methods, complex regions such as the repetitive ones and segmental duplications found in the CR have been difficult to resolve (Heyer *et al.* 2001; Bronstein *et al.* 2018; Formenti *et al.* 2021). In theory, when repeats longer than the sequencing reads are present, assemblies are constrained within the confines of these repetitive elements (Picardi and Pesole 2012).

Currently, mitogenome assemblies have a low margin of error and are highly accurate (Formenti *et al.* 2021; Nachtigall *et al.* 2021; Uliano-Silva *et al.* 2023). Comparisons between mitogenomes facilitate the retrieval of phylogenetic relationships within the study group. The quantity, quality, and diversity of complete mitogenome assemblies and datasets available for mammals enable a precise phylogenetic comparison of sequence data and assembly approaches to describe it and enable the development of a new line of research in the field of mammalian genomics.

Mitogenomes have been widely used in phylogenomics of mammals, to obtain a better understanding of relationships between species and within species (Castellanos-Morales and Gutiérrez-Guerrero 2025). A study obtained 93 mitogenomes for six species of the genus *Dasyprocta* (Ruiz-García *et al.* 2022) and found that this genus requires taxonomic revision. Several species may be constituted by more than one lineage, while others were not supported by the analysis. These results are relevant for conservation as some of the taxa that require revisions are endemic to islands and may be endangered.

Whole genome sequencing (WGS) and Pangenomics

WGS is a comprehensive technique used to sequence the complete DNA of the genome (Figure 1). WGS covers the entire genome, including nuclear and mitochondrial DNA, allowing us to study a full picture of genetic variation (Ng and Kirkness 2010).

Covering the entire genome of an organism offers insights into both coding and non-coding regions that regulate gene expression or have other important functions. WGS allows researchers to examine all types of genetic variation, from single nucleotide polymorphisms (SNPs) to larger structural variants like insertions, deletions, and duplications (Ekblom and Wolf 2014). As provided in the previous section, through NGS technologies, short and long-read technologies (i.e. Illumina, PacBio) facilitate the production of high-quality genome assemblies.

In conservation, WGS has proven useful for the identification of population bottlenecks, inbreeding, and

adaptive traits in endangered species. For example, the Tasmanian devil (*Sarcophilus harrisii*) is endangered due to transmissible cancer known as Devil Facial Tumor Disease (DFTP). Through WGS analysis it was possible to identify genetic variants associated with disease resistance, aiding conservation managers to plan breeding programs to enhance the chances of survival for this species (Stahlke *et al.* 2021).

In another study, WGS was implemented to assess inbreeding depression in black bears (*Ursus americanus*), brown bears (*U. arctos*), and polar bears (*U. maritimus*) through runs of homozygosity (ROH). These authors detected higher variance in the amount of inbreeding and detrimental variants within species than between species; smaller, isolated, or recently bottlenecked populations had higher genetic load than larger and connected populations. Overall differences in genetic load between species were related to historic effective population size, where polar bears showed lower genetic load because small historic effective population sizes may have allowed the purge of deleterious alleles. This study also highlights the applicability of WGS in conservation by identifying populations that require management to reduce genetic load (Clendenin *et al.* 2025).

Beyond the single reference genome approach, the emerging field of pangenomics is the study of all genomic content within a species or across populations. Pangenomics includes core genes shared by all individuals and accessory genes that vary between individuals or populations (Tettelin and Medini 2020). Accessory genes can reflect local adaptations or environmental pressures (Whelan *et al.* 2021). Pangenomics captures a broader spectrum of genomic variation, offering a more complete picture of species diversity than single-genome sequencing.

Pangenomics has been more commonly applied in microbial genomics and to study crops, mainly because of the complexity and size of mammalian genomes which can be challenging and costly to sequence to construct a pangenome. The genomes of bacteria and archaea range from 0.6 to 14.3 Mb, while the reported genome sizes in mammals go from 1.6 to 6.3 Gb (Kapusta *et al.* 2017; Martinez-Gutierrez and Aylward 2022); plus, in mammals 40% of the genome is constituted by repetitive elements, while coding regions represent ~2-8%. The latter impacts the availability of high-quality genomes; for example, by March 2024 there were complete genomes available at NCBI for only 1,011 mammalian species; moreover, a small fraction of these genomes have curated annotations (Castellanos-Morales and Gutiérrez-Guerrero 2025).

Pangenomics is starting to be applied in mammalian representatives, such as the case of the domestic pig (*Sus scrofa*) pangenome are now available (Li *et al.* 2023). In a study based on 250 individuals from 32 breeds across Eurasia, it was possible to identify 3,438 novel genes absent from the current reference genome. The catalog sequences were characterized as presence/absence variations (PAVs) within pigs. The authors found that 16.8% of the genes in the pangenome catalog undergo PAV. They also found several genes associated with adaptation that are relevant to immune responses (e.g. swine leukocyte antigen, respiratory syndrome virus) (Li *et al.* 2023). This example highlights the importance of studying pangenomes, which revealed hidden layers in the diversity of pigs, and can be applied to mammalian species with a focus on conservation.

The Human Pangenome Project is another example of current pangenomics that seeks to obtain the pangenome of humans (Wang *et al.* 2022). Pangenome projects face the challenge of managing an enormous amount of data and require robust computational resources and bioinformatics expertise. However, the potential for integrating pangenomics with the other 'omics' approaches (i.e., transcriptomics, epigenomics) could provide a more holistic understanding of species adaptation and resilience, and the link between genotype and phenotype, which could be highly valuable for mammalian conservation efforts.

Pangenomics studies on human genomes and crops have uncovered intraspecific structural variation. Structural variants (SVs) change the total amount of DNA such as gene duplications, insertions and deletions, or change the sequence of DNA such as translocation, inversions, and fissions/fusions (Smeds *et al.* 2024). These studies highlight the importance of SVs in functional genomic variation, molecular evolution, and rapid adaptation to environmental changes. Therefore, obtaining multiple high-quality genomes for endangered species will allow performing analyses on SVs to better understand fitness-associated traits of conservation interest (Wold *et al.* 2021). Implementing this approximation for the study of wildlife is still methodologically challenging, but steps are being taken with promising results. For example, in Scandinavian wolves (*Canis lupus*) it has been demonstrated that in a small, isolated and inbred population, SVs increased genetic load and may play a role in inbreeding depression—as this type of variants will have significant effects on protein function—, while immigration reduced genetic load and provided a means for genetic rescue (Smeds *et al.* 2024).

Another approach is to obtain low-coverage genomes. lcWCS allows for cost-effective population screening. This approach focuses on overall population characteristics such as allele frequencies and patterns of variation across SNP throughout the genome, patterns of linkage disequilibrium, identity by descent segments, selection scans to detect signatures of selection and adaptive divergence, among others (Lou *et al.* 2021).

One of the main constraints to applying lcWGS to non-model organisms is the need for a reference genome to map short-sequence reads, but if a reference genome for the target species is not available, a reference genome of a closely related species can be used. An alternative is using a reference transcriptome to map short-reads. There are still several limitations and challenges for the implementation

of lcWGS to wildlife (e.g. required quantity and quality of DNA, need of bioinformatic skills and access to a computer cluster to conduct analyses), but this approach may be particularly useful to study rare or endangered species where obtaining a large sample size could be difficult (Lou *et al.* 2021). This approach can also help take advantage of samples from mammalogical collections, where a few samples per locality may be available, depending on the species of interest.

A study compared results from mid-coverage WGS (30x), lcWGS (9x) and RRS (RADseq) data regarding the population structure and historical demography of the North American mountain gout (Martchenko and Shafer 2023). All data sets (WGS and RADseq) revealed similar results for population differentiation, demographic history, and signals of adaptation, suggesting that the long-term adaptive capabilities of the North American mountain gout may be compromised as the species has low genetic variation (Martchenko and Shafer 2023). According to these authors, WGS provides certain advantages over RADseq as it is more adequate for inferring adaptive processes and for calculating inbreeding through ROH.

Metagenomics

Metagenomics refers to the production of comprehensive genomic data from samples that contain more than one taxon, such as environmental samples (soil, water, or fecal samples) or individual samples (swaps, blood, urine, feces). Initially, metagenomics was developed to study communities of microorganisms. Currently, metagenomics' application has extended because it provides valuable information about genome-wide variation of communities and taxonomic groups (Seeber and Epp 2022).

Metagenomics is being used to study spatial and temporal changes in biological communities, to record rare species that are difficult to sample or observe in the wild, for early detection of invasive species, to analyze the microbiome and its relationship with health or susceptibility to disease, to characterize diet items, etc. (Bohman *et al.* 2014; Thomsen and Willerslev 2015; Ruppert *et al.* 2019). In this section, we will focus on two applications of metagenomics: (a) metabarcoding (amplification of a specific DNA region to identify taxa) to study mammalian communities or specific taxa through a single sample, and (b) the study of the mammalian microbiome (communities of microorganisms associated with mammals).

Moreover, it is now possible to assemble complete mitochondrial genomes from metagenomic data by performing NGS of total DNA extracted from environmental or fecal samples; for example, the mitochondrial genomes of four large vertebrates (giant panda (*Ailuropoda melanoleuca*), Asian black bear (*Ursus thibetanus*), Sunda pangolin (*Manis javanica*) and North Atlantic right whale (*Eubalaena glacialis*) were assembled from metagenomics of scat samples (Baeza *et al.* 2023). This is a valuable tool for monitoring rare, inconspicuous, and endangered mammals.

Metagenomics has emerged as a powerful tool in ecological studies and species monitoring, garnering significant interest from molecular ecologists (Ruppert *et al.* 2019; Liu *et al.* 2020). Although this type of analysis may not identify all species with absolute certainty, it provides valuable data for ecological inference, assessing species responses to current environmental changes, and monitoring invasive species and disease vectors of public health concern (Liu *et al.* 2020). Metagenomics enables to evaluate the impact of anthropogenic activities on mammalian communities, the functional characterization of microbiomes and their implications for mammalian health, to record the presence/absence of endangered species and to obtain mitochondrial genomes for rare, inconspicuous and elusive species, from environmental and paleontological samples.

Metabarcoding. Metabarcording of environmental DNA (eDNA) is a useful, rapid, and non-invasive tool to recognize mammalian communities, populations and species that are endangered, invasive, or common species that are difficult to observe in an ecosystem by traditional field methods such as footprints, camera traps or scats (Bohmann *et al.* 2014; Harper *et al.* 2019). Environmental DNA (eDNA) is obtained from a sample of water, sediment, or free DNA that organisms transfer to the environment through feces, secretions, sperm, blood, urine, leaves, roots, pollen, or fruit that contains a mixture of genetic material from different organisms (Bohmann *et al.* 2014; Thomsen and Willerslev 2015). Through eDNA we can analyze ecological and evolutionary processes of aquatic or terrestrial biodiversity, rare taxa or environmental information and answer research questions from areas such as molecular biology, paleontology, and environmental sciences (Thomsen and Willerslev 2015; Aivelo and Medlar 2018).

DNA metabarcoding methods change slightly depending on the organisms and on the type of sample (Aivelo and Medlar 2018; Brassea-Pérez *et al.* 2019; Harper *et al.* 2019; Liu *et al.* 2020). There are several steps to implement an eDNA metabarcoding methodology for the study of mammals (Bohmann *et al.* 2014; Thomsen and Willerslev 2015; Haarsma *et al.* 2016; Ruppert *et al.* 2019; Liu *et al.* 2020; Hassan *et al.* 2022, Figure 2). First, identify the eDNA barcoding region to answer the research question and build a reference database of all possible DNA barcodes that may occur in the study area with barcode repositories or specimens from natural history museums, scientific collections or research institutions (Haarsma *et al.* 2016). When selecting an appropriate DNA barcode, several key factors must be considered. The barcode should be a universal and highly conserved region to facilitate sequence alignment across diverse species (Yang *et al.* 2018). Additionally, a short fragment (<1000 bp) DNA is recommended to ensure amplification, even from degraded samples (Yang *et al.* 2018; Ruppert *et al.* 2019). Ideally, the selected region should exhibit low intraspecific variation but high interspecific variation

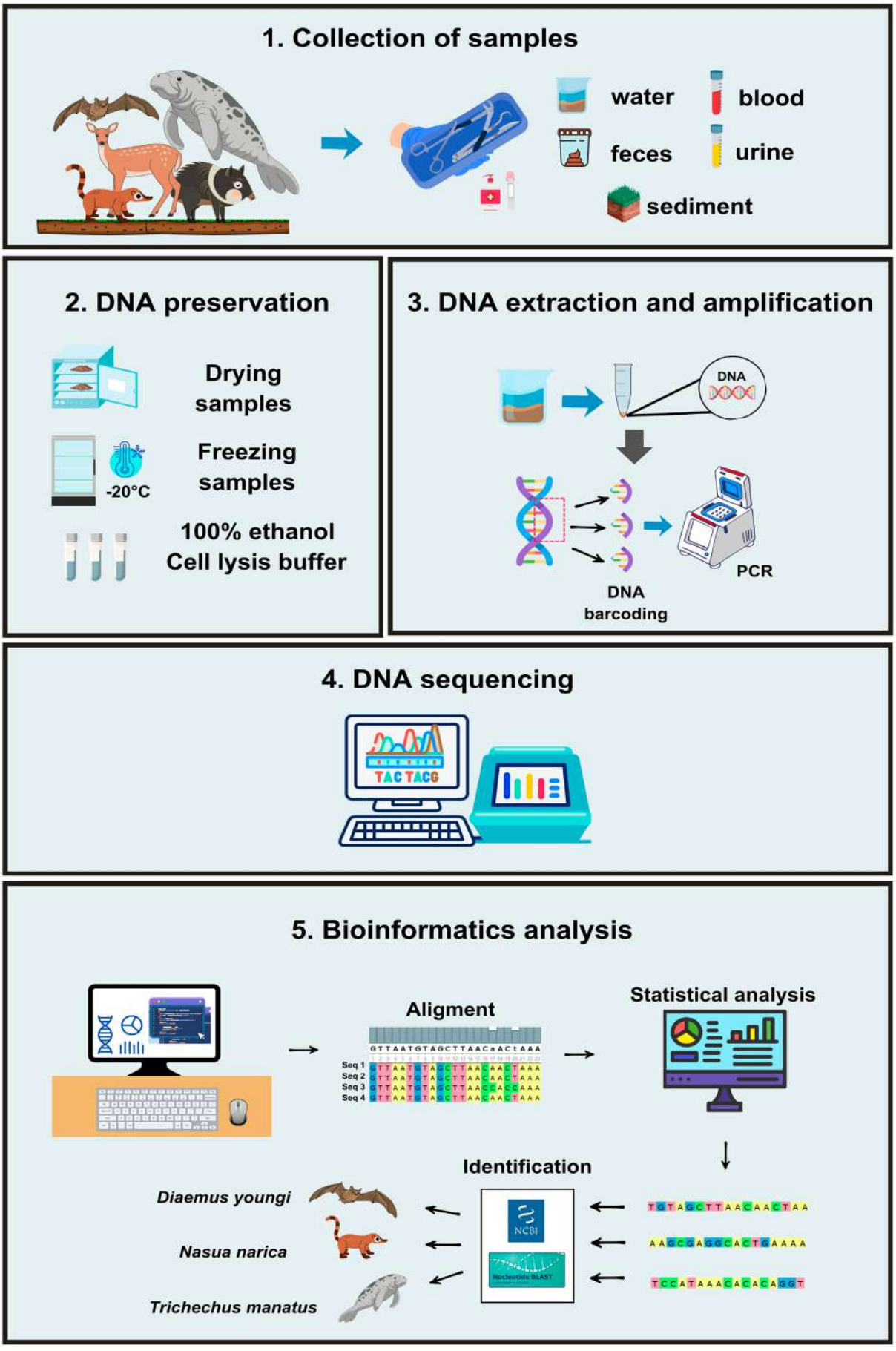

Figure 2. Overview of steps needed to conduct a metagenomics study of mammals.

to identify the target group (Ruppert *et al.* 2019). The barcode sequence commonly used in mammals and other vertebrates is the cytochrome c oxidase subunit I (COI or COX) from mtDNA (Ivanova *et al.* 2012). There are international repositories such as BOLD database (boldsystem.org) and NCBI's GenBank where reference sequences are deposited (www.ncbi.nlm.nih.gov).

Several details should be considered when sampling to optimize detection (depending on type of substrate), and to minimize contamination with exogeneous DNA (Seeber and Epp 2022). To ensure eDNA sample quality and minimize contamination, sterile equipment should be used, washed with soapy water or ethanol between samples, and accompanied by gloves, sterile vials, and a negative control (Aivelo and Medlar 2018; Liu *et al.* 2020). Proper storage is crucial as temperature, pH, and light exposure influence DNA degradation (Ruppert *et al.* 2019). For drying samples, freezing at -20°C is recommended to prevent DNA degradation (Creer *et al.* 2016, Figure 2).

After sample collection, DNA is extracted and a target DNA segment corresponding to a barcode is amplified via polymerase chain reaction (PCR); PCR products are purified and sequenced (Ruppert *et al.* 2019). The obtained DNA sequences are analyzed using bioinformatics tools and databases like BOLD and NCBI, or a reference database can be built for a specific study, to search for similarity and identify the taxa in the samples (Thomsen and Willerslev 2015; Chaves *et al.* 2025). Methods for obtaining eDNA are improved continuously as new technological advancements are incorporated (Thomsen and Willerslev 2015).

The analysis and alignment of metabarcoding data are essential steps for identifying organisms within a sample (Galhardo *et al.* 2018). The application of eDNA with other traditional field tools has improved biodiversity monitoring and has enabled the detection of species, such as the rare longfinned pilot whale (*Globicephala melas*) and the endangered hellbender salamander (*Cryptobranchus alleganiensis*), which were detected from water samples (Bohmann *et al.* 2014). The eDNA method is an efficient approach for biodiversity assessment because it offers a less invasive sampling method, and facilitates the identification of rare or endangered species, while minimizing stress to study organisms (Bohmann *et al.* 2014; Thomsen and Willerslev 2015; Liu *et al.* 2020).

Metabarcoding has been successfully used to detect mammals in a tropical forest, when compared to other commonly used sampling techniques such as mist-nets, pitfalls, grids and camera traps which are designed for certain focal groups. Accordingly, non-invasive eDNA sampling complements conventional sampling techniques and allows conducting rapid assessments for monitoring, management and conservation of mammals. This approach allows evaluating changes in the composition of mammalian communities through space and time, for example, contrasting different types of habitats, contrasting sites in a habitat perturbation gradient, or monitoring the effect of management and restoration programs (Coutant *et al.* 2021; Mena *et al.* 2021).

Metabarcoding from fecal samples has been used to determine animal diets. For example, this approach was used to assess dietary range and overlap between co-occurring mammals to assess potential competition (Kanishka *et al.* 2025). Another study used eDNA from scats to assess changes in diet of the yellow footed antechinus (*Anthechinus flavipes*), heath mouse (*Pseudomys shortridge*) and bush rat *(Rattus fuscipes*) after fire in a woodland ecosystem in Australia. This method was time-effective and successful to determine the baseline diet of the three species, and to detect changes in diet associated with the availability of critical food resources after a fire. Accordingly, these analyses allow considering the effect of fire management actions in the identified food resources (Wanniarachchi *et al.* 2022).

Microbiome. Metagenomics can also be used to study the mammalian microbiome. The microbiome is the community of microorganisms (bacteria, viruses, protozoa and fungi) that inhabit in or reside on an organism. The microbiome has influenced the course of mammalian adaptation and diversification. It has been associated with dietary transitions to herbivory, specialization and resistance to toxic food items, phenotypic plasticity and the evolution of innate and adaptive immune mechanisms in mammals. In some species, there is even host dependence on its microbiome to perform certain functions (Moeller and Sanders 2020).

There can be differences in the microbiome between individuals, and even between parts of the body. Moreover, there is a close interaction between the host and its microbiome (via structural elements, metabolites and signal molecules), and the microbiome composition of an individual may affect many of the individual's attributes (health, nutrition, physiology, immunity and development) and its fitness. The microbiome changes in response to differences in environmental conditions, for example, between lowland and highland populations or between captive and wild populations (Bahrndorff *et al.* 2016; Ange-Stark *et al.* 2023; Wang *et al.* 2025). Also, it has been suggested that captivity disrupts the gut microbiome of organisms because of changes in diet, the use of antibiotics, homogeneous environment, increased stress and close contact with humans (Dallas and Warne 2023; Dai *et al.* 2025). This, in turn, may affect the prevalence of pathogenic bacteria and the immune response of organisms (Dai *et al.* 2025). Differences in gut microbiome between captive and wild populations have been linked to low fecundity in captivity. Microbiome studies are useful for the development of prebiotics and probiotics for the reintroduction and management of threatened populations (Dallas and Warne 2023; Wang *et al.* 2025).

A study on black rhinoceros (*Diceros bicornis*) compared the microbiome of wild and captive animals. There were differences in beta diversity between captive and wild

rhinoceros. In captive individuals, some microbes were replaced with microbes typically found in livestock. Moreover, analysis of the microbiome found different functional bacterial communities, with higher abundance of glycolysis and amino acid synthesis pathways in captive rhinoceros, which results in differences in the acquisition of certain nutrients from the diet. Accordingly, management of the captive population should include changes in diet, and the administration of probiotics or fecal transplants to restore gut microbiome diversity (Gibson *et al.* 2019).

Analyzing the microbiome of wild mammals may be challenging, but methodological advancements make it feasible nowadays. Comparative studies on the gut microbiome of small mammals suggested that diet may influence the composition of the gut microbiome. In this case, sympatric species showed similarities in their microbiome composition; other aspects such as diet, life history, and phylosymbiosis may influence microbiome composition (Moeller and Sanders 2020; Li *et al.* 2022). In addition, microbiomes are being studied in relation to susceptibility to disease, such as the white nose syndrome (caused by *Pseudogymnoascus destructans*), a fungal pathogen responsible for mass mortality of bats in North America (Vanderwolf *et al.* 2021). In this sense, even if the effects of the white nose syndrome on bat microbiomes vary between bat hosts, it has been demonstrated that the presence of certain microorganisms may influence host resistance (Vanderwolf *et al.* 2021; Ange-Stark *et al.* 2023).

Transcriptomics

Transcriptomics focuses on the study of the products of the transcription of the genome from DNA to RNA in any of its forms (mRNA, rRNA, tRNA and noncoding RNA), to characterize molecular responses to external stimuli such as ecological, environmental or anthropogenic factors. This discipline allows characterizing genetic expression profiles, and to identify and quantify genes that turn on or off under certain conditions; taking into consideration that each organism has an evolutionary history that influences the genetic expression of gene profiles under different environmental conditions (Jaris *et al.* 2012). Transcriptomics allows studying the molecular mechanisms of adaptation, and to use this information in management and conservation planning to conserve the adaptive potential of species (Alvarez *et al.* 2015; Theissinger *et al.* 2023).

Species respond to environmental changes through two main mechanisms: phenotypic plasticity and changes in the genome that confer adaptation (Bernatchez *et al.* 2024). Phenotypic plasticity is the ability of one genotype to face environmental changes by expressing an alternative phenotype; phenotypic plasticity could become fixed as permanent changes that improve species fitness (Aubin-Horth and Renn 2009; Weeks *et al.* 2022; Yeaman 2022). Genetic adaptation involves heritable changes in the allele frequencies of genes that impact fitness (Yeaman 2022). In this sense, transcriptomics arises as an approximation to understand the role of gene expression in the responses of organisms to different environmental conditions, which drives evolutionary adaptation (He *et al.* 2016) and ecological divergence during speciation (Jeukens *et al.* 2010; Pavey *et al.* 2010).

RNA-seq technology was developed to characterize complete transcriptomes, without information from a reference genome, to identify the gene profiles with downregulated or upregulated expression in a specific condition, to identify the use of alternative splicing, secondary structures of RNA, to characterize metabolic pathways, and the genetic regulation process. Additionally, this methodology allows the quantification of gene expression with high accuracy even from genes with low expression (Wang *et al.* 2009; Loeffler *et al.* 2023).

Regarding population genotyping, RNA-seq allows us to characterize and quantify the variation in gene expression at a population level (Jaris *et al.* 2012; Lopez-Maestre *et al.* 2016). Such variation occurs not only on the coding sequences (it is estimated that 60% of the adaptive sites associated with selection signals occur in these regions), but also on *cis* and *trans* regulation elements (such as promoters, enhancers, silencers, binding sites for transcription factors, miRNA, etc.), which contribute to phenotypic or adaptive divergence of species (Jehl *et al.* 2021).

The integration of gene expression and population genomics to identify genetic variants such as SNPs from RNA sequences also enables estimating genetic diversity parameters (nucleotide diversity, structure, differentiation, and gene flow) for making evolutionary inferences (Jaris *et al.* 2012; Yu *et al.* 2023). For example, adaptation to altitudinal variation has been studied in the deer mice (*Peromyscus maniculatus*). This study found differential abundance in 11.7% of evaluated genes between individuals from highland (n = 10) and lowland populations (n = 10), and differences in gene expression in 0.7% of the genes. Few differentially expressed genes were associated with the response to differences in altitude. In this case, regulatory plasticity contributed to physiological adaptation to highlands. Accordingly, regulatory plasticity may play an important role in niche breadth and in potential response to environmental changes (Cheviron *et al.* 2013).

Another application of transcriptomics analyses is in landscape transcriptomics, which refers to the study of fluctuations in genome expression across populations in response to environmental gradients to establish management. This approach provides interesting information about adaptive local responses and the potential resilience of populations to rapid environmental change. Also, anthropogenic perturbations may lead to genetic differentiation between wild populations, and changes in connectivity, which could drive species to extinction (Keagy *et al.* 2023).

The potential of this tool is clear; however, there are many more reports of its use for studying the response to stress or environmental changes in model plants, fish, and

insects than for non-model mammals. Initially, one of the main limitations for the applicability of transcriptomics for the study of mammals and particularly endangered species, was that it required euthanizing individuals to obtain samples from specific organs or tissues, such as the brain, the kidneys, the lungs, the heart or the liver, to mention a few, depending on the research question (Huang *et al.* 2016). Nonetheless, thanks to technological advances, nowadays it is possible to conduct single-cell transcriptomics or to study the transcriptome from blood samples, making it feasible to study endangered species (Huang *et al.* 2016; 2019; Hilton *et al.* 2019).

Here we highlight some interesting studies that used RNA-seq to study ecological-evolutionary processes, such as identifying conserved sequences, expansion or contraction of gene families in specific lineages implicated in molecular evolution, genome complexity which drives species adaptation to new environments, and signals of selection. For example, 39 differentially expressed genes (DEG) were identified to be under positive selection in lung tissue of the yak (*Bos grunniens*) when compared with cattle (*Bos taurus*). The yak is a unique bovine that can live in high-altitude regions such as the Tibetan Plateau; accordingly, identified DEGs were associated with survival in oxygen-deficient environments (Lan *et al.* 2018).

Another study found that, in some cattle lineages, selective pressures have relaxed on traits associated with behavior in wildlife. In addition, there was an increase in the strength of positive selection in genes associated with amino acid metabolism, immune response, reproductive traits, hormone biosynthesis, and response to stress associated with an increase in temperature. The latter, together with non-conserved sequences in genes associated with lipid metabolism, could be used to improve the production and quality of meat (Cortez *et al.* 2022).

Transcriptomics allows to identify biomarkers that are indicative of the amount of genetic variation within and between populations to gain a better assessment of functional variability; this is useful information when defining management units and when identifying populations with low adaptive potential (Xu *et al.* 2014; 2016). The use of biomarkers allows monitoring population health, levels of genetic diversity, detection and prevalence of disease, and the response to environmental stress (He *et al.* 2016; Tarlinton *et al.* 2021). These aspects are highly relevant when selecting individuals for reintroduction and for implementing assisted reproduction techniques (Bowen *et al.* 2022; Gad *et al.* 2024); particularly for endangered mammals that require higher precision and efficacy in their management (Gao *et al.* 2022; Theissinger *et al.* 2023).

An RNA-seq approach was used to identify a biomarker for detecting kidney disease in koalas (*Phascolarctos cinereus*). The koala is a vulnerable species that is distributed in Australia, where two genetic clusters have been identified, a northern and a southern cluster. The southern cluster shows low levels of genetic variation, and individuals are carriers of several diseases that impact fitness. The gene *SLC26A6* was differentially expressed when comparing the northern and southern populations, and differential expression was associated with kidney disease; thus, this gene may function as a biomarker to detect susceptibility to kidney disease in koalas (Tarlinton *et al.* 2021).

In the bighorn sheep (*Ovis canadensis*), several genes (TGFb, AHR, IL1b and MX1) were associated with the initial phases of pneumonia, which cause a mortality rate of 90%. These genes can be used as biomarkers for monitoring populations for early detection of the disease, and to implement an adequate management plan (Bowen *et al.* 2022).

Transcriptomic data have also been used to develop biomarkers that allow assessing ecological risks for the presence of toxins in the marine surface, changes in temperature regimes, and the presence of pathogens in the bottlenose dolphin (*Tursiops truncatus*) from Bahía Sur de Baja California. In this case, two genes (UBQLN4 and TXNDC11) were associated with response to environmental stress such as fluctuations in temperature (Trego *et al.* 2019).

Finally, the characterization of the transcriptome in early embryonic development provides information that allows optimizing the process for embryo selection, fertilization, and the selection for individuals for *ex situ* conservation and reintroduction (Chitwood *et al.* 2017; Gad *et al.* 2024). The southern population of white rhinoceros (*Ceratotherium simum*) consists of only two non-reproductive individuals; in this case, assisted reproduction may be a viable alternative to increase population size. This analysis showed that four miRNA (miR-149b, miR-148a, miR-451 and miR-21) are highly active during embryonic development; these loci may be key for implementing successful assisted reproduction (Gad *et al.* 2024).

The application of transcriptomics for mammal conservation is only starting, but this approach is promising for gaining a better understanding of species' capacity to respond to environmental changes. In addition, obtaining transcriptomic data has a lower cost than obtaining genomic data; therefore, this approach represents a viable alternative for laboratories with restricted budgets.

Challenges and perspectives

There are still some challenges in implementing genomics for the study and conservation of mammals. A strong population genetics' theoretical background is advisable to implement adequate analyses and to help interpret the data. In this sense, population genetics courses for managers must be designed.

Another challenge is building technical capabilities (both in equipment and human resources) for the construction of genomic libraries and gaining access to next-generation sequencing technologies, particularly in countries from the global south. In this sense, expertise in bioinformatics is needed to conduct data analyses and develop user-friendly software that provides easier access

to data analysis for non-experts. The latter comes hand in hand with access to high-performance computer clusters because genomic approaches produce a large amount of data that cannot be analyzed on a personal computer.

Finally, translating complicated technical language into an accessible language for non-experts and grounding research findings in their practical implications and applications for conservation will help raise awareness in the public. Moreover, this is a crucial step in linking scientific researchers with wildlife managers and decision-makers.

The transition from conservation genetics to genomics will become increasingly common as massive sequencing costs decrease and technologies become more accessible. The application of genomics in combination with non-invasive sampling is still challenging, as DNA from this type of sampling is usually found in low concentrations and it is degraded. Although there have been advances in these areas, future efforts should optimize the application of genomic tools to non-invasive samples (Russello *et al.* 2015; Andrews *et al.* 2018; Ramírez-García *et al.* 2025) and museum specimens, which hold valuable information about historical patterns of genetic diversity (Card *et al.* 2021; Raxworthy and Smith 2021; Fong *et al.* 2023). In addition, genomics, transcriptomics, epigenetics and other omics (such as metabolomics and proteomics) will contribute with a better understanding of how species, populations and biological communities will respond to climate change and to address the biodiversity crisis (Tiwari and Rajwanshi 2022; De León *et al.* 2023; Bernatchez *et al.* 2024). In conjunction with environmental data and future projections of niche models, genomics and other omics will help predict potential allele turnover, dispersal potential, and the role of gene flow to climate change (Fitzpatrick and Keller 2015; Capblancq *et al.* 2020; Aguirre-Liguori *et al.* 2021; Bernatchez *et al.* 2024); as well inbreeding and inbreeding depression, hybridization and adaptive introgression. We hope that mammalogists (current and future) found this review useful as a starting point for implementing genomics studies for the conservation of mammals.

Acknowledgements

Authors greatly appreciate editor's invitation to contribute to this special issue that celebrates the academic trajectory of Dr. Livia León Paniagua. The first author of this manuscript (GCM) gives a very special thanks to Dr. Livia León Paniagua for her continuous guidance and support. Dr. Livia León Paniagua introduced me to the fascinating world of mammals as a teacher in an optative course on Deutorostomes imparted as part of the Bachelor's degree syllabus at the Faculty of Sciences, UNAM. Later on, Dr. Livia accompanied me during my Master's in Science studies as thesis reviewer. Since I first met her, Dr. Livia demonstrated to be a warm-hearted person, as well as having a high level of openness and willingness to collaborate, to the point that after many years we continue to collaborate with the mammalogical collection from the "Museo de Zoología Alfonso L. Herrera" at the Faculty of Sciences, UNAM. There is no doubt that Dr. Livia León Paniagua is a reference and inspiration for me and many Mexican women in science.

Declaration of Artificial Intelligence use

The authors declare that no AI was used in the preparation of this manuscript.

Author contributions

Gabriela Castellanos-Morales led the writing and development of the present manuscript. Gabriela Castellanos-Morales and Jorge Ortega were responsible for manuscript conceptualization. All authors performed literature searches and revision for different sections and writing of original draft. Anahí Canedo-Texón composed the abbreviature and concept lists, Jesús Antonio Rocamontes-Morales prepared Table 1 and Katia Hernández-Bolaños prepared figures. All authors contributed to reviewing and editing of previous versions of the manuscript. All authors approved the final version of this manuscript.

Supplementary Data

SD1. List of abbreviations used in the present article.
SD2. List of concepts frequently used in genomic studies.

Literature cited

Aguirre-Liguori JA, Ramírez-Barahona S, and Gaut BS. 2021. The evolutionary genomics of species' responses to climate change. *Nature Ecology & Evolution* 5:1350–1360. https://doi.org/10.1038/s41559-021-01526-9

Ahrens CW, Rymer PD, Sow A, Bragg J, Dillon S, Umbers KDL, *et al*. 2018. The search for loci under selection: trends, biases and progress. *Molecular Ecology* 27:1342–1356. https://doi.org/10.1111/mec.14549

Aivelo T, and Medlar A. 2018. Opportunities and challenges in metabarcoding approaches for helminth community identification in wild mammals. *Parasitology* 145:608–621. https://doi.org/10.1017/S0031182017000610

Allendorf FW. 2017. Genetics and the conservation of natural populations: allozymes to genomes. *Molecular Ecology* 26:420–430. https://doi.org/10.1111/mec.13948

Allendorf FW, Hohenlohe PA, and Luikart G. 2010. Genomics and the future of conservation genetics. *Nature Reviews Genetics* 11:697–709. https://doi.org/10.1038/nrg2844

Alvarez M, Schrey AW, and Richards CL. 2015. Ten years of transcriptomics in wild populations: what have we learned about their ecology and evolution? *Molecular Ecology* 24:710–725. https://doi.org/10.1111/mec.13055

Andrews KR, De Barba M, Russello MA, and Waits LP. 2018. Advances in using non-invasive, archival, and environmental samples for population genomic studies. In: Hohenlohe P, and Rajora OP, editors. *Population genomics: wildlife*. Cham (CHE): Springer; p 63–99. https://doi.org/10.1007/13836_2_018_45

Andrews KR, Good JM, Miller MR, Luikart G, and Hohenlohe PA. 2016. Harnessing the power of RADseq for ecological

and evolutionary genomics. *Nature Reviews Genetics* 17:81–92. https://doi.org/10.1038/nrg.2015.28

Ange-Stark M, Parise KL, Cheng TL, Hoyt JR, Langwig KE, Frick WF, *et al*. 2023. White-nose syndrome restructures bat skin microbiomes. *Environmental Microbiology* 11:1–15. https://doi.org/10.1128/spectrum.02715-23

Attardi G, and Schatz G. 1988. Biogenesis of mitochondria. *Annual Review of Cell and Developmental Biology* 4:289–333. https://doi.org/10.1146/annurev.cb.04.110188.001445

Aubin-Horth N, and Renn SCP. 2009. Genomic reaction norms: using integrative biology to understand molecular mechanisms of phenotypic plasticity. *Molecular Ecology* 18:3763–3780. https://doi.org/10.1111/j.1365-294X.2009.04313.x

Avise JC, and Ellis D. 1986. Mitochondrial DNA and the evolutionary genetics of higher animals. *Proceedings of the Royal Society B* 312:325–342. https://doi.org/10.1098/rstb.1986.0011

Baeza JA, Barata R, Rajapakse D, Penaloza J, Harrison P, and Haberski A. 2023. Mitochondrial genomes assembled from non-invasive eDNA metagenomic scat samples in critically endangered mammals. *Genes* 14:657. https://doi.org/10.3390/genes030657

Bahrndorff S, Alemu T, Alemneh T, and Nielsen JL. 2016. The microbiome of animals: implications for conservation biology. *International Journal of Genomics* 2016:5304028. https://doi.org/10.1155/2016/5304028

Baird NA, Etter PD, Atwood TS, Currey MC, Shiver AL, Lewis ZA, *et al*. 2008. Rapid SNP discovery and genetic mapping using sequenced RAD markers. *PLoS One* 3(10):e3376. https://doi.org/10.1371/journal.pone.0003376

Bernatchez L, Ferchaud AL, Berger CS, Venney CJ, and Xuereb A. 2024. Genomics for monitoring and understanding species responses to global climate change. *Nature Reviews Genetics* 25:165–183. https://doi.org/10.1038/s41576-023-00657-y

Bohling J. 2020. Evaluating the effect of reference genome divergence on the analysis of empirical RADseq datasets. *Ecology and Evolution* 10:7585–7601. https://doi.org/10.1002/ece3.6483

Bohmann K, Evans A, Gilbert MTP, Carvalho GR, Creer S, Knapp M, *et al*. 2014. Environmental DNA for wildlife biology and biodiversity monitoring. *Trends in Ecology & Evolution* 29:358–367. https://doi.org/10.1016/j.tree.2014.04.003

Botero-Castro F, Tilak M-K, Justy F, Catzeflis F, Delsuc F, and Douzery EJP. 2018. In cold blood: compositional bias and positive selection drive the high evolutionary rate of vampire bats mitochondrial genomes. *Genome Biology and Evolution* 10:2218–2239. https://doi.org/10.1093/gbe/evy120

Bowen L, Manlove K, Roug A, Waters S, and LaHue N. 2022. Using transcriptomics to predict and visualize disease status in bighorn sheep (*Ovis canadensis*). *Conservation Physiology* 10:coac046. https://doi.org/10.1093/conphys/coac046

Brassea-Pérez E, Schramm Y, Heckel G, Chong-Robles J, and Lago-Lestón A. 2019. Metabarcoding analysis of the Pacific harbor seal diet in Mexico. *Marine Biology* 166:106. https://doi.org/10.1007/s00227-019-3555-8

Bronstein O, Kroh A, and Haring E. 2018. Mind the gap! The mitochondrial control region and its power as a phylogenetic marker in echinoids. *BMC Evolutionary Biology* 18:80. https://doi.org/10.1186/s12862-018-1198-x

Calabrese FM, Balacco DL, PresteR, Diroma MA, Forino R, Ventura M, *et al*. 2017. Numts colonization in mammalian genomes. *Scientific Reports* 7:16357. https://doi.org/10.1038/s41598-017-16750-2

Capblancq T, Fitzpatrick MC, Bay RA, Exposito-Alonso M, and Keller SR. 2020. Genomic prediction of (mal)adaptation across current and future climatic landscapes. *Annual Review of Ecology, Evolution and Systematics* 51:245–269. https://doi.org/10.1146/annuev-ecolsys-020720-042553

Card DC, Shapiro B, Giribert G, Moritz C, and Edwards SV. 2021. Museum genomics. *Annual Reviews of Genetics* 55:633–659. https://doi.org/10.1146/annurev-genet-071719-020506

Castellanos-Morales G, and Gutiérrez-Guerrero YT. 2025. Phylogenomics for the study of speciation and diversification in Neotropical mammals. In: Melletti M, Tirira DG, Gallina Tessaro S, and Ortega J, editors. *Mammals of Middle and South America: History, Biogeography, Conservation*. Cham (CHE): Springer Nature. https://link.springer.com/book/9783032107664

Chaves BRN, Santos-Junior JE, and Santos FR. 2025. Metabarcoding markers and a reference database for neotropical mammals. *Conservation Genetics Resources* 17:283–297. https://doi.org/10.1007/s12686-025-01404-7

Cheviron ZA, Connaty AD, McClelland GB, and Storz JF. 2013. Functional genomics of adaptation to hypoxic cold-stress in high-altitude deer mice: transcriptomic plasticity and thermogenic performance. *Evolution* 68:48–62. https://doi.org/10.1111/evo.12257

Chitwood JL, Burruel VR, Halstead MM, Meyers SA, and Ross PJ. 2017. Transcriptome profiling of individual *rhesus macaque* oocytes and preimplantation embryos. *Biology of Reproduction* 97:353–364. https://doi.org/10.1093/biolre/iox114

Clendenin HR, Pollard MD, and Puckett EE. 2025. Linking measures of inbreeding and genetic load to demographic histories across three species of bears. *Evolutionary Applications* 18:e70133. https://doi.org/10.1111/eva.70133

Coutant O, Richard-Hansen C, de Thoisy B, Ecotte J-B, Valentini A, Dejean T, *et al*. 2021. Amazonian mammal monitoring using aquatic environmental DNA. *Molecular Ecology Resources* 21:1875–1888. https://doi.org/10.1111/1755-0998.13393

Cortez T, Montenegro H, Coutinho LL, Regitano LCA, and Andrade SCS. 2022. Molecular evolution and signatures of selective pressures on Bos, focusing on the Nelore breed (*Bos indicus*). *Plos One* 17:e0279091. https://doi.org/10.1371/journal.pone.0279091

Creer S, Deiner K, Frey S, Porazinska D, Taberlet P, Thomas WK, *et al*. 2016. The ecologist's field guide to sequence-based identification of biodiversity. *Methods in Ecology and Evolution* 7:1008–1018. https://doi.org/10.1111/2041-210X.12574

Crossman CA, Hamilton, PK, Brown MW, Conger LA, George RC, Jackson KA, Radvan SN, Frasier TR. 2024. Effects of inbreeding on reproductive success in endangered North Atlantic right whales. *Royal Society Open Science* 11:240490. http://doi.org/10.1098/rsos.240490

Cuber P, Chooneea D, Geeves C, Salatino S, Creedy TJ, Griffin C, *et al*. 2023. Comparing the accuracy and efficiency of third generation sequencing technologies, Oxford Nanopore Technologies, and Pacific Biosciences, for DNA barcode sequencing applications. *Ecological Genetics and Genomics* 28:100181. https://doi.org/10.1016/j.egg.2023.100181

da Fonseca RR, Johnson WE, O'Brien SJ, Ramos MJ, and Antunes A. 2008. The adaptive evolution of the mammalian mitochondrial genome. *BMC Genomics* 9:119. https://doi.org/10.1186/1471-2164-9-119

Dai Z, Xie B, Xie C, Xiang J, Wang X, Li J, Zheng R, and Wang Y. 2025. Comparative metagenomic analysis of the gut microbiota of captive pangolins: a case study of two species. *Animals* 15:57. https://doi.org/10.3390/ani15010057

Dallas JW, and Warne RW. 2023. Captivity and animal microbiomes: potential roles of microbiota for influencing animal conservation. *Microbial Ecology* 85:820–838. https://doi.org/10.1007/s00248-022-01991-0

Davey JW, Hohenlohe PA, Etter PD, Boone JQ, Catchen JM, and Blaxter ML. 2011. Genome-wide genetic marker discovery and genotyping using next-generation sequencing. *Nature Reviews Genetics* 12:499–510. https://doi.org/10.1038/nrg3012

Davey JW, Cezard T, Fuentes-Utrilla P, Eland C, Gharbi K, and Blaxter ML. 2013. Special features of RAD sequencing data: implications for genotyping. *Molecular Ecology* 22:3151–3164. https://doi.org/10.1111/mec.12084

De León LF, Silva B, Avilés-Rodríguez KJ, and Buitrago-Rosas D. 2023. Harnessing the omics revolution to address the global biodiversity crisis. *Current Opinion in Biotechnology* 80:102901. https://doi.org/10.1016/j.copbio.2023.102901

Donath A, Jühling F, Al-Arab M, Bernhart SH, Reinhardt F, Stadler PF, *et al*. 2019. Improved annotation of protein-coding genes boundaries in metazoan mitochondrial genomes. *Nucleic Acids Research* 47:10543–10552. https://doi.org/10.1093/nar/gkz833

Ekblom R, and Wolf JBW. 2014. A field guide to whole-genome sequencing, assembly and annotation. *Evolutionary Applications* 7:1026–1042. https://doi.org/10.1111/eva.12178

Fernández-Silva P, Enriquez JA, and Montoya J. 2004. Replication and transcription of mammalian mitochondrial DNA. *Experimental Physiology* 88:41–56. https://doi.org/10.1113/eph8802514

Fitzpatrick MC, and Keller MC. 2015. Ecological genomics meets community-level modelling of biodiversity: mapping the genomic landscape of current and future environmental adaptation. *Ecology Letters* 18:1–16. https://doi.org/10.1111/ele.12376

Fong JJ, Blom MPK, Aowphol A, McGuire JA, Sutcharit C, and Soltis PS. 2023. Editorial: recent advances in museomics: revolutionizing biodiversity research. *Frontiers in Ecology and Evolution* 11:1188172. https://doi.org/10.3389/fevo.2023.1188172

Formenti G, Rhie A, Balacco J, Hasse B, Maountcastle J, Fedrigo O, *et al*. 2021. Complete vertebrate mitogenomes reveal widespread repeats and gene duplications. *Genome Biology* 22:120. https://doi.org/10.1186/s13059-021-02336-9

Frankham R. 2003. Genetics and conservation. *Comptes Rendus Biologies* 326:S22–S29. https://doi.org/10.1016/S1631-0691(03)00023-4

Frankham R. 2005. Genetics and extinction. *Biological Conservation* 126:131–140. https://doi.org/10.1016/j.biocon.2005.05.002

Frankham R. 2010. Challenges and opportunities of genetic approaches to biological conservation. *Biological Conservation* 143:1919–1927. https://doi.org/10.1016/j.biocon.2010.05.011

Fu Y-B, Peterson GW, and Dong Y. 2016. Increasing genome sampling and improving SNP genotyping for genotyping-by-sequencing with new combinations of restriction enzymes. *Genes Genomes Genetics* 6:845–856. https://doi.org/10.1534/g3.115.025775

Fuentes-Pardo AP, and Ruzzante DE. 2017. Whole-genome sequencing approaches for conservation biology: Advantages, limitations and practical recommendations. *Molecular Ecology* 26:5369–5406. https://doi.org/10.1111/mec.14264

Fusco NA, Consentino BJ, Gibbs JP, Allen ML, Blumenfeld AJ, Boettner GH, *et al*. 2023. Population genomic structure of a widespread, urban-dwelling mammal: the eastern grey squirrel (*Sciurus carolinensis*). *Molecular Ecology* 33:e17230. https://doi.org/10.1111/mec.17230

Gad A, Menjivar NG, Felton R, Durrant B, Tesfaye D, and Ruggeri E. 2024. Mapping the follicle-specific regulation of extracellular vesicle-mediated microRNA transport in the southern white rhinoceros (*Ceratotherium simum simum*). *Biology of Reproduction* 111:376–390. https://doi.org/10.1093/biolre/ioae081

Galhardo M, Fonseca N, Egeter B, Paupério J, Ferreira S, Oxelfelt F, *et al*. 2018. Deliverable 4.5 (D4.5): Protocol for the processing of DNA sequence data generated by next-gen platforms, EnMetaGen project

(Grant Agreement No 668981). *Zenodo*. https://doi.org/10.5281/ZENODO.2586889

Gao X, Wang S, Wang YF, Li S, Wu S-X, Yan R-G, *et al*. 2022. Long read genome assemblies complemented by single cell RNA-sequencing reveal genetic and cellular mechanisms underlying the adaptive evolution of yak. *Nature Communications* 13:4887. https://doi.org/10.1038/s41467-022-32164-9

Gibson A, Gowri-Shankar V, Higgs PG, and Rattray M. 2004. A comprehensive analysis of mammalian mitochondrial genome base composition and improved phylogenetic methods. *Molecular Biology and Evolution* 22:251–264. https://doi.org/10.1093/molbev/msi012

Gibson KM, Nguyen BN, Neumann LM, Miller M, Buss P, Daniels S, *et al*. 2019. Gut microbiome differences between wild and captive black rhinoceros – implications for rhino health. *Scientific Reports* 9:7570. https://doi.org/10.1038/s41598-019-43875

Goodwin S, McPherson JD, and McCombie WR. 2016. Coming of age: ten years of next-generation sequencing technologies. *Nature Reviews in Genetics* 17:333–351. https://doi.org/10.1038/nrg.2016.49

Haarsma A, Siepel H, and Gravendeel B. 2016. Added value of metabarcoding combined with microscopy for evolutionary studies of mammals. *Zoologica Scripta* 45:37–49. https://doi.org/10.1111/zsc.12214

Harper LR, Lawson Handley L, Carpenter AI, Ghazali M, Di Muri C, Macgregor CJ, *et al*. 2019. Environmental DNA (eDNA) metabarcoding of pond water as a tool to survey conservation and management priority mammals. *Biological Conservation* 238:108225. https://doi.org/10.1016/j.biocon.2019.108225

Hassan S, Sabreena, Poczai P, Ganai BA, Almalki WH, Gafur A, *et al*. 2022. Environmental DNA metabarcoding: a novel contrivance for documenting terrestrial biodiversity. *Biology* 11:1297. https://doi.org/10.3390/biology11091297

Hassanin A, Léger N, and Deutsch J. 2005. Evidence for multiple reversals of asymmetric mutational constraints during the evolution of the mitochondrial genome of Metazoa, and consequences for phylogenetic inferences. *Systematic Biology* 54:277 https://doi.org/10.1080/10635150590947843

He X, Johansson ML, and Heath DD. 2016. Role of genomics and transcriptomics in selection of reintroduction source populations. *Conservation Biology* 30:1010–1018. https://doi.org/10.1111/cobi.12674

Hedrick PW, and Garcia-Dorado A. 2016. Understanding inbreeding depression, purging, and genetic rescue. *Trends in Ecology & Evolution* 31:940–952. https://doi.org/10.1016/j.tree.2016.09.005

Heyer E, Zietkiewicz E, Rochowski A, Yotova V, Puymirat J, and Labuda D. 2001. Phylogenetic and familial estimates of mitochondrial substitution rates: study of control region mutations in deep-rooting pedigrees. *American Journal of Human Genetics* 69:1113–11126. https://doi.org/10.1086/324024

Hilton HG, Rubinstein ND, Janki P, Ireland AT, Bernstein N, Fong NL, *et al*. 2019. Single-cell transcriptomics of the naked mole-rat reveals unexpected features in mammalian immunity. *Plos Biology* 17:e3000528. https://doi.org/10.1371/journal.pbio.3000528

Hu T, Chitnis N, Monos D, and Dinh A. 2021. Next-generation sequencing technologies: An overview. *Human Immunology* 82:801–811. https://doi.org/10.1016/j.humimm.2021.02.012

Huang Z, Gallot A, Lao NT, Puechmaille SJ, Foley NM, Jebb D, *et al*. 2016. A nonlethal sampling method to obtain, generate and assemble whole blood transcriptomes from small, wild mammals. *Molecular Ecology Resources* 12:150–162. https://doi.org/10.1111/1755-0998.12447

Huang Z, Whelan CV, Foley NM, Jebb D, Touzalin F, Petit EJ, *et al*. 2019. Longitudinal comparative transcriptomics reveals unique mechanisms underlying extended healthspan in bats. *Nature Ecology & Evolution* 3:1110–1120. https://doi.org/10.1038/s41559-019-0913-3

Hurst GDD, and Jiggins FM. 2005. Problems with mitochondrial DNA as a marker in population, phylogeographic and phylogenetic studies: the effects of inherited symbionts. *Proceedings of the Royal Society B* 272:1525–1534. https://doi.org/10.1098/rspb.2005.3056

Ivanova NV, Clare EL, and Borisenko AV. 2012. DNA barcoding in mammals. In: Kress WJ, and Erickson DL, editors. *DNA Barcodes. Methods and protocols*. Cham (CHE): Springer Nature; p 153–182. https://doi.org/10.1007/978-1-61779-591-6_8

Jaris H, Therkildsen NO, Morikawa M, and Palumbi SR. 2012. The simple fool's guide to population genomics via RNA-Seq: an introduction to high-throughput sequencing data analysis. *Molecular Ecology Resources* 12:1058–1067. https://doi.org/10.1111/1755-0998.12003

Jehl F, Degalez F, Bernard M, Lecerf F, Lagoutte L, Désert C, *et al*. 2021. RNA-Seq data for reliable SNP detection and genotype calling: interest for coding variant characterization and *cis*-regulation analysis by allele-specific expression in livestock species. *Frontiers in Genetics* 12:655707. https://doi.org/10.3389/fgene.2021.655707

Jin J, Yu W, Yang J, Song Y, de Pamphilis CW, Yi T, *et al*. 2020. GetOrganelle: a fast and versatile toolkit for accurate de novo assembly of organelle genomes. *Genome Biology* 21(241):1–31. https://doi.org/10.1186/s13059-020-02154-5

Jeukens J, Renaut S, St-Cyr J, Nolte AW, and Bernatchez L. 2010. The transcriptomics of sympatric dwarf and normal lake whitefish (*Coregonus clupeaformis* spp., Salmonidae) divergence as revealed by next-generation sequencing. *Molecular Ecology* 19:5389–403. https://doi.org/10.1111/j.1365-294X.2010.04934.x

Kanishka AM, MacGregor C, Neaves LE, Evans MJ, Robinson NM, Dester N, *et al*. 2025. Quantifying the dietary overlap of two co-occurring mammal species using DNA

metabarcoding to assess potential competition. *Ecology and Evolution* 15(4):e71274. https://doi.org/10.1002/ece3.71274

Kapusta A, Suh A, and Feschotte C. 2017. Dynamics of genome size evolution in birds and mammals. *Proceedings of the National Academy of Science* 114(8):E1460–E1469. https://doi.org/10.1073/pnas.1616702114

Keagy J, Drummond CP, Gilbert KJ, Grozinger CM, Hamilton J, Hines HM, *et al*. 2023. Landscape transcriptomics as a tool for addressing global change effects across diverse species. *Molecular Ecology Resources* 25:e13796. https://doi.org/10.1111/1755-0998.13796

Konrad A, Thompson O, Waterston RH, Moerman DG, Keightley PD, Bergthorsson U, *et al*. 2017. Mitochondrial mutation rate, spectrum and heteroplasmy in *Caenorhabditis elegans* spontaneous mutation accumulation lines of differing population size. *Molecular Biology and Evolution* 34:1319–1334. https://doi.org/10.1093/molbev/msx051

Ladoukakis ED, and Zouros E. 2017. Evolution and inheritance of animal mitochondrial DNA: rules and exceptions. *Journal of Biological Research-Thessaloniki* 24:1–7. https://doi.org/10.1186/s40709-017-0060-4

Lan D, Xiong X, Ji W, Li J, Mipam TD, Ai Y, *et al*. 2018. Transcriptome profile and unique genetic evolution of positively selected genes in yak lungs. *Genetica* 146:151–160. https://doi.org/10.1007/s10709-017-0005-8

Li F, Yang S, Zhang L, Qiao L, Wang L, He S, *et al*. 2022. Comparative metagenomics analysis reveals how the diet shapes the gut microbiota in several small mammals. *Ecology and Evolution* 12:e8470. https://doi.org/10.1002/ece3.8470

Li LF, Cushman SA, He YX, and Li Y. 2020. Genome sequencing and population genomics modeling provide insights into the local adaptation of weeping forsythia. *Horticulture Research* 7:130. https://doi.org/10.1038/s41438-020-00352-7

Li Z, Liu X, Wang C, Li Z, Jiang B, Zhang R, *et al*. 2023. The pig pangenome provides insights into the roles of coding structural variations in genetic diversity and adaptation. *Genome Research* 33:1833–1847. https://doi.org/10.1101/gr.277638.122

Liu M, Clarke LJ, Baker SC, Jordan GJ, and Burridge CP. 2020. A practical guide to DNA metabarcoding for entomological ecologists. *Ecological Entomology* 45:373–385. https://doi.org/10.1111/een.12831

Loeffler C, Zhang J, Muszyńska A, Munteanu V, Yang H, Rotman J, *et al*. 2023. RNA-seq data science: From raw data to effective interpretation. *Frontiers in Genetics* 13:14:997383. https://doi.org/10.3389/fgene.2023.997383

Lopez-Maestre H, Brinza L, Marchet C, Kielbassa J, Bastien S, Boutigny M, *et al*. 2016. SNP calling from RNA-seq data without a reference genome: identification, quantification, differential analysis and impact on the protein sequence. *Nucleic Acids Research* 44:48. https://doi.org/10.1093/nar/gkw655

Lou RN, Jacobs A, Wilder AP, and Therkildsen NO. 2021. A beginner's guide to low-coverage whole genome sequencing for population genomics. *Molecular Ecology* 30:5966–5993. https://doi.org/10.1111/mec.16077

Lu H, Giordano F, and Ning Z. 2016. Oxford Nanopore MinION Sequencing and Genome Assembly. *Genomics Proteomics Bioinformatics* 14:265–279. https://doi.org/10.1016/j.gpb.2016.05.004

Luikart G, Kardos M, Hand BK, Rajora OP, Aitken SN, and Hohenlohe PA. 2019. Population genomics: advancing understanding of nature. In: Rajora OP, editor. *Population genomics: concepts, approaches and applications*. Cham (CHE): Springer Nature. https://link.springer.com/chapter/10.1007/13836_2018_60

Martchenko D, and Shafer ABA. 2023. Contrasting whole-genome and reduced representation sequencing for population demographic and adaptive inference: an alpine mammal case study. *Heredity* 131:273–281. https://doi.org/10.1038/s41437-023-00643-4

Martinez-Gutierrez CA, and Aylward FO. 2022. Genome size in bateria and archae are strongly linked to evolutionary historyu at broad phylogenetic scales. *Plos Genetics* 18(5):e1010220. https://doi.org/10.1371/journal.pgen.1010220

Mastretta-Yanes A, Arrigo N, Alvarez N, Piñero D, and Emerson B. 2014. Restriction site-associated DNA sequencing, genotyping error estimation and *de novo* assembly optimization for population genetic inference. *Molecular Ecology Resources* 15:28–41. https://doi.org/10.1111/1755-0998.12291

Meganathan PR, Pagan HJT, McCulloch ES, Stevens RD, and Ray DA. 2012. Complete mitochondrial genome sequences of three bats species and whole genome mitochondrial analyses reveal patterns of codon bias and lend support to a basal split in Chiroptera. *Gene* 492:121–129. https://doi.org/10.1016/j.gene.2011.10.038

Mena JL, Yagui H, Tejeda V, Bonifaz E, Bellemain E, Valentini A, *et al*. 2021. Environmental DNA metabarcoding as a useful tool for evaluating terrestrial mammal diversity in tropical forests. *Ecological Applications* 31(5):e02335. https://doi.org/10.1002/eap.2335

Miller MR, Dunham JP, Amores A, Cresko WA, and Johnson EA. 2007. Rapid and cost-effective polymorphism identification and genotyping using restriction site associated DNA (RAD) markers. *Genome Research* 17:240–248. https://doi.org/10.1101/gr.5681207

Moeller AH, and Sanders JG. 2020. Roles of the gut microbiota in the adaptive evolution of mammalian species. *Philosophical Transactions of the Royal Society B* 375(1808):20190597. https://doi.org/10.1098/rstb.2019.0597

Mohammadi Z, Shahabi S, Ghorbani F, and Khajeh A. 2019. Efficiency of the mitochondrial DNA markers (COI, cyt b) and a nuclear DNA marker (RAGI) in molecular identification of zoonotic diseases' hosts. *Journal of*

Health Sciences & Surveillance System 7:86–93. https://doi.org/10.30476/jhsss.2020.84774.1042

Nachtigall PG, Grazziotin FG, and Junqueira-de-Azevedo ILM. 2021. MITGARD: an automated pipeline for mitochondrial genome assembly in eukaryotic species using RNA-seq data. *Brief Bioinformatics* 22:bbaa429. https://doi.org/10.1093/bib/bbaa429

Ng PC, and Kirkness EF. 2010. Whole Genome Sequencing. In: Barnes MR, and Breen G, editors. *Genetic Variation*. Vol. 628. Totowa, NJ (EEUU): Springer (*Methods in Molecular Biology*); p. 215–226. https://doi.org/10.1007/978-1-60327-367-1_12

Nicholls TJ, and Minczuk M. 2014. In D-loop: 40 years of mitochondrial 7S DNA. *Experimental Gerontology* 56:175–181. https://doi.org/10.1016/j.exger.2014.03.027

O'Leary SJ, Puritz JB, Willis SC, Hollenbeck CM, and Portnoy DS. 2018. These aren't the loci you'e looking for: principles of effective SNP filtering for molecular ecologists. *Molecular Ecology* 27:3193–3206. https://doi.org/10.1111/mec.14792

Ouborg NJ, Pertoldi C, Loeschcke V, Bijlsma R, and Hedrick PW. 2010. Conservation genetics in transition to conservation genomics. *Trends in Genetics* 26:177–187. https://doi.org/10.1016/j.tig.2010.01.001

Paris JR, Stevens JR, and Catchen JM. 2017. Lost in parameter space: a road map for Stacks. *Methods in Ecology and Evolution* 8:1360–1373. https://doi.org/10.1111/2041-210X.12775

Pavey SA, Collin H, Nosil P, and Rogers SM. 2010. The role of gene expression in ecological speciation. *Annals of the New York Academy of Sciences* 1206:110–29. https://doi.org/10.1111/j.1749-6632.2010.05765.x

Payne N, Andersen D, Davis R, Mollohan C, Baldwin K, LeCount AL, *et al*. 2025. Evidence of extensive home range sharing among mother-daughter bobcat pairs in the wildland-urban interface of the Tucson Mountains. *Journal of Heredity* 116:408–421. https://doi.org/10.1093/jhered/esae072

Peterson BK, Weber JN, Kay EH, Fisher HS, and Hoekstra HE. 2012. Double digest RADseq: an inexpensive method for *de novo* SNP discovery and genotyping in model and non-model species. *Plos One* 7:e37135. https://doi.org/10.1371/journal.pone.0037135

Picardi E, and Pesole G. 2012. Mitochondrial genomes gleaned from human whole-exome sequencing. *Natural Methods* 9:523–524. https://doi.org/10.1038/nmeth.2029

Quintero-Galvis JF, Saenz-Agudel P, Délia G, and Nespolo RF. 2024. Local adaptation of *Dromiciops* marsupials (Microbiotheriidae) from southern South America: implications for species management facing climate change. *Ecology and Evolution* 14:e70355. https://doi.org/10.1002/ece3.70355

Ramírez-García JG, Maciel-Torres SP, Hernández-Rodríguez M, Arenas-Báez P, Orzuna-Orzuna JF, and Granados-Rivera LD. 2025. Non-invasive sampling for population genetics of wild terrestrial mammals (2015-2025): a systematic review. *Diversity* 17:760. https://doi.org/10.3390/d17110760

Raxworthy CJ, and Smith BT. 2021. Mining museums for historical DNA: advances and challenges in museomics. *Trends in Ecology & Evolution* 36:1049–1060. https://doi.org/10.1016/j.tree.2021.07.009

Rocamontes-Morales JA, Baeza JA, Martínez-Cárdenas A, Ortega J, and Castellanos-Morales G. 2025. Mitochondrial selection and evolutionary insights into nectarivory in Glossophaginae (New world leaf-nosed bats). *Molecular Biology Reports* 52:720. https://doi.org/10.1007/s11033-025-10782-y

Ruiz-García M, Cáceres AM, Luengas-Villamil K, Aliaga-Rossel E, Zeballos H, Singh MD, *et al*. 2022. Mitogenomic phylogenetics and population genetics of several taxa of agouties (*Dasyprocta* sp., Dasyproctidae, Rodentia): molecular nonexistencie of some claimed endemic taxa. *Mammal Research* 67:367–397. https://doi.org/10.1007/s13364-022-00626-6

Ruppert KM, Kline RJ, and Rahman MS. 2019. Past, present, and future perspectives of environmental DNA (eDNA) metabarcoding: a systematic review in methods, monitoring, and applications of global eDNA. *Global Ecology and Conservation* 17:e00547. https://doi.org/10.1016/j.gecco.2019.e00547

Russello MA, Waterhouse MD, Etter PD, and Johnson EA. 2015. From promise to practice: pairing non-invasive sampling with genomics in conservation. *PeerJ* 3:e1106. https://doi.org/10.7717/peerj.1106

Schlötterer C. 2004. The evolution of molecular markers – just a matter of fashion? *Nature Reviews Genetics* 5:63–69. https://doi.org/10.1038/nrg1249

Seeber PA, and Epp LS. 2022. Environmental DNA and metagenomics of terrestrial mammals as kwystone taxa of recent and past ecosystems. *Mammal Review* 52:538–553. https://doi.org/10.1111/mam.12302

Selkoe KA, and Toonen RJ. 2006. Microsatellites for ecologists: a practical guide to using and evaluating microsatellite markers. *Ecology Letters* 9:615–629. https://doi.org/10.1111/j.1461-0248.2006.00889.x

Shafer ABA, Wolf JBW, Alves PC, Bergström L, Bruford MW, Brännström I, *et al*. 2015. Genomics and the challenging translation into conservation practice. *Trends in Ecology & Evolution* 30:78–87. https://doi.org/10.1016/j.tree.2014.11.009

Shen YY, Liang L, Zhu ZH, Zhou WP, Irwin DM, and Zhang YP. 2010. Adaptive evolution of energy metabolism genes and the origin of flight in bats. *Proceedings of the National Academy of Science USA* 107:8666–8671. https://doi.org/10.1073/pnas.0912613107

Simon SA, Zhai J, Nandety RS, McCormick KP, Zeng J, Mejia D, *et al*. 2009. Short-read sequencing technologies for transcriptional analyses. *Annual Reviews in Plant Biology* 60:305–333. https://doi.org/10.1146/annurev.arplant.043008.092032

Smeds L, Huson LSA, and Ellegren H. 2024. Structural genomic variation in the inbred Scandinavian wolf population contributes to the realized genetic load but is positively affected by immigration. *Evolutionary Applications* 17:e13652. https://doi.org/10.1111/eva.13652

Soares P, Abrantes D, Rito T, Thomson N, Radivojac P, Li B, *et al*. 2013. Evaluating purifying selection in the mitochondrial DNA of various mammalian species. *Plos One*, 8:e58993. https://doi.org/10.1371/journal.pone.0058993

Stahlke AR, Epstein B, Barbosa S, Margres MJ, Patton A, Hendricks SA, *et al*. 2021. Contemporary and historical selection in Tasmanian devils (*Sarcophilus harrisii*) support novel, polygenic response to transmissible cancer. *Proceedings of the Royal Society B* 288(1951):2021.0577. https://doi.org/10.1098/rspb.2021.0577

Sunnucks P. 2000. Efficient genetic markers for population biology. *Trends in Ecology and Evolution* 15:199–203. https://doi.org/10.1016/S0169-5347(00)01825-5

Supple MA, and Shapiro B. 2018. Conservation of biodiversity in the genomics era. *Genome Biology* 19:131. https://doi.org/10.1186/s13059-018-1520-3f

Tarlinton RE, Fabijan J, Hemmatzadeh F, Meers J, Owen H, Sarker N, *et al*. 2021. Transcriptomic and genomic variants between koala populations reveal underlying genetic components to disorders in a bottlenecked population. *Conservation Genetics* 22:329–340. https://doi.org/10.1007/s10592-021-01340-7

Tettelin H, and Medini D, editors. 2020. *The pangenome: diversity, dynamics and evolution of genomes*. Cham (CHE): Springer International Publishing. [accessed 2024 Sep 25]. https://link.springer.com/10.1007/978-3-030-38281-0

Theissinger K, Fernandes C, Formenti G, Bista I, Berg PR, Bleidorn C, *et al*. 2023. How genomics can help biodiversity conservation. *Trends in Genetics* 39:545–559. https://doi.org/10.1016/j.tig.2023.01.005

Thomsen PF, and Willerslev E. 2015. Environmental DNA – an emerging tool in conservation for monitoring past and present biodiversity. *Biological Conservation* 183:4–18. https://doi.org/10.1016/j.biocon.2014.11.019

Tiwari S, and Rajwanshi R. 2022. Overview of omics-assisted techniques for biodiversity conservation. In: Kumar A, Choudhury B, Dayanandan S, and Khan ML, editors. *Molecular genetics and genomics tools in biodiversity conservation*. Cham (CHE): Springer; p 63–78. https://doi.org/10.1007/978-981-16-6005-4_4

Toews DPL, and Brelsford A. 2012. The biogeography of mitochondrial and nuclear discordance in animals. *Molecular Ecology* 21(16):3907–3930. https://doi.org/10.1111/j.1365-294X.2012.05664.x

Trego ML, Whitehead A, Kellar NM, Lauf M, and Lewison RL. 2019. Tracking transcriptomic responses to endogenous and exogenous variation in cetaceans in the Southern California Bight. *Conservation Physiology* 7:coz018. https://doi.org/10.1093/conphys/coz018

Uliano-Silva M, Ferreira JGRM, Krasheninnikova K, Darwin Tree of Life Consortium, Formenti G, Abueg L, *et al*. 2023. MitoHiFi: a python pipeline for mitochondrial genome assembly from PacBio high fidelity reads. *BMC Bioinformatics* 24:288. https://doi.org/10.1186/s12859-023-05385-y

Uvizl M, Puechmaille SJ, Power S, Pippel M, Carthy S, Haerty W, *et al*. 2023. Comparative genome microsynteny illuminates the fast evolution of nuclear mitochondrial segments (NUMTs) in mammals. *Molecular Biology and Evolution* 41:msad278. https://doi.org/10.1093/molbev/msad278

Vanderwolf KJ, Campbell LJ, Goldberg TL, Blehert DS, and Lorch JM. 2021. Skin fungal assemblages of bats vary based on susceptibility to white-nose syndrome. *The ISME Journal* 15:909–920. https://doi.org/10.1038/s41396-020-00821-w

Wanniarachchi S, Swan M, Nevil P, and York A. 2022. Using eDNA metabarcoding to understand the effect of fire on the diet of small mammals in a woodland ecosystem. *Ecology and Evolution* 12:e9457. https://doi.org/10.1002/ece3.9457

Wang T, Antonacci-Fulton L, Howe K, Lawson HA, Lucas JK, Phillippy AM, *et al*. 2022. The Human Pangenome Project: a global resource to map genomic diversity. *Nature* 604:437–446. https://doi.org/10.1038/s41586-022-04601-8

Wang Z, Gerstein M, and Snyder M. 2009. RNA-Seq: a revolutionary tool for transcriptomics. *Nature Reviews Genetics* 10:57–63. https://doi.org/10.1038/nrg2484

Wang L, Huang G, Li G, Yuan S, and Wei F. 2025. Updating conservation metagenomics on the gut microbiome of threatened mammals. *IScience* 28:113000. https://doi.org/10.1016/j.isci.2025.113000

Weeks BC, Klemz M, Wada H, Darling R, Dias T, O'Brien BK, *et al*. 2022. Temperature, size and developmental plasticity in birds. *Biology Letters* 18:20220357. http://doi.org/10.1098/rsbl.2022.0357

Whelan FJ, Hall RJ, and McInerney JO. 2021. Evidence for selection in the abundant accessory gene content of a prokaryote pangenome. Agashe D, editor. *Molecular Biology and Evolution* 38:3697–3708. https://doi.org/10.1093/molbev/msab139

Whibley A, Kelley JL, and Narum SR. 2021. The changing face of genome assemblies: Guidance on achieving high-quality reference genomes. *Molecular Ecology Resources* 21:641–652. http://doi:10.1111/1755-0998.13312

Whiteley AR, Fitzpatrick SW, Funk WC, and Tallmon DA. 2010. Genetic rescue to the rescue. *Trends in Ecology & Evolution* 30:42–49. https://doi.org/10.1016/j.tree.2014.10.009

Wold J, Koepfli K-P, Galla SJ, Eccles D, Hogg CJ, Le Lec MF, *et al*. 2021. Expanding the conservation genomics toolbox: incorporating structural variants to enhance genomic studies for species of conservation concern. *Molecular Ecology* 30:5949–5965. https://doi.org/10.1111./mec.16141

Xu Q, Xing S, Zhu C, Liu W, Fan Y, Wang Q, *et al*. 2014. Population transcriptomics reveals a potentially positive role of expression diversity in adaptation. *Journal of Integrative Plant Biology* 57:284–299. https://doi.org/10.1111/jipb.12287

Xu Q, Zhu C, Fan Y, Song Z, Xing S, Liu W, *et al*. 2016. Population transcriptomics uncovers the regulation of gene expression variation in adaptation to changing environment. *Scientific Reports* 6:25536. https://doi.org/10.1038/srep25536

Xue Y, Prado-Martinez J, Sudmant PH, Narasimhan V, Ayub Q, Szpak M, *et al*. 2015. Mountain gorilla genomes reveal the impact of long-term population decline and inbreeding. *Science* 348:242–245. https://doi.org/10.1126/science.aaa3952

Yang F, Ding F, Chen H, He M, Zhu S, Ma X, *et al.* 2018. DNA Barcoding for the identification and authentication of animal species in traditional medicine. *Evidence-Based Complementary and Alternative Medicine* 2018:5160254. https://doi.org/10.1155/2018/5160254

Yeaman S. 2022. Evolution of polygenic traits under global *vs* local adaptation. *Genetics* 220:iyab134. https://doi.org/10.1093/genetics/iyab134.

Yu X, Chen F, Chen Z, Wei P, Song X, Liu C, *et al*. 2023. Genetic diversity and gene expression diversity shape the adaptive pattern of the aquatic plant *Batrachium bungei* along an altitudinal gradient on the Qinghai-Tibet plateau. *Plant Molecular Biology* 111:275–290. https://doi.org/10.1007/s11103-022-01326-0

Zhang D-X, and Hewitt GM. 1996. Nuclear integrations: challenges for mitochondrial DNA markers. *Trends in Ecology & Evolution* 11:247–251. https://doi.org/10.1016/0169-5347(96)10031-8

Associated editors: Giovani Hernández Canchola and Pablo Colunga Salas
Submitted: November 11, 2025; Reviewed: December 17, 2025
Accepted: March 21, 2026; Published online: May 29, 2026

THERYA, 2026, Vol. 17(2):191-200 DOI: 10.12933/therya.2026.6270 ISSN 2007-3364

Mammals as engines of diversification: revisiting the evolutionary history of the *Trypanosoma cruzi* clade

Javier Juárez-Gabriel[1,2*], Spenser J. Babb-Biernacki[3], and Ingeborg Becker[2]

[1]Programa de Doctorado en Ciencias Biomédicas, Universidad Nacional Autónoma de México, Ciudad de México, México.
[2]Centro de Medicina Tropical, División de Investigación, Facultad de Medicina, Universidad Nacional Autónoma de México, Ciudad de México, México. E-mail: becker@unam.mx (IB)
[3]Museum of Natural Science and Department of Biological Sciences, Louisiana State University, Baton Rouge, Louisiana, United States of America. E-mail: sbiern1@lsu.edu (SJB-B)
[*]Corresponding author: javiergabriel@ciencias.unam.mx

The *Trypanosoma cruzi* clade represents one of the most complex and ecologically diverse assemblages of mammalian trypanosomes. Although the group's human pathogenic member *T. cruzi* is best known as the etiological agent of Chagas disease, its evolutionary origins remain debated. Two main hypotheses attempt to explain the diversification of the *T. cruzi* clade: the supercontinent hypothesis, which proposes an ancient co-diversification with South American marsupials, and the bat-seeding hypothesis, which suggests a more recent origin through host-switching from bat trypanosomes. Here, we combined parasite and host phylogenies with global-fit cophylogenetic analyses to evaluate whether mammalian diversification has influenced the evolutionary history of the *T. cruzi* clade. Using PACo and ParaFit, we detected a weak but statistically significant global correspondence between mammal and trypanosome phylogenies. This correspondence was primarily associated with bat-trypanosome relationships, whereas associations involving non-bat mammals showed limited phylogenetic concordance. Together, these findings suggest that mammalian diversification may have influenced trypanosome evolution across multiple evolutionary contexts and timescales.

Keywords: bats, Chiroptera, Chagas disease, cophylogeny, host-switching, Trypanosomatids

El clado *Trypanosoma cruzi* representa uno de los ensambles más complejos y ecológicamente diversos de tripanosomas que infectan mamíferos. Aunque el miembro patógeno para humanos del grupo, *T. cruzi*, es ampliamente conocido como el agente etiológico de la enfermedad de Chagas, sus orígenes evolutivos continúan siendo motivo de debate. Dos hipótesis principales intentan explicar la diversificación del clado *T. cruzi:* la hipótesis del supercontinente, que propone una co-diversificación antigua con los marsupiales sudamericanos, y la hipótesis de "bat seeding", que sugiere un origen más reciente mediante cambios de hospedero a partir de tripanosomas asociados a murciélagos. En este estudio combinamos filogenias de parásitos y hospederos con análisis cofilogenéticos de ajuste global para evaluar si la diversificación de los mamíferos ha influido en la historia evolutiva del clado *T. cruzi*. Utilizando PACo y ParaFit, detectamos una correspondencia global débil pero estadísticamente significativa entre las filogenias de mamíferos y tripanosomas. Esta correspondencia estuvo asociada principalmente a las relaciones murciélago–*Trypanosoma*, mientras que las asociaciones que involucran a mamíferos no quirópteros mostraron una concordancia filogenética limitada. En conjunto, estos patrones sugieren que la diversificación de los mamíferos pudo haber influido en la evolución de los tripanosomas a través de múltiples contextos y escalas evolutivas.

Palabras clave: cambio de hospedero, Chiroptera, cofilogenia, enfermedad de Chagas, murciélagos, Tripanosomátidos

Mammals host a remarkable diversity of kinetoplastid parasites, among which the *Trypanosoma cruzi* clade (subgenus *Schyzotrypanum*) has received heightened attention due to its medical relevance. However, this attention from the medical community has nevertheless failed to resolve the evolutionary origin of *Schizotrypanum*. Determining how *T. cruzi* and its closest relatives emerged, either as relics of ancient Gondwanan lineages or as descendants of bat-associated trypanosomes, is essential for understanding how harmful human parasites originate, as well as reconstructing mammal-parasite coevolution more broadly (Stevens and Gibson 1999; Hamilton and Stevens 2012).

Genomic advances in molecular systematics have benefited our understanding of *Trypanosoma* evolution, revealing repeated transitions between aquatic and terrestrial hosts, frequent host-switching, and instances of recombination and hybridization (Westenberger *et al.* 2005; Simpson *et al.* 2006; Kaufer *et al.* 2017). However, parasite-based phylogenies must be contextualized within the broader evolutionary and biogeographic history of mammals, whose diversification and ecological variation fundamentally constrain and shape parasite radiation (Hamilton *et al.* 2012; Lima *et al.* 2015).

Although trypanosomes in general include taxa that can infect a variety of animals, all known species within *Schizotrypanum* exclusively infect mammals, suggesting a long and dynamic history of adaptation to mammal hosts (Hamilton and Stevens 2010; Lima *et al.* 2013; Cottontail *et al.* 2014; Juárez-Gabriel *et al.* 2024). Two major hypotheses

attempt to explain the origin of this mammal-exclusive clade. The supercontinent hypothesis proposes that the lineage diversified alongside South American marsupials and Triatominae vectors during the breakup of Gondwana, representing a deep Mesozoic ancestry (Stevens and Gibson 1999; Hamilton and Stevens 2012). In contrast, the bat-seeding hypothesis does not propose a single transmission event from bats to other mammals, but rather that bats acted as the primary ancestral hosts and evolutionary reservoir of the *T. cruzi* clade, from which multiple lineages diversified and subsequently colonized other mammalian groups through repeated host-switching events (Hamilton *et al.* 2012; Lima *et al.* 2013; Lima *et al.* 2015).

Aspects of mammalian diversification and observed trypanosome diversity correspond with both hypotheses. Marsupials retain long-standing associations with *T. cruzi*, a pattern historically interpreted as consistent with a Gondwanan origin of the clade [based largely on ecological persistence rather than explicit phylogenetic congruence] (Stevens and Gibson 1999; Hamilton and Stevens 2012). However, bats exhibit unparalleled trypanosome diversity and dispersal capacity, supporting their role as primary contributors to diversification within *Schizotrypanum* (Hamilton *et al.* 2012; Cottontail *et al.* 2014; Lima *et al.* 2015). Against the backdrop of both hypotheses, rodents, carnivores, and primates appear to have acquired *T. cruzi* through more recent and ecologically mediated host-switch events (Rocha *et al.* 2013; Jansen *et al.* 2015). By integrating molecular phylogenies and global-fit cophylogenetic analysis, the aim of this study was to analyze how mammalian evolution has influenced the origin and diversification of the *T. cruzi* clade.

Materials and methods

Trypanosoma spp. and mammalian hosts sequence dataset. We compiled publicly available sequences belonging to members of the *T. cruzi* clade. Sequences were retrieved from GenBank from studies that explicitly reported natural infections in mammals. Only accessions with confirmed host origin in the original publication were included. We used a fragment of the *18S rDNA* gene because it is widely available and informative for resolving relationships within *Trypanosoma*.

Redundant, low-quality (<500 bp), chimeric, or environmental sequences lacking host information were excluded. The final dataset consisted of 19 parasite species or lineages (see Supplementary Table S1).

To reconstruct host phylogeny, we assembled mitochondrial *cytochrome b* (*Cytb*) sequences exclusively from mammalian species in which trypanosomes have been molecularly confirmed. Sequences were obtained from peer-reviewed publications. When multiple sequences were available, we prioritized those from the same locality where the associated parasite was reported. The final host dataset included 58 species across different orders from Mammalia (see Supplementary Table S2).

Phylogenetic analysis and host-parasite matrix. Parasite and host datasets were aligned independently using MAFFT v7 with the L-INS-i algorithm. Resulting alignments were visually inspected and manually trimmed in AliView to remove ambiguously aligned regions and ensure positional homology.

Phylogenetic trees were inferred using IQ-TREE v2, implementing the best-fit substitution model selected by ModelFinder based on Bayesian Information Criterion (BIC). For *Trypanosoma* tree we used 19 sequences with 878 nucleotid sites, and the Best-fit model calculated was: TIM3e+I+G4. On the other hand, for host tree, we used 58 sequences with 1140 nucleotid sites, and the Best-fit model according to BIC was: GTR+F+I+G4. Nodal support was assessed using 1,000 ultrafast bootstrap replicates (UFBoot) and SH-aLRT tests. Trees were visualized and edited in FigTree v.1.4.4.

We constructed a binary host–parasite association matrix. Each parasite sequence was matched to its corresponding host species based on published reports. Only associations explicitly supported by primary literature were included; ambiguous or assumed associations were excluded (see Supplementary Table S3).

Cophylogenetic analyses. To assess whether mammal phylogeny influences the diversification of trypanosomes in the *T. cruzi* species complex, we tested whether there is a statistically significant global fit between host and parasite trees. To accomplish this, we first converted the phylogenetic trees of the *T. cruzi* species complex and their mammal hosts into distance matrices using the "*cophenetic.phylo*" function from the R package *ape* (v 5.8-1) (Paradis and Schliep 2019) as implemented in R Studio (v. 4.5.0), applying a cailliez correction to account for negative eigenvalues. We then tested the global congruence of these trees using two cophylogenetic fitting methods: PACo (Balbuena *et al.* 2013), in which we performed 10,000 permutations to generate a null distribution, and ParaFit (Legendre *et al.* 2002), in which we performed 999 permutations. For the PACo results, we also analyzed how strongly individual host-parasite relationships influenced the global congruence of host and parasite trees by performing jackknife estimation of their square residuals with the "*paco_links*" function. We assessed whether individual host-parasite relationships were statistically significantly correlated using the "*ParaFitLink1*" function in ParaFit.

To determine if bat:trypanosome relationships contributed disproportionately to the global signal of cophylogenetic concordance detected by PACo, we sorted the PACo residuals into two groups that represented bat:trypanosome and non-bat:trypanosome associations. We then performed a one-tailed two-sample *t*-test to assess whether bats and their trypanosomes had significantly lower residuals than non-bats, which would suggest they disproportionately drive the global cophylogenetic signal in the dataset.

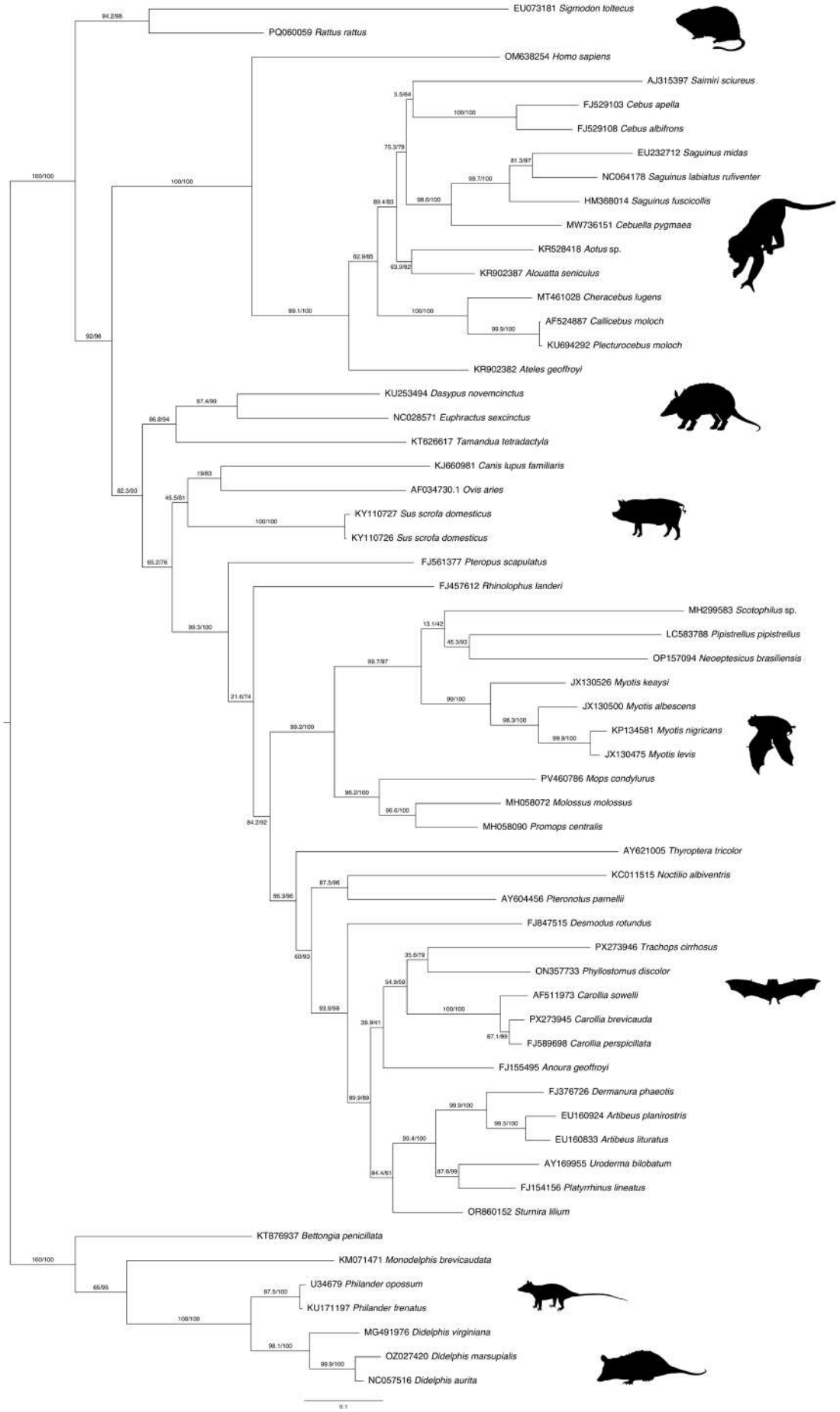

Figure 1. Phylogenetic relationships among mammalian hosts included in this study, inferred from mitochondrial (*Cytb*) sequences. Only ≥70 branch support values are shown.

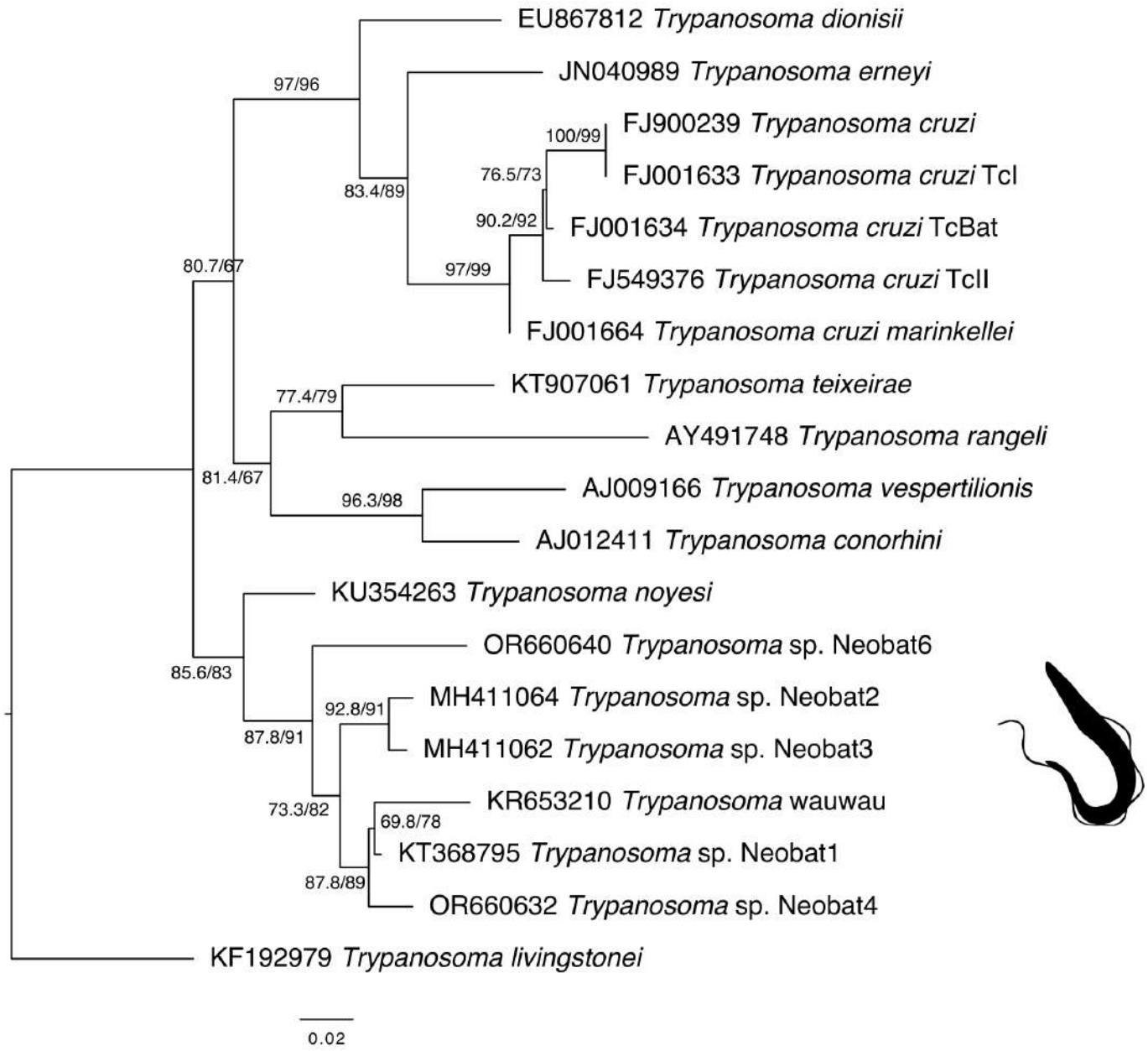

Figure 2. Phylogenetic relationships among *Trypanosoma cruzi* clade species inferred from partial *18S rDNA* sequences.

Results

The mammalian phylogeny inferred from the *Cytb* sequences recovered well-supported relationships across the major mammalian groups included in the analysis (Figure 1). These comprised Artiodactyla, Carnivora, Chiroptera, Marsupialia, Rodentia, and Xenarthra, each forming distinct and largely well-supported clades consistent with established mammalian phylogenies. Within Chiroptera, representatives of Phyllostomidae (*Artibeus, Carollia, Dermanura, Phyllostomus, Sturnira, Uroderma, Anoura, Trachops, Desmodus, Pteronotus*), Molossidae (*Molossus, Promops, Mops*), Vespertilionidae (*Myotis, Eptesicus, Pipistrellus, Scotophilus*), Rhinolophidae (*Rhinolophus*), Pteropodidae (*Pteropus*) and, Thyropteridae (*Thyroptera*), were recovered as monophyletic or near-monophyletic groups, with generally high branch nodal support value (>85%).

Marsupials clustered into a coherent clade including Didelphidae (*Didelphis, Philander, Monodelphis*), and Potoroidae (*Bettongia*), while placental mammals were distributed among expected orders. Although some deeper relationships showed moderated support (Figure 1), overall tree topology was congruent with previously published mitochondrial-based mammalian phylogenies, *i.e.* Primates were represented by multiple Neotropical lineages spanning Atelidae, Cebidae, Pitheciidae, Callitrichidae, Aotidae, and Hominidae, indicating that the host tree provides an appropriate framework for subsequent cophylogenetic analysis.

Phylogenetic reconstruction of trypanosomes based on *18S rDNA* sequences resolved the *T. cruzi* clade as a well-supported monophyletic group (Figure 2). Within this clade, bat associated trypanosomes occupied several basal

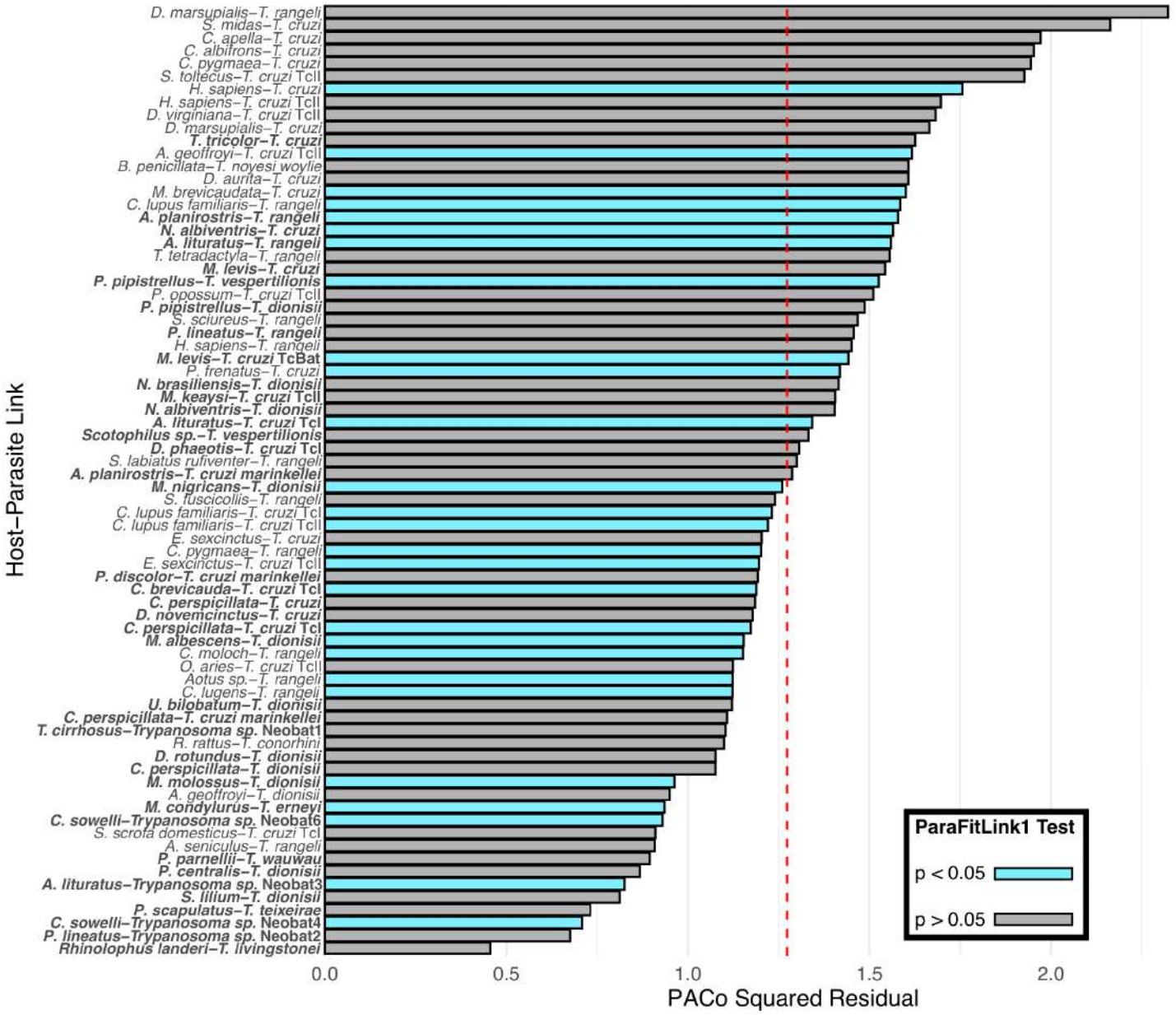

Figure 3. PACo jackknifed squared residuals of each host-parasite link between mammal hosts and trypanosome parasites included in this analysis. Lower residual values (bars) correspond to greater cophylogenetic signal of that host-parasite link. Bars are colored according to whether a given host-parasite link was found to exhibit statistically significant cophylogenetic signal according the ParaFitLink1 test. Red dashed line denotes the overall median PACo squared residual value.

and early diverging positions. Species such as *T. dionisii*, *T. erneyi*, *T. cruzi*, *T. livingstonei*, and multiple Neotropical bat-associated lineages formed distinct, well-supported subclades. Together, the reconstructed mammalian and trypanosome phylogenies provide the basis for evaluating patterns of host-parasite phylogenetic correspondence using global-fit cophylogenetic analyses.

Both PACo and ParaFit detected a weak but statistically significant global correspondence between host and parasite trees when compared to random permutations (PACo: m2 = 33.4040, p = 0.0004; ParaFit: ParaFitGlobal = 2.1457, p = 0.003). The weak global fit suggests that this statistical significance is driven by a few strongly correlated host-parasite associations amidst largely incongruent host-parasite trees, which was recapitulated by individual jackknifed squared residual values calculated in PACo, as well as tests of association significance in ParaFit. PACo residual values appeared to demonstrate that bat trypanosomes were the biggest drivers of this (Figure 3): of the 10 host-parasite associations contributing the most to the global cophylogenetic signal (lowest squared residuals), 8 involve bats, while none of the 10 associations with the highest squared residuals involve bat hosts. A one-tailed two sample *t*-test confirmed the statistical significance of this pattern, as bat:trypanosome relationships were characterized by PACo residuals that were significantly lower than those of non-bat:trypanosome relationships (p < 0.001, Cohen's d = 0.95) (Figure 4). This supports bats and their resident trypanosomes as the primary drivers of global cophylogenetic signal between these two trees.

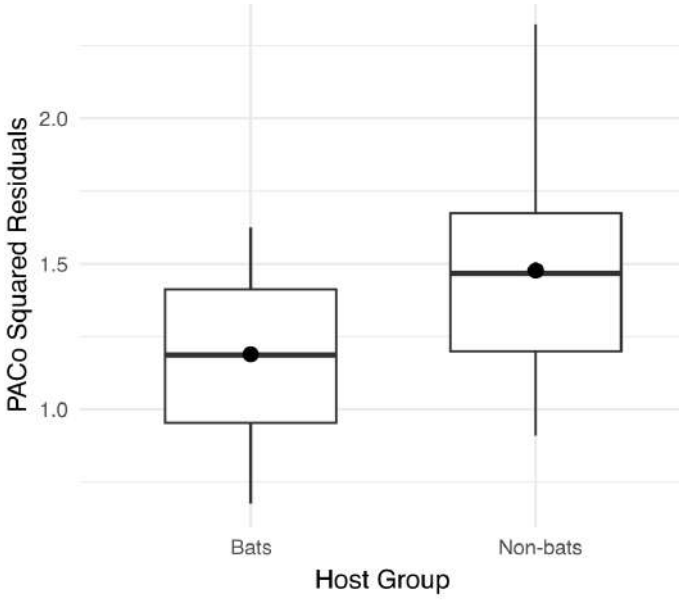

Figure 4. Distribution of PACo jackknifed squared residual values of host-trypanosome links in bat vs. non-bat hosts. Mean residual values added to plots as a black dot. Lower residuals indicate greater contribution to global cophylogenetic signals. Bats and their associated trypanosomes exhibit significantly lower residuals when compared to non-bat hosts ($p < 0.001$, Cohen's d = 0.95).

However, the identification of significant relationships using ParaFitLink1 did not strongly favor bat-trypanosome associations as drivers of the cophylogenetic signal. Instead, it was more likely to identify trypanosome taxa with very broad host ranges, such as *T. cruzi* infecting hosts as distantly related as the placental *Homo sapiens* (humans) and the marsupial *Monodelphis brevicaudata* (northern red-sided opossum), as exhibiting significant cophylogenetic concordance. Significant ParaFit *p*-values were also not strongly correlated with low squared PACo residuals (Figure 3), consistent with previous findings that ParaFit frequently identifies associations with very high PACo residuals to be nevertheless statistically significant.

Discussion

The evolutionary origin of the *T. cruzi* clade remains one of the most debated topics in kinetoplastid systematics, with two dominant competing hypotheses: a Gondwanan origin associated with early South American marsupials (Hoare 1972; Stevens and Gibson 1999; Hamilton and Stevens 2012), and a more recent origin arising from bat-associated trypanosomes (Hamilton *et al.* 2012). By explicitly testing patterns of host-parasite phylogenetic correspondence across mammalian hosts with confirmed infections, this study contributes new evidence to clarify how mammalian diversification shaped the evolutionary trajectory of the *T. cruzi* clade.

Our cophylogenetic analyses detected global cophylogenetic signal between host and parasite phylogenetic trees, suggesting mammal diversification does influence diversification of this trypanosome clade, as well as providing some support for the bat-seeding hypothesis. Although the program ParaFit did not find evidence of bats driving cophylogenetic signal, its assumption of cophylogenetic symmetry likely limits how well the analysis can assess biological reality. PACo, meanwhile, assumes asymmetric dependence, in which the parasite phylogeny is unidirectionally influenced by the host phylogeny (Balbuena *et al.* 2013), which better represents how host-parasite clades tend to evolve. This asymmetric analysis instead produced a strong and statistically significant finding that bat:trypanosome relationships are the primary drivers of cophylogenetic signal in this host-parasite assemblage. This concordance between bat and parasite phylogenies supports the hypothesis that bat diversification shaped trypanosome evolution, while the relative lack of cophylogenetic signal in non-bat:trypanosome associations is consistent with host switching leading to colonization of other hosts. Furthermore, marsupial:trypanosome links corresponded to some of the highest residuals in the PACo analysis, suggesting a lack of cophylogenetic signal and arguing against a marsupial-associated Gondwanan origin of *Schizotrypanum* from a cophylogenetic perspective.

Nevertheless, the disagreement between PACo and ParaFit results highlights the difficulties of applying traditional cophylogenetic analyses to systems that include broadly generalist parasites, such as *T. cruzi* and *T. rangeli,* which infect hosts as distantly related as marsupials and placentals. Such extreme generalists complicate cophylogenetic analysis and can lead to erroneous findings of congruence such as those presumably inferred by ParaFit in this work (Refrégier *et al.* 2008; de Vienne *et al.* 2013). It is also possible that sampling bias has made some taxa, such as the clade of novel Neotropical bat trypanosomes, appear more host-specific than they truly are (Sweet *et al.* 2016; Dallas *et al.* 2017). Further sampling of Mammalia may uncover these novel taxa in other hosts and dilute the cophylogenetic signal associated with bats. While we encourage improved sampling of trypanosomes across mammal diversity to address this concern, cophylogenetic analysis of all currently known taxa in the *Schizotrypanum* clade favors bat-seeded origins.

Multiple multilocus phylogenies have demonstrated that *Schizotrypanum* is a monophyletic group composed exclusively of mammalian parasites (Hamilton and Stevens 2010; Hamilton *et al.* 2012; Austen and Barbosa 2021). Within this clade, bat trypanosomes such as *T. dionisii*, *T. cruzi marinkellei*, *T. erneyi*, and *T. livingstonei* consistently occupy basal positions, indicating that the earliest diversification events occurred within bats rather than in marsupials or other terrestrial hosts (Marcili *et al.* 2009; Lima *et al.* 2013; Cottontail *et al.* 2014; Dos Santos *et al.* 2018). This recurrent phylogenetic pattern forms the conceptual core of the bat-seeding hypothesis, which proposes bats as the primary ancestral hosts rather than incidental reservoirs.

Furthermore, the discovery of *T. livingstonei* in African bats provides additional support for the idea that the origins of the *T. cruzi* clade may be older and geographically

broader than initially assumed (Lima *et al.* 2013; Pereira *et al.* 2022). Rather than being strictly Neotropical and tightly tied to South American marsupials, ancestral lineages may have diversified in bats across multiple continents, consistent with the high mobility and global distribution of these mammals. In addition, the persistence of the bat-restricted TcBat lineage, even in regions where other *T. cruzi* DTUs circulate broadly among terrestrial mammals, reinforces the notion that bats constitute an ancestral reservoir and continue to harbor unique parasite lineages (Marcili *et al.* 2009; Lima *et al.* 2015).

These phylogenetic insights are consistent with the ecological characteristics of bats. Their ability to fly, form dense colonies, migrate long distances, and exploit a wide range of habitats create ideal conditions for parasite transmission, diversification, and geographic expansion (Cottontail *et al.* 2014; Austen and Barbosa 2021; Peixoto *et al.* 2019). Consequently, bats act not only as hosts but also as evolutionary engines, repeatedly generating opportunities for host-switch events and shaping the structure of the *T. cruzi* clade.

On the other hand, marsupials, particularly didelphid opossums, are well established as key components of contemporary sylvatic cycles of *T. cruzi* in the Neotropics (Jansen *et al.* 2015; Jansen *et al.* 2018). Their high infection rates and capacity to support parasite development have long been cited as evidence for a deep evolutionary association. However, recent phylogenetic studies of didelphids show that most of their diversification occurred during the Miocene (Jansa *et al.* 2013), well after the breakup of Gondwana. This temporal mismatch weakens the plausibility of a strict Gondwanan co-diversification scenario, suggesting that marsupials are more likely to represent long-standing ecological reservoirs rather than ancestral hosts.

Similarly, numerous other mammalian groups, including rodents, carnivores, xenarthrans, and primates, are frequently infected by *T. cruzi* in sylvatic environments (Rocha *et al.* 2013; Gürtler *et al.* 2015; Jansen *et al.* 2018). While these associations highlight the ecological flexibility of the parasite, they do not imply a primary evolutionary role for these hosts. Instead, the available evidence suggests that these mammals' function mainly as secondary or bridge hosts, particularly in disturbed or anthropogenic landscapes, contributing more to parasite maintenance and spread than to its early diversification (Hamilton *et al.* 2012; Jackson 2015).

Recognizing bats as central to the origin of the *T. cruzi* clade has important implications for both evolutionary biology and disease ecology. It underscores the deep evolutionary flexibility of the parasite and suggests that novel host associations may continue to arise. It also highlights the need for expanded sampling of bat trypanosomes worldwide, particularly in Africa and Asia, where basal lineages remain poorly characterized (Pinto *et al.* 2015; Austen and Barbosa 2021).

Although this study refines the evolutionary context of the *T. cruzi* clade, several limitations remain. Genomic sampling of bat-associated trypanosomes is still incomplete, deep-time calibration of host and parasite phylogenies remains uncertain, and vector–host interactions are poorly resolved in many regions. Future work integrating genome-scale data, expanded host sampling, and time-calibrated cophylogenetic frameworks will be essential to fully reconstruct the origins and diversification of *T. cruzi* clade.

Acknowledgements

We gratefully acknowledge Dr. Livia León-Paniagua for her profound influence on the development of mammalogy in Mexico and for her invaluable role as a mentor, colleague, and scientific leader. Her contributions to the study of mammalian systematics and biogeography, together with her commitment to academic training, have shaped multiple generations of researchers. For the authors, her guidance, generosity, and passion for science have had a lasting impact on our academic and professional trajectories, making this contribution particularly fitting for this commemorative issue. This work was supported by UNAM-PAPIIT IG200924.

Declaration of Artificial Intelligence use

Artificial intelligence was used only to assist with English grammar and manuscript wording (Grammarly Pro). All suggestions were carefully reviewed by the authors, who take full responsibility for the final version of the manuscript. The original manuscript, with all ideas, is original to the authors.

Author contributions

Javier Juárez-Gabriel: conceptualization, methodology, investigation, data curation, formal analysis, visualization. Spenser J. Babb-Biernacki: methodology, formal analysis and visualization. Ingeborg Becker: conceptualization and supervision. All authors made substantial contributions to the design, development, analysis, and writing, reviewing and editing of the manuscript, approved the final version, and agreed to be accountable for all aspects of the work.

Data availability

All DNA sequences used in this study were obtained from public databases and are available in GenBank. The corresponding accession numbers are listed in Supplementary Table S1.

The sequence alignments used for phylogenetic reconstruction of hosts (*Cytb*, Supplementary Data S1) and parasites (*18S rDNA*, Supplementary Data S2), as well as the host–parasite association matrices employed in the cophylogenetic analyses (Supplementary Table S3), are provided as Supplementary Material accompanying this manuscript.

Supplementary data

SDT1. Accession numbers of mammalian *Cytb* sequences used in this study.

SDT2. Accession numbers of trypanosomatid *18S rDNA* sequences used in this study.

SDT3. Host–parasite association matrices for cophylogenetic analyses.

SD1. FASTA-formatted alignment of mammalian *Cytb* sequences used in this study.

SD2. FASTA-formatted alignment of trypanosomatid *18S rDNA* sequences used in this study.

Literature cited

Austen JM, and Barbosa AD. 2021. Diversity and Epidemiology of Bat Trypanosomes: A One Health Perspective. *Pathogens* 6:1148. https://doi.org/10.3390/pathogens10091148

Balbuena JA, Míguez-Lozano R, and Blasco-Costa I. 2013. PACo: a novel Procrustes application to cophylogenetic analysis. *PLoS One* 8:e61048. https://doi.org/10.1371/journal.pone.0061048

Cottontail VM, Kalko EKV, Wellinghausen N, Tschapka M, Perkins SL, and Pinto CM. 2014. High local diversity of *Trypanosoma* in a common bat species and implications for the biogeography and taxonomy of the *T. cruzi* clade. *PLoS One* 9:e108603. https://doi.org/10.1371/journal.pone.0108603

Dallas T, Huang S, Nunn CL, Park AW, and Drake JM. 2017. Estimating parasite host range. *Proceedings of the Royal Society B: Biological Sciences* 284:20171250. https://doi.org/10.1098/rspb.2017.1250

de Vienne DM, Refrégier G, López-Villavicencio M, Tellier A, Hood ME, and Giraud T. 2013. Cospeciation vs host-shift speciation: methods for testing, evidence from natural associations and relation to coevolution. *New Phytologist* 198:347–385. https://doi.org/10.1111/nph.12150

Dos Santos FCB, Lisboa CV, Xavier SCC, Dario MA, Verde RS, Calouro AM, *et al.* 2018. *Trypanosoma* sp. diversity in Amazonian bats (Chiroptera; Mammalia) from Acre State, Brazil. *Parasitology* 145:828–837. https://doi.org/10.1017/S0031182017001834

Gürtler RE, Cecere MC, Lauricella MA, Cardinal MV, and Kitron U. 2015. Domestic dogs and cats as sources of *Trypanosoma cruzi* infection in rural northwestern Argentina. *Parasitology* 142:181–191. https://doi.org/10.1017/S003118201400150X

Hamilton PB, Cruickshank C, Stevens JR, Teixeira MMG, and Mathews F. 2012. Parasites reveal movement of bats between the New and Old Worlds. *Molecular Phylogenetics and Evolution* 63:521–526. https://doi.org/10.1016/j.ympev.2012.01.013

Hamilton PB, and Stevens JR. 2010. Classification and phylogeny of *Trypanosoma cruzi*. In: Telleria J, and Tibayrenc M, editors. *American trypanosomiasis: Chagas disease one hundred years of research*. London (UK): Elsevier; p. 321–338. https://doi.org/10.1016/B978-0-12-384876-5.00013-7

Hamilton PB, and Stevens JR. 2012. The evolution of *Trypanosoma cruzi*: the bat-seeding hypothesis. *Trends in Parasitology* 26:190–196. https://doi.org/10.1016/j.pt.2010.01.006

Hoare CA. 1972. The Trypanosomes of Mammals. *Blackwell, Oxford*. 749.

Jackson AP. 2015. The evolution of parasite genomes and the origins of parasitism. *Parasitology* 142:S40–S56. https://doi.org/10.1017/S0031182014000894

Jansa SA, Barker FK, and Voss RS. 2013. The early diversification history of didelphid marsupials: a window into South America's splendid isolation. *Evolution* 68:684–695. https://doi.org/10.1111/evo.12290

Jansen AM, Xavier SC, and Roque ALR. 2015. The multiple and complex scenarios of *Trypanosoma cruzi* sylvatic transmission. *Acta Tropica* 151:1–15. https://doi.org/10.1016/j.actatropica.2015.07.018

Jansen AM, Xavier SCDC, and Roque ALR. 2018. *Trypanosoma cruzi* transmission in the wild and its most important reservoir hosts in Brazil. *Parasites & Vectors* 11:502. https://doi.org/10.1186/s13071-018-3067-2

Juárez-Gabriel J, Alegría-Sánchez D, Yáñez-Aguirre D, Grostieta E, Álvarez-Castillo L, Torres-Castro M, *et al.* 2024. Unraveling the diversity of *Trypanosoma* species from Central Mexico: molecular confirmation of *Trypanosoma dionisii* and novel Neobat lineages. *Acta Tropica* 251:106875. https://doi.org/10.1016/j.actatropica.2023.107113

Kaufer A, Ellis J, Stark D, and Barratt J. 2017. The evolution of trypanosomatid taxonomy. *Parasites & Vectors* 10:287. https://doi.org/10.1186/s13071-017-2204-7

Legendre P, Desdevises Y, and Bazin E. 2002. A Statistical Test for Host-Parasite Coevolution. *Systematic Biology* 51:217–234. https://doi.org/10.1080/10635150252899734

Lima L, Espinosa-Álvarez O, Hamilton PB, Neves L, Takata CSA, Campaner M, *et al.* 2013. *Trypanosoma livingstonei*: a new species from African bats supports the bat-seeding hypothesis for the *Trypanosoma cruzi* clade. *Parasites & Vectors* 6:221. https://doi.org/10.1186/1756-3305-6-221

Lima L, Espinosa-Álvarez O, Pinto CM, Cavazzana M Jr, Pavan AC, Carranza JC, *et al.* 2015. New insights into the evolution of the *Trypanosoma cruzi* clade from a novel trypanosome tightly linked to *Pteronotus* bats and related to an Australian lineage of trypanosomes. *Parasites & Vectors* 8:657. https://doi.org/10.1186/s13071-015-1255-x

Marcili A, Lima L, Cavazzana M, Junqueira AC, Veludo HH, Maia Da Silva F, *et al.* 2009. A new genotype of *Trypanosoma cruzi* associated with bats evidenced by phylogenetic analyses using SSU rDNA, cytochrome b and Histone H2B genes and genotyping based on ITS1 rDNA. *Parasitology* 136:641–55. https://doi.org/10.1017/S0031182009005861

Paradis E, and Schliep K. 2019. ape 5.0: an environment for modern phylogenetics and evolutionary analyses in

R. *Bioinformatics* 35:526–528. https://doi.org/10.1093/bioinformatics/bty633

Peixoto FP, Braga PHP, and Peixoto PM. 2018. A synthesis of ecological and evolutionary determinants of bat diversity across spatial scales. *BMC Ecology* 18:18. https://doi.org/10.1186/s12898-018-0174-z

Pereira SS, Jackson AP, and Figueiredo LM. 2022. Evolution of the variant surface glycoprotein family in African trypanosomes. *Trends in Parasitology* 38:39–52. https://doi.org/10.1016/j.pt.2021.07.012

Pinto CM, Ocaña-Mayorga S, Tapia EE, Lobos SE, Zurita AP, Aguirre-Villacís F, *et al.* 2015. Bats, trypanosomes, and triatomines in Ecuador: new insights into the diversity, transmission, and origins of *Trypanosoma cruzi*. *PLoS One* 10:e0139999. https://doi.org/10.1371/journal.pone.0139999

Refrégier G, le Gac M, Jabbour F, Widmer A, Shykoff JA, Yockteng R, *et al.* 2008. Cophylogeny of the anther smut fungi and their caryophyllaceous hosts: prevalence of host shifts and importance of delimiting parasite species for inferring cospeciation. *BMC Evolutionary Biology* 8:100. https://doi.org/10.1186/1471-2148-8-100

Rocha FL, Roque ALR, Lima JS, Cheida CC, Lemos FG, Azevedo FC, *et al.* 2013. *Trypanosoma cruzi* infection in Neotropical wild carnivores (Mammalia: Carnivora): at the top of the *Trypanosoma cruzi* transmission chain. *PLoS One* 8:e67463. https://doi.org/10.1371/journal.pone.0067463

Simpson AG, Stevens JR, and Lukes J. 2006. The evolution and diversity of kinetoplastid flagellates. *Trends in Parasitology* 2:168–74. https://doi.org/10.1016/j.pt.2006.02.006

Stevens JR, and Gibson WC. 1999. The evolution of pathogenic trypanosomes. *Cadernos de Saúde Pública* 15:673–684. https://doi.org/10.1590/S0102-311X1999000400002

Sweet AD, Boyd BM, and Johnson KP. 2016. Cophylogenetic patterns are uncorrelated between two lineages of parasites on the same hosts. *Biological Journal of the Linnean Society* 118:813–828. https://doi.org/10.1111/bij.12771

Westenberger SJ, Barnabé C, Campbell DA, and Sturm NR. 2005. Two hybridization events define the population structure of *Trypanosoma cruzi*. *Genetics* 171:527–43. https://doi.org/10.1534/genetics.104.038745

Associated editors: Giovani Hernández Canchola and Pablo Colunga Salas
Submitted: December 31, 2025; Reviewed: March 5, 2026
Accepted: March 23, 2026; Published online: May 29, 2026

THERYA, 2026, Vol. 17(2):201-212 DOI: 10.12933/therya.2026.6275 ISSN 2007-3364

Status and shortfalls in the availability of genetic sequences and associated metadata for Mexican mammals

Luis D. Verde Arregoitia[1*], Martín Y. Cabrera Garrido[1], Julia Saravia[2,3], Lillian Draper Parker[4], and Fabricio Villalobos[1]

[1]Red de Biología Evolutiva, Instituto de Ecología A.C, Xalapa, Veracruz 91073, Mexico. Email: martin.cabrera@posgrado.ecologia.edu.mx (MYCG); fabricio.villalobos@inecol.mx (FV)
[2]Instituto de Ciencias Marinas y Limnológicas, Universidad Austral de Chile, Valdivia, Chile
[3]Millenium Institute Biodiversity of Antarctic and Subantarctic Ecosystems, BASE. E-mail: saraviajulia@gmail.com (JS)
[4]Laboratories of Molecular Anthropology and Microbiome Research, Department of Anthropology, University of Oklahoma, Norman, OK, USA. E-mail: lilly.parker@gmail.com (LDP)
[*]Corresponding author: luis@liomys.mx

Genetic information represents an important dimension of biodiversity beyond species or ecosystems, and genetic sequences are essential for all themes in biodiversity research. Genetic data are not exempt from gaps and biases, particularly in the tropics. Even for well-studied groups like mammals, many species remain understudied, and the completeness of underlying metadata for existing sequences is largely unknown. We quantified genetic data availability for 548 species of Mexican land mammals in the NCBI Nucleotide database. We evaluated the status and completeness of metadata regarding dates, locations, and voucher information associated with sequences, noting endemic species. We located genetic data for 90% of species, including sequences for 77% of Mexican endemics. Availability was skewed, with most species having very few sequences. In our sample, 316 of 496 species (64%) had at least one record with location, date, and voucher information, yet metadata quality was highly variable, and most records lacked key spatiotemporal details. We identified highly biased coverage in nucleotide sequence availability and relatively poor metadata quality for Mexican land mammals. Despite decades of sampling, decreasing costs, and advances in museomics and sequencing, major gaps and disparities remain. At a time of open science and open data, we insist on a research culture where sampling, sequencing, and adequate metadata recording happen concurrently.

Keywords: bioinformatics, entrez, GenBank, molecular, reproducibility

La información genética representa una dimensión clave de la diversidad más allá de especies o ecosistemas, y las secuencias son esenciales para investigar sobre biodiversidad. Los datos genéticos presentan vacíos y sesgos, especialmente en regiones tropicales. Incluso en grupos bien estudiados como los mamíferos, muchas especies permanecen poco estudiadas, y se desconoce la integridad de los metadatos asociados a sus secuencias. En el presente trabajo, cuantificamos la disponibilidad de datos genéticos para 548 especies de mamíferos terrestres mexicanos en la base de datos 'Nucleotide' de NCBI, evaluando la completitud de los metadatos sobre fechas, localidades e información de ejemplares asociada a las secuencias, tomando en cuenta la situación particular de las especies endémicas. Encontramos datos genéticos para el 90% de las especies, incluyendo 77% de las endémicas, con un sesgo en la disponibilidad, ya que la mayoría de las especies contaba con muy pocas secuencias. Encontramos que 316 de 496 especies (64 %) tenían al menos un registro con localidad, fecha, y ejemplar, aunque la calidad de los metadatos fue variable y la mayoría carecía de datos espaciotemporales. A pesar de décadas de muestreo, costos decrecientes y avances en museómica y secuenciación, persisten los vacíos. Identificamos un sesgo en la disponibilidad de secuencias nucleotídicas y una calidad relativamente deficiente en los metadatos para los mamíferos de México. En una era de ciencia y datos abiertos, insistimos en una cultura de investigación donde muestreo, secuenciación y registro adecuado de metadatos ocurran en paralelo.

Palabras clave: bioinformática, entrez, GenBank, molecular, reproducibilidad

Globally, DNA sequence data have been generated, collected, and aggregated for over 35 years. This endeavor has been supported and promoted by various national and international initiatives, including specialized infrastructure to collate and share this important information online (Arita *et al.* 2021). These collections of open genetic resources have an unquestionable role in answering research questions in phylogenetics, evolution, ecology, and conservation (Blaxter *et al.* 2022). For example, the GenBank (Benson *et al.* 2013) sequence database is a prime example of globally-centralized and standardized repositories of nucleotide sequence data meant for archiving, reuse, and re-analysis. GenBank is one of multiple primary repositories in the International Nucleotide Sequence Database Collaboration (INSDC), alongside nodes such as the European Nucleotide Archive (ENA) and the DNA DataBank of Japan (DDBJ); through international collaboration, all members synchronize and share their data to form a unified global resource. GenBank is produced and maintained by the National Center for Biotechnology Information (NCBI; part of the National Institutes of Health in the USA). GenBank is public and freely and openly accessible, and it has become a key component of modern biodiversity research (Leray *et al.* 2019).

Sequence data alone is incredibly valuable, but it is also a sensible scientific practice to record and share supporting metadata related to sample provenance, such

as spatiotemporal information regarding sampling location and date, to achieve its full potential (Dunnum *et al.* 2020). GenBank originated as and remains a public archive of genetic sequences and annotations and increased over time in the amount and nature of secondary information that can be recorded. As an archive for sequences produced across multiple disciplines (e.g., biomedical research, synthetic biology, human health, and molecular function), its metadata focuses on documenting the sequences compactly. However, these limited metadata meant to at least record a sampling location, remain useful for biodiversity science. Since 2005, GenBank has had the option for recording location data (country, locality, latitude, and longitude) for sequences in a dedicated metadata field, which can connect sequence data to the geographical locations where samples were collected (Gratton *et al.* 2017). Linking sequences to the museum vouchers sampled for sequencing (when applicable) is also possible. Vouchers in this context are the crucial link between nucleotide sequences, the taxonomic identity of the referred sequence, and physical specimens that are preserved, cataloged, and curated following standardized protocols (Buckner *et al.* 2021). When sequences are derived from physical specimens in scientific collections, these specimens can and should provide additional individual-level information such as sex, age, or body size.

Accurate documentation and usable metadata are crucial for enhancing the utility and reproducibility of molecular datasets (Galvao Elias *et al.* 2024). However, recording spatiotemporal and voucher metadata was optional when uploading sequences to databases like GenBank until late 2024 (NCBI Staff 2023). Even when this information adds context, value, and usability to primary molecular data, these data may not be shared—even when it was recorded. Such reluctance can be due to a variety of reasons relating to technical workflows, journal or funding body requirements (or lack thereof), or research culture (Sidlauskas *et al.* 2010). These issues are pervasive and not limited to metadata for genetic sequences, and work is underway to understand and lower the different barriers to data-sharing (Pope *et al.* 2015; Verde Arregoitia *et al.* 2020).

Existing studies have already revealed important gaps in metadata for nucleotide sequence data. In 2013, most sequences on GenBank lacked fundamental data such as geographical and vouchering information (Marques *et al.* 2013). Even when geographic information is provided for sequence data, it is often not precise enough for repurposing in spatially explicit analyses, mainly because coordinates or unambiguous locality details are not provided (Pope *et al.* 2015). In addition, missing temporal information also affects subsequent analyses. For example, a 2020 study of global genetic diversity in time and space had to focus on a small subset of sequences relative to all data available on GenBank because of lacking collection years in the metadata (Millette *et al.* 2020). Missing metadata for existing sequences undermines the lasting reuse and integration of public data and depletes massive amounts of resources in terms of funds, time, and wasted opportunities such as unique samples destroyed and expensive reagents consumed. Even when substantial efforts have been made to cross-reference available repositories of geographic and genetic information and ultimately bring spatial context to sequences (Pelletier *et al.* 2022), this is technically and computationally challenging. Cross-referencing massive batches of data from disparate sources involves interacting with application programming interfaces (APIs) and working efficiently with big data, and ultimately this process would need to be repeated periodically.

In addition to gaps in metadata for existing nucleotide sequences, there is great variation in the taxa or places that are better represented in public databases of genetic information (Pitogo 2025). A recent evaluation of public sequence data found that one quarter of terrestrial vertebrates worldwide had no genetic data and that mammals were the most sampled group, with 81% of species represented with at least one gene (Šmíd 2022). This study found that unsampled mammals tend to be taxa from Equatorial Africa, New Guinea, Sumatra, and inland Australia. Taxonomically, the least-sequenced families are Abrocomidae and Dasyproctidae (both Rodentia), with only 40% of their species sampled, followed by Gliridae (48%) and other less speciose families, including Tragulidae and Nycteridae, at ~50% completeness (Šmíd 2022).

In general, the species that remain unsampled are important to investigate, since they are not a random subset of diversity. Entire clades, regions, or countries may be altogether missing molecular data (Lim 2012). These unsampled taxa follow known gaps in biodiversity knowledge in which highly diverse tropical regions are less studied (Hughes *et al.* 2021). Research effort is also biased towards larger-bodied and more widely distributed species (Moura *et al.* 2024). It is also possible for regions or taxa to have high-quality genetic or genomic data, but without adequate metadata. This disconnect confounds the true nature of knowledge gaps and reduces the value of existing sequences, potentially compromising the results and inferences made with incomplete information.

Despite their high genetic sampling relative to other vertebrate groups, mammals are a group worth investigating in regard to the availability of nucleotide sequence data, as well as the status of the underlying metadata for existing sequences. In particular, terrestrial mammals that occur in Mexico represent an important opportunity for study given the high species richness and endemism (Vázquez and Gaston 2004) and worrying conservation status (Zamora-Gutierrez *et al.* 2019; Kennerley *et al.* 2021). Mexico is a megadiverse country and a tropical diversity hotspot for multiple vertebrate groups (Arita 1997; Nieves Delgado 2024), in addition to also having a rich cultural diversity (Flores-Santiago *et al.* 2024). Like most megadiverse countries, Mexico faces scientific challenges related to limited resources and funding in a context of

rapid biodiversity loss (Vilaça *et al.* 2024). Incomplete or biased data can misguide conservation, policy, and restoration efforts, since biodiversity conservation depends on the expansion of taxonomy and systematics research (Ruedas and Gardner 2025), which in turn relies heavily on molecular information (Hoban *et al.* 2024). It is therefore a pressing matter to quantify which species have sequences and which do not, gauge the size of the knowledge gap, and identify hidden shortfalls in quality that ultimately reduce the potential for existing sequences to be reused in future research.

Here, we assessed the status and availability of nucleotide sequence information and associated metadata for the land mammals of Mexico in the NCBI-GenBank Nucleotide database. After taxonomic harmonization, we ran a species-by-species search for any existing sequences and examined the underlying metadata. For each sequence, we checked whether the metadata included date, location, and associated voucher and, for those with location, if the sample was from Mexico. We found that ~10% of Mexican land mammals lack public nucleotide sequence data, while many others have very few sequences, and that many Mexican endemic species are critically undersampled. When evaluating metadata quality, we determined that the associated metadata for a significant proportion of existing sequences remains largely incomplete. Concerted efforts are urgently needed to increase sampling and sequencing and to improve metadata quality during deposition.

Materials and methods

We focused on extant, non-marine mammals (i.e., 'land mammals', which includes bats) known to occur in Mexico using the taxonomic scheme from the American Society of Mammalogists' Mammal Diversity Database (MDD) version 2.1. This database uses distributional data to track the native distribution of species in countries and continents. Accordingly, we filtered species on the 'countryDistribution' field, keeping only records that contained 'Mexico'. Of 590 species that met this condition, we excluded 38 cetaceans but retained pinnipeds except for the Galapagos fur seal *Arctocephalus galapagoensis* which is only recorded in Mexico from transient individuals (Tamayo-Millán *et al.* 2021). We also excluded the pocket mouse *Chaetodipus lineatus* which is listed in MDD 2.1, but following recent work, we considered this taxon a synonym of *Chaetodipus nelsoni* (Light *et al.* 2025). The taxonomic scheme that we followed also includes two extinct or possibly extinct species of rice rats (*Oryzomys nelsoni* and *Oryzomys peninsulae*), which we also excluded as they lack fundamental data and are absent from the NCBI taxonomy.

For the remaining 548 nonmarine species of Mexican mammals, we harmonized the scientific names using functions from the R package taxize (Chamberlain and Szocs 2013), matching and standardizing the taxon names to the taxonomy used by NCBI. This workflow matched the species names against the Global Names Verifier service (https://gni.globalnames.org/). We also used details on recent taxonomic revisions provided in the Mammal Diversity Database to find the corresponding identifiers for taxa in the NCBI taxonomy. In MDD v2.1, several taxa are recognized as distinct species because of recent taxonomic revisions, including species splits and the elevation of previously recognized subspecies to species status. This information is not typically reflected in the underlying NCBI taxonomy, so there is no straightforward way to link these taxa with an existing NCBI identifier. Additionally, linking existing sequences that ultimately correspond to newly recognized species involves extensive 'detective work' in the supporting data and figures of the publications linked to the taxonomic changes. For example, in many cases the updated identities of existing sequences are only reported secondarily in dendrograms, maps, appendices, or lists of specimens examined. We omitted 52 species in this situation from our search of sequences and metadata but provide this list as supplementary data.

With a final list of scientific names for the land mammals of Mexico and their corresponding NCBI unique identifiers when we could locate one, we used the R package rentrez v 1.2.4 (Winter 2017) to search the GenBank nucleotide database and then download and parse the metadata for each result. These search parameters were meant to return all available sequence data for a given taxon, from short fragments to complete genomes, including full/partial gene sequences, mRNA, tRNA, rRNA, genomic DNA, cDNA, expressed sequence tags, whole genome shotgun, and transcriptome shotgun assemblies (Sayers *et al.* 2019). We tailored our searches to exclude computationally generated (predicted) mRNA sequences and viral cRNA sequences associated with our target species because of internal host-pathogen links in the databases, because these two types of results are not informative for species-level biodiversity studies for our focal species. All programmatic queries of the entrez API were performed in batches between December 4 and December 9, 2025.

We searched for all available sequences for our study taxa, but when parsing the metadata for each result, we focused on three key pieces of information: the location of genetic sampling, the date, and the associated vouchers (i.e., permanently preserved specimens stored and maintained in an accessible collection) when applicable. These metadata are of central importance to most studies in ecology and evolution and the most likely to influence the reuse or repurposing of the nucleotide sequence data (Pope *et al.* 2015). We considered sequences produced from any type of sample but checked for voucher information given the importance of linking sequences to physical specimens. Sequences are also produced from other sources such as tissue or blood samples, scats, hair, or environmental DNA, and sample source or type was not a criterion in our searches.

In an age of high-throughput or massively parallel sequencing, it is commonplace to sometimes find tens of

thousands of sequences for a given species, which may be misleading for our purposes if these are small DNA or RNA fragments obtained from a single sample or specimen and uploaded separately to GenBank. These results may misrepresent the research interest for a species or region. Fortunately, entries derived from high-throughput methods in the Nucleotide database are usually linked with entries in the NCBI BioSample database, which keeps a record of biological isolates with unique physical properties. BioSample entries generally relate to multiple sequences, and a single BioSample may link to tens of thousands of DNA or RNA fragments. We attempted to link all our results with entries in BioSample so we could deduplicate observations by keeping only one sequence at random from a group of sequences from the same BioSample. This way we could make better comparisons of research interest and sequence availability across species by not having a small number of samples with tens of thousands of derived sequences mislead our inferences. All our reported numbers of sequences per species refer to unique BioSample entries and not raw fragment counts.

Additionally, we examined the GenBank accession numbers in our results using regular expressions to detect sequential patterns such as identifiers with the same prefixes and consecutive numerical suffixes (e.g., BV389079, BV389080, BV389081 and so on until BV399201 where "BV" is the prefix). These accession identifiers indicate batch submissions from a single study or project and likely reflect assembly sequences from a single sample rather than extensive species-level sampling efforts. We checked the accessions in our results for batches greater than 1000 sequences, which were then checked manually on the NCBI web portal to determine if these were Genome or Transcriptome assembly sequences. Assembly sequences were also deduplicated by keeping only one sequence from a batch (chosen at random) as long as these entries could be linked to a single study and all shared the same metadata.

For each accession in our final deduplicated dataset, we retrieved the full GenBank record in XML format. These records were parsed to extract the molecule type, organelle annotation (to infer genomic location), and gene name(s) from the gene qualifier of annotated features. When no explicit gene qualifier was present, we used the feature key itself as a descriptor (e.g., D-loop, rRNA, tRNA). We retained multi-gene records, which were primarily mitogenomes and multi-locus amplicons, as delimited strings. Lastly, we standardized all gene names to uppercase and unified common synonyms (e.g., COI/CO1 to COX1; CYT-B/cytochrome B to CYTB, etc.).

Results

Our final list of land mammals that occur in Mexico included 548 species, of which 203 are endemic. After taxonomic harmonization and manual standardization, we worked with 496 species. This set of 496 species spanned 12 orders and 39 families. Similar to global patterns, rodents (249 species, 50.2%) and bats (141 species, 28.4%) accounted for nearly 80% of all species. The best represented families in these two orders were Cricetidae (146 spp.), Phyllostomidae (58 spp.), Vespertilionidae (44 spp.), Heteromyidae (42 spp.), and Sciuridae (34 spp.). The remaining diversity includes various orders: Carnivora (40 spp.), Eulipotyphla (29 spp.), Lagomorpha (11 spp.), and few representatives each from Artiodactyla, Didelphimorphia, Primates, Cingulata, Pilosa, and Perissodactyla. Of these 496 species, 157 are endemic to Mexico. Rodents make up most of the endemism (119 species, 75.8%), followed by Chiroptera (17 spp.) and Eulipotyphla (15 spp.). For families, Cricetidae accounts for more than half of all endemics (82 spp.) and other rodent families Geomyidae (13 spp.), Heteromyidae (13 spp.), and Sciuridae (11 spp.) also contribute substantially. Non-rodent endemics are sparse, including mainly shrews (14 spp.), and small numbers of lagomorphs, carnivorans, and didelphids.

These 496 species all had at least one record in the Nucleotide database, meaning that the remaining 52 species or approximately 10% of species in our chosen taxonomic scheme, have no nucleotide sequence data, or none that are readily accessible. In total, we located 98,327 sequences after deduplicating entries linked to the same BioSample. We reduced this total further to 79,419 by deduplicating batch submissions linked to a Whole Genome Shotgun assembly for *Canis latrans* (10,123 sequences) and a Transcriptome Shotgun Assembly for *Desmodus rotundus* (8,787 sequences).

The 52 species with no sequences under our methods and search criteria spanned 5 orders (Rodentia: 22 species, Eulipotyphla: 17 species, Chiroptera: 5 species, Didelphimorphia: 4 species, and Lagomorpha: 4 species) and 9 families (Didelphidae, Leporidae, Cricetidae, Heteromyidae, Dasyproctidae, Sciuridae, Soricidae, Vespertilionidae, and Phyllostomidae), and was mainly represented by shrews and rodents. These unsampled species represent a combination of species in groups that are in constant taxonomic flux and well-recognized taxa that have simply not been sequenced yet. Roughly half of the species without sequences were rodents, and a third were shrews (*Sorex, Cryptotis, Notiosorex*). A small number of bats, rabbits, and opossum species also lacked sequences under our methods, mainly resulting from a lack of information to link existing sequences with now-outdated identities with their new taxonomic assignments. For a limited number of species, we found mentions of molecular data used in publications (e.g., studies reported amplifying gene fragments in their methods and using the resulting sequences in their analyses) without corresponding data on GenBank, the respective supplementary materials, or any other public platform or archive.

Sequence availability. The number of sequences per species varied greatly. The median number of sequences was 43, and these totals ranged from 1 to 3296. The distribution of total sequences per species was highly

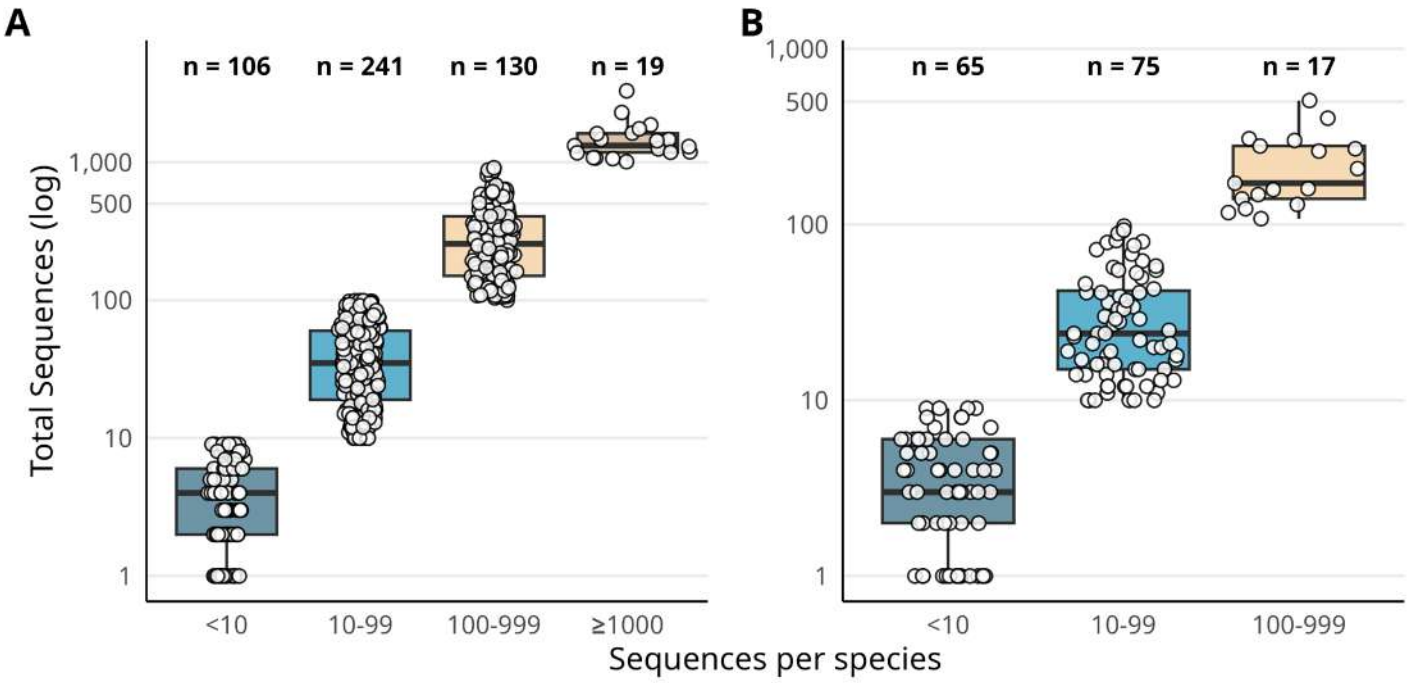

Figure 1. Distribution of nucleotide sequence counts per species, binned using cutpoints at 10, 100, 500, and 1,000 sequences. (A) All 496 species. (B) Mexican endemic species only. Box plots show medians and interquartile ranges; individual species are overlaid as points. Sample sizes per bin are indicated above boxes.

skewed—70% of species had fewer than 100 sequences, and a small remainder (~4%) made up the long tail of taxa with >1000 sequences (Figure 1A). Mexican endemics showed a similar skew: the median number of sequences was 13 (min 1, max 508) and 90% of species had fewer than 100 sequences (Figure 1B). No endemic species had more than 1000 sequences, although the deer mouse *Peromyscus mexicanus* had 508 sequences (driven mainly by 368 COX1 barcoding submissions), followed by the harvest mouse *Reithrodontomys sumichrasti* (403 sequences, mainly CTYB and COX1 but also a full mitogenome and nuclear markers) and the rice rat *Casiomys chapmani* (308 sequences in which nuclear markers such as CD14, RBP3, FUT4, DXS254E, NUP160, PRKC1 notably outnumber mitochondrial ones).

In general, there was a massive disparity in total sequences per species: a few widespread or abundant species received far more attention, while the bottom tier of species with only one or two sequences are mainly rare and endemic rodents and shrews. The species with the most hits in our searches were wide-ranging taxa that have historically attracted greater research interest relative to other mammals, including the white-tailed deer *Odocoileus virginianus,* the short-tailed bat *Carollia perspicillata*, the vampire bat *Desmodus rotundus,* and the deer mouse *Peromyscus leucopus* (Table 1). On the other hand, some species with only one sequence included threatened endemics such as the Zempoaltepec vole *Microtus umbrosus* and the surprising result of only finding one hit (a partial

Table 1. Top 20 mammal species by nucleotide sequence availability, ranked by total number of sequences.

Rank	Species	Family	Total Sequences	Rank	Species	Family	Total Sequences
1	*Odocoileus virginianus*	Cervidae	3,296	11	*Procyon lotor*	Procyonidae	1,299
2	*Carollia perspicillata*	Phyllostomidae	2,294	12	*Odocoileus hemionus*	Cervidae	1,251
3	*Desmodus rotundus*	Phyllostomidae	1,868	13	*Ateles geoffroyi*	Atelidae	1,189
4	*Peromyscus leucopus*	Cricetidae	1,749	14	*Phoca vitulina*	Phocidae	1,182
5	*Canis latrans*	Canidae	1,627	15	*Tamiasciurus douglasii*	Sciuridae	1,172
6	*Eptesicus fuscus*	Vespertilionidae	1,613	16	*Ursus americanus*	Ursidae	1,080
7	*Bos bison*	Bovidae	1,466	17	*Peromyscus truei*	Cricetidae	1,077
8	*Artibeus jamaicensis*	Phyllostomidae	1,461	18	*Artibeus lituratus*	Phyllostomidae	1,062
9	*Taxidea taxus*	Mustelidae	1,434	19	*Molossus molossus*	Molossidae	1,010
10	*Dasypus mexicanus*	Dasypodidae	1,321	20	*Sorex monticolus*	Soricidae	912

Table 2. Mammal species with a single nucleotide sequence (n = 21 species). Congeneric species are grouped for space. Flag indicates species endemic to Mexico (n = 16 of 21 species).

Species with 1 Sequence		
Species[1]	**Family**	**Order**
Cryptotis 🇲🇽 *(2 spp.): griseoventris, soricinus*	Soricidae	Eulipotyphla
Cryptotis goodwini	Soricidae	Eulipotyphla
Ictidomys mexicanus 🇲🇽	Sciuridae	Rodentia
Microtus 🇲🇽 *(3 spp.): oaxacensis, quasiater, umbrosus*	Cricetidae	Rodentia
Neotoma insularis 🇲🇽	Cricetidae	Rodentia
Peromyscus 🇲🇽 *(4 spp.): madrensis, pembertoni, polius, sagax*	Cricetidae	Rodentia
Procyon pygmaeus 🇲🇽	Procyonidae	Carnivora
Reithrodontomys hirsutus 🇲🇽	Cricetidae	Rodentia
Sciurus alleni 🇲🇽	Sciuridae	Rodentia
Sciurus aureogaster	Sciuridae	Rodentia
Sigmodon zanjonensis	Cricetidae	Rodentia
Sorex emarginatus 🇲🇽	Soricidae	Eulipotyphla
Sorex chiapensis	Soricidae	Eulipotyphla
Trachops coffini	Phyllostomidae	Chiroptera
Tylomys tumbalensis 🇲🇽	Cricetidae	Rodentia

[1] 🇲🇽 indicates Mexican endemic species

cytochrome b sequence) for the ubiquitous Mexican gray squirrel *Sciurus aureogaster* (Table 2).

Sequence types and genetic markers. After deduplication, we fetched and parsed a total of 79,419 accessions. The majority of sequences were genomic DNA (75,898; 95.6%), with smaller proportions of mRNA (2,651; 3.3%) and transcribed or unassigned RNA (692; 0.9%). Mitochondrial sequences accounted for 61.4% of records; the remaining 38.6% were derived from the nuclear genome. By sequence type, 60.1% of records were classified as targeted single-locus or multi-locus gene sequences, 19.1% as mitochondrial control region/D-loop sequences, and 6.4% as nuclear introns. Smaller proportions included mRNA (3.4%), rRNA (2.7%), microsatellites (2.2%), mobile elements (1.0%), and complete mitogenomes (1.0%). The remaining 3.7% could not be assigned to a specific category.

We found gene annotations for 93.4% of records (74,151), of which 7.5% (5,920) contained multiple genes. For single-gene records, the two most common markers were CYTB (n = 12,212) and COX1 (n = 12,119), accounting for almost one third of all annotated records. The D-loop/control region was the next most frequently represented (8,464 records),

followed by nuclear markers including PRNP (2,672), RAG2 (770), FGB (568), RAG1 (462), and IRBP (460).

Metadata. We found that date, location, and voucher data for available sequences were rarely present and highly variable across species. Non-trivial proportions of species had incomplete information on collection date, location, or associated vouchers: 34% of species have no collection dates at all, 44% lack geographic coordinates, and 8% have no associated voucher specimens for any of their sequences.

We found an important gap in temporal information. Only 19% (15,102 of 79,419) of sequences had usable dates recorded in the appropriate metadata field. Sequences with dates were distributed unevenly across species. A concerning 170 species (34%) had no collection dates whatsoever. Most species (356 or 72%) had minimal temporal metadata (dates for < 25% of their sequences), and only 65 species (13%) had ≥ 50% temporal coverage. Parsing the sampling year (the most common time unit shared across sequences), we found that the collection dates span 125 years from 1900 to 2025, although most sequences originate from samples collected between 1980 and 2020. Sequences from historical specimens (pre-1980) are minimal (0.4% of all dated records).

Despite the importance of spatial context for gene sequences, 59% of sequences lack information in the 'country' field (in which more detailed locality information may be stored and not just the country), and 85% lack geographic coordinates. More sequences have locality information (median = 38% of records per species) than coordinates (median = 1.3% per species), and we found that 218 species have no coordinate data for their sequences.

Of all the sequences, roughly 42% (33,075 of 79,419) listed a voucher specimen in the metadata, and most species (455 of 496 or 92%) had at least one sequence with an associated voucher. On average, 60% of a species' sequences had voucher information, and the orders Rodentia and Eulipotyphla had the highest proportions of sequences with vouchers, with 67 and 86%, respectively. Bats (Order Chiroptera) had a lower proportion (43%) of sequences with vouchers despite their high diversity.

Discussion

Genetic data have been generated at an exponential rate for many years now (Pope *et al.* 2015). However, such data is highly taxonomically and geographically biased, and significant gaps remain. We found that a non-trivial proportion (~10%) of Mexican land mammals lack public nucleotide sequence data altogether, and another large fraction is critically undersampled. In general, when sequences do exist, the associated metadata describing vouchers, dates, and locations for existing sequences remains largely incomplete.

Of the 548 species of terrestrial mammals that occur in Mexico, we could not locate usable genetic data for 52, and of the remaining 496, one in five species (21%) have critically low representation (>10 sequences, a rough minimum for achieving usable estimates of diversity, structure, gene flow, or inbreeding, Scaketti *et al.* 2025) in the GenBank Nucleotide database. These low numbers of sequences for a large number of species, especially those endemic to Mexico, are likely insufficient to capture population-level variation, thus limiting the statistical power of the common methods used in evolution, systematics, or conservation (Paz-Vinas *et al.* 2025). These substantial gaps remain despite the boost in sequencing efforts derived from the Mexican Barcode of Life project (MEXBOL), part of a global initiative for establishing a system for species identification and discovery through mitochondrial gene sequences (Alvarez Castañeda *et al.* 2012). Other more recent and ongoing initiatives to generate high-quality genomic data for particular groups such as the Bat1k Project (Teeling *et al.* 2018) include concrete plans to sequence species that occur in Mexico, which should eventually help fill gaps in genetic knowledge.

We found that ~61% of all the sequences for Mexican land mammals target the mitochondrial genome. Two markers in particular (CYTB and COX1) accounted for almost one third of all sequences. This pattern reflects the historic use of mitochondrial phylogenetics and barcoding, but it also means that for many species, sequences are effectively limited to a single genomic compartment and a narrow set of loci. Nuclear markers had a substantial representation of ~38%, covering a heterogeneous assortment of markers that more likely reflect the priorities of different research groups. Nuclear coverage is uneven across taxa: some species may have several nuclear loci sequenced while others have none. Collectively, uneven taxonomic sampling across species is compounded by uneven genomic representation, which limits comparative studies unless these gaps are addressed.

With our approach of first linking taxa from our list of species to NCBI identifiers, we had to exclude 52 species that could not be linked to the NCBI reference taxonomy. This was either because the species have truly not been sequenced or because of recent taxonomic changes, and the distinction is not always clear. This is partly because of the dynamic nature of mammalian systematics and because our chosen taxonomic scheme (MDD) is constantly updated and recognizes taxonomic changes unrelated to molecular data. To help alleviate these issues with taxonomic identities, we call for authors of publications that describe novel taxa or suggest changes to species identities based on molecular data to make explicit links between existing sequences and their assignments in both existing and new taxonomic arrangements.

For Mexican land mammals, we found a skewed distribution of the total number of sequences (regardless of gene or type of sequence) per species, which indicates gaps and biases in research effort. This skew is likely driven in part by the particular agendas of individuals or research groups and by a positive feedback loop in which more data attracts more studies and more funding, which in turn

increases the disparity in sequences between well-studied species relative to undersampled taxa. With this exercise, we were able to identify that not only rare endemics but also widespread and abundant species, including the Mexican gray squirrel (*Sciurus aureogaster*), are being overlooked in molecular studies.

Incomplete metadata for sequences undermines their value and reuse in studies that need spatially and/or temporally explicit information. This includes phylogeographic studies or any efforts to calculate genetic diversity for any kind of spatial unit. Without date information it is also not possible to compare changes in genetic diversity or structure through time or work in modern ecological timescales, which is important for studies of genetic diversity in relation to recent land-use changes. In addition to undersampled taxa, the metadata of existing sequences may lack dates, locations, vouchers, or different combinations of these important fields.

We found numerous sequences that in their current version on GenBank are essentially disconnected from physical specimens, sampling locations, and temporal references. In a striking case, the blackish deer mouse *Peromyscus furvus* had 270 sequences (mainly mitochondrial markers CYTB and ND3 and a smaller complement of nuclear markers consistent with Sanger sequencing-based phylogeography or systematics studies), but none had any usable information about location (no coordinates, country, or locality) or date, and only 6 sequences had an associated voucher. This pattern is unlike other deer mouse species, which generally had high proportions of sequences with linked vouchers, as is often the case for rodents. Two bat species showed a similar problematic pattern: *Vampyrum spectrum* and *Macrotus californicus* both had fewer than 400 sequences but a less than 3% voucher rate and near-zero location/date data.

A key inference from this work is to state the need for further molecular sampling of Mexican mammals, either from new field work or using existing materials in natural history collections. We identified numerous species with either zero or critically low numbers of sequences (>10), which are mainly rodents and shrews and include multiple endemic taxa. Their low genetic representation on GenBank could make them priority species for sequencing, but other factors may be taken into consideration as well, including conservation status (prioritize threatened taxa), phylogenetic position (prioritize taxa in unresolved clades), or geographic range (prioritize missing parts of species' ranges).

It is worth mentioning that we aimed to quantify sequence availability and metadata completeness. In doing so, we deduplicated multiple reads from high-throughput sequencing methods from the same NCBI BioSample identifier and from shotgun assemblies and excluded predicted sequences and those of the parasites or pathogens associated with our species of interest. However, we did not filter our data by type of molecule, and thus our summary statistics include direct-submission entries from mRNA converted to cDNA and amplified for sequencing. These individual uploads may lack a BioSample identifier, either because they predate the introduction of the BioSample database in 2011 (Barrett *et al.* 2012) or because the submitting researchers are explicitly treating this information as sequence-only data not linked to a physical sample. These mRNA sequences may contribute to the skewed sequence counts and could be examined in more detail in future studies. Similarly, the resulting sequences may be refined further to only include molecular markers compatible with taxonomic, systematics, and biodiversity conservation studies, rather than sequences derived from physiological or immunological research.

Without question, we support existing calls for those involved in generating and submitting sequence data to record and carefully upload metadata such as collection date and location, at minimum, when depositing sequences. In a promising change, as of late 2024, databases in the International Nucleotide Sequence Database Collaboration (including GenBank) require submitters to include minimum information about sample locations and dates, which should ultimately improve the quality and completeness of metadata for future submissions. In parallel, research communities, journals, and funding agencies are requiring deposition of vouchers and sharing specimen information for publications built on biological materials (Colella *et al.* 2021). These changes in culture and policy should ultimately improve metadata quality, addressing part of the shortfalls that we identified for Mexican mammals. We encourage submitters and data managers to follow the increasingly detailed and user-friendly documentation for the relevant databases and to follow best practice guides (Renner *et al.* 2024), considering how to ensure that the sequences submitted can be reused in the future.

Policy changes are promising, but they do not solve the issue of incomplete metadata for hundreds of thousands of existing sequences. Although it is possible for the original depositors of sequences to directly update the metadata on their uploads, this is additional work, and updates like these are rare (Deck *et al.* 2017; Crandall *et al.* 2023). For case studies like ours that focused on a discrete and manageable set of species, it may be possible to take advantage of the voucher identifiers provided for a substantial number of species to enrich the metadata. Leveraging recent initiatives to digitize and publish information from biocollections into online platforms (Guralnick *et al.* 2016), dates and locations may be parsed and linked with nucleotide sequences. Numerous species had good voucher coverage but poor spatiotemporal metadata, such as *Peromyscus truei, Sturnira parvidens, Chaetodipus intermedius, Megascapheus umbrinus,* and *Peromyscus hylocetes*, which all have >250 sequences and >90% vouchering information but no sampling dates at all. Similarly, various rodents (many of which are endemic), including *Heteromys nelsoni, Megascapheus sheldoni, Megascapheus atrovarius,*

Chaetodipus goldmani, *Peromyscus truei*, and *Chaetodipus intermedius* all have high proportions of sequences with vouchers but no locations.

We found nucleotide sequence data for 90% of species of Mexican land mammals. However, this seemingly high proportion conceals gaps, biases, and incomplete metadata. These issues compromise the use we can give to these molecular data, especially when published sequences lack spatiotemporal context. Moving forward, we need to fill taxonomic gaps by generating new sequences with special care in recording the metadata that gives them biological meaning. Thanks to preserved specimens, it may be possible to enrich sequences with their missing context, but we insist on a shift in research culture towards rigorous and open recording of metadata. This will maximize the value of public molecular data in a way that can truly help us understand and conserve the mammals of this megadiverse country.

Acknowledgments

We dedicate this work to Livia S. León Paniagua, in appreciation for the mentorship and guidance that was instrumental for the personal and professional development of those of us fortunate enough to have been her students. We also wish to acknowledge Livia's contributions to the study of mammals in Mexico and towards establishing a healthy, friendly, and productive collaborative network. We would also like to thank Maximiliano M. Maronna for his active role in understanding and closing gaps in genetic sequence data and metadata that inspired this work and for feedback on this manuscript. Financial support: ANID Fondecyt Postdoctorado Grant Number 3230234 and SECIHTI scholarship 778388.

Declaration of Artificial Intelligence use

Initial data exploration was assisted by Databot, an LLM-based coding assistant integrated within Positron (version 2025.10.1, Posit PBC), using the Claude Sonnet 4.5 model (Anthropic PCB) served through a GitHub Copilot. All AI-generated R code was reviewed and validated before use.

Author contributions

Luis Darcy Verde Arregoitia and Fabricio Villalobos conceptualized the ideas and aims of the manuscript. Luis Darcy Verde Arregoitia and Martín Y. Cabrera Garrido collected the data. Luis Darcy Verde Arregoitia analyzed the data. Julia Saravia, Lillian Draper Parker, and Luis Darcy Verde Arregoitia interpreted the results. All authors contributed substantially to the final manuscript text and gave approval for submission and publication.

Supplementary data

Supplementary datasets including the species examined and their corresponding NCBI identifiers, plus the processed results for each sequence located, are available on OSF (https://doi.org/10.17605/OSF.IO/K4QNP).

Literature cited

Alvarez Castañeda ST, Lorenzo C, Rios Mendoza EP, Cortes-Calva P, Gutierrez ME, Ortega J, *et al*. 2012. DNA barcoding of mammals in Mexico: Implications for biodiversity. *The Open Zoology Journal* 5:18–26. https://doi.org/10.2174/1874336601205010018

Arita HT. 1997. The non-volant mammal fauna of Mexico: species richness in a megadiverse country. *Biodiversity and Conservation* 6:787–795. https://doi.org/10.1023/B:BIOC.0000010402.08813.ab

Arita M, Karsch-Mizrachi I, Cochrane G, on behalf of the International Nucleotide Sequence Database Collaboration. 2021. The international nucleotide sequence database collaboration. *Nucleic Acids Research* 49(D1):D121–D124. https://doi.org/10.1093/nar/gkaa967

Barrett T, Clark K, Gevorgyan R, Gorelenkov V, Gribov E, Karsch-Mizrachi I, Kimelman M, *et al*. 2012. BioProject and BioSample databases at NCBI: facilitating capture and organization of metadata. *Nucleic Acids Research* 40(Database issue):D57–D63. https://doi.org/10.1093/nar/gkr1163

Benson DA, Cavanaugh M, Clark K, Karsch-Mizrachi I, Lipman DJ, Ostell J, *et al*. 2013. GenBank. *Nucleic Acids Research 41*(Database issue):D36–D42. https://doi.org/10.1093/nar/gks1195

Blaxter M, Archibald JM, Childers AK, Coddington JA, Crandall KA, Di Palma F, *et al*. 2022. Why sequence all eukaryotes? *Proceedings of the National Academy of Sciences* 119:e2115636118. https://doi.org/10.1073/pnas.2115636118

Buckner JC, Sanders RC, Faircloth BC, and Chakrabarty P. 2021. The critical importance of vouchers in genomics. *eLife* 10:e68264. https://doi.org/10.7554/eLife.68264

Chamberlain S, and Szocs E. 2013. taxize - taxonomic search and retrieval in R. F1000Research.

Colella JP, Stephens RB, Campbell ML, Kohli BA, Parsons DJ, and Mclean BS. 2021. The Open-Specimen Movement. *BioScience* 71:405–414. https://doi.org/10.1093/biosci/biaa146

Crandall ED, Toczydlowski RH, Liggins L, Holmes AE, Ghoojaei M, Gaither MR, *et al*. 2023. Importance of timely metadata curation to the global surveillance of genetic diversity. *Conservation Biology* 37:e14061. https://doi.org/10.1111/cobi.14061

Deck J, Gaither MR, Ewing R, Bird CE, Davies N, Meyer C, *et al.* 2017. The Genomic Observatories Metadatabase (GeOMe): A new repository for field and sampling event metadata associated with genetic samples. *PLOS Biology* 15:e2002925. https://doi.org/10.1371/journal.pbio.2002925

Dunnum J, Malaney J, Cook J, Dunnum J, Malaney J, Cook J. 2020. Sustained impact of holistic specimens for mammalogy and parasitology in South America: Sydney Anderson's legacy. *Therya* 11:347–358. https://doi.org/10.12933/therya-20-1011

Flores-Santiago I, Baena ML, Delfín-Alfonso CA, Silva-Rivera E, and Pérez-Chacón JL. 2024. Perception and uses about mammals in México: a literature review. *Ethnobiology and Conservation* 13:25. https://doi.org/10.15451/ec2024-08-13.22-1-12

Galvao Elias S, Cervieri Guterres D, Weingart Barreto R, and Mario Martins do Vale H. 2024. GeneConnector: Unlocking the full potential of Genbank metadata. *IEEE Latin America Transactions* 22:99–105. https://doi.org/10.1109/TLA.2024.10412034

Gratton P, Marta S, Bocksberger G, Winter M, Trucchi E, and Kühl H. 2017. A world of sequences: Can we use georeferenced nucleotide databases for a robust automated phylogeography? *Journal of Biogeography 44: 475–486.* https://doi.org/10.1111/jbi.12786

Guralnick RP, Zermoglio PF, Wieczorek J, LaFrance R, Bloom D, and Russell L. 2016. The importance of digitized biocollections as a source of trait data and a new VertNet resource. *Database* 2016:baw158. https://doi.org/10.1093/database/baw158

Hoban S, Paz-Vinas I, Shaw RE, Castillo-Reina L, da Silva JM, DeWoody JA, *et al*. 2024. DNA-based studies and genetic diversity indicator assessments are complementary approaches to conserving evolutionary potential. *Conservation Genetics* 25:1147–1153. https://doi.org/10.1007/s10592-024-01632-8

Hughes AC, Orr MC, Ma K, Costello MJ, Waller J, Provoost P, *et al*. 2021. Sampling biases shape our view of the natural world. *Ecography* 44:1259–1269. https://doi.org/10.1111/ecog.05926

Kennerley RJ, Lacher Jr. TE, Hudson MA, Long B, McCay SD, Roach NS, *et al*. 2021. Global patterns of extinction risk and conservation needs for Rodentia and Eulipotyphla. *Diversity and Distributions* 27:1792–1806. https://doi.org/10.1111/ddi.13368

Leray M, Knowlton N, Ho S-L, Nguyen BN, and Machida RJ. 2019. GenBank is a reliable resource for 21st century biodiversity research. *Proceedings of the National Academy of Sciences* 116:22651–22656. https://doi.org/10.1073/pnas.1911714116

Light JE, Siciliano-Martina L, Morley L, Castellanos AA, LaMonica L, and Hafner DJ. 2025. Taxonomic status of *Chaetodipus lineatus* and phylogeography of the *Chaetodipus nelsoni* species group. *Journal of Mammalogy* 106:1187–1198. https://doi.org/10.1093/jmammal/gyaf052

Lim BK. 2012. Preliminary Assessment of Neotropical Mammal DNA Barcodes: An Underestimation of Biodiversity. *The Open Zoology Journal* 5:10–17. https://doi.org/10.2174/1874336601205010010

Marques AC, Maronna MM, and Collins AG. 2013. Putting GenBank Data on the Map. *Science* 341(6152):1341–1341. https://doi.org/10.1126/science.341.6152.1341-a

Millette KL, Fugère V, Debyser C, Greiner A, Chain FJJ, and Gonzalez A. 2020. No consistent effects of humans on animal genetic diversity worldwide. *Ecology Letters* 23:55–67. https://doi.org/10.1111/ele.13394

Moura MR, Ceron K, Guedes JJM, Chen-Zhao R, Sica YV, Hart J, *et al*. 2024. A phylogeny-informed characterisation of global tetrapod traits addresses data gaps and biases. *PLOS Biology* 22:e3002658. https://doi.org/10.1371/journal.pbio.3002658

NCBI Staff. 2023. Coming Soon! Including Sample Location and Collection Date and Time for Sequences Submitted to GenBank and SRA. NCBI Insights. [accessed 14 Jan 2026] https://ncbiinsights.ncbi.nlm.nih.gov/2023/05/01/sequences-genbank-sra/

Nieves Delgado A. 2024. "México es un país megadiverso": Biocultural Heritage and Exceptionality in Mexican Ethnobiology. History of Anthropology Review. [accessed 5 Mar 2026] https://histanthro.org/notes/mexico-megadiverso/

Paz-Vinas I, Vandergast AG, Schmidt C, Leigh DM, Blanchet S, Clark RD, *et al*. 2025. Sparse genetic data limit biodiversity assessments in protected areas globally. *Frontiers in Ecology and the Environment* 23:e2867. https://doi.org/10.1002/fee.2867

Pelletier TA, Parsons DJ, Decker SK, Crouch S, Franz E, and Ohrstrom J. 2022. phylogatR: Phylogeographic data aggregation and repurposing. *Molecular Ecology Resources* 22:2830–2842. https://doi.org/10.1111/1755-0998.13673

Pitogo KME. 2025. Gaps and biases in vertebrate wildlife genetics from a global biodiversity hotspot. *Environmental Conservation* 52:127–138. https://doi.org/10.1017/S0376892925000141

Pope LC, Liggins L, Keyse J, Carvalho SB, and Riginos C. 2015. Not the time or the place: the missing spatio-temporal link in publicly available genetic data. *Molecular Ecology* 24:3802–3809. https://doi.org/10.1111/mec.13254

Renner SS, Scherz MD, Schoch CL, Gottschling M, and Vences M. 2024. Improving the gold standard in NCBI GenBank and related databases: DNA sequences from type specimens and type strains. *Systematic Biology* 73:486–494. https://doi.org/10.1093/sysbio/syad068

Ruedas LA, and Gardner SL. 2025. Biodiversity conservation depends on the expansion of taxonomy and systematics research. *Journal of Mammalogy* 106:1495–1512. https://doi.org/10.1093/jmammal/gyaf067

Sayers EW, Cavanaugh M, Clark K, Ostell J, Pruitt KD, Karsch-Mizrachi I. 2019. GenBank. *Nucleic Acids Research* 47(D1):D94–D99. https://doi.org/10.1093/nar/gky989

Scaketti M, Sujii PS, Alves-Pereira A, Schwarcz KD, Francisconi AF, Moro MS, *et al.* 2025. Sample Size Impact (SaSii): An R script for estimating optimal sample sizes in population genetics and population genomics studies. *PLOS One* 20:e0316634. https://doi.org/10.1371/journal.pone.0316634

Sidlauskas B, Ganapathy G, Hazkani-Covo E, Jenkins KP, Lapp H, McCall LW, *et al*. 2010. Linking big: The continuing promise of evolutionary synthesis. *Evolution* 64:871–880. https://doi.org/10.1111/j.1558-5646.2009.00892.x

Šmíd J. 2022. Geographic and taxonomic biases in the vertebrate tree of life. *Journal of Biogeography* 49:2120–2129. https://doi.org/10.1111/jbi.14491

Tamayo-Millán CJ, Ahumada-Sempoal MÁ, Cortés-Gómez A, Chacón-Romo Leroux IM, Bermúdez-Díaz D, *et al*. 2021. Molecular identification of the first Galapagos fur seal (*Arctocephalus galapagoensis*) reported on the central coast of Oaxaca. *Ciencias Marinas* 47:201–209. https://doi.org/10.7773/cm.v47i3.3184

Teeling EC, Vernes SC, Dávalos LM, Ray DA, Gilbert MTP, Myers E, *et al*. 2018. Bat biology, genomes, and the Bat1K Project: To generate chromosome-level genomes for all living bat species. *Annual Review of Animal Biosciences* 6:23–46. https://doi.org/10.1146/annurev-animal-022516-022811

Vázquez L-B, and Gaston KJ. 2004. Rarity, commonness, and patterns of species richness: the mammals of Mexico. *Global Ecology and Biogeography* 13:535–542. https://doi.org/10.1111/j.1466-822X.2004.00126.x

Verde Arregoitia LD, Teta P, and D'Elía G. 2020. Patterns in research and data sharing for the study of form and function in caviomorph rodents. *Journal of Mammalogy* 101:604–612. https://doi.org/10.1093/jmammal/gyaa002

Vilaça ST, Vidal AF, Pavan AC, Silva BM, Carvalho CS, Povill C, *et al*. 2024. Leveraging genomes to support conservation and bioeconomy policies in a megadiverse country. *Cell Genomics* 13:4. https://doi.org/10.1016/j.xgen.2024.100678

Winter DJ. 2017. rentrez: an R package for the NCBI eUtils API. *The R Journal* 9:520–526.

Zamora-Gutierrez V, Amano T, and Jones KE. 2019. Spatial and taxonomic biases in bat records: Drivers and conservation implications in a megadiverse country. *Ecology and Evolution* 9:14130–14141. https://doi.org/10.1002/ece3.5848

Associated editors: Giovani Hernández Canchola and Pablo Colunga Salas
Submitted: January 16, 2026; Reviewed: March 3, 2026
Accepted: April 11, 2026; Published online: May 29, 2026

THERYA, 2026, Vol. 17(2):213-224 DOI: 10.12933/therya.2026.6244 ISSN 2007-3364

Diversity of rodents in three altitudinal zones in Cloudbridge Nature Reserve, Costa Rica

Rebeca Jiménez-Gómez[1, 4*], Bernal Rodríguez-Herrera[2], Lilliana Piedra-Castro[3], and José D. Ramírez-Fernández[4]

[1]Universidad Nacional, Heredia, Costa Rica.
[2]Centro de Investigación en Biodiversidad y Ecología Tropical (CIBET), Universidad de Costa Rica. San Pedro, Montes de Oca, CP. 2060. San José, Costa Rica. E-mail: bernal.rodriguez@ucr.ac.cr (BR-H)
[3]Laboratorio de Recursos Naturales y Vida Silvestre (LARNAVISI), Escuela de Ciencias Biológicas, Universidad Nacional, 36-3000, Heredia, Costa Rica. E-mail: lilliana.piedra.castro@una.cr (LP-C)
[4]OneHealth Costa Rica Alliance (OHCRA), San José, Costa Rica. E-mail: josed-rf@hotmail.com (JDR-F)
[*]Corresponding author: rebecajimgom@gmail.com

Elevation is a natural gradient that shapes wildlife and vegetation communities. Therefore, spatial, climatic and ecological hypotheses have been proposed to describe the diversity of rodents in the altitudinal gradient. Our objective was to describe the biological diversity of rodents at three elevations in relation to microhabitat characteristics and seasonality. We captured rodents using Sherman traps in three altitudinal zones (1600, 1800, 2000 m.a.s.l.) during the dry and rainy season. We measured five microhabitat characteristics at each elevation. We compared the species diversity using coverage-based rarefaction and extrapolation curves and the composition of the rodent's community using the similarity indices of Jaccard and Bray – Curtis. In addition, we identify the species that contributed most to the differences in the community. Through Generalized Linear Models (GLM) we evaluate 1) the rodent occurrence by elevation, seasonality and microhabitat characteristics and 2) the variation of microhabitat characteristics by elevation and seasonality. In 2100 night-trap effort we captured 200 individuals of nine species. The most abundant species was *Peromyscus nudipes*. We found that the species diversity decreases with elevation and in the dry season. In terms of species composition, the low elevation between seasons and the high elevation between seasons were more similar. However, when we analyze the abundance, the 2000 m elevation were more similar between seasons. Rodent occurrence depends on the elevation. Finally, the microhabitat characteristics vary by elevation and seasonality. In conclusion, at Cloudbridge Nature Reserve the elevation influences the diversity and the presence of rodents by changing the microhabitat characteristics. Therefore, sites with microhabitat characteristics that could provide protection against predators and potential food sources harbor more rodent diversity.

Keywords: Central America, microhabitat, mountains, rodents, seasonality, species richness

La elevación es un gradiente natural que moldea las comunidades faunísticas y florísticas. Por lo tanto, se han propuesto hipótesis espaciales, climáticas y ecológicas para describir la diversidad de ratones en el gradiente altitudinal. Nuestro objetivo fue describir la diversidad biológica de las especies de ratones en tres elevaciones en relación con las características del microhábitat y la época. Se capturaron ratones, utilizando trampas Sherman, en un gradiente altitudinal (1600, 1800, 2000 m.s.n.m.) durante la época seca y la lluviosa. Se midieron cinco características de microhábitat en cada elevación. La diversidad de especies se comparó por medio de curvas de rarefacción y extrapolación basadas en la cobertura de muestra y la composición de la comunidad mediante los índices de similitud de Jaccard y Bray – Curits. Además, se identificaron las especies que más contribuían a las diferencias en la comunidad. Por medio de modelos lineales generalizados se evaluó 1) la presencia de ratones por elevación, época y características del microhábitat y 2) la variación de las características de microhábitat por elevación y época. Con un esfuerzo de muestreo de 2100 noches trampa se capturaron 200 individuos de nueve especies. La especie más abundante fue *Peromyscus nudipes*. Se encontró que la diversidad de especies disminuyó con la elevación y en la época seca. En términos de composición de especies, la elevación baja entre épocas y la elevación alta entre épocas fueron más similares. Sin embargo, cuando se analizó la abundancia, la elevación de 2000 m fue más similar entre épocas. La presencia de ratones dependió de la elevación. Finalmente, las características del microhábitat varían según la elevación y la época. En conclusión, en la Reserva Natural Cloudbridge la elevación influye en la diversidad y la presencia de roedores al cambiar las características del microhábitat. Por lo tanto, los sitios con características de microhábitat que podrían brindar protección contra depredadores y posibles fuentes de alimento albergan una mayor diversidad de roedores.

Palabras clave: Centroamérica, microhábitat, montañas, ratones, riqueza de especies, temporalidad

Elevation constitutes a powerful ecological gradient that influences the structure and composition of wildlife and plant communities across restricted spatial scales. It shapes patterns of species dispersal, colonization, speciation, and extinction, often giving rise to biodiversity hotspots and endemic-rich zones (Brown 2001; Lomolino 2001; Rahbek *et al.* 2019a, 2019b). To explain these distributional dynamics, a range of spatial, climatic, and ecological hypotheses have been proposed in the context of elevational gradients (McCain and Grytnes 2010).

From the climatic point of view, precipitation affects positively and indirectly the richness and abundance of non-volant rodents because it influences productivity, habitat heterogeneity, plant biomass, and food availability (Nor 2001; McCain and Grytnes 2010). Regarding the habitat heterogeneity, the microhabitat characteristics that might influence the presence of rodents are those that help them search for food or shelter, such as canopy coverage, presence of rocks, logs, live trees, leaf litter depth, density of shrubs, proximity of

water bodies and food resources (e.g., Ramírez-Bautista and Williams 2019; Sakane *et al.* 2019; Karasov-Olson and Kelt 2020; Benedek *et al.* 2021).

Costa Rica is a mountainous country, although there are few studies related to altitudinal gradient, microhabitat characteristics and rodents. Regarding the altitudinal gradient, McCain (2004, 2006) concluded that the diversity of rodents in Monteverde Cloud Forest Biological Reserve and Children's Eternal Rainforest was higher at mid-elevations, apparently due to productivity gradients and climatic conditions such as precipitation, temperature, and cloud distance that were higher at mid-elevation.

In terms of microhabitat characteristics at Cerro de la Muerte Biological Station (CMBS) and the paramo, Ramírez-Fernández (2023a) found that *Peromyscus nudipes* was more abundant in the montane forest that had more bushes and less luminosity because this habitat provides greater structural diversity, food resources, and protection against predators.

As a result of climate change and habitat loss, the mountain ecosystem and the species that inhabit it are being affected (Yanahan and Moore 2019; Barras *et al.* 2021). In Costa Rica climate projections indicate a significant reduction in mountain life zones (Birkel *et al.* 2022), and modeled scenarios suggest changes in the spatial distribution of birds, lizards, and anurans in the mountains (Pounds *et al.* 1999; Liu *et al.* 2023). Because not all organisms can adapt to climatic and habitat variations, it is necessary to know the species that live in the mountains and establish actions that allow the permanence of individuals. In Costa Rica, there are 17 endemic species of mice, most restricted to mountainous ecosystems at elevations greater than 1500 m.a.s.l. (McPherson 1985; Rodríguez-Herrera *et al.* 2014; Ramírez-Fernández *et al.* 2023b). However, there are gaps in information about ecology and natural history; therefore, we aim to describe the biological diversity of rodents at three elevations in relation to microhabitat characteristics and seasonality.

Materials and methods

Study area. The study was conducted in the Cloudbridge Nature Reserve (CNR), located in the montane oak forest within Talamanca Mountain range, in San Gerardo de Rivas, San José, Costa Rica (9°28'20" N, 83°34'39" W). The CNR presents an area of 255 ha, including 28 ha of primary forest and secondary forest at different levels of regeneration. The CNR connects with the Chirripó National Park at the highest elevations and has an altitudinal gradient of 1500 to 2600 m.a.s.l. (Figure 1). The average daily temperature oscillates between 16 and 19°C. The mean precipitation changes drastically between the dry season and the rainy season (113 to 2470 mm) (Powell *et al.* 2022). The life zones are humid to rainy forests in the Premontane and Lower Montane altitudinal belts (Holdridge 1967).

Rodents trapping. We selected three trapping stations along the Jilguero trail, at 1600, 1800 and 2000 m.a.s.l. We captured rodents using Sherman live traps (5 × 6 × 16 cm; H. B. Sherman Traps, Inc., Florida) baited with a homogeneous mix of oatmeal, banana, peanut butter, and vanilla extract. We placed the traps in a paired linear transect with a distance of ca. 10 m between traps, and each trap was georeferenced using a GPSMAP Garmin 64sx. Each station was sampled for five consecutive nights per elevation. During the dry season (February – March) we set 30 traps at each elevation (15 paired stations) for a total of 900 night-traps, while in the rainy season (June – July) we set 40 traps at each elevation (20 paired stations) for a total of 1200 night-traps. The number of traps was increased during the rainy season because no rodents were captured at 1800 m during the dry season. Despite the difference in sampling effort between seasons, sample coverage analyses indicated that the sampling effort was sufficient to characterize the rodent diversity in both seasons. Finally, we identified captured individuals to the species level using the key published by Villalobos-Chaves *et al.* (2016). Voucher specimens of taxonomically debatable species were collected as a reference (Supplementary Data SD1).

Microhabitat characteristics. We measured five vegetative variables at 15 random well-spaced trapping points within each station. We quantified (1) the number of fallen logs > 50 cm long and ≥ 10 cm diameter, and (2) the number of trees with ≥ 10 cm diameter at breast height, in a perimeter of 3 and 5 m around the trap. We measured (3) understory density/cover using a densimeter placed just above the trap and (4) leaf litter depth at the four sides of the trap using a ruler. Finally, (5) ground cover was measured using a 50 x 50 cm grid divided into 100 cells placed on the ground next to the trapping point. We estimated the percentage of ground cover occupied by leaf litter, rocks, herbaceous vegetation, woody material, and bare ground by quantifying the number of cells occupied by each material.

Data analysis. To compare samples of different sizes, we assessed rodents' diversity across elevations and seasonality by generating coverage-based rarefaction and extrapolation sampling curves using Hill numbers. Following the recommendation of Chao and Jost (2012), we determined the base coverage as the minimum coverage among compared groups. For comparisons across elevations, we used a minimum coverage of 0.76 and for seasonal comparisons we used 0.98. Specifically, the diversity indices q0 (species richness), q1 (Shannon diversity) and q2 (dominant species abundance, derived from the Simpson index) were calculated following Chao and Jost (2012) implemented via the *vegan* (Oksanen *et al.* 2022) and *iNEXT* (Hsieh *et al.* 2016) R packages.

To evaluate compositional differences between elevation and seasonality, we applied an Analysis of Similarity (ANOSIM) and constructed two dendrograms based on Jaccard (presence/absence) and Bray–Curtis (abundance) dissimilarity indices, employing average linkage clustering. To further dissect the patterns of community dissimilarity, we conducted a Similarity Percentage (SIMPER) analysis to identify the species

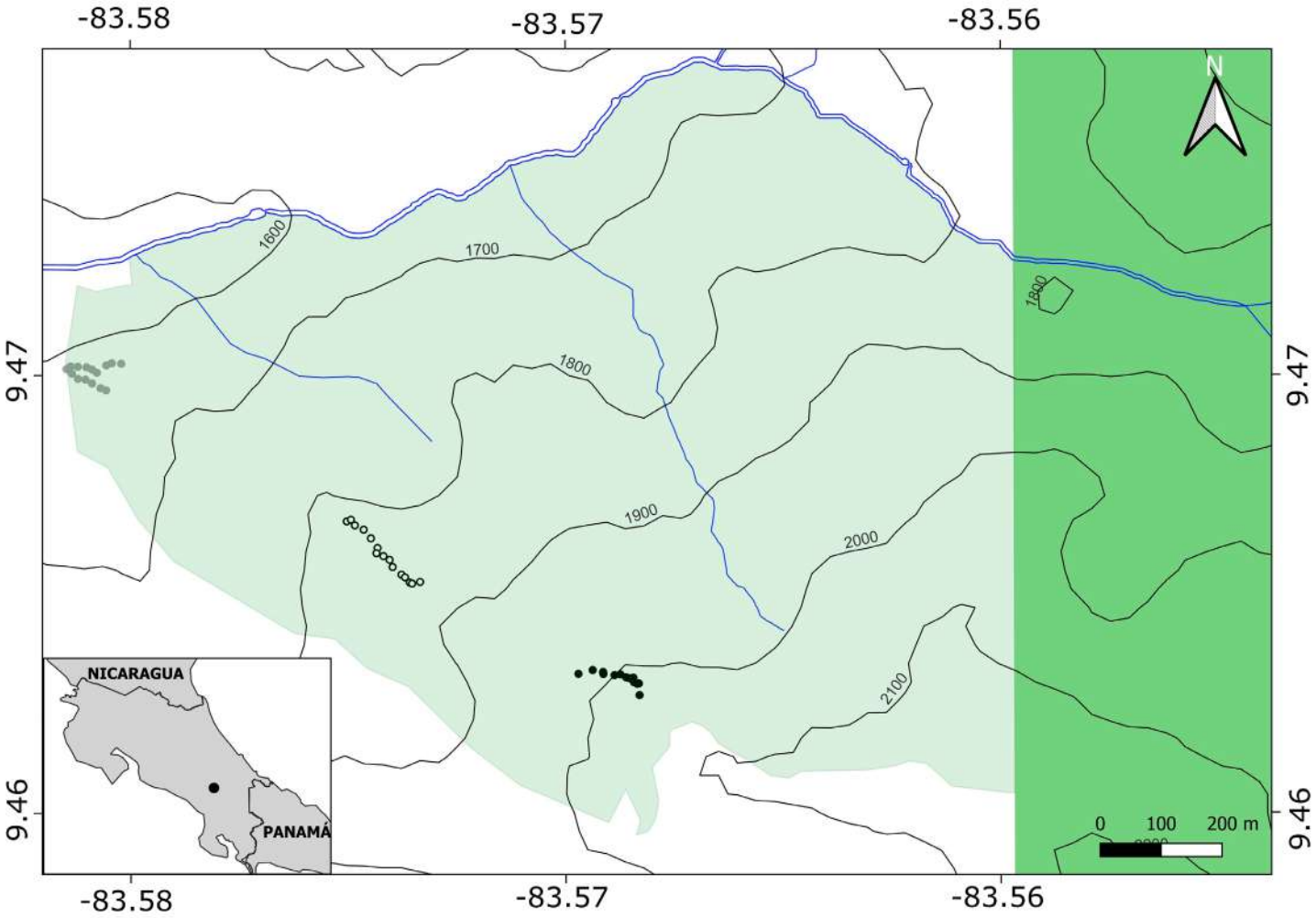

Figure 1. Geographical distribution of sampling sites along an elevational gradient in Cloudbridge Nature Reserve, Talamanca Mountain Range, Costa Rica (2023). Gray, white and black dots represent sampling stations at 1600, 1800, 2000 m.a.s.l., respectively. The light green area indicates the Cloudbridge Nature Reserve; dark green corresponds to Chirripó National Park.

contributing most to differences among sites. To explain if the probability of rodent occurrence was determined by the elevation and microhabitat characteristics, we analyzed the data separately for each season and fitted Generalized Linear Models (GLMs) (family = binomial, link = logit). The most parsimonious model was selected using stepwise model selection based on the lowest Akaike Information Criterion (AIC), for the selected models we report parameter estimate (β) and 95 % confidence intervals (CI).

Also, microhabitat characteristics were analyzed using Generalized Linear Models (GLMs) (family = gaussian, link = identity and family = poisson, link = log), with elevation and seasonality as fixed effects. The best-fitting models were selected based on the Akaike Information Criterion (AIC) (Supplementary Data SD2), and post-hoc comparisons were performed using Tukey's tests to determine pairwise differences.

All statistical analyses were executed in R version 4.4.2 (R Core Team 2024). A significance level of 0.05 was applied to all tests, except for the ANOSIM procedure, where a threshold of 0.1 was used to account for limitations in sample size. This analytical framework allowed for robust evaluation of biodiversity and environmental gradients within the study region.

Ethical statement. Research and handling with live animals followed ASM guidelines (Sikes *et al.* 2016). This study is framed under MINAE and CONAGEBIO research permits (resolutions SINAC-ACC-PI-R-044-2020, R-SINAC-PNI-ACLAP-028-2020, and R-001-2021-OT-CONAGEBIO).

Results

A total of 200 captures of nine species distributed in three families were captured in 2100 night-trap effort. Of the nine species captured, three are endemic to the Talamanca Mountain range in Costa Rica and Panamá. Two captures corresponded to the mouse opossum *Marmosa zeledoni*, and those were excluded from all the analyses (Table 1). Only *Scotinomys teguina* was present at the three elevations. One species, *Nyctomys sumichrasti*, was only captured at 1800 m. While at 2000 m two unique species, *Nephelomys devius* and *Tylomys watsoni* were captured. The most abundant species was *P. nudipes* with 111 captures, and the least abundant were *N. sumichrasti* and *T. watsoni* with only one individual captured. In terms of seasonality, we captured fewer rodents during the dry season compared to the rainy season (Table 1).

Table 1. Abundance of small mammals captured along three elevations in Cloudbridge Nature Reserve, Talamanca Mountain range, Costa Rica (2023), during the dry and rainy season. Endemic species to the Talamanca Mountain range are marked with asterisk (*).

Family	Species	Elevation m.a.s.l.			Total abundance	Season	
		1600	1800	2000		Dry	Rainy
Didelphidae							
	Marmosa zeledoni E. A. Goldman, 1911	1	1	0	2	0	2
Cricetidae							
	Scotinomys teguina (Alston, 1877)	9	2	18	29	2	27
	* *Peromyscus nudipes* (J. A. Allen, 1891)	6	0	105	111	44	67
	Reithrodontomys "mexicanus"[a] Saussure, 1880	19	0	4	23	3	20
	* *Nephelomys devius* (Bangs, 1902)	0	0	5	5	3	2
	Oligoryzomys costaricensis (J. A. Allen, 1893)	24	1	0	25	4	21
	Nyctomys sumichrasti (Saussure, 1860)	0	1	0	1	0	1
	* *Tylomys watsoni* O. Thomas, 1899	0	0	1	1	1	0
Heteromyidae							
	Heteromys desmarestianus Gray, 1868	0	2	1	3	0	3
	Total abundance	59	7	134	200	57	143

A this species is denoted in quotation marks because it represents a species cryptic complex (Martínez-Borrego *et al.* 2023); while the species ID is likely to be *Reithrodontomys garichensis* or *Reithrodontomys brevirostris*, we did not perform any molecular analysis to confirm its taxonomy. Two specimens were collected and preserved in a scientific collection for further analysis and proper identification (Supplementary Data SD1).

Sample coverage varied with elevation. At 2000 m elevation it was 0.98, at 1800 m was 0.76, and at 1600 m was 1. For all diversity orders, at both high and low elevations, the sample coverage suggests adequate sampling, as our sample captured most of the diversity. However, at 1800 m elevation, the sample coverage value suggests that a larger sample is required. We found no significant differences when comparing all Hill numbers (q0, q1, q2), between 1800 m and the other two elevations (Figure 2). Also, we did not find a dominant species and the abundances of the captured species were very similar (Table 1), which may explain the greater variability in the standard errors. When comparing low and high elevations, the 1600 m elevation showed greater species richness (q0), greater diversity of common (q1) and abundant species (q2). In contrast, at 2000 m the community was strongly dominated by *P. nudipes*. At low elevation, the community showed a more balanced structure, with the dominance of *Reithrodontomys "mexicanus"* and *Oligoryzomys costaricensis*.

On the other hand, the sample coverage was very similar for seasonality 0.98 in the dry season and 0.99 in the rainy season. We found a low diversity (q1, q2) during the dry season, however, in species richness (q0) there were no differences between seasons (Figure 3). Also, in the dry season the community was dominated by *P. nudipes*. While during the rainy season yielded a broader spectrum of rare species, including *N. sumichrasti* and *Heteromys desmarestianus*. These temporal shifts underscore the role of climatic variability in shaping rodent assemblages along tropical elevational gradients.

The species composition at the CNR showed a weak tendency to vary by elevation (*Figure 4*, ANOSIM: $R2 = 0.44$, $P < 0.1$), while no differences were detected between seasons (*Figure 4*, ANOSIM: $R2 = -0.11$, $P = 0.8$). According to the Jaccard index, rodent species composition at 1600 m was nearly identical between seasons and at 2000 m also show high seasonal similarity. On the other hand, both elevations were highly dissimilar from the 1800 m elevation. When we compared the abundance of rodents using the Bray – Curtis index the highest similarity between seasons was observed at 2000 m, whereas overall dissimilarity among elevations remained high. In both indices, the rodent community from the 1800 m elevation dry season form a distinct group because there were no captures (Figure 4).

When we compared the species that contribute most to dissimilarity, we found that between low and mid elevations *P. nudipes* contributes most significantly to the dissimilarity, with a contribution of 81 %, followed by *R. "mexicanus"* with 65 %. This high contribution is due to the absence of both species at 1800 m elevation. On the other hand, *O. costaricensis*, which is present at both low and mid elevations, contributes 36 % to the similarity between these two elevations. In contrast, between 1800 and 2000 m elevations only *P. nudipes* contributes to dissimilarity, by 80 %.

In addition, the probability of rodent occurrence during the dry season was positively related with the elevation ($\beta = 0.007$, CI 95 % = 0.004 – 0.011). To better understand this variable, we describe the microhabitat characteristics that varied by elevation and seasonality. Rodent occurrence decreased with increasing the number of trees ($\beta = -0.163$,

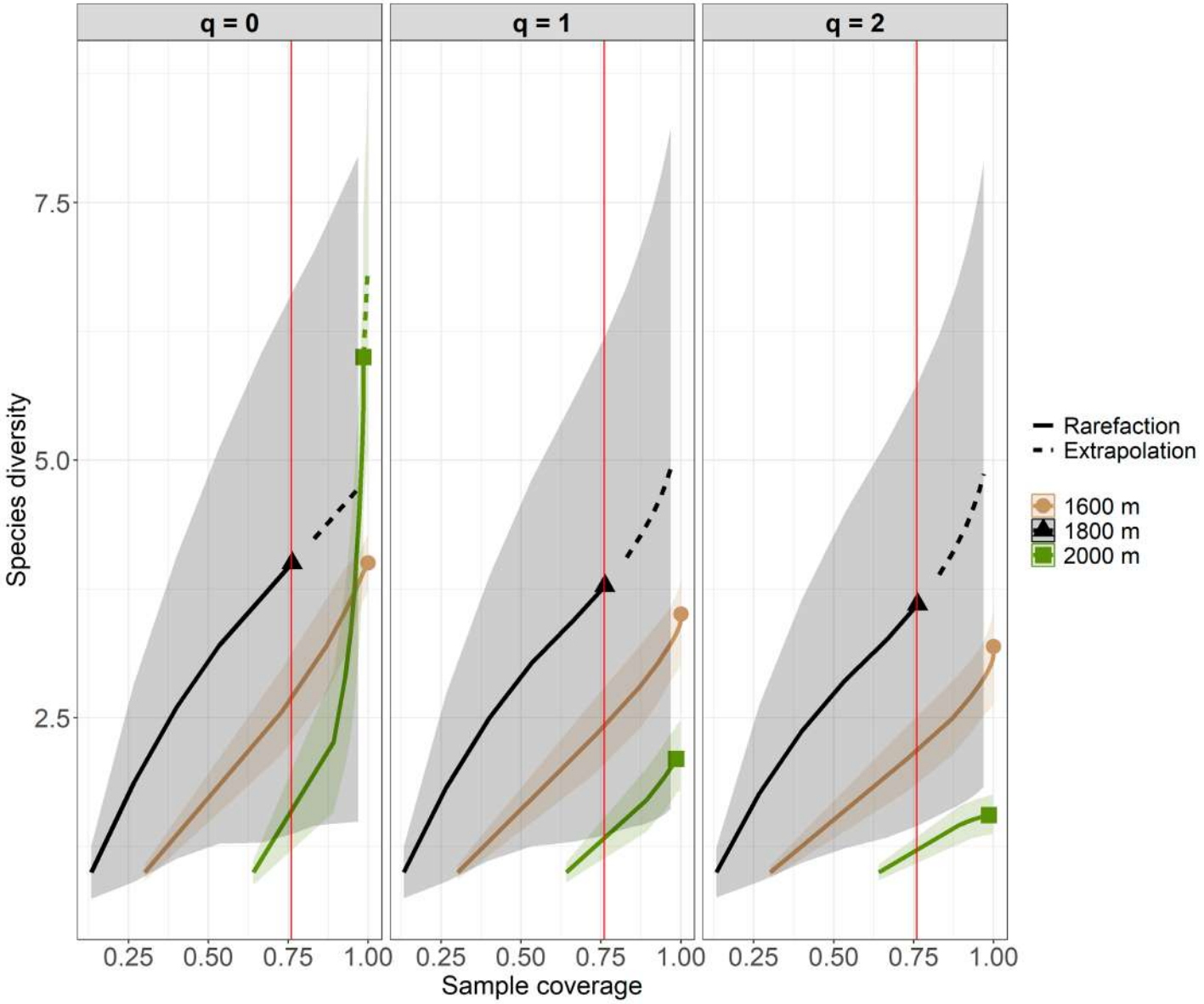

Figure 2. Coverage-based rarefaction and extrapolation sampling curves for q0 (species richness), q1 (Shannon diversity) and q2 (dominant species abundance, derived from the Simpson index) across three elevations at Cloudbridge Nature Reserve, Talamanca Mountain range, Costa Rica (2023). Shaded areas represent standard error, dotted lines indicate extrapolation, red line indicate the minimum coverage.

CI 95 % = - 0.329 – -0.030). During the rainy season, rodent presence decreased with increasing bare ground (β = -0.109, CI 95 % = -0.228 – -0.013) and leaf litter (β = -0.026, CI 95 % = -0.053 – -0.001, Table 2).

Specifically, we found more logs at mid elevation (β = 1.61, SE = 0.34, z = 4.67, P < 0.001) and high (β = 1.55, SE = 0.34, z = 4.56, P < 0.001) elevations during the dry season. There were more trees at mid elevation (β = 0.842, SE = 0.72, z = 11.64, P < 0.001; post-hoc Tukey's tests P < 0.001) and during the dry season (β = 2.50, SE = 0.57, t = 4.36, P < 0.001). Leaf litter depth was higher in the dry season (β = 0.56, SE = 0.12, t = 4.67, P < 0.001), and at both 1800 m and 2000 m elevations, but there was no significant difference between mid and high elevations (post-hoc Tukey's tests P = 0.6, Table 3). Finally, we found that the understory density/cover was higher at 2000 m elevation (β = 4.02, SE = 0.84, t = 4.81, P < 0.001; post-hoc Tukey's tests P = 0.010) and during the rainy season (Table 3).

Regarding the ground cover, we found more herbaceous coverage at 1600 m elevation (β = 66.10, SE = 5.78, t = 11.43, P < 0.001). Additionally, herbaceous coverage was higher

Table 2. Parameters of Generalized Linear Models (GLMs) assessing the probability of rodent occurrence by the elevation and microhabitat characteristics separated by seasonality at Cloudbridge Nature Reserve, Talamanca Mountain Range, Costa Rica (2023). We represent the confidence intervals (CI) at 95%.

Seasonality	Coefficient	Estimate	Standard error	CI 95 %
Dry	Intercept	-11.806	3.203	-18.602 – -5.895
	Elevation	**0.007**	**0.002**	**0.004 – 0.011**
	Trees number	**-0.163**	**0.076**	**-0.329 – -0.030**
	Woody material	-0.053	0.028	-0.112 – 0.0005
Rainy	Intercept	-3.393	2.817	-9.066 – 2.068
	Elevation	0.002	0.002	-0.0006 – 0.006
	Trees number	0.154	0.091	-0.020 – 0.340
	Bare ground	**-0.109**	**0.054**	**-0.228 – -0.013**
	Leaf litter	**-0.026**	**0.013**	**-0.053 – -0.001**

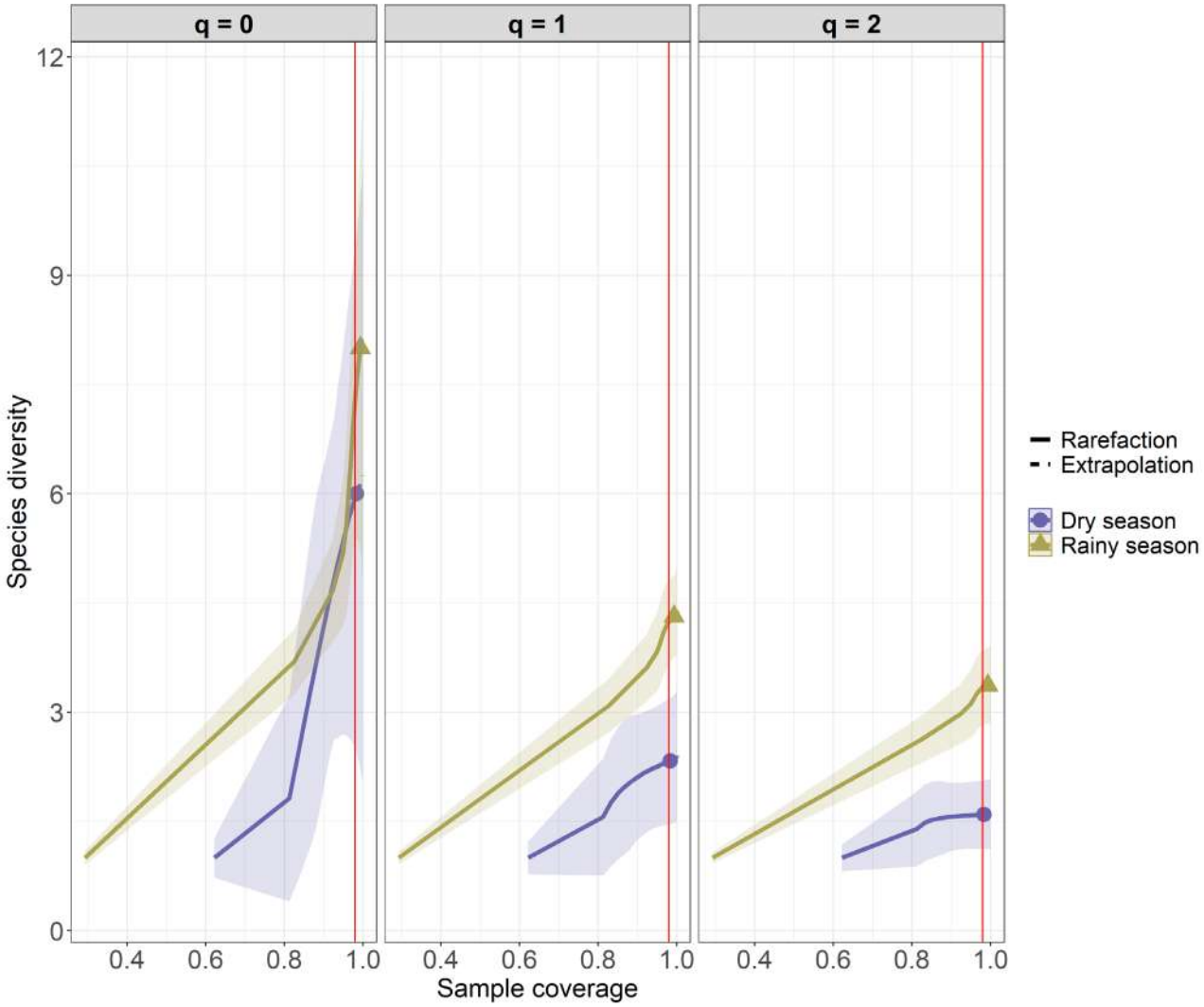

Figure 3. Coverage-based rarefaction and extrapolation sampling curves for q0 (species richness), q1 (Shannon diversity), and q2 (dominant species abundance, derived from the Simpson index) during the dry and rainy seasons at Cloudbridge Nature Reserve, Talamanca Mountain range, Costa Rica (2023). Shaded areas represent standard error, dotted lines indicate extrapolation, red line indicate the minimum coverage.

Table 3. Parameters of Generalized Linear Models (GLMs) assessing the effects of elevation and seasonality on structural microhabitat characteristics at Cloudbridge Nature Reserve, Talamanca Mountain Range, Costa Rica (2023). Int: Intercept.

Variable	Coefficient	Estimate	Standard error	Test statistic	P value
Logs number	1 600 m, Rainy season (Int)	0.693	0.129	z = 5.369	<0.001
	1 800 m elevation	0.569	0.162	z = 3.523	<0.001
	2 000 m elevation	0.847	0.154	z = 5.491	<0.001
	Dry season	-1.609	0.316	z = -5.089	<0.001
	1 800 m elevation x Dry season	1.6094	0.345	z = 4.668	<0.001
	2 000 m elevation x Dry season	1.551	0.339	z = 4.578	<0.001
Trees number	1 600 m, Rainy season (Int)	1.318	0.064	z = 25.870	<0.001
	1 800 m elevation	0.842	0.072	z =11.639	<0.001
	2 000 m elevation	0.243	0.080	z = 3.002	0.003
	Dry season	0.362	0.057	z = 6.317	<0.001
Leaf litter depth	1 600 m, Rainy season (Int)	1.599	0.119	t = 13.403	<0.001
	1 800 m elevation	0.305	0.146	t = 2.083	0.039
	2 000 m elevation	0.440	0.146	t = 3.011	0.003
	Dry season	0.557	0.119	t = 4.669	<0.001
Understory density/cover	1 600 m, Rainy season (Int)	93.765	0.682	t = 137.524	<0.001
	1 800 m elevation	1.539	0.835	t = 1.843	0.067
	2 000 m elevation	4.018	0.835	t = 4.812	<0.001
	Dry season	-2.342	0.682	t = -3.435	<0.001

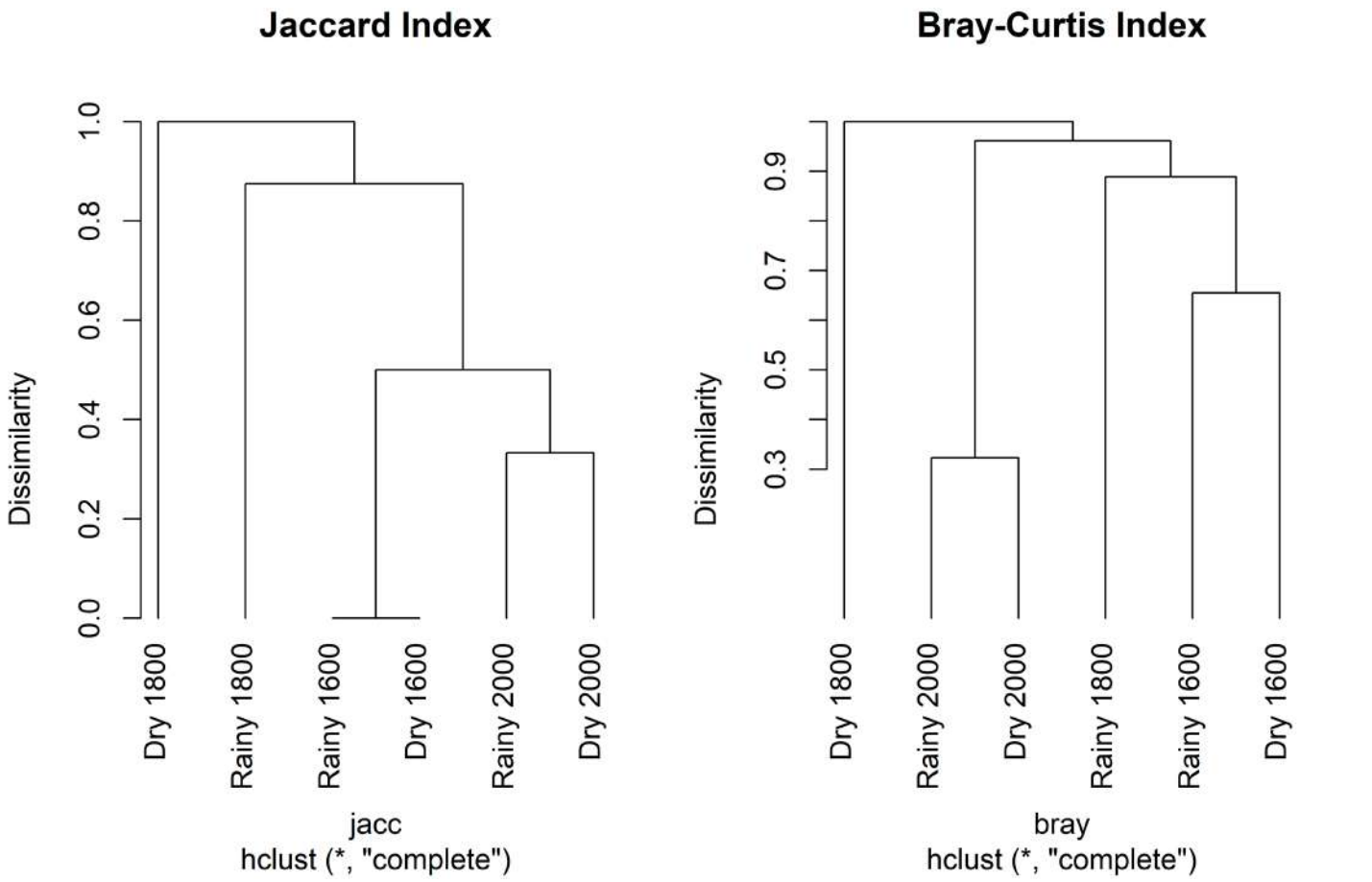

Figure 4. Dissimilarity in rodent assemblages at Cloudbridge Nature Reserve, Talamanca Mountain range, Costa Rica (2023). Based on Presence/Absence (Jaccard index) and Species Abundance (Bray – Curtis index).

at mid elevation during the dry season compared to the other elevations during the same season (β = 30.60, SE = 11.57, t = 2.65, P < 0.009). The presence of rocks was higher at the 2000 m elevation compared to the other elevations (β = 14.78, SE = 2.73, t = 5.42, P < 0.001; post-hoc Tukey's tests P = 0.0001). The presence of leaf litter was higher at mid elevation and during the rainy season (Table 4), with no difference between mid and high elevations (post-hoc Tukey's tests P = 0.09). However, we found more leaf litter at high elevation during the dry season compared to the other elevations during the same season (β = 56.00, SE = 12.64, t = 4.42, P < 0.001). The average amount of woody material (β = 11.83, SE = 2.96, t = 4.02, P < 0.001) and bare ground (β = 54.26, SE = 4.75, t = 11.42, P < 0.001) was higher during the dry season, with bare ground being more abundant at low elevation during the dry season (Table 4).

Discussion

Precipitation has been associated with increased rodents' diversity due to greater habitat heterogeneity (Sánchez-Cordero 2001; Ramírez-Bautista and Williams 2019). Our results support this pattern by documenting higher understory density; this is a habitat feature frequently selected by rodents to feed, shelter, or avoid predation (Brown 2001; Williams *et al.* 2002; Fardell *et al.* 2021). Furthermore, it has been reported that rodents are more active under the rain since it could reduce the risk of predation for two reasons: (1) the rain dissipates the smell of the rodents (Vickery and Bider 1981), and (2) it hides the sounds of movement when walking on leaf litter or branches (Barnum *et al.* 1992). However, we found that the rodent presence decreased as leaf litter increased, suggesting that further studies are needed to better understand this pattern.

On the other hand, the low diversity and presence of rodent during the dry season, could be due to the high density of trees, which can reduce light availability, thus limiting the development of understory density cover (Klinka *et al.* 1996). Therefore, bare ground may reduce rodent occurrence, because they are more exposed to predators and could be easily detected and predated (Schulte-Hostedde and Brooks 1997; Roche *et al.* 1999).

Rodent's presence was associated with elevation, suggesting that changes in microhabitat characteristics along the three elevations might influence rodent distribution and composition at CNR. The 1600 m elevation has open areas within the forest because it has microhabitat characteristics such as herbaceous cover and bare ground. These explain the most abundant species, *O. costaricensis* and *R. "mexicanus"*, because they prefer secondary forest, but also forest glades (Pardiñas *et al.* 2017).

Table 4. Parameters of Generalized Linear Models (GLMs) evaluating the effects of elevation and seasonality on ground cover microhabitat characteristics at Cloudbridge Nature Reserve, Talamanca Mountain Range, Costa Rica (2023). Int: Intercept.

Variable	Coefficient	Estimate	Standard error	T value	P value
Herbaceous	1600 m, Rainy season (Int)	66.100	5.783	11.430	<0.001
	1 800 m elevation	-47.800	8.178	-5.845	<0.001
	2 000 m elevation	-27.733	8.178	-3.391	0.001
	Dry season	-8.967	8.178	-1.096	0.274
	1 800 m elevation x Dry season	30.600	11.566	2.646	0.009
	2000 m elevation x Dry season	-0.800	11.566	-0.069	0.945
Rocks	1600 m, Rainy season (Int)	-0.589	2.228	-0.264	0.792
	1 800 m elevation	2.917	2.729	1.069	0.287
	2 000 m elevation	14.783	2.729	5.417	<0.001
	Dry season	1.178	2.228	0.529	0.598
Woody material	1600 m, Rainy season (Int)	25.611	2.958	8.658	<0.001
	1 800 m elevation	6.167	3.623	1.702	0.091
	2 000 m elevation	0.233	3.623	0.064	0.949
	Dry season	11.878	2.958	4.015	<0.001
Leaf litter	1600 m, Rainy season (Int)	105.200	6.325	16.633	<0.001
	1 800 m elevation	31.867	8.945	3.563	<0.001
	2 000 m elevation	1.933	8.945	0.216	0.829
	Dry season	-61.533	8.945	-6.879	<0.001
	1 800 m elevation x Dry season	23.800	12.649	1.881	0.062
	2 000 m elevation x Dry season	56.000	12.649	4.427	<0.001
Bare ground	1600 m, Rainy season (Int)	4.267	3.360	1.270	0.206
	1 800 m elevation	3.333	4.752	0.702	0.484
	2 000 m elevation	8.800	4.752	1.852	0.0657
	Dry season	54.267	4.752	11.421	<0.001
	1 800 m elevation x Dry season	-49.700	6.720	-7.396	<0.001
	2 000 m elevation x Dry season	-56.967	6.720	-8.477	<0.001

At 2000 m elevation, the greater density of understory vegetation and increased rock cover likely create favorable microhabitats for forest-dwelling rodents such as *N. devius, P. nudipes,* and *T. watsoni*. The structural complexity of the terrain enhances concealment opportunities, with rock formations offering reliable shelter from predators, a behavior well documented in *Peromyscus* spp. (Dooley and Dueser 1990; Millus and Stapp 2008). These microhabitat features may play a key role in shaping community composition at higher elevations.

The notable abundance of *P. nudipes* at this elevation is plausibly linked to trophic specialization, particularly its association with oak (*Quercus* spp.) seed consumption (Rojas and Barboza 2007; Ramírez-Fernández 2019), a food resource encountered exclusively at 2000 m elevation in this study. This dietary preference underscores the influence of vegetation composition on species distribution and highlights the importance of integrating habitat and resource availability when interpreting elevational patterns in rodent assemblages.

The low rodent capture at 1800 m elevation could be due to rodents reducing their activity. This is because logs and leaf litter cover/depth were found at this elevation. Additionally, there was herbaceous coverage at mid elevation during the dry season. These microhabitat characteristics could be used by rodents to hide from predators, and semi-arboreal species could move more easily through trees. However, our results suggest that more sampling effort is needed to better understand which variables affect the rodent presence at mid-elevation.

The singing mouse *S. teguina* was the only one found in the three elevations in both seasons. This could be due to its flexibility on habitat selection since it occurs within the forest, as well as in disturbed sites with grass or herbs (Hooper and Carleton 1976; Ribble and Rathbun 2018). Changes in food availability could also play a role, as it is a primarily insectivorous species (Hooper 1972; Hooper and Carleton 1976). The three elevations had leaf litter and logs, which are suitable microhabitats for larval development and the presence of various beetles in both seasons (Gossner *et al.* 2013; Cole *et al.* 2016), which are preferred by *Scotinomys* spp. (Hooper and Carleton 1976). However, this factor was not directly evaluated in the present study.

Mountain ecosystems are characterized by a high level of endemism. At CNR, we captured three endemic species; this reinforces the importance of highlands conservation and protection (Sakane *et al.* 2019). Our results suggest that elevation indirectly influences species diversity and occurrence through changes in microhabitat characteristics. Therefore, maintaining forested areas with understory

density/cover, rocks, and leaf litter favors the diversity of rodents and the permanence of endemic species, possibly because it provides diverse food resources and protection against predators. However, this relationship should be explicitly evaluated in future studies.

Acknowledgements

Querida Livia, desde Costa Rica te agradezco todo tu aporte al conocimiento de la mastofauna de la región. También admiro tu impacto como formadora de excelentes profesionales. Muchas gracias por tanta dedicación y cariño en tu trabajo. Bernal Rodríguez-Herrera. We thank the staff and volunteers of Cloudbridge Nature Reserve for logistical support, the Oncilla Conservation project of the Costa Rica Wildlife Foundation for financial support. The Laboratorio de Recursos Naturales y Vida Silvestre (LARNAVISI) of the UNA for loan of equipment. Eduardo Chacón for the help in the statistical analysis. David Vela as a field assistant. This work is part of Rebeca undergraduate research project (Licenciatura) at Universidad Nacional de Costa Rica.

Declaration of Artificial Intelligence use

Authors used ChatGPT for grammar checking.

Author contributions

Rebeca Jiménez-Gómez: conceptualization, study design and fieldwork planning, data collection, analysis and interpretation of the results, and preparation of the first draft of the manuscript. Bernal Rodríguez-Herrera: conceptualization, study design, and fieldwork planning; reviewed and provided critical revisions to the manuscript. Lilliana Piedra-Castro: conceptualization, reviewed, and provided critical revisions to the manuscript. José D. Ramírez-Fernández: conceptualization, study design and fieldwork planning, funding acquisition, reviewed and provided critical revisions to the manuscript.

Supplementary data

SD1. Catalog of voucher specimens of some of the species captured at the Cloudbridge Nature Reserve deposited in the Zoology Museum University of Costa Rica.

SD2. Generalized Linear Models (GLM) evaluating the effects of the elevation and the season on microhabitat characteristics at three elevations of the Cloudbridge Nature Reserve, Talamanca Mountain Range, Costa Rica (2023). The model with the best fit, based on the Akaike Information Criterion (AIC), is indicated in bold.

Literature cited

Barnum SA, Manville CJ, Tester JR, and Carmen WJ. 1992. Path selection by *Peromyscus leucopus* in the presence and absence of vegetative cover. *Journal of Mammalogy* 73:797–801. https://doi.org/10.2307/1382198

Barras AG, Braunisch V, and Arlettaz R. 2021. Predictive models of distribution and abundance of a threatened mountain species show that impacts of climate change overrule those of land use change. *Diversity and Distributions* 27:989–1004. https://doi.org/10.1111/ddi.13247

Benedek AM, Sîrbu I, and Lazăr A. 2021. Responses of small mammals to habitat characteristics in Southern Carpathian forests. *Scientific Reports* 11:1–13. https://doi.org/10.1038/s41598-021-91488-6

Birkel C, Dehaspe J, Chavarría-Palma A, Venegas-Cordero N, Capell R, and Durán-Quesada AM. 2022. Projected climate change impacts on tropical life zones in Costa Rica. *Progress in Physical Geography: Earth and Environment* 46:180–200. https://doi.org/10.1177/03091333211047046

Brown JH. 2001. Mammals on mountainsides: elevational patterns of diversity. *Global Ecology and Biogeography* 10:101–109. https://doi.org/10.1046/j.1466-822x.2001.00228.x

Chao A, and Jost L. 2012. Coverage-based rarefaction and extrapolation: standardizing samples by completeness rather than size. *Ecology* 93:2533 –2547. https://doi.org/10.1890/11-1952.1

Cole RJ, Holl KD, Zahawi RA, Wickey P, and Townsend AR. 2016. Leaf litter arthropod responses to tropical forest restoration. *Ecology and Evolution* 6:5158–5168. https://doi.org/10.1002/ece3.2220

Dooley JL and Dueser RD. 1990. An experimental examination of nest-site segregation by two *Peromyscus* species. *Ecology* 71:788–796. https://doi.org/10.2307/1940330

Fardell LL, Nano CE, Pavey CR, and Dickman CR. 2021. Small prey animal habitat use in landscapes of fear: effects of predator presence and human activity along an urban disturbance gradient. *Frontiers in Ecology and Evolution* 9:1–17. https://doi.org/10.3389/fevo.2021.750094

Gossner MM, Floren A, Weisser WW, and Linsenmair KE. 2013. Effect of dead wood enrichment in the canopy and on the forest floor on beetle guild composition. *Forest Ecology and Management* 302:404–413. http://dx.doi.org/10.1016/j.foreco.2013.03.039

Holdridge LR. 1967. Life Zone Ecology. San José (CR): Tropical Science Center. Available at: https://app.ingemmet.gob.pe/biblioteca/pdf/Amb-56.pdf

Hooper ET. 1972. A synopsis of the rodent genus *Scotinomys*. *Occasional Papers of the Museum of Zoology, University of Michigan* 665:1–32.

Hooper ET, and Carleton MD. 1976. Reproduction, growth and development in two contiguously allopatric rodent species, genus *Scotinomys*. *Miscellaneous Publications Museum of Zoology, University of Michigan* 151:1–60.

Hsieh TC, Ma KH, and Chao A. 2016. iNEXT: An R package for rarefaction and extrapolation of species diversity (Hill numbers). *Methods in Ecology and Evolution* 7:1451–1456. https://doi.org/10.1111/2041-210X.12613

Karasov-Olson A, and Kelt DA. 2020. Small mammal assemblage composition and habitat associations across an elevational gradient in southern California. *Journal of Mammalogy* 101:92–106. https://doi.org/10.1093/jmammal/gyz178

Klinka K, Chen HY, Wang Q, and de Montigny L. 1996. Forest canopies and their influence on understory vegetation in early-seral stands on West Vancouver Island. *Northwest Science* 70:193–200.

Liu Z, Sandoval L, Sherman LB, and Wilson AM. 2023. Vulnerability of elevation-restricted endemic birds of the Cordillera de Talamanca (Costa Rica and Panama) to climate change. *Neotropical Biodiversity* 9:115–127. https://doi.org/10.1080/23766808.2023.2261196

Lomolino MV. 2001. Elevation gradients of species-density: historical and prospective views. *Global Ecology and Biogeography* 10:3–13. https://doi.org/10.1046/j.1466-822x.2001.00229.x

Martínez-Borrego D, Arellano E, González-Cózatl FX, Ospina-Gárces S, and Rogers DS. 2023. Species delimitation and integrative taxonomy of the *Reithrodontomys mexicanus* (Rodentia: Cricetidae) cryptic complex. *Ecology and Evolution* 13:1–18. https://doi.org/10.1002/ece3.10355

McCain CM. 2004. The mid-domain effect applied to elevational gradients: species richness of small mammals in Costa Rica. *Journal of Biogeography* 31:19–31. https://doi.org/10.1046/j.0305-0270.2003.00992.x

McCain CM. 2006. Do elevational range size, abundance, body size patterns mirror those documented for geographic ranges? A case study using Costa Rican rodents. *Evolutionary Ecology Research* 8:435–454.

McCain CM, and Grytnes JA. 2010. Elevational gradients in species richness. *Encyclopedia of Life Sciences* 1–10. https://doi.org/10.1002/9780470015902.a0022548

McPherson AB. 1985. A biogeographical analysis of factors influencing the distribution of Costa Rican rodents. *Brenesia* 23:97–273.

Millus SA, and Stapp P. 2008. Interactions between seabirds and endemic deer mouse populations on Santa Barbara Island, California. *Canadian Journal of Zoology* 86:1031–1041. https://doi.org/10.1139/Z08-081

Nor SM. 2001. Elevational diversity patterns of small mammals on Mount Kinabalu, Sabah, Malaysia. *Global Ecology and Biogeography* 10:41–62. https://doi.org/10.1046/j.1466-822x.2001.00231.x

Oksanen J, Simpson G, Blanchet F, Kindt R, Legendre P, Minchin P, *et al*. 2022. Vegan: Community Ecology Package. R package version 2.6-4.

Pardiñas U, Myers P, León-Paniagua L, Ordóñez-Garza N, Cook J, Kryštufek B, *et al.* 2017 Family Cricetidae (true hamsters, voles, lemmings and New World rats and mice). In: Wilson DE, Lacher TE, Mittermeier, RA, editors. *Handbook of the mammals of the world.* Vol. 7, *Rodents II*. Barcelona (SPA): Lynx Edicions; p. 204–535.

Pounds JA, Fogden MPL, and Campbell JH. 1999. Biological response to climate change on a tropical mountain. *Nature* 398:161–167. https://doi.org/10.1038/19297

Powell JR, Slifkin JP, Spooner FT, Roth J, Allnatt L, Andrews R, *et al*. 2022. Bird species inventory in secondary tropical montane cloud forest at Cloudbridge Nature Reserve, Talamanca Mountains, Costa Rica. *Check List* 18:17–65. https://doi.org/10.15560/18.1.17

R Core Team. 2024. *R: A language and environment for statistical computing. R Foundation for Statistical Computing*. R Foundation for Statistical Computing. V. 4.4.2. Vienna (Austria). https://www.R-project.org/

Rahbek C, Borregaard MK, Antonelli A, Colwell RK, Holt BG, Nogues-Bravo D, *et al.* 2019a. Building mountain biodiversity: geological and evolutionary processes. *Science* 365:1114–1119. https://doi.org/10.1126/science.aax0151

Rahbek C, Borregaard MK, Colwell RK, Dalsgaard BO, Holt BG, Morueta-Holme N, *et al.* 2019b. Humboldt's enigma: what causes global patterns of mountain biodiversity? *Science* 365:1108–1113. https://doi.org/10.1126/science.aax0149

Ramírez-Bautista A, and Williams JN. 2019. The importance of productivity and seasonality for structuring small rodent diversity across a tropical elevation gradient. *Oecologia* 190:275–286. https://doi.org/10.1007/s00442-018-4287-z

Ramírez-Fernández JD. 2019. *Uso del hábitat y estructura poblacional de Peromyscus nudipes (Rodentia: Cricetidae) en las zonas altas de la Cordillera de Talamanca, Costa Rica.* [Undergraduate thesis]. [San Pedro (CR)]: University of Costa Rica.

Ramírez-Fernández JD, Barrantes G, Sánchez-Quirós C, and Rodríguez-Herrera B. 2023a. Habitat use, richness, and abundance of native mice in the highlands of the Talamanca Mountain range, Costa Rica. *Therya* 14:49–54. https://doi.org/10.12933/therya-23-2227

Ramírez-Fernández JD, Sánchez R, May-Collado LJ, González-Maya FJ, and Rodríguez-Herrera R. 2023b. Revised checklist and conservation status of the mammals of Costa Rica. *Therya* 14:1–12. https://doi.org/10.12933/therya-23-2142

Ribble DO, and Rathbun GB. 2018. Preliminary observations on home ranges and natural history of *Scotinomys teguina* in Costa Rica. *Mammalia* 82:490–493. https://doi.org/10.1515/mammalia-2017-0065

Roche BE, Schulte-Hostedde AI, and Brooks RJ. 1999. Route choice by deer mice (*Peromyscus maniculatus*): reducing the risk of auditory detection by predators. *The American Midland Naturalist* 142:194–197. https://doi.org/10.1674/0003-0031(1999)142[0194:RCBDMP]2.0.CO;2

Rodríguez-Herrera B, Ramírez-Fernández JD, Villalobos-Chaves D, and Sánchez R. 2014. Actualización de la lista de especies de mamíferos vivientes de Costa Rica. *Mastozoología Neotropical* 21:275–289.

Rojas RL, and Barboza RM. 2007. Ecología poblacional del ratón *Peromyscus mexicanus* (Rodentia: Muridae) en el Parque Nacional Volcán Poás, Costa Rica. *Revista de Biología Tropical* 55:1037–1050.

Sakane KK, Percequillo AR, and Setz EZF. 2019. Community of small mammals along an elevational gradient in Biological Reserve of Serra do Japi, municipality of

Jundiaí-SP, Brazil. *Austral Ecology* 44:1236–1244. https://doi.org/10.1111/aec.12801

Sánchez-Cordero V. 2001. Elevation gradients of diversity for rodents and bats in Oaxaca, Mexico. *Global Ecology and Biogeography* 10:63–76. https://doi.org/10.1046/j.1466-822x.2001.00235.x

Schulte-Hostedde AI, and Brooks RJ. 1997. An experimental test of habitat selection by rodents of Algonquin Park. *Canadian Journal of Zoology* 75:1989–1993. https://doi.org/10.1139/z97-831

Sikes RS, Bryan II JA, Byman D, Danielson BJ, Eggleston J, Gannon MR, *et al.* 2016. Guidelines of the American Society of Mammalogists for the use of wild mammals in research. *Journal of Mammalogy* 97:663–688. https://doi.org/10.1093/jmammal/gyw078

Vickery WL, and Bider JR. 1981. The influence of weather on rodent activity. *Journal of Mammalogy* 62:140–145. https://doi.org/10.2307/1380484

Villalobos-Chaves D, Ramírez-Fernández JD, Chacón-Madrigal E, Pineda-Lizano W, and Rodríguez-Herrera B. 2016. Clave para la identificación de los roedores de Costa Rica. Escuela de Biología, Universidad de Costa Rica. San José, Costa Rica.

Williams SE, Marsh H, and Winter J. 2002. Spatial scale, species diversity, and habitat structure: small mammals in Australian tropical rain forest. *Ecology* 83:1317–1329. https://doi.org/10.1890/0012-9658(2002)083[1317:SSSDAH]2.0.CO;2

Yanahan AD, and Moore W. 2019. Impacts of 21st-century climate change on montane habitat in the Madrean Sky Island Archipelago. *Diversity and Distributions* 25:1625–1638. https://doi.org/10.1111/ddi.12965

Associated editors: Giovani Hernández Canchola and Pablo Colunga Salas
Submitted: Noviembre 1, 2025; Reviewed: December 16, 2025
Accepted: April 11, 2026; Published online: May 29, 2026

THERYA, 2026, Vol. 17(2):225-234 DOI: 10.12933/therya.2026.6243 ISSN 2007-3364

Resolving the taxonomic status of *Abrothrix andina* (Rodentia, Cricetidae): evidence from topotypic specimens

Mauro N. Tammone[1], Erika Cuellar Soto[2], Carola Cañón[3], Jonathan A. Guzmán[4], and Ulyses F.J. Pardiñas[5*]

[1]Instituto de Investigaciones en Biodiversidad y Medioambiente, CONICET-UN Comahue, Bariloche, Argentina. E-mail: mtammone@comahue-conicet.gob.ar (MNT).
[2]Department of Biology, College of Science, Sultan Qaboos University, Muscat, Oman. E-mail: e.soto@squ.edu.om (ECS).
[3]Cape Horn International Center for Global Change Studies and Biocultural Conservation (CHIC), Puerto Williams; Pontificia Universidad Católica de Chile, Facultad de Ciencias Biológicas, Departamento de Ecología; and Instituto Milenio Centro de Regulación del Genoma (CRG), Santiago, Chile. E-mail: carolacanonv@gmail.com (CC).
[4]Laboratorio de Historia Natural (LAHN), Universidad de Concepción, Campus Los Ángeles, Chile. E-mail: jguzman@udec.cl (JAG).
[5]Instituto de Diversidad y Evolución Austral (IDEAus-CONICET), Puerto Madryn, Argentina; and Instituto Nacional de Biodiversidad (INABIO), Quito, Ecuador.
[*]Corresponding author: ulyses@cenpat-conicet.gob.ar

Recent studies have demonstrated that the Andean sigmodontine rodent *Abrothrix andina* (Sigmodontinae, Abrotrichini) is neither widespread nor a senior synonym of several nominal taxa (i.e., *dolichonyx*, *cinnamomea*, *jucundus*, *gossei*, and *polius*) described from Argentina, Chile, and Peru since the 19th century. However, a comprehensive taxonomic and nomenclatural reassessment requires the examination of type material. Here, we address this by analyzing topotypic specimens collected from three Andean localities near Santiago de Chile (Chile), the type locality of *A. andina*. *Cytochrome b* sequences from these specimens cluster within *Abrothrix olivacea*. These results support treating *Abrothrix andina* (Philippi in Philippi & Landbeck, 1858) as a junior synonym of *Abrothrix olivacea* (Waterhouse, 1837). Additionally, the nominal form *Abrothrix gossei* (Thomas, 1920) warrants recognition as a distinct species of *Abrothrix*, sister to *A. olivacea*. Although this study appears to complete the taxonomic reassessment of *A. andina*, a remote possibility remains that its holotype, currently lost, represents a still-unsampled Andean highland population, now extinct or extremely rare due to climate change.

Keywords: *Abrothrix gossei; Abrothrix olivacea*; Argentina; Chile; *cytochrome b*; topotype.

Estudios recientes han demostrado que el roedor sigmodontino andino *Abrothrix andina* (Sigmodontinae, Abrotrichini) no es ni una especie de amplia distribución, ni un sinónimo principal de varios taxones nominales (i.e., *dolichonyx*, *cinnamomea*, *jucundus*, *gossei* y *polius*) descritos desde el siglo XIX en Argentina, Chile y Perú. Sin embargo, una reevaluación taxonómica y nomenclatural integral requiere el examen del material tipo. Aquí abordamos esta cuestión mediante el análisis de especímenes topotípicos recolectados en tres localidades andinas cercanas a Santiago de Chile (Chile), la localidad tipo de *A. andina*. Las secuencias del *citocromo b* de estos especímenes se agrupan dentro de *Abrothrix olivacea*. Estos resultados respaldan tratar a *Abrothrix andina* (Philippi in Philippi & Landbeck, 1858) como sinónimo junior de *Abrothrix olivacea* (Waterhouse, 1837). Además, la forma nominal *Abrothrix gossei* (Thomas, 1920) merece ser reconocida como una especie distinta de *Abrothrix*, hermana de *A. olivacea*. Aunque este estudio parece completar la reevaluación taxonómica de *A. andina*, persiste la posibilidad remota de que su holotipo, actualmente perdido, represente una población altoandina aún no muestreada, hoy extinta o extremadamente rara debido al cambio climático.

Palabras clave: *Abrothrix gossei; Abrothrix olivacea*; Argentina; Chile; *citocromo b*; topotipo.

Since the late 20th century, sigmodontine rodents have received renewed taxonomic attention, leading not only to the description of new taxa but also to the revision of well-established species. In many cases, such revisions have resulted in the resurrection of nominal forms previously regarded as synonyms, thereby expanding the recognized diversity of the group (e.g., Myers *et al.* 1990; Jayat *et al.* 2016; Rocha *et al.* 2018) and demonstrating that some supposedly widespread species are, in fact, composite taxa. Less frequently, recent taxonomic reassessments have shown that supposedly widespread species, long maintained under taxonomic stasis, are actually composites of erroneously synonymized nominal forms.

The Andean cricetid *Abrothrix andina* (Philippi in Philippi & Landbeck 1858) has recently emerged as a paradigmatic example of the latter case. Historically, this member of the subgenus *Angelomys* was considered a widespread species ranging from central-western Argentina and Chile to southern Peru (e.g., Patterson *et al.* 2015; Pardiñas 2017; Teta *et al.* 2017; Tammone *et al.* 2025a; 2025b). This taxon was notable not only for its broad latitudinal distribution, spanning approximately 10 degrees, but also for its historically inclusive concept, which subsumed five nominal forms described between the late 19th and early 20th centuries. These are, in chronological order: *Hesperomys dolichonyx* Philippi, 1896, *Hesperomys dolichonyx cinnamomea* Philippi, 1896, *Akodon jucundus* Thomas, 1913, *Akodon gossei* Thomas, 1920, and *Akodon andinus polius* Osgood, 1944 (Philippi 1896; Thomas 1913; 1920; Osgood 1943; 1944). Within this general taxonomic

framework, *A. andina* has also been studied in other contexts, such as physiology, ecology, and natural history (e.g., Bozinovic 1993; Bozinovic *et al.* 1988; 1990; 1999; Rosenmann and Ruiz 1993; López-Cortés *et al.* 2007).

From a taxonomic perspective, Mann (1978) suggested that *A. andina* might be conspecific with *Abrothrix olivacea* (Waterhouse 1837). However, it was not until recently that two studies employing *cytochrome b* sequences provided key insights into the taxonomy of *A. andina* and *A. olivacea*. Tammone *et al.* (2025a) showed that topotypes of *A. gossei* from Mendoza (Argentina) form the sister group to *A. olivacea*, whereas individuals assigned to *A. polius* from southern Peru were nested within *A. olivacea*. Subsequently, Tammone *et al.* (2025b) confirmed that *A. jucundus* and *A. dolichonyx*, two other nominal taxa included under *A. andina*, also clustered within *A. olivacea*. However, a crucial piece of this taxonomic puzzle is to determine the status of the populations of *A. andina* inhabiting the Andes near Santiago de Chile, as this region corresponds to the type locality of the species (Philippi and Landbeck 1858; Philippi 1900).

Here, we focus on the status of these high-Andean populations of *A. andina* from localities near Santiago de Chile in order to assess Mann's (1978) hypothesis. Sequencing of topotypic specimens provides further evidence supporting the synonymy of *A. andina* with *A. olivacea*. The main taxonomic and nomenclatural implications of these findings are discussed.

Materials and methods

Sampled localities correspond to Andean ranges in central and northern Chile, in the Region Metropolitana and Tarapacá, respectively (Table 1; Figure 1 and Figure 2). Specimens were secured following the guidelines established by the American Society of Mammalogists (Sikes *et al.* 2016). Collections were authorized by the Servicio Agrícola y Ganadero de Chile (SAG) RESOLUCIÓN EXENTA Nº: 6230/2024 to JG. Primary taxonomic identification was based on geographic distribution and external morphology. Vouchers were deposited in the Laboratorio de Estudios de Mamíferos, Universidad Nacional de Concepción (LEM-UCLA, Los Ángeles, Chile). Currently, they are cataloged under the field number JG (= collector number of Jonathan Guzman), which will be updated to LEM once the numbering process is completed.

Genomic DNA was extracted using the DNeasy Blood and Tissue kit (Qiagen, Valencia, California), following the manufacturer's instructions. PCR amplification of the entire *cytochrome b* (*cyt b*) locus (1,140bp) was achieved using two pairs of primers: MVZ05-16, MVZ23-14. Mastermix, and thermocycling conditions were the same as detailed previously (Smith and Patton 1999; Tammone *et al.* 2016). Sequencing was performed at Macrogen Inc (Seoul, South Korea). The obtained sequences (GenBank accession numbers PX116190-PX116201) were used to perform a phylogenetic analysis in combination with 53 sequences retrieved from GenBank, representing all known populations of *Abrothrix* from central and northern Andean ranges from Chile and Argentina. The complete dataset includes our newly sampled topotypes of *A. andina*, plus samples from all nominal forms recognized within *A. olivacea* (Quiroga-Carmona *et al.* 2022; Tammone *et al.* 2025a), *A. gossei* (Tammone *et al.* 2025a), as well as other five species of *Abrothrix* (i.e., *hirta*, *illutea*, *lanosa*, *longipilis*, and *sanborni*; Supplementary Data SD1). Sequences of *Geoxus valdivianus* and *Paynomys macronyx* were used as outgroup.

Phylogenetic trees were generated by maximum likelihood algorithms (ML; RAxML v.8, Stamatakis 2014) and Bayesian inference (BI; MrBayes 3.2.7a; Ronquist *et al.* 2012), using the CIPRES Getaway portal (Miller *et al.* 2010). ML analysis was run 1,000 times using the rapid Bootstrap protocol, followed by identification of the tree with the best ML score. BI analysis was run for 2 million generations

Table 1. Basic data of the specimens of *Abrothrix andina* analyzed in this paper. References: **JG** = collector number of Jonathan Guzman. Numbers (#) correspond to those in Figure 1.

#	Field no.	Locality	Region	Lat	Long	Alt (m)
4	JG 001	Quebrada de Choja	Tarapacá	-21.085278°	-68.867222°	3400
15	JG 459	El Colorado, Farellones	Metropolitana	-33.343293°	-70.294183°	2780
15	JG 465	El Colorado, Farellones	Metropolitana	-33.343293°	-70.294183°	2780
15	JG 466	El Colorado, Farellones	Metropolitana	-33.343293°	-70.294183°	2780
15	JG 467	El Colorado, Farellones	Metropolitana	-33.343293°	-70.294183°	2780
15	JG 468	El Colorado, Farellones	Metropolitana	-33.343293°	-70.294183°	2780
15	JG 471	El Colorado, Farellones	Metropolitana	-33.343293°	-70.294183°	2780
16	JG 473	Lomas del Viento, Farellones	Metropolitana	-33.358908°	-70.326116°	2436
16	JG 474	Lomas del Viento, Farellones	Metropolitana	-33.358908°	-70.326116°	2436
16	JG 475	Lomas del Viento, Farellones	Metropolitana	-33.358908°	-70.326116°	2436
16	JG 476	Lomas del Viento, Farellones	Metropolitana	-33.358908°	-70.326116°	2436
18	JG 479	2 km E El Volcán, Cajón del Maipo	Metropolitana	-33.828802°	-70.046349°	1850

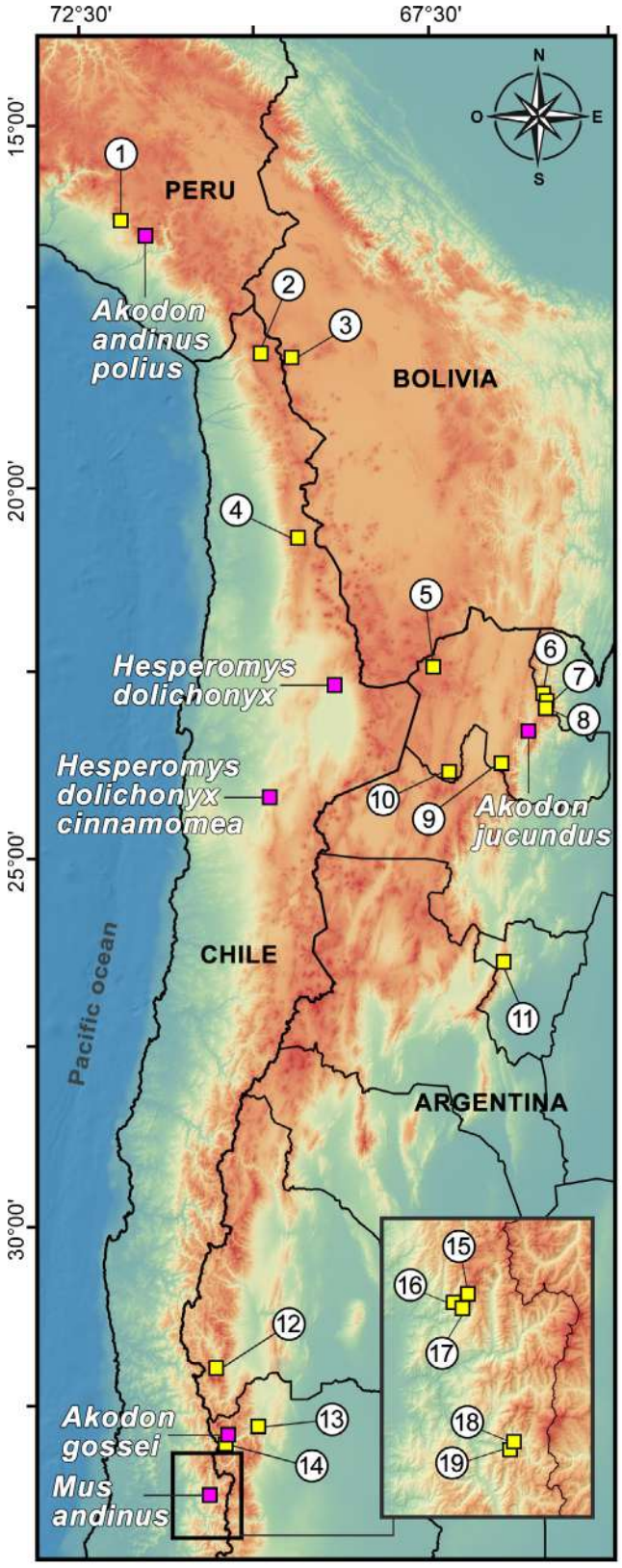

Figure 1. Map of the central Andes depicting type localities of the nominal forms (purple squares) traditionally associated to *Abrothrix andina* and the localities represented by sequences in the phylogenetic analyses (yellow squares). From north to south, type localities are: Salinas, Peru (*polius*); San Pedro de Atacama, Chile (*dolichonyx*); Campo Laguna, Argentina (*jucundus*); Leoncitos, Chile (*cinnamomea*); Puente del Inca, Argentina (*gossei*); and the Andes near Santiago, Chile (*andinus*). Localities represented by sequences are: (1) Arequipa; (2) Putre; (3) PN Sajama; (4) Quebrada de Choja; (5) Laguna de Vilama; (6) Abra de Zenta; (7) Abra Colorada; (8) Laguna Verde; (9) Nevado del Chañi; (10) Volcán Tuzgle; (11) Lagunas de Huaca Huasi; (12) Cerro Mercedario; (13) Uspallata; (14) Cristo Redentor; (15) El Colorado; (16) Lomas del Viento; (17) Valle Nevado; (18) Cajón del Maipo; and (19) Lo Valdés.

with sampling every 1,000 generations using one cold and three hot chains. Twenty-five percent of sampled trees were removed as a conservative measure of burn-in, which was assessed using Tracer 1.7 (Rambaut *et al.* 2018). This analysis was repeated four times using different numbers of initial seeds, after which the convergence of the resulting trees was assessed. We use the GTR+F+I+G4 substitution model as estimated by Corrected Akaike Information Criterion using ModelFinder (Kalyaanamoorthy *et al.* 2017). Strongly supported clades are considered those with posterior probabilities (PP) ≥ 0.95 for BI and bootstrap values (MLB) ≥ 75% for ML. Following identification of well-supported nodes, percent sequence divergence (p-distance; Nei and Kumar 2000) was calculated among and within clades using a pairwise deletion mode for missing data in MEGA 11 (Tamura *et al.* 2021).

Taxonomic inference in this study follows an integrative, lineage-based approach, in which species are interpreted as independently evolving evolutionary lineages identifiable through multiple lines of evidence (de Queiroz 2007; Fujita *et al.* 2012). Given the scope of the present work, focused on resolving the identity of a nominal taxon based on topotypic material, we do not implement algorithmic species delimitation methods. Instead, taxonomic decisions are based on the concordance of: (i) phylogenetic placement of topotypic or near-topotypic populations; (ii) relative levels of genetic divergence in comparison with recognized species and clades within *Abrothrix*, and (iii) consistency with available phenotypic and historical taxonomic evidence. Under this framework, the absence of genealogical exclusivity, combined with low genetic divergence and lack of consistent phenotypic differentiation, is interpreted as evidence against species-level distinction.

Results

Topotypes of *Abrothrix andina* from Andean localities near Santiago de Chile (Farellones and Cajón del Maipo; Table 1, Figure 1) are phylogenetically nested within *Abrothrix olivacea*, forming a well-supported clade (PP = 0.98; MLB = 89%; Figure 3). This clade also includes typical *A. olivacea* from Valparaíso and populations extending from La Serena to Parinacota in northern Chile (Figure 3: "central-north" *A. olivacea* clade). This "central-north" clade is sister to a group comprising *A. olivacea* from central to southern Patagonia in Argentina and Chile (PP = 0.98; MLB = 77%; Figure 3: "central-south" clade).

A third well-supported clade of *A. olivacea* (PP = 0.98; MLB = 77%) includes two distinct groups: one from Mendoza Province, Argentina (Las Leñas, Las Loicas, and La Valenciana; Figure 3: "Mendoza" clade), and another from Tierra del Fuego (Argentina and Chile; Figure 3: "south" clade). Two additional *A. olivacea* clades were identified in the Altiplano. One (PP = 1; MLB = 99%) comprises the new sequence from Tarapacá (Quebrada de Choja) together with samples from southern Peru, Bolivia, and Argentina (Figure 3: "dolichonyx-polius" clade). The other (PP = 1; MLB

Figure 2. Sampled localities of typical *Abrothrix andina* and external appearance of selected specimens. (A) Landscape view of Farellones, Chile; (B) Lo Valdés, Chile; (C–F) topotype of *A. andina* (JG 479), photographed fresh-dead: (C) dorsal view, (D) lateral view, (E) ventral view, and (F) detail of tail and hind foot. Photographs by Jonathan A. Guzmán Sandoval.

= 100%) consists exclusively of samples from Salta and Jujuy, Argentina (Figure 3: "jucundus" clade).

Percent sequence divergence within the clade including topotypes of *A. andina* (Farellones and Cajón del Maipo) and typical *A. olivacea* (Valparaíso) was 1.5% (Figure 4). Comparable values were observed within other *A. olivacea* clades and among other species of *Abrothrix* (e.g., *A. hirta* = 1.4%; Figure 4). Divergence between clades of *A. olivacea* ranged from 4.4% to 6.5%, whereas divergence among recognized species of *Abrothrix* varied from 10% to 13% (Figure 4). These patterns support the conspecificity of topotypic *A. andina* with *A. olivacea*.

Phenotypically, topotypes of *A. andina* from the high Andes near Santiago de Chile are indistinguishable from *A. olivacea* (e.g., Osgood 1943; Mann 1978; Pine *et al.* 1979; Rodríguez-Serrano *et al.* 2006, 2008; Figure 2). These rodents are small (total length = 167 mm; tail = 67 mm; hind foot with claw = 23 mm; ear = 16 mm; weight = 33 g; Supplementary Data SD2), with grayish-brown dorsal pelage tinged with olive, grayish ventral fur, moderate countershading, and an inconspicuous lateral line.

The eyes are small, surrounded posteriorly by a subtle ring of lighter, very short hairs, producing a soft contrast with the dark eye. The ears are rounded and moderately haired, lacking distinct pre-auricular whitish patches but occasionally showing subtle lighter hairs. The tail is sharply bicolored. The manus and pes are sparsely haired, with acute claws slightly longer than those of typical *A. olivacea* (cf. Osgood 1943). Overall, both molecular and morphological evidence indicate that the type-locality populations of *A. andina* are fully nested within *A. olivacea*.

Discussion

Abrothrix andina was originally described as *Mus andinus* from a single specimen (Philippi and Landbeck 1858). It was characterized as a small rodent with dark-gray dorsal

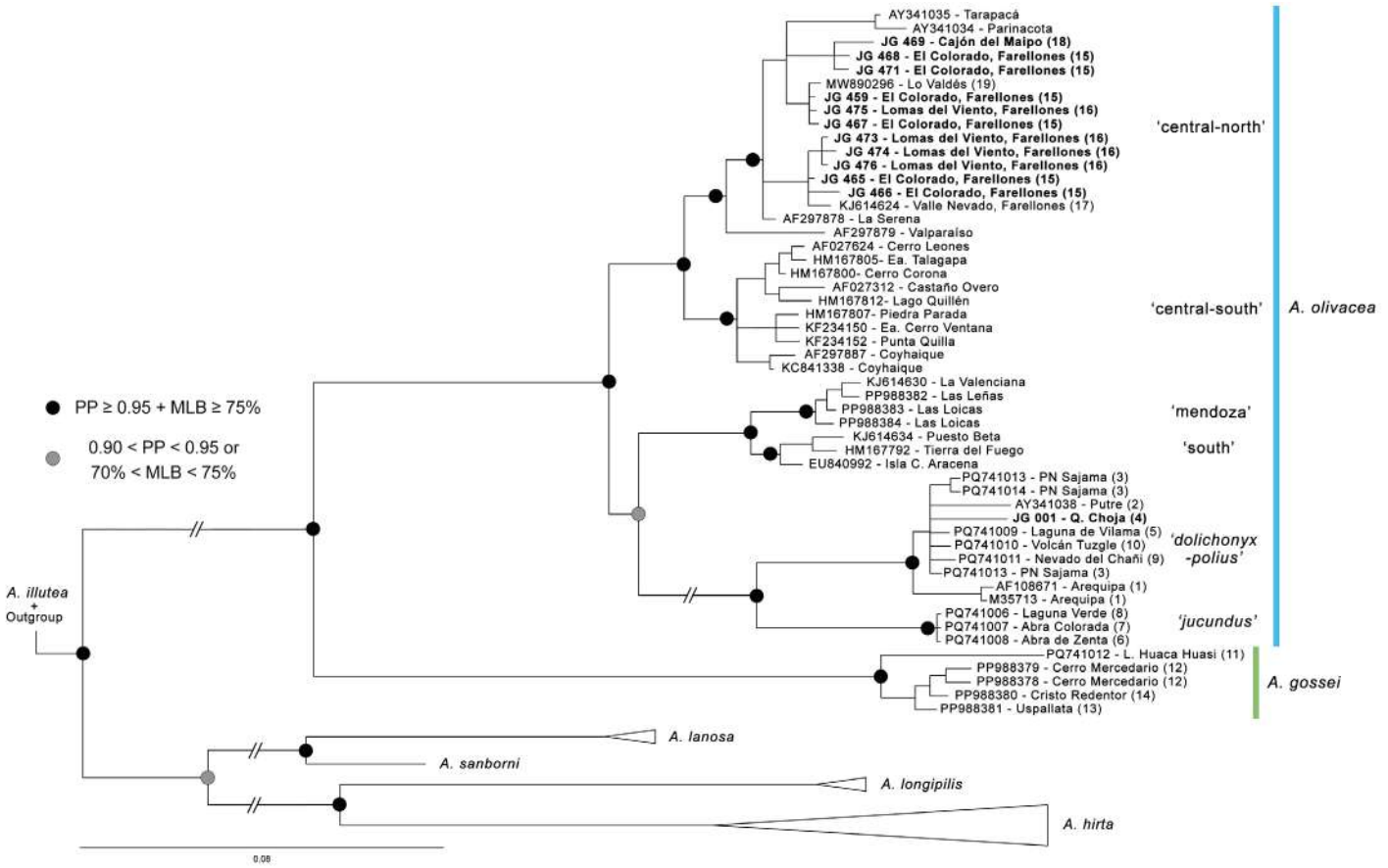

Figure 3. Phylogenetic reconstruction derived from new and available *cyt b* sequences of *Abrothrix*, represented by the final Bayesian 50% majority-rule consensus tree.

fur, similar to *Mus musculus*, and a bluish-white ventral surface. Ears were well-haired but short, barely reaching the distance between the eye and the ear; the tail was approximately half the head-body length, blackish above and white below, densely haired; and the feet were covered with white fur, with elongated, compressed claws on both manus and pes. Original measurements reported were: head and body length ~100 mm; tail length ~50 mm; ear length ~10 mm; hind foot with claws ~20 mm; and claws ~4 mm (Philippi and Landbeck 1858). The description emphasized the soft and lax nature of the fur, the much longer claws compared to *M. musculus*, and the overall resemblance to *Abrothrix longipilis* (cited as *Mus longipilis*) and *A. olivacea* (cited as *Mus rengeri* [sic]). This account was later translated into Spanish and supplemented with a color illustration of the living animal (Philippi 1900).

Thomas (1920), describing *Akodon gossei* from the Andes of Mendoza Province, emphasized differences from *M. andinus*, including larger size, gray (not rufous) dorsal coloration, elongated claws, and the absence of light ear patches. He concluded that *M. andinus* was "evidently quite a different animal" (Thomas 1920). However, Osgood (1943) was the first to examine the original material directly and synonymized *A. gossei* under *A. andina*, rejecting color and metric differences proposed by Thomas (1920). Osgood (1943) also redescribed *dolichonyx*, from northern Chile, and later *A. andinus polius* from Salinas, Arequipa, Peru (Osgood 1944). These studies laid the foundation for the concept of *Abrothrix andina* as a widespread, polytypic high-Andean sigmodontine, a view maintained by subsequent authors (e.g., Mann 1978; Patterson *et al.* 2015; Pardiñas 2017; Teta *et al.* 2017).

Despite its historical and nomenclatural significance, typical *A. andina* remained largely unexamined. The holotype has not been subject to modern taxonomic reassessment since its redescription by Osgood (1943). This omission is notable given that the type locality, "Andibus elevatis prov. Santiago" (Philippi and Landbeck 1858) falls within a region of intense research on *Abrothrix* and other sigmodontines. Consequently, *A. andina* has been overlooked or misinterpreted in several studies, including Pine *et al.* (1979), Reise and Venegas (1987), Gallardo *et al.* (1988), Barrantes *et al.* (1993), Smith and Patton (1999), and more recent systematic studies (Cañón *et al.* 2014; D'Elía *et al.* 2015).

The topotypes sampled in this study from Farellones and Cajón del Maipo (Andes near Santiago de Chile) correspond morphologically and metrically to both the original holotype description (Philippi and Landbeck 1858) and Osgood (1943) redescription. These specimens are small *Abrothrix* (total length ≈ 167 mm; tail ≈ 67 mm; hind foot with claw ≈ 23 mm; ear ≈ 16 mm). Dorsally, the pelage is gray to gray-olivaceous, ventrally washed whitish, and countershading is moderate. Ears are rounded, well-haired, and lack post-auricular whitish patches. The tail is sharply bicolored, and manus and pes are sparsely haired with

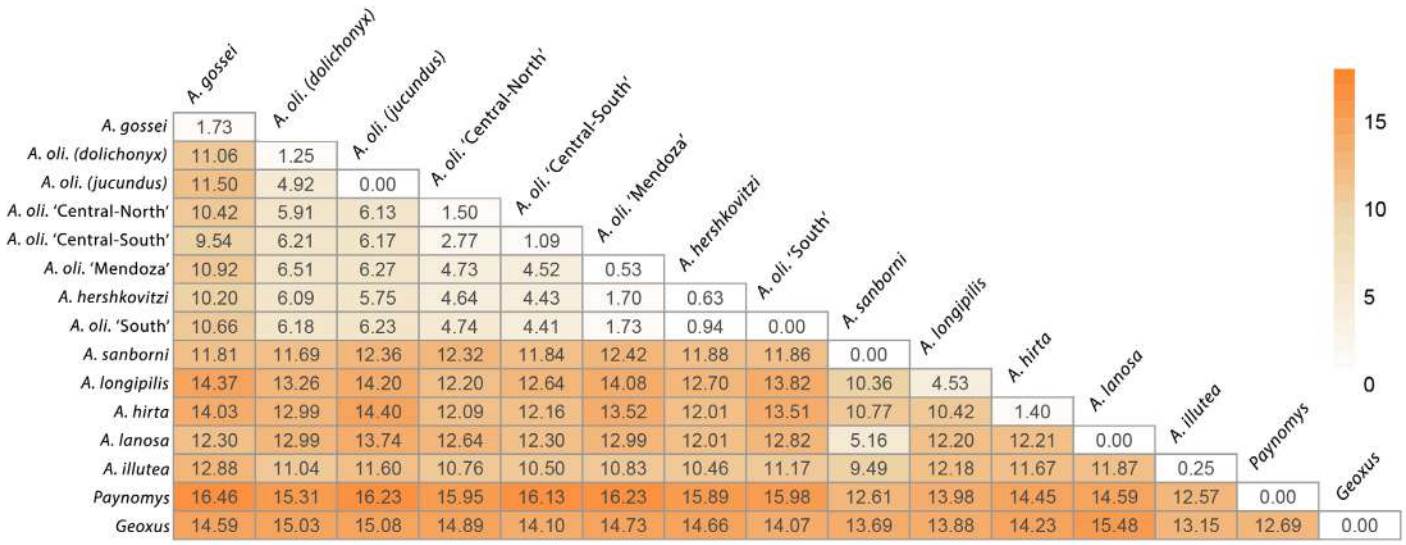

	A. gossei	A. oli. (dolichonyx)	A. oli. (jucundus)	A. oli. 'Central-North'	A. oli. 'Central-South'	A. oli. 'Mendoza'	A. hershkovitzi	A. oli. 'South'	A. sanborni	A. longipilis	A. hirta	A. lanosa	A. illutea	Paynomys	Geoxus
A. gossei	1.73														
A. oli. (dolichonyx)	11.06	1.25													
A. oli. (jucundus)	11.50	4.92	0.00												
A. oli. 'Central-North'	10.42	5.91	6.13	1.50											
A. oli. 'Central-South'	9.54	6.21	6.17	2.77	1.09										
A. oli. 'Mendoza'	10.92	6.51	6.27	4.73	4.52	0.53									
A. hershkovitzi	10.20	6.09	5.75	4.64	4.43	1.70	0.63								
A. oli. 'South'	10.66	6.18	6.23	4.74	4.41	1.73	0.94	0.00							
A. sanborni	11.81	11.69	12.36	12.32	11.84	12.42	11.88	11.86	0.00						
A. longipilis	14.37	13.26	14.20	12.20	12.64	14.08	12.70	13.82	10.36	4.53					
A. hirta	14.03	12.99	14.40	12.09	12.16	13.52	12.01	13.51	10.77	10.42	1.40				
A. lanosa	12.30	12.99	13.74	12.64	12.30	12.99	12.01	12.82	5.16	12.20	12.21	0.00			
A. illutea	12.88	11.04	11.60	10.76	10.50	10.83	10.46	11.17	9.49	12.18	11.67	11.87	0.25		
Paynomys	16.46	15.31	16.23	15.95	16.13	16.23	15.89	15.98	12.61	13.98	14.45	14.59	12.57	0.00	
Geoxus	14.59	15.03	15.08	14.89	14.10	14.73	14.66	14.07	13.69	13.88	14.23	15.48	13.15	12.69	0.00

Figure 4. Heatmap showing percent sequence divergence at the *cyt b* locus between clades of *Abrothrix* identified in the phylogenetic analysis, generated using the pheatmap R package.

slightly elongated claws. These traits clearly distinguish them from *A. gossei*, which has conspicuous white ear patches (Thomas 1920; Contreras and Rosi 1981; Tammone *et al.* 2025a; Figure 5).

The conducted phylogenetic analyses recover topotypes of *A. andina* within a well-supported clade that also includes typical *A. olivacea* from Valparaíso and populations extending from La Serena to Parinacota in northern Chile. Percent sequence divergence within the topotype-inclusive clade is 1.5%, similar to within-species divergence in other *Abrothrix* (e.g., Cañón *et al.* 2014; D'Elía *et al.* 2015; Quiroga-Carmona *et al.* 2022).

Taken together, molecular and morphological data indicate that the studied topotypes belong to the same taxon as the *M. andinus* holotype, supporting synonymy with *A. olivacea*. Recognizing *A. andina* as junior synonym of *A. olivacea* reveals the remarkable complexity of this species. *A. olivacea* spans ~40° latitude from southern Peru to Tierra del Fuego, making it one of the most geographically widespread sigmodontines (Patterson *et al.* 2015; Cañón *et al.* 2024; Cairampoma *et al.* 2024; Tammone *et al.* 2025a; 2025b). Historically, over 30 nominal taxa, have been subsumed under *A. olivacea* (Philippi and Landbeck 1858; Thomas 1913; 1920; Osgood 1944; Rodríguez-Serrano *et al.* 2006; Teta *et al.* 2017; Tammone *et al.* 2025a; 2025b). This extensive synonymy is unparalleled among widespread abrotrichines, such as *A. jelskii* or *A. hirta* (e.g., Patterson *et al.* 2015).

An alternative to considering *Abrothrix olivacea* as a polytypic species is to recognize it as a complex of cryptic or still poorly known species. Similar cases have been documented in sigmodontine rodents, where species once thought to be widespread and singular were later found to comprise multiple distinct units. In such instances,

Figure 5. External appearance of two *Abrothrix* from high Andean ranges. (A) individual attributed to *A. andina* photographed in wild at Embalse del Yeso, 50 km southeast of Santiago de Chile. (B) individual of *A. gossei* photographed in wild at Refugio Andino Cerro Mercedario, San Juan, Argentina. Photographs by T. Aronson and M. Tammone.

molecular markers have played a central role in shaping new taxonomic hypotheses. For example, following Hershkovitz's (1962) influential revision of *Calomys*, several large-bodied populations previously assigned to different nominal forms within this phyllotine genus were grouped under a single species, *Calomys callosus*. Today, *C. callosus* is understood as a species complex comprising at least seven distinct taxa (e.g., González-Ittig *et al.* 2022). The history of sigmodontine taxonomy reflects shifts between expansive and restrictive classifications. Over the past two centuries, taxonomic schools have alternatively expanded species concepts—subsuming nominal forms as synonyms—or refined them, reinstating previously synonymized taxa as valid species. This pattern is exemplified by taxa such as *Akodon boliviensis* and *Oligoryzomys flavescens* (see Myers *et al.* 1990; González-Ittig *et al.* 2010). Recent studies, including the present contribution, suggest that *A. olivacea* exhibits a geographically structured genealogy composed of monophyletic clades, with inter-clade genetic divergences ranging from 1% to 7% (e.g., Lessa *et al.* 2010; Giorello *et al.* 2021; Quiroga-Carmona *et al.* 2022; 2023; Tammone *et al.* 2025b: Figure 4). Additionally, phenotypic differences among populations are evident, as past researchers have distinguished *A. andina* from *A. olivacea* in northern Chile (e.g., Palma *et al.* 2005), or *A. xanthorhina* from *A. olivacea* in Argentine Patagonia (e.g., Lozada *et al.* 1996; Smith *et al.* 2001). However, despite being a moderately well-studied sigmodontine, *A. olivacea* inhabits an extensive and environmentally heterogeneous range, leaving substantial gaps in its known distribution. Some monophyletic groups identified in the current *cyt b* phylogeny may simply reflect inadequate sampling rather than true evolutionary lineages. For instance, north of Santiago, a ~1,000 km region remains unsampled (Figure 1). At the other end of the species' range, haplotypes from the southernmost Chilean populations have only recently been reported (Cañón *et al.* 2024) and await integrative analysis. In summary, whether *A. olivacea* will ultimately be divided into multiple species remains uncertain. If taxonomic partitioning occurs, numerous available names could be used to designate new binomial or trinomial combinations (e.g., Smith *et al.* 2001; Rodríguez-Serrano *et al.* 2006).

Politically, recognizing *A. andina* as a junior synonym of *A. olivacea* reduces by one the number of species recorded in Chile, lowering the count from eight to seven (D'Elía *et al.* 2020). Despite this reduction, *Abrothrix* remains the most diverse sigmodontine genus in Chile, nearly doubling the species richness of its closest competitor, the phyllotine *Eligmodontia* (D'Elía *et al.* 2020). However, this issue is not settled, as an additional *Abrothrix* species, *A. gossei*, is likely present in west-central Chile. Its known distribution extends to Las Cuevas and Cristo Redentor, being both localities in Mendoza Province, very near the Chilean border (Da Rosa *et al.* 2020; Tammone *et al.* 2025a). The continuous Andean habitat along the Mendoza River strongly suggests its occurrence in Chile. Notably, Thomas (1920) reported *A. gossei* in "Chili," based on a specimen labeled as *Mus andinus*, received from R. Philippi.

Abrothrix gossei, previously considered a synonym of *A. andina*, is now confirmed as a valid species and the sister taxon to *A. olivacea*. Its distribution extends from northern Mendoza to Tucumán, with specimens characterized by small size (total length ~140 mm; weight ~18 g), dense pelage, small rounded ears with prominent post-auricular white patches, large claws, and short bicolored tails (Thomas 1920; Osgood 1943; Contreras and Rosi 1981; Ferro and Barquez 2008; Tammone *et al.* 2025a; 2025b). According to Thomas (1920), the species is also entering in Chile. The karyotype of *A. gossei* has been described from Mendoza and San Juan populations (Da Rosa *et al.* 2020).

A remote possibility remains that the holotype of *M. andinus* represents a taxon distinct from here studied topotypes. Collected in 1857 during the Little Ice Age (Villalba 1994), environmental conditions may have supported populations now extirpated. Glacial retreat in the Andes has accelerated over the past century (Masiokas *et al.* 2008; Lopez *et al.* 2010), and altitudinal shifts in small mammal assemblages have been documented (Mann 1944; Mella 2006), including also regional extinctions (Cuellar Soto *et al.* 2026). Whether *A. andina* sensu stricto (i.e., restricted to its holotype) persists or has been replaced by *A. olivacea* remains unknown. The loss of the holotype (J. Canto, pers. comm.) prevents direct testing, but museomic approaches could clarify this historical uncertainty.

Conclusions

Based on the evidence presented herein, we consider *Mus andinus*, currently referred to as *Abrothrix andina*, to be a junior synonym of *Abrothrix olivacea*.

This conclusion is supported by: (1) Topotypic specimens of *A. andina* are nested within *A. olivacea* and do not form a distinct lineage; (2) Low divergence (~1.5%) between topotypic *A. andina* and *A. olivacea* falls within intraspecific variation and is far below interspecific levels; (3) No consistent phenotypic differences distinguish topotypic *A. andina* from *A. olivacea*; and (4) Sampled populations correspond to the type region and agree with historical descriptions.

Acknowledgments

During the process of reassessing *Abrothrix andina*, we benefited from the generous collaboration of many individuals who facilitated fieldwork and museum studies. We are especially grateful to Raúl Briones for supporting the logistics of field campaigns in the Metropolitan Region. We also thank colleagues who contributed through discussions and feedback, including Pablo Valladares, José Urquizo, Agustina Murgia, Damián Voglino, and Ignacio Ferro. Two anonymous reviewers provided constructive comments that significantly improved the clarity of this work. Finally, we acknowledge ChatGPT for assistance in refining the linguistic accuracy and grammatical style of the manuscript.

This study was financially supported by Agencia Nacional de Promoción de la Investigación, el Desarrollo Tecnológico y la Innovación grant #2020-2068 (to UFJP).

Declaration of Artificial Intelligence use

Artificial intelligence was used exclusively to assist with language editing and stylistic refinement of the manuscript. Specifically, the authors used ChatGPT (OpenAI; model version GPT-5.2) to improve clarity, grammar, coherence, and consistency of academic English. ChatGPT is accessible via: https://openai.com/chatgpt. AI tools were not used for data generation, data analysis, figure preparation, image manipulation, statistical analyses, or interpretation of results. All scientific content, analyses, conclusions, and final editorial decisions are entirely the responsibility of the authors.

Author contributions

The authors accepted responsibility for the entire content of this manuscript and approved its submission. Mauro N. Tammone: laboratory analysis, investigation, writing–original draft. Erika Cuellar Soto: investigation. Carola Cañón: laboratory analysis. Jonathan Alexi Guzman Sandoval: data collection. Ulyses F.J. Pardiñas: conceptualization, investigation, supervision, writing–original draft. All the authors: Writing–review and editing.

Supplementary data

SD1. List of sequences downloaded from GenBank that were used to construct the phylogeny.

SD2. External measurements of the specimens sequenced as part of this study. Collector: Jonathan A. Guzman Sandoval.

Data availability

The studied material is available in public collections. Genetic data can be accessed in the public database GenBank (accession numbers PX116190-PX116201). Additional raw data can be found in the supplementary material files or obtained upon request from the corresponding author.

Literature cited

Barrantes GE, Ortells MO, and Reig OA. 1993. New studies on allozyme genetic distance and variability in akodontine rodents (Cricetidae) and their systematic implications. *Biological Journal of the Linnean Society* 48:283–298. https://doi.org/10.1111/j.1095-8312.1993.tb02092.x

Bozinovic F. 1993. Nutritional ecophysiology of the Andean mouse *Abrothrix andinus: energy requirements, food quality and turnover time. Comparative Biochemistry and Physiology Part A: Molecular & Integrative Physiology* 104:601–604. https://doi.org/10.1016/0300-9629(93)90471-F

Bozinovic F, Lagos JA, and Marquet PA. 1999. Geographic energetics of the Andean mouse, *Abrothrix andinus. Journal of Mammalogy* 80:205–209. https://doi.org/10.2307/1383220

Bozinovic F, Novoa FF, and Veloso C. 1990. Seasonal changes in energy expenditure and digestive tract of *Abrothrix andinus (Cricetidae) in the Andes range. Physiological Zoology* 63:1216–1231. https://doi.org/10.1086/physzool.63.6.30152641

Bozinovic F, Veloso C, and Rosenmann M. 1988. Cambios del tracto digestivo de *Abrothrix andinus* (Cricetidae): efecto de la calidad de dieta y requerimientos de energía. *Revista Chilena de Historia Natural* 61:245–251.

Cañón C, Barroso O, D'Elía G, Vásquez R, and Rozzi R. 2024. Native rodents of the Cape Horn Biosphere Reserve at the southern end of Chile: advances in their knowledge and conservation. *Anales del Instituto de la Patagonia* 52:1–21. https://doi.org/10.22352/AIP202452007

Cañón C, Mir D, Pardiñas UFJ, Lessa E, and D'Elía G. 2014. A multilocus perspective on the phylogenetic relationships and diversification of rodents of the tribe Abrotrichini (Cricetidae: Sigmodontinae). *Zoologica Scripta* 43:443–454. https://doi.org/10.1111/zsc.12069

Contreras JR, and Rosi MI. 1981. Notas sobre los Akodontini argentinos (Rodentia, Cricetidae). II. *Akodon andinus andinus* (Philippi, 1868) en la Provincia de Mendoza. *Historia Natural* 32:233–236.

Cuellar Soto E, Tammone MN, Voglino D, and Pardiñas UFJ. 2026. The plausible extinction of an Andean rodent: a victim of climate change? *Mammalia* 90:120–125. https://doi.org/10.1515/mammalia-2025-0040

D'Elía G, Teta P, Upham NS, Pardiñas UFJ, and Patterson BD. 2015. Description of a new soft-haired mouse, genus *Abrothrix (Sigmodontinae), from the temperate Valdivian rainforest. Journal of Mammalogy* 96:839–853. https://doi.org/10.1093/jmammal/gyv103

D'Elía G, Canto J, Ossa G, Verde-Arregoitia LD, Bostelmann E, Iriarte A, *et al*. 2020. Lista actualizada de los mamíferos vivientes de Chile. *Boletín del Museo Nacional de Historia Natural* 69:67–98. https://doi.org/10.54830/bmnhn.v69.n2.2020.6

Da Rosa FA, Ojeda A, Novillo A, Labaroni C, Buschiazzo M, Teta P, *et al*. 2020. Chromosome variability and evolution in rodents of the tribe Abrotrichini (Rodentia, Cricetidae, Sigmodontinae). *Mammalian Research* 65:59–67. https://doi.org/10.1007/s13364-019-00463-0

De Queiroz K. 2007. Species concepts and species delimitation. *Systematic Biology* 56:879–886. https://doi.org/10.1080/10635150701701083

Ferro LI, and Barquez RM. 2008. Comentarios sobre la distribución de *Abrothrix andinus* y *Calomys lepidus* (Rodentia: Cricetidae) en la provincia de Tucumán, Argentina. *Mastozoología Neotropical* 15:197–201.

Fujita MK, Leaché AD, Burbrink FT, McGuire JA, and Moritz C. 2012. Coalescent-based species delimitation in an integrative taxonomy. *Trends in Ecology & Evolution 27:480–488*. https://doi.org/10.1016/j.tree.2012.04.012.

Gallardo MH, Aguilar G, and Goicoechea O. 1988. Systematics of sympatric cricetid *Akodon (Abrothrix) rodents and*

their taxonomic implications. Medio Ambiente, Ambientes Terrestres 9:65–74.

Giorello FM, D'Elía G, and Lessa EP. 2021. Genomic footprints of Quaternary colonization and population expansion in the Patagonian–Fuegian region rules out a separate southern refugium in Tierra del Fuego. *Journal of Biogeography* 48:2656–2670. https://doi.org/10.1111/jbi.14231

González-Ittig RE, Pinotti JD, Carballo J, Martín ML, Levis S, Calderón G, *et al. 2022. Molecular systematics and biogeographic insights of the Calomys callosus complex (Rodentia, Cricetidae). Zoologica Scripta* 51:498–521. https://doi.org/10.1111/zsc.12556

González-Ittig RE, Salazar-Bravo J, Barquez RM, and Gardenal CN. 2010. Phylogenetic relationships among species of the genus *Oligoryzomys (Rodentia, Cricetidae) from Central and South America. Zoologica Scripta* 39:511–526. https://doi.org/10.1111/j.1463-6409.2010.00446.x

Hershkovitz P. 1962. Evolution of Neotropical cricetine rodents (Muridae) with special reference to the Phyllotine group. *Fieldiana Zoology* 46:1–524.

Jayat JP, Ortiz PE, and D'Elía G. 2016. Taxonomy of the *Phyllotis osilae species group in Argentina; the status of the "Rata de los nogales" (Phyllotis nogalaris Thomas, 1921; Rodentia: Cricetidae). Zootaxa* 4083:397–417. https://doi.org/10.11646/zootaxa.4083.3.5

Kalyaanamoorthy S, Minh BQ, Wong TKF, von Haeseler A, and Jermiin LS. 2017. ModelFinder: fast model selection for accurate phylogenetic estimates. *Nature Methods* 14:587–589. https://doi.org/10.1038/nmeth.4285

Lessa EP, D'Elía G, and Pardiñas UFJ. 2010. Genetic footprints of late Quaternary climate change in the diversity of Patagonian–Fueguian rodents. *Molecular Ecology* 19:3031–3037. https://doi.org/10.1111/j.1365-294X.2010.04734.x

Lopez P, Chevallier P, Favier V, Pouyaud B, Ordenes F, and Oerlemans J. 2010. A regional view of fluctuations in glacier length in southern South America. *Global and Planetary Change* 71:85–108. https://doi.org/10.1016/j.gloplacha.2009.12.009

López-Cortés F, Cortés A, Miranda E, and Rau JR. 2007. Dietas de *Abrothrix andinus*, *Phyllotis xanthopygus* (Rodentia) y *Lepus europaeus* (Lagomorpha) en un ambiente altoandino de Chile. *Revista Chilena de Historia Natural* 80:3–12.

Lozada M, Monjeau A, Heinemann KM, Guthmann N, and Birney EC. 1996. *Abrothrix xanthorhinus*. *Mammalian Species* 540:1–6. https://doi.org/10.2307/3504275

Mann FG. 1944. Dos nuevas especies de roedores. *Biológica (Santiago)* 1:95–113.

Mann FG. 1978. Los pequeños mamíferos de Chile. Marsupiales, quirópteros, edentados y roedores. *Gayana Zoología* 40:1–342.

Masiokas MH, Villalba R, Luckman BH, Lascano ME, Delgado S, and Stepanek P. 2008. 20th-century glacier recession and regional hydroclimatic changes in northwestern Patagonia. *Global and Planetary Change* 60:85–100. https://doi.org/10.1016/j.gloplacha.2006.07.031

Mella JE. 2006. Micromamíferos en el Monumento Natural El Morado: abundancia relativa y cambios estacionales. *Noticiario Mensual, Museo Nacional de Historia Natural, Santiago de Chile* 357:10–18.

Miller MA, Pfeiffer W, and Schwartz T. 2010. Creating the CIPRES Science Gateway for inference of large phylogenetic trees. *Proceedings of the Gateway Computing Environments Workshop (GCE)* 2010: 1–8. https://doi.org/10.1109/GCE.2010.5676129

Myers P, Patton JP, and Smith MF. 1990. A review of the boliviensis group of *Akodon (Rodentia: Sigmodontinae), with emphasis on Peru and Bolivia. Miscellaneous Publications, Museum of Zoology, University of Michigan* 177:iv + 1–104.

Nei M, and Kumar S. 2000. *Molecular Evolution and Phylogenetics*. New York (EEUU): Oxford University Press

Osgood WH. 1943. The mammals of Chile. *Field Museum of Natural History, Zoology Series* 30:1–268.

Osgood WH. 1944. Nine new South American rodents. *Field Museum of Natural History, Zoology Series* 29:191–204.

Cairampoma R, D'Elía G, Pacheco Torres VR, Sánchez-Vendizú P, and Diaz S. 2024. Primer registro de *Abrothrix olivacea* (Waterhouse, 1837) en Perú basado en material histórico de Tacna. *Revista Peruana de Biología* 31:e28882. https://doi.org/10.15381/rpb.v31i3.28882

Palma RE, Marquet PA, and Boric-Bargetto D. 2005. Inter- and intraspecific phylogeography of small mammals in the Atacama Desert and adjacent areas of northern Chile. *Journal of Biogeography* 32:1931–1941. https://doi.org/10.1111/j.1365-2699.2005.01349.x

Pardiñas UFJ. 2017. Genus *Abrothrix* Waterhouse, 1837. In: Wilson DE, Lacher TE Jr, and Mittermeier RA (eds.). *Handbook of the Mammals of the World: Lagomorphs and Rodents I, Volume 6*. Barcelona (SPA): Lynx Editions; p. 230–233.

Patterson BD, Smith MF, Teta P, and D'Elía G. 2015. Genus *Abrothrix* Waterhouse, 1837. In: Patton JL, Pardiñas UFJ, and D'Elía G, editors. *Mammals of South America, Volume 2. Rodents.* Chiago (EEUU): University of Chicago Press; p. 109–127.

Philippi RA. 1896. Descripcion [sic] de los mamíferos traídos del viaje de esploracion [sic] de Tarapacá, hecho por orden del gobierno en el verano de 1884 a 1885, por Federico Philippi. *Anales del Museo Nacional de Santiago de Chile, Zoología* 133:1–7.

Philippi RA. 1900. Figuras i descripciones de los murideos de Chile. *Anales del Museo Nacional de Santiago de Chile, Zoología* 14:1–70.

Philippi RA, and Landbeck L. 1858. Beschreibung einiger neuen Chilenischen Mäuse. *Archiv für Naturgeschichte* 24:77–82.

Pine RH, Miller SD, and Schamberger ML. 1979. Contributions to the mammalogy of Chile. *Mammalia* 43:339–376. https://doi.org/10.1515/mamm.1979.43.3.339

Quiroga-Carmona M, Abud C, Lessa EP, and D'Elía G. 2022.

The mitochondrial genetic diversity of the Olive Field Mouse *Abrothrix olivacea* (Cricetidae; Abrotrichini) is latitudinally structured across its geographic distribution. *Journal of Mammalian Evolution* 29:413–430. https://doi.org/10.1007/s10914-021-09582-5

Quiroga-Carmona M, Teta P, and D'Elía G. 2023. The skull variation of the olive field mouse *Abrothrix olivacea* (Cricetidae: Abrotrichini) is localized and correlated to the ecogeographic features of its geographic distribution. *PeerJ* 11:e15200. https://doi.org/10.7717/peerj.15200

Rambaut A, Drummond AJ, Xie D, Baele G, and Suchard MA. 2018. Posterior summarization in Bayesian Phylogenetics Using Tracer 1.7. *Systematic Biology* 67:901–904. https://doi.org/10.1093/sysbio/syy032

Reise D, and Venegas W. 1987. Catalogue of records, localities and biotopes from research work on small mammals in Chile and Argentina. *Gayana Zoología* 51:103–130.

Rocha RG, Duda R, Flores T, Rossi R, Sampaio I, Mendes-Oliveira AC, *et al*. 2018. Cryptic diversity in the *Oecomys roberti* complex: revalidation of *Oecomys tapajinus* (Rodentia, Cricetidae). *Journal of Mammalogy* 99:174–186. https://doi.org/10.1093/jmammal/gyx149

Rodríguez-Serrano E, Cancino RA, and Palma RE. 2006. Molecular phylogeography of *Abrothrix olivaceus* (Rodentia: Sigmodontinae) in Chile. *Journal of Mammalogy* 87:971–980. https://doi.org/10.1644/05-MAMM-A-393R2.1

Rodríguez-Serrano E, Hernández CE, and Palma RE. 2008. A new record and an evaluation of the phylogenetic relationships of *Abrothrix olivaceus markhami* (Rodentia: Sigmodontinae). *Mammalian Biology* 73:307–317. https://doi.org/10.1016/j.mambio.2007.10.003

Ronquist F, Teslenko M, van der Mark P, Ayres DL, Darling A, Höhna S, *et al*. 2012. MrBayes 3.2: efficient Bayesian phylogenetic inference and model choice across a large model space. *Systematic Biology* 61:539–542. https://doi.org/10.1093/sysbio/sys029

Rosenmann M, and Ruiz G. 1993. Seasonal changes of blood values in the Andean mouse *Abrothrix andinus*. *Comparative Biochemistry and Physiology Part A: Molecular & Integrative Physiology* 105:119–122. https://doi.org/10.1016/0300-9629(93)90182-4

Sikes RS, and The Animal Care and Use Committee of the American Society of Mammalogists. 2016. Guidelines of the American Society of Mammalogists for the use of wild mammals in research. *Journal of Mammalogy* 92:235–253. https://doi.org/10.1093/jmammal/gyw078

Smith MF, and Patton JL. 1999. Phylogenetic relationships and the radiation of sigmodontine rodents in South America: evidence from *cytochrome b*. *Journal of Mammalian Evolution* 6:89–128. https://doi.org/10.1023/A:1020668004578

Smith MF, Kelt DA, and Patton JL. 2001. Testing models of diversification in mice in the *Abrothrix olivaceus/xanthorhinus* complex in Chile and Argentina. *Molecular Ecology* 10:397–405. https://doi.org/10.1046/j.1365-294X.2001.01183.x

Stamatakis A. 2014. RAxML version 8: a tool for phylogenetic analysis and post-analysis of large phylogenies. *Bioinformatics* 30:1312–1313. https://doi.org/10.1093/bioinformatics/btu033

Tammone MN, Lavin BR, Pardiñas UFJ, and Lacey EA. 2016. Post-extinction discovery of a population of the highly endemic colonial tuco-tuco (*Ctenomys sociabilis*). *Journal of Mammalogy* 97:1753–1761. https://doi.org/10.1093/jmammal/gyw146

Tammone MN, Cuellar Soto E, Voglino D, and Pardiñas UFJ. 2025a. New genetic data unveil taxonomic complexity in the high-Andean sigmodontine *Abrothrix andina* (Rodentia, Cricetidae). *Mammal Research* 70:159–165. https://doi.org/10.1007/s13364-024-00772-z

Tammone M, Cuellar Soto E, Voglino D, Urquizo JH, Ferro I, *et al*. 2025b. Deconstructing the high-Andean sigmodontine *Abrothrix andina* (Rodentia, Cricetidae): taxonomic insights from northwestern Argentinean and western Bolivian populations. *Mammalia Aequatorialis* 7:29–42. https://doi.org/10.59763/mam.aeq.v7i2.119

Tamura K, Stecher G, and Kumar S. 2021. MEGA11: Molecular Evolutionary Genetics Analysis Version 11. *Molecular Biology and Evolution* 38:3022–3027. https://doi.org/10.1093/molbev/msab120

Teta P, Cañón C, Patterson BD, and Pardiñas UFJ. 2017. Phylogeny of the tribe Abrotrichini (Cricetidae, Sigmodontinae): integrating morphological and molecular evidence into a new classification. *Cladistics* 33:153–182. https://doi.org/10.1111/cla.12164

Thomas O. 1913. On small mammals collected in Jujuy by Señor E. Budin. *Annals and Magazine of Natural History* 11:136–143.

Thomas O. 1920. On small mammals from the Famatina Chain, North-western Rioja. *Annals and Magazine of Natural History* 5:417–422.

Villalba R. 1994. Tree-ring and glacial evidence for the medieval warm epoch and the Little Ice Age in southern South America. *Climatic Change* 26:183–197. https://doi.org/10.1007/BF01092413

Waterhouse GR. 1837. Characters of new species of the genus *Mus*, from the collection of Mr. Darwin. *Proceedings of the Zoological Society of London* 1837 (part V):15– 21, 27–32.

Associated editors: Giovani Hernández Canchola and Pablo Colunga Salas
Submitted: October 29, 2025; Reviewed: January 28, 2026
Accepted: April 22, 2026; Published online: May 29, 2026

THERYA, 2026, Vol. 17(2):235-246 DOI: 10.12933/therya.2026.6246 ISSN 2007-3364

Hair microstructure in peromyscine rodents revealed by multiscale microscopy

Alina Nashiely Rendón-Lugo

Secretaría de Ciencia, Humanidades, Tecnología e Innovación (SECIHTI), México.
Corresponding author: alina.rendon@secihti.mx

The structural characteristics of dorsal guard hair were analyzed in twelve cricetid rodent species, including eleven peromyscine and one sigmodontine species, using optical microscopy, scanning electron microscopy (SEM), and transmission electron microscopy (TEM). Hairs were collected from the dorsal region of adult specimens, prepared according to standard protocols, and examined to describe cuticular and medullary morphology. Optical microscopy revealed irregular mosaic-scale patterns with interspecific variation in density and contour. SEM confirmed diagnostic differences in scale size and arrangement, while TEM revealed variation in internal medullary organization. The combined use of these techniques provided morphological criteria useful for taxonomic assessment, particularly at higher taxonomic levels and established a comparative methodological framework for mammalogical studies. Our findings highlight the value of multitechnique hair analysis for taxonomic identification and for understanding structural adaptations in Neotropical rodents.

Keywords: hair morphology, medullary structure, mammal hair, microscopy techniques, Neotropical rodents, Peromyscine.

Se analizaron las características estructurales del pelo de guarda dorsal en doce especies de roedores cricétidos, incluyendo once especies peromiscinas y un sigmodontino, mediante microscopía óptica, microscopía electrónica de barrido (SEM) y microscopía electrónica de transmisión (TEM). Los pelos fueron recolectados de la región dorsal de ejemplares adultos, preparados de acuerdo con protocolos estándar y examinados con el fin de describir la morfología cuticular y medular. La microscopía óptica reveló patrones de escamas en mosaico irregular, con variación interespecífica en la densidad y el contorno. El uso de SEM confirmó diferencias diagnósticas en el tamaño y la disposición de las escamas, mientras que la TEM evidenció variaciones en la organización interna de la médula. El uso combinado de estas técnicas proporcionó criterios morfológicos útiles para la evaluación taxonómica, particularmente a niveles taxonómicos superiores y estableció un marco metodológico comparativo para estudios mastozoológicos. Los hallazgos destacan el valor del análisis multitécnico del pelo para la identificación taxonómica y para la comprensión de las adaptaciones estructurales en roedores neotropicales.

Palabras clave: estructura medular, morfología del pelo, pelo de mamíferos, Peromyscine, roedores neotropicales, técnicas microscópicas.

Hair is an epidermal appendage composed of keratinized cells, extensively studied since the late 18th and early 19th centuries. It has been considered the most important diagnostic feature of mammals, as it appears at least during some stage of life and in both sexes. Moreover, it possesses characteristics and properties that make it useful in studies across various fields of biological sciences (Hausman 1920; 1930; Arita and Aranda 1987; Teerink 2003).

The resilience and stability of hair and all its components, along with its ease of collection and handling, have made it an excellent element for biological, forensic (Deedrick and Koch 2004; Tremori *et al.* 2018) and archaeological research (Tridico 2015; Wygal *et al.* 2024). Optical microscopy is the technique responsible for the development of hair studies, or trichology, since the discovery and description of its morphological constituents, which are organized into three main layers: the innermost part, called the medulla, composed of remnants of keratinized cells arranged in columns; the cortex, the intermediate layer, made up of spindle-shaped cells and containing pigment granules that give hair its color; and the cuticle, the outer region, formed by plates of cells arranged in scales (Hausman 1920, 1924, 1930, 1932; Williams 1938; Stoves 1942; Oyer 1946; Noback 1951).

Analysis of these microscopic hair structures revealed morphological differences in medullary cells and cuticular scales among various mammalian species, which is why hair has been widely used for genus and even species identification (Arita and Aranda 1987; Amman 2002; Baca and Sánchez-Cordero 2004).

Nevertheless, meticulous study of morphological differences that enabled taxonomic identification and the publication of guidelines made necessary the use of electron microscopes (Short 1978; Clement *et al.* 1981; Quadros and Monteiro-Filho 1998; Amman 2002; Teerink 2003; Debelica and Thies 2009), mainly due to the advantage of directly observing cuticular morphology in greater detail thanks to their high resolution and depth of field. Thus, using both scanning and transmission electron microscopes made it possible to observe structural details useful not only for taxonomy but also for histological studies of important structures such as the hair follicle, medulla, and pigment granules or melanosomes (Birbeck *et al.* 1956; Birbeck and Mercer 1957; Chernova 2002, 2003, 2006; De Cássia *et al.* 2007; Borovansky 2011).

Currently, although hair studies undeniably require optical microscopes, they are incomplete without more

sophisticated tools such as electron microscopes, this is because, despite appearing to be a simple structure, more microstructural details with significant adaptive, physiological, and genetic implications continue to be discovered (Russell 1946; Birbeck and Mercer 1957; Alibardi 2004a, 2004b).

In hair studies, as in many areas of biological sciences, different microscopic techniques prove complementary—from the simplest, which helps to understand the structure of the hair fiber, to the most sophisticated, which reveal details of its micro- and ultrastructure and their respective biological implications. This work presents the hair structure of several peromyscine rodents (Family Cricetidae, Tribe Peromyscini), including species of the genus Peromyscus and related genera, using light and electron microscopy, as well as the differences in observations and scope with each technique. Peromyscine rodents constitute one of the most diverse groups of small mammals in Mexico and represent a taxonomically cohesive group for evaluating hair microstructure. However, the diagnostic value of hair at the species level remains uncertain among closely related taxa. The selection of Peromyscini allowed the evaluation of hair microstructure within a closely related group, facilitating the assessment of its diagnostic value and the comparative advantages of different microscopic techniques.

Materials and methods

The selection of the tribe Peromyscini aimed to conduct the analysis within a taxonomically cohesive group, allowing a clearer assessment of the diagnostic value of hair among closely related taxa. This approach, combined with the use of complementary microscopic techniques, makes it possible to evaluate both the usefulness of hair as a taxonomic character and the advantages and scope of different levels of microscopic analysis.

One sigmodontine species (*Sigmodon mascotensis*) was included to provide a comparative framework within Cricetidae. This species was examined exclusively using optical microscopy, as medullary patterns have traditionally been considered one of the primary taxonomic characters in hair-based identification. The inclusion of this species allowed comparison of medullary organization at a broader familial scale, without extending the analysis to higher-resolution techniques.

Sample Collection, Preparation, and Optical Microscopy. Hair samples from the dorsal guard region were taken from specimens housed at the "Alfonso L. Herrera" Zoology Museum, Faculty of Sciences, Universidad Nacional Autónoma de México (UNAM), from the following genera and species: 1) *Habromys* (*H. ixtlani* and *H. lophurus*); 2) *Megadontomys* (*M. cryophilus* and *M. nelsoni*); 3) *Osgoodomys banderanus;* 4) *Onychomys leucogaster*; 5) *Peromyscus* (*P. mexicanus*, *P. difficilis*, and *P. eremicus*); 6) *Neotomodon alstoni*; 7) *Reithrodontomys chrysopsis;* and 8) *Sigmodon mascotensis*

For each analyzed species, ten individual hairs were washed with absolute ethanol to remove impurities and grease and subsequently mounted on slides using Canada balsam. Preparations for each genus were observed under a Leica DM 2000 optical microscope equipped with an integrated CCD camera (charge-coupled device), which was used to capture micrographs at 20X.

The analyzed regions of each sample included the distal and proximal portions of the hair, as well as the spatula region (widest part). Due to structural variation along the hair shaft, the medulla in the spatula region was considered the primary reference. Morphology was analyzed according to Hausman's classification (1920).

Scanning Electron Microscopy (SEM). Scanning electron microscopy (SEM) was used to analyze the surface morphology of the hair shaft, with particular emphasis on cuticular scale patterns and features relevant for interspecific comparison. Hair samples were mounted in cylinder aluminum stubs and adhered with conductive double-side carbon tape.

SEM observations were conducted using a JEOL JSM-5900LV (low vacuum/variable pressure) microscope on dorsal guard hairs from the following species: *H. simulatus*, *H. ixtlani*, *O. banderanus*, *P. mexicanus*, *P. difficilis*, *P. hylocetes*, *P. eremicus*, *M. cryophilus*, *M. nelsoni*, and *N. alstoni*. The regions selected for observation were the shaft near the root and the midsection or spatula. All observations were performed at an accelerating voltage of 20 kV, which was kept constant for all species.

Several regions of the hair were examined, including the shaft near the root and the midsection or spatula. However, interspecific comparisons were primarily based on observations of the midshaft region, where cuticular patterns are more stable and comparable among species. To observe scale morphology, whole hairs were mounted flat on carbon tape and coated with Au (gold) using a sputtering evaporation system, as fresh observations were hindered by electrical charging due to the non-conductive nature of the samples.

To determine and quantify the percentage of each element present in mammalian hair, energy-dispersive X-ray spectroscopy (EDS) microanalysis was performed on uncoated hair samples from *H. ixtlani*, *P. mexicanus*, *P. difficilis*, *P. hylocetes*, *M. cryophilus* and *M. nelsoni* , using a JEOL JSM-5900LV microscope equipped with an Oxford detector (ISIS model).

Dual Beam Microscopy (FIB). Focused ion beam scanning electron microscopy (FIB-SEM) was employed to obtain high-resolution cross sections of the hair shaft and to examine the internal microstructure of the cuticle, cortex, and medulla. The objective of using this technique was to complement light microscopy and conventional SEM observations by providing detailed information on internal morphology and three-dimensional structural relationships that cannot be observed from surface images alone. Due to the difficulty of preparing transverse and

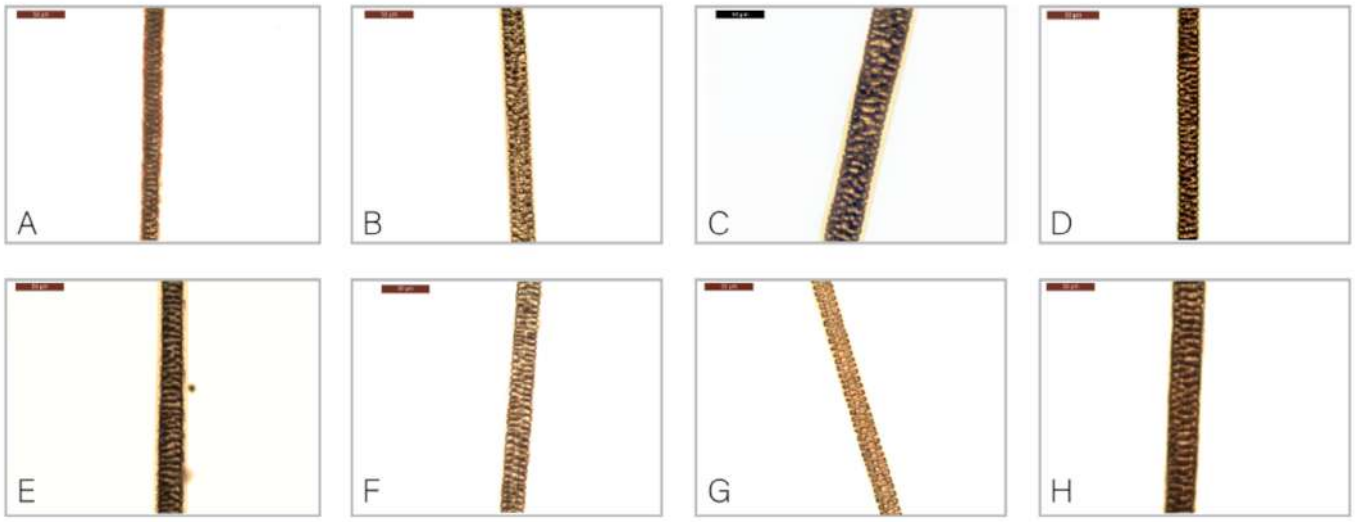

Figure 1. Optical micrographs (20X) showing the medullary patterns of dorsal guard hairs from eight rodent species. (a) *Peromyscus mexicanus*; (b) *Peromyscus eremicus*; (c) *Sigmodon mascotensis*; (d) *Habromys lophurus*; (e) *Neotomodon alstoni*; (f) *Osgoodomys banderanus*; (g) *Onychomys leucogaster*; and (h) *Reithrodontomys chrysopsis*.

longitudinal sections using conventional methods such as ultramicrotomy, a morphological exploration was conducted on hair samples from *P. mexicanus* using a Dual Beam Nova 200 Nanolab station. Hair samples were mounted on aluminum stubs using conductive copper tape to ensure both mechanical stability and electrical continuity between the specimen and the holder.

FIB-SEM analysis was performed on a limited number of samples due to the restricted availability of instrument time and the high cost associated with this technique; therefore, these observations were intended to complement optical and surface analyses rather than to provide a comparative analysis among species. Milling was performed using a gallium ion beam, and scanning images were obtained using the electron beam operated at 20 kV with an Everhart–Thornley detector, allowing visualization of the internal structure of the three layers composing the hair shaft.

Transmission Electron Microscopy (TEM). Transmission electron microscopy (TEM) was employed to examine the internal ultrastructure of the hair shaft. Ultrathin sections were obtained by ultramicrotomy, allowing detailed observation of the cuticle, cortex, and medulla at high resolution.

For TEM analysis, hair from *M. cryophilus* was embedded in EPON resin after being washed in propylene oxide and placed in a pre-embedding mixture of the same substance and resin. Samples were then transferred to embedding molds, filled with resin, and cured in an oven at temperatures ranging from 30 to 60°C for 48 hours. Hardened preparations were used to obtain fine and semi-thin sections with a Leica EM UC6 ultramicrotome.

Samples were observed using a FEI F30 field emission microscope operating at 300 kV. Measurements of observed structures were performed using Digital Micrograph software version 3.11.0 (GATAN 2007). The photographs presented correspond to species exhibiting general patterns found across all analyzed specimens.

Results

Optical Microscopy. The dorsal guard hair micrographs correspond to twelve species of rodents housed in the mammal collection of the "Alfonso L. Herrera" Museum, Faculty of Sciences, UNAM. The analyzed hairs consist of a proximal depigmented shaft region and a distal region containing the widest and most pigmented part of the shaft (shield), which provides the characteristic coloration of each species.

At 20X magnification (Figure 1), the medullary pattern was clearly visible without the need for bleaching procedures. In peromyscine species such as *P. mexicanus* (Fig. 1A), *P. eremicus* (Fig. 1B), and *H. lophurus* (Fig. 1D), the medulla spans the entire width of the hair shaft and is compound, typically biseriate along most of its length. In the widest regions of the shield, it may become triseriate, with a central rounded cell flanked by two elongated, flattened cells. In some areas, these cells partially fuse, forming poorly defined transverse bands.

Similar patterns were observed in *N. alstoni* (Fig. 1E), *O. banderanus* (Fig. 1F), *O. leucogaster* (Fig. 1G), and *R. chrysopsis* (Fig. 1H), although variation in shaft width and pigmentation intensity was evident. The most marked deviation from this pattern was observed in *S. mascotensis* (Fig. 1C), whose hairs are wider, longer, and more heavily pigmented, with a multiseriate medulla composed of rounded cells that fuse to form more defined transverse bands. Overall, optical microscopy reveals a highly conserved medullary architecture among the analyzed taxa. The observed variation was insufficient to establish diagnostic characters at the species level within the family Cricetidae.

Scanning Electron Microscopy. Scanning electron microscopy enabled direct observation of cuticular scale morphology across the examined taxa (Figure 2A–F). In peromyscine mice, as in most mammalian species,

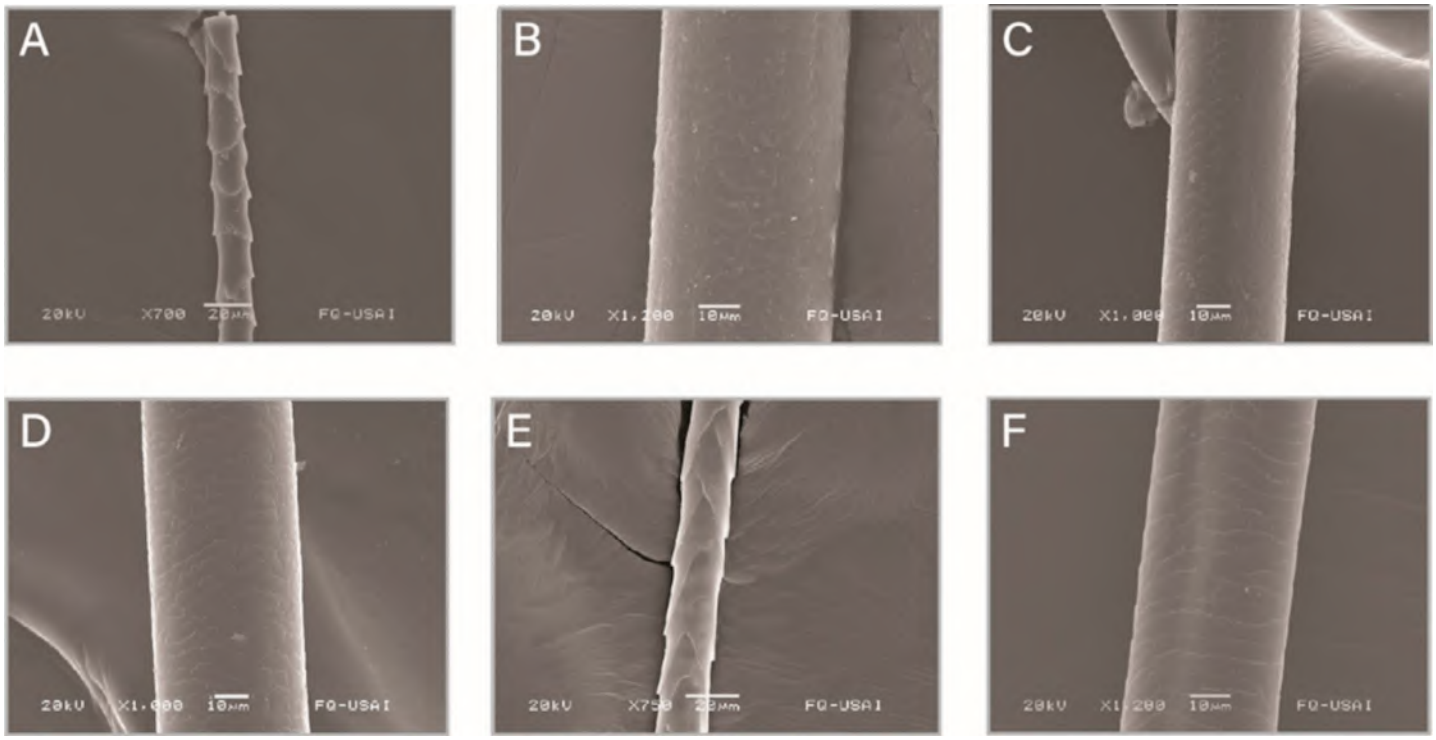

Figure 2. Scanning electron micrographs showing cuticular scale morphology in cricetid rodents. (A–B) *Peromyscus difficilis*; (C) *Peromyscus mexicanus*; (D) *Megadontomys nelsoni*; and (E–F) *Habromys ixtlani*. Images illustrate variation in imbricate scale arrangement, marginal crenation, and spacing along the hair shaft.

the thinner regions near the root tend to exhibit a predominantly coronal arrangement, whereas the wider regions of the shaft are characterized by imbricate scales.

In *P. difficilis* (Figure 2A–B), the shaft displays imbricate scales with relatively regular, overlapping margins. Toward the wider regions, the free edges become more defined, although the general pattern remains symmetrical and moderately spaced. In *P. mexicanus* (Figure 2C), the imbricate pattern is maintained, but the scales in the widest region are distinctly crenate, with large, symmetrical undulations along their distal margins.

A similar imbricate organization is observed in *M. nelsoni* (Figure 2D), whose scales resemble those of *Peromyscus* species in their general arrangement, though they appear broader and more uniformly distributed, with less pronounced marginal undulation. In *H. ixtlani* (Figure 2E–F), the scales are also imbricate but tend to be more widely spaced and smoother, exhibiting gently curved margins with reduced crenation. In some regions, the pattern appears less symmetrical along the shaft, while in broader portions the scales remain symmetrical but comparatively non-undulated and more separated.

Overall, although all species share the imbricate configuration characteristic of cricetid rodents, variation in cuticular morphology is influenced not only by interspecific differences but also by changes in hair shaft thickness, as observed in *H. ixtlani* and *P. difficilis*, where scale configuration shifts between thinner and wider regions of the hair. Interspecific variation is evident in scale width, spacing, and degree of marginal crenation; however, these differences are subtle and partially overlapping among taxa. This suggests that cuticular morphology alone may provide limited diagnostic resolution at the species level within closely related cricetids and may be more informative when interpreted in combination with additional microscopic characters.

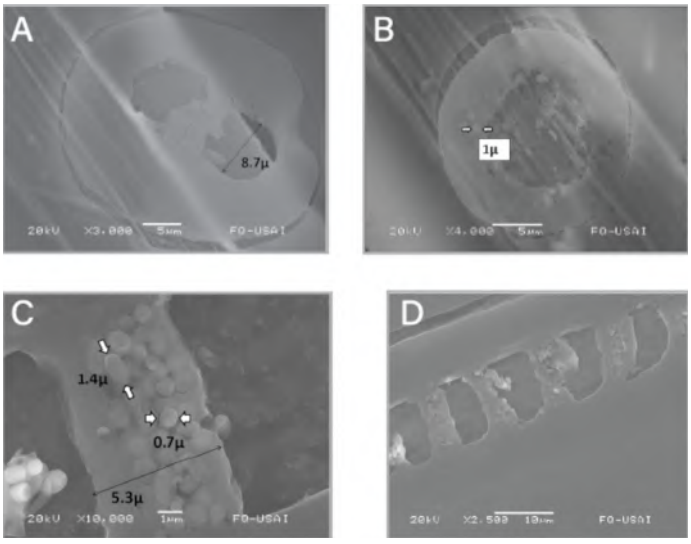

Figure 3. Ultramicrotome sections of *Megadontomys cryophilus* hair. (A–B) Transverse sections showing medullary compartments and central cavities. (C–D) Longitudinal sections displaying a discontinuous, staircase-like medulla with spherical (pheomelanin-type) and ellipsoidal (eumelanin-type) melanosomes.

Ultramicrotomy Sections. Ultramicrotome sections of *M. cryophilus* allowed observation of the internal organization of the hair shaft (Figure 3A–D). Transverse sections (Figure 3A–B) reveal a relatively simple medulla composed of distinct compartments or voids, with central cavities bordered by cortical material. Longitudinal sections (Figure 3C–D)

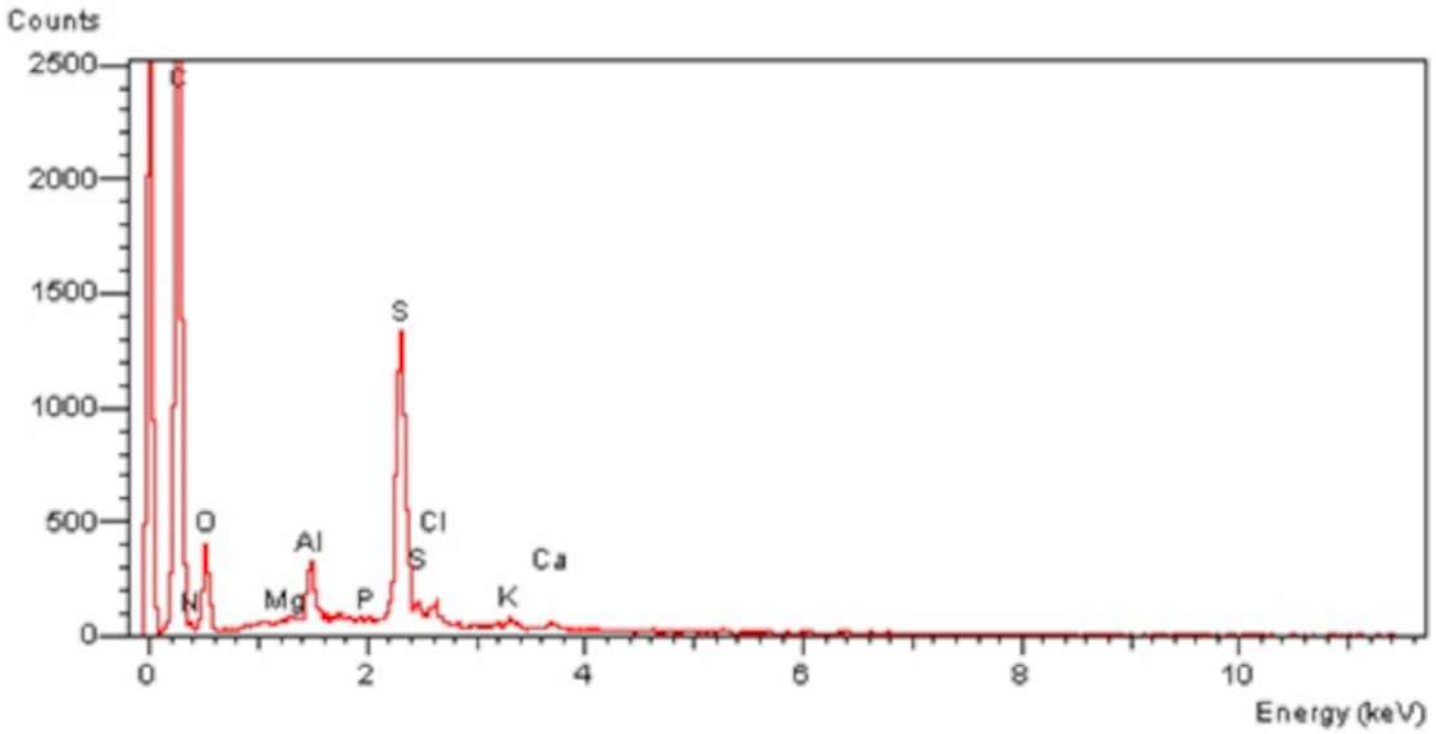

Figure 4. EDS spectrum of *Peromyscus mexicanus*.

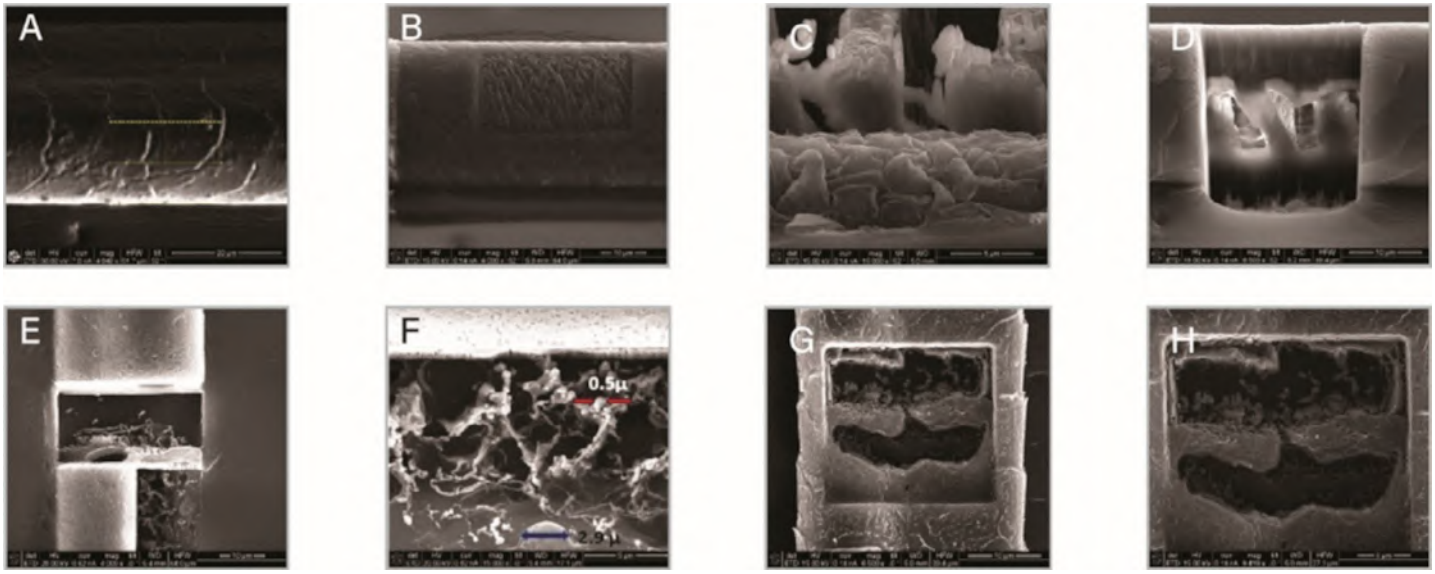

Figure 5. FIB–SEM micrographs of dorsal guard hair from *Peromyscus mexicanus*, showing sequential ion beam milling and cross-sectional exposure of the internal structure. (A–C) Trench excavation and exposure of the internal region. (D–H) Polished cross-sections revealing cortical and medullary organization at increasing magnification.

show a discontinuous, staircase-like medulla containing numerous pigment granules. Two main morphologies are evident: spherical bodies measuring approximately 0.7–1.0 µm in diameter and elongated to ovoid bodies up to 1.4–1.5 µm in length. These correspond morphologically to pheomelanin (spherical) and eumelanin (ellipsoidal) melanosomes, respectively.

Energy-Dispersive X-ray Spectroscopy (EDS). Energy-dispersive X-ray spectroscopy (EDS) analysis performed on a localized region near the hair root confirmed that the elemental composition of the shaft is dominated by carbon (C) and oxygen (O), with a well-defined sulfur (S) peak (Figure 4). The high carbon and oxygen signals are consistent with the organic keratin matrix of mammalian hair, while the sulfur peak reflects the presence of sulfur-containing amino acids (*e.g.*, cysteine) characteristic of keratinized structures.

In addition to these major elements, minor peaks corresponding to sodium (Na), magnesium (Mg), aluminum (Al), silicon (Si), chlorine (Cl), potassium (K), and calcium (Ca) were detected at lower intensities. Among these, potassium and calcium were comparatively more evident in some samples, particularly in Peromyscus mexicanus. These elements likely represent trace constituents either structurally associated with the hair matrix or adsorbed from environmental exposure.

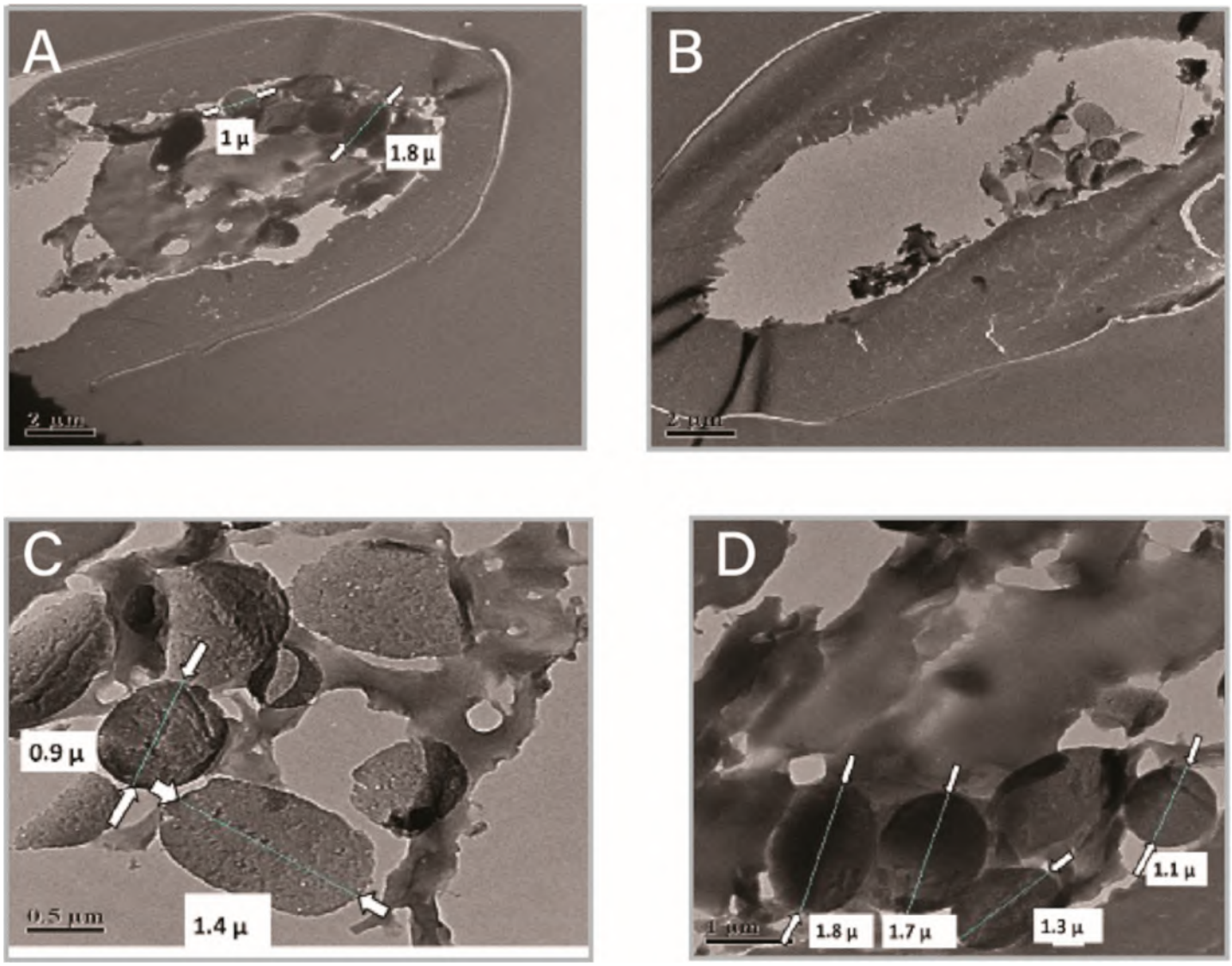

Figure 6. TEM micrographs of transverse sections of dorsal guard hair of *Megadontomys cryophilus*. (A–B) General view of the shaft showing cortical region and partially deteriorated medulla. (C–D) Detail of cortical organization with electron-dense spherical and ovoid bodies.

Overall, the elemental profiles were broadly consistent across analyzed specimens, with no marked interspecific differences in the dominant components.

Dual Beam Microscopy (FIB). Morphological exploration using dual-beam microscopy was conducted on Peromyscus mexicanus. Milling was performed in the midsection of the hair shaft. The sequential stages of trenching and exposure of the internal structures are illustrated in figure 5 (figure A–E). The selected milling area and initial trench opening are shown in Figure 5 A, followed by progressive removal of material to expose the internal face of the fiber (Figure 5 B). Higher magnification images (Figure 5 C) reveal the compact external cuticle and the underlying cortical region.

Continued milling produced a well-defined rectangular window (Figure 5 D–E), clearly exposing the three principal layers of the hair shaft. The cuticle appears as a dense, continuous outer layer; beneath it, the cortex shows a compact arrangement of cortical cells; and centrally, the medulla is visible as a less compact region with internal structural heterogeneity.

Detailed examination of the exposed cavity (Figure F) revealed additional structures associated with the inner cuticle boundary. A globular body measuring approximately 2.9 µm in diameter was observed attached to the internal wall, together with a tangled filamentous network containing small spherical elements of approximately 0.5 µm. These structures were not evident using optical microscopy or conventional SEM and became distinguishable only after focused ion beam milling.

The final milled views (Figure G–H) provide a clearer cross-sectional perspective of the internal organization of the shaft, confirming the stratified arrangement of cuticle, cortex, and medulla, and highlighting the three-dimensional architecture revealed by the FIB-generated window. This technique, unlike ultramicrotomy or chemical preparation methods, allows step-by-step observation of the milling process, enabling detailed imaging of each layer and a better understanding of hair fiber structure.

The filamentous network and associated globular elements observed at the inner cuticle boundary represent

features that became discernible only after focused ion beam milling. Although their biological nature cannot be determined at this stage, their presence highlights the analytical potential of dual-beam FIB-SEM for revealing submicron-scale internal structures that remain inaccessible using conventional optical or scanning electron microscopy. These findings underscore the need for further systematic application of this technique to evaluate the reproducibility and structural significance of such features.

Transmission Electron Microscopy. Transverse sections of *M. cryophilus* dorsal guard hair prepared by ultramicrotomy were examined under TEM (Figure 6). The shaft shows an outer cortex and an internal medullary region. Because the sections were not coated, progressive beam-induced deterioration was observed, mainly affecting the medulla. The medullary region appeared fragmented and was gradually lost during observation, whereas the cortex remained comparatively preserved. In several sections, the shaft appeared as a hollow oval structure with residual medullary fragments attached to the inner wall.

The cortex displayed a spongy appearance with apparent intercellular spaces (Figure 6 C–D). However, FIB–SEM sections showed cohesive cortical organization, suggesting that some separations observed here may be beam-related artifacts. Electron-dense spherical and ovoid bodies were observed within the cortex (Figure 6 A–D). Their size ranged up to 1.1 µm in spherical forms and up to 1.8 µm in ovoid forms. Based on morphology and correspondence with SEM observations, these structures are compatible with melanosomes.

Discussion

A methodological aspect that should be considered is that the observations performed using different microscopic techniques were not always conducted on the same species. This situation was determined both by the availability of suitable material for each type of preparation and by the technical requirements—and in some cases the partially destructive nature—of certain methodologies. However, since the primary objective of this study was to characterize hair microstructure and to evaluate the type of information that can be obtained at different levels of resolution, this approach does not affect the general interpretation of the results.

Moreover, the basic organization of hair in cricetid rodents follows a broadly conserved structural plan, allowing comparable patterns to be recognized among closely related species and enabling the use of different specimens to document morphological features representative of the group. In this sense, the use of different species across distinct techniques provided a complementary illustration of the structural variability and complexity of hair, as well as of the analytical capabilities of each method.

Optical Microscopy. Optical microscopy is undoubtedly the foundation for exploring the morphological patterns present in hair, and according to Teerink (2003), it has been used in trichological studies since the mid-19th century. The main structural elements of the hair shaft were clearly described using light microscopy, although indirect methods were required for some structures such as the cuticle, which could be observed by imprinting the scales onto materials like commercial nail polish (Hausman 1920, 1924, 1930, 1932; Apgar 1930; Mathiak 1938; Williams 1938; Stoves 1942; Oyer 1946; Noback 1951).

Despite the limitations of this type of observation, Hausman (1920, 1924, 1930) proposed that cuticular morphology is more closely related to hair thickness than to taxonomic grouping. This tendency was also observed in the rodent hair examined here, where scales near the shaft—*i.e.*, the thinnest region—are coronal, while in the wider midsection they are consistently imbricate. This same association between cuticular pattern and shaft diameter can be observed in other mammalian taxa, including *Loxodonta africana* (Hausman, 1920), *Didelphis virginiana* (Juárez-Sánchez *et al.* 2010), and *Cryptotis mexicana* (Baca and Sánchez, 2004). Although additional comparative studies would be needed to determine how general this pattern is across mammals, its presence in phylogenetically distant groups suggests that hair thickness may play a stronger role than fine-scale taxonomic differences in shaping cuticular structure.

The medulla has been considered the most important hair structure due to its species-specific patterns, particularly in the widest region, which has enabled the publication of numerous taxonomic identification keys using optical microscopy as the primary tool (Mathiak 1938; Mayer 1952; Quadros and Monteiro-Filho1998; Teerink 2003; Debelica and Thies 2009).

In peromyscine mice, no well-differentiated medullary morphological types were observed that would allow reliable species-level identification. While previous studies have shown that medullary patterns can be useful for distinguishing taxa at broader hierarchical levels, such as families or genera (*e.g.*, Pech-Canché *et al.* 2009), the present results indicate that their resolution decreases among closely related species. Some degree of variation may reflect ecological influences and phenotypic plasticity (Chernova 2006), particularly in traits such as coloration or shaft dimensions; however, the fundamental medullary organization remains relatively conserved within the group. These adaptive traits primarily support thermoregulation, as evidenced by the presence of different hair types and pigmentation patterns in guard hairs, such as those in the subgenus *Haplomylomys*, where pigmentation is restricted to the final third of the shaft. The presence of coronal scales near the root also appears to be related to thermoregulation, as their open structure allows air to be trapped between shafts, functioning as thermal insulation.

The inclusion of *S. mascotensis* provided a broader perspective on medullary organization within Cricetidae. Despite belonging to a different lineage within the family Cricetidae, its medullary pattern did not exhibit radical

structural divergence from those observed in peromyscines. Instead, variation in medullary configuration appeared to be more closely associated with hair shaft width than with fine-scale taxonomic distinctions. This finding supports the idea that medullary architecture is constrained by structural and dimensional factors, which may limit its usefulness for distinguishing closely related peromyscine species. Consequently, the similarity of qualitative medullary patterns across taxa helps explain the reduced diagnostic resolution of hair morphology at the species level. The advantages of optical microscopy in hair studies include its ease of use for rapid and straightforward exploration of various hair traits, especially medullary morphology.

Scanning Electron Microscopy (SEM). SEM has been a fundamental tool in trichological research due to its high resolution and depth of field, allowing detailed observation of cuticular morphology (Reimer 1993; Vázquez-Nin and Echeverría 2000; Egerton 2005). Cuticular scale patterns, including dentate or crenate margins, are clearly resolved with this technique (Chernova 2002). Although SEM-based keys have relied heavily on scale morphology for taxonomic identification (Ahmed *et al.* 2018; Lee *et al.* 2014; Debelica and Thies 2009; Teerink 2003), some authors consider scales to have limited diagnostic value when used alone (Mayer 1952; Homan and Genoways 1978; Short 1978). In peromyscine rodents, the imbricate configuration predominates, and identification may depend on the combined interpretation of multiple hair characters (Teerink 2003).

Beyond taxonomy, SEM reveals functional aspects of the cuticle, including its interaction with environmental particles. Highly open coronal scales in nectarivorous bats, for example, facilitate pollen retention (Howell and Hodgkin 1976; Vaughan 1988; Chernova 2002; Meyer *et al.* 2002), whereas the more tightly appressed imbricate scales observed here suggest different ecological adaptations.

Ultramicrotome sections. Ultramicrotome sections provide controlled visualization of internal hair architecture (De Cássia *et al.* 2007). In *M. cryophilus*, transverse and longitudinal sections revealed a relatively simple, discontinuous medulla containing two morphologically distinct pigment granule types: spherical and ellipsoidal bodies.

These correspond to pheomelanin and eumelanin melanosomes, respectively, consistent with established ultrastructural descriptions (Ito and Wakamatsu 2003). Hair coloration reflects the relative abundance and distribution of these pigments (Ozeki *et al.* 1995; Rees 2003; Fan *et al.* 2010; Delevoye *et al.* 2011). The coexistence of both morphotypes suggests pigment heterogeneity integrated within the keratinized medullary framework (Borovansky 2011).

These correspond to pheomelanin and eumelanin melanosomes, respectively, consistent with established ultrastructural descriptions (Ito and Wakamatsu 2003). Hair coloration reflects the relative abundance and distribution of these pigments (Ozeki *et al.* 1995; Rees 2003; Fan *et al.* 2010; Delevoye *et al.* 2011). The coexistence of both morphotypes suggests pigment heterogeneity integrated within the keratinized medullary framework (Borovansky 2011).

Energy-Dispersive X-ray Spectroscopy (EDS). EDS analysis confirmed that hair is primarily composed of carbon and oxygen, consistent with keratin and melanin polymers, and showed a strong sulfur signal indicative of cysteine-rich α-keratin (Robbins 2012). While EDS does not allow direct chemical discrimination between eumelanin and pheomelanin at the resolution employed, the morphological differentiation of melanosomes supports compositional heterogeneity within the medulla.

Melanosomes are also capable of binding metallic elements and toxins (Tobin 2008; Kintz and Villain 2005). SEM combined with EDS therefore offers the potential to assess localized elemental accumulation and contaminant particles associated with hair (Lee and von Lehmden 1973), providing complementary structural and microanalytical insights.

Focused Ion Beam (FIB) Microscopy. The application of FIB milling provided access to internal features that were not clearly distinguishable using the other microscopy techniques employed. Progressive material removal permitted controlled exposure of the cuticular scales, which exhibited a sponge-like internal appearance, and of the cortex, composed of quadrangular, hyaline cells that are inherently difficult to visualize (Hausman 1920).

One of the most remarkable findings of this study was the identification of spherical structures associated with a dense network of disorganized filaments, resembling a tangled skein of yarn, revealed through FIB-SEM analysis. To my knowledge, this structural arrangement has not been previously described in the literature on mammalian hair ultrastructure. Although its biological nature requires further investigation, the detection of this complex internal organization highlights the capacity of advanced ion-beam–assisted microscopy to uncover previously unrecognized features, even in tissues that have been extensively studied for decades. This observation emphasizes the importance of applying novel high-resolution methodologies to revisit classical biological materials, as they may still harbor undocumented structural complexity.

Interpretation of the exposed internal structures must be approached with caution. Certain filamentous or globular features may reflect modifications induced during ion milling, including redeposition effects, beam-induced damage, or partial collapse of internal components, rather than representing intrinsic morphological traits of the hair shaft. Beam-induced damage and material redeposition are well-documented phenomena in FIB processing (Giannuzzi and Stevie 1999; Mayer *et al.* 2007; Volkert and Minor 2007). Consequently, additional replicates and complementary techniques will be necessary to distinguish genuine biological organization from potential preparation artifacts inherent to the FIB process.

Additionally, through characteristic X-ray analysis (EDS), it was possible to directly verify the elemental composition of hair across its layers. In the outermost layers—namely, the cuticle and cortex—a high concentration of sulfur was detected, in contrast to the medulla, which lacked this element, as confirmed in this study using this analytical tool.

The FIB-SEM analysis was conducted on a single representative sample, reflecting the practical constraints inherent to this technique, including extended preparation and acquisition times, the need for highly specialized infrastructure, and its partially destructive nature due to progressive ion milling. Although the number of samples analyzed was limited, the aim of incorporating FIB-SEM was not to evaluate interspecific or interindividual variation, but to explore the three-dimensional organization and microstructural arrangement of the hair shaft at high resolution. Within this context, the use of a single sample proved sufficient to document structural features that are not accessible through conventional sectioning or surface imaging techniques.

Given that hair in cricetid rodents follows a broadly conserved structural plan, the features observed can be interpreted as representative of the general architectural organization of the group. The ultrastructural information obtained through FIB-SEM is particularly valuable for understanding keratinized tissues, as it allows the integration of observations across different scales of resolution and facilitates more precise interpretation of cuticular, cortical, and medullary organization. Thus, rather than serving a comparative purpose, the application of FIB-SEM in this study provides a methodological contribution by demonstrating the analytical potential of high-resolution three-dimensional imaging to complement optical and conventional electron microscopy approaches.

Transmission Electron Microscopy. Transmission electron microscopy enabled the observation of morphological details in the structures previously examined using other techniques. The oval shape of hair, clearly visible in transverse sections, has been described since the earliest studies, which also reported other forms such as dorsoventrally flattened and peanut-shaped hairs (Hausman 1920, 1924; Williams 1938). The key difference lies in the microstructural details that are lost with optical microscopy, such as the fibrillar structure of hair, the spherical and ovoid bodies, and their thin membranes. These bodies match in size those observed in longitudinal sections under scanning electron microscopy.

Such structures may be identified as pigment granules, since according to Fan *et al.* (2010), eumelanosomes are elongated and ellipsoidal, with a diameter of 0.9 *μm*. In contrast, pheomelanosomes are packed into spherical bodies approximately 0.7 *μm* in diameter, as reported by the same author. Furthermore, it has been suggested that the aggregation pattern of pigment granules is genetically regulated and taxon-specific (Hausman 1920; Ito and Wakamatsu 2003). Transmission electron microscopy is essential for observing these melanosome aggregation patterns, which represent an entire line of research whose adaptive and phylogenetic implications remain largely unexplored.

Conclusions

The combined use of optical microscopy and electron microscopy allowed the characterization of hair morphology in species of the genus *Peromyscus* at multiple levels of structural organization. Optical microscopy provided a general assessment of hair types, banding patterns, and the distribution of the cuticle, cortex, and medulla, whereas SEM, TEM, and FIB-SEM revealed detailed surface and internal microstructural features.

The results indicate that cuticular scale morphology and medullary organization show consistent patterns at the genus level. However, in the peromyscine rodents analyzed, intra- and interspecific overlap in morphological characters limits the reliability of hair as a diagnostic trait at the species level.

The integration of light and electron microscopy techniques proved essential for relating general morphology to fine structural organization. In particular, FIB-SEM enabled high-resolution three-dimensional visualization of internal architecture, confirming the continuity and spatial arrangement of medullary chambers and cuticular transitions. Although applied to a limited number of samples, this approach demonstrated the analytical potential of high-resolution microscopy for studying keratinized structures in micromammals.

Overall, hair morphology in cricetid rodents constitutes a useful structural trait for identification at higher taxonomic levels and for comparative and functional analyses, while its diagnostic value at the species level remains limited within closely related taxa.

Acknowledgments

I am deeply grateful to Dr. Livia León Paniagua, who served as my advisor during both my Master's and Ph.D. studies, for her guidance, academic rigor, and intellectual generosity. Her enthusiasm for the study of mammals and her commitment to training new generations of specialists across a wide diversity of topics were decisive in the development of this line of research. Her influence endures at every stage of this work, which reflects the mark she has left on Mexican mammalogy through teaching, research, and scientific mentorship. I want to thank the Instituto de Física, Universidad Nacional Autónoma de México for facilitating the laboratory used in the sample preparation. Special thanks to the MZFC-M for providing the samples and Guadalupe Zavala Padilla for her technical assistance in sample preparation. SEM was conducted at the Instituto Mexicano del Petróleo (IMP) and at the Laboratorio de Microscopía Electrónica USAII-FQ, UNAM. I thank Vicente Garibay Febles, Eduardo Palacios González and Iván Puente-Lee for their technical assistance.

Declaration of Artificial Intelligence use

The artificial intelligence tool ChatGPT was used solely to assist with the preliminary translation of the manuscript from Spanish into English. All generated text was subsequently reviewed, edited, and validated by the author.

Literature cited

Ahmed E, Pienaar R, and Moolman H. 2018. Morphological identification of southern African rodent species based on scanning electron microscopy of hair. *Journal of Morphology* 279:1741–1753. https://doi.org/10.1002/jmor.20878

Alibardi L. 2004a. Fine structure of marsupial hairs, with emphasis on trichohyalin and the structure of the inner root sheath. *Journal of Morphology* 261:390–402. https://doi.org/10.1002/jmor.10257

Alibardi L. 2004b. Comparative aspects of the inner root sheath in adult and developing of mammals in relation to the evolution of hairs. *Journal of Anatomy* 205:179–200. https://doi.org/10.1111/j.0021-8782.2004.00324

Amman BR. 2002. Utility of hair structure for taxonomic discrimination in bats, with an example from the bats of Colorado. *Occasional Papers, The Museum, Texas Tech University* 216:1–16. https://doi.org/10.5962/bhl.title.156835

Apgar CS. 1930. A comparative study of the pelage of three forms of *Peromyscus*. *Journal of Mammalogy* 11:485–493. https://doi.org/10.2307/1373972

Arita HT, and Aranda M. 1987. Técnicas para el estudio y clasificación de los pelos. Cuadernos de divulgación INIREB No. 32. Xalapa (MEX): Instituto Nacional de Investigaciones sobre Recursos Bióticos.

Baca II, and Sánchez-Cordero V. 2004. Catálogo de pelos de guardia dorsal en mamíferos del estado de Oaxaca, México. *Anales del Instituto de Biología. Serie Zoológica* 72:383–427.

Birbeck MSC, Mercer EH, and Barnicot NA. 1956. The structure and formation of pigment granules in human hair. *Experimental Cell Research* 10:505–514. https://doi.org/10.1016/0014-4827(56)90022-2

Birberck MSC, and Mercer E. 1957. The electron microscopy of the human hair follicle. *The Journal of Biophysical and Biochemical Cytology* 3: 203–230.

Borovansky J. 2011. History of melanosome research. In: Borovansky J, and Riley PA, editors. *Melanins and melanosomes: biosynthesis, structure, physiological and pathological functions*. Hoboken (EEUU): John Wiley & Sons; p. 1–19. https://doi.org/10.1002/9783527636150.ch1

Chernova OF. 2002. Architectonic and diagnostic significance of hair cuticle. *Izvestiya Akademii Nauk, Seriya Biologicheskaya* 29:238–247. https://doi.org/10.1023/A:101548243043

Chernova OF. 2003. Architectonic and diagnostic significance of hair cortex and medulla. *Akademii Nauk, Seriya Biologicheskaya* 30:53–62.

Chernova OF. 2006. Evolutionary aspects of hair polymorphism. *Akademii Nauk, Seriya Biologicheskaya* 33:43–52. https://doi.org/10.1134/S1062359006010067

Clement JL, Hagege R, Le Pareux A, Connet J, and Gastaldi G. 1981. New concepts about hair identification revealed by electron microscope studies. *Journal of Forensic Sciences* 26:447–458. https://doi.org/10.1520/JFS11383J

Debelica A, and Thies M. 2009. Atlas and key to the hair of terrestrial Texas mammals. Lubbock (EEUU): Museum of Texas Tech University. https://doi.org/10.5962/bhl.title.142652

De Cássia R, Kunihiko P, Silveira M, and Joekes I. 2007. Electron microscopic observations of human hair medulla. *Journal of Microscopy* 226:54–62. https://doi.org/10.1111/j.1365-2818.2007.01747.x

Deedrick DW, and Koch SL. 2004. Microscopy of hair part I: A practical guide and manual for animal hairs. *Forensic Science Communications* 6: 1–44

Delevoye C, Giordano F, Marks MS, and Raposo G. 2011. Biogenesis of melanosomas. In: Borovansky J, and Riley PA, editors. *Melanins and melanosomes: biosynthesis, structure, physiological and pathological functions*. Hoboken (EEUU): John Wiley & Sons; p. 247–294. https://doi.org/10.1051/medsci/2011272153

Egerton RF. 2005. Physical principles of electron microscopy: an introduction to TEM, SEM, and AEM. New York (EEUU): Springer. https://doi.org/10.1007/978-3-319-39877-8

Fan R, Yang G, and Dong C. 2010. Study of hair melanins in various hair color alpaca (*Lama pacos*). *Asian-Australasian Journal of Animal Sciences* 23:444–449. https://doi.org/10.5713/ajas.2010.90333

GATAN. 2007. Digital Micrograph. V 3.11.0. California (EEUU). https://www.gatan.com/.

Giannuzzi LA, and Stevie FA. 1999. A review of focused ion beam milling techniques for TEM specimen preparation. *Micron* 30:197–204. https://doi.org/10.1016/S0968-4328(99)00005-0

Hausman LA. 1920. Structural characteristics of the hair of mammals. *The American Naturalist* 54:496–523.

Hausman LA. 1924. Further studies of the relationships of the structural characters of mammalian hair. *The American Naturalist* 58:544–557. https://doi.org/10.1086/280006

Hausman LA. 1932. The cortical fusi of mammalian hair shafts. *The American Naturalist* 66:461–470.

Hausman LA. 1930. Recent studies of hair structure relationships. *Scientific Monthly* 30:258–277.

Homan JA, and Genoways HH. 1978. An analysis of hair structure and its phylogenetic implications among heteromyid rodents. *Journal of Mammalogy* 59:740–760. https://doi.org/10.2307/1380139

Howell DJ, and Hodgkin N. 1976. Feeding adaptations in the hairs and tongues of nectar-feeding bats. *Journal of Morphology* 148:329–339. https://doi.org/10.1002/jmor.1051480305

Ito S, and Wakamatsu K. 2003. Quantitative analysis of eumelanin and pheomelanin in human, mice and

other animals: a comparative review. *Pigment Cell Research* 16:523–531. https://doi.org/10.1034/j.1600-0749.2003.00072.x

Juárez-Sánchez D, Estrada C, Bustamante M, Moreira J, Quintana Y, and López J. 2010. *Guía ilustrada de pelos para la identificación de mamíferos mayores y medianos de Guatemala*. Guatemala (GTM): Dirección General de Investigación (DIGI).

Kintz P, and Villain M. 2005. Hair in forensic toxicology with a special focus on drug-facilitated crimes. In: Tobin DJ, editor. Hair in toxicology: an important bio-monitor. Cambridge (UK): Royal Society of Chemistry; p. 54–80.

Lee RE, and von Lehmden DJ. 1973. Trace metal pollution in the environment. *Journal of the Air Pollution Control Association* 23:853–857. https://doi.org/10.1080/00022470.1973.10469854

Lee SH, Lee MY, and Park YC. 2014. Species identification of mammals using hair morphology: A scanning electron microscopy approach. *Microscopy Research and Technique* 77:468–474.

Mathiak HA. 1938. A key to hairs of the mammals of southern Michigan. *Journal of Wildlife Management* 2:251–268. https://doi.org/10.2307/3795673

Mayer J, Giannuzzi LA, Kamino T, and Michael J. 2007. TEM sample preparation and FIB-induced damage. *MRS Bulletin* 32:400–407. https://doi.org/10.1557/mrs2007.63

Mayer WV. 1952. The hair of California mammals with keys to the dorsal guard hairs of California mammals. *American Midland Naturalist* 48:480–512. https://doi.org/10.2307/2422262

Meyer W, Schnapper A, and Hulmann G. 2002. The hair cuticle and its relationships to functions of the hair coat. *Journal of Zoology* 256:489–494. https://doi.org/10.1017/S0952836902000535

Noback C. 1951. Morphology and phylogeny of hair. *Annals of the New York Academy of Sciences* 53:476–492. https://doi.org/10.1111/j.1749-6632.1951.tb31950.x

Oyer ER. 1946. Identification of mammals from studies of hair structure. *Transactions of the Kansas Academy of Sciences* 49:155–160. https://doi.org/10.2307/3625853

Ozeki H, Ito S, Wakamatsu K, and Hirobe T. 1995. Chemical characterization of hair melanins in various coat-color mutants of mice. *The Society for Investigative Dermatology* 105:361–366. https://doi.org/10.1111/1523-1747.ep12320792

Pech-Canché JM, Sosa-Escalante JE, and Koyoc Cruz ME. 2009. Guía para la identificación de pelos de guardia de mamíferos no voladores del Estado de Yucatán, México. *Revista Mexicana de Mastozoología* 13: 7–33. http://doi:10.22201/ie.20074484e.2009.13.1.33

Quadros J, and Monteiro-Filho ELA. 1998. Revisão conceitual, padrões microestructurais e proposta nomenclatória para os pêlos-guarda de mamíferos brasileiros. *Revisa Brasileira de Zoología* 23:279–292. https://doi.org/10.1590/S0101-81752006000100023

Rees JL. 2003. Genetics of hair and skin color. *Annual Reviews of Genetics* 37:67–90. https://doi.org/10.1146/annurev.genet.37.110801.143233

Reimer L. 1993. *Transmission electron microscopy: physics of image formation and microanalysis*. Berlin (DEU): Springer-Verlag. https://doi.org/10.1007/978-0-387-40093-8

Robbins CR. 2012. *Chemical and physical behavior of human hair*. Berlin (DEU): Springer-Verlag. https://doi.org/10.1007/978-3-642-25611-0

Russell ES. 1946. A quantitative histological study of the pigment found in the coat-color mutants of the house mouse. I. Variable attributes of the pigment granules. *Genetics* 31:327–346. https://doi.org/10.1093/genetics/31.3.327

Short HL. 1978. Analysis of cuticular scales on hairs using the scanning electron microscope. *Journal of Mammalogy* 59:261–268. https://doi.org/10.2307/1379911

Stoves JL. 1942. The histology of mammalian hair. *Analyst* 67:385–387. https://doi.org/10.1039/AN9426700385

Teerink BJ. 2003. *Hair of West European mammals: atlas and identification key*. Cambridge (UK): Cambridge University Press.

Tobin DJ. 2008. Human hair pigmentation-biological aspects. *International Journal of Cosmetic Science* 30:233–257. https://doi.org/10.1111/j.1468-2494.2008.00456.x

Tremori T, Monteiro Garcia F, Montoya Flórez LM, Picado Gonçalves B, Ferraz de Camargo B, Gwinnett C, *et al*. 2018. Hair analysis of mammals of Brazilian wildlife for forensic purposes. *Open Journal of Animal Sciences* 8:335–345. https://doi.org/10.4236/ojas.2018.83025

Tridico S. 2015. Morphological and molecular approaches to characterize modifications relating to mammalian hairs in archaeological, paleontological and forensic contexts [PhD thesis]. [Perth (Australia)]: Murdoch University.

Vaughan TA. 1988. *Mamíferos*. Mexico City (MEX): Interamericana McGrawHill.

Vázquez-Nin G, and Echeverría O. 2000. *Introducción a la microscopía electrónica aplicada a las ciencias biológicas*. Mexico City (MEX): Universidad Nacional Autónoma de México/Fondo de Cultura Económica.

Volkert C A, and Minor AM. 2007. Focused ion beam microscopy and micromachining. *MRS Bulletin* 32:389–399. https://doi.org/10.1557/mrs2007.62

Williams CS. 1938. Aids to the identification of mole and shrew hairs with general comments on hair structure and hair determination. *The Journal of Wildlife Management* 2:239–250. https://doi.org/10.2307/3795672

Wygal BT, Krasinski KE, Metcalfe JZ, McMahan D, Holmes CE, Crass BA, *et al*. 2024. Archaeological recovery of Late Pleistocene hair and environmental DNA from interior Alaska. *Environmental Archaeology* 29:265–280. https://doi.org/10.1080/14614103.2022.2031836

Associated editors: Giovani Hernández Canchola and Pablo Colunga Salas
Submitted: October 31, 2025; Reviewed: January 8, 2026
Accepted: April 16, 2026; Published online: May 29, 2026

THERYA, 2026, Vol. 17(2):247-258 DOI: 10.12933/therya.2026.6277 ISSN 2007-3364

Recognizing chorotypes for terrestrial Mexican mammals: contrasting datasets and units of analysis, and ecological implications

Tania Escalante[1], Oscar Campos[1], and Juan J. Morrone[2*]

[1]Laboratorio de Biogeografía de la Conservación, Departamento de Biología Evolutiva, Facultad de Ciencias, Universidad Nacional Autónoma de México (UNAM), 04510 Mexico City, Mexico. E-mail: tescalante@ciencias.unam.mx (TE); ocampos667@gmail.com (OC).

[2]Museo de Zoología "Alfonso L. Herrera", Departamento de Biología Evolutiva, Facultad de Ciencias, Universidad Nacional Autónoma de México (UNAM), 04510 Mexico City, Mexico.

[*]Corresponding author: morrone@ciencias.unam.mx

Chorotypes are groups of species that share a similar distribution within a study area. Their identification depends on the geographic units and the taxa analyzed. For the terrestrial Mexican mammals, identification of chorotypes has not been explored yet. Our objectives are (1) to identify chorotypes for the species of terrestrial Mexican mammals using two different datasets (Map of Life [MOL] and International Union for Conservation of Nature [IUCN]), (2) to compare the results using biogeographic provinces, and (3) to discuss the relevance of the chorotypes for ecological regionalization. More than 400 species of mammals were used to identify 33 chorotypes in four different analyses: MOL and IUCN with the whole Chihuahuan province, and MOL and IUCN splitting it into Northern and Southern Chihuahuan. For the 33 chorotypes, one was recovered in all analyses, one was shared by three analyses, seven were shared by two, and 24 were unique for one. We demonstrate the importance of the use of different datasets of geographic distribution of mammals, as well as pre-defined units of analyses, and their influence on the results of a chorotype analysis. Most of the chorotypes identified the mixture of Nearctic and Neotropical biotas in the Mexican territory, but more interestingly, the affinity of ecological patterns of lowland and highland areas.

Keywords: affinity, biogeography, pattern, process, regionalization.

Los corotipos son grupos de especies que comparten una distribución similar dentro de un área de estudio. La identificación de estos depende de las unidades geográficas y los taxones analizados. Para los mamíferos terrestres mexicanos aún no se ha explorado la identificación de corotipos. Nuestros objetivos son: (1) identificar corotipos para las especies de mamíferos terrestres mexicanos empleando dos conjuntos de datos diferentes (Map of Life [MOL] e International Union for Conservation of Nature [IUCN]), (2) comparar los resultados utilizando provincias biogeográficas, y (3) analizar la relevancia de los corotipos para la regionalización ecológica. Para ello, se utilizaron más de 400 especies de mamíferos para identificar 33 corotipos en cuatro análisis diferentes: MOL y IUCN con la provincia Chihuahuense completa, y MOL y IUCN separando el Norte y Sur de la misma. De los 33 corotipos, uno se recuperó en todos los análisis, uno estuvo compartido por tres análisis, siete de ellos por dos y 24 resultaron únicos para uno. Demostramos la importancia del uso de diferentes conjuntos de datos de distribución geográfica de mamíferos, así como de unidades de análisis predefinidas, y su influencia en los resultados de un análisis de corotipos. La mayoría de los corotipos identificaron la mezcla de biotas neárticas y neotropicales en el territorio mexicano, pero lo más interesante fue la afinidad de los patrones ecológicos de áreas de tierras bajas y altas.

Palabras clave: afinidad, biogeografía, patrón, proceso, regionalización.

The term "chorotype" has a complex history (see Morrone 2014; Fattorini 2015; 2016; Passalacqua 2015). Fattorini (2015) clarified it, distinguishing between global and regional chorotypes. Global chorotypes correspond to "groups into which species with similar overall ranges can be classified" (Fattorini 2015, p. 2249), whereas regional chorotypes are "groups of species that have a similar distribution within a certain study area" (Fattorini 2015, p. 2250). Interestingly, Fattorini (2015) assimilated the former to "biotas" (taxa inhabiting a particular area) and the latter to "cenocrons" (sets of taxa that share the same biogeographic history, constituting identifiable subsets that dispersed in a given time frame and assembled to a biota) (Morrone 2009; 2014). The quantitative identification of chorotypes was proposed by Baroni-Urbani *et al.* (1978) as a biogeographic pattern of two or more species occupying a similar distributional area. For a brief discussion of Baroni-Urbani *et al.* (1978) algorithm, see Real *et al.* (1992) and Escalante *et al.* (2024).

Distributional patterns are fundamental to propose biogeographic regionalizations of the Earth, but they are dependent on the taxa analyzed, the data and the geographic context. Additionally, it has been found that ecological and biogeographical regions might not always match (Crisci *et al.* 2006). Recently, Zhang *et al.* (2025) suggested that the identification of chorotypes may help refine biogeographic regionalizations, especially for exploring transition zones.

The use of different geographic units and data sources has been briefly explored for chorotypes. Since their formulation, chorotypes have been identified using

artificial units as grid-cells of a particular size (*v. gr.* 1 x 1° latitude-longitude), however, the use of natural units, as biogeographic provinces, could be preferable. Natural units may adjust better to the typical irregular form of the distributional areas, due to ecological and evolutionary barriers. Moreover, many databases of biodiversity try to recover the geographic distribution areas of the species in polygons that could be useful to identify biogeographic patterns. For mammals, which are one of the taxa with more data (Troudet *et al.* 2017) and public databases available (*v. gr.* Wilson and Reeder 2005; International Union for Conservation of Nature (IUCN) 2025; Map of Life [MOL] 2025; Global Biodiversity Information Facility [GBIF.org] 2026; iNaturalist 2026; Mammal Diversity Database 2026), many sources could be used to identify chorotypes (or other distributional patterns). Few analyses assess how different datasets for the same taxon affect the identification of their distributional patterns. Due to taxonomic updates or the use of different taxonomic and nomenclatural authorities based on different species concepts, the current datasets available may influence the chorotype results.

In the case of Mexico, chorotypes have been identified for 264 bird species of the Sierra Madre Oriental (Ferro *et al.* 2017) and for endemic taxa of the Transmexican Volcanic Belt (25 species of amphibians, 89 of insects, 15 mammals, one bird and 37 plants) (Escalante *et al.* 2024). Although there have been many attempts to identify distributional patterns of the terrestrial Mexican mammalian fauna, using numerical methods (Ramírez-Pulido and Castro-Campillo 1990), based on endemism (Escalante *et al.* 2007a; 2009), and diversity (Arita and León-Paniagua 1993; Rodríguez and Arita 2004), there are no analyses identifying chorotypes. For Mexico, some regionalizations have been proposed based on mammals (Ramírez-Pulido and Castro-Campillo 1990; Escalante *et al.* 2013), and they are dependent on the taxa analyzed, the data and the geographic context. For these reasons, our objectives are 1) to identify chorotypes for the species of Mexican mammals using two datasets, Map of Life (MOL 2025) and the IUCN Red List (IUCN 2025); 2) to compare the results using the Mexican biogeographic provinces; and 3) to discuss their implications for ecological distributional patterns.

Material and methods

We followed Fattorini (2015) to identify regional chorotypes. We divided the study area into geographical units and considered the species distributed within each unit; those that were grouped according to their distribution within a unit were considered a chorotype.

To compare two different data sources of mammalian species distributions, we obtained geographical distribution range areas from Map of Life (hereafter MOL; Map of Life 2025; https://mol.org/) and the IUCN Red List (hereafter IUCN; IUCN 2025; https://www.iucnredlist.org/), both in shapefile format. There are 772 mammal species registered in the geopolitical boundaries of Mexico in the MOL database, whereas 663 species are registered for the country in the IUCN database (a difference of 109 species). As both databases possibly overestimate the number of Mexican species (around 600 species according to the taxonomic list of Comisión Nacional para el Conocimiento y Uso de la Biodiversidad (CONABIO); Reséndiz-López 2025), we selected the MOL and IUCN species names following an updated list provided by García-Trujano and collaborators. Therefore, our final species lists have 487 species in MOL and only 416 species in IUCN, excluding the marine mammal species and species with uncertain taxonomy.

Polygons in shapefile format of distribution ranges for the selected species of both databases were intersected in QGIS 3.34 (QGIS Development Team 2023) with the complete boundaries of the 14 biogeographic provinces shapefiles of Mexico (Morrone *et al.* 2017; Escalante *et al.* 2025; https://americas.atlasbiogeografico.com/). The Chihuahuan province has the biggest surface of all provinces, and some authors have recognized at least two provinces or areas of endemism for mammals (Ramírez-Pulido and Castro-Campillo 1990; Escalante *et al.* 2003; 2007b) and other species (Morrone *et al.* 2022a). Thus, we decided to test the Chihuahuan province as a natural unit, dividing it into two sub-units, provisionally named Northern and Southern Chihuahuan. The limits used for this division correspond to Ramírez-Pulido and Castro-Campillo (1990) and applied with a shapefile provided by Reaño-Jiménez (pers. comm.). Therefore, two more intersections were carried out considering 15 provinces. All geographic analyses were done in QGIS 3.34.

For each of the four geographical intersections, we built a presence-absence matrix for all species, where a species' presence in each province was coded as '1' and its absence as '0'. Therefore, four matrices were analyzed and named: MOL - Chihuahuan, MOL - N & S Chihuahuan, IUCN – Chihuahuan, and IUCN - N & S Chihuahuan.

To identify the chorotypes, we used the RMACOQUI package for R software (Olivero *et al.* 2011; R Core Team 2023), which classifies distributional areas using Baroni-Urbani and Buser's (1976) index. The index provides a table of critical values which are used to perform exact randomization tests comparing the observed similarity values with all possible outcomes to detect significant similarities (Olivero *et al.* 2011). Then, a dendrogram was built with the agglomerative unweighted pair-group method using arithmetic averages (UPGMA) and branches that exhibited significant positive within-branch shared distributions and significantly disjunct from adjoining branches were identified. An index of internal homogeneity (IH) and distinctness was derived considering pairwise comparisons of the proportion of significant similarity and significant dissimilarity in every branch. A given branch was considered a chorotype if IH = 1 or positive, higher than subsequent nested clusters and statistically significant. Significance was evaluated comparing the frequency of significant similarities within a tested cluster and the most

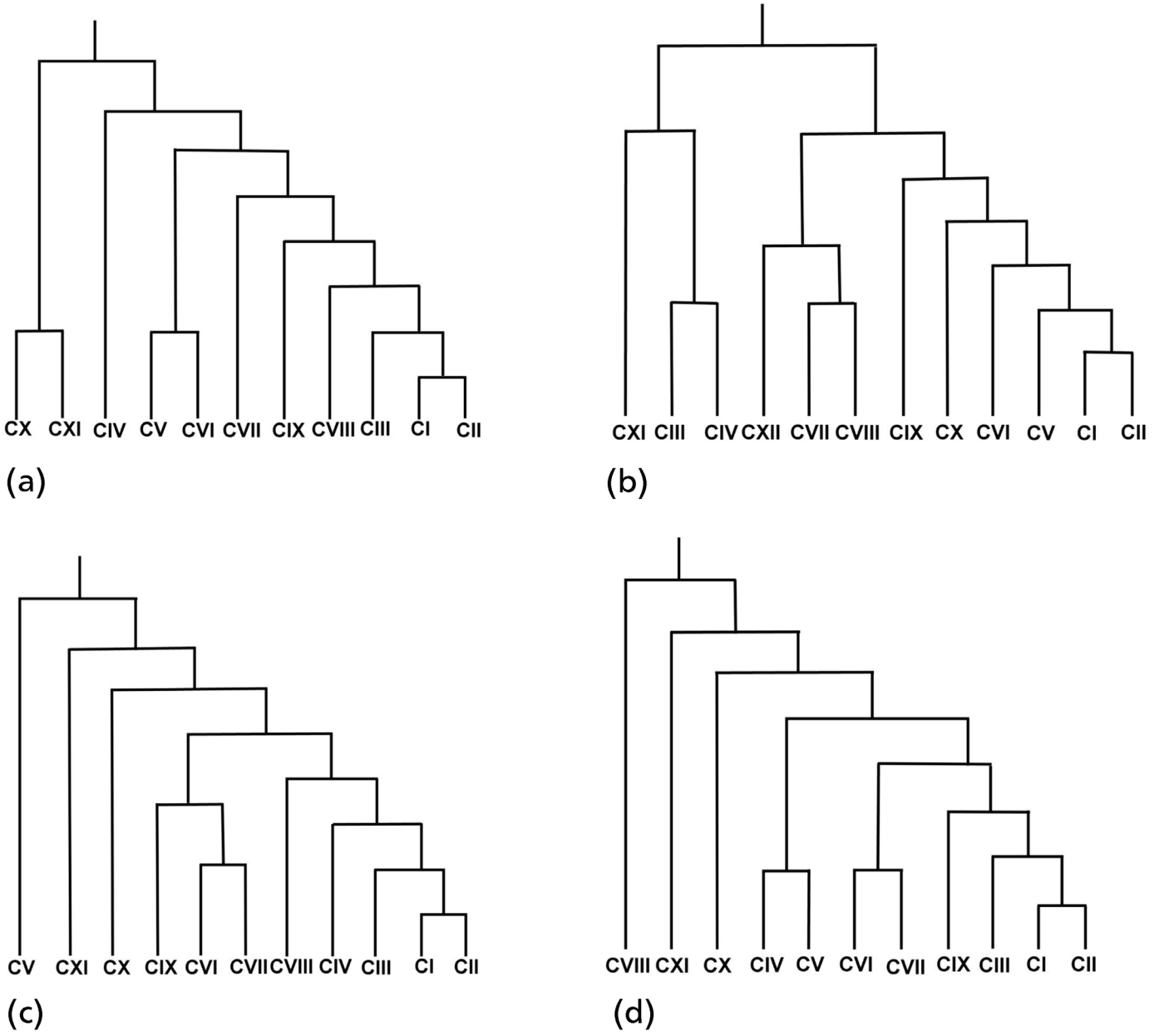

Figure 1. Dendrograms with the individual chorotypes obtained for the four datasets: (a) Map of Life (MOL) with the complete Chihuahuan province, (b) MOL with Northern and Southern Chihuahuan, (c) IUCN with the complete Chihuahuan, and (d) IUCN with Northern and Southern Chihuahuan.

similar branch of the dendrogram by means of a G-test of independence. Finally, a series of fuzzy logic parameters was computed based on the average of similarities between each species distribution and all the distributions in a chorotype, to evaluate the degree of membership of any particular distribution to every chorotype, the overlap between chorotypes and the degree to which a chorotype was included into another chorotype (Olivero *et al.* 2011).

We used the script provided by Ferro (2024) for the R 4.3.2 software (R Core Team 2023) and RStudio (Posit team 2025), based on the chorological affinity, which refers to the similarity between the geographic distribution areas of the taxa without reference to any predefined geographic area (Ferro *et al.* 2017). To identify the chorotypes, we consulted the output file named Chorotype Report, where the number of each chorotype is shown (C1, C2, C3, etc.) and the location of each one in the dendrogram is indicated, with the node number and the left branch as "A" or the right branch as "B" (Ferro 2024). If there were species whose distribution do not overlap significantly with another distribution (which means that they did not belong to any chorotype), their degree of membership in each chorotype was evaluated using the output file named Macoqui Degree of Membership. Because there is no formal procedure for the nomenclature of chorotypes, we followed Olivero *et al.* (2011) numbering the main chorotypes as they were shown in the output file.

Finally, we compared the provinces and species composition of all individual chorotypes (from each single analysis) obtained and summarized their coincidences. When we found the same chorotype in more than one analyses, they were grouped into a general chorotype,

which was named with Roman numerals. Also, we used QGIS to select the polygons of the provinces of each chorotype species with significantly overlapping distribution and they were identified with the same color on a map.

Results

The results of the four different analyses of chorotypes, considering both datasets (MOL and IUCN) and two alternative numbers of provinces, are shown in Table 1. In Table 2, the individual chorotypes for each matrix are named with capital letter 'C' and Arabic numerals in the corresponding column with their number of species. From them, we identified 33 general chorotypes named with Roman numerals, regarding the numerical codes of the biogeographic provinces. The general chorotype IV was identical for all alternatives; chorotype I was shared by three matrices; seven chorotypes were shared by two datasets (V, XIII, XIV, XVI, XX, XXI, and XXXII; Table 2), all of which will be analyzed and discussed; and 24 were unique chorotypes for some datasets (which will not be described in detail).

The main features of each dendrogram with the relationship between their individual chorotypes are as follows:

For the MOL - Chihuahuan matrix, the dendrogram (Figure 1a) showed a first dichotomy segregating the mainly coastal provinces from the Pacific (C10) and the Baja Californian biogeographic provinces (C11). Then, the species distributed in the Chihuahuan and Tamaulipas provinces (C4) are separated from the rest. Next, provinces in northern and central Mexico (C5) and the Chiapas Highlands and Pacific Lowlands provinces (C6) are grouped together. The next division separates some highland and lowland provinces in southern Mexico (C7), followed by C9, which encompasses the Chihuahuan province with two central provinces. Then, a chorotype with all the provin-ces is separated (C8), C1 and C2 are the next, in a group with mostly lowland provinces. Finally, the last individual chorotype, C3, presents a mixture of highland and lowland provinces.

Compared to the previous matrix, MOL - N & S Chihuahuan showed one more individual chorotype, resulting in 12 chorotypes (Figure 1b). Only two of these chorotypes are the same and the branches in the dendrograms are not completely equivalent. For this matrix, some chorotypes are recovered including only one of the two sub-units, Northern and Southern Chihuahuan, like in Southern Chihuahuan and Tamaulipan (C8), Southern Chihuahuan and Baja Californian (C11), Northern Chihuahuan, Pacific Lowlands and Sonoran (C4), and Northern Chihuahuan and other central provinces (C10). Although we expected to recover the chorotypes of the previous matrix, this did not happen, but some variations and nesting of the previous chorotypes were discovered. For example, C3 is similar to the previous C10; and C5 includes almost all the provinces of the previous C8 but excludes the complete Baja California Peninsula. All the differences and maps are shown in the Supplementary Material S1 and S2.

Table 1. Results of the four analyses of chorotypes, using the MOL and IUCN databases of geographic distribution areas, with the complete Chihuahuan province and its northern and southern parts. Individual chorotypes refer to the results of single analysis. MOL - Chihuahuan= Map of Life database with the complete Chihuahuan province, MOL - N & S Chihuahuan= Map of Life database with the Chihuahuan province divided in northern and southern parts, IUCN - Chihuahuan= IUCN database with the complete Chihuahuan province, and IUCN - N & S Chihuahuan= IUCN database with the Chihuahuan province divided in northern and southern parts.

Results / Tests	MOL - Chihuahuan	MOL - N & S Chihuahuan	IUCN - Chihuahuan	IUCN - N & S Chihuahuan
Number of species analyzed	487	487	416	416
Number of individual chorotypes	11	12	11	11
Number of species in no chorotype	178	7	158	111
Number of species in all chorotypes	309	480	258	305

For the IUCN - Chihuahuan matrix, the dendrogram (Figure 1c) showed a first dichotomy separating the Baja California province (C5) from the rest, and it was recovered in the MOL - Chihuahuan database. Next, C11 is separated from the rest, joining the Chihuahuan province with two lowland provinces and the Transmexican Volcanic Belt. The following individual chorotype includes the Sierra Madre del Sur and Veracruzan provinces (C10). Next, two groupings are formed: one including C6, C7 and C9, and other with C1, C2, C3, C4 and C8. In the first one the northern provinces are separated first (C9). Then, C6 and C7 are separated: C6 is similar to C9 but also includes highland provinces. Finally, C7 includes only the Pacific Lowlands and Sierra Madre del Sur provinces. On the second branch, two groups are discovered: the mainly lowland provinces (C8) and the other four chorotypes in another branch. Then, C4 is separated from the rest, grouping all the provinces together, similar to the chorotypes obtained in the MOL databases (C8 and C6). Finally, C3 is separated, having a mixture of lowland and highland provinces, the same as C2 but including mainly central provinces, and C1 but including northern provinces.

When comparing the results of the IUCN - N & S Chihuahuan with the previous one, more similarities are noticed in the dendrogram (Figure 1d). Eight chorotypes are exactly the same (73%), being the branches in both dendrograms similar. The main differences are in C10, which includes the Balsas Basin, Sonoran and Veracruzan provinces; C2, which is very similar to C5 of the MOL - N & S Chihuahuan; and C5, which includes only the Californian, Northern Chihuahuan and Tamaulipan provinces. All the differences and maps are shown in the Supplementary Material S1 and S2.

We also compared the taxonomic composition and biogeographic provinces included in the chorotypes shared by four, three and two different analyses (Table 2). The only chorotype shared by the four analyses, chorotype IV, includes all the Mexican biogeographic provinces, but it is important to note that the chorotypes from the MOL and

Table 2. General chorotypes (Roman numerals) obtained through a consensus of the individual chorotypes, using the MOL and IUCN databases of geographic distribution areas, with the complete Chihuahuan province and its northern and southern parts. The name of each individual chorotype is shown in Arabic numerals, as the number of species in each chorotype per dataset, ordered by biogeographic provinces included. Biogeographic provinces: (1) Baja Californian, (2) Balsas Basin, (3) Californian, (4) Chiapas Highlands, (5) Chihuahuan, (5a) Northern Chihuahuan, (5b) Southern Chihuahuan, (6) Pacific Lowlands, (7) Sierra Madre del Sur, (8) Sierra Madre Occidental, (9) Sierra Madre Oriental, (10) Sonoran, (11) Tamaulipas, (12) Transmexican Volcanic Belt, (13) Veracruzan and (14) Yucatán Peninsula. MOL - Chihuahuan= Map of Life database with the complete Chihuahuan province, MOL - N & S Chihuahuan= Map of Life database with the Chihuahuan province divided in northern and southern parts, IUCN - Chihuahuan= IUCN database with the complete Chihuahuan province, and IUCN - N & S Chihuahuan= IUCN database with the Chihuahuan province divided in northern and southern parts.

General horotype name	Biogeographic provinces	Individual chorotype names and number of species included in parentheses			
		MOL - Chihuahuan	MOL - N & S Chihuahuan	IUCN - Chihuahuan	IUCN - N & S Chihuahuan
I	1	C11 (9)		C5 (10)	C8 (10)
II	2, 5, 12	C9 (10)			
III	2, 7, 13				C10 (7)
IV	1, 2, 3, 4, 5a, 5b, 6, 7, 8, 9, 10, 11, 12, 13, 14	C8 (49)	C6 (107)	C4 (41)	C3 (85)
V	1, 3, 5, 6, 8, 9 10, 11			C6 (39)	C6 (36)
VI	1, 3, 5a, 5b, 6, 8, 10		C3 (38)		
VII	1, 3, 6, 8, 10, 11	C10 (48)			
VIII	1, 5b		C11 (11)		
IX	2, 4, 5, 7, 8, 9, 11, 12, 13	C3 (18)			
X	2, 4, 5a, 5b 6, 7, 8, 10, 12, 13, 14				C2 (14)
XI	2, 4, 5a, 5b, 6, 7, 8, 9, 10, 11, 12, 13, 14		C5 (105)		
XII	2, 4, 6, 7, 12, 13			C2 (14)	
XIII	2, 4, 6, 7, 13, 14			C8 (73)	C9 (73)
XIV	2, 5, 6, 12			C11 (12)	C11 (only 5b) (13)
XV	2, 5, 6, 7, 8, 9, 10, 12			C1 (15)	
XVI	2, 5, 6, 7, 9, 11, 12, 13			C3 (13)	C1 (only 5b) (14)
XVII	2, 5, 6, 7, 8, 9, 10, 12, 13, 14	C1 (26)			
XVIII	2, 5a, 5b, 6, 7, 8, 9, 10, 12, 13		C1 (28)		
XIX	2, 5b, 9, 12		C10 (10)		
XX	2, 6, 7, 12, 13	C2 (24)	C2 (24)		
XXI	3, 5, 8, 9, 10, 11, 13			C9 (29)	C4 (21)
XXII	3, 5a, 11				C5 (6)
XXIII	3, 5a, 5b, 8, 10, 11, 12		C12 (35)		
XXIV	3, 5a, 5b, 8, 9, 10, 11, 12, 13		C7 (24)		
XXV	4, 6	C6 (7)			
XXVI	4, 6, 7, 13, 14	C7 (75)			
XXVII	4, 6, 7, 9, 12, 13, 14		C9 (83)		
XXVIII	5, 11	C4 (9)			
XXIX	5, 6, 8, 9, 10, 11,12	C5 (34)			
XXX	5a, 11		C8 (10)		
XXXI	5a, 6, 10		C4 (5)		
XXXII	6, 7			C7 (7)	C7 (7)
XXXIII	7, 13			C10 (5)	

IUCN datasets were very similar using only the complete Chihuahuan province, with 49 and 41 species, respectively, and also using the partitioned Chihuahuan, with 107 and 85 species, respectively. We found 36 species shared by MOL and IUCN with the complete Chihuahuan province and 78 species shared between MOL and IUCN with the partitioned Chihuahuan province.

For the general chorotype I (Figure 2a), which was the only one shared by three matrices (except MOL - N & S Chihuahuan), almost 100% of the species were shared in all chorotypes, showing a high affinity to the Baja Californian province. The next seven general chorotypes were shared by two datasets. Chorotype V (Figure 2b) was diagnosed by both IUCN datasets, including eight biogeographic

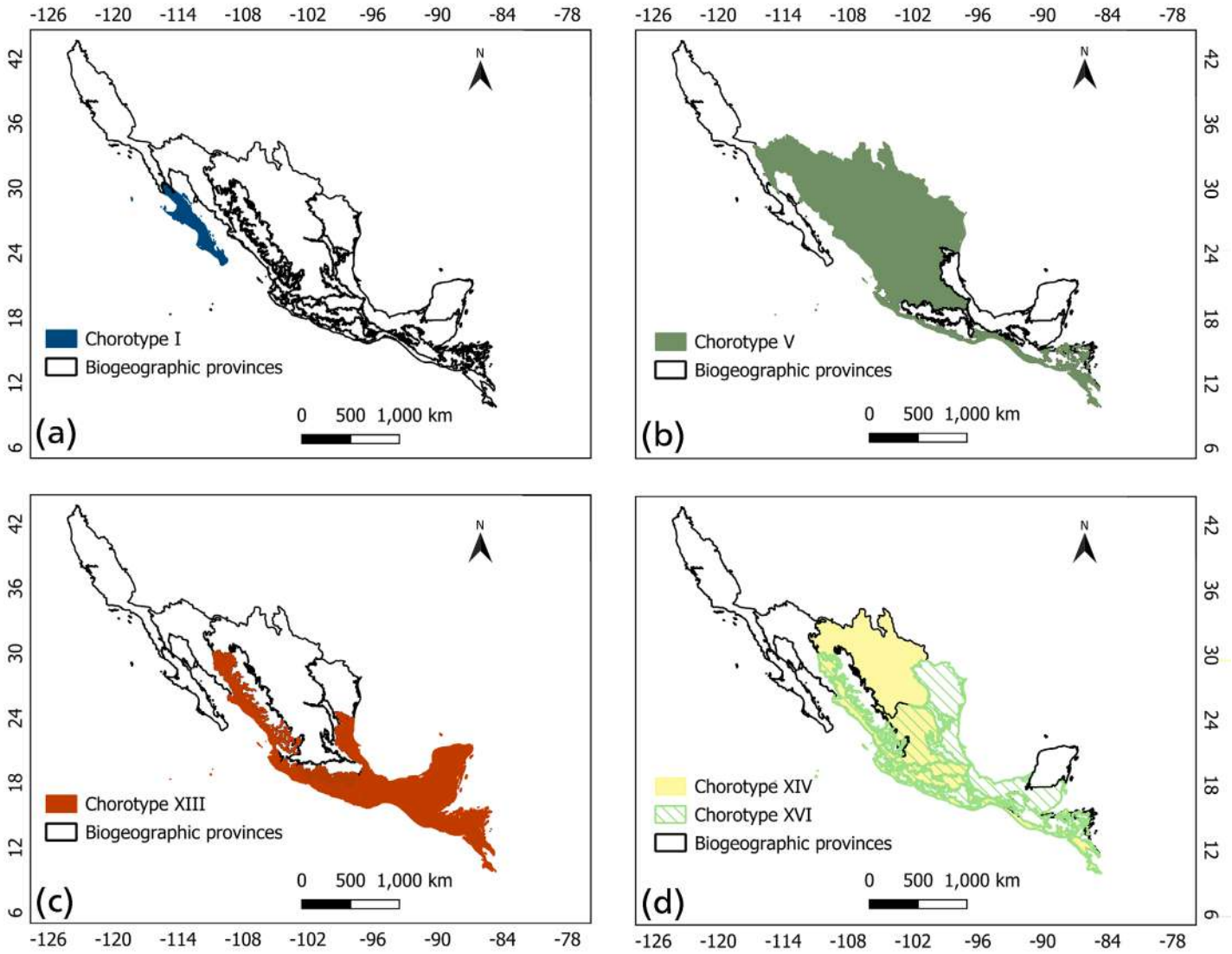

Figure 2. General chorotypes, which are shared by two or more analyses. (a) General chorotype I, shared by three analyses, represented by the individual chorotype C11 from the MOL database with the complete Chihuahuan province. (b) Chorotype V, shared by two analyses, represented by the individual chorotype C6 from the IUCN database with the complete Chihuahuan province. (c) Chorotype XIII, shared by two matrices, from both IUCN datasets. (d) Chorotypes XIV and XVI, shared by two IUCN matrices. Chorotype XIV is a subset of chorotype XVI.

provinces: the five Nearctic provinces, both mountainous chains that border those provinces at eastern and western sides, and a lowland province, the Pacific Lowlands. Chorotype XIII (Figure 2c) was also diagnosed by both IUCN datasets, but for central and southern provinces mainly, mixing Neotropical lowlands with highlands of the Mexican Transition Zone. The next general chorotypes shared by two datasets are XIV and XVI (Figure 2d), both chorotypes recognized by the IUCN matrix. Regarding the provinces involved in them, the chorotype XIV is a subset of XVI (with four and eight provinces, respectively), but in the IUCN - N & S Chihuahuan matrix, only the northern part of the Chihuahuan province was involved.

Chorotype XX, only identified by both MOL databases, occupies central Mexico, with lowland and highland provinces (Figure 3a). The next chorotype (XXI) was diagnosed by seven provinces in the IUCN - N & S Chihuahuan database (Figure 3b). The last chorotype, XXXII, was shared in two IUCN databases with only two biogeographic provinces: Pacific Lowlands and Sierra Madre del Sur (Figure 3c).

Discussion

Chorotypes are useful for organizing knowledge on the geographical distribution of taxa (Passalacqua 2015). When identifying chorotypes, as well as areas of endemism, the problem of using different datasets is not trivial. In this study, we show the relevance of using different datasets of geographic distribution of mammals, as well as pre-defined units of analyses, and their influence on the results of a chorotype analysis.

The differences among the four analyses led to the identification of a total of 33 different general chorotypes (coming from the individual chorotypes), but most of them were unique for one analysis. For the unique general chorotype (IV) obtained in the four analyses, MOL and IUCN had many species shared (~40 species); however, the use of a divided province (Chihuahuan) in two different units (Northern and Southern) duplicated the number of species (~80). These findings can reveal important implications for the universal application of data sources and units of analyses.

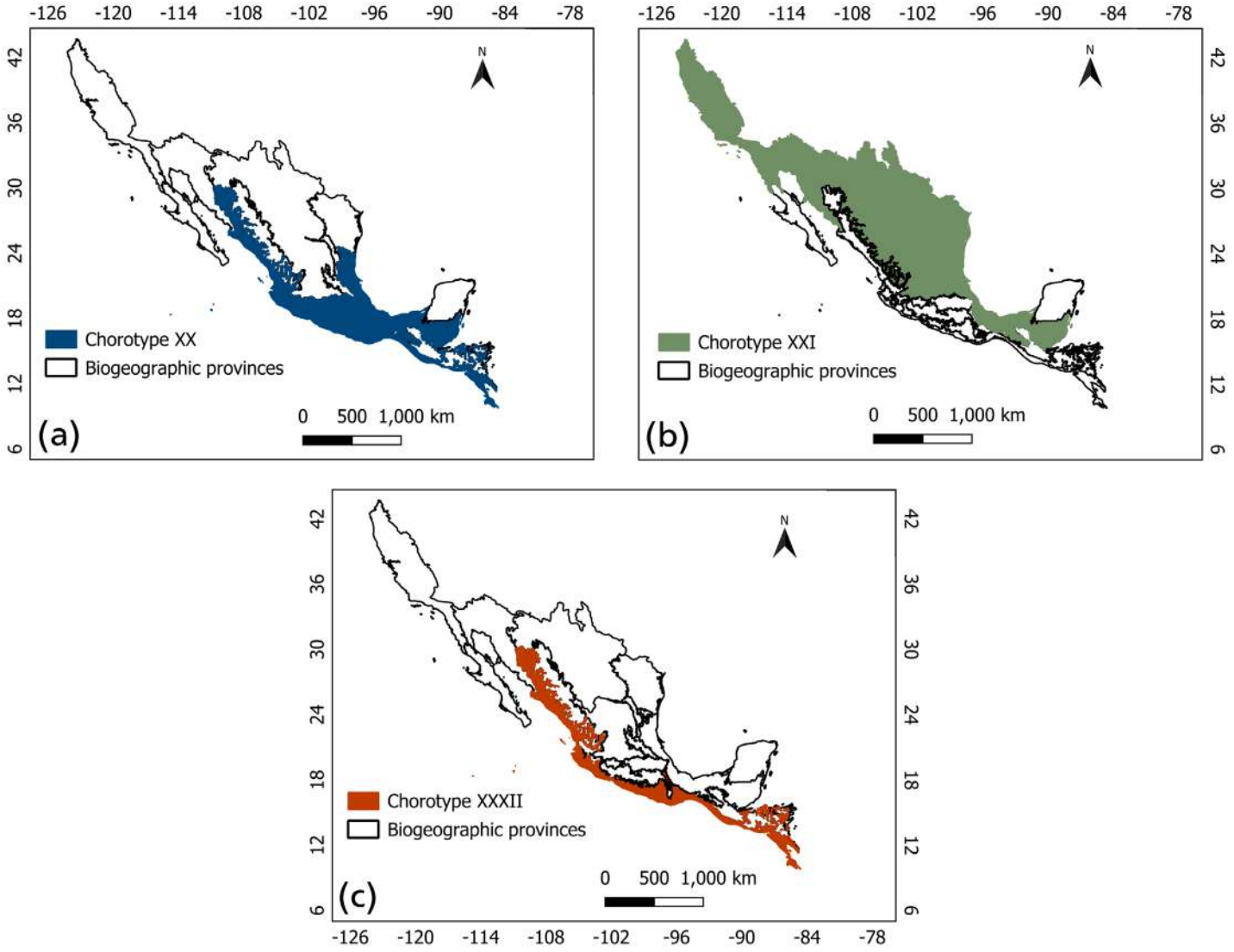

Figure 3. General chorotypes shared by two matrices. (a) General chorotype XX, identified by both MOL databases, (b) Chorotype XXI, shared by two matrices from the IUCN database, and (c) Chorotype XXXII, shared by two IUCN databases.

Chorotype IV, that includes all the Mexican biogeographic provinces, may result from the mixture of the Nearctic and Neotropical biotas in the Mexican Transition Zone. The biota of the Mexican Transition Zone was assembled through the successive dispersal of four cenocrons from North and South America that assembled to the original Paleoamerican biota (Morrone 2020): (1) the Mexican Plateau cenocron dispersed to southern North America from South America (Gondwana) in the Late Cretaceous-Paleocene; (2) the Mountain Mesoamerican cenocron dispersed from South America to the mountain forests of Central America and southern Mexico in the Oligocene-Miocene and then northward in the Pliocene; (3) the Nearctic cenocron dispersed from northern North America to the Mexican Transition Zone in the Miocene-Pliocene; and (4) finally, in the Pleistocene the Typical Neotropical cenocron dispersed from the Neotropical region. Some of the species defining chorotype IV are widely distributed in the country (distributed in at least two biogeographic provinces). For instance, *Lynx rufus, Myotis volans* and *Odocoileus hemionus* are distributed mainly in lowlands and highlands in the Nearctic region. These species, despite belonging to different orders, have high dispersal abilities and may constitute a "subchorotype" within a bigger one, as was defined by Flores *et al.* (2004). Other species can reach more southern areas, like *Eptesicus fuscus, Procyon lotor* and *Puma concolor*, the latter even exceeding the Neotropical region to the Andean region in South America. Their dispersal abilities have allowed them to colonize successfully lowlands and highlands, producing a mixture that could be useful in ecological regionalization, but would be useless for an evolutionary biogeographic regionalization.

Chorotype I (Figure 2a) confirmed the identity of the Baja California province biota, conformed by at least 10 species whose geographic distributions are not randomly shared: *Chaetodipus ammophilus, C. siccus, Neotoma insularis, Peromyscus caniceps, P. dickeyi, P. eva, P. guardia, P. sejugis, P. slevini* and *P. stephani*. Although it was not recovered in the MOL - N & S Chihuahuan database, in the C11 of this database,

all of them are present together with *Myotis vivesi*, which is also distributed in the Sonoran province (Otárola-Ardila *et al.* 2013). The biota of the Baja California province is a result mainly of the geographical isolation of the peninsula, which had happened over the last 4 or 5 million years, as result of a complex tectonic origin and ecological transformation (Grismer 2000).

Chorotype V is based on 36 species distributed in nine provinces, most of them belonging to the order Rodentia. Moreover, three species were not shared by the two datasets, only diagnosed for the IUCN - Chihuahuan matrix: *Euderma maculatum*, *Perognathus amplus* and *Peromyscus boylii*. From them, in fact, *P. amplus* is distributed only in the Sonoran province, while the other two species diagnosed the whole Chihuahuan province. Other species, like *Neotoma albigula,* even avoid the Chihuahuan province, probably also representing subchorotypes, or *Callospermophilus madrensis*, which is exclusive to the Sierra Madre Occidental. Other species, like *Cynomys ludovicianus,* are only marginally distributed in this chorotype, which is an effect of the possible overestimation of the polygons. Other problems were shown for species with some uncertainty in their distributions and taxonomy, like *Neotamias durangae*. This species has only one continuous population in the MOL database, but two allopatric populations in the IUCN database. Therefore, this chorotype was not identified by the MOL analyses, even partitioning the Chihuahuan province. It is interesting that *N. durangae* is present in C5 of the MOL - Chihuahuan and C12 of the MOL - N & S Chihuahuan matrices (corresponding to general chorotypes XXIX and XXIII in Table 2). These chorotypes represent variations with 34 and 35 species, respectively, and variations between the provinces involved.

Similarly in general chorotype XIII, which has 73 species, some are typically found in colder highlands (*v. gr.,* species of *Cryptotis*, *Habromys* or *Sorex*), whereas other species are typically from hotter lowlands (*v. gr.,* species of *Alouatta*, *Heteromys* or *Phyllostomus*). This chorotype also includes species with very restricted habitats and geographic distributions, but also species widely distributed.

General chorotype XIV is a subset of chorotype XVI. It is defined by 12 species, most of them belonging to the order Rodentia. In general, these species have distributional areas very restricted to mountainous chains (*v. gr.*, *Cratogeomys fulvescens*, *C. perotensis* and *Habromys delicatulus*). Some of them have been diagnosed as endemic taxa of one biogeographic province (*v. gr.*, *Romerolagus diazi* and *Sorex oreopolus* endemic to the Transmexican Volcanic Belt); however, the chorotype analysis was not able to identify these subtle differences. For the largest general chorotype XVI, there were also 12 species, but with a different composition, with the genus *Peromyscus* being the most representative. Some species are distributed in two or more mountainous provinces, but also the polygons could be overestimating the distributions to lowlands (*v. gr.*, *Peromyscus furvus* and *Sciurus oculatus*), like the Veracruzan province. Again, the chorotypes could identify patterns useful for ecological regionalization, diagnosing roughly species more restricted to lowland and highland environments.

General chorotype XX grouped 24 species distributed in central Mexico. Some of them are typical of lowlands (*Musonycteris harrisoni*, *Notocitellus annulatus* and *Tlacuatzin balsasensis*), and others typical of highlands (*Cryptotis magnus*, *Peromyscus melanurus* and *Sorex ixtlanensis*). In this chorotype, we may diagnose some subchorotypes, separating both sets of species; however, at this time, identification of this pattern is not clear.

Chorotype XXI was identified by 21 species, some of them distributed in north-central provinces (*v. gr., Ammospermophilus interpres*, *Cratogeomys castanops* and *Myotis planiceps*) and others from northeastern provinces (*Nycticeius humeralis*, *Onychomys leucogaster* and *Sciurus alleni*). In general, these species are distributed in lowlands of the Nearctic provinces, although marginally extend to both mountain chains at eastern and western sides. In this chorotype there are species with Nearctic and Neotropical affinities that belong to the Mexican Plateau cenocron.

The last general chorotype, XXXII, encompasses seven species, three of them of the order Lagomorpha: *Lepus flavigularis*, *Sylvilagus graysoni* and *S. insonus*. In particular, *S. graysoni* is an insular species, belonging to the Pacific Lowlands province; moreover, its distribution is allopatric from lowland continental ones like *L. flavigularis*. Other species in this chorotype, like *Rheomys mexicanus* and *Peromyscus madrensis,* are distributed in the highlands of the Sierra Madre del Sur province.

Olivero *et al.* (2011) have suggested that chorotypes may result from environmental conditions shared by several species or from historical events biasing certain taxa to different areas. Thus, chorotypes may enhance the search for global processes influencing distribution of biodiversity. For the Mexican mammals, chorotypes were uninformative for evolutionary patterns mainly based on vicariance, which are used for evolutionary biogeographic regionalizations. In contrast, patterns influenced by dispersal or ecological processes are diagnosed herein, which could be useful for ecological regionalizations.

The biogeographical regionalization of Mexico currently recognizes the Nearctic and Neotropical regions, and the Mexican Transition Zone as an area of biotic assembly (*e.g.*, Morrone *et al.* 2017; 2022a; Morrone 2019). This mixture could be recognized, but more than the recovery of those patterns, chorotypes may identify mixed patterns based on environments associated with altitude. None of the identified mammal chorotypes corresponds to Morrone *et al.* (2022b) division of the Trans-Pecos and Mapimian districts within the Chihuahuan province; however, we found that this division affected the results, although not decisively. Also, only one biogeographic province was recognized (Baja Californian province), which allows in this particular case to integrate ecological and evolutionary

processes in a natural regionalization. The incorporation of other taxa with different evolutionary and ecological histories as well as the temporal component, will allow to improve the understanding of the processes that produce the complex evolutionary and ecological biogeographic patterns of the country.

Conclusions

We demonstrate the possible effects of the use of different sources of geographic distributional data and operational units, where even small variations may modify the number of chorotypes obtained, and the species and units involved. In total, we identified 33 chorotypes, but subchorotypes also should be analyzed, to diagnose possible lowland and highland patterns within them. Finally, chorotypes seem to recognize more closely ecological patterns rather than evolutionary ones, even mixing species with different affinities in the same pattern, showing that the Mexican mammal fauna is a result of a complex history.

Acknowledgments

We thank Erick García-Trujano and collaborators for providing the current list of Mexican mammals and Claudia Reaño-Jiménez for the shapefile of the Chihuahuan province. We thank Pablo Colunga Salas and Giovani Hernández Canchola for inviting us to contribute to this special issue of *Therya* honoring Livia León Paniagua. We would like to highlight Livia's many contributions to the systematics and biogeography of the Mexican mammals and her friendship.

Declaration of Artificial Intelligence use

No artificial intelligence tools were used in the preparation of this manuscript.

Author contributions

Conceptualization & Methodology: Tania Escalante, Juan J. Morrone. Investigation & Data Curation: Oscar Campos. Formal Analysis & Validation: Tania Escalante, Oscar Campos. Writing & Reviewing: Tania Escalante, Juan J. Morrone.

Supplementary data

S1. Similarities and differences between the 33 chorotypes obtained from each database, regarding the biogeographic provinces involved in each one.

S2. Maps of the 33 chorotypes resulting from the four datasets and the Mexican biogeographic provinces.

Literature cited

Arita HT, and León-Paniagua L. 1993. Diversidad de mamíferos terrestres. *Ciencias* 7:13–22.

Baroni-Urbani C, and Buser NW. 1976. Similarity of binary data. *Systematic Zoology* 25:251–259. https://doi.org/10.2307/2412493

Baroni-Urbani C, Ruffo S, and Vigna Taglianti A. 1978. Materiali per una biogeografia italiana fondata su alcuni generi di coleotteri Cicindelidi, Carabidi e Crisomelidi. *Memorie della Società Entomologica Italiana* 56:35–92.

Crisci JV, Sala OE, Katinas L, and Posadas P. 2006. Bridging historical and ecological approaches in biogeography. *Australian Systematic Botany* 19:1–10. https://doi.org/10.1071/SB05006

Escalante, T, Elguea-Manrique LM and Espiritu-Guerrero PC. 2024. Chorotypes and geographical relationships among endemic species of the Transmexican Volcanic Belt, Mexico. *Revista Mexicana de Biodiversidad* 95:e955329. https://doi.org/10.22201/ib.20078706e.2024.95.5319

Escalante T, Espinosa D, and Morrone JJ. 2003. Using parsimony analysis of endemicity to analyze the distribution of Mexican land mammals. *Southwestern Naturalist* 48:563–578. https://doi.org/10.1894/0038-4909(2003)048<0563:UPAOET>2.0.CO;2

Escalante T, Morrone JJ, Noguera-Urbano EA, Rodríguez-Tapia G and Sandoval-Salinas ML. 2025. Biogeographic regions, provinces and ecoregions: Integrating mammalian patterns from the Chihuahuan Desert to the Magellanic Moorland. In: Melleti M, Gallina-Tessaro SA, Ortega, J and Tirira D, editors. *Mammals of Middle and South America: History, Biogeography, Conservation. Handbook of the Mammals of Middle and South America*. Cham (CHE): Springer, Nature; p. 1-16. https://doi.org/10.1007/978-3-031-43163-0_26-1

Escalante T, Morrone JJ, and Rodríguez G. 2007a. La distribución de los mamíferos terrestres y la regionalización biogeográfica natural de México. In: Sánchez-Rojas G, and Rojas-Martínez AE, editors. *Tópicos en Sistemática, Biogeografía, Ecología y Conservación de Mamíferos*. Pachuca (MEX): Universidad Autónoma del Estado de Hidalgo; p. 9–17.

Escalante T, Morrone JJ, and Rodríguez-Tapia G. 2013. Biogeographic regions of North American mammals based on endemism. *Biological Journal of the Linnean Society* 10:485–499. https://doi.org/10.1111/bij.12142

Escalante T, Sánchez-Cordero V, Morrone JJ, and Linaje M. 2007b. Areas of endemism of Mexican terrestrial mammals: A case study using species' ecological niche modeling, Parsimony Analysis of Endemicity and Goloboff fit. *Interciencia* 32:151–159.

Escalante T, Szumik C, and Morrone JJ. 2009. Areas of endemism of Mexican mammals: Re-analysis applying the optimality criterion. *Biological Journal of the Linnean Society* 98:468–478. https://doi.org/10.1111/j.1095-8312.2009.01293.x

Fattorini S. 2015. On the concept of chorotype. *Journal of Biogeography* 42: 2246–2251. https://doi.org/10.1111/jbi.12589

Fattorini S. 2016. A history of chorological categories. *History and Philosophy of the Life Sciences* 38:1-13. https://doi.org/10.1007/s40656-016-0114-1

Ferro I. 2024. Detección de zonas de transición mediante deconstrucción biótica con base en afinidades corológicas. In: Escalante T, Morrone JJ, and García Trejo

EA, editors. *Biogeografía práctica*. Mexico City (MEX): Las Prensas de Ciencias, Universidad Nacional Autónoma de México; p. 61–62.

Ferro I., Navarro-Sigüenza AG, and Morrone JJ. 2017. Biogeographical transitions in the Sierra Madre Oriental, Mexico, shown by chorological and evolutionary biogeographical affinities of passerine birds (Aves: Passeriformes). *Journal of Biogeography* 44:2145–2160. https://doi.org/10.1111/jbi.13015

Flores T, Puerto MA, and Barbosa AM. 2004. Agrupación en corotipos de los anfibios de la provincia de Ciudad Real (España). *Revista Española de Herpetología* 18:41–53.

GBIF.org. 2026. GBIF. [Accessed January 12th, 2026]. https://www.gbif.org

Grismer LL. 2000. Evolutionary biogeography on Mexico's Baja California peninsula: A synthesis of molecules and historical geology. *Proceedings of the National Academy of Science of the United States of America* 97:14017–14018, https://doi.org/10.1073/pnas.260509697

iNaturalist. 2026. [Accessed January 12, 2026]. https://www.inaturalist.org

International Union for Conservation of Nature (IUCN). 2025. The IUCN Red List of Threatened Species. 6.3 version. [Accessed November 20th, 2025]. https://www.iucnredlist.org.

Mammal Diversity Database. 2026. Mammal Diversity Database (Version 2.4) [Data set]. Zenodo. https://doi.org/10.5281/zenodo.17033774

Map of Life. 2025. Mammal range maps harmonised to the Mammals Diversity Database [Class Mammalia]. [Accessed February 1st, 2015]. https://doi.org/10.48600/MOL-48VZ-P413.

Morrone JJ. 2009. *Evolutionary biogeography: An integrative approach with case studies*. New York (EEUU): Columbia University Press.

Morrone JJ. 2014. On biotas and their names. *Systematics and Biodiversity* 12:386–392. https://doi.org/10.1080/14772000.2014.942717

Morrone JJ. 2019. Regionalización biogeográfica y evolución biótica de México: Encrucijada de la biodiversidad del Nuevo Mundo. *Revista Mexicana de Biodiversidad* 90:1–68. https://doi.org/10.22201/ib.20078706e.2019.90.2980

Morrone JJ. 2020. *The Mexican Transition Zone: A natural biogeographic laboratory to study biotic assembly*. Cham: Springer. https://doi.org/10.1007/978-3-030-47917-6

Morrone JJ, Escalante T, and Rodríguez-Tapia G. 2017. Mexican biogeographic provinces: Map and shapefiles. *Zootaxa* 4277:277–279. https://doi.org/10.11646/zootaxa.4277.2.8

Morrone JJ, Escalante T, Rodríguez-Tapia G, Carmona A, Arana M, and Mercado-Gómez JD. 2022a. Biogeographic regionalization of the Neotropical region: New map and shapefile. *Anais da Academia Brasileira de Ciências* 94:e20211167. https://doi.org/10.1590/0001-3765202220211167

Morrone JJ, Acosta R, and Fernández JA. 2022b. Biogeographic units in the Chihuahuan Desert: Implications for regionalization and area nomenclature. *Revista Mexicana de Biodiversidad* 93:1–24. https://doi.org/10.22201/ib.20078706e.2022.93.3907

Olivero J, Real R, and Márquez AL. 2011. Fuzzy chorotypes as a conceptual tool to improve insight into biogeographic patterns. *Systematic Biology* 60:645–660. https://doi.org/10.1093/sysbio/syr026

Otárola, Ardila A, Herrera-Montalvo G, and Flores Martínez JJ. 2013. Marine and terrestrial food sources in the diet of the fish-eating myotis (*Myotis vivesi*). *Journal of Mammalogy* 94:1102–1110. https://doi.org/10.1644/12-MAMM-A-281.1

Passalacqua NG. 2015. On the definition of element, chorotype and component in biogeography. *Journal of Biogeography* 42:611–618. https://doi.org/10.1111/jbi.12473

Posit team. 2025. *RStudio: Integrated Development Environment for R*. Boston (EEUU): Posit Software, PBC. http://www.posit.co/

QGIS Development Team. 2023. *QGIS Geographic Information System*. Beaverton (EEUU): Open Source Geospatial Foundation Project. https://qgis.org/

R Core Team. 2023. *R: A Language and Environment for Statistical Computing*. R Foundation for Statistical Computing, Vienna. https://www.R-project.org/

Ramírez-Pulido J, and Castro-Campillo A. 1990. Provincias mastofaunísticas Escala 1: 4 000 000 Mapa IV.8.8A. Atlas Nacional de México. Vol. 2. Mexico City (MEX): Instituto de Geografía, Universidad Nacional Autónoma de México.

Real R, Guerrero JC, and Vargas JM. 1992. Análisis biogeográfico de clasificación de áreas y especies. *Monografías Herpetológicas, Asociación Herpetológica Española* 2:73–84.

Reséndiz-López MA. 2025. Listado taxonómico de mamíferos con distribución en México. Version 1.3. No organization. Checklist dataset. [Accessed March 14th, 2025]. https://www.snib.mx/iptconabio/resource?r=mamiferos

Rodríguez P, and Arita TH. 2004. Beta diversity and latitude in North American mammals: Testing the hypothesis of covariation. *Ecography* 27:547–556. https://doi.org/10.1111/j.0906-7590.2004.03788.x

Troudet J, Grandcolas P, Blin A, Vignes-Lebbe R, and Legendre F. 2017. Taxonomic bias in biodiversity data and societal preferences. *Scientific Reports* 7:9132. https://doi.org/10.1038/s41598-017-09084-6

Wilson DE, and Reeder DAM. 2005. *Mammal Species of the World. A Taxonomic and Geographic Reference (3rd ed)*. Baltimore (EEUU): Johns Hopkins University Press.

Zhang B, Zhou M, Xie Z, Zhang L, Duan H, Yu J, *et al*. 2025. Updated chorotypes of terrestrial vertebrates shed new light on zoogeographical regions in China. *Integrative Zoology* 2025:1–12. https://doi.org/10.1111/1749-4877.70025

Associated editors: Giovani Hernández Canchola and Pablo Colunga Salas
Submitted: January 20, 2026; Reviewed: March 21, 2026
Accepted: April 23, 2026; Published online: May 29, 2026

THERYA, 2026, Vol. 17(2):259-276 DOI: 10.12933/therya.2026.6252 ISSN 2007-3364

Analyzing the adaptive potential of the long-nosed bat, *Leptonycteris nivalis*, in the face of climate change

Roberto-Emiliano Trejo-Salazar[1,2], Jaime Gasca-Pineda[*1,3], Rosalinda Tapia López[3], and Luis E. Eguiarte[3]

[1]Secretaría de Ciencias, Humanidades, Tecnología e Innovación (SECIHITI), Estancias Posdoctorales por México. E-mail: remilianotrejo@ciencias.unam.mx (RET-S)
[2]Departamento de Biología Evolutiva, Facultad de Ciencias, Universidad Nacional Autónoma de México (UNAM).
[3]Departamento de Ecología Evolutiva, Instituto de Ecología, Universidad Nacional Autónoma de México. Ciudad Universitaria, Ciudad de México, México. E-mail: rtapia@ecologia.unam.mx (RTL); fruns@unam.mx (LEE)
[*]Corresponding author: jaimegasca@yahoo.com

Tequila or magueyero bats (*i.e.,* the genus *Leptonycteris*) play a very important role as pollinators in most Mexican and southern US ecosystems, which is why they have recently been given greater attention. Female members of *Leptonycteris nivalis* populations exhibit migratory behavior associated with nectar consumption and pollination of ecologically important *Agave* species in Mexico, and with their reproductive events. Such migratory behavior makes them susceptible to the consequences of climate change. In this study, we explored how the distribution and the adaptive potential of *L. nivalis* may be affected by possible global warming scenarios. We obtained samples from six locations across the distribution of *L. nivalis.* Using parallel massive-sequencing techniques, we obtained 13,112 filtered SNPs (single-nucleotide polymorphisms). Just two of these SNPs were associated with a climatic variable, but we detected associations between heterozygosity and climate change in two sites. Models of future distribution under climate change indicated a reduction in climatic stable areas favorable to this bat's presence. Our results will support the implementation of protection strategies for bats and the ecosystems they inhabit, which are the most representative in Mexico. Also, it is very important to maintain connectivity between the localities and refuges occupied by the magueyero bat, as well as to maintain populations within areas of greatest thermodynamic stability, where the most favorable conditions for bat presence are predicted. Based on our analysis, we believe the species has the potential to withstand changes in temperature and precipitation patterns, which may support its conservation.

Keywords: Chihuahuan Desert, climate change, conservation genomics, Mexico, nectar-feeding bats, potential adaptive, potential distribution, population genomics, SNP

Los murciélagos del género *Leptonycteris*, a veces llamados tequileros o magueyeros, desempeñan un papel muy importante como polinizadores en la mayoría de los ecosistemas mexicanos y del sur de Estados Unidos, por lo que recientemente se les ha prestado mayor atención. La especie de murciélago *Leptonycteris nivalis* muestra un comportamiento migratorio en parte de sus hembras, que está asociado al consumo del néctar de especies ecológicamente importantes en México en particular del género *Agave,* y a los eventos reproductivos del murciélago. Estas características los hacen susceptibles a las consecuencias del cambio climático. En este estudio, exploramos cómo la distribución y el potencial adaptativo de *Leptonycteris nivalis* podrían verse afectados por posibles escenarios de calentamiento global. Para ello, obtuvimos muestras en seis localidades en la distribución de *L. nivalis*. Mediante técnicas de secuenciación masiva, obtuvimos 13,112 SNP (polimorfismos de un solo nucleótido) filtrados. En total sólo dos se asociaron con una variable climáticas, pero encontramos una relación estadística entre dos sitios y la susceptibilidad de la heterocigosis a cambios climáticos. Los modelos de distribución futura mostraron una reducción de las áreas climaticamente estables donde este murciélago podría sobrevivir. Pensamos que nuestros resultados respaldarán la implementación de estrategias de protección para los murciélagos y los ecosistemas que habitan. Es muy importante mantener la conectividad entre las localidades y los refugios ocupados por el murciélago magueyero. Es importante mantener espacios dentro del área de mayor estabilidad termodinámica, donde se prevén las condiciones más favorables para la presencia de murciélagos. Basándonos en nuestros análisis, creemos que la especie tiene el potencial de soportar cambios en los patrones de temperatura y precipitación, y estas circunstancias pueden favorecer la conservación de la especie.

Palabras clave: cambio climático, Desierto Chihuahuense, distribución potencial genómica de la conservación, genómica de poblaciones, murciélagos nectarívoros, potencial adaptativo, SNP

Every species across all biomes is affected by global climate change, potentially harming the persistence and functioning of each ecosystem (Meek *et al.* 2023). Changes in temperature driven by global warming and the greenhouse effect directly affect organisms by challenging their physiological limits or altering their phenology or reproductivity cycles (Hayes *et al.* 2009). The consequences may include an expansion of the distribution range of pathogens, increased disease severity, and the introduction of invasive species into new ecosystems (Elad and Pertot 2014; Gona and More 2022; Mora *et al.* 2022).

The accelerated pace of climate change may prevent many populations from responding adequately, thus increasing the rate of decline and extinction (McLaughlin *et al.* 2002; Cahill *et al.* 2013; Bestion *et al.* 2015). Even if populations persist in their habitats and respond to these rapid changes, they still need to maintain levels of genetic diversity that allow the expression of alleles associated with adaptive characteristics (Waldvogel *et al.* 2020). The ability to respond to new environmental conditions is referred to as 'evolvability' or 'adaptive potential' (Houle 1992). In the context of climate change or global warming, there is a risk

of reduced evolvability, as extinction could be accelerated by an inability to respond to selection pressures (Blows and Hoffmann 2005; Davis *et al.* 2005).

Species can avoid extinction by shifting their geographic distribution or moving to more favorable habitats, acclimating to stressful conditions through phenotypic plasticity (the ability of a genotype to express different phenotypes in different environments), or by adapting through genetic changes (Thomas 2010). However, understanding how and under what circumstances eco-evolutionary responses will occur, and differentiating among these responses to identify the adaptive potential in species with low adaptive capacity, is challenging (Urban *et al.* 2024).

One factor that promotes local adaptation is maintaining a species' genetic diversity. Generally, greater genetic diversity reflects a greater adaptive potential of species to respond to extreme situations. This is why it is important to maintain genetic variants that can cope with different or changing ecological conditions (Whitlock 2015). Then, a relationship may also be established between climate change and genetic diversity and adaptive potential of natural populations (Pauls *et al.* 2013; Wanjala *et al.* 2023).

Nowadays, vulnerability to climate change is commonly assessed using forecasts generated by suitability models that project probable future scenarios (Levinsky *et al.* 2007; Rebelo *et al.* 2010; Deb *et al.* 2020; McGowan *et al.* 2021; Moura *et al.* 2023). Among the various genetic and epigenetic tools that enable the study of local adaptations, we used mass sequencing for SNP genotyping that allowed us to explore for potential local adaptations in the genome's coding regions that could produce advantageous forms in response to changing environmental conditions, such as climate change, the greenhouse effect and global warming (Franks and Hoffmann 2012; Aguirre-Liguori *et al.* 2021; Hoffmann *et al.* 2021; Lancaster *et al.* 2022). This approach has recently become more common due to its importance in conservation biology, as it enables us to anticipate possible scenarios in the context of current climate change (Hayes *et al.* 2009; Kumar *et al.* 2016; Jordan *et al.* 2017; Luo *et al.* 2024; Klichowska *et al.* 2025).

Local adaptations are generally the result of divergent selection on one or more traits. These adaptations play a crucial role in determining populations' ability to respond to environmental changes (Henriques *et al.* 2018; Cummins *et al.* 2019; Meek *et al.* 2023). However, this approach has not yet been applied to bats. Detecting candidate alleles under selection enables the use of statistical methods to associate their presence and frequency in natural populations with specific environmental variables (Beji *et al.* 2020; Guillaume *et al.* 2024), thus providing insights about the populations' capabilities to face abrupt changes in environmental conditions (Hansen *et al.* 2012; Marková *et al.* 2023).

In this sense, maintaining the genetic diversity of populations is important because it provides the basis for adaptive responses to surrounding environments (Whitlock 2014; Kardos *et al.* 2021). Understanding the mechanisms behind the formation and maintenance of diversity and adaptive potential is essential for improving conservation and species management plans and programs.

Climate-related local extinctions have been recorded in hundreds of species (Wiens 2016). Wild mammals exhibit different degrees of vulnerability to climate change, some species have very specialized characteristics, which may cause them to disappear due to temperature changes that affect physiological processes, habitat loss, or resource loss (Boutin and Lane 2014; Hetem *et al.* 2014; McCain and King 2014; Chattopadhyay *et al.* 2019; Wells *et al.* 2022; de Castro *et al.* 2024).

The Chiroptera order is especially susceptible to ecological disturbances because most species have adapted to specific habitats and feeding habits, and most of them are susceptible to population decrease with an associated risk of extinction (Sherwin *et al.* 2012; Chattopadhyay *et al.* 2019; Gonçalves *et al.* 2021; McGowan *et al.* 2021; Festa *et al.* 2023). In Mexico, there are about 138 registered bat species, but only 21 are nectar-feeding (Medellín *et al.* 2008). Nectarivorous bats are responsible for pollinating many plant species that are considered ecologically important in the country's most representative ecosystems, like the scrubland and low deciduous forest (Koleff *et al.* 2018). For instance, *Leptonycteris nivalis*, the long-nosed bat, murciélago magueyero mayor, or tequila bat, is one of the main pollinators of *Agave* plants (Hensley and Wilkins 1988). This chiropteran is distributed across central and northern Mexico, and in southern New Mexico, United States (Hensley and Wilkins 1988). It is the largest nectar-feeding bat in North America, and it is grouped into populations ranging from a few dozen to over 10,000 individuals (Hensley and Wilkins 1988). Besides many species of *Agave, Leptonycteris nivalis* pollinates several plant species of the Leguminosae and Cactaceae families, plants whose presence is found throughout Mexico and the southern United States in practically all ecosystems (Sánchez and Medellín 2007). In addition to its specialized nectar-consumption behavior, *L. nivalis* has another distinguishing characteristic: some of its females perform migratory movements from Central Mexico maternity shelters in the northern part of their distribution range, in Nuevo León, Mexico, and Texas, USA (Moreno-Valdez *et al.* 2000). The migration is directly related to their reproductive behavior during the spring and summer, coupling with the blooming season of various *Agave* species. This guarantees the availability of resources to feed during gestation and offspring rearing at the northern part of their distribution range (Bogan *et al.* 2017; Burke *et al.* 2019). However, these characteristics underscore the long-nosed bat's vulnerability to extreme temperature variations and habitat changes and degradation (Sánchez and Medellín 2007).

In Mexico, *L. nivalis* is classified as endangered in the official list of species, known as NOM-059-SEMARNAT-2010, which includes species under some form of wildlife protection, based on the Ley General de Vida Silvestre,

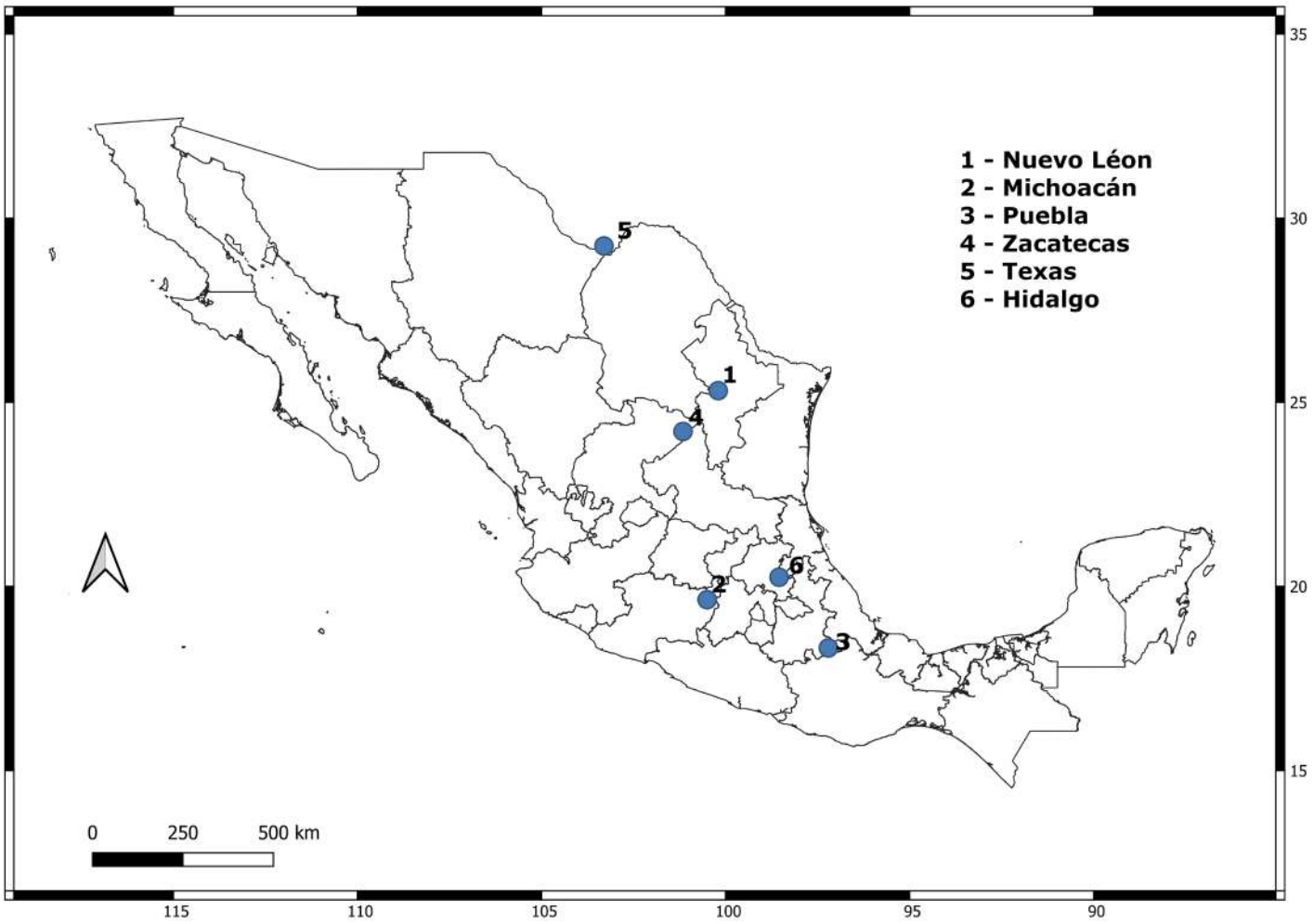

Figure 1. Map of sampled locations; the number associated with each blue dot corresponds to the location number in Table 1.

Conservación y Aprovechamiento Sustentable (D.O.F. 2014). It has also been listed as endangered under the U.S. Endangered Species Act since 1988, and the International Union for Conservation of Nature (IUCN; Medellín 2016).

Leptonycteris nivalis evolutionary genetics and migration were recently studied using mitochondrial genetic markers (Trejo-Salazar *et al.* 2025). It was estimated that the species has undergone recent population growth, associated with an increase in global temperature following a decrease during the Pleistocene (Trejo-Salazar *et al.* 2023; Trejo-Salazar *et al.* 2025). This increase was supported using distribution models from the Last Interglacial, Last Maximum Glacial, Holocene, and Current epochs, in which the distribution extends to the north (Trejo-Salazar *et al.* 2025). Here, we describe a new set of 13,112 filtered SNPs (single-nucleotide polymorphisms) obtained using massive sequencing techniques from six locations throughout the distribution of *L. nivalis*. In addition, we generated models for the future potential distribution of *L. nivalis* under global warming. Thus, our main objective was to associate the genetic diversity of *L. nivalis* with changes in climatic conditions to support future management of conservation programs and maintain pollination services in Mexico's most representative ecosystems. We expect that our results will enable the potential impacts of climate change on the tequila bat species, *L. nivalis*.

Materials and methods

Sampling. Forty-seven samples were taken from six localities in roosting caves and mist nests on field feeding-sites along *L. nivalis* distribution from 2014 to 2016 (Figure 1, Table 1), with sampling permit Secretaría del Medio Ambiente y Recursos Naturales (SEMARNAT) SGPA/DGVS/07161/15 (Supplemental File SD1), following the Animal Care and Use protocols of the American Society of Mammalogists (Sikes

Table 1. Sample sizes by location are shown, along with genetic diversity, observed heterozygosity (*Ho*), and expected heterozygosity (*He*) and Inbreeding coeficient *Fis*.

	Locality	n	Ho	He	F_{IS}
1	Nuevo León (nl)	14	0.1913	0.2123	0.0757
2	Michoacán (mich)	7	0.1867	0.2113	0.0793
3	Puebla (pue)	1	-	-	-
4	Zacatecas (zac)	1	-	-	-
5	Texas (tex)	19	0.2041	0.2157	0.0457
6	Hidalgo (hid)	5	0.1900	0.2122	0.0502
	Overall	47	0.1866	0.2112	0.1097

et al. 2016). Tissue samples were taken with a 3 mm^2 biopsy wing punch in an area of the wing with no blood capillaries or nerve terminals. Wing biopsies were fixed in 90% ethanol at environmental temperature and then stored at -20°C until DNA extraction.

DNA Extraction and Genotyping. Total genomic DNA was extracted following Gasca-Pineda *et al.* (2015). Genomic DNA was genotyped by nextRAD sequencing libraries (SNPsaurus LLC, Eugene, OR, USA) as described by Russello *et al.* (2015). DNA was fragmented using Nextera reagent (Illumina, San Diego, CA, USA), which also ligates short adapter sequences to the ends of the fragments. The DNA was amplified for 27 cycles at 74°C, and libraries were sequenced on an Illumina HiSeq 4000 150 bp single-end line (University of Oregon, Eugene, OR, USA).

Raw data processing. Raw reads were trimmed by quality with trimmomatic v0.35 (Bolger *et al.* 2014), using the following parameters: LEADING:5 TRAILING:5 SLIDINGWINDOW:4:20 MINLEN:75. To remove Nextera Adapters, we used the bbduk module of the BBTools v37.87 software (https://sourceforge.net/projects/bbmap/files/). Filtered reads quality was evaluated using FASTQC v0.11.5 (Andrews 2010). Single Nucleotide Polymorphisms (SNPs) were obtained in ipyrad v0.979 (Eaton and Overcast 2020) using as a reference the previously published genome of *Leptonycteris yerbabuenae* (Gutierrez-Guerrero *et al.* 2020). We applied the following parameters: a minimum depth of six for statistical base calling, two maximum alleles per site in consensus sequences, 0.05 maximum uncalled bases in consensus, 0.05 maximum heterozygotes in consensus, four as the minimum number of samples per locus, 0.2 as the maximum SNPs per locus, and 0.5 as the maximum shared heterozygous sites per locus. After testing multiple filtering schemes, we implemented the following filtering parameters using VCFtools v 0.1.16 software (Danecek *et al.* 2011): a maximum missing data per locus of 20%, a Hardy-Weinberg test with $p \leq 0.01$, and a maximum alleles per locus of two. Because outlier methods may be sensitive to linkage disequilibrium and rare variants (Frichot and François 2015; Luu *et al.* 2017), we implemented a more stringent filtering scheme, including a MAC filter of 3 to recover SNPs present in at least 2 individuals and a thinning of 450 pb. This filtering recovered 13,112 SNPs.

Genetic Diversity and Population Genetic Structure. We estimated the basic summary statistics, *He*, *Ho,* and *FIS*, using the adegenet 2.1.11 (Jombart 2008; Jombart and Ahmed 2011) and hierfstat 0.5-11 (Goudet and Jombart 2022) R 4.5.1 packages (R Core Team 2025). To detect possible genetic structuring, we implemented Admixture v1.3.0 (Alexander *et al.* 2009) to assess the number of genetic groups (*K*) in the collected samples. We tested for 1-20 *K* groups, and the optimal *K* value was determined by the lowest 50-fold CV error (Alexander and Lange 2011). As the genetic structure of this species is unknown, we opted to use a superior *K* value that accounts for the possible genetic groups represented in the sample. We also performed a principal component analysis (PCA) using the R package adegenet to summarize genetic similarities among individuals.

To detect genetic structuring between sampling locations, we performed a paired *FST* analysis. The test was performed using a 10,000 bootstrap test; if 95% of the intervals did not reach zero, we considered the value significant. As there was only one individual in the Puebla and Zacatecas populations, these sites were removed from the analyses to obtain summary statistics and pairwise FST. In turn, we used Nei's distances to represent the genetic differences between sampling locations using the Ward clustering method. An isolation-by-distance (IBD) analysis was performed to assess whether geographic distance between sampling locations influences genetic differentiation in *Leptonycteris nivalis*. This analysis was based on the correlation between genetic and geographic distances between pairs of sites, using only the set of previously identified neutral markers (SNPs) to avoid bias from potential natural selection. Nei's distance, calculated from the allele frequencies at each location, was used as a measure of genetic distance. To strengthen the analysis at the individual level, we also used Euclidean distances between individuals derived from the first two principal components (PCs) of a principal component analysis (PCA). Geographic distance was calculated as the straight-line Euclidean distance (in kilometers) between the sampling sites' geographic coordinates. The correlation between the genetic and geographic distance matrices was evaluated using a Mantel test with 10,000 permutations to determine the p-value. A p-value of less than 0.05 was considered to be evidence of a correlation, indicating that genetic differentiation increases with geographic distance (see below).

Additionally, we used the kinship analysis in VCFtools to evaluate kinship relationships within the study sample. Specifically, the '--relatedness2' command was used to calculate a matrix of kinship estimates for all pairs of individuals from the genotype data contained in the source VCF file. This estimator is based on the correlation of allele states across multiple genetic markers between individuals, providing a robust measure that is relatively insensitive to population structure. VCFtools generates a tabulated file (.relatedness2) as output for this analysis, containing the estimated kinship values (commonly denoted as RELATEDNESS_PHI) for each pair of individuals. These values quantify the proportion of genetic material two individuals are expected to share by descent. This allows family relationships to be identified, such as duplicates/sampling errors, full siblings, and first- and second-degree relatives.

Suitability models and Future Scenarios. We obtained the environmental data from the WorldClim database (Fick and Hijmans 2017). To avoid redundancy among variables, we applied a Variance Inflation Factor (VIF) test and retained variables with a VIF below 10 using the AlleleShift

R package (Kindt 2020). The final data set included: Bio.2 (Mean Diurnal Temperature Range), Bio.3 (Isothermality), Bio.8 (Mean Temperature of Wettest Quarter), Bio.9 (Mean Temperature of Driest Quarter), Bio.14 (Precipitation of Driest Month), Bio.15 (Precipitation Seasonality), Bio.16 (Precipitation of Wettest Quarter), Bio.18 (Precipitation of Warmest Quarter) and Bio.19 (Precipitation of Coldest Quarter). Then, we used the R package FactoMineR (Le *et al.* 2008) to implement a PCA analysis to evaluate the relative contribution of each variable.

Distribution models were constructed using a set of nine bioclimatic variables. For future projections, we used MIROC6 from the Coupled Model Intercomparison Project Phase 6 (CMIP6) for the intervals 2041-2060, 2061-2080, and 2081-2100, available from the WorldClim database (www.worldclim.org). To evaluate different climate change scenarios, we included the Shared Socio-economic Pathways models ssp126 and 585. The first is a more conservative model that predicts a lower increase in global temperatures, while the second predicts the highest increase (Fick and Hijmans 2017). Models and future projections were generated using the R library biomod2 v 4.2-6-2 (Thuiller *et al.* 2025). The ensemble models were created using the committee-averaging criteria (Araújo and New 2007; Qiao *et al.* 2015). Models were computed using the generalized boosted model (GBM; Friedman 2001) and random forest (RF; Breiman 2001). For each computed algorithm, five independent pseudo-absence sets of 1000 points were generated with two replicates, using 70% of the records to train the model and 30% to evaluate performance. We assessed model performance using the area under the receiver operating characteristic curve (AUC; Swets 1988) and true skill statistic (TSS; Allouche *et al.* 2006). The ensemble computation was performed using the committee average criterion restricted to models with AUC > 0.9 and TSS > 0.8. Ensembles were transformed to presence/absence values using the TSS metric (in our runs, ROC and TSS performed almost equally; we selected TSS binary because it yielded more conservative models).

Outlier detection and GenomeEnvironment Association analysis. We implemented three different approaches to evaluate loci under selection. First, we used the R package pcadapt 4.4.1(Luu *et al.* 2017; Privé *et al.* 2020). This method identifies outlier loci using principal component analysis (PCA), computing K vectors of z-scores to infer the statistical association of each SNP with the *K* principal components. To select the optimal value of *K*, we used the "screeplot" option, followed by inspection of the paired plots of the recovered components to ensure they reflected sample genetic grouping. Outlier loci were selected using the Bonferroni correction for multiple comparisons, considering an alpha threshold of ≤ 0.1.

Second, we implemented a GenomeEnvironment Association (GEA) method using Redundancy Analysis (RDA) to identify outlier SNPs associated with environmental variables, following Capblancq and Forester (2021). Initially, we used the same variable data set as in the suitability models; however, to avoid overfitting, we excluded variables identified as collinear by the RDA analysis. The RDA was performed using the R package vegan (Oksanen *et al.* 2025) using SNPs as response variables and the three selected environmental variables as explanatory variables (Bio.3, Bio.9, Bio.14). RDA requires a genotype matrix without missing data; therefore, missing values were imputed using the frequency of the most common allele (the mode). Outlier SNPs were identified on each of the first three constrained axes using a threshold of 2 standard deviations. Then, we evaluated the association between each outlier and the environmental variables, estimating the Pearson correlation coefficient. We retained SNPs with correlation values of 0.5 or greater.

Third, we used a latent factor mixed model (LFMM; Frichot *et al.* 2013) implemented in the LEA v3.20.0 R package (Frichot and François 2015; Gain and François 2021). This method performs statistical tests to identify loci associated with environmental gradients (Frichot *et al.* 2013). The analysis was run using the environmental variables previously selected for each analysis. Outliers were selected using the Bonferroni correction with a threshold of ≤ 0.1.

We opted for these methods because they do not require an a priori definition of genetic groups, unlike *FST*-based methods. Considering all loci detected by the three methods, we generated a neutral data set for the genetic structure analysis. To annotate outlier loci, we considered only loci shared by at least two methods. Then, loci were mapped to the reference genome and extracted 500 bp in both directions (a total of 1,000 bp). We also performed a blast search (Altschul *et al.* 1997) against the UniProtKB database (https://www.uniprot.org/) and only hits with an e-value < $1x10^{-5}$ were considered.

We calculated the risk of non-adaptation (RONA) using pyRONA v0.4.3 (Rellstab *et al.* 2016; Pina-Martins *et al.* 2019). This method is based on the association between current allele frequencies and current climatic variables, and the estimation of the differences between current and future expected allele frequencies. For this analysis, we used the outlier loci detected by the three methods, all based on the same data set of environmental variables used in the LEA and RDA outlier detection methods. A high RONA value suggests a greater likelihood of maladaptation to climate change. For this analysis, we implemented the MIROC6 Coupled Model Intercomparison Project Phase 6 ssp585 for the interval 2081-2100.

Results

Genetic Diversity and Population Structure. We obtained an overall of 2,776,591 raw SNPs. After filtering, we identified 13,112 SNPs distributed across 2,065 scaffolds in the *Leptonycteris yerbabuenae* reference genome. The observed heterozygosity for the overall sample was *Ho* = 0.1866 (s.d. = 0.259), whereas the average expected heterozygosity

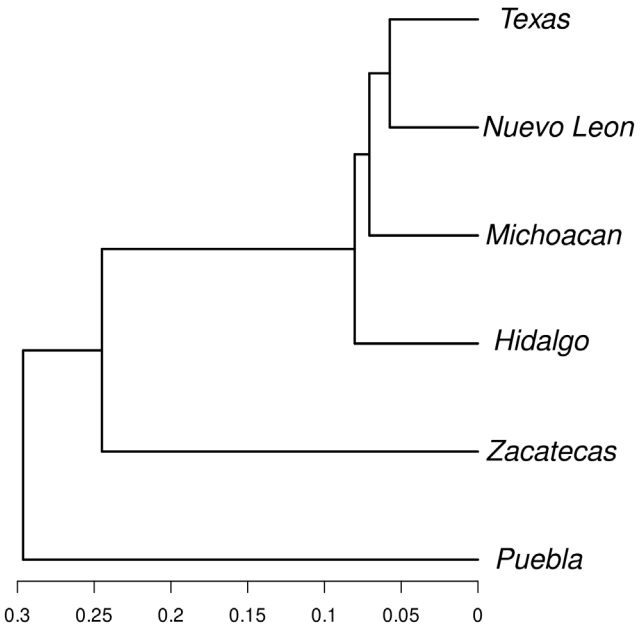

Figure 2. Dendrogram of Euclidean distances illustrating genetic relationships among collection sites. The dendrogram was constructed using Euclidean distances calculated from genome-wide SNP data. Each terminal branch represents a site. The tree structure depicts the hierarchical clustering of sites based on genetic similarity, with shorter branches indicating greater genetic proximity. This analysis provides insights into population structure and the genetic differentiation among sampled localities.

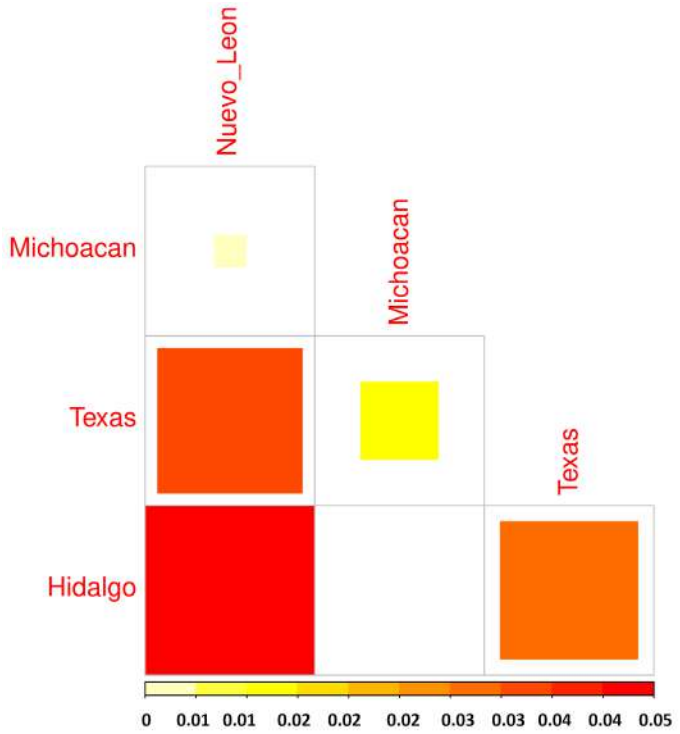

Figure 3. Heatmap of pairwise *FST* values among sampled localities. *FST* estimates are shown for comparisons involving Nuevo León, Michoacán, Texas, and Hidalgo. Color intensity reflects the degree of genetic differentiation, with darker shades indicating higher *FST* values. Localities represented by a single individual (Zacatecas and Puebla) were excluded from the analysis to ensure reliable estimates. The heatmap provides a visual summary of population structure and genetic divergence across sampling sites.

was *He* = 0.2112 (s.d. = 0.1815) and the *FIS* was 0.1097 (s.d. = 0.3101). The genetic-distance dendrogram revealed a genetic grouping irrespective of the geographical distance between sampling locations (Figure 2). Furthermore, the analysis of *FST* between the different locations showed similar patterns (Figure 3), with low but > 0.05 values (except for Michoacan vs. Hidalgo; Table SD2, supplementary materials). The principal component analysis revealed a homogeneous population, consistent with the *FST*-based analyses (Figure 4).

Relatedness analysis. Our analysis of relatedness among all individuals revealed minimal kin relationships among two pairs of individuals in the same locality (Figure 5). Only individuals ln70-ln73, and individuals ln64-ln69, who are all from Nuevo León, and the degree of relationship in the two pairs of individuals reflects a close kinship similar to that between uncles and nephews. The first pair exhibits a higher degree of relatedness between its members (Figure 5).

To complete these results, the Admixture analysis showed no genetic structuring (*K* = 1, Figure SD2 supplemental materials). Moreover, worth noting that the plots with higher *K* values showed no admixture between individuals (SD3 supplemental material). The distance-based isolation analysis for the samples (SD4 supplemental material) did not show a correlation between geographic distance and genetic distance ($p > 0.3$).

Potential Distribution Model in Future Scenarios. Our models projecting the potential distribution of the migratory bat, *L. nivalis*, in future climate change scenarios show contraction in areas of greater climate suitability. In the most optimistic scenario (Figure 6a, SSP1-2.6), this contraction is minimal and concentrated in the northern part of *L. nivalis*' distribution, where temperatures would not rise by more than the global average increase of approximately 1.8 °C by the year 2100 compared to pre-industrial levels.

By contrast, in the most pessimistic scenario (SSB585; Figure 6b), which projects a temperature increase of 4.4 °C (with a probable range of 3.3 to 5.7 °C) above pre-industrial levels by 2100, the contraction of climatic stable areas mainly occurs in the north of the distribution range, particularly affecting areas where maternity caves are located, primarily in Nuevo León in Mexico and Texas in the United States. The area that showed the greatest climatic suitability across the three time periods is in the center and southern parts of the current distribution. This means that even in the scenario of the greatest global warming, the center of distribution and part of the south would remain suitable for the species.

Outlier detection and SNP annotation. The three methods yielded an overall of 582 outlier SNPs. The PCAdapt analysis recovered 123 outlier SNPs, RDA 254 SNPs, and LEA 213; from them, only two SNPs were shared by at least two methods. (Figure 7) Of the outlier loci, only one had a match with uncharacterized proteins from species of the Vespertilionidae family.

Risk of non-adaptedness. RONA analysis shows an association between heterozygosity and changes in three climate variables in the context of projected global change (Figure 8). In other words, current heterozygosity maintains

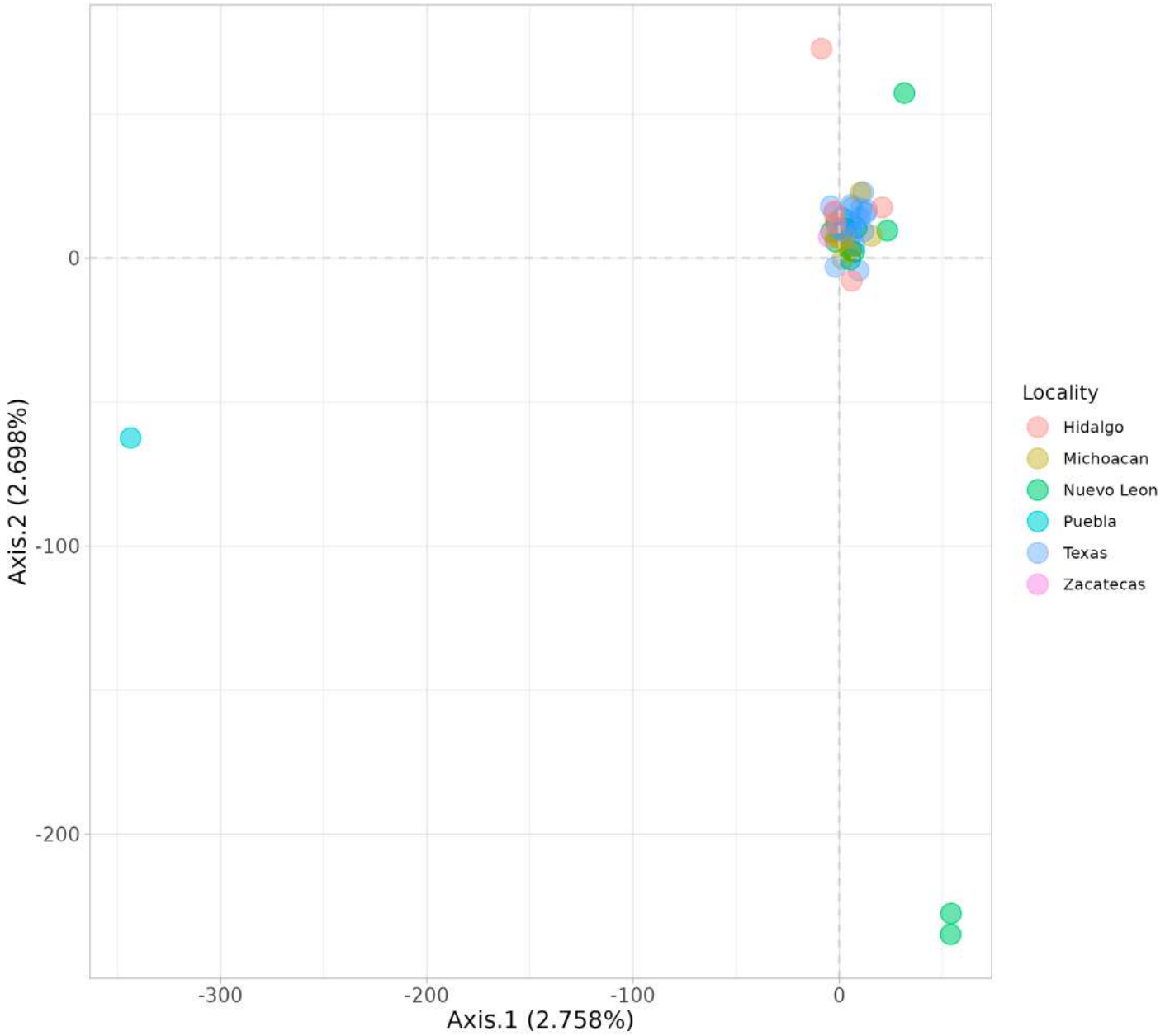

Figure 4. Principal Component Analysis (PCA) of 47 individuals based on 13,112 SNPs. Each point represents an individual, colored by sampling locality: Hidalgo, Michoacán, Nuevo León, Puebla, Texas, and Zacatecas. The first two principal components (Axis1 and Axis5) are shown, explaining 2.758% and 2.698% of the total genetic variance, respectively. The analysis reveals population structure and genetic relationships among localities, with individuals from the same geographic region tending to cluster together.

adaptive potential under present conditions; however, changing some of these variables may compromise this potential in response to environmental conditions. The most significant risk relationship in the context of climate change is that between heterozygosity and the Bio.9 variable, 'Mean Temperature of Driest Quarter'. However, this risk is more pronounced in the northern part of the species' distribution, specifically in Texas (0.93415) in the United States and, to a lesser extent, in Nuevo León, Mexico (0.5362). The Bio.3 variable, 'Isothermality', and the Bio.14 variable, 'Precipitation of Driest Month', showed average RONA values at sites in the center and south of the long-nosed bat's distribution range. For Bio.3, the three sites at greatest risk were Texas (0.45894), Zacatecas (0.44286) and Puebla (0.3934). Meanwhile, the highest values for Bio.14 were found in Puebla (0.55603) in the south and in Texas (0.38008) in the north (see all values in Supplemental Data SD5).

Discussion

The genetic diversity, expressed as expected heterozygosity (*Ho*), is considered a parameter that can help us predict the adaptive potential of species in the face of rapidly emerging adverse conditions (Schmidt and Russello 2025), as is currently being observed during the Anthropocene. While this parameter does not precisely identify the genes and alleles under local selection and adaptation, it provides an overview of the populations' adaptive potential. We initially assumed that *L. nivalis*, if it had low levels of heterozygosity, would be vulnerable to the abrupt changes expected in the

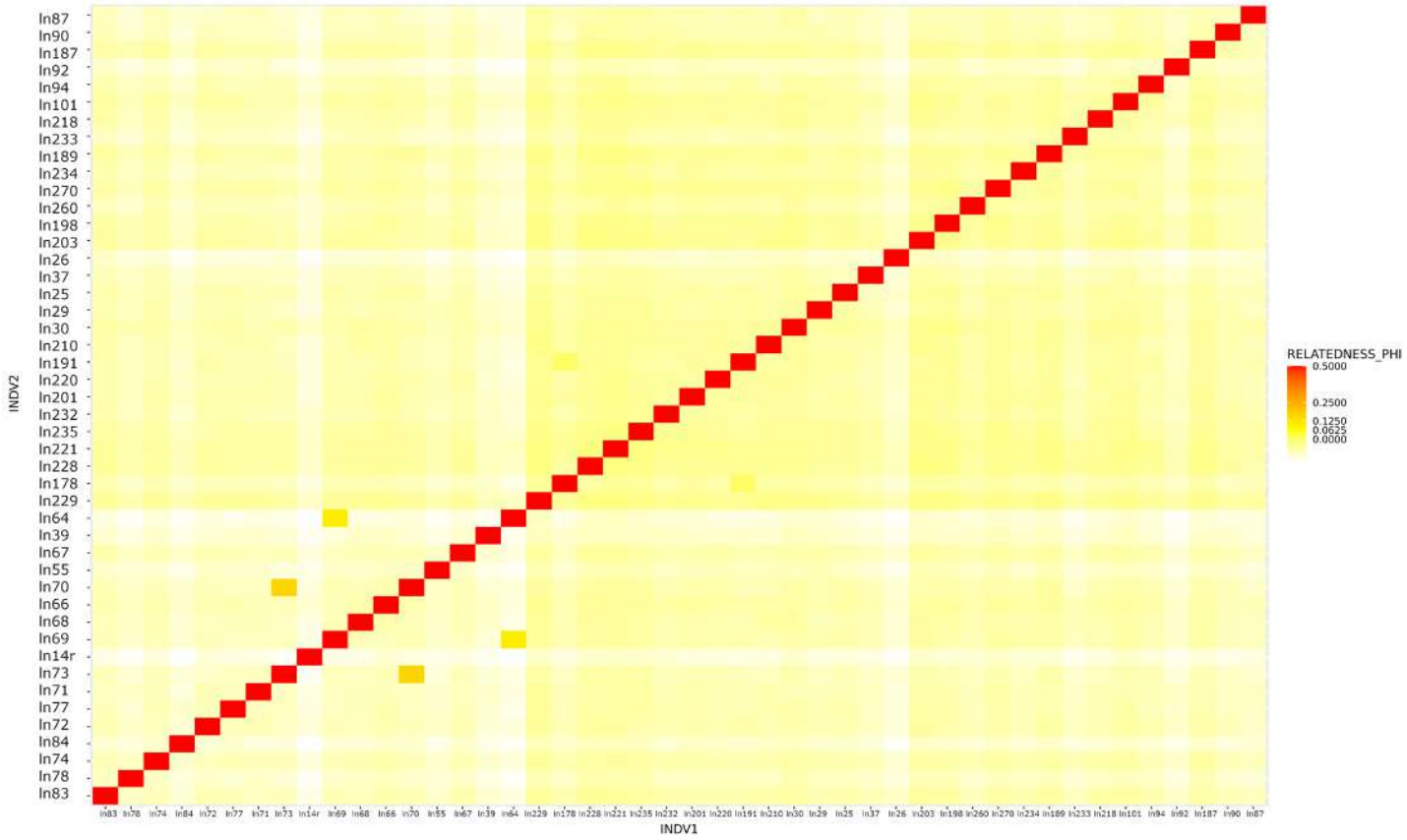

Figure 5. Heatmap of pairwise relatedness estimates among 187 individuals. Relatedness coefficients were calculated using VCFtools based on genome-wide SNP data. The color gradient represents the degree of genetic relatedness, with warmer colors (e.g., red) indicating higher relatedness and cooler colors (e.g., white) indicating lower relatedness or unrelated individuals. Individuals are ordered along both axes by sample ID, and the matrix is symmetric, reflecting bidirectional pairwise comparisons. This analysis provides insights into familial relationships and population structure within the sampled cohort.

near future, in particular if their distribution in maternity caves found in the northern part of the species' range--primarily in Nuevo León in Mexico and Texas in the United States during spring-summer seasons-- would be affected by the climatic changes. For this reason, it is important to explore the optimal conditions for the species' migratory and reproductive dynamics.

Maintaining heterozygosity is therefore extremely important in *L. nivalis*, given that its genetic diversity is low (*Ho* = 0.1866) compared to that of other bat species considered for national and/or international protection, such as the sister species, the lesser long-nosed bat, *L. yerabuenae* (*Ho*= 0.292; Peralta *et al.* 2025), even with a larger sample analyzed in our study. Heterozygosity of *L. nivalis* is also lower than in *Myotis lucifugus* (*Ho*= 0.247-0.263; Lilley *et al*. 2020) *Myotis grisescens* (*Ho*= 0.183; Nagel *et al.* 2023). *Myotis sodalis* (*Ho*= 0.083) (Nagel *et al.* 2023), as well as *Miniopterus schreibersii* (Dufresnes *et al.* 2023), and *Myotis septentrionalis* (*Ho* = 0.000086 -0.000115; Grimshaw *et al.* 2024).

Given the geographic distribution of the species, we consider our sampling to be adequate of a genomic study (were the large number of genetic makers can compensate the smaller samples of individuals, see simulations of Aguirre-Liguori *et al.* 2020), although we recognize that there is a bias towards northern locations, Texas and Nuevo León, as well as shortage in one locality at the center and one locality at southern of *L. nivalis* distribution. However, bias and a small sample size may have prevented the detection of genetic differences between populations or genetic structure.

Based on previous work, we expected to detect population genetic structure, given that evidence of distinct genetic groups had been reported in a recent study using two mitochondrial markers and one associated-chromosome Y gene data (Trejo-Salazar *et al.* 2025). This is important for associating outlier alleles with local adaptations and for proposing conservation strategies that prioritize sites where individuals carry these alleles. However, our results did not detect any genetic structure. Genetic structure analyses in this study and previous studies (Pourshoushtari and Ammerman 2021; Trejo-Salazar *et al.* 2025) suggest that genetic flow remains strong and constant, preventing genetic differentiation between refugees and locations inhabited by the species. Therefore, it appears that females maintain this genetic flow when they return to the south-central part of the species' distribution during the autumn-winter season, keeping the sites or populations as a single unit.

Despite the absence of genetic population structure and the relatively large sample size, we detected only two candidate alleles under selection that are statistically correlated with the climatic variables used for distribution model projections. But they are not clearly representatives of maladaptations or of any potential adaptation related to

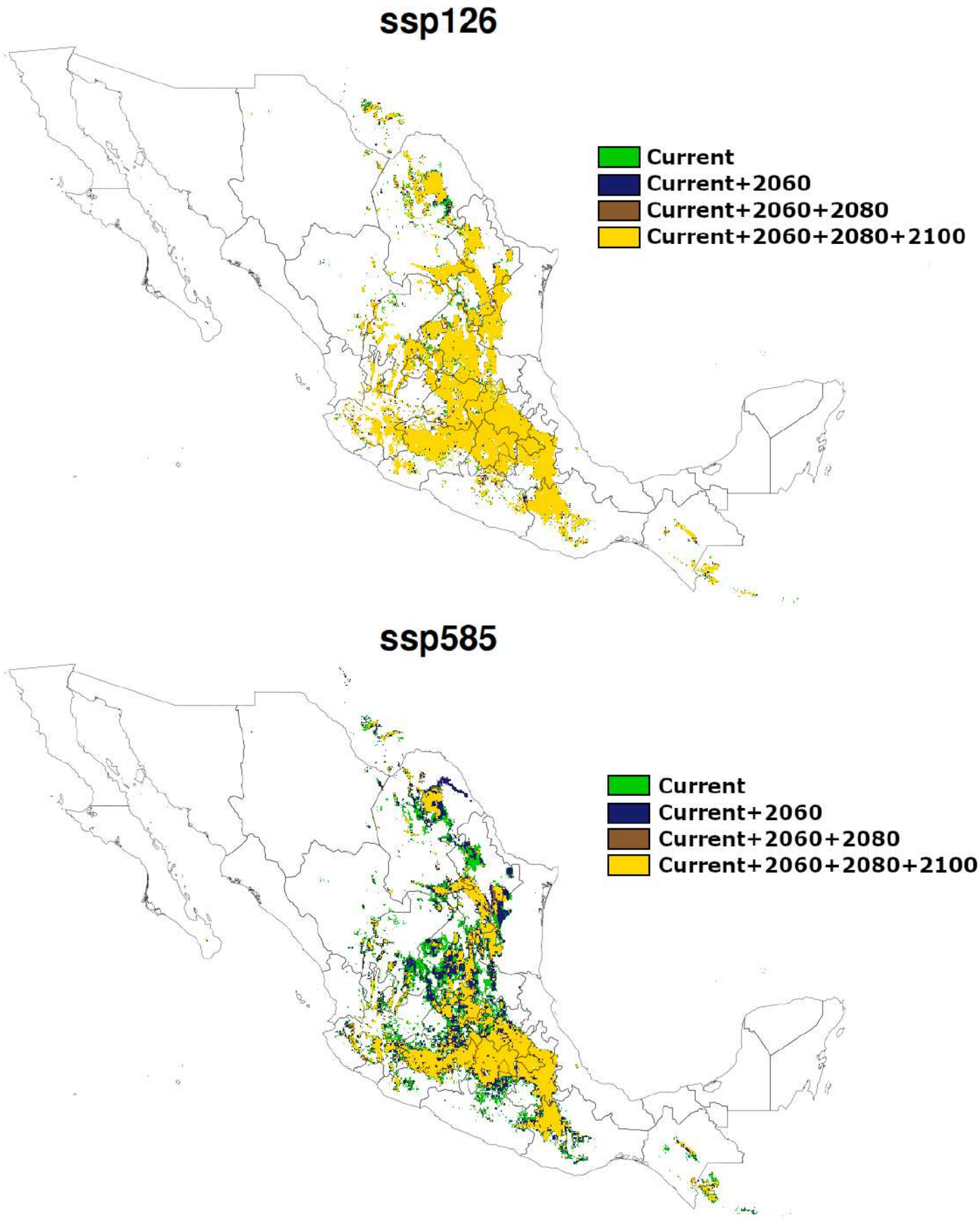

Figure 6. Maps show the suitability models for the *L. nivalis* species for the present (in green) and three future time periods, with major climate stability, until the end of the century. The colors blue, brown, and yellow represent the time periods that overlap.

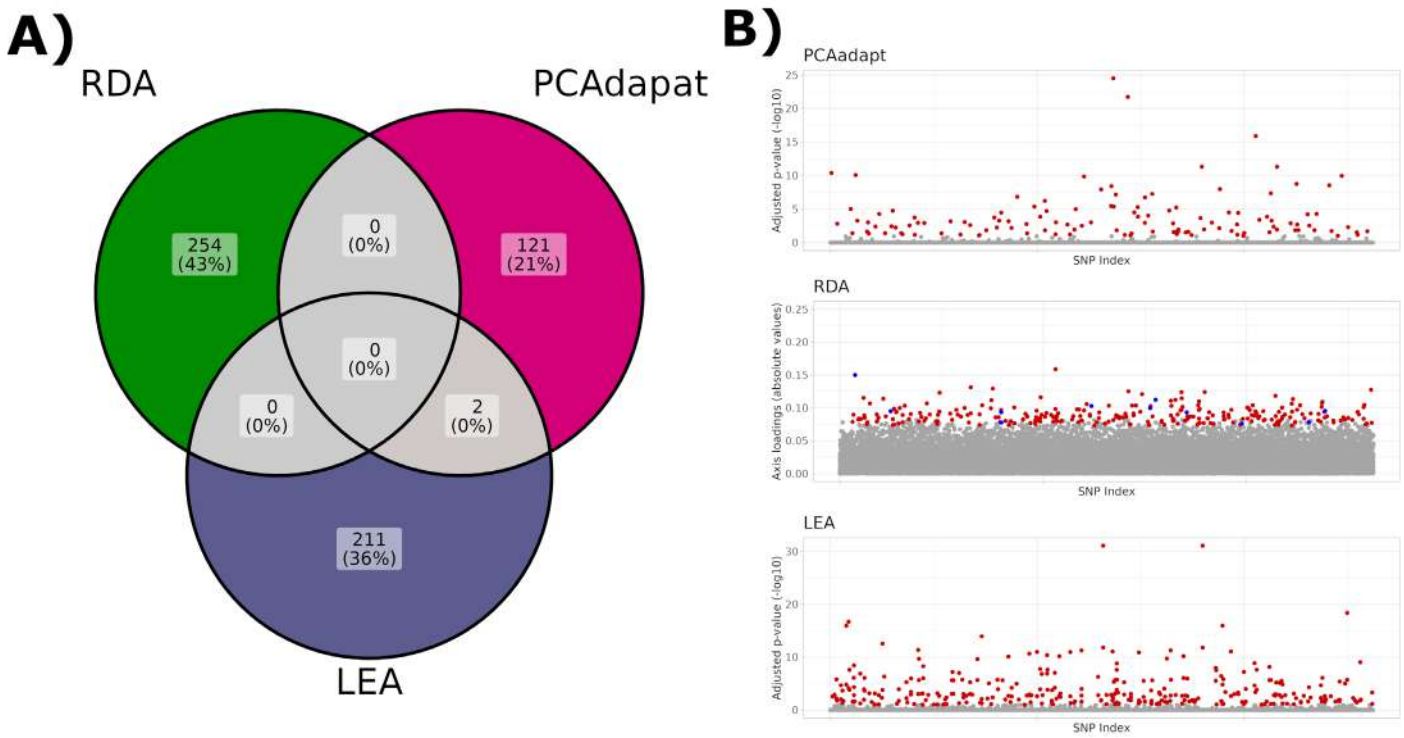

Figure 7. A) Venn diagram showing the number of SNPs identified by three different filtering methods. RDA, PCAdapt, and LEA yielded 254 (43%), 121 (21%), and 211 (36%) SNPs, respectively. The overlapping regions indicate the number of SNPs shared between methods. Only two SNPs (<1%) were common to all three approaches. B) Adjusted *p*-values (-log10) are shown for each method, with values of 0 indicating strong statistical support after correction. Percentages represent the proportion of SNPs relative to the total number of unique SNPs identified across all methods.

climate change. In other words, we identified alleles related to climatic conditions, temperature, and precipitation, we did not find local adaptations that would allow us to prioritize the protection of one area over another. We also detected a positive correlation between genetic diversity and four climatic variables. This result is relevant, as it enables us to predict the future of tequila bat populations and prioritize connectivity between sites, migratory routes, and the conservation of heterozygosity levels for the species.

Thus, environmental pressures or resource scarcity can affect the entire population of a species, pushing it into a complex situation. Based on our results, Nuevo León is among the most susceptible locations to climate change. According to RONA's analysis, there is a closer relationship between diversity and the precipitation-related climate variable (Bio9) in this location. In Nuevo Léon, at the El Infierno cave, both sexes gather to form shelters for mating and raising offspring. The long-nosed bat is present there alongside at least five species of the genus *Agave* during their flowering stage. Furthermore, the presence of *L. nivalis* in this area is positively related to ambient temperature (Moreno-Valdez *et al.* 2004), so any variation in temperature could negatively affect the species' ecological dynamics and, consequently, its primary food source.

On the other hand, we think that the lack of population structure helps to explain the distant kinship relationships between individuals in our sample. In other words, the absence of population structure means that it is less likely that close relatives will be found in small population samples (Weir and Goudet 2017). A larger sample size would likely yield more detailed information on both genetic population structure and kinship relationships, and apparently, genetic flow between refuges has remained constant. However, gene flow must be maintained to ensure that the adaptive potential and the outlier loci remain part of the species' gene pool (Chhina *et al.* 2024). Nevertheless, intense selective pressures, such as climate change or global warming, could cause a bottleneck (Jangjoo *et al.* 2016) and affect the parameters addressed in this study, thereby impacting genetic diversity and the adaptive potential stored in this genomic variation.

We consider our analysis for detecting outlier loci under selection to be representative, as, in general terms, this sampling reflects the species' distribution. Nevertheless, among the 13,112 SNPs used for outlier detection, fewer than 5% were identified as outliers by any of the three methods, and only two were shared across methods. We considered that our results are similar to those found in previous studies in mammals. For instance, for the sister species, *L. yerbabuenae,* Peralta *et al.* (2025) reported 17,732 SNPs after filtering, of which 7,172 were useful for demographic analyses with 32 individuals, compared with our sample of 47 individuals. In 288 individual samples of the American pika (*Ochotona princeps*), Henry and Russello (2013) detected 68 outlier loci under selection, and 15 of these were statistically associated with at least one climatic variable. In the arboreal Australian mammal *Petauroides volans*, Knipler *et al.* (2023) detected 66 loci associated with climatic variables using an 85-individual sample.

As for studies focused on the Chiroptera group,

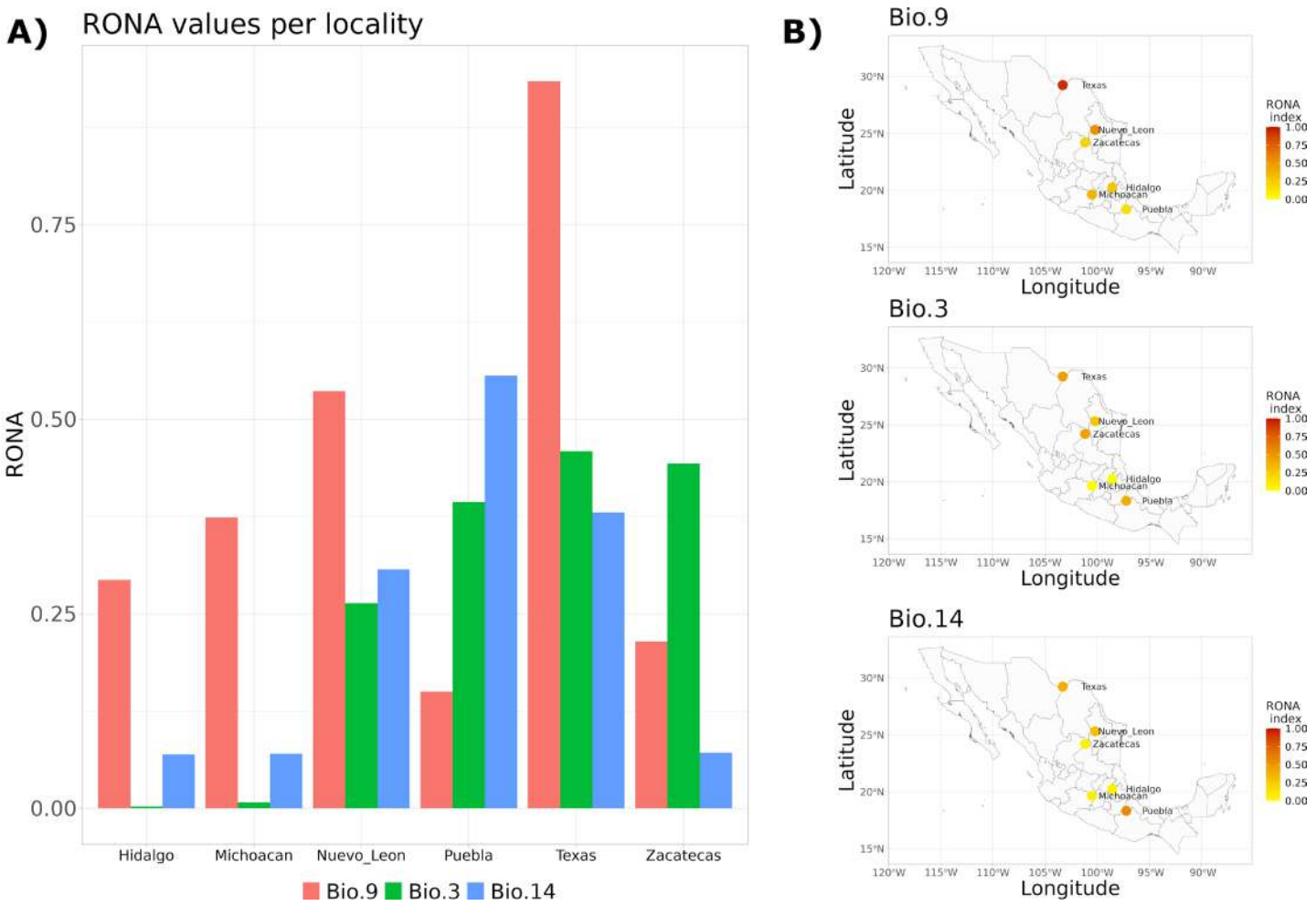

Figure 8. Risk of non-adaptedness (RONA) analysis across sampling localities for three bioclimatic variables (Bio.9, Bio.3, Bio.14). A) Bar plots showing RONA values per locality, representing the statistical association between heterozygosity and the risk of maladaptation under future climate change scenarios for each bioclimatic variable. B) Geographic distribution of RONA values across the sampled range. Warmer colors (closer to red) indicate localities with a higher risk of non-adaptedness if the associated climatic variable changes. Values for selected representative localities (Bio.9, Bio.3, Bio.14) are shown to illustrate spatial variation in climate-associated genetic vulnerability.

despite many species being considered vulnerable due to ecological characteristics, morphological features, and physiological specializations, there is insufficient information to predict likely scenarios using genomic tools and to establish preventive or corrective measures in response to climate change. One of the few studies to address the adaptive potential of the European bat, *Plecotus austriacus,* was Razgour *et al.* (2018), which examined a sample of 83 individuals and detected 24 single-nucleotide polymorphisms (SNPs) associated with extreme temperature and summer precipitation variables. In contrast, we detected statistically significant associations with just two SNPs and climatic variables: temperature during the driest month and precipitation of the warmest quarter. However, these were merely statistical correlations, and we did not find a biological association.

Regarding the potential distribution of the species under global warming scenarios, the most pessimistic scenario predicts a global temperature increase of around 4.4°C relative to pre-industrial levels. This would lead to a contraction of *L. nivalis* current distribution, mainly affecting migratory areas during the breeding season (Moreno-Valdez *et al.* 2000). Nevertheless, this species has already experienced similar dynamics in the past (Trejo-Salazar *et al.* 2025), during the climate changes from the Last Interglacial to the Holocene and Current time. Thus, we consider that *L. nivalis* populations can adjust to seasonal changes in climatic conditions through migratory movements. However, these changes have occurred in the past over longer periods than those we are expecting in the Anthropocene, so we cannot be sure that species will be able to withstand such predicted radical changes in less than 100 years.

Despite their obvious importance, relatively few studies have incorporated local adaptation into predictions of how species' distributions and abundances will be affected by climate change (Smith *et al.* 2019) or have taken local adaptation into account when designing conservation and recovery plans (Peterson *et al.* 2019). Managed (assisted) gene flow and the incorporation of local adaptation into conservation plans can provide options for populations that have become increasingly maladapted to their environment, due to reduced genetic diversity or rapidly changing environments, or for restoring resilient populations in places where they have become locally extinct.

Conclusions

The future distribution of the long-nosed bat may be compromised in areas that are crucial for its reproductive behavior, particularly in places where it establishes maternity roosts during the spring and summer seasons. By inferring and predicting the distribution patterns and consequences for the adaptive potential of this nectarivorous bat, we can suggest possible scenarios of particular relevance, considering, for instance, that some plant species depend on pollination by these mammals. In other words, this way we can predict possible consequences at the ecosystem level due to climate change in Mexico.

It is possible that *L. nivalis* will adapt to these future climate scenarios. However, it must still be considered that current global warming is very rapid, and although bats of the genus *Leptonycteris* have survived and adapted to similar -but slower- climatic changes of the planet, it is not possible to ensure that in such a short time the current populations will manage to maintain a large enough size.

Regarding climate change scenarios, two predictions were made. The one we consider most optimistic forecasts an increase of approximately 1.8°C by the end of this century. In that case, the changes in climatic conditions favorable to bat presence are minor, and therefore, we believe the consequences may be barely noticeable. However, in the most pessimistic scenario, with a warming of around 4.4°C above pre-industrial global temperatures, the situation is more catastrophic, both for bats and, as will surely be the case, for the plants that depend on pollination by these bats.

Acknowledgments

This work is dedicated to Dra. Livia León Paniagua in recognition of her contributions to Mexican mammalogy. She played a fundamental role in training human resources and studying Mexican bats and rodents. We would like to express our gratitude for her hard work curating one of the country's largest zoological collections for over 40 years. On a personal level, Dra. Livia supported Roberto Trejo's academic, professional and personal development, always offering words of encouragement and demonstrating her humanity. Without her presence and support, we would not have been able to finish this work or other previous publications. We admire her as a person and an academic because she has always supported and collaborated with those in need, promoting an atmosphere of respect and professionalism with her positive and often maternal attitude. Author thanks Dra. Erika Aguirre Planter for technical support in laboratory, Dra. Edén Rodríguez and Mc S. Dulce Hernández for supporting DNA extraction. Gasca-Pineda J. received a post-doctoral fellowship from "Estancias Posdoctorales por México para la Formación y Consolidación de las y los Investigadores por México" (SECIHTI , formerly CONAHCYT, CVU: 172925); Trejo-Salazar RE received a post-doctoral fellowship from "Estancias Posdoctorales por México para la Formación y Consolidación de las y los Investigadores por México" (SECIHTI , formerly CONAHCYT, CVU: 249584). Proyecto Conacyt Investigación en Fronteras de la Ciencia 2015, número 177, Genómica de la Diversidad de Vertebrados Mexicanos 1: Leptonycteris y la evolución de la nectarivoría en murciélagos y aves.

Declaration of Artificial Intelligence use

The authors declare that we have not used any artificial intelligence tools at any stage of the preparation of this manuscript.

Author contributions

Roberto-Emiliano Trejo-Salazar designed the project, collect samples, database construction, analyses and drafting the manuscript; Jaime Gasca-Pineda participated in the database construction, computational analyses and drafting manuscript; Rosalinda Tapia López contributed with DNA extraction and laboratory support and drafting manuscript; Luis E. Eguiarte helped with the logistics and drafted and corrected the manuscript.

Supplementary data

Supplementary materials are available at Therya online and https://doi.org/10.5281/zenodo.17613255

SD1. Permit to collect biological samples.

SD2. Pairwise *FST* values between the sampled locations and Bootstrap values for paired comparisons of *FST* between sampled locations.

SD3. CV values for different *K* values in the admixture analysis.

SD4. Distance isolation analysis.

SD5. RONA analysis values for each location.

Literature cited

Alexander DH, Novembre J, and Lange, K. 2009. Fast model-based estimation of ancestry in unrelated individuals. *Genome Research* 19:1655-1664. https://doi.org/10.1101/gr.094052.109

Alexander DH, and Lange K. 2011. Enhancements to the ADMIXTURE algorithm for individual ancestry estimation. *BMC Bioinformatics* 12:246. https://doi.org/10.1186/1471-2105-12-246

Aguirre-Liguori JA, Luna-Sánchez JA, Gasca-Pineda J, and Eguiarte LE. 2020. Evaluation of the minimum sampling design for population genomic and microsatellite studies: An analysis based on wild maize. *Frontiers in Genetics* 11:870. https://doi.org/10.3389/fgene.2020.00870

Aguirre-Liguori JA, Ramírez-Barahona S, and Gaut BS. 2021. The evolutionary genomics of species' responses to climate change. *Nature Ecology & Evolution* 5:1350-1360. https://doi.org/10.1038/s41559-021-01526-9

Allouche O, Tsoar A, and Kadmon R. 2006. Assessing the

accuracy of species distribution models: prevalence, kappa and the true skill statistic (TSS). *Journal of Applied Ecology* 43:1223–1232. https://doi.org/10.1111/j.1365-2664.2006.01214.x

Altschul SF, Madden TL, Schaffer AA, Zhang J, Zhang Z, Miller W, *et al*. 1997. Gapped BLAST and PSI-BLAST: a new generation of protein database search programs. *Nucleic Acids Resources* 25:3389–3402. https://doi.org/10.1093/nar/25.17.3389

Andrews S. 2010. FastQC: a Quality Control Tool for High Throughput Sequence Data. [Accessed October 10th, 2024]. http://www.bioinformatics.babraham.ac.uk/projects/fastqc

Araújo M, and New M. 2007. Ensemble forecasting of species distributions. *Trends in Ecology & Evolution* 22:42–47. https://doi.org/10.1016/j.tree.2006.09.010

Beji S, Fontaine V, Devaux R, Thomas, M, Negro, SS, Bahrman, N, *et al*. 2020. Genome-wide association study identifies favorable SNP alleles and candidate genes for frost tolerance in pea. *BMC Genomics* 21:536. https://doi.org/10.1186/s12864-020-06928-w

Bestion E, Teyssier A, Richard M, Clobert J, and Cote J. 2015. Live fast, die young: experimental evidence of population extinction risk due to climate change. *PLoS Biology* 13:e1002281. https://doi.org/10.1371/journal.pbio.1002281

Blows MW, and Hoffmann AA. 2005. A reassessment of genetic limits to evolutionary change. *Ecology* 86:1371–84. https://doi.org/10.1890/04-1209

Bolger AM, Lohse M, and Usadel B. 2014. Trimmomatic: a flexible trimmer for Illumina sequence data. *Bioinformatics* 30: 2114–2120. https://doi.org/10.1093/bioinformatics/btu170

Boutin S, and Lane JE. 2014. Climate change and mammals: evolutionary versus plastic responses. *Evolutionary Applications* 7:29–41. https://doi.org/10.1111/eva.12121

Bogan MA, Cryan PM, Weise CD, and Valdez EW. 2017. Landscape movements by two species of migratory nectar-feeding bats (*Leptonycteris*) in a northern area of seasonal sympatry. *Western North American Naturalist* 77:317–330. https://doi.org/10.3398/064.077.0305

Burke RA, Frey JK, Ganguli A, and Stoner KE. 2019. Species distribution modelling supports "nectar corridor" hypothesis for migratory nectarivorous bats and conservation of tropical dry forest. *Diversity and Distributions* 25:1399–1415. https://doi.org/10.1111/ddi.12950

Breiman L. 2001. Random forests. *Machine Learning* 45:5–32. https://doi.org/10.1023/A:1010933404324

Cahill AE, Aiello-Lammens ME, Fisher-Reid MC, Hua X, Karanewsky CJ, Yeong R, *et al*. 2013. How does climate change cause extinction? *Proceedings of the Royal Society B: Biological Sciences* 280(1750): 20121890. https://doi.org/10.1098/rspb.2012.1890

Capblancq T, and Forester BR. 2021. Redundancy analysis: A Swiss Army knife for landscape genomics. *Methods in Ecology and Evolution* 12:2298–2309. https://doi.org/10.1111/2041-210X.13722

Chattopadhyay B, Garg KM, Ray R, and Rheindt FE. 2019. Fluctuating fortunes: genomes and habitat reconstructions reveal global climate-mediated changes in bats' genetic diversity. *Proceedings of the Royal Society B* 286(1911):20190304. https://doi.org/10.1098/rspb.2019.0304

Chhina AK, Abhari N, Mooers A, and Lewthwaite JMM. 2024. Linking the spatial and genomic structure of adaptive potential for conservation management: a review. *Genome* 67:403–423. https://doi.org/10.1139/gen-2024-0036

Cummins D, Kennington WJ, Rudin-Bitterli T, and Mitchell NJ. 2019. A genome-wide search for local adaptation in a terrestrial-breeding frog reveals vulnerability to climate change. *Global Change Biology* 25:3151–3162. https://doi.org/10.1111/gcb.14703

Danecek P, Auton A, Abecasis G, Albers CA, Banks E, DePristo MA, *et al*. 2011. The variant call format and VCFtools. *Bioinformatics* 27:2156–2158. https://doi.org/10.1093/bioinformatics/btr330

Davis MB, Shaw RG, and Etterson JR. 2005. Evolutionary responses to changing climate. *Ecology* 86:1704–1714. https://doi.org/10.1890/03-0788

Deb JC, Forbes G, and MacLean DA. 2020. Modelling the spatial distribution of selected North American woodland mammals under future climate scenarios. *Mammal Review* 50:440–452. https://doi.org/10.1111/mam.12210

de Castro Evaldt BH, Leite YLR, and Loss AC. 2024. Climate change impact on small mammals from two Neotropical hotspots. *Biological Journal of the Linnean Society* 143(3): blae014. https://doi.org/10.1093/biolinnean/blae014

Diario Oficial de la Federación. 05-03-2014. Norma Oficial Mexicana – 059 (NOM-059). Acuerdo por el que se da a conocer la lista de especies y poblaciones prioritarias para la conservación. Estados Unidos Mexicanos. Mexico City (MEX): Secretaría de Medio Ambiente y Recursos Naturales.

Dufresnes C, Dutoit L, Brelsford A, Goldstein-Witsenburg F, Clément L, López-Baucells, *et al*. 2023. Inferring genetic structure when there is little: population genetics versus genomics of the threatened bat *Miniopterus schreibersii* across Europe. *Scientific Reports* 13:1523. https://doi.org/10.1038/s41598-023-27988-4

Eaton DA, and Overcast I. 2020. ipyrad: Interactive assembly and analysis of RADseq datasets. *Bioinformatics* 36:2592–2594. https://doi.org/10.1093/bioinformatics/btz966

Elad Y, and Pertot I. 2014. Climate change impacts on plant pathogens and plant diseases. *Journal of Crop Improvement* 28:99–139. https://doi.org/10.1080/15427528.2014.865412

Festa F, Ancillotto L, Santini L, Pacifici M, Rocha R, Toshkova N, *et al*. 2023. Bat responses to climate change: a systematic review. *Biological Reviews* 98:19–33. https://doi.org/10.1111/brv.12893

Fick SE, and Hijmans RJ. 2017. WorldClim 2: new 1-km spatial resolution climate surfaces for global land areas. *International Journal of Climatology* 37:4302–4315. https://doi.org/10.1002/joc.5086

Franks SJ, and Hoffmann AA. 2012. Genetics of climate change adaptation. *Annual Review of Genetics* 46:185–208. https://doi.org/10.1146/annurev-genet-110711-155511

Friedman JH. 2001. Greedy function approximation: a gradient boosting machine. *Annals of Statistics* 29:1189–1232. https://www.jstor.org/stable/2699986

Frichot E, Schoville SD, Bouchard G, and François O. 2013. Testing for associations between loci and environmental gradients using latent factor mixed models. *Molecular Biology and Evolution* 30:1687–1699. https://doi.org/10.1093/molbev/mst063

Frichot E, and François O. 2015. LEA: An R package for landscape and ecological association studies. *Methods in Ecology and Evolution* 6:925–929. https://doi.org/10.1111/2041-210X.12382

Gain C, and François O. 2021. LEA 3: Factor models in population genetics and ecological genomics with R. *Molecular Ecology Resources* 21:2738–2748. https://doi.org/10.1111/1755-0998.13366

Gasca-Pineda J. 2015. Genética de la conservación del bisonte de la pradera (*Bison bison bison*) y del borrego cimarrón (*Ovis canadensis*) en México. [PhD thesis]. [Mexico City (MEX)]: Universidad Nacional Autónoma de México.

Gona PN, and More AF. 2022. Bacterial pathogens and climate change. *The Lancet* 400:2161–2163.

Gonçalves F, Sales LP, Galetti M, and Pires MM. 2021. Combined impacts of climate and land use change and the future restructuring of Neotropical bat biodiversity. *Perspectives in Ecology and Conservation* 19:454–463. https://doi.org/10.1016/j.pecon.2021.07.005

Goudet J, and Jombart T. 2022. hierfstat: Estimation and Tests of Hierarchical F-Statistics. <ttps://doi.org/10.32614/CRAN.package.hierfstat>, R package version 0.5-11, https://CRAN.R-project.org/package=hierfstat

Grimshaw JR, Donner D, Perry R, Ford WM, Silvis A, Garcia CJ, *et al*. 2024. Disentangling genetic diversity of *Myotis septentrionalis*: population structure, demographic history, and effective population size. *Journal of Mammalogy* 105:854–864. https://doi.org/10.1093/jmammal/gyae056

Guillaume AS, Leempoel K, Rogivue A, Gugerli F, Parisod C, and Joost S. 2024. Integrating very high resolution environmental proxies in genotype–environment association studies. *Evolutionary Applications* 17:e13737. https://doi.org/10.1111/eva.13737

Gutierrez-Guerrero YT, Ibarra-Laclette E, Martínez del Río C, Barrera-Redondo J, Rebollar EA, Ortega J, *et al*. 2020. Genomic consequences of dietary diversification and parallel evolution due to nectarivory in leaf-nosed bats. *Gigascience* 9:giaa059. https:// doi.org/10.1093/gigascience/giaa059

Hansen MM, Olivieri I, Waller DM, Nielsen EE, and GeM Working Group. 2012. Monitoring adaptive genetic responses to environmental change. *Molecular Ecology* 21:1311–1329. https://doi.org/10.1111/j.1365-294X.2011.05463.x

Hayes BJ, Bowman PJ, Chamberlain AJ, Savin K, van Tassell CP, Sonstegard TS, *et al*. 2009. A Validated Genome Wide Association Study to Breed Cattle Adapted to an Environment Altered by Climate Change. *PLoS One* 4:e6676. https://doi:10.1371/journal.pone.0006676

Henriques D, Wallberg A, Chávez-Galarza J, Johnston JS, Webster MT, and Pinto MA. 2018. Whole genome SNP-associated signatures of local adaptation in honeybees of the Iberian Peninsula. *Scientific Reports* 8:11145. https://doi.org/10.1038/s41598-018-29469-5

Henry P, and Russello MA. 2013. Adaptive divergence along environmental gradients in a climate-change-sensitive mammal. *Ecology and Evolution* 3:3906–3917. https://doi.org/10.1002/ece3.776

Hensley AP, and Wilkins KT. 1988. *Leptonycteris nivalis*. *Mammalian Species* 307:1–4. https://doi.org/10.1644/797.1

Hetem RS, Fuller A, Maloney SK, and Mitchell D. 2014. Responses of large mammals to climate change. *Temperature* 1:115–127. https://doi.org/10.4161/temp.29651

Hoffmann AA, Weeks AR, and Sgrò CM. 2021. Opportunities and challenges in assessing climate change vulnerability through genomics. *Cell* 184:1420–1425. https://doi.org/10.1016/j.cell.2021.02.006

Jangjoo M, Matter SF, Roland J, and Keyghobadi N. 2016. Connectivity rescues genetic diversity after a demographic bottleneck in a butterfly population network. *Proceedings of the National Academy of Sciences* 113:10914–10919. https://doi.org/10.1073/pnas.160086511

Houle D. 1992. Comparing evolvability and variability of quantitative traits. *Genetics* 130:195-204. https://doi.org/10.1093/genetics/130.1.195

Jombart T. 2008. adegenet: a R package for the multivariate analysis of genetic markers. *Bioinformatics* 24: 1403–1405. https://doi:10.1093/bioinformatics/btn129

Jombart T, and Ahmed I. 2011. adegenet 1.3-1: new tools for the analysis of genome-wide SNP data. *Bioinformatics* 27: 3070–3071. https://doi:10.1093/bioinformatics/btr521

Jordan R, Hoffmann AA, Dillon SK, and Prober SM. 2017. Evidence of genomic adaptation to climate in *Eucalyptus microcarpa*: Implications for adaptive potential to projected climate change. *Molecular Ecology* 26:6002–6020. https://doi.org/10.1111/mec.14341

Kardos M, Armstrong EE, Fitzpatrick SW, Hauser S, Hedrick PW, Miller JM, *et al*. 2021. The crucial role of genome-wide genetic variation in conservation. *Proceedings of the National Academy of Sciences* 118:e2104642118. https://doi.org/10.1073/pnas.2104642118

Kindt R. 2020. AlleleShift: an R package to predict and visualize population-level changes in allele frequencies

in response to climate change. *PeerJ* 9:e11534. https://10.7717/peerj.11534

Knipler ML, Gracanin A, and Mikac KM. 2023. Conservation genomics of an endangered arboreal mammal following the 2019–2020 Australian megafire. *Scientific Reports* 13:480. https://doi.org/10.1038/s41598-023-27587-3

Klichowska E, Wróbel A, Nowak A, and Nobis M. 2025. Eco-evolutionary genomics reveal mountain range-specific adaptation and intraspecific variation in vulnerability to climate change of alpine endemics. *Molecular Ecology* 34:e70113. https://doi.org/10.1111/mec.70113

Koleff P, Urquiza-Haas T, Ruiz-González SP, Hernández-Robles DR, Mastretta-Yanes A, Quintero E, *et al*. 2018. Biodiversity in Mexico: State of knowledge. In: Pullaiah T, editor. *Global Biodiversity Volume 4: Selected Countries in the Americas and Australia* 1st Edition. New York (EEUU): Apple Academic Press; p. 285–337.

Kumar S, Banks TW, and Cloutier S. 2016. SNP discovery through next-generation sequencing and its applications. In: Kumar S. editor. *Crop Breeding Bioinformatics and Preparing for Climate Change*. New York (EEUU): Apple Academic Press; p. 209–244.

Lancaster LT, Fuller ZL, Berger D, Barbour MA, Jentoft S, and Wellenreuther M. 2022. Understanding climate change response in the age of genomics. *Journal of Animal Ecology* 91:1056–1063. https://doi.org/10.1111/1365-2656.13711

Le S, Josse J, and Husson F. 2008. FactoMineR: An R Package for Multivariate Analysis. *Journal of Statistical Software* 25:1-18. https://doi.org/10.18637/jss.v025.i01

Levinsky I, Skov F, Svenning JC, and Rahbek C. 2007. Potential impacts of climate change on the distributions and diversity patterns of European mammals. *Biodiversity and Conservation* 16:3803–3816. https://doi.org/10.1007/s10531-007-9181-7

Lilley TM, Wilson IW, Field KA, Reeder DAM, Vodzak ME, Turner GG, *et al*. 2020. Genome-Wide Changes in Genetic Diversity in a Population of *Myotis lucifugus* Affected by White-Nose Syndrome. *G3 Genes|Genomes|Genetics* 10:2007–2020. https://doi.org/10.1534/g3.119.400966

Luo Y, Qin W, Yan Y, Yin K, Zang R, and Du FK. 2024. Climate change vulnerability and conservation strategies for tertiary relict tree species: Insights from landscape genomics of *Taxus cuspidata*. *Evolutionary Applications* 17(9):e13686. https://doi.org/10.1111/eva.13686

Luu K, Bazin E, and Blum MG. 2017. pcadapt: an R package to perform genome scans for selection based on principal component analysis. *Molecular Ecology Resources* 17:67–77. https://doi.org/10.1111/1755-0998.12592

Marková S, Lanier HC, Escalante MA, da Cruz MO, Horníková M, Konczal M, *et al*. 2023. Local adaptation and future climate vulnerability in a wild rodent. *Nature Communications* 14:7840. https://doi.org/10.1111/1755-0998.12592

McCain CM, and King SR. 2014. Body size and activity times mediate mammalian responses to climate change. *Global Change Biology* 20:1760–1769. https://doi.org/10.1111/gcb.12499

McGowan NE, Roche N, Aughney T, Flanagan J, Nolan P, Marnell F, *et al*. 2021. Testing consistency of modelled predictions of the impact of climate change on bats. *Climate Change Ecology* 2:100011. https://doi.org/10.1016/j.ecochg.2021.100011

McLaughlin JF, Hellmann JJ, Boggs CL, and Ehrlich PR. 2002. Climate change hastens population extinctions. *Proceedings of the National Academy of Sciences* 99:6070–6074. https://doi.org/10.1073/pnas.052131199

Medellín RA, Arita HT, and Sánchez O. 2008. Identificación de los murciélagos de México: Clave de campo (2ª ed.). Mexico City (MEX): Asociación Mexicana de Mastozoología, A.C., Instituto de Ecología, Universidad Nacional Autónoma de México.

Medellín R. 2016. *Leptonycteris nivalis*. *The IUCN Red List of Threatened Species* 2016: e.T11697A22126172. [Accessed on 30 June 2025]. https://dx.doi.org/10.2305/IUCN.UK.2016-1.RLTS.T11697A22126172.en

Meek MH, Beever EA, Barbosa S, Fitzpatrick SW, Fletcher NK, Mittan-Moreau, *et al*. 2023. Understanding local adaptation to prepare populations for climate change. *Bioscience* 73:36–47. https://doi.org/10.1093/biosci/biac101

Mora C, McKenzie T, Gaw IM, Dean JM, von Hammerstein H, Knudson TA, *et al*. 2022. Over half of known human pathogenic diseases can be aggravated by climate change. *Nature Climate Change* 12:869–875. https://doi.org/10.1038/s41558-022-01426-1

Moura MR, Oliveira GA, Paglia AP, Pires MM, and Santos BA. 2023. Climate change should drive mammal defaunation in tropical dry forests. *Global Change Biology* 29:6931–6944. https://doi.org/10.1111/gcb.16979

Moreno-Valdez A, Grant WE, and Honeycutt RL. 2000. A simulation model of Mexican long-nosed bat (*Leptonycteris nivalis*) migration. *Ecological Modelling* 134:117–127. https://doi.org/10.1016/S0304-3800(00)00253-2

Moreno-Valdez A, Honeycutt RL, and Grant WE. 2004. Colony dynamics of *Leptonycteris nivalis* (Mexican Long-Nosed Bat) related to flowering *Agave* in Northern Mexico. *Journal of Mammalogy* 85:453–459. https://doi.org/10.1644/1383942

Nagel JJ, Nelson DM, and Gugger PF. 2023. Population genetic structure and effective size of two endangered cave bat species. *Acta Chiropterologica* 25:203–211. https://doi.org/10.3161/15081109ACC2023.25.2.001

Oksanen J, Simpson G, Blanchet F, Kindt R, Legendre P, Minchin P, *et al*. 2025. Package 'vegan'. *Community Ecology Package, version*, 2:1–295

Pauls SU, Nowak C, Bálint M, and Pfenninger M. 2013. The impact of global climate change on genetic diversity within populations and species. *Molecular Ecology* 22:925–946. https://doi.org/10.1111/mec.12152

Peralta DM, Jaramillo-Correa JP, Hernández-Rosales HS, Túnez JI, Gasca-Pineda J, Medellín RA, *et al*. 2025. To Migrate or not to migrate? Exploring the genomic basis of partial mi-

gratory behavior in bats *Genome Biology and Evolution* 17: evaf203. https://doi.org/10.1093/gbe/evaf203

Peterson ML, Doak DF, and Morris WF. 2019. Incorporating local adaptation into forecasts of species' distribution and abundance under climate change. *Global Change Biology* 25:775–793. https://doi.org/10.1111/gcb.14562

Pina-Martins F, Baptista J, Pappas GJr, and Paulo OS. 2019. New insights into adaptation and population structure of cork oak using genotyping by sequencing. *Global Change Biology* 25:337–350. https://doi.org/10.1111/gcb.14497

Pourshoushtari RD, and Ammerman LK. 2021. Genetic variability and connectivity of the Mexican long-nosed bat between two distant roosts. *Journal of Mammalogy* 102:204–219. https://doi.org/10.1093/jmammal/gyaa138

Privé F, Luu K, Vilhjálmsson BJ, and Blum MG. 2020. Performing highly efficient genome scans for local adaptation with R package pcadapt version 4. *Molecular Biology and Evolution* 37:2153–2154. https://doi.org/10.1093/molbev/msaa053

Qiao H, Soberón J, and Peterson AT. 2015. No silver bullets in correlative ecological niche modelling: insights from testing among many potential algorithms for niche estimation. *Methods in Ecology and Evolution* 6:1126–1136. https://doi.org/10.1111/2041-210X.12397

R Core Team (2025). R: A Language and Environment for Statistical Computing. R Foundation for Statistical Computing, Vienna, Austria. https://www.R-project.org/

Razgour O, Taggart JB, Manel S, Juste J, Ibañez C, Rebelo H, *et al*. 2018. An integrated framework to identify wildlife populations under threat from climate change. *Molecular Ecology Resources* 18:18–31. https://doi.org/10.1111/1755-0998.12694

Rebelo H, Tarroso P, and Jones G. 2010. Predicted impact of climate change on European bats in relation to their biogeographic patterns. *Global Change Biology* 16:561–576. https://doi.org/10.1111/j.1365-2486.2009.02021.x

Rellstab C, Zoller S, Walthert L, Lesur I, Pluess AR, Graf R, *et al*. 2016. Signatures of local adaptation in candidate genes of oaks (*Quercus spp*.) with respect to present and future climatic conditions. *Molecular Ecology* 25:5907–5924. https://doi.org/10.1111/mec.13889

Russello MA, Waterhouse MD, Etter PD, and Johnson EA. 2015. From promise to practice: pairing non-invasive sampling with genomics in conservation. *PeerJ* 3:e1106. https://doi: 10.7717/peerj.1106

Sánchez R, and Medellín RA. 2007. Food habits of the threatened bat *Leptonycteris nivalis* (Chiroptera: Phyllostomidae) in a mating roost in Mexico. *Journal of Natural History* 41:1753–1764. https://doi.org/10.1080/00222930701483398

Schmidt DA, and Russello MA. 2025. Genomic Vulnerability of a Sentinel Mammal Under Climate Change. *Molecular Ecology* 34:e17688. https://doi.org/10.1111/mec.17688

Sherwin HA, Montgomery WI, and Lundy MG. 2012. The impact and implications of climate change for bats. *Mammal Review* 43:171–182. https://doi: 10.1111/j.1365-2907.2012.00214.x

Swets JA. 1988. Measuring the accuracy of diagnostic systems. *Science* 240:1285–1293. https://doi.org/10.1126/science.3287615

Sikes RS. the Animal Care and Use Committee of the American Society of Mammalogists. 2016. Guidelines of the American Society of Mammalogists for the use of wild mammals in research and education. *Journal of Mammalogy* 97:663–688. https://doi.org/10.1093/jmammal/gyw078

Smith AB, Beever EA, Kessler AE, Johnston AN, Ray C, Epps CW, *et al*. 2019. Alternatives to genetic affinity as a context for within-species response to climate. *Nature Climate Change* 9:787–794. https://doi.org/10.1038/s41558-019-0584-8

Thomas CD. 2010. Climate, climate change and range boundaries. *Diversity and Distributions* 16:488–495. https://doi.org/10.1111/j.1472-4642.2010.00642.x

Thuiller W, Georges D, Gueguen M, Engler R, Breiner F, Lafourcade B. *et al*. 2025. biomod2: Ensemble Platform for Species Distribution Modeling. https://doi:10.32614/CRAN.package.biomod2

Trejo-Salazar RE, Gámez N, Escalona-Prado E, Scheinvar E, Medellín RA, Moreno-Letelier A, *et al*. 2023. Historical, temporal, and geographic dynamism of the interaction between *Agave* and *Leptonycteris* nectar-feeding bats. *American Journal of Botany* 110:e16222. https://doi.org/10.1002/ajb2.16222

Trejo-Salazar RE, Gasca-Pineda J, Hernández-Bolaños K, Hernández-Rosales DC, Tapia-López R, Aguirre-Planter E, *et al*. 2025. High genetic variation, low differentiation, and Pleistocene expansions of the migratory and endangered long-nosed tequila bat, *Leptonycteris nivalis*, inferred using both maternal and paternal genetic markers. *PLoS One* 20:e0316530. https://doi.org/10.1371/journal.pone.0316530

Urban MC, Swaegers J, Stoks R, Snook RR, Otto SP, Noble DW, *et al*. 2024. When and how can we predict adaptive responses to climate change? *Evolution Letters* 8:172–187. https://doi.org/10.1093/evlett/qrad038

Waldvogel AM, Feldmeyer B, Rolshausen G, Exposito-Alonso M, Rellstab C, Kofler R, *et al*. 2020. Evolutionary genomics can improve prediction of species' responses to climate change. *Evolution Letters* 4: 4–18. https://doi.org/10.1002/evl3.154

Wanjala G, Astuti PK, Bagi Z, Kichamu N, Strausz P, and Kusza S. 2023. A review on the potential effects of environmental and economic factors on sheep genetic diversity: Consequences of climate change. *Saudi Journal of Biological Sciences* 30:103505. https://doi.org/10.1016/j.sjbs.2022.103505

Wells CP, Barbier R, Nelson S, Kanaziz R, and Aubry LM. 2022. Life history consequences of climate change in hibernating mammals: a review. *Ecography* 2022: e06056. https://doi.org/10.1111/ecog.06056

Weir BS, and Goudet J. 2017. A Unified Characterization of Population Structure and Relatedness. *Genetics* 206:2085–2103. https://doi.org/10.1534/genetics.116.198424

Wiens JJ. 2016. Climate-related local extinctions are already widespread among plant and animal species. *PLoS Biology* 14:e2001104. https://doi.org/10.1371/journal.pbio.2001104

Whitlock R. 2014. Relationships between adaptive and neutral genetic diversity and ecological structure and functioning: a meta-analysis. *Journal of Ecology* 102:857–872. https://doi.org/10.1111/1365-2745.12240

Whitlock MC. 2015. Modern approaches to local adaptation. *American Naturalist* 186:S1–S4. https://doi.org/10.1086/682933

Associated editors: Giovani Hernández Canchola and Pablo Colunga Salas
Submitted: November 18, 2025; Reviewed: December 17, 2025
Accepted: May 8, 2026; Published online: May 29, 2026

THERYA, 2026, Vol. 17(2):277-294 DOI: 10.12933/therya.2026.6265 ISSN 2007-3364

Genomic evidence of a previously undetected *Peromyscus truei* invasion on San Clemente Island, California

Madeleine A. Becker[123], Kayce C. Bell[4], Selena Lopez-Ortiz[2], Jesús E. Maldonado[2,3], Cody W. Edwards[1,3], and Susette Castañeda-Rico[1,2,3,*].

[1]Smithsonian-Mason School of Conservation, Front Royal, VA, USA. E-mail: beckerm@si.edu (MAB); cedward7@gmu.edu (CWE).
[2]Center for Conservation Genomics, Smithsonian National Zoo and Conservation Biology Institute, Washington, DC, USA. E-mail: lopezortizs@si.edu (SLO), maldonadoj@si.edu (JEM).
[3]College of Science, George Mason University, Fairfax, VA, USA.
[4]Natural History Museum of Los Angeles County, Los Angeles, CA, USA. E-mail: kbell@nhm.org (KCB).
[*]Corresponding author: susetteazul@gmail.com; castanedaricos@si.edu

Museum genomics (museomics) provide powerful tools for detecting cryptic diversity in natural history collections, including previously undetected invasions. We analyzed genomic and morphological data from 75 *Peromyscus* specimens collected during the Channel Islands Biological Survey (1939-1941), a series of expeditions on the California Channel Islands spearheaded by the Natural History Museum of Los Angeles County (LACM). Most of these specimens were confirmed as native Channel Island deer mice (*P. gambelii* subspp.), but two specimens from San Clemente Island (SCL) were re-identified as *P. truei*, a species never reported before on the Channel Islands. Using study skins, complete mitogenomes, and low coverage whole-genome data, we confirmed these identifications, and our phylogenetic analyses determined that these *P. truei* individuals are closely related to California mainland populations. We also placed these species within the subfamily Neotominae, including the first mitogenome of a native Channel Island deer mouse. Additional morphological data reveal several more likely *P. truei* specimens, indicating the existence of a substantial populations of this species in 1939. Combined with the presence of other non-native rodents on San Clemente Island (*Reithrodontomys megalotis* and *Microtus californicus*), these findings suggest a possible co-introduction from San Diego County during the 1930s via hay shipments. Our results have important implications for conservation management on San Clemente Island, and potentially Santa Rosa Island, where some specimens appear phenotypically inconsistent with *P. gambelii*. This study highlights the value of molecular tools for reassessing historic collections, especially in dynamic systems subject to high levels of anthropogenic modification.

Keywords: Channel Islands, cryptic diversity, island invasion, museomics, *Peromyscus*.

El estudio genómico de ejemplares de museo (museómica) es una herramienta poderosa para detectar diversidad críptica en colecciones de historia natural, incluidas invasiones previamente no detectadas. Obtuvimos datos genómicos y morfológicos de 75 ejemplares de *Peromyscus* colectados durante el Channel Islands Biological Survey (1939-1941), una serie de expediciones a las Islas del Canal de California encabezadas por el Natural History Museum de Los Angeles County (LACM). La mayoría de estos ejemplares fueron confirmados como ratones ciervo nativos de las Islas del Canal (*P. gambelii* subsp.), excepto dos ejemplares de la Isla San Clemente (SCL) que fueron reidentificados como *P. truei*, una especie nunca antes reportada para las Islas del Canal. El análisis de pieles de estudio, mitogenomas completos y datos del genoma completo de baja cobertura, permitió confirmar estas identificaciones. Los análisis filogenéticos mostraron que los ejemplares de *P. truei* están estrechamente relacionados con poblaciones continentales de California. Asimismo, incluimos estas especies dentro de la subfamilia Neotominae, incorporando el primer mitogenoma del ratón ciervo de las Islas del Canal. Datos morfológicos adicionales indicaron que varios ejemplares probablemente corresponden a *P. truei*, lo que sugiere la existencia de una población sustancial en 1939. Junto con la presencia de otros roedores no nativos en SCL (*Reithrodontomys megalotis* y *Microtus californicus*), estos hallazgos sugieren una posible co-introducción desde el Condado de San Diego durante la década de 1930 mediante envíos de pacas de heno. Nuestros resultados tienen implicaciones importantes para la gestión y conservación en SCL y, potencialmente en Isla Santa Rosa, donde algunos ejemplares parecen ser fenotípicamente inconsistentes con *P. gambelii*. Este estudio destaca el valor de las herramientas moleculares para reevaluar colecciones históricas, especialmente en sistemas dinámicos con altos niveles de modificación antropogénica.

Palabras clave: Diversidad críptica, invasión insular, Islas del Canal, museómica, *Peromyscus*.

Natural history collections (NHC) house irreplaceable records of global biodiversity spanning more than two centuries and increasingly provide the context needed to establish pre-perturbation baselines for threatened populations (Suarez and Tsutsui 2004; Benham and Bowie 2022). By coupling specimens with modern analytical tools, NHC enable retrospective assessments of changes of geographic distribution, phenology, morphology, and genetic diversity over time, often driven by anthropogenic impacts (Meineke *et al.* 2019). Critically, museum genomics (museomics) of historical DNA can also pinpoint the origins and pathways of non-native taxa, resolving the number of introductions, their timing and spread (Kim *et al.* 2023), informing conservation responses to pathogens, disease vectors, and other biosecurity threats (e.g., O'Hanlon *et al.* 2018). As genetic barcoding and genomic tools are applied more broadly, NHC are revealing cryptic invasions events that have gone unrecognized in the natural history literature, and consequently, unaccounted for in conservation management decisions (e.g., Provan *et al.* 2008; Goedknegt *et al.* 2018).

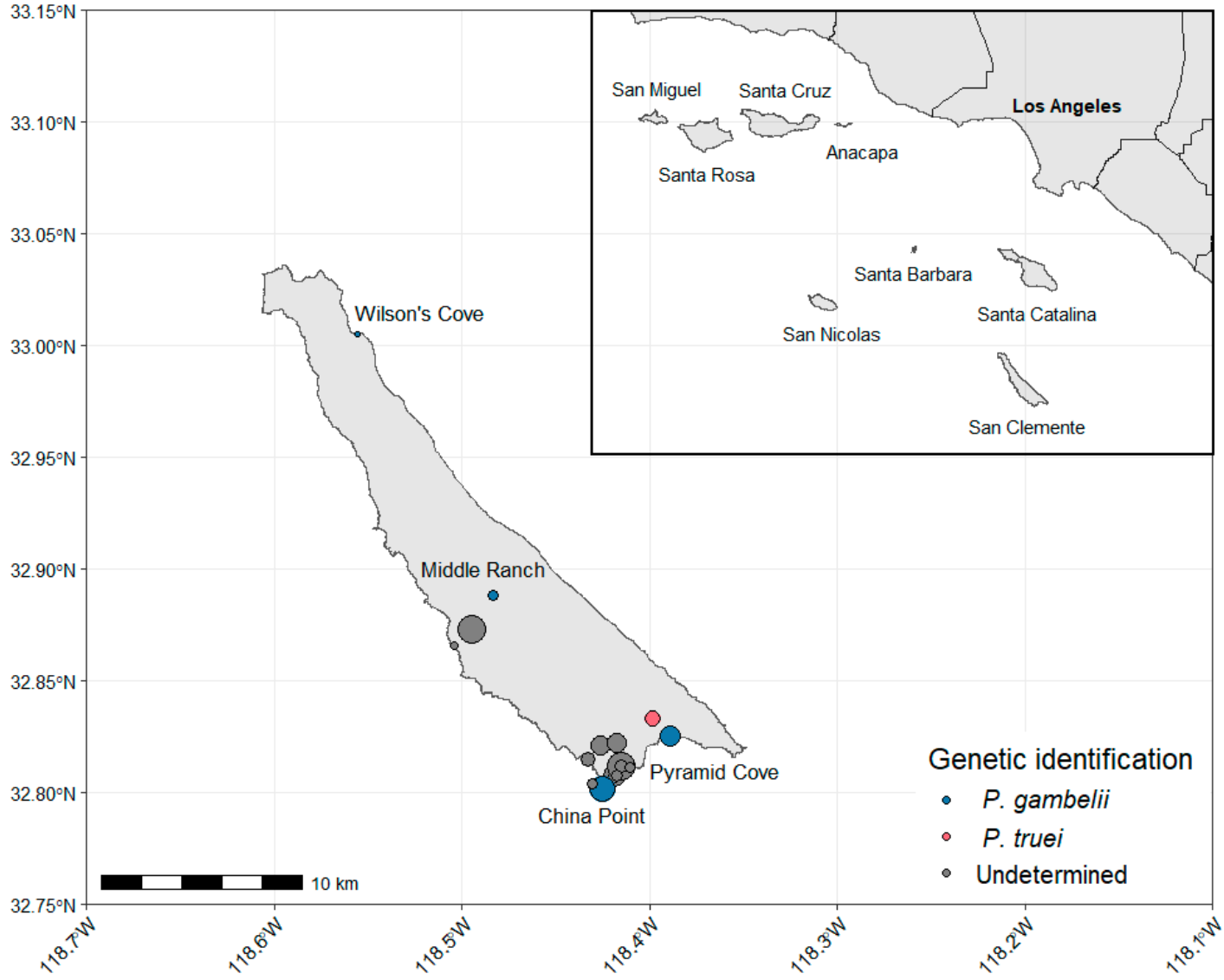

Figure 1. Collecting localities of 287 *Peromyscus* specimens from San Clemente Island, USA, during the Channel Islands Biological Survey (1939-1941). Dot size indicates the number of specimens collected at each site. Colors denote whether sequenced specimens were genetically identified as endemic *P. gambelii clementis* or introduced *P. truei*. Inset: Map of the Channel Islands Archipelago relative to mainland southern California.

The California Channel Islands, an isolated, near-shore archipelago, harbor exceptional endemic biodiversity and a rich archeological record reflecting over 13,000 years of human occupation on the northern islands and at least 9,500 years on the southern islands (Erlandson *et al.* 2011). Despite never being connected to the mainland, long-term human use, historical ranching, and 20th-century military activity have produced complex biogeographic legacies, including introduction of commensal and domestic animals and episodic translocations among islands and with the mainland.

Within this context, the Channel Islands Biological Survey (CIBS; 1939–1941) conducted the only comprehensive archipelago-wide survey to date, leading 13 expeditions and collecting thousands of specimens now curated at the Natural History Museum of Los Angeles County (LACM). San Clemente Island (SCL), the first island visited by CIBS, has experienced intensive sheep/goat ranching and US Navy activity, with documented ecological degradation followed by substantial eradication and restoration efforts (Keegan *et al.* 1994). These histories make CIBS holdings particularly valuable for reconstructing mid-20th century species composition and for detecting previously unrecognized introductions to the islands.

Island deer mice (*Peromyscus gambelii* sensu Greenbaum *et al.* 2017; 2019; Bradley *et al.* 2019) occur on all eight Channel Islands, each with morphologically and genetically distinct subspecies (Gill 1980; Ashley and Wills 1989; Pergams and Ashley 2002). Six island mouse subspecies had been described by the time of CIBS (Mearns 1897; Elliot 1903; Mearns 1907; Nelson and Goldman 1931), and CIBS mammalogist Jack von Bloeker would go on to describe the last two (von Bloeker Jr 1940; 1941). Their extensive Holocene history stretches at least 11,000 years, (Shirazi *et al.* 2018), likely driven by natural and human assisted dispersal, in addition to later contact with mainland lineages on the southern islands (Ashley and Wills 1989; Becker *et al.* 2025).

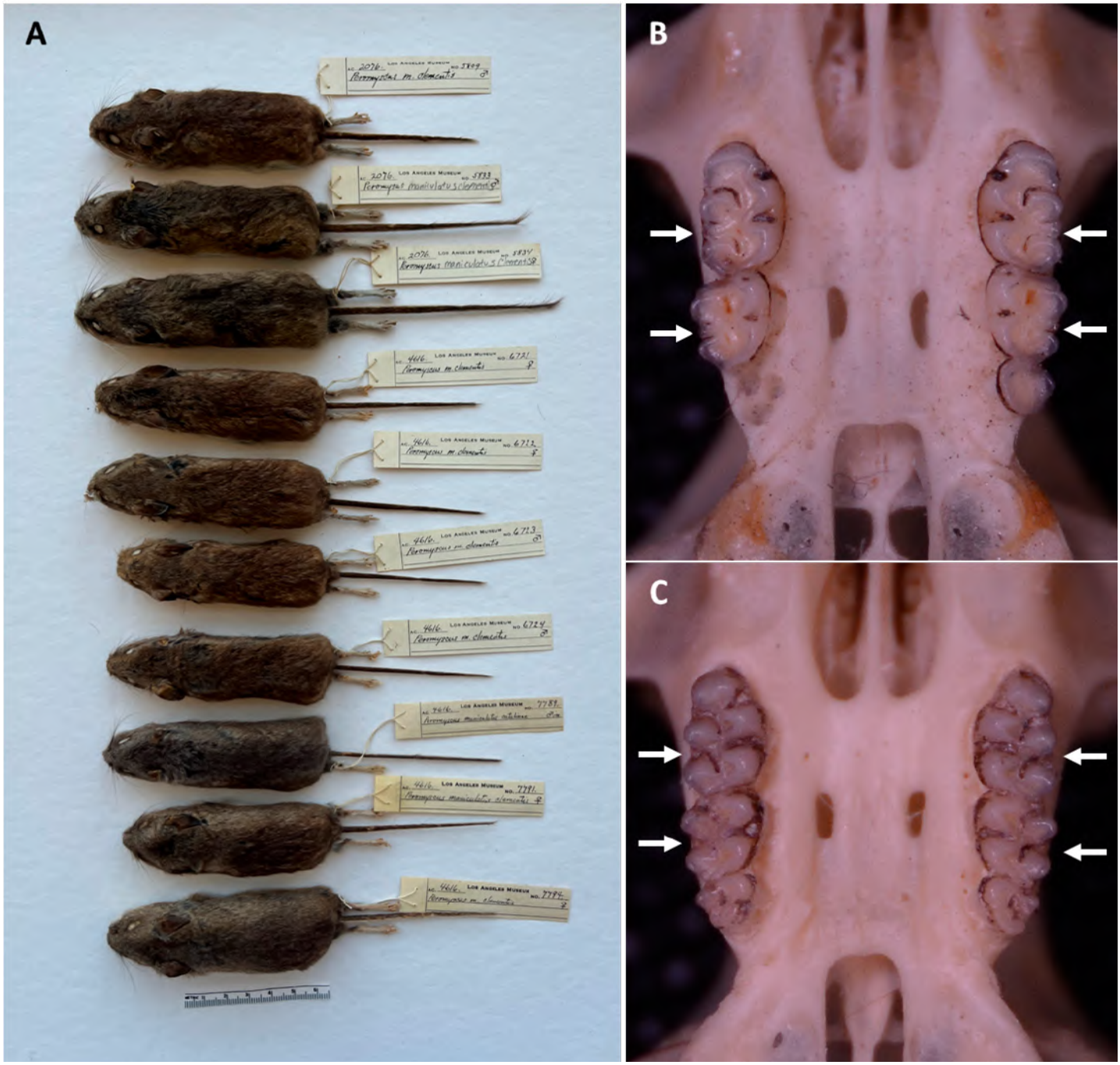

Figure 2. A) *Peromyscus* specimens from San Clemente Island, USA, collected during the Channel Islands Biological Survey (1939-1941) and housed at the Natural History Museum of Los Angeles County. Specimens LACM 5833 and LACM 5834 (second and third from the top, respectively) were re-identified as *P. truei* with genomic data. These specimens show morphological traits distinguishing them from the endemic *P. gambelii*, including longer tails with more densely furred tips, larger total body sizes, and larger ears. Original identifications from collector and CIBS mammalogist Jack von Bloeker appear in pen, while the specific and subspecific epithets in pencil were likely erroneously added later to LACM 5833 and LACM 5834. B) Upper molars of LACM 5834 exhibit diagnostic accessory cusps associated with *P. truei* (white arrows). C) Upper molars of LACM 6722 do not include these accessory cusps (absence indicated by white arrows), consistent with *P. gambelii* identification.

Recent introductions from other *Peromyscus* lineages have not been recorded on the Channel Islands, but given the archipelago's dynamic anthropogenic footprint and the presence of other introduced rodents (von Bloeker Jr 1967; Rick 2013), they may be under-documented. *Peromyscus* are a diverse group of morphologically similar animals which have been difficult to resolve with traditional tools (Platt *et al.* 2015; Castañeda-Rico *et al.* 2025), and contain frequently misidentified lineages (e.g., Light *et al.* 2021). Furthermore, field identification within *Peromyscus* relies on the geographic and ecological context of collection—information which is no longer useful in novel insular contexts. Lastly, rapid morphological adaptation to novel island habitats is common in rodents (e.g., Pergams *et al.* 2015), further impeding accurate identification of newly established populations and raising the possibility of cryptic introductions.

While conducting population genomic research with Channel Island deer mouse specimens (Becker in prep.), we recovered genomic data from two individuals on SCL (Figure

1) that were inconsistent with identification as *P. gambelii*. Here, we revisit the CIBS collections with museomics and morphology to interrogate this finding and reassess CIBS *Peromyscus* specimens. We analyze mitogenomes, low coverage whole-genome data, and study skins and skulls from 75 specimens collected during the CIBS to: 1) test for non-native *Peromyscus* lineages within historic Channel Island collections; 2) phylogenetically place newly identified lineages; 3) evaluate introduction pathways and management implications. We report the first evidence of *P. truei* on the Channel Islands, identify additional likely *P. truei* specimens on SCL consistent with an invasion of multiple individuals, and infer a probable co-introduction pathway via hay bales shipped from San Diego County on the California mainland. Our study demonstrates the power of genetic identification in dynamic systems such as the Channel Islands and underscores the importance of revisiting historical collections with genomic tools.

Materials and methods

Specimen subsampling. We subsampled 75 *Peromyscus* study skins housed in Natural History Museum of Los Angeles County (LACM) mammal collections (Supplemental Data SD1A), primarily to study historical *P. gambelii* population genomics (Becker in prep.). Using sterile techniques, we performed whole claw excision due to documented high performance for this sample type in rodent study skins (McDonough *et al.* 2018). These specimens were originally collected across the eight California Channel Islands during the Channel Islands Biological Survey from 1939-1941. All specimens were catalogued as *Peromyscus maniculatus*, with original specific locality data matching each corresponding island subspecies. Specimens were not morphologically examined during subsampling, since native island mice are the only extant recorded *Peromyscus* occurring on any of the Channel Islands. Ten specimens were sampled from San Clemente Island, including two that we are presently re-identifying as *P. truei* based on morphological and genomic evidence (Figure 2).

Laboratory processing. Specimen subsamples were processed in a specialized ancient DNA facility with no exposure to PCR products or modern DNA. All laboratory work was conducted at the Center for Conservation Genomics (CCG), Smithsonian National Zoo and Conservation Biology Institute. We extracted samples with a modified ancient DNA silica-column protocol (McDonough *et al.* 2018), using either MinElute columns (Qiagen Inc., Valencia, CA, USA) or Zymo Spin Columns (Zymo Research, Irvine, CA, USA). DNA was quantified with 1x dsDNA High Sensitivity Qubit assays (Thermo Fisher, Waltham, MA, USA), and genomic libraries were prepared with the Santa Cruz Reaction customized for each sample's input quantity (Kapp *et al.* 2021). Libraries were indexed with KAPA uracil-tolerant polymerase (Roche Kapa Biosystems, Wilmington, MA, USA) in a modern DNA facility, using Tru-seq style indices. Indexing PCR cycle number was determined by performing quantitative PCR on diluted pre-PCR libraries (Kapp *et al.* 2021). In addition to these specimens, we also prepared genomic libraries with the same methods from a *P. truei truei* tissue sample (USNM 603235, coll. 2017) sheared DNA extract, which was previously sequenced for captured ultraconserved elements and the mitochondrial genome (Castañeda-Rico *et al.* 2025). Genomic libraries were quantified with Qubit and Tapestation High Sensitivity (Agilent Technologies, Santa Clara, CA, USA), equimolarly pooled with other projects, and quality controlled for insert size with Blue Pippin (Sage Science Inc., Beverly, MA, USA). Final pools were submitted for low-coverage paired-end sequencing (150bp PE, 300 cycles) on an Illumina NovaSeq X 25B flow cell (Illumina Inc., San Diego, CA, USA) at the Oklahoma Medical Research Foundation's Clinical Genomics Center.

Mitochondrial genome assembly and initial species identification. Raw sequences were trimmed for adapter content, quality, and length with default parameters in Trim Galore v0.6.10 (Martin 2011), and exact duplicates were removed with prinseq-lite.pl v0.20.4 (Schmieder and Edwards 2011). Mitochondrial genomes (mitogenomes) were assembled from the processed shotgun sequencing data in Geneious Prime® 2025.0.3 using the Geneious mapping algorithm with default parameters and up to five iterations. Initially, all sequences were mapped to the *Peromyscus maniculatus bairdii* reference mitogenome NC_039921, but final versions of the LACM 5833 and LACM 5834 *P. truei* mitogenomes were mapped to the reference *P. truei* mitogenome PP818778 (USNM 603235) for increased mapping quality. Any sites under 5X depth and all ambiguous bases in the consensus sequences for these mitogenomes were called as N. Annotations were transferred from the reference mitogenomes in Geneious and checked for premature stop codons and the presence of nuclear copies of mitochondrial DNA (NUMTs). Cytochrome *b* gene sequences were extracted from mitogenome assemblies for species identification and/or downstream analysis, since only one *P. truei* mitogenome (PP818778) and no island mouse (*P. gambelii* spp.) mitogenomes have previously been published. Initial species identifications were made by querying NCBI's core nucleotide database (core_nt) with cytochrome *b* sequences using BLASTN v2.17.0+ (Camacho *et al.* 2009). Of the confirmed island mouse specimens, we only included data from one SCL specimen (LACM 6722) in further molecular analyses to investigate differences between the *P. truei* collected with native *Peromyscus* on this island.

Nuclear DNA species identification. Since we obtained shotgun sequencing data from LACM 5833 and LACM 5834 as well as the specimen associated with the *P. truei* reference mitogenome (USNM 603235), we wanted to ensure that nuclear DNA also supported the species identification obtained from mitochondrial DNA. To do this, we used Kraken2 v2.1.3 (Wood and Salzberg 2014) to construct a custom database containing all available reference

genomes within the Neotominae subfamily: *P. maniculatus. bairdii* (HU_Pman_2.1), *P. m. sonoriensis* (mPerMan1.0.p), *P. leucopus* (UCI_PerLeu_2.1), *P. eremicus* (PerEre_H2_v1), *P. californicus* (ASM782708v3), *P. polionotus* (HU_Ppol_2), *P. melanophrys* (Pmel_10x_v1), *P. attwateri* (Patt_10x_v1), *P. nudipes* (Pnud_10x_v1), *P. aztecus* (Pazt_10x_v1), *Onychomys torridus* (mOncTor1.1), *O. arenicola* (OncAre_H1_v1), *O. leucogaster* (OncLeu_H2_v1), *Reithrodontomys megalotis* (mReiMeg1.0.p), *Neotoma floridana* (mNeoFlo1.hap1), *N. lepida* (ASM167557v1), *Scotinomys teguina* (ASM4990163v1). Since shotgun sequencing of museum specimens also frequently includes common contaminants, we also added the pre-made "bacteria", "human", and "UniVec_Core" libraries to prevent false hits. Because a genome for *P. truei* has not yet been assembled, we added the quality-checked, merged reads of the USNM 603235 tissue sample as representative sequences of this species. All validated reads from LACM 5833, 5834, and 6722 were queried against this custom database, and krakentools v1.2 (Lu *et al.* 2022) and krona v2.8.1 (Ondov *et al.* 2011) were used to visualize the results.

Whole mitogenome analysis and molecular dating. We conducted multiple whole mitogenome phylogenetic analyses with the three novel mitogenomes and previously published data to 1) robustly confirm the initial *P. truei* species identification of LACM 5833 and LACM 5834, 2) resolve the relationship between these specimens' mitochondrial haplotypes and closely related taxa, 3) and establish the position of *P. gambelii clementis* (LACM 6722).

We used MAFFT v7.490 plugin (Katoh and Standley 2013) in Geneious to align complete mitogenomes generated in this study and in Castañeda-Rico *et al.* (2025). Phylogenetic trees were obtained using Maximum Likelihood (ML) in IQTree v2.3.1 (Minh *et al.* 2020) and Bayesian Inference (BI) in MrBayes v3.2.7a (Ronquist and Huelsenbeck 2003) on partitioned mitogenome alignments. We used ModelFinder, as implemented in IQTree, to find the best-fit model for the ML analysis. IQTree was run with the best-fit models and partitions (TIM2+F+R4, GTR+F+I+R4, GTR+F+I+R5, GTR+F+I+R6, GTR+F+R4; five partitions) and 1000 ultrafast bootstrap replicates, with values of >95 indicating support. We used PartitionFinder 2.1.1 (Lanfear *et al.* 2017) with linked, corrected Akaike Information Criterion (AICc), and greedy parameters, to select the best model and partition scheme for the alignment. The search was limited to the models available in MrBayes. We defined the data block by codon position, tRNA, rRNA and D-loop selection. MrBayes was run with the best-fit model and partitions (GTR+I+G for each of the six partitions) for 50 million generations, with a burn-in of 25%, a sample frequency of 1000 generations, and 4 Markov chains Monte Carlo (MCMC). Posterior probabilities and final topologies result from 50% majority rule consensus trees, with a probability of >0.95 indicating support.

We estimated divergence times in BEAST2 v2.6.7 (Bouckaert *et al.* 2019) using a partitioned alignment. The best-fit model and partition scheme were selected with PartitionFinder 2.1.1, restricted to models available in BEAST and using linked, AICc, and greedy parameters. The data block was defined by codon position, tRNA, rRNA and D-loop selection. We ran the analysis with the best-fit models and partitions (GTR+I+G+X, TRN+I+G; six partitions) under an uncorrelated lognormal relaxed molecular clock model, a calibrated Yule speciation processes model, and with a randomly generated starting tree as priors. Calibrations were based on fossil records of 1) *Onychomys* sp. at ca. 4.85 million years ago (mya), 2) *Peromyscus* sp. at ca. 4.85 mya, and 3) *Reithrodontomys wetmori* at ca. 4.5 mya (see Castañeda-Rico *et al.* 2025). We performed two independent runs of 50 million iterations each, with sample frequency of 1000 iterations. Tracer v1.7.1 (Rambaut *et al.* 2018) was used to check convergence for the Effective Sample Size (ESS), and 25% burn-in was performed in each run. LogCombiner v2.6.6 and Tree Annotator v2.6.2, both packages in BEAST, were used to combine trees and to compile a maximum clade credibility tree with node heigh distribution.

All analyses were performed on the Smithsonian Institution High Performance Computing Cluster (Smithsonian Institution, https://doi.org/10.25572/SIHPC). Trees were visualized with ggtree (Yu *et al.* 2017) in R version R v.4.5.1 (R Core Team 2021).

Phylogeographic analysis of Peromyscus truei with cytochrome b. We conducted phylogeographic analysis with extracted cytochrome *b* genes of LACM 5833 and LACM 5834 and previously published *Peromyscus truei* sequences to infer the origins of the introduction of *P. truei* to SCL. We downloaded all sequenced cytochrome *b* gene fragments greater than 1000 bp from NCBI Genbank (n=82), which were all sequenced from wild-caught museum specimens with locality information. We only analyzed unique haplotypes (n=67) in addition to LACM 5833, LACM 5834, and the *P. truei* reference PP818778 (USNM 603235). We chose related outgroups based on the Neotominae mitogenome phylogeny (Castañeda-Rico *et al.* 2025): *P. gratus gratus* (AY376421), *P. gratus gentilis* (AY376420), *P. gratus zapotecae* (AY376423), *P. ochraventer* (PP818776), *P. attwateri* (ON528112), *P. nasutus* (PP818775). *P. pectoralis* (KY707309), and *Habromys ixtlani* (KY707304). The resulting dataset (n=78) was aligned with the MAFFT v7.490 plugin in Geneious.

Phylogenetic trees were built using ML (IQTree v2.3.1) and BI (MrBayes v3.2.7a) on unpartitioned cytochrome *b* alignments. We also used ModelFinder as implemented within IQTree to find the best models for both analyses. IQTree was run with the best-fit model (TIM2+F+G4) and 1000 ultrafast bootstraps, with a score of >95 indicating support. We ran MrBayes with the best-fit model (GTR+F+G4) for 20 million generations with a burn-in of 25%, a sample frequency of 1000, and 4 MCMC. Posterior probabilities and final topologies result from 50% majority rule consensus trees, with a probability of >0.95 indicating support.

Morphological analysis. We examined study skins of the SCL specimens included in our genomic analyses (Figure

2) and compared their original measurements to those of genetically confirmed *P. gambelii* and *P. truei* to other *Peromyscus* specimens collected during the CIBS across the Channel Islands. The goals of the morphological analyses were: 1) to determine whether LACM 5833 and LACM 5834 skins comported with morphological characters consistent with the genetic identification of *P. truei*, and 2) to detect any other putative misidentifications present in LACM Channel Island deer mice collections. We also examined a subset of skulls to assess dental traits diagnostic of *P. truei*, specifically the presence of accessory cusps (mesolophs) on upper molars (Ingles 1965).

Of the total 709 *Peromyscus* specimens collected during the CIBS and housed at LACM, we restricted analyses to the 703 specimens prepared by Jack von Bloeker to ensure measurement consistency. Juveniles and subadults were retained due to inconsistent age class labels, but two extreme outliers in tail or total length (due to tail damage) were removed, resulting in a final dataset of n=701 (Supplemental Data SD1B). This dataset includes 277 specimens caught on SCL, including those sequenced for genomic analysis. Since *P. truei* typically exhibits larger body size with longer tails proportional to their body size and larger ears compared to *P. gambelii*/*maniculatus* (Ingles 1965), we plotted the distribution of these traits using von Bloeker's original measurement data. Each island was treated as a separate population, and genetically confirmed individuals were concurrently plotted to visualize where *P. gambelii* and *P. truei* fell within island-specific distributions. These analyses were not performed to compare *P. gambelii* and *P. truei* specimens, but to better understand how our genetically identified individuals compared to the morphological variation found in each island *Peromyscus* population. To assess potential confounding effects of sexual dimorphism, pregnancy, and immaturity, we also plotted trait distributions by sex, known reproductive status, and recorded age class. All calculations and plots were made in R v.4.5.1 with tidyverse packages (Wickham *et al.* 2019).

Six specimens collected on SCL during the CIBS and now housed at the Santa Barbara Museum of Natural History were also examined, but were ultimately not included in this dataset as three of these specimens were originally identified as *Onychomys* and mistakenly re-labeled as *P. maniculatus*. We also examined 157 Channel Island *Peromyscus* specimens housed at the Smithsonian National Museum of Natural History (USNM) and collected in 1892-1931, prior to the CIBS. These specimens were largely collected before mammal body measurements were standardized, with many incomplete datapoints including few ear measurements. They were also prepared by several different collectors at multiple time points, so they were not included in the CIBS dataset. However, these collections remain an important reference point, and were still checked for diagnostic *P. truei* external characters such as high tail to body size ratios and tail tip fur density (Ingles 1965).

Results

Mitochondrial genome assembly and initial species identification. Mitogenomes from LACM 5833, 5834, and 6722 were successfully recovered from assembled shotgun data, with average depths of 70-104.4X (Supplemental Data SD2). However, likely structural variation in the D-loop led to low depth and poor assembly at the end of this region for the two *P. truei* samples. Reads were re-assembled with GetOrganelle to try to recover mitochondrial genomes without these small ambiguous regions, but this method resulted in 3-6 short contigs and did not cover the entire mitochondrial genome. Nonetheless, the final Geneious assemblies only contained 34-51 ambiguities, and variants in the rest of the mitochondrial genome were sufficient for downstream analysis. Annotated mitogenomes for these three specimens have been deposited in GenBank (PZ213495-PZ213497), and raw reads for these specimens and USNM 603235 can be found on the Sequence Read Archive (SRR37837849-SRR37837852; Supplemental Data SD1C).

The mitogenomes of LACM 5833 and LACM 5834 differed by 159 nucleotide positions, corresponding to a pairwise identity of 99.0%. Both haplotypes returned the same top BLAST hit: the *P. truei* reference mitochondrial genome (GenBank accession PP818778; voucher USNM 603235), with 96.04-96.22% pairwise identity. In contrast, the SCL island deer mouse (LACM 6722) matched most closely with a *P. maniculatus rufinus* voucher (USNM 603271, Figure 3), with a 96.25% pairwise identity. Pairwise identity between the *P. truei* collected on SCL and the *P. gambelii clementis* (LACM 6722) mitogenome was 86.5-86.7%.

The cytochrome *b* sequences extracted from LACM 5833 and 5834 were also unique, differing by nine nucleotide positions across a 1,144 bp region. Assemblies in this region were of high quality, with an average sequencing depth of 83-104X and a minimum depth of 53-55X. Neither haplotype had an identical match in the NCBI core_nt BLAST database; however, both showed high percent identity to multiple available vouchered *P. truei* specimens from California. The top BLAST hit for LACM 5833 was MVZ:Mamm:198610, a *Peromyscus truei montipinoris* collected in Kern County, CA (99.56%), with 30 total hits over 99% percent identity. For LACM 5834, the top BLAST hits were MVZ:Mamm:157332 and MVZ:Mamm:157330 (*Peromyscus truei gilberti)* collected in Berkeley, CA with 99.48% identity and 10 total hits over 99% percent identity.

The cytochrome *b* sequence extracted from LACM 6722 was 99.83% identical to previously sequenced island deer mice from San Clemente and Santa Catalina Islands (Becker *et al.* 2025). All other LACM *Peromyscus* subsampled from the CIBS expedition harbored either identical or very closely related haplotypes to previously reported Channel Island deer mouse cytochrome *b* sequences. Nine novel haplotypes were identified and deposited on GenBank (PZ213486-PZ213494; Supplemental Data SD1C). These sequences were generated primarily to confirm species identification in morphological re-examination of

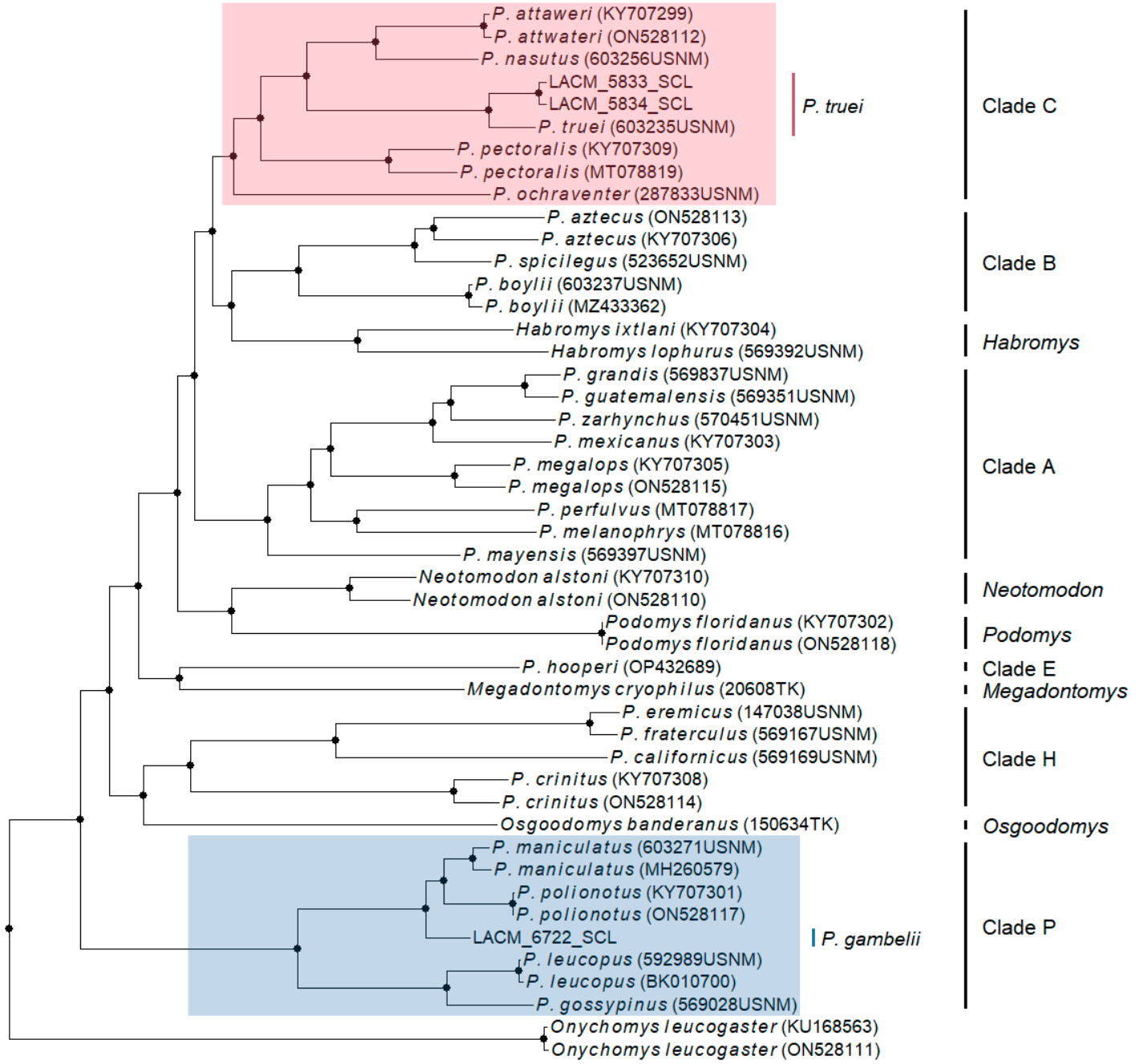

Figure 3. Bayesian mitogenome consensus tree showing positions of LACM 5833 and LACM 5834 (*P. truei*) and LACM 6722 (*P. gambelii clementis*), subset to the tribe Peromyscini and its sister genus (*Onychomys*). The *Peromyscus truei* species group is highlighted in red, and the *Peromyscus maniculatus* species group is highlighted in blue. Clade names and sequences are replicated from Castañeda-Rico *et al.* 2025. Nodes with black dots indicate high support with posterior probabilities >0.95.

specimens; no further molecular analysis were conducted on these samples.

Nuclear DNA identification. Validated shotgun reads from LACM 5833, 5834, and 6722 all contained high amounts of cricetid DNA (81-87%) according to the Kraken2 custom database search. Each library contained small numbers of human and bacterial reads and a significant number of unclassified reads (13-19%). This contamination is consistent with the age and preservation of the specimens (coll. 1939), and the unclassified reads may likely include fungi or other eukaryotic microbes found on study skins or pests present in collections (Raxworthy and Smith 2021). The highest species-resolved hit for LACM 5833 and 5834 was *P. truei*, with 31% of reads classified to this species. Despite our biased method of adding *P. truei* shotgun sequencing data to the custom database versus using an assembled genome like the other rodents, 22% of *P. gambelii clementis* reads were successfully classified as most related taxon of *Peromyscus maniculatus*, with a higher percentage of reads only classified to the genus level (43%). 1% of LACM 6722 reads were classified as *P. truei*, and 2% of LACM 5833 and 5834 reads were classified as *P. maniculatus*. These numbers are comparable to other Neotominae off-target classifications and seem likely driven by conserved regions of the genome between related species, rather than cross-contamination or hybridization (Supplemental Data SD3).

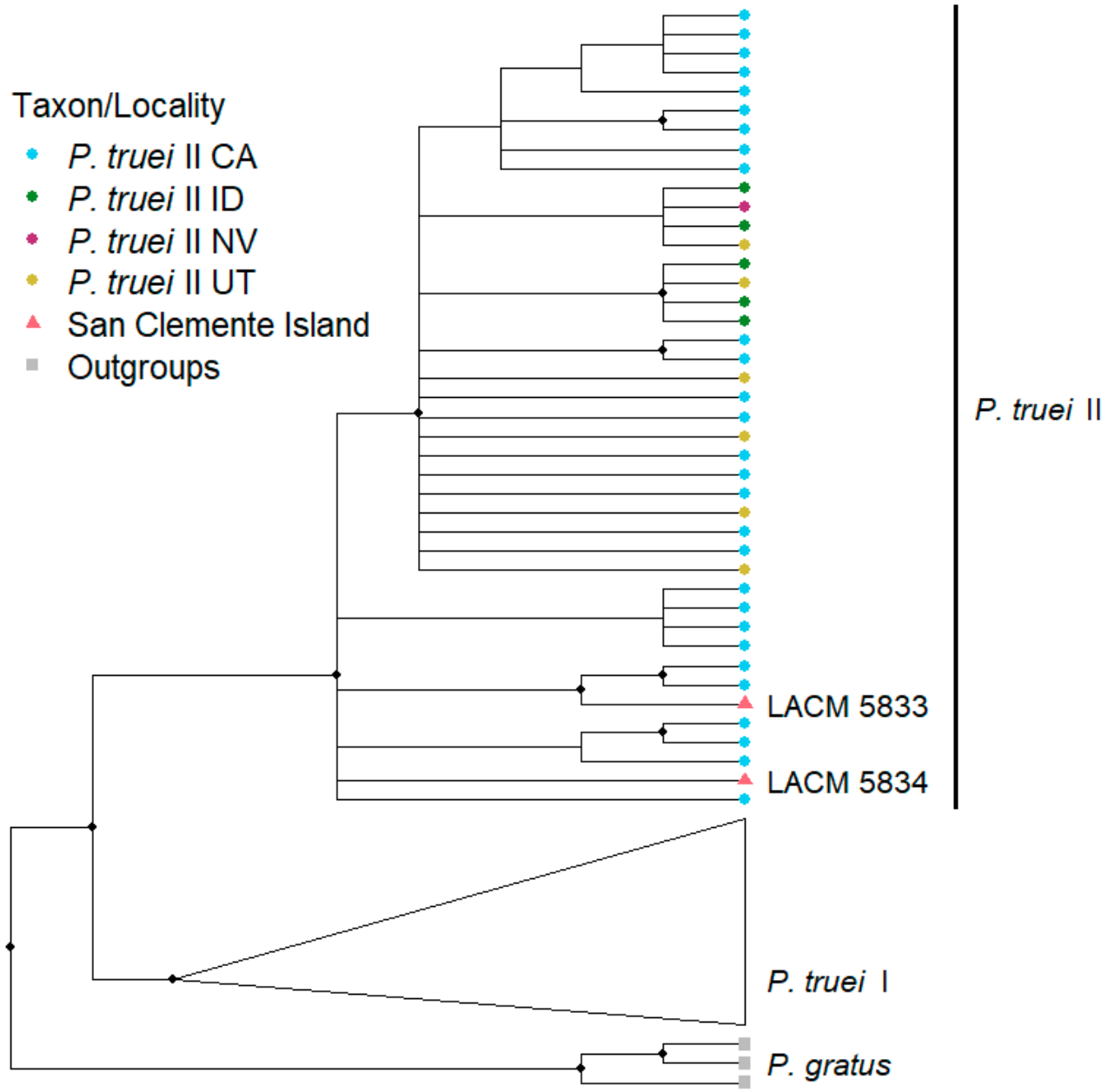

Figure 4. Bayesian cytochrome *b* consensus tree showing positions of LACM 5833 and LACM 5834 within *Peromyscus truei*. Clades are labeled in accordance with Hernández-Canchola *et al.* (2022). The *P. truei* II clade includes all haplotypes sequenced from California specimens. This phylogenetic tree has been subset to *P. truei* and its sister (*P. gratus*) for relevance. Nodes with black dots indicate high support with posterior probabilities >0.95.

Mitogenome phylogenetic analysis and molecular dating. In both BI and ML trees, LACM 5833 and LACM 5834 were recovered as sisters to each other and then sister to the *P. truei* reference mitogenome (USNM 603235), confirming the species identification as *P. truei* (Figure 3, Supplemental Data SD4-5). The reference genome is *P. truei truei*, which has previously been shown to belong to a separate clade from the western subspecies of *P. truei* (Hernández-Canchola *et al.* 2022). BEAST dated the split between the *P. truei truei* mitogenome and the LACM haplotypes to 512-670 kya, demonstrating significant distance between these two clades (Supplemental Data SD4).

LACM 6722 was recovered within the *Peromyscus maniculatus* species group (Clade P), sister to a clade of samples identified as *P. maniculatus rufinus*, *P. maniculatus bairdii*, and *P. polionotus* (1.0 posterior probability; 100 UF bootstrap). This position is consistent with previous placement of *P. gambelii* (Bradley *et al.* 2019; Greenbaum *et al.* 2019) and Channel Island mice specifically (Becker *et al.* 2025) within the *Peromyscus maniculatus* species group using cytochrome *b*. However, this position is not stable, since the relationship between *P. maniculatus* and *P. polionotus* is not resolved in the ML tree (92 UF bootstrap, Supplemental Data SD5), and in the BEAST tree, LACM 6722 is recovered as sister to the *P. maniculatus* mitogenomes only. This complex in general has been difficult to resolve and requires more loci to fully disentangle these relationships (Bradley *et al.* 2019; Castañeda-Rico *et al.* 2025). Nonetheless, BEAST dates the split between *P. gambelii clementis* and its sisters to 554-745 kya. This is

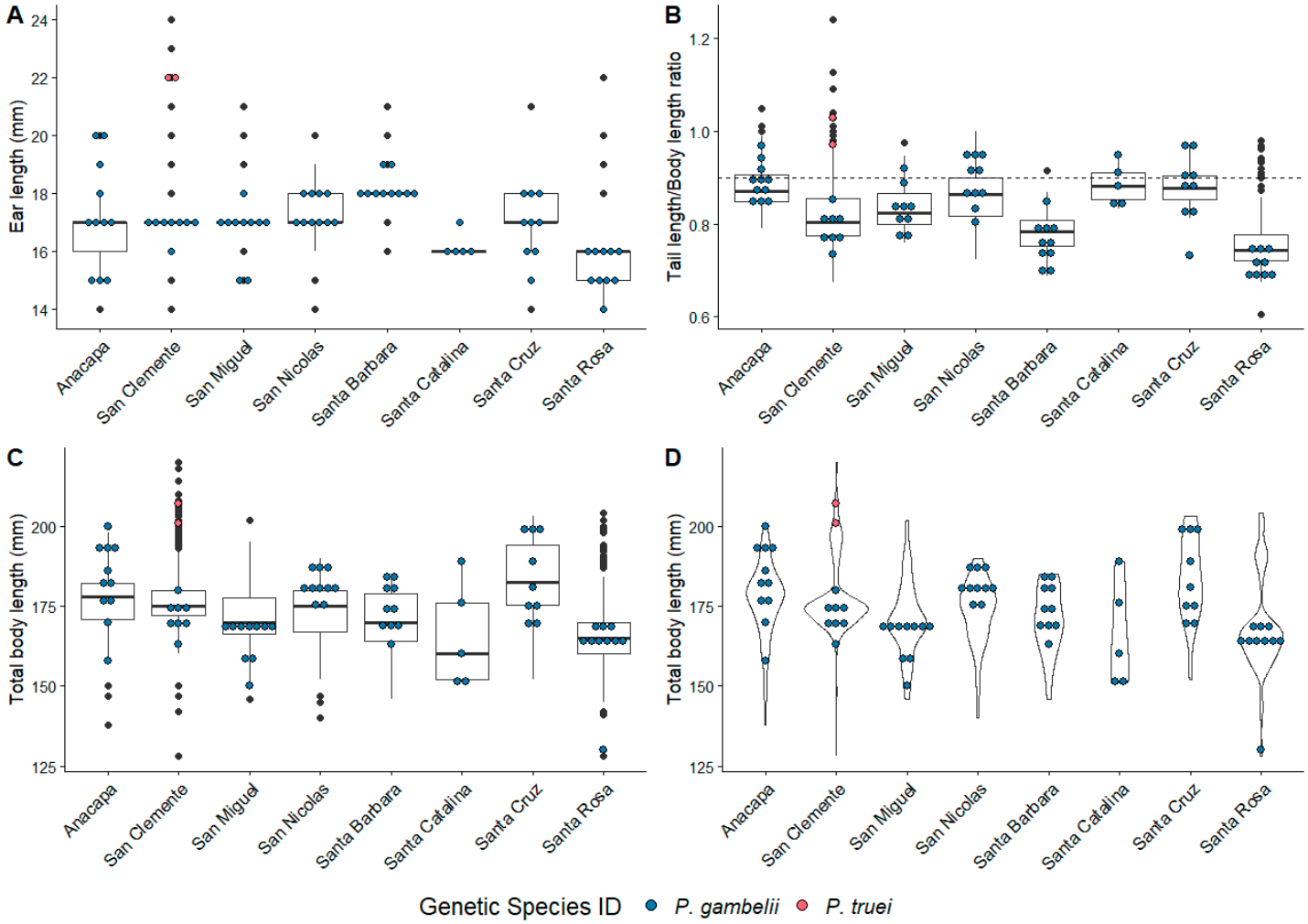

Figure 5. Distribution of study skin measurements recorded from Channel Islands Biological Survey specimens (n=701) prepared by Jack von Bloeker, including 75 genetically identified individuals, endemic *P. gambelii* (blue) and introduced *P. truei* (red), across each of the Channel Islands. A) Boxplot of ear length (mm). B) Boxplot of tail length to body length ratio; dashed line at 0.9 indicates threshold distinguishing *P. truei* from *P. gambelii* (Ingles 1965). C) Boxplot of total body length including tail (mm). D) Violin plot of total body length including tail (mm).

notably a shorter time than the 1.8 mya split previously estimated with cytochrome *b* (Bradley *et al.* 2019).

Cytochrome b phylogeographic analysis. Phylogenetic analysis of *P. truei* cytochrome *b* haplotypes recovered the two major clades identified by Hernández-Canchola *et al.* (2022). The *P. truei* I clade includes the *P. t. truei* reference mitogenome from New Mexico and other specimens from Arizona, Colorado, New Mexico, Oklahoma, Texas, and Utah (Figure 4). The *P. truei* II clade comprises specimens from California, Idaho, Nevada, and Utah. While we did not examine these specimens to verify their subspecies assignment within each clade, the observed geographic structuring is consistent with previous findings (Hernández-Canchola *et al.* 2022). The *P. truei* I clade was not resolved in the ML tree (Supplemental Data SD6), but *P. truei* II was supported in both ML and BI trees.

LACM 5833 and LACM 5834 were recovered in the *P. truei* II clade, which also contained all other specimens collected in California. We did not recover fine phylogeographic structure within the major clades, with polytomies in both ML/BI trees, limiting our ability to identify a source population for the *P. truei* caught on SCL. LACM 5833 is sister to haplotypes associated with MVZ specimens caught in Berkeley, CA, as suggested by the BLAST search, but this relationship only had support in the BI tree. The phylogenetic position of LACM 5834 was not resolved within the *P. truei* II clade.

Morphological analysis. LACM 5833 and LACM 5834 are much larger than the other SCL *Peromyscus* we sequenced (Figure 2) and have diagnostic features associated with *P. truei*. Their total body sizes are over 200 mm in total length (201, 207), with high tail to body ratios (0.97, 1.0), large ears (22 mm each), and visibly denser fur at the tip of the tail (Figure 2A). While the teeth of LACM 5833 were too worn for analysis, LACM 5834 exhibits distinct mesolophs/accessory cusps on its molars (Figure 2B), consistent with *P. truei* dental characters (Ingles 1965). By contrast, the specimens genetically confirmed as *P. gambelii clementis* have a median total body size of 172 ± 5.2 mm, a tail to body ratio of 0.79 ± 0.04, an ear length of 17 ± 0.4 mm, no tail tufting, and no accessory cusps (Figure 2C). The median measurements for these values across the 277 SCL specimens are relatively consistent with these specimens, but with high standard deviations: 175 ± 12.2 mm total length, 0.80 ± 0.08 tail/

body ratio, and 17 ± 2.0 mm ear length. Boxplots of this population demonstrate that abnormally large specimens are not limited to LACM 5833 and LACM 5834; there are a significant number of outliers with much larger total body lengths, tail ratios, and ear sizes (Figure 5A-C). In fact, this distribution is nearly bimodal, with few specimens of intermediate size, and the genetically identified *P. truei* specimens clustering with other outliers (Figure 5D). We did observe densely furred tail tips in some of these specimens, but this character is inconsistent and dependent on specimen preparation and preservation.

Across the Channel Islands, median measurements and distributions differed between island populations, consistent with prior morphological studies. While SCL specimens were either distributed solidly below or above the 0.9 tail/body length ratio used in differentiating *P. truei* and *P. maniculatus* (Ingles 1965), this value overlapped with the distribution of other islands. Santa Cruz Island contained the largest individuals, with total body size of genetically confirmed *P. gambelii* specimens comparable to the outliers on SCL. Some sporadic large specimens with long tails collected on Anacapa, San Nicolas, Santa Barbara, and Santa Catalina were also genetically confirmed as *P. gambelii*. By contrast, the median measurements of Santa Rosa Island deer mice were the smallest of any island, but also contained many large outlier specimens, none of which were sequenced. The measurements of these outliers were generally not as high as the SCL outliers and overlapped with distributions on other islands (Figure 5C). Nonetheless, the violin plot of Santa Rosa Island total body length was the only other island to show a more bimodal distribution like SCL (Figure 5D). Some outliers for total body length on SCL, Anacapa, San Miguel, and San Nicolas were pregnant when collected (Supplemental Data SD7A), but sexual dimorphism did not explain any general size distribution patterns (Supplemental Data SD8). Many, but not all, small-bodied outliers were recorded as immature, and three outliers for high total body length on SCL were also immature individuals (Supplemental Data SD7B).

Study skins housed at the Smithsonian National Museum of Natural History and collected before the CIBS contain few abnormally large specimens, except on Santa Cruz Island (Supplemental Data SD9), where large-bodied island mice have previously been documented. Of the six specimens from the Santa Barbara Museum of Natural History Museum collected during the CIBS, three were *Onychomys* specimens which had been incorrectly re-labeled as P. maniculatus (SBMNH:MAM:7621; SBMNH:MAM:9202-9203; Supplemental Data SD10). Of the *Peromyscus* specimens, two (SBMNH:MAM:7619, SBMNH:MAM:7620) were large-bodied (total length 198, 192 mm, respectively) with large ears (19 mm) and intermediate tail size (0.9, 0.88 tail/body ratio; Supplemental Data SD11). These measurements are consistent with descriptions of both *P. maniculatus* and *P. truei* (Ingles 1965). Neither specimen displayed dense fur at their tail tips of (Supplemental Data SD10), yet both were substantially larger than the median SCL island deer mouse.

Discussion

Mitochondrial genomes, low coverage nuclear data, and morphological characters of LACM 5833 and LACM 5834 confirm their identity as *P. truei*, not the endemic SCL deer mouse *P. gambelii clementis*. These specimens represent the first assembled mitogenomes from the western "*P. truei* Clade II" (*P.* cf. *martirensis*; Hernández-Canchola *et al.* 2022), which we estimate diverged from "*P. truei* Clade I" ~512-670 kya. Distinct mitogenome haplotypes indicate multiple individuals were introduced rather than a single pregnant female. Morphometric analysis of other CIBS specimens revealed additional individuals with ear and tail measurements consistent with *P. truei*, suggesting breeding *P. truei* populations on SCL in the 1930s. Although limited phylogeographic resolution at cytochrome *b* precludes pinpointing a source population of the detected invasion, the closest related haplotypes derived from mainland California *P. truei*. This pattern aligns with historical accounts of hay shipments introducing other rodents, including *Microtus californicus* and *Reithrodontomys megalotis* (von Bloeker Jr 1967), and underscores how human-mediated movements repeatedly reshaped island faunas.

Anthropogenic history of Channel Island rodents and San Clemente Island. The archaeological record shows that *P. gambelii* arrived on the Channel Islands after or concurrently with humans (Shirazi *et al.* 2018), suggesting that deer mice were inadvertently introduced some 13,000 years ago. Trade networks between the mainland and among the Island Chumash and Gabrielino/Tongva peoples living on the Channel Islands likely provided further opportunities for translocation (Johnson *et al.* 1983), which may also explain Holocene introductions of harvest mice (*Reithrodontomys megalotis*) on Santa Catalina and Santa Cruz Islands (Ashley 1989). Other mammals, such as the island fox and the Catalina ground squirrel, may have been intentionally translocated by Indigenous people (Collins 1991a; 1991b; Rick *et al.* 2009; 2019; 2024). However, in addition to these species which have lived on the Channel Islands for thousands of years, several rodents were repeatedly introduced during 19th-20th centuries along with other commensal and domestic animals: *Rattus norvegicus* on Catalina; *Rattus rattus* on Catalina, San Clemente, San Miguel, and Anacapa Island; *Mus musculus* on Catalina and San Clemente; *Microtus californicus* on Catalina and San Clemente, and *Reithrodontomys megalotis* on San Clemente (Rick 2013). While many islands experienced agricultural activity and mainland connectivity during this period, this especially rich rodent diversity on the SCL including adept island invaders like *Rattus* and *Mus* is striking.

While considered federal land since 1850, SCL was used primarily for private ranching operations until the US Navy assumed control in 1934. Today, Naval Base Coronado administers military operations on SCL, including extensive training facilities and the US Navy's last remaining ship-to-shore live firing range. Increasing military development during the 1930s was a motivating factor for the CIBS

team to begin expeditions on SCL as quickly as possible, according to their initial proposal for the survey (Laverty 2020). However, there had already been a long history of ecological deterioration on the island due to the impact of sheep and goat ranching. The San Clemente sheep company operated from at least 1879, grazing tens of thousands of sheep on the island. Feral goats, likely the most destructive of the animals introduced to SCL, were finally eradicated in 1991 by the US Navy, with over 29,000 total goats removed since 1972 (Keegan *et al.* 1994). CIBS botanist Meryl Dunkle wrote that, "The heavy grazing of sheep and goats in the past gave such a desolate appearance to the island that it seemed superficially of but little interest to the botanist" (Dunkle 1943). However, SCL is recognized today for harboring the highest number of endemic plants in the Channel Islands archipelago (Raven 1963), aided by Navy conservation and restoration efforts.

Today, proactive biosecurity measures are in place on the Channel Islands (e.g., Brenner *et al.* 2025), as stakeholders understand the potential for invasive species undermining meticulous conservation restoration efforts. Millions of dollars have been spent eradicating feral animals left behind from the ranching period, especially as these species have threatened charismatic endemics: feral goats on SCL degraded habitats for the loggerhead shrike (*Lanius ludovicianus mearnsi*) and island night lizard (*Xantusia riversiana reticulata*) (Scott and Morrison 1990; Keegan *et al.* 1994); feral ungulates on the northern Channel Islands indirectly led to hyperpredation on island foxes from golden eagles (Roemer *et al.* 2001; Coonan *et al.* 2014); feral cats on Santa Barbara and rats on Anacapa predated on the rare Scripps's murrelet (*Synthliboramphus scrippsi*) (McChesney and Tershy 1998; Whitworth *et al.* 2013). Invasive species and habitat degradation on Anacapa and SCL have also impacted island deer mice, resulting in the State of California recognizing these two subspecies, *P. g. anacapae* and *P. g. clementis*, as critically imperiled (California Natural Diversity Database 2026). Monumental eradication efforts led by collaborations between National Park Services, the US Navy, and conservation organizations have led to the recovery and delisting of many Channel Islands species from the endangered species act, including the island fox and island night lizard (US Fish and Wildlife Service 2014; 2016), and recently on SCL, a unique Bell's sparrow subspecies (*Artemisiospiza belli clementeae*) and four endemic plants (US Fish and Wildlife Service 2023).

Timing and pathways of introduction. Mammalogist Jack von Bloeker collected both native and introduced mammals during the CIBS, and attempted to infer their colonization histories in his comprehensive list of Channel Island mammals (von Bloeker Jr 1967). For example, he examined 28 *M. californicus* and 36 *R. megalotis* specimens from SCL, and determined that they were indistinguishable from geographically proximate mainland species (von Bloeker Jr 1967). He hypothesized that both of these species were inadvertently introduced by imported hay from San Diego County: "In April, 1939, I obtained information which supports this suggestion from a conversation with Mr. Theodore Murphy, United States Marshal, who was stationed on the island at that time and was the recipient of the hay as feed for his horse which he used in patrolling the island" (von Bloeker Jr 1967). These *Microtus* and *Reithrodontomys* were collected in geographic proximity to both confirmed *P. gambelii* and *P. truei* on southern SCL. In addition, six *Onychomys* specimens were also collected by von Bloeker in this area (LACM 6593- 6594, LACM 6596; SBMNH:MAM:7621, SBMNH:MAM:9202-9203), which are the only *Onychomys* individuals ever recorded on any of the Channel Islands (Knapp *et al.* 2021).

The co-localized collection of non-native *Microtus*, *Reithrodontomys*, and *Onychomys* on southern SCL indicates an active route for wild (not just commensal) rodent invasions from mainland California during the Channel Islands ranching era. Furthermore, von Bloeker's correspondence with Theodore Murphy, who was ranching on SCL prior to serving as US Marshal, supports hay shipments as the introduction pathway for at least two of these species. If *P. truei* arrived contemporaneously, its introduction likely occurred after 1926 when Murphy began activity on SCL. This timeline is concordant with earlier *Peromyscus* specimens (n=37) collected on SCL between 1894-1897 by Mearns, Anthony, and Gaylord from the International Boundary Commission, which are phenotypically consistent with *P. gambelii* (Supplemental Data SD9). Because localities for these earlier specimens are unrecorded, and CIBS sampling was concentrated at the island's southern end, our ability to infer the distribution or spread of *P. truei* remains limited.

Specimen identification and historical notes. Given von Bloeker's extensive experience collecting and identifying rodents across California, it is notable that he did not classify any SCL specimens as *P. truei*. Specimens such as LACM 5833 and 5834 exhibit distinct tail tips, diagnostic dental characters, and body size significantly larger than both Mearns's descriptions and von Bloeker's average *Peromyscus* specimens. Unfortunately, von Bloeker's complete field notes are unavailable, and because SCL mice had already been described as a subspecies, he did not formally analyze them as he did for Santa Rosa and Anacapa Islands. However, original tag labels suggest he may have recognized some of these large mice as atypical: while most were labeled "*Peromyscus maniculatus clementis*" or "*Peromyscus m. clementis*", the original pen labels of LACM 5833, 5834, and other specimens were solely labeled "*Peromyscus*" (Figure 2). Later curatorial staff added species and subspecies epithets in pencil, but von Bloeker himself appears not to have resolved these identifications. Notes from a 1941 expedition to SCL further support this interpretation: "Jack von Bloeker secured … a considerable number of the San Clemente white-footed mouse, *Peromyscus maniculatus clementis*. In addition, several examples of *Peromyscus*, *Reithrodontomys* and *Microtus*, not yet

determined, were taken, and are being given further study" (Comstock 1946). Some pencil annotations even list the species epithet such as "*boylii*" or "*californicus*", though no diagnostic characters for these species were observed in the specimens we examined. Nonetheless, we recommend molecular identification for these specimens, especially those with damaged teeth or without skulls, to definitively resolve this issue without further misidentifications.

Several unusually large *Peromyscus* specimens from Santa Rosa and Anacapa Islands share similar labeling patterns to those on San Clemente, with pen-labeled "*Peromyscus*" and pencil-marked "*boylii*". On Anacapa, four such specimens (LACM 7394-7397) were genetically confirmed *P. gambelii*, along with other individuals with outlier total body lengths (Figure 5C). von Bloeker himself noted large body sizes and tail lengths in his description of the Anacapa subspecies (von Bloeker Jr 1941), and large body sizes and tail lengths on Santa Cruz Island are consistent with known subspecific traits (Nelson and Goldman 1931), with multiple outliers for total body length genetically confirmed as *P. gambelii*.

Santa Rosa Island presents a more ambiguous case. A significant series of large-bodied specimens collected in 1939 from Elderberry and Cherry Canyons were not genetically tested, and dental characters were inconclusive. von Bloeker described *P. m. sanctaerosae* as one of the smallest island mouse subspecies with uniquely short tails (von Bloeker Jr 1940), yet our morphological analysis identified several outliers exceeding 170 mm in total length. Comparing von Bloeker's reported specimen counts to current LACM holdings suggests that these outliers were excluded from his subspecies description, possibly because he did not consider them *P. m. sanctaerosae*. Their collection near Vail Ranch, where calves were routinely shipped for nearly a century, provides a plausible introduction pathway via livestock transport. Without genetic data or field notes, the identity of these large Santa Rosa mice remains unresolved.

Although we detected evidence of non-native *Peromyscus* on San Clemente and possibly Santa Rosa Islands using standard measurements, morphological identification in this group is inherently challenging. *Peromyscus* is highly diverse, with unresolved species complexes and substantial phenotypic variation that complicates differentiation among sympatric lineages (Rich *et al.* 1996; Platt *et al.* 2015; Castañeda-Rico *et al.* 2025). Channel Island deer mice also exhibit mild island gigantism making them larger than mainland forms (Collins *et al.* 1979; Gill 1980). These size differences reduce the utility of identification keys based on mainland *Peromyscus*, as exemplified by the many genetically confirmed island mice with a tail to body ratio of exceeding 0.9 (Figure 5C). Morphological plasticity on the Channel Islands further complicates identification (Pergams and Ashley 1999), though we minimized this by restricting analyses to specimens collected during the same three-year survey period. While von Bloeker likely suspected that unusually large *Peromyscus* on San Clemente were atypical, similar suspicions may have applied to outlier Anacapa and Santa Cruz specimens.

Implications and further directions. LACM 5833, LACM 5834, and other specimens may not have been correctly identified as *P. truei* because this species is not typically associated with island invasions. In fact, insular forms of *P. truei*, native or introduced, have never been reported. While some subspecies specialize in piñon-juniper habitats, California *P. truei* occupy a diversity of habitats, including chaparral on canyon slopes (Hoffmeister 1981), suggesting suitable habitat exists on the Channel Islands, even on comparatively depauperate SCL. Limited post-CIBS collecting makes it unclear whether *P. truei* populations persisted past the 1940s. Although *P. truei* is absent from published records and platforms like iNaturalist (Knapp *et al.* 2021), it is likely that Channel Island rodent identifications are rarely scrutinized beyond the generic level with only one known local *Peromyscus* species. Determining whether *P. truei* remains extant on SCL is critical, as introduced rodents may thrive in degraded habitats and threaten the critically imperiled endemic *P. gambelii clementis*. Monitoring is essential as restoration progresses to assess shifts in rodent communities. While eradication of black rats on Anacapa succeeded without negatively affecting native island deer mice populations (Howald *et al.* 2010; Ozer *et al.* 2011), similar efforts for *P. truei* on SCL would be impractical due to the island's large size and *P. truei*'s morphological similarity to native island deer mice.

Over 80 years after the CIBS, museum genomics has resolved long standing misidentifications within *Peromyscus*, confirming that large-bodied Anacapa and Santa Cruz specimens belong to endemic subspecies, while revealing a cryptic invasion of *P. truei* on SCL. Cytochrome *b* comparisons link these specimens to mainland California populations, consistent with the hypothesis that hay bales imported from San Diego during the 1930s may have inadvertently translocated multiple species of wild rodents (von Bloeker Jr 1967). Morphological evidence suggests *P. truei* may have formed substantial populations on SCL, and perhaps on Santa Rosa Island. We recommend molecular screening and comprehensive morphological analysis in collections and targeted field surveys to test identifications and better understand the scope of these introductions. Accurate identification is essential for conservation management on the Channel Islands, and for collections-based research in this taxonomically complex group.

Acknowledgements

This manuscript is dedicated to Dr. Livia León-Paniagua, whose research, mentorship, and leadership have profoundly shaped the field of mammalogy and created a lasting legacy in the study of Mexican mammals. We are deeply grateful for her unwavering commitment to training new generations of mammalogists and for the collaborative spirit that has distinguished her work with students and colleagues.

Thanks also to LACM for a Student Collections Study Award which enabled initial sampling of museum specimens for this study. Additional thanks to Shannen Robson (LACM), Melissa Hawkins and Darrin Lunde (USNM), and Ally Coconis and Krista Fahy (SBMNH) for access to the collections and specimens examined. This work was supported by CCG, Smithsonian National Zoo and Conservation Biology Institute federal funding, the Smithsonian-Mason School of Conservation, George Mason University, an American Genetics Association EECG Award, the American Society of Mammalogists Grants-in-Aid and Horner Awards, a Society of Systematic Biologists Graduate Student Research Award, an American Wildlife Conservation Foundation Grant, and a Cosmos Scholar Grant. Digitization of specimen traits from study skin tags was funded by the National Science Foundation (DBI 2228388 to KCB). MAB was also supported by an SMSC Fellowship through the Jacquemin Family Foundation and by the George Mason University Graduate Division. This project is supported in part by federal funding from the Latino Initiatives Pool, administered by the National Museum of the American Latino. This funding supports the UCSB-Smithsonian Scholars Program and SLO's internship. Thanks to Mario Castellanos and Melani Castellanos for support of UCSB-Smithsonian Scholars. Additional thanks to Nancy McInerney and CCG lab members for support, including feedback on this project. We are grateful to Jesús A. Fernández and an anonymous reviewer for providing valuable input and improving the quality of this manuscript.

Declaration of Artificial Intelligence use

No generative AI tools were used in the preparation of this manuscript.

Author contributions

Madeleine A. Becker: Conceptualization, Formal Analysis, Funding Acquisition, Investigation, Visualization, Writing – Original Draft Preparation, Writing – Review & Editing; Kayce C. Bell: Data Curation, Investigation, Writing – Review & Editing; Selena Lopez-Ortiz: Formal Analysis, Visualization, Writing – Review & Editing; Jesús E. Maldonado: Conceptualization, Funding Acquisition, Resources, Supervision, Writing – Review & Editing; Cody W. Edwards: Funding Acquisition, Supervision, Writing – Review & Editing; Susette Castañeda-Rico: Conceptualization, Formal Analysis, Supervision, Visualization, Writing – Original Draft Preparation, Writing – Review & Editing.

Supplementary data

SD1. A) Measurements from Natural History Museum of Los Angeles County (LACM) Channel Island *Peromyscus* specimens collected during the Channel Islands Biological Survey (1939-1941), which were genetically sampled and morphologically examined. All metadata are derived from original study skin tags, except for tail to body size ratio, which was calculated from these measurements. B) Measurements from Natural History Museum of Los Angeles County (LACM) Channel Island Peromyscus specimens collected during the Channel Islands Biological Survey (1939-1941), which were morphologically examined but not genetically sampled. All metadata are derived from original study skin tags, except for tail to body size ratio, which was calculated from these measurements. C) GenBank and Sequence Read Archive accession numbers for annotated mitochondrial genomes, novel cytochrome b haplotypes, and shotgun genomic data generated.

SD2. Shotgun sequencing and mito-chondrial genome assembly statistics for San Clemente Island *P. truei* specimens (LACM 5833, LACM 5834), San Clemente Island mouse (*P. gambelii clementis*; LACM 6722), and reference *P. truei truei* (USNM 603235).

SD3. Kronagrams displaying classi-fication results of low coverage whole genome data, restricted to reads classified as *Peromyscus* at the genus level: A) LACM 5833 (*P. truei*), B) LACM 5834 (*P. truei*), and C) LACM 6722 (*P. gambelii clementis*).

SD4. Time-scaled mitogenome tree inferred by BEAST, showing the positions of LACM 5833 and LACM 5834 (*P. truei*) and LACM 6722 (*P. gambelii clementis*), subset to the tribe Peromyscini and its sister genus (*Onychomys*). Nodes are labeled with median estimated divergence time in millions of years, with green bars displaying the 95% confidence interval.

SD5. Maximum Likelihood mito-genome consensus tree showing positions of LACM 5833 and LACM 5834 (*P. truei*), and LACM 6722 (*P. gambelii clementis*), subset to the tribe Peromyscini and its sister genus (*Onychomys*). The *Peromyscus truei* species group is highlighted in red, and the *Peromyscus maniculatus* species group is highlighted in blue. Clade names and sequences are replicated from Castañeda-Rico *et al.* 2025. Nodes with black dots indicate high Ultrafast bootstrap support >95.

SD6. Maximum Likelihood cytochrome *b* consensus tree showing positions of LACM 5833 and LACM 5834 within *Peromyscus truei*. Clades are labeled in accordance with Hernández-Canchola *et al.* (2022). The *P. truei* II clade includes all haplotypes sequenced from California specimens. This phylogenetic tree has been subset to *P. truei* and its sister (*P. gratus*) for relevance. Nodes with black dots indicate high Ultrafast bootstrap support >95.

SD7. Distribution of study skin measurements from Channel Islands Biological Survey specimens (n=701) prepared by Jack von Bloeker. Boxplots of total body size by island (mm) with A) pregnant females foregrounded according to reproductive status as originally recorded on tags by von Bloeker, B) immature individuals foregrounded according to age class as originally recorded on tags by von Bloeker.

SD8. Distribution of study skin measurements from Channel Islands Biological Survey specimens (n=701) prepared by Jack von Bloeker. Boxplots of total body size (mm) by island and by sex.

SD9. Measurements from National Museum of Natural History (USNM) Channel Island *Peromyscus* specimens collected before the Channel Islands Biological Survey. All

metadata are derived from original study skin tags, except for tail to body size ratio, which was calculated from these measurements. Many specimen tags did not include complete metadata, resulting in missing data.

SD10. Santa Barbara Museum of Natural History (SBMNH) *Peromyscus* (SBMNH:MAM:7619-7620, SBMNH:MAM:7622) and *Onychomys* (SBMNH:MAM:7621, SBMNH:MAM:9202-9203;) specimens originally collected on San Clemente Island during the Channel Islands Biological Survey. *Onychomys* specimens had been erroneously re-labeled as *P. maniculatus* in collections.

SD11. Measurements of Santa Barbara Museum of Natural History (SBMNH) *Peromyscus* and *Onychomys* specimens originally collected on San Clemente Island during the Channel Islands Biological Survey. *Onychomys* specimens had previously been re-labeled as *P. maniculatus* in collections. All metadata are derived from original study skin tags, except for tail to body size ratio, which was calculated from these measurements.

Literature cited

Ashley MV. 1989. Absence of differentiation in mitochondrial DNA of island and mainland harvest mice, *Reithrodontomys megalotis*. *Journal of Mammalogy* 70:383–386. https://doi.org/10.2307/1381523

Ashley MV, and Wills C. 1989. Mitochondrial-DNA and allozyme divergence patterns are correlated among island deer mice. *Evolution* 43:646–650.

Becker MA, Carrasco C, Kautt AF, Castañeda-Rico S, Orrock JL, Maldonado JE, *et al*. 2025. Phylogenetics of Channel Island deer mice based on the cytochrome *b* gene sheds light on multiple colonization events and supports current taxonomy. *Western North American Naturalist* 85:293–309. https://doi.org/10.3398/064.085.0215

Becker MA. In preparation. *Evolutionary Genomics of Channel Island Peromyscus*. [PhD thesis]. [Virginia (EEUU)]: George Mason University.

Benham PM, and Bowie RCK. 2022. Natural history collections as a resource for conservation genomics: Understanding the past to preserve the future. *Journal of Heredity* 114:367–384. https://doi.org/10.1093/jhered/esac066

Bouckaert R, Vaughan TG, Barido-Sottani J, Duchêne S, Fourment M, Gavryushkina A, *et al*. 2019. BEAST 2.5: an advanced software platform for Bayesian evolutionary analysis. *PLoS Computational Biology* 15(e1006650). https://doi.org/10.1371/journal.pcbi.1006650

Bradley RD, Francis JQ, Platt II RN, Soniat TJ, Alvarez D, and Lindsey LL. 2019. Mitochondrial DNA sequence data indicate evidence for multiple species within *Peromyscus maniculatus*. *Special Publications, Museum of Texas Tech University* 70:1–59.

Brenner LJ, Rindlaub N, Matos J, Meyler S, Pollock S, Schuetzenmeister F, *et al*. 2025. Real-time island biosecurity surveillance: Evaluating a wireless camera network for AI-assisted early detection of invasive mammals on Santa Cruz Island, CA. *Western North American Naturalist* 85:365–375. https://doi.org/10.3398/064.085.0220

California Natural Diversity Database [CNDDB]. 2026. *Special Animals List*. Sacramento (CA, EEUU): California Department of Fish and Wildlife; April 2026. [Accessed May 11th, 2026]. https://nrm.dfg.ca.gov/FileHandler.ashx?DocumentID=109406

Camacho C, Coulouris G, Avagyan V, Ma N, Papadopoulos J, Bealer K, *et al*. 2009. BLAST+: Architecture and applications. *BMC Bioinformatics* 10:421. https://doi.org/10.1186/1471-2105-10-421

Castañeda-Rico S, Maldonado JE, Hawkins MTR, and Edwards CW. 2025. Unveiling hidden diversity: Phylogenomics of neotomine rodents and taxonomic implications for the genus *Peromyscus*. *Molecular Phylogenetics and Evolution* 203:108233. https://doi.org/10.1016/j.ympev.2024.108233

Collins PW, Storrer J, and Rindlaub K. 1979. XI. Vertebrate zoology: biology of the deer mouse, A natural resources study of the Channel Islands National Park, California. In: Power DM, editor. *Final Technical Report to the Denver Service Center, National Park Service*, Denver, CO (EEUU); p. 11.1–11.74.

Collins PW. 1991a. Interaction between island foxes (*Urocyon littoralis*) and Indians on islands off the coast of southern California: I. Morphologic and archaeological evidence of human assisted dispersal. *Journal of Ethnobiology* 11:51–81.

Collins PW. 1991b. Interaction between island foxes (*Urocyon littoralis*) and Native Americans on islands off the coast of southern California: II. Ethnographic, archaeological, and historical evidence. *Journal of Ethnobiology* 11:205–229.

Comstock JA. 1946. Contributions from the Los Angeles museum—Channel Islands Biological Survey--33. Brief notes on the expeditions conducted between March 16, 1940 and December 14, 1941. *Bulletin, Southern California Academy of Sciences* 45:94–107.

Coonan TJ, Bakker V, Hudgens B, Boser CL, Garcelon DK, and Morrison SA. 2014. On the fast track to recovery: Island foxes on the northern Channel Islands. *Monographs of the Western North American Naturalist* 7:373–381. https://doi.org/10.3398/042.007.0128

Dunkle MB. 1943. Contributions from the Los Angeles Museum-Channel Islands Biological Survey No. 28: Three new plants from San Clemente Island. *Bulletin of the Southern California Academy of Sciences* 42:31–33.

Elliot DG. 1903. Descriptions of apparently new species and subspecies of mammals from California, Oregon, the Kenai Peninsula, Alaska, and Lower California, Mexico. *Field Columbian Museum Publication* 74:141–149.

Erlandson JM, Rick TC, Braje TJ, Casperson M, Culleton B, Fulfrost B, *et al*. 2011. Paleoindian seafaring, maritime technologies, and coastal foraging on California's Channel Islands. *Science* 331:1181–1185. https://doi.org/10.1126/science.1201477

Gill AE. 1980. Evolutionary genetics of California islands *Peromyscus*. In: Power DM, editor. *The California Islands: Proceedings of a multidisciplinary symposium*. Santa Barbara Museum of Natural History, Santa Barbara, CA (EEUU); p. 719–743.

Goedknegt MA, Thieltges DW, Van Der Meer J, Wegner KM, and Luttikhuizen PC. 2018. Cryptic invasion of a parasitic copepod: Compromised identification when morphologically similar invaders co-occur in invaded ecosystems. *PLoS ONE* 13:e0193354. https://doi.org/10.1371/journal.pone.0193354

Greenbaum IF, Chirhart SE, Walker ML, and Honeycutt RL. 2017. Molecular phylogenetics of western deer mice (*Peromyscus*): Taxonomic and biogeographic implications. *The Southwestern Naturalist* 62:129–137. https://doi.org/10.1894/0038-4909-62.2.129

Greenbaum IF, Honeycutt R, and Chirhart S. 2019. Taxonomy and phylogenetics of the *Peromyscus maniculatus* species group. *Special Publications, Museum of Texas Tech University* 71:559–575.

Hernández-Canchola G, León-Paniagua L, and Esselstyn JA. 2022. Mitochondrial DNA and other lines of evidence clarify species diversity in the *Peromyscus truei* species group (Cricetidae: Neotominae). *Mammalia* 86:380–392. https://doi.org/10.1515/mammalia-2021-0146

Hoffmeister DF. 1981. *Peromyscus truei*. *Mammalian Species* 161:1–5.

Howald GR, Donlan CJ, Faulkner KR, Ortega S, Gellerman H, Croll DA, *et al*. 2010. Eradication of black rats *Rattus rattus* from Anacapa Island. *Oryx* 44:30–40. https://doi.org/10.1017/S003060530999024X

Ingles LG. 1965. *Mammals of the pacific states: California, Oregon, and Washington*. Redwood City (EEUU): Stanford University Press.

Johnson DL. 1983. The California continental borderland: Landbridges, watergaps and biotic dispersals. In: Master PM, and Flemming NC, editors. *Quaternary Coastlines and Marine Archaeology: Towards the Prehistory of Land Bridges and Continental Shelves*. Academic Press, London (UK) and New York, NY (EEUU); p. 481–527.

Kapp JD, Green RE, and Shapiro B. 2021. A fast and efficient single-stranded genomic library preparation method optimized for ancient DNA. *Journal of Heredity* 112:241–249. https://doi.org/10.1093/jhered/esab012

Katoh K, and Standley DM. 2013. MAFFT multiple sequence alignment software version 7: improvements in performance and usability. *Molecular Biology and Evolution* 30:772-780. https:// doi.org/10.1093/molbev/mst010

Keegan DR, Coblentz BE, and Winchell CS. 1994. Feral goat eradication on San Clemente Island, California. *Wildlife Society Bulletin* 22:56–61.

Kim AS, Kreiner JM, Hernández F, Bock DG, Hodgins KA, and Rieseberg LH. 2023. Temporal collections to study invasion biology. *Molecular Ecology* 32:6729–6742. https://doi.org/10.1111/mec.17176

Knapp DA, Collins PW, and Etter K. 2021. *Channel Islands mammals: A gap analysis of specimen and observation data. Unpublished final report prepared for The Nature Conservancy by the Santa Barbara Botanic Garden, Santa Barbara, California*. Santa Barbara (CA, EEUU): Santa Barbara Botanic Garden; October, 2021. [Accessed May 11th, 2026]. https://sbbotanicgarden.org/wp-content/uploads/2022/06/MAMMALS-gap-analysis-final.pdf

Lanfear R, Frandsen PB, Wright AM, Senfeld T, and Calcott B. 2017. PartitionFinder 2: New methods for selecting partitioned models of evolution for molecular and morphological phylogenetic analyses. *Molecular Biology and Evolution* 34:772–773. https://doi.org/10.1093/molbev/msw260

Laverty CH. 2020. *North America's Galapagos: The Historic Channel Islands Biological Survey*. Salt Lake City (EEUU): University of Utah Press.

Light JE, Siciliano-Martina L, Dohlanik E, Vielleux G, Hafner D, Lawing AM, *et al*. 2021. Morphological differentiation of *Peromyscus leucopus* and *P. maniculatus* in East Texas. *Therya* 12:369–387. https://doi.org/10.12933/therya-21-1116

Lu J, Rincon N, Wood DE, Breitwieser FP, Pockrandt C, Langmead B, *et al*. 2022. Metagenome analysis using the Kraken software suite. *Nature Protocols* 17:2815–2839. https://doi.org/10.1038/s41596-022-00738-y

Martin M. 2011. Cutadapt removes adapter sequences from high-throughput sequencing reads. *EMBnet.Journal* 17:10–12. https://doi.org/10.14806/ej.17.1.200

McChesney GJ, and Tershy BR. 1998. History and status of introduced mammals and impacts to breeding seabirds on the California Channel and northwestern Baja California islands. *Colonial Waterbirds* 21:335–347. https://doi.org/10.2307/1521646

McDonough MM, Parker LD, Rotzel McInerney N, Campana MG, and Maldonado JE. 2018. Performance of commonly requested destructive museum samples for mammalian genomic studies. *Journal of Mammalogy* 99:789–802. https://doi.org/10.1093/jmammal/gyy080

Mearns EA. 1897. Descriptions of six new mammals from North America. *Proceedings of the United States National Museum* 19:719–724.

Mearns EA. 1907. Mammals of the Mexican boundary of the United States. *United States National Museum Bulletin* 56:1–530.

Meineke EK, Davies TJ, Daru BH, and Davis CC. 2019. Biological collections for understanding biodiversity in the Anthropocene. *Philosophical Transactions of the Royal Society B: Biological Sciences* 374:20170386. https://doi.org/10.1098/rstb.2017.0386

Minh BQ, Schmidt HA, Chernomor O, Schrempf D, Woodhams MD, von Haeseler A, *et al*. 2020. IQ-TREE 2: New models and efficient methods for phylogenetic inference in the genomic era. *Molecular Biology and Evolution* 37:1530–1534. https://doi.org/10.1093/molbev/msaa015

Nelson EW, and Goldman EA. 1931. Six new white-footed mice (*Peromyscus maniculatus* group), from islands off

the Pacific Coast. *Journal of the Washington Academy of Sciences* 21:530–535.

O'Hanlon SJ, Rieux A, Farrer RA, Rosa GM, Waldman B, Bataille A, *et al*. 2018. Recent Asian origin of chytrid fungi causing global amphibian declines. *Science* 360:621–627. https://doi.org/10.1126/science.aar1965

Ondov BD, Bergman NH, and Phillippy AM. 2011. Interactive metagenomic visualization in a Web browser. *BMC Bioinformatics* 12:385. https://doi.org/10.1186/1471-2105-12-385

Ozer F, Gellerman H, and Ashley MV. 2011. Genetic impacts of Anacapa deer mice reintroductions following rat eradication: Anacapa island mouse reintroduction. *Molecular Ecology* 20:3525–3539. https://doi.org/10.1111/j.1365-294X.2011.05165.x

Pergams ORW, and Ashley MV. 1999. Rapid morphological change in Channel Island deer mice. *Evolution* 53:1573–1581. https://doi.org/10.1111/j.1558-5646.1999.tb05420.x

Pergams ORW, and Ashley MV. 2002. California Island deer mice: Genetics, morphometrics, and evolution. In: Browne DR, Mitchell KL, and Chaney HW, editors. *Proceedings of the Fifth California Islands Symposium*. Santa Barbara, CA (EEUU): Santa Barbara Museum of Natural History; p. 278–288.

Pergams ORW, Byrn D, Lee KLY, and Jackson R. 2015. Rapid morphological change in black rats (*Rattus rattus*) after an island introduction. *PeerJ* 3:e812. https://doi.org/10.7717/peerj.812

Platt RN, Amman BR, Keith MS, Thompson CW, and Bradley RD. 2015. What Is *Peromyscus*? Evidence from nuclear and mitochondrial DNA sequences suggests the need for a new classification. *Journal of Mammalogy* 96:708–719. https://doi.org/10.1093/jmammal/gyv067

Provan J, Booth D, Todd NP, Beatty GE, and Maggs CA. 2008. Tracking biological invasions in space and time: Elucidating the invasive history of the green alga *Codium fragile* using old DNA. *Diversity and Distributions* 14:343–354. https://doi.org/10.1111/j.1472-4642.2007.00420.x

R Core Team. 2021. *R: A language and environment for statistical computing.* R Foundation for Statistical Computing. V. 2.14.2. Vienna (Austria). https://www.R-project.org/.

Raven PH. 1963. A flora of San Clemente Island, California. *Aliso: A Journal of Systematic and Floristic Botany* 5:289–347.

Rambaut A, Drummond AJ, Xie D, Baele G, and Suchard MA. 2018. Posterior summarization in Bayesian phylogenetics using Tracer 1.7. *Systematic Biology* 67:901–904. https://doi.org/10.1093/sysbio/syy032

Raxworthy CJ, and Smith BT. 2021. Mining museums for historical DNA: Advances and challenges in museomics. *Trends in Ecology and Evolution* 36:1049–1060. https://doi.org/10.1016/j.tree.2021.07.009

Rich SM, Kilpatrick CW, Shippee JL, and Crowell KL. 1996. Morphological differentiation and identification of *Peromyscus leucopus* and *P. maniculatus* in northeastern North America. *Journal of Mammalogy* 77:985–991. https://doi.org/10.2307/1382779

Rick TC. 2013. Hunter-gatherers, endemic island mammals, and the historical ecology of California's Channel Islands. In: Thompson VD, and Waggoner JC, editors. *The Archaeology and Historical Ecology of Small Scale Economies*. Gainseville (EEUU): University Press of Florida; p. 41–64. https://doi.org/10.5744/florida/9780813042428.003.0003

Rick TC, Erlandson JM, Vellanoweth RL, Braje RJ, Collins PW, Guthrie DA, *et al*. 2009. Origins and antiquity of the island fox (*Urocyon littoralis*) on California's Channel Islands. *Quaternary Research* 71:93–98. https://doi.org/10.1016/j.yqres.2008.12.003

Rick TC, Hofman CA, and Reeder-Myers LA. 2019. Why Translocate? Evaluating the evidence and reasons for ancient human introductions of wildlife to California's Islands. In: Gill KM, Fauvelle M, Erlandson JM, editors. *An Archaeology of Abundance: Reevaluating the Marginality of California's Islands*. Gainseville (EEUU): University Press of Florida; p. 248–272. https://doi.org/10.5744/florida/9780813056166.003.0009

Rick TC, Radde HD, Teeter WG, Elliott Smith EA, Alvitre CM, Dagtas ND, *et al*. 2024. Enhancing biodiversity: Historical ecology and biogeography of the Santa Catalina Island ground squirrel, *Otospermophilus beecheyi nesioticus*. *Royal Society Open Science* 11:240726. https://doi.org/10.1098/rsos.240726

Roemer GW, Coonan TJ, Garcelon DK, Bascompte J, and Laughrin L. 2001. Feral pigs facilitate hyperpredation by golden eagles and indirectly cause the decline of the island fox. *Animal Conservation* 4:307–318. https://doi.org/10.1017/S1367943001001366

Ronquist F, and Huelsenbeck JP. 2003. MrBayes 3: Bayesian phylogenetic inference under mixed models. *Bioinformatics* 19:1572–1574. https://doi.org/10.1093/bioinformatics/btg180

Schmieder R, and Edwards R. 2011. Quality control and preprocessing of metagenomic datasets. *Bioinformatics* 27:863–864. https://doi.org/10.1093/bioinformatics/btr026

Scott TA, and Morrison ML. 1990. Natural history and management of the San Clemente Loggerhead Shrike. *Proceedings of the Western Foundation of Vertebrate Zoology* 4:23–57.

Shirazi S, Rick TC, Erlandson JM, and Hofman CA. 2018. A tale of two mice: A trans-Holocene record of *Peromyscus nesodytes* and *Peromyscus maniculatus* at Daisy Cave, San Miguel Island, California. *The Holocene* 28:827–833. https://doi.org/10.1177/0959683617744266

Suarez AV, and Tsutsui ND. 2004. The value of museum collections for research and society. *BioScience* 54:66–74. https://doi.org/10.1641/0006-3568(2004)054[0066:TVOMCF]2.0.CO;2

US Fish and Wildlife Service [USFWS]. 2014. Final rule removing the island night lizard from the federal

list of endangered and threatened wildlife. *United States Federal Register* 79:18190–18210. https://www.fws.gov/sites/default/files/federal_register_document/2014-06576.pdf

US Fish and Wildlife Service [USFWS]. 2016. Final rule: Removing the San Miguel island fox, Santa Rosa island fox, and Santa Cruz island fox from the federal list of endangered and threatened wildlife, and reclassifying the Santa Catalina island fox from endangered to threatened. *United States Federal Register* 81:53315–53333. https://www.fws.gov/sites/default/files/federal_register_document/2016-18778.pdf

US Fish and Wildlife Service [USFWS]. 2023. Endangered and threatened wildlife and plants; removing five species that occur on San Clemente Island from the federal lists of endangered and threatened wildlife and plants. *United States Federal Register* 88:4761–4792. https://www.fws.gov/sites/default/files/federal_register_document/2023-01400.pdf

von Bloeker Jr JC. 1940. Contributions from the Los Angeles Museum-Channel Islands Biological Survey No. 11: A new race of white-footed mouse from Santa Rosa Island, California. *Bulletin of the Southern California Academy of Sciences* 39:172–174.

von Bloeker Jr JC. 1941. Contributions from the Los Angeles Museum-Channel Islands Biological Survey No. 22: A new subspecies of white-footed mouse from the Anacapa Islands, California. *Bulletin of the Southern California Academy of Sciences* 40:161–162.

von Bloeker Jr JC. 1967. Land mammals of the southern California islands. In Philbrick RN, editor. *Proceedings of the Symposium on the Biology of the California Islands*. Santa Barbara, CA (EEUU): Santa Barbara Botanic Garden; p. 245–264.

Whitworth DL, Carter HR, and Gress F. 2013. Recovery of a threatened seabird after eradication of an introduced predator: Eight years of progress for Scripps's murrelet at Anacapa Island, California. *Biological Conservation* 162:52–59. https://doi.org/10.1016/j.biocon.2013.03.026

Wickham H, Averick M, Bryan J, Chang W, McGowan L, François R, *et al*. 2019. Welcome to the Tidyverse. *Journal of Open Source Software* 4:1686. https://doi.org/10.21105/joss.01686

Wood DE, and Salzberg SL. 2014. Kraken: Ultrafast metagenomic sequence classification using exact alignments. *Genome Biology* 15:R46. https://doi.org/10.1186/gb-2014-15-3-r46

Yu G, Smith DK, Zhu H, Guan Y, and Lam TT. 2017. ggtree: An r package for visualization and annotation of phylogenetic trees with their covariates and other associated data. *Methods in Ecology and Evolution* 8:28–36. https://doi.org/10.1111/2041-210X.12628

Associated editors: Giovani Hernández Canchola and Pablo Colunga Salas
Submitted: December 19, 2025; Reviewed: March 22, 2026
Accepted: May 8, 2026; Published online: May 29, 2026

THERYA, 2026, Vol. 17(2):295-306 DOI: 10.12933/therya.2026.6269 ISSN 2007-3364

The genus *Habromys*: an untold biogeographic history

Deborah V. Espinosa-Martínez[1,3], César A. Ríos-Muñoz[2*], and Joaquín Arroyo-Cabrales[3]

[1]Posgrado en Ciencias del Mar y Limnología, Universidad Nacional Autónoma de México, Ciudad de México, México. E-mail: dvem@ciencias.unam.mx (DVE-M)
[2]Facultad de Ciencias, Universidad Nacional Autónoma de México, Ciudad Universitaria, CP 04510, Ciudad de México, México.
[3]Laboratorio de Arqueozoología, Subdirección de Laboratorios y Apoyo Académico, Instituto Nacional de Antropología e Historia, Moneda 16 Centro, CP 06060, Ciudad de México, México. E-mail: joaquin_arroyo@inah.gob.mx (JA-C)
[*]Corresponding author: cesar.rios@unam.mx

The genus *Habromys* includes seven species of rodents restricted to Mesoamerican cloud forests across the mountain systems of central and eastern Mexico and northern Central America. Previous studies have suggested that diversification within the genus largely shaped by vicariant scenarios in which range expansion was followed by isolation driven by habitat fragmentation. However, these hypotheses have not been formally evaluated within a time-calibrated framework using explicit model-based approaches. Here, we reconstructed the biogeographic history of *Habromys* using a time-calibrated phylogeny based on mitochondrial genes, previously used in published studies, and evaluated alternative parametric biogeographic models implemented in BioGeoBEARS. The DEC+j was the best-supported model explaining geographic range evolution, indicating that founder-event speciation and within-area cladogenesis (narrow and subset sympatry) were the most frequent processes shaping diversification, whereas vicariance and anagenetic dispersal/extinction were inferred as comparatively uncommon. Divergence-time estimates suggest that crown diversification in *Habromys* began during the Pliocene, whereas most interspecific divergences occurred during the middle Pleistocene. These patterns are consistent with a biogeographic history driven by climatic oscillations that periodically increased connectivity among cloud forest habitats and later promoted isolation in montane regions. Overall, our results support a scenario in which repeated colonization and isolation events associated with Pliocene–Pleistocene climatic fluctuations played a greater role than vicariant processes linked to mountain building.

Keywords: Ancestral reconstruction area, cloud forest, Cricetidae, distribution, Mesoamerica, parametric biogeography.

El género *Habromys* incluye siete especies de roedores restringidas a los bosques mesófilos de montaña de Mesoamérica, distribuidos en los sistemas montañosos del centro y este de México y el norte de Centroamérica. Estudios previos han sugerido que la diversificación dentro del género estuvo determinada principalmente por escenarios vicariantes, en los cuales una expansión del área de distribución fue seguida por aislamiento impulsado por la fragmentación del hábitat. Sin embargo, estas hipótesis no han sido evaluadas formalmente dentro de un marco temporal calibrado ni mediante enfoques explícitos basados en modelos. En este estudio reconstruimos la historia biogeográfica de *Habromys* utilizando una filogenia calibrada temporalmente basada en genes mitocondriales previamente empleados en estudios publicados, y evaluamos modelos biogeográficos paramétricos alternativos implementados en BioGeoBEARS. El modelo DEC+j fue el mejor soportado para explicar la evolución del rango geográfico, indicando que la especiación por efecto fundador y la cladogénesis dentro de área (simpatría estrecha y simpatría por subconjunto) fueron los procesos más frecuentes que moldearon su diversificación, mientras que la vicarianza y la dispersión/extinción anagenética fueron inferidas como relativamente poco comunes. Las estimaciones de tiempo de divergencia sugieren que la diversificación en *Habromys* inició durante el Plioceno, mientras que la mayoría de las divergencias interespecíficas ocurrieron durante el Pleistoceno medio. Estos patrones son consistentes con una historia biogeográfica impulsada por oscilaciones climáticas que incrementaron periódicamente la conectividad entre los bosques mesófilos y posteriormente promovieron el aislamiento en regiones montañosas. En conjunto, nuestros resultados apoyan un escenario en el que eventos repetidos de colonización y aislamiento asociados a las fluctuaciones climáticas del Plioceno–Pleistoceno desempeñaron un papel más importante que procesos vicariantes vinculados al levantamiento de los sistemas montañosos.

Palabras clave: Biogeografía paramétrica, bosques mesófilos de montaña, Cricetidae, distribución, Mesoamérica, reconstrucción de áreas ancestrales.

The genus *Habromys* Hooper and Musser 1964 (Cricetidae: Neotominae) includes seven species of rodents (*H. chinanteco*, *H. delicatulus*, *H. ixtlani*, *H. lepturus*, *H. lophurus*, *H. schmidlyi*, and *H. simulatus*), all endemic and ecologically restricted to Mesoamerican cloud forest from central and eastern Mexico to northern Central America (León-Paniagua *et al.* 2007; Ceballos 2014; Ramírez-Pulido *et al.* 2014; Contreras-Medina *et al.* 2024). The species are considered unique due to their arboreal habits and high ecological specialization (Colunga Salas 2014; 2016; Marines-Macías *et al.* 2018). In some species, populations may occur at low densities (Colunga Salas 2016; Castañeda-Rico *et al.* 2023) and small home ranges (Marines-Macías *et al.* 2018), which has contributed to their recognition as threatened at the national level (*H. simulatus*: subject to special protection, SEMARNAT 2010) and the international level (*H. delicatulus*: endangered, *H. ixtlani*: critically endangered, and *H. lophurus*: near threatened, [Vázquez 2017; Álvarez-Castañeda *et al.* 2018; Emmons *et al.* 2019]).

The geographic distribution of *Habromys* species is restricted or highly fragmented. *H. delicatulus* and *H. schmidlyi* occur in the Trans-Mexican Volcanic Belt (Romo-Vázquez *et al.* 2005); *H. simulatus* has a disjunct distribution in the Sierra Madre Oriental and eastern Trans-Mexican

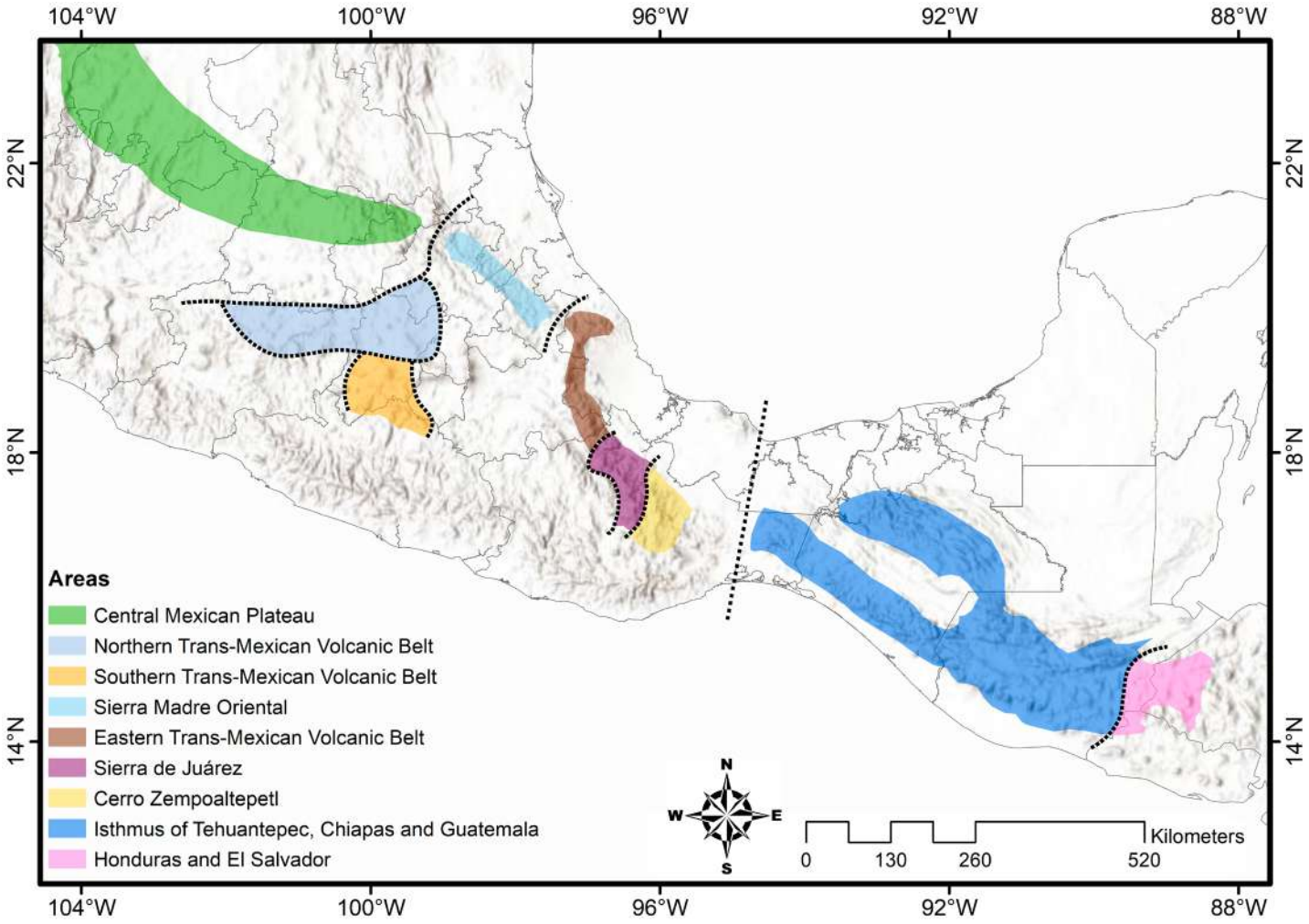

Figure 1. Distribution areas of the species included in the analysis: *Peromyscus boylii* (Central Mexican Plateau), *Habromys delicatulus* (Northern Trans-Mexican Volcanic Belt), *H. schmidlyi* (Southern Trans-Mexican Volcanic Belt), *H. simulatus* (Sierra Madre Oriental and eastern Trans-Mexican Volcanic Belt), *H. ixtlani* and *H. chinanteco* (Sierra de Juárez), *H. lepturus* (Cerro Zempoaltepetl), *H. lophurus* (Isthmus of Tehuantepec, Chiapas, Guatemala, Honduras, and El Salvador). *Peromyscus slevini* (not illustrated) is found only on Santa Catalina Island in the Gulf of California.

Volcanic Belt (León-Paniagua *et al.* 2007; Castañeda-Rico *et al.* 2011); while *H. chinanteco* and *H. ixtlani* are found in the Sierra de Juárez and *H. lepturus* in Cerro Zempoaltepetl, all part of the Sierra Madre de Oaxaca (León-Paniagua *et al.* 2007; Contreras-Medina *et al.* 2024); and *H. lophurus* is distributed in the mountains east of the Isthmus of Tehuantepec in southeastern Mexico (Chiapas), through southern and central Guatemala (Sierra de las Minas), to El Salvador (Hall 1981; León-Paniagua *et al.* 2007; Contreras-Medina *et al.* 2024) (Figure 1).

In addition to formal descriptions of the species (Merriam 1898; Osgood 1904; Goodwin 1964; Robertson and Musser 1976; Carleton *et al.* 2002; Romo-Vázquez *et al.* 2005), published works have focused on identifying new distributional records (Briones-Salas *et al.* 2012), ecological aspects and genetic diversity for some species (Castañeda-Rico *et al.* 2011; 2023; Colunga Salas 2014; 2016; Marines-Macías *et al.* 2018), analyzing the effect of Pleistocene climate change (León-Paniagua and Guevara 2019), and understanding phylogenetic relationships within the genus (León-Paniagua *et al.* 2007; Rogers *et al.* 2007; Castañeda-Rico *et al.* 2011; 2023). Nevertheless, studies have emphasized phylogenetic relationships and distributional patterns rather than explicit hypothesis testing of biogeographic processes.

The first phylogenetic hypotheses for *Habromys* were presented by Rogers *et al.* (2007), based on the complete mitochondrial cytochrome-b gene (1143 bp), and by León-Paniagua *et al.* (2007), based on mitochondrial *ND3*, *tRNA-Arg*, *ND4L*, and *ND4* sequences (1131 bp). Both studies supported the monophyly of *Habromys* using broad taxonomic sampling within Neotominae, and recovered geographically structured lineages largely associated with montane regions of Mexico and northern Central America, suggesting that isolation among cloud forest massifs has promoted diversification. Rogers *et al.* (2007), which included six of the seven recognized species, emphasized the role of the Isthmus of Tehuantepec as a major geographic barrier potentially driving divergence between lineages west and east of the isthmus, and suggested that this vicariant event may predate Pleistocene climatic fluctuations. They also proposed the Cajonos River as a potential vicariant barrier separating *H. ixtlani* and *H. lepturus*. León-Paniagua *et al.* (2007) included all described

species of *Habromys* and additionally documented geographically structured lineages within *H. simulatus* and *H. lophurus*, suggesting a history of range expansion followed by diversification associated with fragmentation of montane forests during climatic oscillations, and suggesting that the Isthmus of Tehuantepec is not a major force in the differentiation of the genus. Subsequent work supported the differentiation of two evolutionary units within *H. simulatus* using microsatellite data (Castañeda-Rico *et al.* 2011), whereas the phylogeographic structure suggested for *H. lophurus* remains untested. However, although these studies provided a critical phylogenetic framework, their biogeographic interpretations were not evaluated under explicit model-based approaches, and the relative roles of biogeographic processes in shaping current distributions remain unclear.

Parametric biogeography provides a statistical framework to test alternative evolutionary scenarios by explicitly modeling biogeographic processes (anagenetic: dispersal, extinction, range switching; and cladogenetic: within-area cladogenesis, vicariance, founder-event) through time, involved in the reconstruction of biogeographic history. In addition to considering a temporal framework that allows identifying the congruence of biogeographic events, and relating them to independent geographic information (Sanmartin 2012). Based on a time-calibrated phylogenetic hypothesis and knowledge of species distributions, the geographic evolution of lineages is modeled using a stochastic process that determines the rate of change between areas, allowing the reconstruction of ancestral areas and inference of processes that shaped the distribution of a given taxon (Sanmartin 2012; Matzke 2013b). Despite the availability of a phylogenetic hypothesis and well-documented geographic distributions, *Habromys* has not been examined using parametric biogeographic methods that explicitly compare alternative evolutionary scenarios.

Given the strong association of *Habromys* with cloud forests, the high fragmentation of these habitats, and the presumably limited dispersal ability of these rodents, we hypothesize that vicariance played an important role in the diversification of the genus among montane regions during climatic fluctuations of the late Neogene and Pleistocene (León-Paniagua *et al.* 2007; Rogers *et al.* 2007; León-Paniagua and Guevara 2019). We evaluated this scenario against alternative processes such as founder-event speciation and within-area cladogenesis. Specifically, we predict that (1) ancestral areas will be reconstructed in eastern Mexican and Central American highlands, (2) diversification events will coincide with major geographic barriers such as the Isthmus of Tehuantepec and the separation of the Trans-Mexican Volcanic Belt, Sierra Madre Oriental, Sierra de Juarez and Cerro Zempoaltepetl, and (3) dispersal events will be limited and mostly restricted to adjacent mountain systems. To test these predictions, we conducted a model-based historical biogeographic analysis using a time-calibrated phylogeny and explicit parametric models. Here we reanalyzed the mitochondrial dataset of León-Paniagua *et al.* (2007), complemented with an additional sequence for *H. simulatus* from Castañeda-Rico *et al.* (2014), to evaluate alternative parametric models of historical biogeography.

Materials and methods

Phylogenetic analysis. We performed a phylogenetic analysis including 31 individuals representing the seven species described for the genus *Habromys* and 14 outgroup species (one individual per species), following the taxon sampling and outgroup selection by León-Paniagua *et al.* (2007). Partial mitochondrial sequences of ND3 and ND4 were obtained from GenBank (Supplementary Material 1), following León-Paniagua *et al.* (2007), with one additional *H. simulatus* sequence from Castañeda-Rico *et al.* (2014). The two gene fragments were concatenated for subsequent analyses. Sequences were aligned in MEGA11 (Tamura *et al.* 2021) with the Multiple Sequence Comparison algorithm based on Log-Expectation (MUSCLE) (Edgar 2004) under default settings.

We inferred a time-calibrated phylogeny using BEAST 2.7.7 (Bouckaert *et al.* 2019). We selected the substitution model by running Modeltest 3.6 on our alignment, which recovered HKY model (Hasegawa *et al.* 1985) with invariant sites, four Gamma categories as the best-fit model, consistent with León-Paniagua *et al.* (2007). To ensure comparability with previous analyses, we implemented this same model in BEAST. We implemented a relaxed log-normal molecular clock, and the Calibrated Yule speciation model (Heled and Drummond 2012). The speciation rate (birthRateY) was modeled using a Gamma distribution with parameters $\alpha = 3$ and $\beta = 0.09$. Node ages were calibrated using four secondary fossil-based constraints taken from León-Paniagua *et al.* (2007). For each calibrated node, we implemented an MRCA (most recent common ancestor) priors with a lognormal distribution and enforced monophyly (Table 1), these priors constrain node ages while enforcing monophyly. For the relaxed molecular clock, Gamma distributions were used with parameters $\alpha = 3$ and $\beta = 0.00667$ for the mean (ucldMean), and $\alpha = 4$ and $\beta = 0.05$ for the standard deviation (ucldStdev).

Twenty million generations were run, sampling every 1000 generations. We assessed the stationarity of the Markov

Table 1. Parameters used in the calibration of each internal node. The ages used in the divergence time estimates for the nodes of the *Habromys* genus phylogeny were taken from León-Paniagua *et al.* (2007).

Nodes-Groups	Calibration
Neotominae	14.8 Ma (*M* = 7.1, *S* = 0.01, *mean in real space* = true, *offset* = 7.7)
Onychomys-Peromyscus-Habromys	10.3 Ma (*M* = 4.9, *S* = 0.15, *mean in real space* = true, *offset* = 5.36)
Peromyscus-Habromys	4.69 Ma (*M* = 2.25, *S* = 0.05, *mean in real space* = true, *offset* = 2.44)
Habromys simulatus	0.78 Ma (*M* = 0.4, *S* = 0.1, *mean in real space* = true, *offset* = 0.38)

Table 2. Summary of statistics for selecting the best model obtained in BioGeoBEARS. LnL = likelihood, d = dispersion parameter, e = extinction parameter, j = founder-event parameter, AIC = Akaike Information Criterion, and AIC_wt = weighted Akaike Information Criterion.

Model	LnL	Number of parameters per model	d	e	j	AIC	AIC_wt
DEC	-40.4	2	0.07	0.13	0	84.79	0.000023
*DEC+j	-28.92	3	1E-12	1E-12	0.31	63.85	0.8
DIVALIKE	-37.91	2	0.059	0.026	0	79.82	0.0003
DIVALIKE+j	-30.62	3	0.0064	1E-12	0.14	67.24	0.15
BAYAREALIKE	-46.09	2	0.15	0.54	0	96.19	0.000000076
BAYAREALIKE+j	-31.59	3	0.0007	0.031	0.17	69.18	0.055

Chain Monte Carlo (MCMC) in Tracer v.1.7.2 (Rambaut *et al.* 2018), ensuring that the effective sample sizes (ESS) were > 200 for all priors, indicating adequate sampling of the posterior distribution. The Maximum Clade Credibility Tree (MCCT) and the most probable common ancestor were obtained using TreeAnnotator v.2.7.7, discarding 25% of burn-in. The maximum credibility tree was visualized in FigTree v.1.4.4 (http://tree.bio.ed.ac.uk/software/figtree/).

Ancestral area estimation. The ancestral areas for the genus *Habromys* were estimated using the BioGeoBEARS package (Matzke 2013a) in R v.4.3.3 (R Core Team 2024). To reduce the number of geographic states, we initially retained one representative per species of the genus was initially used. In the case of *H. schmidlyi*, two individuals were considered because they do not form a monophyletic group and one of the individuals is a sibling of *H. delicatulus*. This non-monophyly has been previously reported and may reflect incomplete lineage sorting or taxonomic complexity. On the other hand, for *H. simulatus* and *H. lophurus*, León-Paniagua *et al.* (2007) and Castañeda-Rico *et al.* (2011) report that there are two well-differentiated populations in two different areas in each species, so we decided to retain one individual from each of the populations in order to reconstruct biogeographic processes involved (Figure 1). Considering that BioGeoBEARS analyses have a computational limit associated with the number of states (number of combinations of relationships between the areas used, Matzke 2013a, b), we pruned most outgroups, leaving only *Peromyscus boylii* (distributed in the south and southwest of the United States of America and northern Mexico, up to the Central Mexican Plateau [Kalcounis-Rueppell and Spoon 2009]) and *P. slevini* (distributed on Santa Catalina Island in the Gulf of California [Álvarez-Castañeda and Cortés-Calva 2002]), as both are recovered as a sister lineage to *Habromys* (León-Paniagua *et al.* 2007).

To estimate the biogeographic history of the genus, we considered three sets of biogeographic models implemented in BioGeoBEARS: (1) Dispersal-Extinction-Cladogenesis (DEC, Ree *et al.* 2005; Ree and Smith 2008), (2) the likelihood version of the Dispersal-Vicariance Analysis (DIVALIKE, Matzke 2013a, b), which differs from the original version of DIVA (Ronquist 1997; Ronquist and Sanmartín 2011) in that it is not based on parsimony methods, but rather on a likelihood interpretation, and (3) the likelihood version of the BAYAREA model (BAYAREALIKE, Matzke 2013a, b) which, unlike the original version of BAYAREA (Landis *et al.* 2013), considers cladogenesis as part of the evolutionary process. Likewise, models that consider speciation because of the founder effect (parameter +j, Matzke 2013b, 2014) were also tested: DEC+j, DIVALIKE+j, and BAYAREALIKE+j. The best model was selected based on the likelihood values (LnL) and the Akaike Information Criterion (AIC) values obtained from model fitting (Table 2).

We performed biogeographic stochastic mapping (BSM) under the best-fitting DEC+j model to estimate the frequency of biogeographic events across the evolutionary history of *Habromys*. We generated 50 stochastic map replicates and recorded, for each replicate, the number of inferred events corresponding to anagenetic dispersal, within-area cladogenesis (narrow sympatry), subset sympatry, vicariance, and founder-event speciation. The resulting frequency distributions were used to assess the relative contribution of each process.

Results

Phylogenetic analysis. Our phylogenetic hypothesis recovered the same overall topology as León-Paniagua *et al.* (2007), consistent with the use of the same mitochondrial markers (ND3 and ND4) and substitution model HKY+I+G. Some differences were observed in the relationships among individuals of *H. lophurus*, *H. lepturus*, *H. delicatulus*, *H. schmidlyi*, and *H. simulatus*, reflected in moderate posterior probabilities (0.5–0.8) for several internal nodes (Figure 2).

Divergence-time estimates indicate that the neotomine clade containing *Habromys* diversified during the Miocene, whereas crown diversification within *Habromys* began in the Pliocene, with most interspecific divergences occurring during the Pleistocene.

Ancestral area estimation. DEC+j was the best-supported model explaining the geographic range evolution of *Habromys*, with an AIC weight of 0.80, compared to much lower values for the other six models tested (Table 2). Biogeographic stochastic mapping under this model indicated that founder-event speciation (+J) and within-area cladogenesis (narrow and subset sympatry) were inferred as the most frequent processes shaping range evolution and diversification in *Habromys* in the mountain systems of Mexico and the highlands of northern Central

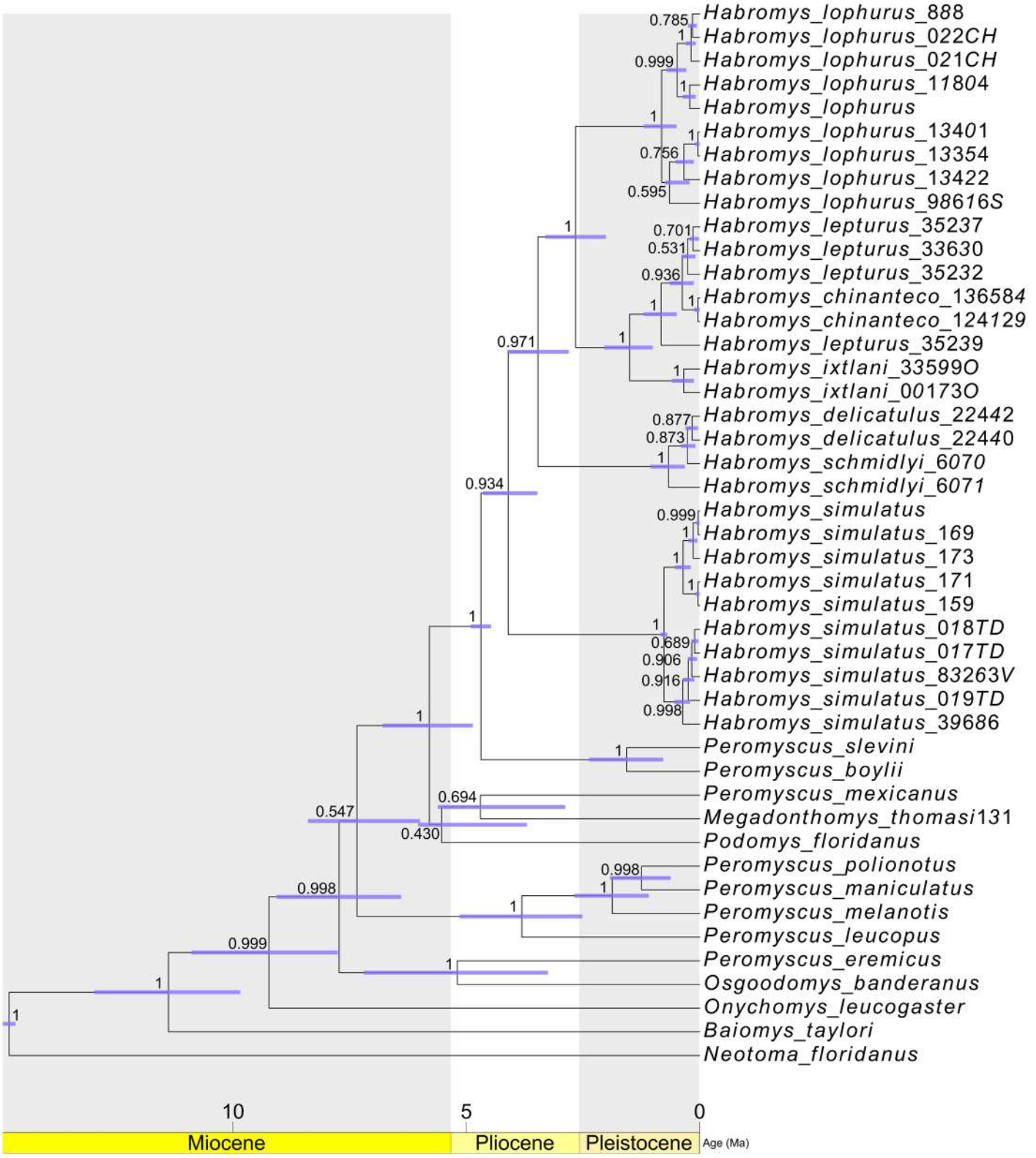

Figure 2. Phylogenetic reconstruction dated for the genus *Habromys* and its external groups based on information from León-Paniagua *et al.* (2007)

America, whereas anagenetic dispersal/extinction and vicariance were comparatively uncommon (Figs. 3 and 4; Supplemented Material 2).

Crown *Habromys* was inferred to originate in the Sierra Madre Oriental (SMO) at 4.69 Ma via founder-event speciation from the outgroup range (Baja California + Central Mexican Plateau) (Figure 3; Supplemented Material 2). The split leading to *H. simulatus* was dated at ~4.1 Ma, and this lineage was inferred to have colonized the eastern Trans-Mexican Volcanic Belt during the Middle Pleistocene (0.77 Ma) through a founder-event (Figure 3, Supplemented Material 2). A subsequent founder-event from the SMO to the southern Trans-Mexican Volcanic Belt (S-TMVB) was inferred at ~4.1 Ma. Within S-TMVB, *H. schmidlyi* was

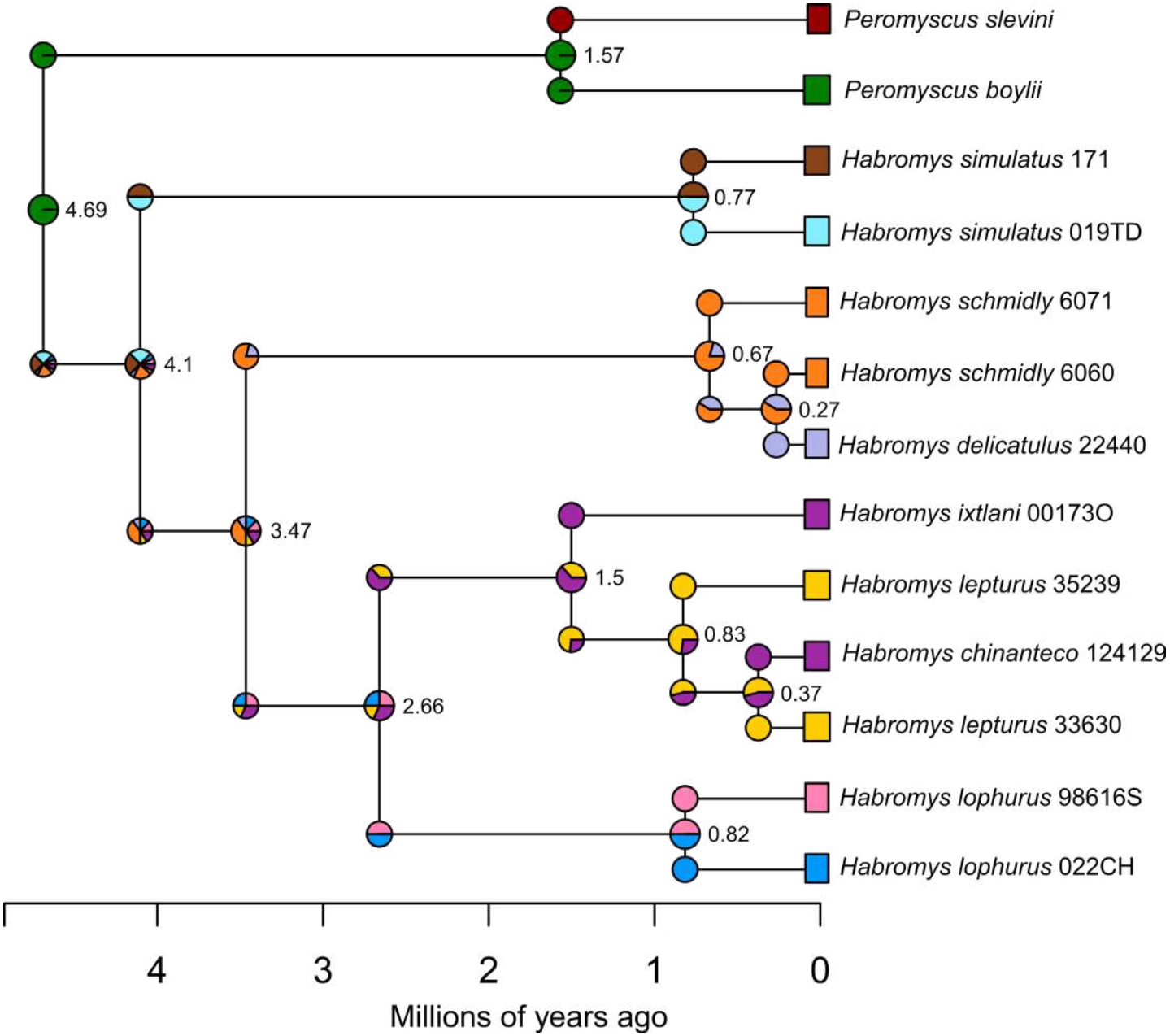

Figure 3. Hypothesis of ancestral area estimation for the genus *Habromys*. The main process involved was the founder-event present in all nodes, with the exception of sympatry events in the species *H. delicatulus* and *H. lepturus*. The colors of the branches correspond to those of the areas in Figure 1.

inferred to originate via within-area cladogenesis (narrow sympatry) at 0.67 Ma, followed by a founder-event into the northern Trans-Mexican Volcanic Belt, where *H. delicatulus* originated at 0.27 Ma (Figure 3; Supplemented Material 2).

A founder-event from the S-TMVB to the Sierra de Juárez (SJ) in the Sierra Madre de Oaxaca was inferred at 3.47 Ma (Figure 3). Within the SJ, diversification among *H. ixtlani*, *H. lepturus*, and *H. chinanteco* was dated at 2.66 Ma at the end of the Pliocene. A founder-event was inferred at 1.5 Ma from the SJ to Cerro Zempoaltepetl, by the lineage that includes *H. lepturus*, whereas *H. ixtlani* remains in SJ. This event was followed by within-area cladogenesis (narrow sympatry) at 0.83 Ma, associated with the divergence of *H. lepturus*. A subsequent founder-event from Cerro Zempoaltepetl back to the SJ was inferred at 0.37 Ma, associated with the divergence of *H. chinanteco* (Figure 3; Supplemented Material 2). Finally, a founder-event from the SJ into the Isthmus of Tehuantepec and the highlands of Chiapas and Guatemala was inferred at 2.66 Ma, followed by colonization of Honduras and El Salvador at 0.82 Ma. Diversification within *H. lophurus* was inferred to occur in these Central American highland areas (Figure 3; Supplemented Material 2).

Discussion

Previous studies on the diversification of the genus *Habromys* suggest that its presence in the mountain systems of central and eastern Mexico and northern Central America is the result of vicariant scenarios, in which range expansion was followed by isolation associated with habitat fragmentation (León-Paniagua *et al.* 2007; Rogers

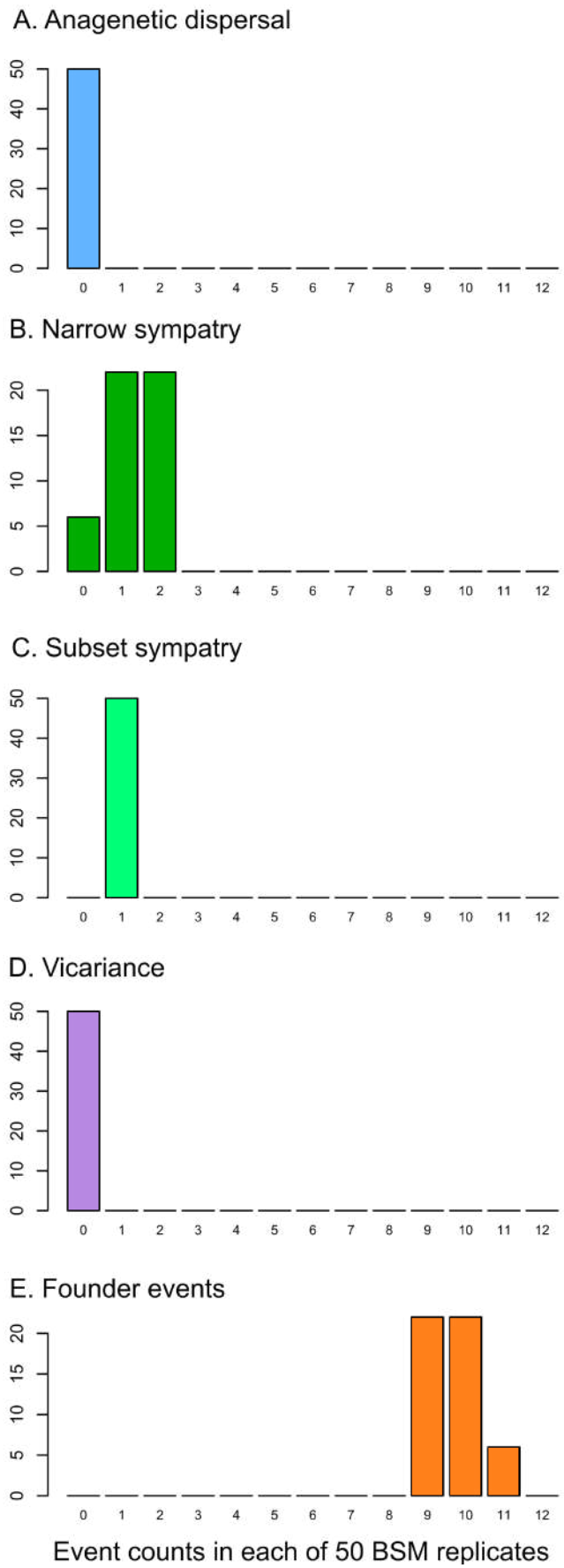

Figure 4. Distribution of biogeographic processes counts across 50 biogeographical stochastic mapping (BSM) replicates under the DEC+J model. Panels show the frequency of inferred events for five processes: (A) Anagenetic dispersal, (B) Narrow sympatry, (C) Subset sympatry, (D) Vicariance, and (E) Founder events. The results indicate a strong predominance of founder-event speciation relative to other biogeographic processes.

et al. 2007). However, these hypotheses were not formally evaluated in a time-calibrated framework that allows explicit comparison among alternative biogeographic processes. Our results indicate that the biogeographic history of *Habromys* is best explained by repeated founder-event speciation, whereas within-area cladogenesis (narrow sympatry) was inferred only for the nodes involving the lineages leading to *H. schmidlyi* and *H. lepturus* (Figure 3; Table 2; Supplemented Material 2).

Founder-event speciation, unlike speciation by vicariance, occurs when a new area is colonized by a small number of individuals through long-distance dispersal or rare dispersal events. Such events may be facilitated when a geographical barrier disappears (due to various factors such as climate changes, continental collisions, the formation of mountain ranges, or changes in sea level). When the barrier reappears or a new one forms, populations on both sides of the barrier begins to separate, reducing gene flow and allowing them to differentiate into different species (geodispersion). Therefore, barriers are not static elements, but rather dynamic throughout history (Lieberman and Eldredge 1996; Matzke 2013c; Wiley and Liberman 2011). In *Habromys*, the best-fitting model (DEC+j, Table 2) supports a biogeographic scenario dominated by multiple founder-events speciation events from the early Pliocene to the middle Pleistocene (Figure 3, Supplemented Material 2), consistent with the climatic oscillations that periodically expanded and contracted cloud forest habitats, and not with the formation of mountain systems. This differs from the scenario proposed by León-Paniagua *et al.* (2007), who interpreted the diversification of *Habromys* and the closely related genera (*Podomys*, *Osgoodomys*, and *Megadontomys*) as the result of an initial range expansion followed by vicariant differentiation driven by climatic fragmentation of montane forests.

The Pliocene has been considered a transitional climatic period characterized by warm climates that changed rhythmically every 40 000 years to large-scale glacial-interglacial periods, which preceded the Pleistocene conditions that occurred with greater frequency and magnitude (Dowsett *et al.* 2010; Lawrence *et al.* 2010; Salzmann *et al.* 2011). In this context, the founding-events occurred during the Pliocene leading to the colonization of the southern Trans-Mexican Volcanic Belt (4.69 Ma), Sierra Madre Oriental (4.1 Ma), Sierra de Juárez (3.47 Ma), and the Isthmus of Tehuantepec, Chiapas, and Guatemala (2.66 Ma), coincide with warm periods of this era (Haywood *et al.* 2009; Salzmann *et al.* 2011; Jennings *et al.* 2025). These have been associated with the dynamics of cloud forests and may have increased their connectivity, which correspond to the habitat of *Habromys* species, whose processes associated solely with the Pliocene have been overshadowed by Pleistocene climate changes (Sosa *et al.* 2016).

Although colonization of the areas began during Pliocene, the diversification of the species that make up *Habromys* within their current ranges took place during

the Middle Pleistocene (1.5–0.27 My) (Figs. 2 and 3). This coincides with the Middle Pleistocene Transition (MPT, 1.2–0.5 My), when the frequency of glacial periods changed from approximately every 41 000 years to approximately every 100 000 years, and remained so until the Late Pleistocene (Head and Gibbard 2005; Head *et al.* 2008; Sun *et al.* 2019; Herbert 2023). In the case of *Habromys*, our divergence-time estimates suggest that their presence distribution areas coincide with glacial periods that took place during the MPT (Cohen and Gibbard 2019; 2022), which coincides with León-Paniagua and Guevara (2019). The colonization of the eastern Trans-Mexican Volcanic Belt from the Sierra Madre Oriental by *H. simulatus* (Figure 3) is temporally consistent with a glacial period that took place 0.77 Ma. Likewise, the colonization southern and northern Trans-Mexican Volcanic Belt, 0.67 and 0.27 Ma respectively (Figure 3), shows that the presence and diversification of *H. schmidlyi* and *H. delicatulus* are also the result of glacial periods that occurred during the MPT (Cohen and Gibbard 2019; 2022).

Unlike the findings of Rogers *et al.* (2007), who argue that the colonization the Sierra de Juárez and Cerro Zempoaltepetl resulted from a single vicariant event occurred in the valley of the Cajonos River, our results suggest a biogeographic scenario were an initial colonization of the Sierra de Juárez by *H. ixtlani* (1.5 Ma) took place during a glacial period prior to the onset of the MPT (Head and Gibbard 2005; Head *et al.* 2008; Cohen and Gibbard 2019; Sun *et al.* 2019; 2022; Herbert 2023); subsequently, the colonization of Cerro Zempoaltepetl (0.83 Ma) and the recolonization of the Sierra de Juárez (0.37 Ma) by *H. chinanteco* and *H. lepturus* also coincide with glacial periods that occurred during the MTP (Cohen and Gibbard 2019; 2022). As for the presence of *H. lophurus* in the Isthmus of Tehuantepec, Chiapas and Guatemala, and Honduras and El Salvador (0.82 Ma) may be associated with the same glacial episode that led to the presence of *H. lepturus* on Cerro Zempoaltepetl. This differs from other studies that have proposed that the presence of *H. lophurus* in the mountain systems of northern Central America is the result of vicariance events due to the presence of the Isthmus of Tehuantepec, which acts has acted as a geographical barrier to the dispersal of *Habromys* and other small mammals (Carleton *et al.* 2002; Rogers *et al.* 2007; León-Paniagua and Guevara 2019). However, it is necessary to consider that the cold and dry conditions that occurred during glacial periods may have promoted the contraction of cloud forests, restricting them to possible refuges, as has been suggested for other periods in Mesoamerica (Toledo 1982; Graham 1999).

The evolution of *Habromys* and its distribution areas is the result of glacial and interglacial events during the Pliocene and Pleistocene epochs. The oldest events allowed the colonization of new areas, while the most recent ones generated isolation and, therefore, the differentiation of each species within its distribution area. This is consistent with the proposal by León-Paniagua and Guevara (2019), who mention that glacial events allowed connections through the formation of corridors between mountainous areas, enabling dispersal events between them, while during warm periods these processes were prevented because valleys and lowlands acted as barriers for species of the genus *Habromys*. However, it is worth mentioning that the climatic changes associated with the Last Glacial Maximum, although they may have had effects on distribution (León-Paniagua and Guevara 2019), did not coincide with major inferred divergence events in our phylogeny.

Our results suggest that the biogeographic history of *Habromys* has been strongly shaped by long-term climatic fluctuations, in which colonization and subsequent isolation processes appear to have played a greater role than vicariant scenarios linked to the formation of Mesoamerican mountain systems. Nevertheless, our inferences are based on a phylogeny reconstructed from mitochondrial genes, which represent a single maternally inherited locus. Mitochondrial datasets may not fully reflect the species tree due to processes such as incomplete lineage sorting, introgression, or sex-biased dispersal, potentially affecting both divergence-time estimates and ancestral-area reconstructions. Therefore, although our results support a founder-event dominated biogeographic scenario, future studies incorporating multilocus nuclear data or phylogenomic datasets will be critical to test the robustness of this hypothesis and to evaluate whether alternative processes such as vicariance or anagenetic dispersal gain support under different phylogenetic reconstructions.

Acknowledgments

We would like to thank the editors for inviting us to contribute to this special issue honoring the academic career of Dr. Livia León-Paniagua. We would also like to thank Dr. Livia León-Paniagua for inspiring so many generations and serving as an example of tenacity and dedication.

Declaration of Artificial Intelligence use

We declare that the authors have not used any Artificial Intelligence in the elaboration of this paper.

Author contributions

Conceptualization: Deborah V. Espinosa-Martínez and César A. Ríos-Muñoz; Methodology: Deborah V. Espinosa-Martínez and César A. Ríos-Muñoz; Supervision: Joaquín Arroyo-Cabrales; Drafting: Deborah V. Espinosa-Martínez, César A. Ríos-Muñoz, and Joaquín Arroyo-Cabrales.

Supplementary data

SD1. Genbank accession numbers of specimens used in the construction of the dated phylogenetic reconstruction. **SD2.** Cladogenetic biogeographic events are inferred from biogeographical stochastic mapping (BSM) under the DEC+J model. The table shows the divergence time (Ma),

process type, ancestral area, descendant areas (1 and 2), and the dispersal areas in founder events. A = X, B =, C =, D =, E =, F =, G =, H =, I = y J =. Geographic areas correspond to those shown in Fig. 1: A = Isthmus of Tehuantepec + Chiapas + Guatemala; B = Honduras + El Salvador; C = Sierra Madre Oriental; D = Eastern Trans-Mexican Volcanic Belt; E = Northern Trans-Mexican Volcanic Belt; F = Southern Trans-Mexican Volcanic Belt; G = Cerro Zempoaltepetl; H = Sierra de Juárez; I = Baja California; J = Central Mexican Plateau.

Literature cited

Álvarez-Castañeda ST, and Cortés-Calva P. 2002. *Peromyscus slevini*. *Mammalian Species* 705:1–2. https://doi.org/10.1644/0.705.1

Álvarez-Castañeda ST, Vázquez E, Castro-Arellano I, and Lacher T. 2018. *Habromys ixtlani*. *The IUCN Red List of Threatened Species* 2018. e.T136582A22376638. [Accessed December 3rd, 2025]. https://dx.doi.org/10.2305/IUCN.UK.2018-2.RLTS.T136582A22376638.en

Bouckaert R, Vaughan, TG, Barido-Sottani J, Duchêne S, Fourment M, Gavryushkina A, *et al*. 2019. BEAST 2.5: an advanced software platform for Bayesian evolutionary analysis. *PLoS Computational Biology* 15:e1006650. https://doi.org/10.1371/journal.pcbi.1006650

Briones-Salas M, Hernández-Allende A, Coronel MM, and Pérez GG. 2012. New records of the endemic Chinanteco deermouse *Habromys chinanteco* (Rodentia: Cricetidae) in the Sierra Madre de Oaxaca, Mexico. *The Southwestern Naturalist* 57:221–222. https://doi.org/10.2307/23258057

Carleton MD, Sánchez O, and Urbano Vidales G. 2002. A new species of *Habromys* (Muroidea: Neotominae) from México with a generic review of species definitions and remarks on diversity patterns among Mesoamerican small mammals restricted to humid montane forests. *Proceedings of the Biological Society of Washington* 115:488–533.

Castañeda-Rico S, León-Paniagua L, Ruedas LA, and Vázquez-Domínguez E. 2011. High genetic diversity and extreme differentiation in the two remaining populations of *Habromys simulatus*. *Journal of Mammalogy* 92:963–973. https://doi.org/10.2307/23259931

Castañeda-Rico S, León-Paniagua L, Vázquez-Domínguez E, and Navarro-Sigüenza AG. 2014. Evolutionary diversification and speciation in rodents of the Mexican lowlands: the *Peromyscus melanophrys* species group. *Molecular Phylogenetics and Evolution* 70:454–463. https://doi.org/10.1016/j.ympev.2013.10.004

Castañeda-Rico S, Parker LD, Sánchez E, Rivas-Trasvina S, Hawkins MTR, Edwards CW, and Maldonado JE. 2023. Novel genomic resources contribute to the systematics of threatened arboreal deer mice of the genus *Habromys* Hooper and Musser, 1964 (Cricetidae, Neotominae) within a neotomine–peromyscine phylogeny. *ZooKeys* 1179: 157–168. https://doi.org/10.3897/zookeys.1179.108759

Ceballos G, editor. 2014. *Mammals of Mexico*. Baltimore (EEUU): Johns Hopkins University Press.

Cohen KM, and Gibbard P. 2019. Global chronostratigraphical correlation table for the last 2.7 million years, version 2019 QI-500. *Quaternary International* 500:20–31. https://doi.org/10.1016/j.quaint.2019.03.009

Cohen KM, and Gibbard P. 2022. *Global chronostratigraphical correlation table for the last 2.7 million years v.2019 (poster version)*. Mendeley Data V5. https://doi.org/10.17632/dtsn3xn3n6.5.

Colunga Salas PF. 2014. Ámbito hogareño y uso de hábitat de *Habromys schmidlyi (Rodentia: Cricetidae)*. [Bachelor's Thesis]. [Mexico City (MEX)]: Universidad Nacional Autónoma de México.

Colunga Salas PF. 2016. *Diversidad genética y patrones ecológicos de Habromys schmidlyi*. [Master's Thesis]. [Mexico City (MEX)]: Universidad Nacional Autónoma de México.

Contreras-Medina R, Santiago-Alvarado M, Espinosa D, Rivas G, and Luna-Vega I. 2024. Distributional patterns and conservation of the genus *Habromys* (Rodentia: Cricetidae) in Mesoamerica. *Studies on Neotropical Fauna and Environment* 59:175–191. https://doi.org/10.1080/01650521.2022.2085071

Dowsett HJ, and Caballero Gill RP. 2010. Pliocene climate. *Stratigraphy* 7:105–110.

Edgar RC. 2004. MUSCLE: multiple sequence alignment with high accuracy and high throughput. *Nucleic Acids Research* 32:1792–1797. https://doi.org/10.1093/nar/gkh340

Emmons L, and Vázquez E. 2019. *Habromys lophurus*. *The IUCN Red List of Threatened Species* 2019. e. T9610A22376801. International Union for Conservation of Nature; December, 2025. [Accessed December 3rd, 2025]. https://dx.doi.org/10.2305/IUCN.UK.2019-3.RLTS.T9610A22376801.en

Goodwin GG. 1964. A new species and a new subspecies of *Peromyscus* from Oaxaca, Mexico. *American Museum Novitates* 2183:1–8.

Graham A. 1999. The tertiary history of the northern temperate element in the northern Latin America biota. *American Journal of Botany* 86:32–38. https://doi.org/10.2307/2656952

Hall ER. 1981. *The mammals of North America*. 2ª ed. Vol. 2. New York (EEUU): The Blackburn Press.

Hasegawa M, Kishino H, and Yano T. 1985. Dating of human-ape splitting by a molecular clock of mitochondrial DNA. *Journal of Molecular Evolution* 22:160–174. https://doi.org/10.1007/BF02101694

Haywood AM, Dowsett HJ, Valdes PJ, Lunt DJ, Francis JE, and Sellwood BW. 2009. Introduction: Pliocene climate, processes and problems. *Philosophical Transactions of the Royal Society A* 367:3–17. https://doi.org/10.1098/rsta.2008.0205

Head MJ, and Gibbard PL. 2005. Early–Middle Pleistocene transitions: an overview and recommendation for

the defining boundary. In: Head MJ, and Gibbard PL, editors. *Early–Middle Pleistocene transitions: the land–ocean evidence*. London (UK): Geological Society, Special Publications; p. 1–18. https://doi.org/10.1144/GSL.SP.2005.247.01.01

Head MJ, Pillans B, and Farquhar SA. 2008. The Early–Middle Pleistocene Transition: characterization and proposed guide for the defining boundary. *Episodes* 31:255–259. https://doi.org/10.18814/epiiugs/2008/v31i2/014

Heled J, and Drummond AJ. 2012. Calibrated tree priors for relaxed phylogenetics and divergence time estimation. *Systematic Biology* 61:138–149.

Herbert TD. 2023. The Mid-Pleistocene Climate Transition. *Annual Review of Earth and Planetary Sciences* 51:389–418. https://doi.org/10.1146/annurev-earth-032320-104209

Hooper ET, and Musser GG. 1964. Notes on classification on the rodent genus *Peromyscus*. *Occasional Papers of the Museum of Zoology, University of Michigan* 635: 1–13.

Jennings CE, Aber JS, Barendregt R, Bierman PR, Mason J, Rovey CW, *et al*. 2025. Middle Pleistocene glaciations in North America. In: Elias S, editor. *Encyclopedia of Quaternary Science*, 3ª ed. London (UK): Elsevier: p. 647–655. https://doi.org/10.1016/B978-0-323-99931-1.00123-9

Kalcounis-Rueppell MC, and Spoon TR. 2009. *Peromyscus boylii* (Rodentia: Cricetidae). *Mammalian Species* 838:1–14. https://doi.org/10.1644/838.1

Landis MJ, Matzke NJ, Moore BR, and Huelsenbeck JP. 2013. Bayesian analysis of biogeography when the number of areas is large. *Systematic Biology* 62:789–804. https://doi.org/10.1093/sysbio/syt040

Lawrence KT, Sosdian S, White HE, and Rosenthal Y. 2010. North Atlantic climate evolution through the Plio-Pleistocene climate transitions. *Earth and Planetary Science Letters* 300:329–342. https://doi.org/10.1016/j.epsl.2010.10.013

León-Paniagua L, and Guevara L. 2019. Quaternary range-shifts of arboreal rodents of the genus *Habromys* (Cricetidae, Neotominae) in Mesoamerica and their evolutionary consequences. *Mammalian Biology* 94:4–10. https://doi.org/10.1016/j.mambio.2018.10.005

León-Paniagua L, Navarro-Sigüenza AG, Hernández-Baños BE, and Morales JC. 2007. Diversification of the arboreal mice of the genus *Habromys* (Rodentia: Cricetidae: Neotominae) in the Mesoamerican highlands. *Molecular Phylogenetics and Evolution* 42:653–664. https://doi.org/10.1016/j.ympev.2006.08.019

Lieberman BS, and Eldredge N. 1996. Trilobite biogeography in the Middle Devonian: geological processes and analytical methods. *Paleobiology* 22:66–79. https://doi.org/10.1017/S009483730001602X

Marines-Macías T, Colunga-Salas P, Verde Arregoitia LD, Narajo EJ, and León-Paniagua L. 2018. Space use by two arboreal rodent species in a Neotropical cloud forest. *Journal of Natural History* 52:1417–1431. https://doi.org/10.1080/00222933.2018.1459921

Matzke NJ. 2013a. *BioGeoBEARS: biogeography with Bayesian (and likelihood) evolutionary analysis in R scripts*. V 0.2.1. R package. https://rdrr.io/cran/BioGeoBEARS/.

Matzke NJ. 2013b. Probabilistic historical biogeography: new models for founder-event speciation, imperfect detection, and fossils allow improved accuracy and model-testing. *Frontiers of Biogeography* 5:242–248. https://doi.org/10.21425/F55419694

Matzke NJ. 2013c. *Probabilistic historical biogeography: new models for founder-event speciation, imperfect detection, and fossils allow improved accuracy and model-testing*. [PhD thesis]. [Berkeley (EEUU)]: University of California.

Matzke NJ. 2014. Model selection in historical biogeography reveals that founder-event speciation is a crucial process in island clades. *Systematic Biology* 63:951–970. https://doi.org/10.1093/sysbio/syu056

Merriam CH. 1898. Descriptions of twenty new species and a new subgenus of *Peromyscus* from Mexico and Guatemala. *Proceedings of the Biological Society of Washington* 12:115–125.

Osgood WH. 1904. Thirty new mice of the genus *Peromyscus* from Mexico and Guatemala. *Proceedings of the Biological Society of Washington* 17:55–77.

R Core Team. 2024. *R: A language and environment for statistical computing*. R Foundation for Statistical Computing. V. 4.4.2. Vienna (Austria). https://www.R-project.org/.

Rambaut A, Drummond AJ, Xie D, Baele G, and Suchard MA. 2018. Posterior Summarization in Bayesian Phylogenetics Using Tracer 1.7. *Systematic Biology* 67:901–904. https://doi.org/10.1093/sysbio/syy032

Ramírez-Pulido J, González-Ruiz N, Gardner AL, and Arroyo-Cabrales J. 2014. List of recent land mammals of Mexico, 2014. *Special Publications, Museum of Texas Tech University* 63:1–69.

Ree RH, and Smith SA. 2008. Maximum likelihood inference of geographic range evolution by dispersal, local extinction, and cladogenesis. *Systematic Biology* 57:4–14. https://doi.org/10.1080/10635150701883881

Ree RH, Moore BR, Webb CO, and Donoghue MJ. 2005. A likelihood framework for inferring the evolution of geographic range on phylogenetic trees. *Evolution* 59:2299–2311. https://doi.org/10.1111/j.0014-3820.2005.tb00940.x

Robertson PB, and Musser GG. 1976. A new species of *Peromyscus* (Rodentia: Cricetidae), and a new specimen of *P. simulatus* from southern Mexico, with comments on their ecology. *Occasional Papers of the Museum of Natural History, The University of Kansas* 47:1–8.

Rogers, DS, Funk CC, Miller JR, and Engstrom MD. 2007. Molecular phylogenetic relationships among crested-tailed mice (genus *Habromys*). *Journal of Mammalian Evolution* 14:37–55. https://doi.org/10.1007/s10914-006-9034-2

Romo-Vázquez E, León-Paniagua L, and Sánchez O. 2005. A new species of *Habromys* (Rodentia: Neotominae) from Mexico. *Proceedings of the Biological Society of*

Washington 118:605–618. https://doi.org/10.2988/0006-324X(2005)118[605:ANSOHR]2.0.CO;2

Ronquist F. 1997. Dispersal–vicariance analysis: a new approach to the quantification of historical biogeography. *Systematic Biology* 46:195–203. https://doi.org/10.1093/sysbio/46.1.195

Ronquist F, and Sanmartín I. 2011. Phylogenetic methods in biogeography. *Annual Review of Ecology, Evolution, and Systematics* 42:441–464. https://doi.org/10.1146/annurev-ecolsys-102209-144710

Salzmann U, Williams M, Haywood AM, Johnson ALA, Kender S, and Zalasiewicz J. 2011. Climate and environment of a Pliocene warm world. *Palaeogeography, Palaeoclimatology, Palaeoecology* 309:1–8. https://doi.org/10.1016/j.palaeo.2011.05.044

Sanmartín I. 2012. Historical biogeography: evolution in time and space. *Evolution: Education and Outreach* 5:555–568. https://doi.org/10.1007/s12052-012-0421-2

SEMARNAT. 2010. Norma Oficial Mexicana NOM-059-ECOL-2010. *Diario Oficial de la Federación* DCLXXXVII (23, 2ª sección). Mexico City (MEX): Secretaría de Medio Ambiente y Recursos Naturales; p. 1–78.

Sosa V, Ornelas JF, Ramírez-Barahona S, and Gándara E. 2016. Historical reconstruction of climatic and elevation preferences and the evolution of cloud forest-adapted tree ferns in Mesoamerica. *PeerJ* 4:e2696. https://doi.org/10.7717/peerj.2696

Sun Y, Yin Q, Crucifix M, Clemens SC, Araya-Melo P, Liu W, *et al.* 2019. Diverse manifestations of the mid-Pleistocene climate transition. *Nature Communications* 10:352. https://doi.org/10.1038/s41467-018-08257-9

Tamura K, Stecher G, and Kumar S. 2021. MEGA 11: molecular evolutionary genetics analysis version 11. *Molecular Biology and Evolution* 38:3022–3027. https://doi.org/10.1093/molbev/msab120

Toledo VM. 1982. Pleistocene changes of vegetation in tropical Mexico. In: Prance GT, editor. *Biological diversification in the tropics*. New York (EEUU): Columbia University Press; p. 93–111.

Vázquez E. 2017. *Habromys delicatulus*. *The IUCN Red List of Threatened Species* 2017. e.T136683A22376548: International Union for Conservation of Nature; December, 2025. [Accessed December 3rd, 2025]. https://dx.doi.org/10.2305/IUCN.UK.2017-2.RLTS.T136683A22376548.en.

Wiley EO, and Lieberman BS. 2011. *Phylogenetics: theory and practice of phylogenetic systematics*. New Jersey (EEUU): Wiley-Blackwell.

Associated editors: Giovani Hernández Canchola and Pablo Colunga Salas
Submitted: December 30, 2025; Reviewed: February 9, 2026
Accepted: May 8, 2026; Published online: May 29, 2026

THERYA, 2026, Vol. 17(2):307-326 DOI: 10.12933/therya.2026.6273 ISSN 2007-3364

Protected area effectiveness for conserving rodent diversity in the Sierra Madre Oriental under climate change

Diana López-Higareda[1*], Susette Castañeda-Rico[2,3,4], Elisa Paulina Zaragoza-Quintana[5], and Zamira A. Ávila-Valle[6,7,8]

[1]Dirección de Cooperación e Implementación en Biodiversidad, Comisión Nacional para el Conocimiento y Uso de la Biodiversidad, C.P. 14010, Ciudad de México, México.
[2]Smithsonian-Mason School of Conservation, C.P. 22630, Front Royal, Virginia, Estados Unidos.
[3]Center for Conservation Genomics, Smithsonian National Zoo and Conservation Biology Institute, C.P. 20008, Washington DC, Estados Unidos.
[4]College of Science, George Mason University, C.P. 22030, Fairfax, Virgina, Estados Unidos. E-mail: susetteazul@gmail.com, castanedaricos@si.edu (SCR)
[5]Facultad de Ciencias Forestales, Universidad Autónoma de Nuevo León, C.P. 67700, Linares, Nuevo León, México. E-mail: nasuanarik@yahoo.com.mx (EPZQ)
[6]Departamento de Biología, División de Ciencias Biológicas y de la Salud, Universidad Autónoma Metropolitana, Unidad Iztapalapa, C.P. 09340, Ciudad de México, México.
[7]Facultad de Ciencias, Universidad Nacional Autónoma de México, C.P. 04510, Ciudad de México, México.
[8]Carrera de Biología, Facultad de Ciencia y Tecnología, Universidad Simón Bolívar México, C.P. 03920, Ciudad de México, México. E-mail: zamira@xanum.uam.mx, zaav@ciencias.unam.mx (ZAAV)
[*]Corresponding author: d.lopezhigareda@gmail.com

Global biodiversity loss is accelerating, driven by multiple factors, including climate change. Protected areas are a cornerstone of conservation strategies; however, their effectiveness is often constrained by limited climate-resilience planning and taxonomic biases that often overlook ecologically important but non-charismatic groups, such as rodents. We analyzed rodent species richness in the Sierra Madre Oriental, Mexico, evaluating conservation effectiveness within protected areas (which cover 29% of the region) under climate change scenarios. Potential species richness for 85 rodent species was estimated using ensemble species distribution models under current conditions and future climate scenarios (RCP4.5 and RCP8.5) for projections to 2030, 2050, and 2070. Temporal trends in potential species richness were evaluated by Mann-Kendall trend test. Additional comparisons included bioclimatic corridors and functional groups (generalists and specialists). Results suggest that protected areas currently encompass all modeled rodent species in the Sierra Madre Oriental (excluding *Dipodomys spectabilis*, *Geomys personatus* and *Sigmodon mascotensis*), however, they do not fully overlap with areas of highest species richness, which are located in the southern Sierra Madre Oriental. Also, an overall decline in high-richness areas by 2070, particularly under the RCP8.5 scenario, where species losses in some protected areas could reach up to 35 species. Although generalist species exhibit relative stability, an overall decreasing trend in species richness is expected in most protected areas, with significant compositional changes projected for specialist species. Notably, bioclimatic corridors were found to host species currently absent from protected areas and to support the same proportion of species classified as at risk. Implementing climate-smart strategies, such as establishing and reinforcing bioclimatic corridors to improve connectivity, is recommended to mitigate biodiversity loss and enhance conservation resilience in the Sierra Madre Oriental.

Keywords: climate scenarios, conservation planning, Global Biodiversity Framework, Mexico, small mammals, species richness

La pérdida global de biodiversidad se está acelerando debido a factores como el cambio climático. Las áreas protegidas son la piedra angular de las estrategias de conservación, pero su efectividad se ve limitada por una planificación insuficiente de la resiliencia climática y por sesgos taxonómicos que omiten grupos ecológicamente importantes, como los roedores. Analizamos la riqueza de especies de roedores en la Sierra Madre Oriental, México, y evaluamos la conservación de las áreas protegidas (29% de la región) bajo escenarios de cambio climático. Se estimó la riqueza potencial de 86 especies de roedores mediante ensambles de modelos de distribución para condiciones actuales y escenarios climáticos futuros (RCP4.5 y RCP8.5), con proyecciones para 2030, 2050 y 2070. Se utilizó la prueba de tendencia de Mann-Kendall para evaluar tendencias temporales de la riqueza potencial de especies y se realizaron comparaciones entre corredores bioclimáticos y grupos funcionales (generalistas y especialistas). Los resultados sugieren que, si bien actualmente las áreas protegidas albergan casi todas las especies modeladas (salvo *Dipodomys spectabilis, Geomys personatus* y *Sigmodon mascotensis*), no se ubican en las zonas de mayor riqueza, al sur de la región. También hay un declive general en las áreas de alta riqueza para 2070, particularmente bajo el escenario RCP8.5, donde las pérdidas en algunas áreas protegidas podrían alcanzar 35 especies. Mientras las especies generalistas muestran estabilidad, se espera una tendencia decreciente en la mayoría de las áreas protegidas, con cambios composicionales significativos en las especies especialistas. También se encontró que los corredores bioclimáticos albergan especies actualmente ausentes en las áreas protegidas y la misma proporción de especies en riesgo. Es recomendable implementar estrategias climáticamente inteligentes, como establecer corredores bioclimáticos para mejorar la conectividad, mitigar la pérdida de biodiversidad y fortalecer la resiliencia de la conservación en la Sierra Madre Oriental.

Palabras clave: escenarios climáticos, mamíferos pequeños, Marco Mundial de Biodiversidad, México, planeación de la conservación, riqueza de especies

Biodiversity is declining at an unprecedented rate in human history, driven primarily by land-use change, resource extraction, pollution, invasive species, and climate change, which together have severely altered 75% of the Earth's land surface (IPBES 2019). Protected areas (PAs) have long been a cornerstone of global conservation policy, serving as a primary strategy for safeguarding ecosystems and species (PNUD and CONANP 2019). The strategic importance of PAs has reached a new milestone under the Kunming-Montreal Global Biodiversity Framework (KMGBF), adopted in December 2022 following significant progress by the Convention on Biological Diversity (CBD). The KMGBF sets an agenda to halt biodiversity loss and restore ecosystems by 2050 (McGowan *et al.* 2024; Zurrell *et al.* 2025). Its flagship objective, Target 3 (known as "30 × 30"), aims to conserve at least 30% of terrestrial, inland water, and marine areas by 2030 (CBD 2022; Rey *et al.* 2024; Steigerwald *et al.* 2024; Buenafe *et al.* 2025; Hutchinson *et al.* 2025).

Despite global consensus on the urgency of avoiding further biodiversity loss, a substantial implementation gap persists between academic research and policy implementation (Hutchinson *et al.* 2025), underscoring the need to integrate biodiversity conservation objectives with global climate challenges through climate-smart conservation planning (Buenafe *et al.* 2025). An important tool in this process is the use of Species Distribution Models (SDMs) to assess potential climate change impacts. Grounded in niche theory (Hutchinson 1957), these models utilize climate change scenarios (plausible, simplified representations of future conditions) derived from General Circulation Models (GCM) to identify shifting suitable ranges over time (McGowan *et al.* 2024; Rey *et al.* 2024; Buenafe *et al.* 2025; Zurrell *et al.* 2025). This approach highlights the importance of protecting both large-scale climate refugia and localized micro-refuges, and of establishing climate corridors that maintain connectivity between current and future suitable habitats (Buenafe *et al.* 2025).

The success of such modeling and connectivity efforts must also take into account the varying adaptive capacities of species, which are closely linked to their functional diversity. While generalist species with broad niches may adapt to or even benefit from climatic shifts by expanding their geographic ranges, specialists with restricted niches often face drastic range contractions (Bravo-Cadena *et al.* 2011; Munguía *et al.* 2016). These specialists are particularly vulnerable to extinction as their specific environmental requirements disappear or shift beyond their dispersal capabilities. The heightened vulnerability of these specialist taxa underscores the critical shortcomings of current conservation infrastructure.

Despite their importance, the overall effectiveness of current PA networks is often limited. Many PAs fail to adequately include rare species, threatened habitats, and unique evolutionary lineages (Beresford *et al.* 2011; Dinerstein *et al.* 2024; Mouillot *et al.* 2024; Revollo-Cadima and Salazar-Bravo 2024; Pulido-Chadid *et al.* 2025). Furthermore, while more than half of mammal habitats worldwide are highly threatened, PAs are frequently established in areas with low human pressure rather than in regions of high conservation priority, driven by the ease of establishment and management rather than systematic conservation planning (Nori *et al.* 2020; Chacón-Prieto *et al.* 2021; Pulido-Chadid *et al.* 2025). Beyond these representativeness gaps, these areas often remain isolated; the absence of mechanisms to reduce ecosystem fragmentation exacerbates connectivity loss and edge effects, negatively impacting preserved areas (SEMARNAT *et al.* 2025). Consequently, identifying complementary areas to enhance the effectiveness and climate resilience of existing PA networks is strongly recommended (Chacón-Prieto *et al.* 2021; Delso *et al.* 2021). The lack of representativeness is often rooted in the specific criteria used for PA design, particularly a strong taxonomic bias that focuses attention and resources on charismatic megafauna, using them as surrogates for general biodiversity (Urquiza-Haas *et al.* 2019; Steigerwald *et al.* 2024). This bias is especially problematic for small, non-charismatic mammals, even though groups such as rodents are among the most diverse and ecologically important taxa, playing key roles as seed dispersers, prey, and contributors to nutrient cycling (Verde-Arregoitia 2016; Formoso and Teta 2019; Zúñiga *et al.* 2021; Lindsø *et al.* 2025). Alarmingly, more than 25% of globally threatened rodent genera and species are not included within recognized biodiversity hotspots (Amori *et al.* 2011).

Furthermore, while conservation status is often assessed using national-level criteria, the impacts of habitat loss often operate at regional scales, indicating that the scale of analysis can influence estimates of threat intensity (Botello *et al.* 2015; Urquiza-Haas *et al.* 2019). Therefore, the effectiveness of conservation efforts depends on the selection of appropriate surrogates and targets. Addressing gaps in the global PA network and ensuring resilience under climate change, requires conducting regional-level assessments focused on underrepresented indicator groups, such as rodents, to identify critical areas, and inform local conservation planning (Amori *et al.* 2011; Formoso and Teta 2019; Revollo-Cadima and Salazar-Bravo 2024).

Given Mexico's environmental diversity, regional precision is essential for effective conservation, with PAs being the main public policy instrument for biodiversity protection since 1917 (SEMARNAT *et al.* 2025). The National Commission of Natural Protected Areas (CONANP) currently administers 232 federal PAs (192 terrestrial/freshwater) and 609 Voluntary Conservation Areas (ADVC; SEMARNAT *et al.* 2025). However, many PAs, particularly in Central Mexico, do not adequately address critical pressures such as climate and land-use changes. Although approximately 54% of established PAs overlap with top-priority conservation areas, 70% of high-priority areas remain entirely unprotected (Chacón-Prieto *et al.* 2021). Additionally, 78% of Mexico's marine, continental, and terrestrial ecosystems are underrepresented within federal and subnational PA networks, with less than 30%

of each ecosystem's area protected, as suggested by the KMGBF (SEMARNAT *et al.* 2025).

To address these systemic deficiencies, some studies suggest a shift toward species-specific impact assessments conducted at regional scales for anticipating local extinction risks and informing the design of targeted conservation actions (Botello *et al.* 2015; Rodríguez-Ruíz *et al.* 2025). This regional approach is particularly important for the Sierra Madre Oriental (SMO) of Mexico, a volcanic mountain range in the country's east, of exceptional biological importance due to its structural complexity and taxonomic richness, including a high mammalian diversity. The SMO hosts approximately 40% of the country's terrestrial mammals, and near 36% of Mexican rodent species (León-Paniagua *et al.* 2004). Although federal authority PAs in the region have increased by 200% over the past two decades (León-Paniagua *et al.* 2004; SEMARNAT *et al.* 2025), ecosystems and species remain highly vulnerable to the dual pressures of climate change and habitat fragmentation (CONANP and GIZ 2013).

Therefore, the objectives of the present study were: (1) evaluate the richness of rodent species currently represented within PAs relative to the overall richness of the SMO region; and (2) assess how well the PAs would perform to maintain rodent species richness under climate change scenarios.

Materials and methods

Study area. The SMO is the second largest mountain system in Mexico, encompassing the states of Coahuila, Guanajuato, Hidalgo, Nuevo León, Puebla, Querétaro, San Luis Potosí, Tamaulipas and Veracruz; this mountain range, with a wetter eastern side, has an irregular, elongated shape, spanning 800 km in length and varying in width from 80 to 100 km (CONANP and GIZ 2013; Goyenechea Mayer-Goyenechea *et al.* 2025). The three priority ecosystems for the SMO are temperate pine and oak forest, low forest and mesophilic mountain forest (CONANP and GIZ 2013). Given the lack of consensus regarding SMO boundaries, we adopted the mastofaunistic province of the SMO (Ramírez-Pulido and Castro-Campillo 1990) as the regionalization framework for this study (Figure 1), instead of the biogeographical provinces (CONABIO 1997; Morrone 2020), or the ecoregions (INEGI *et al.* 2008). Although biogeographic provinces aim to integrate multiple criteria, they exhibit the same methodological inconsistencies of each of these and do not necessarily constitute natural units (Ruíz-Jiménez *et al.* 2004), particularly for mammals whose patterns of endemism and distribution lack natural coherence within the biogeographic province (Goyenechea Mayer-Goyenechea *et al.* 2025). On the other hand, the mastofaunistic province is explicitly defined based on mammalian species distributions and represents a continuous polygon with simple edges that covers both slopes of the mountain range, delimited by the coordinates -101.7357 W, -97.38466 W, 19.63502 N, 26.53433 N, covering approximately 82,667 km^2 (Ramírez-Pulido and Castro-Campillo 1990).

Data. The occurrence records of 91 rodent species (Table 1) were obtained from the National System of Biodiversity Information (SNIB; CONABIO 2024), following the last accepted taxonomy for each species. The initial national-scale dataset was curated to include only records located within the SMO polygon (Ramírez-Pulido and Castro-Campillo 1990). Selection was restricted to records associated with voucher specimens identified to the species level. After removing fossil records and synonyms, the final curated dataset included 2,767 records.

Species distribution models. We used the cumulative projections of potential species distributions under current and climate change scenarios from Ureta *et al.* (2022), who applied ecological niche modeling to assess species exposure and adaptive capacity to climate change. Their SDMs incorporate two Global Circulation Models (GCMs) and corresponding Shared Socioeconomic Pathways (SSPs): a mid-optimistic representative concentration pathway (RCP) scenario (RCP4.5) and a pessimistic scenario (RCP8.5), for three time horizons (2030, 2050, and 2070). Because climate scenarios represent plausible future pathways rather than climate forecasts, we followed established recommendations to always use more than one GCM, more than one time horizon, and more than one RCP (INECC 2021). These data were selected due to the robustness of the modelling approach (Verde-Arregoitia 2016; Thuiller *et al.* 2019), the consistency of the data source with our occurrence dataset, and their thorough representation of Mexico (Urquiza–Haas *et al.* 2019).

Protected area polygons. The list of PAs was compiled from several sources, including the national authority (CONANP), the National Commission for the Knowledge and Use of Biodiversity (CONABIO), and state authorities. The dataset includes federal and subnational level PAs (state and municipal authorities) as well as ADVC, which are under federal authority but have a distinct legal status (CONABIO 2020; CONANP 2024; Garza-Torres *et al.* 2024). The final list comprised 46 PAs covering 23,838 km2 (Table 2). All PA polygons were merged into a single vector layer for spatial analyses.

Species richness. All analyses were performed in R v.4.5.1 (R Core Team 2021) using *terra* (Hijmans 2023), *sf* (Pebesma and Bivand 2023), and *Kendall* (McLeod 2022) packages. Binary ensembled rasters for each rodent species preliminarily identified for the SMO, were sourced from Ureta *et al.* (2022); these maps were binarized by maximizing the True Skill Statistic (TSS) value. The rasters were then cropped to the study area's extent under all scenarios and cropped to the SMO polygon. All maps used the WGS84 coordinate system.

Potential Species Richness (PSR) was calculated as the cross-species overlap value for rodents in the SMO, obtained by summing the cropped binary ensemble models (current potential distribution and under all climate change

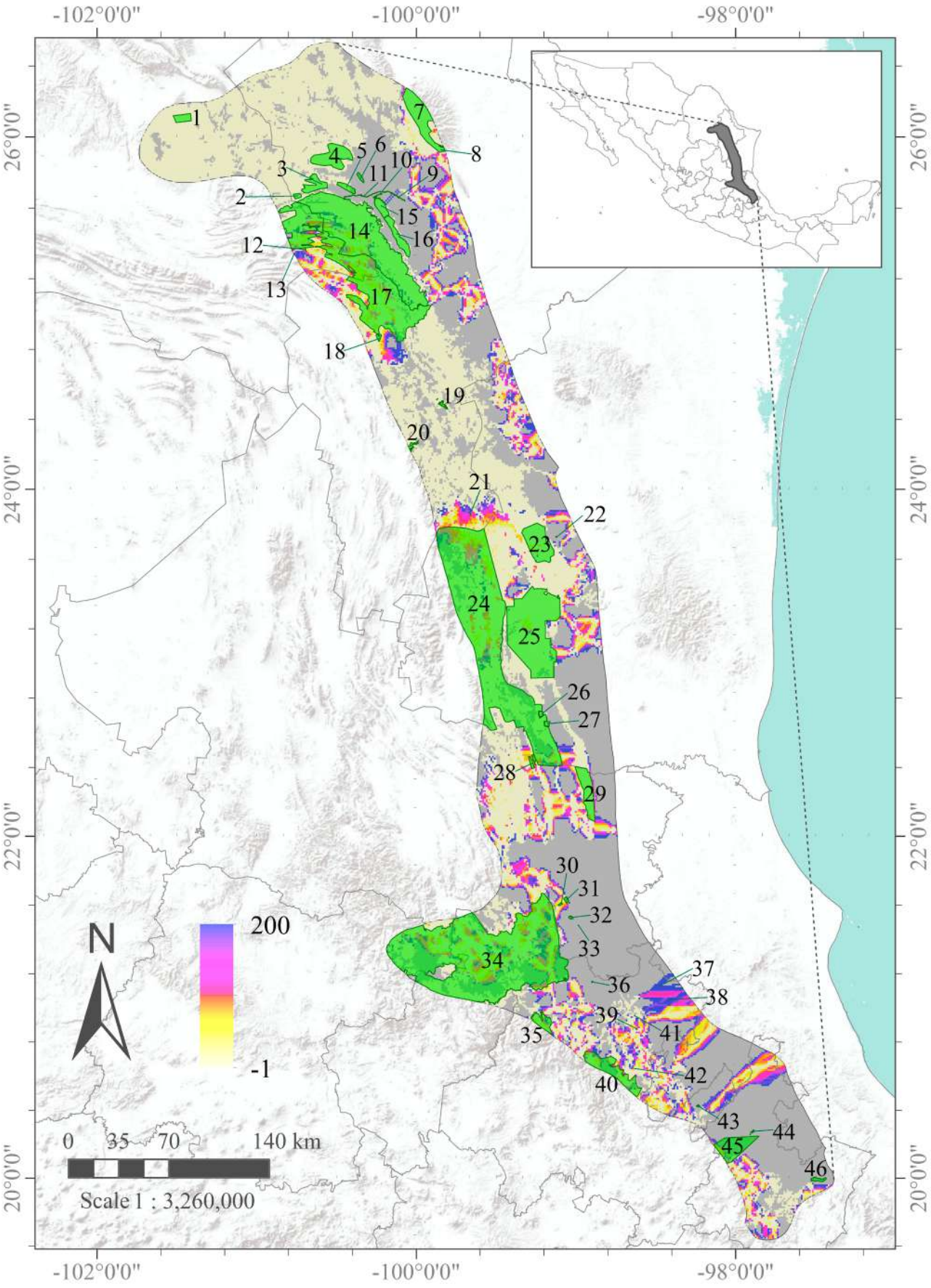

Figure 1. Location of the study area. The Sierra Madre Oriental (SMO) is shown in light grey, and protected areas (PAs) are highlighted in bright green (identified by the numbers provided in Table 2). The color gradient represents bioclimatic corridors (BCCs), with values ranging from -1 (areas with primary vegetation) to 200 (areas with the highest exposure). The inset in the upper-right corner shows a map of Mexico, indicating the location of the SMO (dark grey).

Table 1. Rodent species distributed in the Sierra Madre Oriental (SMO) based on occurrence records. Feeding versatility is classified as generalist (G) or specialist (S). Distribution status indicates that the species is endemic (En). Risk status follows NOM-059-SEMARNAT-2010 (A = threatened, P = endangered, and Pr = subject to special protection) and the IUCN Red List (EN = endangered, CR = critically endangered, and VU = vulnerable). Asterisk (*) denotes species with dispersal ability. Bold type indicates species whose modeled distribution does not show suitability.

id	Rodent species	id	Rodent species	id	Rodent species
1	*Baiomys musculus* (G), (En)	32	***Neotamias durangae*** (S), (En)	63	*Peromyscus leucopus* (G)
2	*Baiomys taylori* (G)	33	*Neotoma albigula* (S) *	64	*Peromyscus levipes* (G), (En)
3	*Chaetodipus eremicus* (S)	34	*Neotoma angustapalata* (S), (En) *	65	*Peromyscus maniculatus* (G),
4	*Chaetodipus hispidus* (S)	35	*Neotoma goldmani* (S), (En) *	66	*Peromyscus melanocarpus* (G), EN
5	***Chaetodipus intermedius*** (S)	36	*Neotoma leucodon* (S) *	67	*Peromyscus melanophrys* (G), (En)
6	*Chaetodipus nelsoni* (S), (En)	37	*Neotoma mexicana* (S) *	68	*Peromyscus melanotis* (G), (En)
7	*Chaetodipus penicillatus* (S)	38	*Neotoma micropus* (S) *	69	*Peromyscus mexicanus* (G), (En)
8	*Coendou mexicanus* (S), A	39	*Neotomodon alstoni* (S), (En)	70	*Peromyscus ochraventer* (G), (En), EN
9	*Cratogeomys castanops* (S)	40	*Nyctomys sumichrasti* (S) *	71	*Peromyscus pectoralis* (G), (En)
10	*Cratogeomys fumosus* (S), (En), A	41	*Oligoryzomys fulvescens* (S)	72	***Peromyscus perfulvus*** (G), (En)
11	*Cratogeomys goldmani* (S), (En)	42	*Onychomys arenicola* (S)	73	*Peromyscus truei* (G)
12	*Cratogeomys merriami* (S), (En)	43	*Onychomys leucogaster* (S)	74	*Reithrodontomys chrysopsis* (S), (En)
13	*Cuniculus paca* (S)	44	*Onychomys torridus* (S)	75	*Reithrodontomys fulvescens* (S)
14	***Cynomys ludovicianus*** (S), P	45	*Heterogeomys hispidus* (S)	76	*Reithrodontomys megalotis* (S)
15	*Cynomys mexicanus* (S), (En), P, EN	46	*Casiomys alfaroi* (S)	77	*Reithrodontomys mexicanus* (S)
16	*Dipodomys merriami* (S)	47	*Casiomys chapmani* (S), (En), VU	78	*Reithrodontomys sumichrasti* (S), (En)
17	*Dipodomys nelsoni* (S), (En)	48	*Oryzomys couesi* (S)	79	*Sciurus alleni* (S), (En)
18	*Dipodomys ordii* (S)	49	*Casiomys melanotis* (S), (En)	80	*Sciurus aureogaster* (S)
19	*Dipodomys phillipsii* (S), (En), Pr	50	*Oryzomys palustris* (S),	81	*Sciurus deppei* (S)
20	*Dipodomys spectabilis* (S)	51	*Casiomys rostratus* (S)	82	***Sciurus griseus*** (S), A
21	*Geomys personatus* (S), A	52	*Otospermophilus variegatus* (S)	83	*Sciurus oculatus* (S), (En), Pr
22	***Geomys tropicalis*** (S), (En), A, EN	53	*Perognathus flavescens* (S)	84	*Sigmodon hispidus* (S)
23	*Glaucomys volans* (S), A	54	*Perognathus flavus* (S)	85	*Sigmodon leucotis* (S), (En)
24	*Habromys simulatus* (S), (En), Pr, CR	55	*Perognathus merriami* (S)	86	*Sigmodon mascotensis* (S), (En)
25	*Heteromys irroratus* (S)	56	*Peromyscus aztecus* (G), (En)	87	*Sigmodon toltecus* (S)
26	*Heteromys pictus* (S)	57	*Peromyscus beatae* (G)	88	*Thomomys bottae* (S)
27	*Ictidomys mexicanus* (G), (En)	58	*Peromyscus boylii* (G)	89	*Thomomys umbrinus* (S)
28	*Megadontomys nelsoni* (G), (En), A, EN	59	*Peromyscus difficilis* (G), (En)	90	*Tylomys nudicaudus* (S)
29	*Microtus mexicanus* (S)	60	*Peromyscus eremicus* (G)	91	*Xerospermophilus spilosoma* (S)
30	*Microtus quasiater* (S), (En), Pr	61	*Peromyscus furvus* (G), (En)		
31	*Neotamias bulleri* (S), (En), VU *	62	*Peromyscus gratus* (G)		

scenarios and projections). This quantifies the number of rodent species with potential distributions within each pixel of the analyzed area and serves as a proxy for species richness. Although this metric does not account for species-level interactions, it can yield reliable biodiversity information over extended periods (Coro *et al.* 2024). Raster cells with undefined values (NA) were replaced with 0.

For the PAs, the SMO species richness raster was cropped with the PAs vector; then raster values within each PA polygon were obtained with zonal statistics. To assess shifts in PSR across the different climate scenarios, the PA species richness raster was reclassified into high, medium, and low categories. These categories were defined using an equal-interval approach based on the maximum species richness observed for the current PSR. By maintaining these fixed interval thresholds across all future projections, we ensured a consistent basis for approximating the expansion or contraction of high-richness areas over time. To evaluate changes in the PSR of PAs across projected time periods, we applied a Mann–Kendall trend test which indicates the direction of the trend: positive, neutral or negative; a positive (*Tau*) value indicates an upward trend, and a negative value indicates a downward trend. While the test does not assess the magnitude of change, it evaluates whether the observed trend is statistically significant; given the limited length of the time series for the analysis (comprising the current projection and three-future time horizons), we adopted a significance level of $p = 0.1$ (corresponding to a 90% confidence interval) (Wang *et al.* 2020; McLeod 2022; Garcia *et al.* 2025).

Species gains and losses across the SMO and within PAs were evaluated by generating presence-absence matrices derived from zonal statistics calculated for each PA polygon under current and climate change scenarios. We then compared these matrices across scenarios. The same approach was applied to functional groups defined

Table 2. Protected areas within the Sierra Madre Oriental, their authority, and their states of location. Authority codes are: S = state; V = voluntary; E = ejidal; M = municipal; F = federal.

id	Protected areas	State	id	Protected areas	State
1	La Viga (E)	Coahuila	24	De la Mariposa Monarca (S)	Tamaulipas
2	Sierra Corral de los Bandidos (S)	Nuevo León	25	El Cielo (S)	Tamaulipas
3	Cerro La Mota (S)	Nuevo León	26	Rancho Regalo de Dios (V)	Tamaulipas
4	Sierra El Fraile y San Miguel (S)	Nuevo León	27	Rancho San Pedro (V)	Tamaulipas
5	Sierra Las Mitras (S)	Nuevo León	28	Sierra del Este y Sierra de Enmedio (S)	San Luis Potosí
6	Cerro El Topo (S)	Nuevo León	29	Sierra del Abra Tanchipa (F)	San Luis Potosí
7	Sierra Picachos (S)	Nuevo León	30	Cuevas de Mantetzulel (S)	San Luis Potosí
8	Cerro El Peñón (S)	Nuevo León	31	El Sótano de las Golondrinas (S)	San Luis Potosí
9	Parque Lineal (S)	Nuevo León	32	Cuevas Sagradas del Viento y de la Fertilidad (S)	San Luis Potosí
10	Nuevo Parque Ecológico La Pastora (S)	Nuevo León	33	La Hoya de las Huahuas (S)	San Luis Potosí
11	Cerro del Obispado (S)	Nuevo León	34	Sierra Gorda (F)	Querétaro, Guanajuato, San Luis Potosí
12	Las Delicias (S)	Coahuila	35	Los Mármoles (F)	Hidalgo
13	La Reforma (S)	Coahuila	36	Cerro el Aguacatillo (M)	Hidalgo
14	Cumbres de Monterrey (F)	Nuevo León, Coahuila	37	El Limonar (S, M)	Hidalgo
15	Cerro de la Silla (F)	Nuevo León	38	Pirámides de Ecuatitla (M)	Hidalgo
16	Sierra Cerro de la Silla (S)	Nuevo León	39	Zacatepec (M)	Hidalgo
17	C.A.D.N.R. 026 Bajo Río San Juan (F)	Coahuila, Nuevo León	40	Barranca de Metztitlán (F)	Hidalgo
18	Cerro El Potosí (S)	Nuevo León	41	Finca Tegolome (S)	Hidalgo
19	La Purísima (S)	Nuevo León	42	Plan Grande (M)	Hidalgo
20	Sandía El Grande (S)	Nuevo León	43	Chicamole (M)	Hidalgo
21	Santa Marta de Abajo (S)	Nuevo León	44	Carmen Serdán (F)	Puebla
22	El Refugio (S)	Tamaulipas	45	Z.P.F.V. la Cuenca Hidrográfica del Río Necaxa (F)	Hidalgo, Puebla
23	Altas Cumbres (S)	Tamaulipas	46	Kowtahyolo (F)	Puebla

by feeding versatility (generalists vs. specialists), following classifications previously used in studies of mammalian functional diversity (Munguía *et al.* 2016; Ureta *et al.* 2022). For each functional group, analyses were repeated using only species within that category.

Bioclimatic corridors. Bioclimatic corridors (BCCs) are shorter, low-impact routes that avoid abrupt climate transitions, thereby facilitating species movement as the climate changes. To assess their conservation potential relative to PAs, we utilized the BCC raster generated by CONABIO *et al.* (2019), which ranks landscape bioclimatic connectivity on a scale from -1 to 200. In this framework values of -1 correspond to fragments of primary vegetation; a value of 0 marks the central, optimal portions (or routes) of the corridors -areas with less climatic variation and less human impact- while values close to 200 occur at the periphery and represent the most exposed areas to anthropogenic pressures (CONABIO *et al.* 2019). The BCC raster was first cropped to the SMO extent and then reclassified into three categories (high, medium, and low). We then overlaid each PSR raster map with the reclassified BCC raster. Species richness within the SMO was analyzed by calculating zonal statistics for the PSR raster for each climate scenario and for the reclassified BCC raster. Finally, we compared species richness between PAs and BCCs.

Results

While 91 rodent species were initially identified through occurrence records from SNIB, the potential distribution models from Ureta *et al.* (2022) projected suitability for only 85 species in the SMO (Table 1). For the remaining six species (*Chaetodipus intermedius, Cynomys ludovicianus, Geomys tropicalis, Peromyscus perfulvus, Sciurus griseus* and *Neotamias durangae*) the models indicated no climatic suitability within the study area under the current projection, despite occurrence records. However, as suitability change in the future under climate change scenarios, *C. intermedius* and *P. perfulvus* gain shift into the SMO in 2070 under RCP4.5 scenario.

We identified 46 PAs comprising 10 under federal authority, 27 state, 5 municipal, 2 ADVC, 1 ejidal, and 1 state/municipal (Figure 1, Table 2) that represent 29% of the SMO total area. The spatial distribution of rodent PSR shows a latitudinal gradient, with richness increasing from north to south along the SMO. The highest PSR values are concentrated in the southern portion of SMO, below the 21° N latitude, primarily within the states of Hidalgo and Puebla, where PSR ranges from 31 and 46 species (Figure 2). The highest PSR do not fully coincide with the largest PAs, as the five most extensive (bigger than a thousand square kilometers) lie above 21° N latitude: C.A.D.N.R. 026 Bajo Río San Juan and Cumbres de Monterrey in state of Nuevo León (PSR of 28 and 38, respectively); De la Mariposa Monarca and El Cielo in state of Tamaulipas (PSR of 27 and 39, respectively); and Sierra Gorda in state of Querétaro, Guanajuato and San Luis Potosí (PSR of 30) (Figures 1 and 2). These large extension PAs, where the PSR is rather medium (between 15 and 30 species) on the

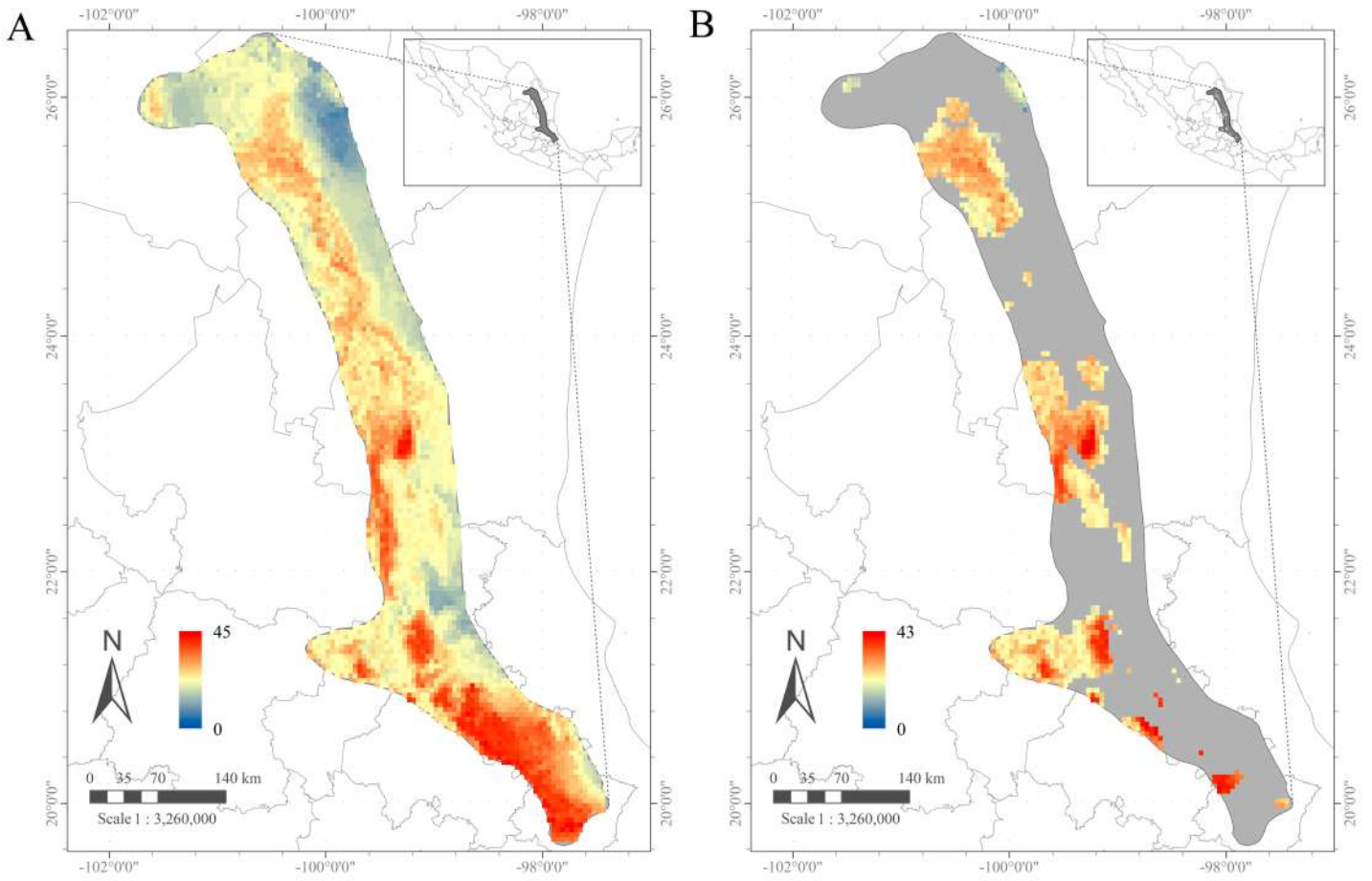

Figure 2. Potential species richness (PSR). A) Sierra Madre Oriental (SMO); B) protected areas (PAs). The color gradient (lower left) indicates the number of rodent species potentially present per pixel across the analyzed area.

western side of the SMO, coincide with areas of rugged topography and temperate forests.

The zone of maximum PSR in Hidalgo, Puebla and Veracruz coincides with BCCs that show intermediate to high exposure values (Figures 1 and 2). The BCCs exhibit also a latitudinal gradient in their landscape integrity, starting in the north of the SMO (states of Coahuila and Nuevo León) where PAs of federal authority Cumbres de Monterrey and C.A.D.N.R. 026 Bajo Río San Juan, are linked by large and optimal areas that facilitate the movement of species. This pattern extends slightly to the south, towards the central section of the SMO (states of Tamaulipas and San Luis Potosí), where a high density of BCCs is found, specifically around the polygons of the PAs De la Mariposa Monarca, El Cielo and Sierra del Este y Sierra de Enmedio, all of them under state authority.

Meanwhile, in the central section of the SMO, Sierra Gorda (states of Querétaro, Guanajuato and San Luis Potosí, federal authority) serves as a major anchor site that bridges the BCCs in the north with the increasingly fragmented southern sections, acting as a primary source for species dispersal. By contrast, the southern section of the SMO (states of Hidalgo, Puebla and Veracruz) reveals notably narrow and fragmented BBCs, with the prevalence of areas of high exposition to impact around polygons of the PAs Finca Tegolome, Plan Grande, Chicamole (the three under municipal authority), Carmen Serdán, Z.P.F.V. la Cuenca Hidrográfica del Río Necaxa, and Kowtahyolo (under federal authority), indicating intense anthropogenic pressure and a greater risk of isolation for local species.

Based on presence/absence data from their potential distribution, only three species with potential distribution in the SMO were not represented within any PA: *Dipodomys spectabilis, Geomys personatus*, and *Sigmodon mascotensis*. Regarding species richness per PA, Barranca de Meztitlán (state of Hidalgo) is the most diverse area, potentially hosting 72 species, whereas Santa Marta de Abajo (state of Nuevo León) hosts only 15 species. Almost 46% of the PAs (21) contain between 15 and 28 species, 71% of which are under state authority.

Regarding shifts in PSR under climate change projections, not only will species richness be reduced, but the area where high richness is maintained will also be reduced; high-richness areas within the SMO (those with PSR from 31-45 species) decline over time losing 50% of the area by 2030, 75% by 2050, and up to 87% in the distant horizon (2070) under RCP4.5 scenario, with a decrease on PSR from 45 to 42, 41 and 40 over the same period. These impacts are further intensified under the high-emission RCP8.5 scenario, where area losses reach 60% by 2030, 79% by 2050, and 97% in 2070, decreasing in PSR from 45, to 42, 39 up to 35 species, respectively. Whereas low-richness

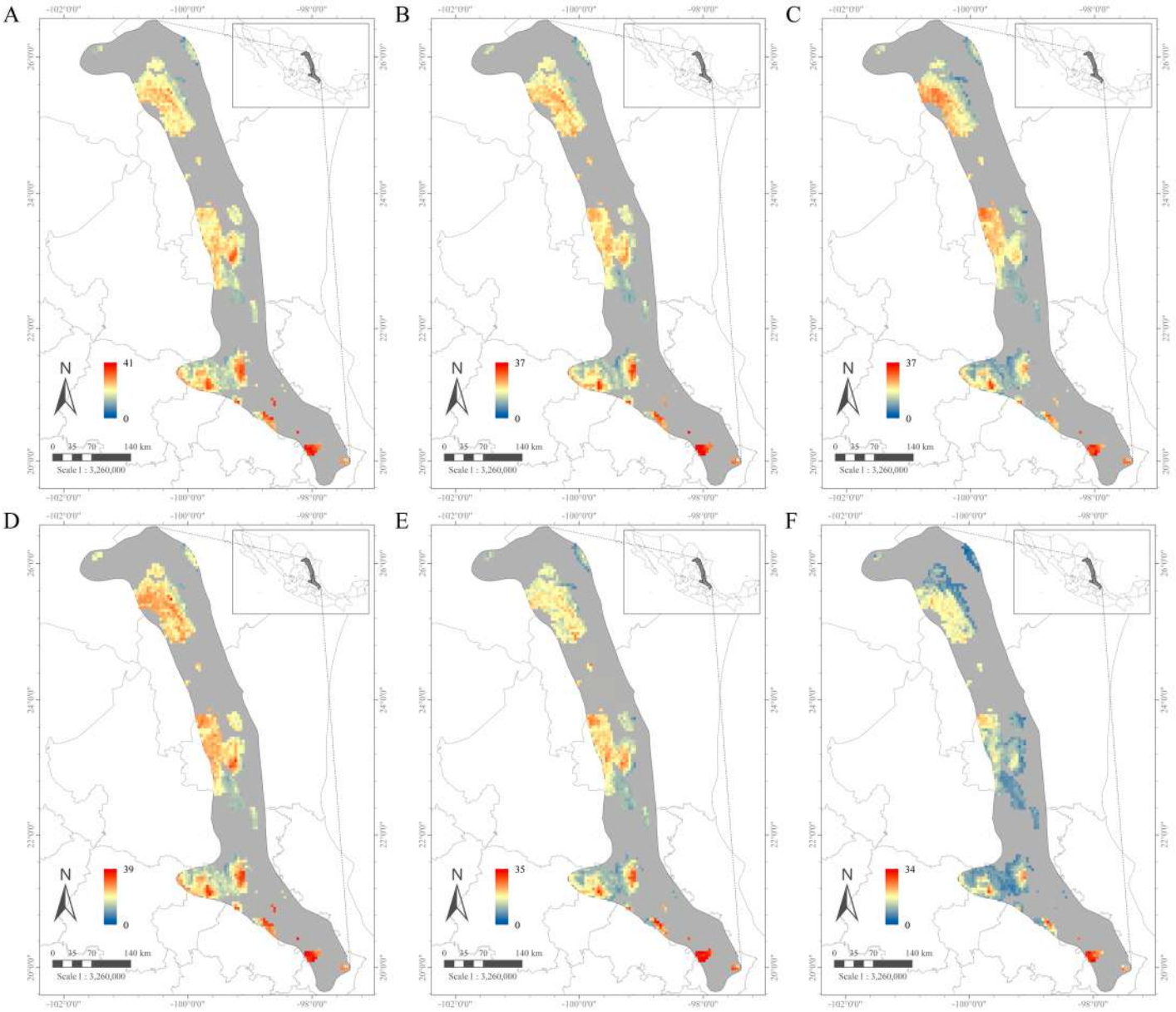

Figure 3. Potential species richness (PSR) under climate change scenarios. A) Representative conservation pathway (RCP) 4.5 in 2030; B) RCP4.5 in 2050; C) RCP4.5 in 2070; D) RCP8.5 in 2030; E) RCP8.5 in 2050; F) RCP8.5 in 2070. The color gradient (lower left) represents the number of rodent species potentially per pixel across the analyzed area.

areas (where PSR is of 16-30 species) expand under both climate scenarios (up to 813% for the 2070 projection under RCP4.5 and 1,149% for the same projected period under RCP8.5 scenario).

Similar trends are observed within PAs; however, in this case, the magnitude of the changes is greater. High-richness areas decline from 70% in 2030, and 85% by 2050, to 93% by 2070, with a decrease in PSR from 41 to 37 species under RCP4.5, while under RCP8.5 loses are 75% by 2030, 89% by 2050, and 98% by 2070, and a loss in PSR from 39 to 34. For both scenarios, the largest reductions in high-richness areas in PAs occur between current and 2030 projections (above 70% of the area), while in the SMO in general, the reduction is of 50-60% (Figures 3 and 4). These patterns of high-richness area contractions persist when generalist and specialist species are analyzed separately (Figure 4). Nevertheless, changes in PSR values over time for PAs, exhibit a difference when considering generalists species: PSR stay almost constant from 17 species under current projection to 18 by 2030, 16 by 2050, and 17 by 2070 under RCP4.5 scenario, and similar for RCP8.5 scenario, to 17 species by 2030, 16 by 2050 and 14 by 2070.

The Mann-Kendall test confirms significant decreasing trends in PSR for 63% of the PAs (*Tau* = -1, $p = 0.089$) under RCP4.5 scenario (Figure 5A); exceptions include Cerro El Potosí (*Tau* = 0.183, $p = 1$), Sierra Corral de Los Bandidos (*Tau* = 0.408, $p = 1$), and La Reforma (*Tau* = 0.183, $p = 0.699$), all located in the northwestern SMO (states of Nuevo León and Coahuila); however, these trends are non-significant ($p > 0.1$). Under RCP8.5, significant decreasing trends are observed for 76% of the PAs (*Tau* = -1, $p = 0.089$; Figure 5B). When considering only generalist species, under the RCP4.5 scenario, the Mann-Kendall test indicates significant negative PSR trends over time, in nine PAs (*Tau* = -1, $p = 0.089$):

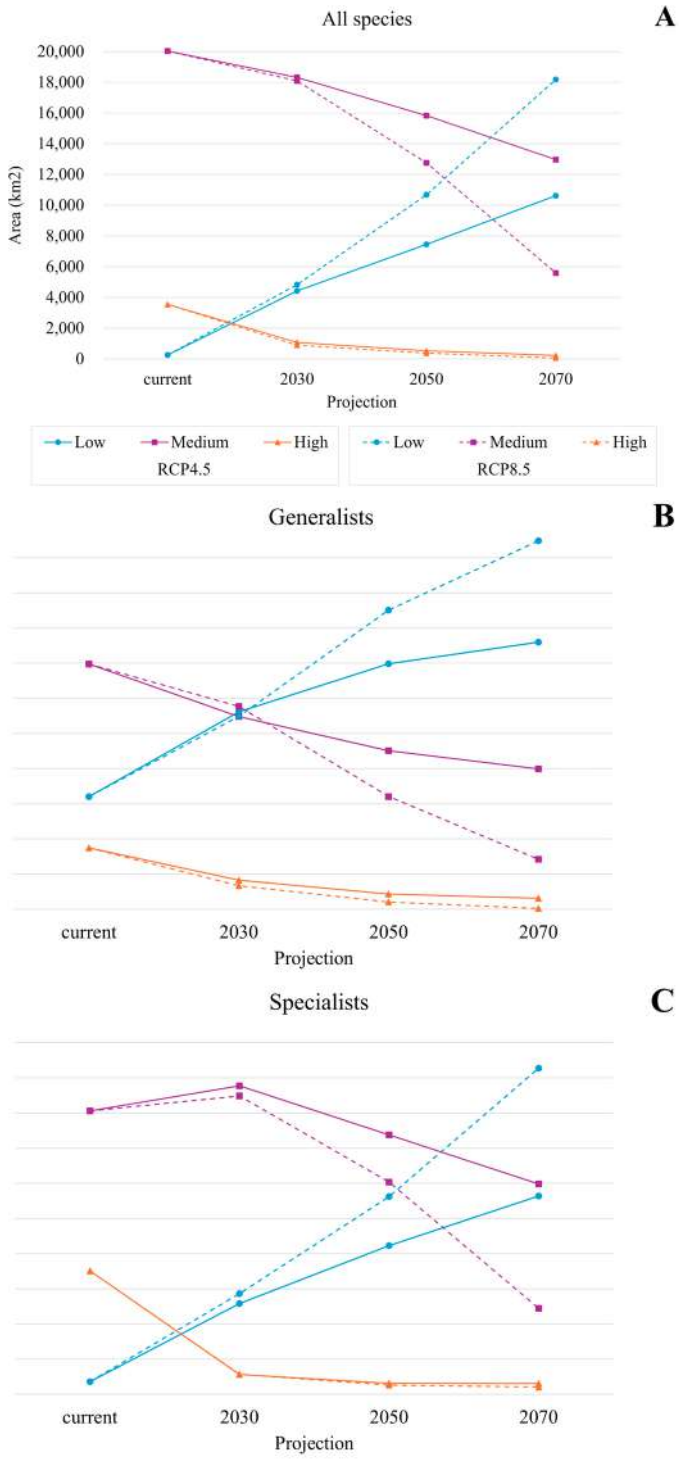

Figure 4. Changes in species richness under climate change scenarios. Increase or decrease in the extent of low (blue), medium (purple), and high richness (orange) areas across projected periods. Solid lines represent the Representative Concentration Pathway (RCP) 4.5 scenario, and dotted lines represent the RCP8.5 scenario. A) All species; B) generalists; C) specialists.

Sierra Las Mitras, Sierra Picachos (state of Nuevo León), El Refugio (state of Tamaulipas), La Hoya de la Huahuas, Sierra del Abra Tanchipa, Sierra del Este y Sierra de Enmedio (state of San Luis Potosí), Sierra Gorda (state of Querétaro), Z.P.F.V. la Cuenca Hidrográfica del Río Necaxa (state of Hidalgo), and Kowtahyolo (state of Puebla); although the positive trend is strong for Sierra Cerro de la Silla and Sierra Corral de los Bandidos (both in the state of Nuevo León), these trends are non-significant (*Tau* = 1, *p* = 1; Figure 6A). Under RCP8.5, the test shows negative values for all the PAs, while the trends are significant for 41% of them (*Tau* = -1, *p* = 0.089), 11 in the states of Coahuila, Nuevo León and Tamaulipas (Figure 6B). The test on specialist species shows a bigger percentage of PAs with decreasing PSR trends conversely generalist species; under the RCP4.5 scenario, trends are significant negative (*Tau* = -1, *p* = 0.089) for 76% of PAs, even though a neutral trend (Tau = 0) is observed for Zacatepec (state of Hidalgo), the trend is no significant (*p* = 1; Figure 7A). The same proportion of PAs with decrease of PSR is observed in specialist species under RCP8.5 scenario, where the 76% of the PAs show significant negative trends (*Tau* = -1, *p* = 0.089; Figure 7B). The test applied to BCCs show significant decreasing trends (*Tau* = -1, *p* = 0.089) across all scenarios, except for the conserved areas under RCP4.5 scenario (for both generalist and specialist species) where decreasing trends are statistically non-significant (*Tau* > -1, *p* > 0.1).

Comparisons of species presence within each PA between the current and 2070 projections, based on potential distribution models, show that under the RCP4.5 scenario, the largest species losses occur in Pirámides de Ecuatitla (12 species, municipal authority, state of Hidalgo) and El Refugio (11 species, state authority, state of Tamaulipas; on the other hand Barranca de Meztitlán (federal authority, Hidalgo), Carmen Serdán (federal authority, Puebla), Cerro de la Silla (federal authority, Nuevo León), and De la Mariposa Monarca (state authority, Tamaulipas), remain among the ones with the highest potential presence of species during the three periods projected. Under the RCP8.5 scenario, the PAs with largest potential species losses are El Limonar (35 species, state and municipal authority, state of Hidalgo), and Cuevas Sagradas del Viento y de la Fertilidad (27 species, state authority, state of San Luis Potosí). Regarding those that maintain the highest potential presence of species during the three projected periods under this pessimistic scenario, they are also Barranca de Meztitlán, and De la Mariposa Monarca.

While the total number of species potentially present in PAs remains relatively without change over time under the RCP4.5 scenario, species composition turnover occurs by 2070 (Table 3). At this horizon, *Cynomys mexicanus* and

Table 3. Projected gains and losses of rodent species within the study area under two climate scenarios (RCP4.5 and RCP8.5) for three period projections (2030, 2050, and 2070).

Scenario	Projection	Species lost	Species gained/regained
RCP4.5	2030	*Reithrodontomys chrysopsis* *Sigmodon leucotis*	*Sigmodon mascotensis*
	2070	*Chaetodipus intermedius* *Peromyscus perfulvus*	*Cynomys mexicanus* *Habromys simulatus*
RCP8.5	2030	*Reithrodontomys chrysopsis* *Sigmodon leucotis*	*Sigmodon mascotensis*
	2050	*Chaetodipus penicillatus* *Cratogeomys tylorhinus* *Neotomodon alstoni*	*Chaetodipus intermedius*
	2070	*Dipodomys phillipsii* *Neotamias bulleri* *Neotoma angustapalata* *Neotoma goldmani*	*Chaetodipus penicillatus*

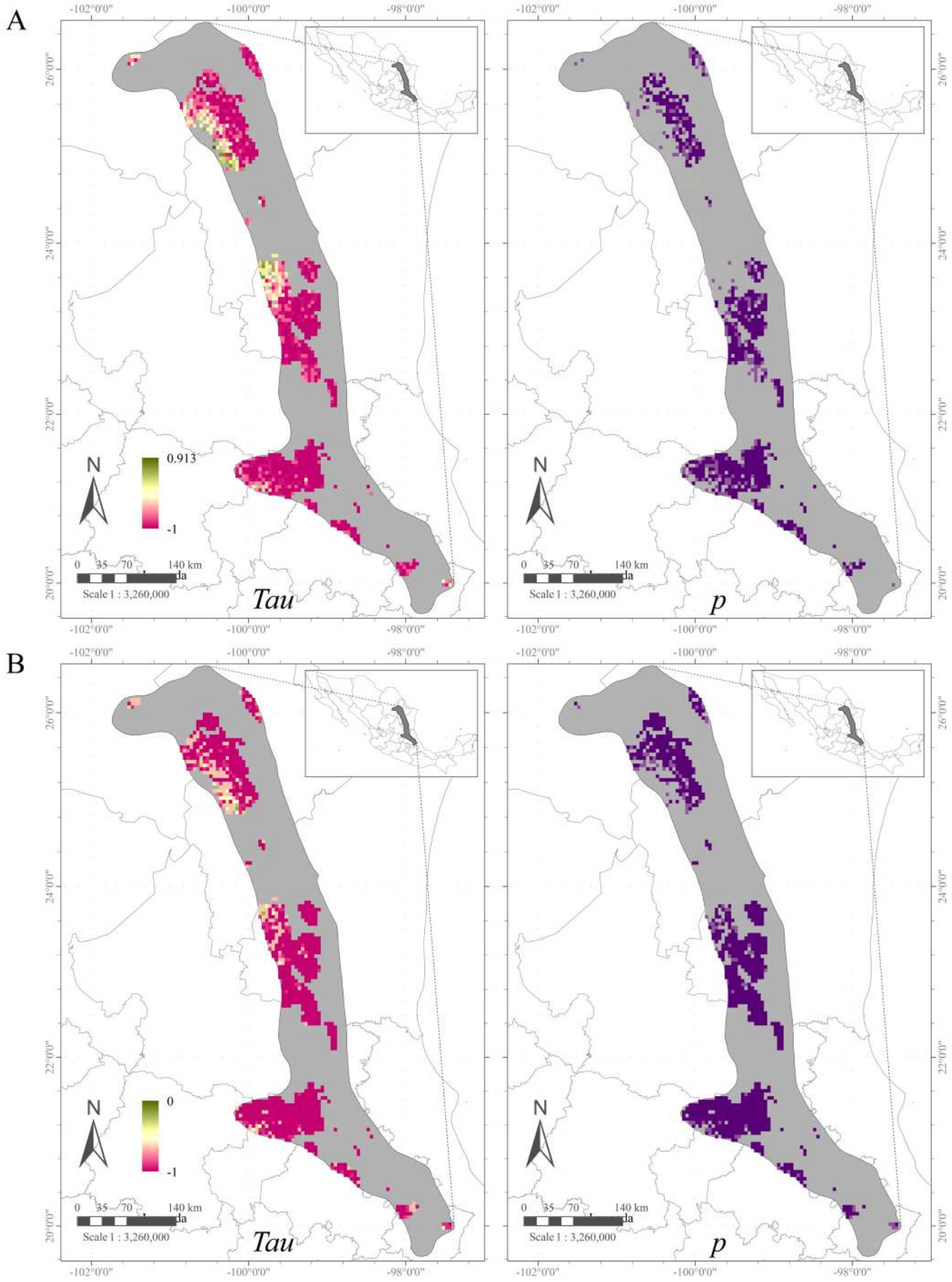

Figure 5. Temporal trends in potential species richness (PSR): Mann-Kendall test results, *Tau* values (left, trend direction indicated by the color scale), and *p*-values (right, purple areas denote statistical significance). A) Representative conservation pathway (RCP) 4.5 scenario; B) RCP8.5 scenario.

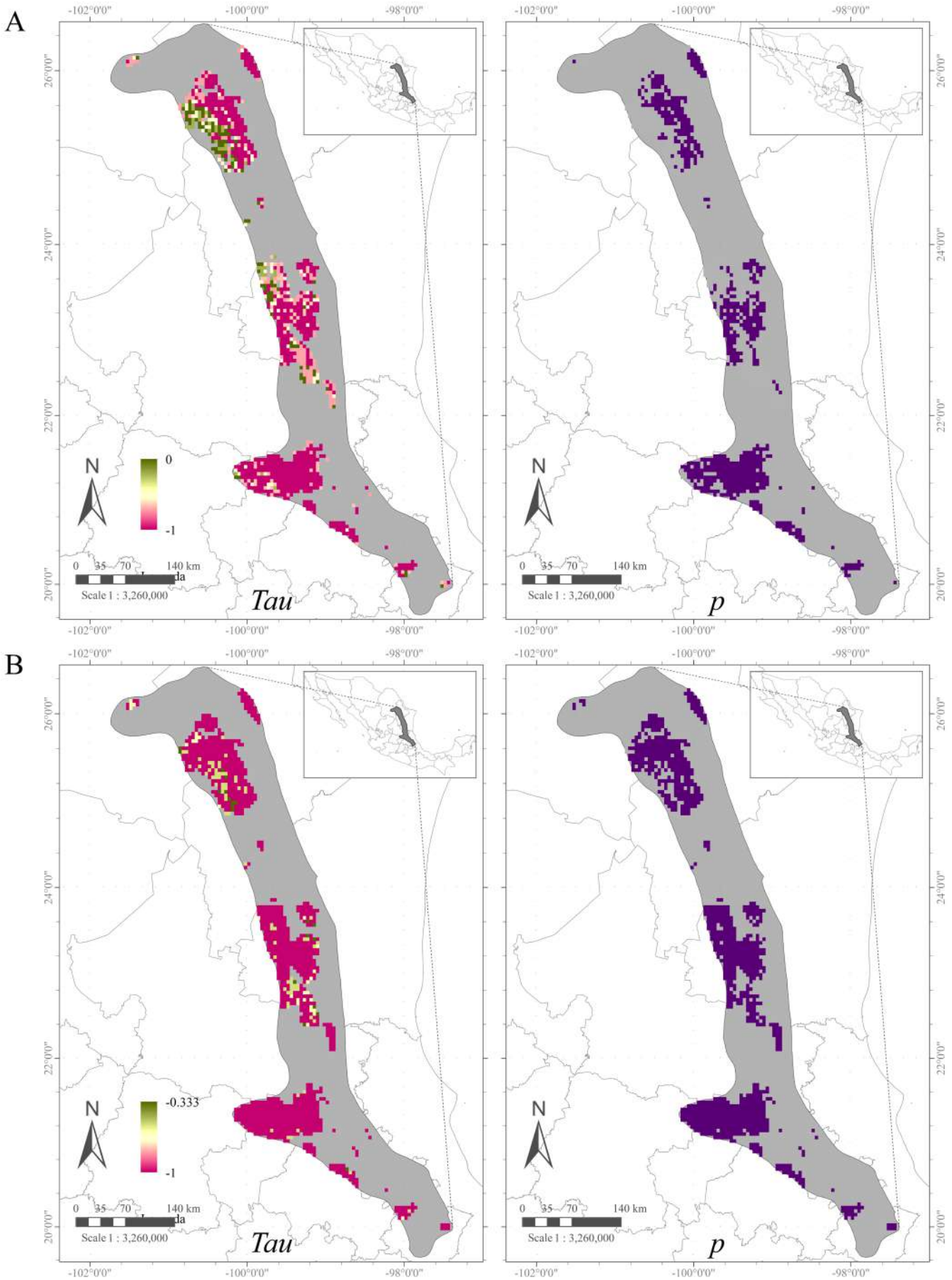

Figure 6. Temporal trends in potential species richness (PSR) for generalist species: Mann-Kendall test results, *Tau* values (left, trend direction indicated by the color scale), and *p*-values (right, purple areas denote statistical significance). A) Representative conservation pathway (RCP) 4.5 scenario; B) RCP8.5 scenario.

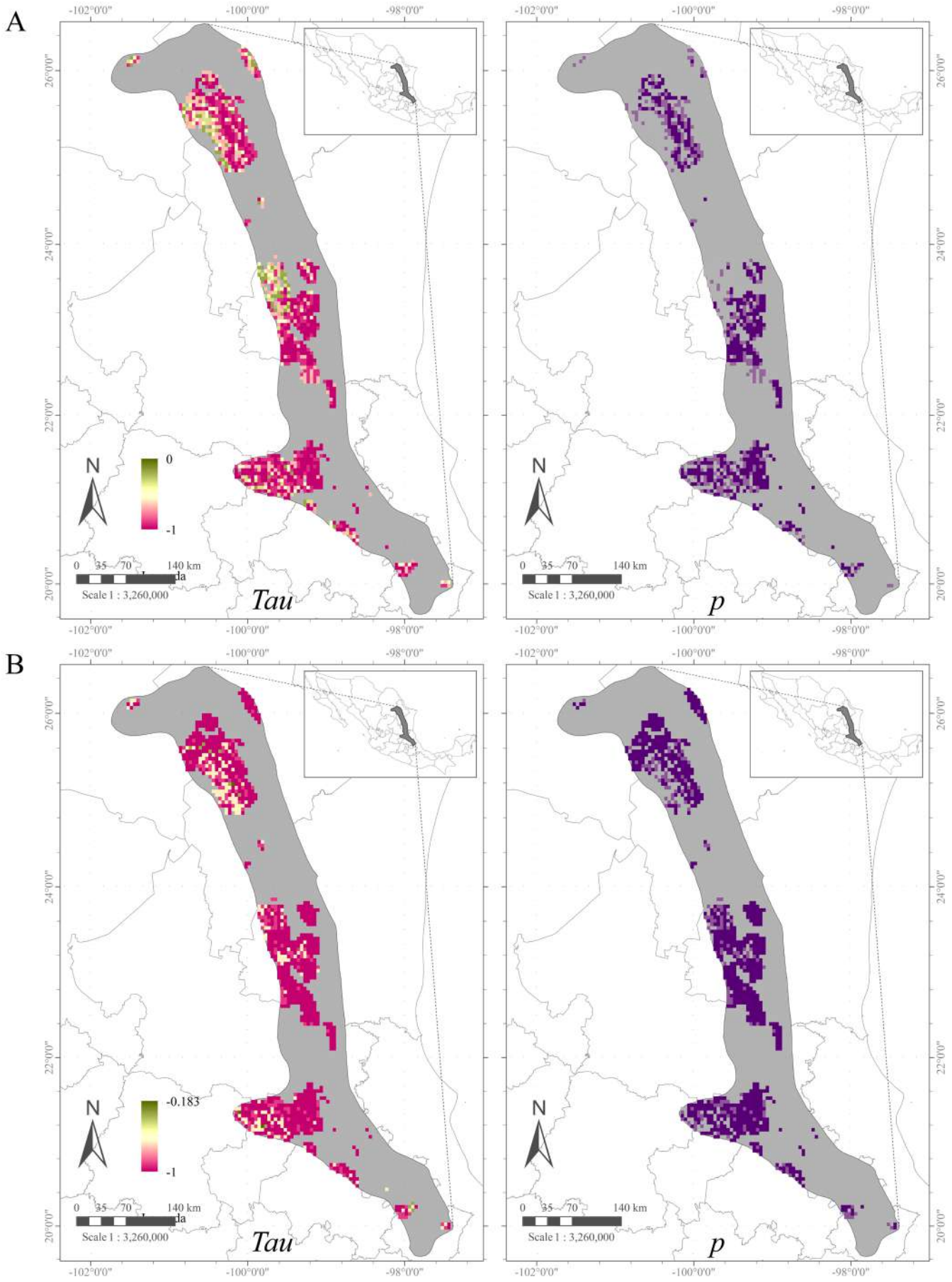

Figure 7. Temporal trends in potential species richness (PSR) for specialist species: Mann-Kendall test results, *Tau* values (left, trend direction indicated by the color scale), and *p*-values (right, purple areas denote statistical significance). A) Representative conservation pathway (RCP) 4.5 scenario; B) RCP8.5 scenario.

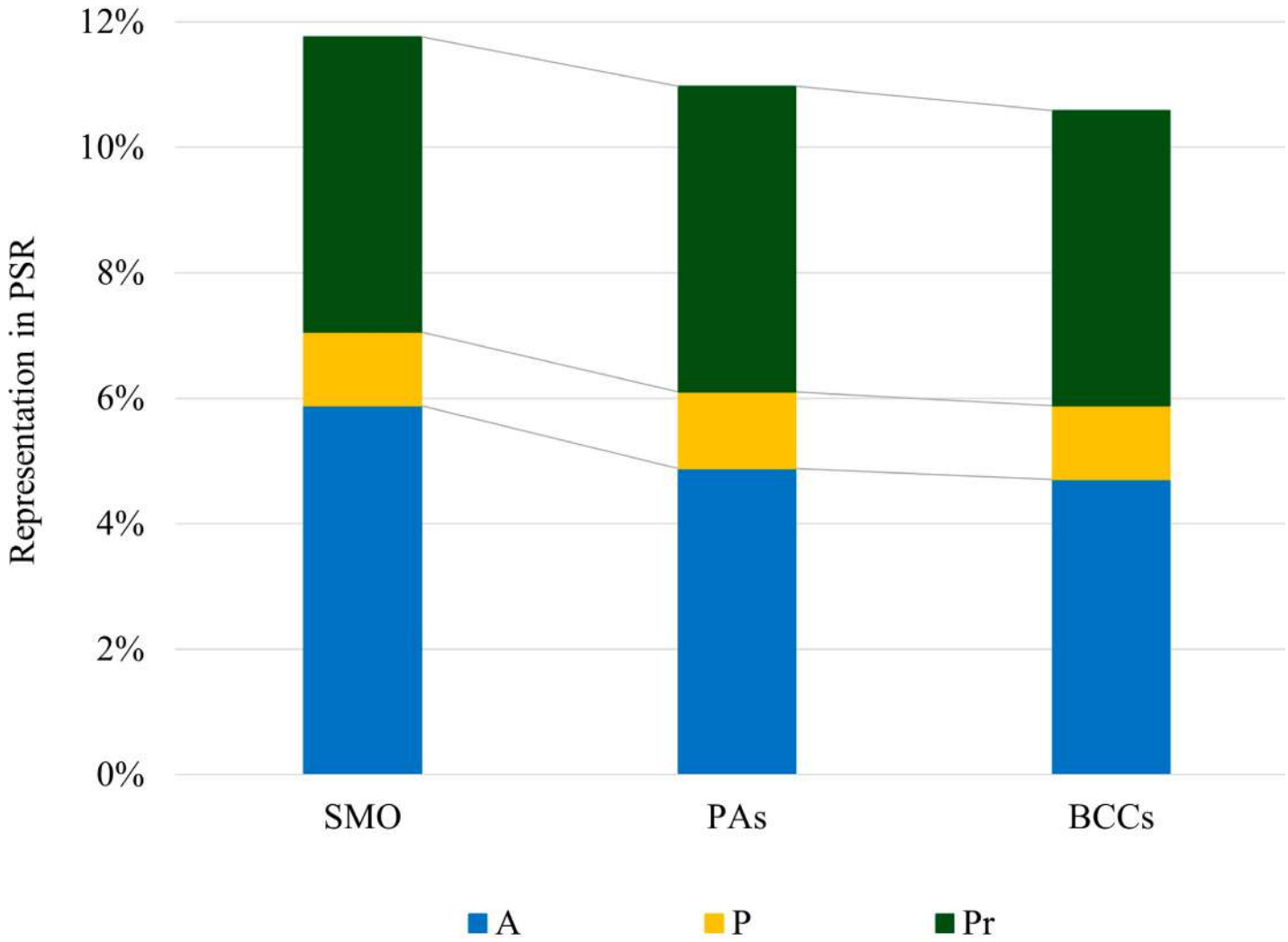

Figure 8. Percentage representation of species in each risk category according to the Official Mexican Standard NOM-059-SEMARNAT-2010 within the potential species richness (PSR) of the Sierra Madre Oriental (SMO), protected areas (PAs), and bioclimatic corridors (BCCs). Risk categories shown are threatened (A, blue), endangered (P, yellow), and subject to special protection (Pr, green).

Habromys simulatus (both specialists) are projected to be lost in the PAs. In contrast, the endemic species *C. intermedius*, is expected to regain presence within PAs: Nuevo Parque Ecológico La Pastora, Cerro del Obispado, and Sierra Picachos (all state authority, in state of Nuevo León), while *P. perfulvus* (which according to the modeled distribution has no climatic suitability under current conditions) regains presence withing Sierra Gorda (federal authority in states of Querétaro, Guanajuato and San Luis Potosí). Under the pessimistic RCP8.5 scenario, overall species presence in PAs declines. By 2050, *Chaetodipus penicillatus*, and *Neotomodon alstoni* (both specialists) are projected to be extirpated, while *C. intermedius* shows recovery in Parque Lineal, Nuevo Parque Ecológico La Pastora, and Cerro del Obispado (all state authority, in state of Nuevo León). By 2070, additional losses include *Dipodomys phillipsii*, *N. bulleri*, *Neotoma angustapalata*, and *N. goldmani*. Notably, *C. penicillatus* despite its initial loss, is projected to regain suitability in Sierra Las Mitras (state authority in state of Nuevo León).

It is important to mention that under all scenarios, *Reithrodontomys chrysopsis* and *Sigmodon leucotis* (both endemic and specialist species) are projected to be consistently lost from the PAs in the study area. Conversely, *S. mascotensis*, without suitability under current conditions, regains presence within the PA starting in 2030. Bioclimatic corridors (BCCs) support two additional species (*C. intermedius* and *P. perfulvus*) that according to the current projection, have no climatic suitability in the PAs or the region. The case of *S. mascotensis* is notable because, according to the modeled current projection, it is absent from PAs but has presence within BCCs. Notably, for future projections, the total potential number of species within BCCs remains constant under both scenarios.

Finally, only 10 rodent species within the SMO fall into any risk category of the Official Mexican Standard (NOM-059-SEMARNAT-2010; SEMARNAT 2010): 5 threatened, 1 endangered, and 4 subject to special protection. For PAs the species count is very similar: 4 threatened, 1 endangered, and 4 subject to special protection. Temporal variation across both climate change scenarios indicates loss of species from the SMO for all risk categories: under RCP4.5 scenario there potentially are one less threatened species by 2030, one less species endangered and one less subject to special protection by 2070; while under RCP8.5

there potentially are one less threatened species by 2030, and one less subject to special protection species by 2070. In regard BCCs, they potentially host same species under risk categories as PAs (and in the same categories): 4 threatened, 1 endangered, and 4 subject to special protection (Figure 8).

Discussion

Our results suggest that PAs contribute to the conservation of rodent species and the maintenance of species richness in the SMO, even under projected climate change scenarios. However, although overall species richness may persist, our projections indicate that community composition is likely to change over time as climatic conditions shift.

The PSR pattern is linked to the topographic axis of the mountain range, where high richness follows the mountainous elevations west of the SMO and decreases as the landscape transitions to the adjacent lowlands towards the east of the region. The highest PSR values (up to 46 species) are concentrated in the southern portion of the SMO, specifically across the states of Hidalgo, Puebla, and northern Veracruz, indicating that this region serves as the primary reservoir of rodent biodiversity. In contrast, the northern regions (states of Coahuila and Nuevo León) exhibit lower overall species richness, typically ranging from 2 to 22 species. Our findings regarding this differentiation of the north, center, and south based on PSR patterns and PA efficacy, is similar to the mammalian regionalization described by León-Paniagua *et al.* (2004) for the SMO, who identified a northern clade dominated by arid-adapted species (states of Coahuila and Nuevo León), a southern section characterized by humid mountain forest fauna (states of Querétaro, Hidalgo, Puebla and Veracruz), and a central section of the SMO (states of Tamaulipas and San Luis Potosí) dominated by tropical taxa.

Areas with higher rodent PSR species in the south, are also those facing greater pressure from climate change or fragmentation (CONANP and GIZ 2013). State and municipal PAs in southern SMO act like small islands in a matrix of high climate pressure; specialist species depend on these areas. The high exposure of the surrounding BCCs suggests that, in the event of a climatic shift, these specialist species will have highly degraded or non-existent dispersal pathways, increasing the risk of local extirpation. The PA Sierra Gorda (states of Querétaro, Guanajuato and San Luis Potosí) represents an important area of medium PSR in the center of the SMO where high BCCs values suggest well-preserved primary vegetation; here it is projected that *P. perfulvus* will potentially regain presence by 2070, while the effectiveness of any colonization may depend on maintaining connectivity at the PA boundaries, where limited BCCs zones must not become insurmountable barriers to dispersal. Although PAs in the northern SMO host lower species richness than those in the south, they are associated with BCCs characterized by high stability and low climate exposure. In Nuevo León, the intersection of PAs such as Cumbres de Monterrey, Sierra Picachos, Nuevo Parque Ecológico La Pastora and Cerro del Obispado with low-exposure BCCs suggests these areas may serve as critical refugia (Buenafe *et al.* 2025). While these findings are not novel, and it is well established that climatic trends influence species richness trends (Urquiza-Haas *et al.* 2019; Thompson 2025), they reinforce the need to conduct analyses at smaller spatial scales and improve connectivity between PAs.

When rodent functional groups were analyzed based on feeding versatility, differences between generalist and specialist species were not statistically significant. Nevertheless, generalist species tended to exhibit greater temporal PSR stability across projections. Under the RCP4.5 scenario, southern PAs retain specialist species in the higher parts of the topography at the south of the region, whereas under the pessimistic RCP8.5 scenario, generalist and widely distributed species persist in PAs. This pattern is consistent with expectations, as climatic changes often favor species with broader ecological tolerances, which are better able to colonize novel environments, potentially offsetting local extirpations (Bravo-Cadena *et al.* 2011; Munguía *et al.* 2016; Thompson *et al.* 2025).

We found that neither PA size nor authority (federal, state, municipal, or private) had a significant effect on species conservation outcomes. This result challenges the widespread assumption that only large PAs can conserve biodiversity, an assumption that may lead to suboptimal conservation strategies, particularly for taxa with restricted distributions (Buenafe *et al.* 2025). Although the authority category does not independently define PSR, it is a key determinant of landscape resilience. Notably, state-level PAs showed better performance in potential species recovery under climate change scenarios, highlighting their relevance in regional conservation planning. By shaping the capacity for adaptation and mitigation, these frameworks act as the primary architecture for the region's climate-smart conservation efforts (Amori *et al.* 2011; Formoso and Teta 2019; Revollo-Cadima and Salazar-Bravo 2024). The functional importance of these governance categories is further evidenced by their roles: while federal PAs function as primary anchors of climatic stability, state and municipal PAs, along with ADVC, serve as strategic refugia in areas of high climatic pressure (Bezaury-Creel 2024). Their capacity to facilitate species recovery is exemplified by the persistence of *C. intermedius* in the PAs of Nuevo León.

These findings related to PA size and authority, highlight the importance of subnational level PAs (including ADVC), and suggest the potential utility of other conservation figures, such as the Other Effective Area-Based Conservation Measures (OECM), which have not yet been implemented in Mexico and were therefore not considered in this study (Dinerstein *et al.* 2024; Mouillot *et al.* 2024; Pulido-Chadid *et al.* 2025). The OECM could exploit the climatic stability that functions as BCCs, enabling non-static conservation strategies that remain effective not only under current

conditions but also under more adverse climate scenarios (Nori *et al.* 2020; Bezaury-Creel 2024; Steigerwald *et al.* 2024; Buenafe *et al.* 2025). Climate connectivity can further strengthen established PA networks by incorporating additional areas that link existing protected sites, thereby promoting better-connected, climate-smart conservation planning (Palfrey *et al.* 2022; Steigerwald *et al.* 2024; Buenafe *et al.* 2025).

Regarding the BCCs, our results confirm their key role in preserving habitat connectivity across future climate projections, maintaining their geographic orientation even under changing climatic conditions (CONABIO *et al.* 2019). Habitat connectivity is essential for mammal conservation because it facilitates gene flow, ecological processes, and climate-driven dispersal (Godínez-Gómez *et al.* 2020; Revollo-Cadima and Salazar-Bravo 2024; Buenafe *et al.* 2025; Pulido-Chadid *et al.* 2025). This connectivity allows conservation efforts to extend beyond PA boundaries, addressing threats at the landscape scale (Rey *et al.* 2024; Rahman *et al.* 2025).

Changes in species composition (gains/losses) across projections suggest that to be effective in mitigating the effects of climate change, conservation will require a dynamic approach: responsive management strategies tailored to address the evolving ways biodiversity reacts to environmental shifts, extending beyond the formal boundaries of PAs to ensure functional connectivity across the landscape. It is important to note, however, that while the present study focuses on climatic drivers, land-use change is an equally (or more) important factor to consider for the long-term conservation of rodents and the maintenance of associated ecosystem services (Munguía *et al.* 2016; Zuñiga *et al.* 2021; Ureta *et al.* 2022; Zurell *et al.* 2025). For example, *C. mexicanus* and *H. simulatus*, which are expected to be lost by 2070 under the RCP4.5 scenario (Table 3), are species closely linked to the condition of their habitats. This implies that their needs for resources, shelter, and reproduction are positively influenced by the greater ecosystem quality and stability, which are often more immediately threatened by land-use change than by climate alone (Castañeda-Rico *et al.* 2011; Zaragoza-Quintana *et al.* 2012; Zaragoza-Quintana *et al.* 2022).

Taking into account this link between rodents and their habitats is particularly relevant, not only due the threats these species face, but also because of their ecological importance. In general, the loss of connectivity in the south could affect the natural regeneration of cloud forests, since rodents are the primary seed dispersers of many tree species. However, rodents remain a non-charismatic taxonomic group that is often overlooked in systematic conservation planning (Delso *et al.* 2021). The limited assessment of this group, despite their important ecological and evolutionary roles in ecosystems, is unlikely to improve as emerging low-cost participatory monitoring approaches -such as citizen science- (Hanson *et al.* 2026) may be ineffective for monitoring this type of species. Effective conservation, therefore, requires moving beyond global targets to incorporate local ecological, social, and economic contexts (Mouillot *et al.* 2024). Site-specific, on-the-ground assessments are essential to ensure that PA networks are designed and implemented to address the unique needs and challenges of each region and taxonomic group (Pulido-Chadid *et al.* 2025). A better understanding of local opportunities, enabling conditions, and barriers would guide strategic interventions toward realistic, operationally feasible, and positive long-term conservation outcomes (Mouillot *et al.* 2024).

Our findings further suggest that strategies that combine multiple climate-smart approaches are advisable for mitigating the effects of climate change. These include facilitating climate connectivity through the establishment of corridors and stepping stones that allow species movement (McGowan *et al.* 2024; Buenafe *et al.* 2025). By overlaying current PSR with future climatic suitability, this study provides the empirical basis for these strategies; we demonstrate that BCCs currently overlap with high-PSR areas that lack formal protection under PAs. Consequently, this work could serve as a spatial blueprint for establishing connectivity, specifically identifying the northward and upward pathways required as southern niches become climatically unsuitable. However, climate-smart spatial prioritization is data-intensive and particularly challenging in data-poor regions (Buenafe *et al.* 2025).

It is also important to note that, although SDM may help link actions with outcomes, evaluate future scenarios, and guide decision-making toward achieving KMGBF objectives and targets (Rahman *et al.* 2025; Zurell *et al.* 2025), limited experience and technical capacity to develop such models, which is the common situation in subnational administrations (CONABIO 2016), can lead to inequities in conservation planning (Buschke *et al.* 2023; Zurell *et al.* 2025). This technical gap is particularly critical given the results of the present study, which demonstrate that state-level PAs and those of smaller spatial extent often outperform larger federal reserves in protecting high-richness areas and facilitating species recovery. Despite their smaller size and administrative challenges, these subnational areas act as refugia in the high-exposure zones.

While the roadmap launched by the national authority emphasizes the importance of ensuring that PAs and OECM represent the full range of Mexican ecosystems and thereby meet and exceed Mexico's commitments under the CBD (SEMARNAT *et al.* 2025), our findings indicate that current and future PAs and OECM must be not only representative but also functionally effective in addressing drivers of biodiversity loss, particularly climate change. This includes incorporating the ecological roles of rodents and their interactions with other species into conservation strategies (Formoso and Teta 2019; Zúñiga *et al.* 2021; Lindsø *et al.* 2025). The roadmap further recognizes that biological corridors should be established as mosaics of areas under integrated landscape management, with

varying categories and functionalities, and incorporated into public policy (SEMARNAT *et al.* 2025). Well-connected PA networks facilitate gene flow and the continuity of ecological functions (Revollo-Cadima and Salazar-Bravo 2024; Buenafe *et al.* 2025). Our results suggest that rodent conservation in the SMO region cannot be achieved solely by expanding PAs in the north. Instead, conservation efforts should prioritize mitigating threats to southern corridors, specifically within the states of Hidalgo and Puebla, as previously established by León-Paniagua *et al.* (2004), to ensure the SMO's biodiversity retains functional dispersal pathways to the north.

Specifically, for the SMO, the Sierra Madre Oriental Ecological Corridor (CESMO) can support more effective conservation planning. This initiative focuses on landscape management through reforestation activities to improve connectivity, the promotion of alternative livelihoods to reduce and control the main pressures and threats to local fauna and flora, and the implementation of systematic field monitoring by trained members of local communities within the corridor. Involves collaboration among several states, including San Luis Potosí, Querétaro, Hidalgo, Puebla, Veracruz, and, more recently, Nuevo León (Moreno *et al.* 2015; Rodríguez-Ruiz *et al.* 2025). Beyond the sum of isolated conservation efforts to date, the reactivation of the CESMO could lead to a major regional conservation policy framework that integrates multiple stakeholders and local development plans, thereby enhancing management strategies to maintain landscape connectivity (Moreno *et al.* 2015). This approach would follow the example of the Biocultural Corridor of Central Western Mexico (COBIOCOM), where regional coordination has enabled the design and implementation of broader and more ambitious conservation strategies in western Mexico (Sosa and Ivanova 2025).

Overall, the design and establishment of PAs must evolve toward a functional network approach that addresses the challenges posed by climate change, data gaps, and governance constraints. Climate-smart strategies, dynamic conservation planning, and climate mitigation efforts are essential for building effective and equitable PA networks (Buenafe *et al.* 2025). By drawing on the best available science and evidence, conservation planning and management can better anticipate future challenges and ensure the long-term resilience of ecosystems in a rapidly changing climate.

Achieving the ambitious "30 × 30" target of the KMGBF (CBD 2022) requires coordinated actions across multiple governance levels, aligning local needs, national priorities, and global agreements (CBD 2022; McGowan *et al.* 2024; Zurell *et al.* 2025). These efforts must be grounded in the best available biodiversity data, particularly at local and subnational scales, which often provide more effective conservation strategies than broad global assessments (Sarukhán and Jiménez 2014; Botello *et al.* 2015; McGowan *et al.* 2024). This study demonstrates the use of open access high-quality subnational biodiversity data to develop the multi-scale analyses required to close these gaps and operationalize global targets at the local level. Integrating such evidence into national policy is essential for countries like Mexico, where although the National Biodiversity Strategy and its Action Plan (ENBioMex) includes specific actions to improve connectivity, a stronger legal framework is still needed to ensure connectivity among existing PAs, newly designated PAs, and soon the OECM (CONABIO 2016; SEMARNAT *et al.* 2025).

Acknowledgments

DLH thanks CONABIO for providing open access to high-quality data on Mexican biodiversity, including occurrence records, potential distributions, and GIS layers. EPZQ gratefully acknowledges financial support from the Secretaría de Ciencia, Humanidades, Tecnología e Innovación (SECIHTI) through a postdoctoral fellowship.

This paper is dedicated to Dr. Livia León-Paniagua, in recognition of her outstanding contributions to the study of Mexican mammals and her enduring influence as a mentor. As her students, we received invaluable knowledge about Mexican mammals and their study, including practical insights into species identification, field techniques, and trapping methods (in the most unexpected places). Her legacy, however, goes far beyond the number of specimens collected, articles published, or species described. The most important lesson was her example of life and science: the passion of being a female mammalogist and the inspiration to do science in a different way. She left a profound mark on our academic formation, such that regardless of the paths our careers have taken, we remain connected not only as colleagues, but as a community.

Declaration of Artificial Intelligence use

We declare that the authors have not used any Artificial Intelligence in the elaboration of this paper.

Author contributions

DLH: Conceptualization, design, data curation, analysis & writing-original draft; SCR: analysis, writing-review & editing; EPZQ: analysis, writing-review & editing; ZAAV: analysis, writing-review & editing.

Literature cited

Amori G, Gippoliti S, and Luiselli L. 2011. Do biodiversity hotspots match with rodent conservation hotspots? *Biodiversity and Conservation* 20:3693–3700. https://doi.org/10.1007/s10531-011-0131-z

Beresford AE, Buchanan GM, Donald PF, Butchart SHM, Fishpool LDC, and Rondinini C. 2011. Poor overlap between the distribution of protected areas and globally threatened birds in Africa. *Animal Conservation* 14:99–107. https://doi.org/10.1111/j.1469-1795.2010.00398.x

Bezaury-Creel JE. 2024. Privately protected areas in Mexico, a 2012–2023 update. *Frontiers in Conservation Science*

4:1304771. https://doi.org/10.3389/fcosc.2023.1304771

Botello F, Sánchez-Cordero V, and Ortega-Huerta MA. 2015. Disponibilidad de hábitats adecuados para especies de mamíferos a escalas regional (estado de Guerrero) y nacional (México). *Revista Mexicana de Biodiversidad* 86(1):226-237. https://doi.org/10.7550/rmb.43353

Bravo-Cadena J, Sánchez-Rojas G, and Gelviz-Gelvez SM. 2011. Estudio de la distribución de las especies frente al cambio climático. *Cuadernos de Biodiversidad* 35:12-18. http://dx.doi.org/10.14198/cdbio.2011.35.03

Buenafe KCV, Dunn DC, Metaxas A, Schoeman DS, Everett JD, Pidd A *et al.* 2025. Current approaches and future opportunities for climate-smart protected areas. *Nature Reviews Biodiversity* 1:284–297. https://doi.org/10.1038/s44358-025-00041-0

Buschke FT, Capitani C, Sow EH, Khaemba Y, Kaplin BA, Skowno A *et al.* 2023. Make global biodiversity information useful to national decision-makers. *Nature Ecology & Evolution* 7:1953–1956. https://doi.org/10.1038/s41559-023-02226-2

Castañeda-Rico S, León-Paniagua L, Ruedas LA, Vázquez-Domínguez E. 2011. High genetic diversity and extreme differentiation in the two remaining populations of *Habromys simulatus*. *Journal of Mammalogy* 92(5):963–973. http://dx.doi.org/10.1644/10-MAMM-A-171.1

Chacón-Prieto F, Rodríguez-Soto C, Cuervo-Robayo A, Monroy J, and Alagador D. 2021. Protected areas in Central Mexico - are they fit in promoting species persistence under climate and land use changes? *Biological Conservation* 260:109186. https://doi.org/10.1016/j.biocon.2021.109186

Chase JM, McGill BJ, Thompson PL, Antão LH, Bates AE, Blowes SA *et al.* 2019. Species richness change across spatial scales. *Oikos* 128:1079–1091. https://doi.org/10.1111/oik.05968

Comisión Nacional para el Conocimiento y Uso de la Biodiversidad [CONABIO]. 1997. *Provincias biogeográficas de México. Escala 1:4,000,000*. México, D. F. (MEX): CONABIO.

Comisión Nacional para el Conocimiento y Uso de la Biodiversidad [CONABIO]. 2016. *Estrategia Nacional sobre Biodiversidad de México (ENBioMex) y Plan de Acción 2016-2030*. México: CONABIO.

Comisión Nacional para el Conocimiento y Uso de la Biodiversidad [CONABIO]. 2020. Áreas Naturales Protegidas Estatales, Municipales, Ejidales, Comunitarias y Privadas de México 2020, edición: 1. México: CONABIO; June, 2020. [Accessed June 14th, 2025]. http://geoportal.conabio.gob.mx/metadatos/doc/html/anpest20gw.html

Comisión Nacional para el Conocimiento y Uso de la Biodiversidad [CONABIO]. 2024. *Sistema Nacional de Información sobre Biodiversidad. Registros de ejemplares de mamíferos*. México: CONABIO; February 2024. [Accessed February 7th, 2024]. http://geoportal.conabio.gob.mx/acceso/mamiferos/2024/02/07

Comisión Nacional para el Conocimiento y Uso de la Biodiversidad, Comisión Nacional de Áreas Naturales Protegidas, and Programa de las Naciones Unidas para el Desarrollo [CONABIO, CONANP and PNUD]. 2019. *Corredores bioclimáticos para la conservación de la biodiversidad*. México: CONABIO; May, 2020. [Accessed October 4th, 2025]. http://geoportal.conabio.gob.mx/metadatos/doc/html/clccrecgw.html

Comisión Nacional de Áreas Naturales Protegidas [CONANP]. 2024. Áreas Naturales Protegidas Federales de México, septiembre *de 2024*. México: CONABIO; October, 2024. [Accessed June 14th, 2025]. http://geoportal.conabio.gob.mx/metadatos/doc/html/anpsp2024gw.html

Comisión Nacional de Áreas Naturales Protegidas and Deutsche Gesellschaft für Internationale Zusammenarbeit [CONANP and GIZ]. 2013. *Programa de Adaptación al Cambio Climático Región Central de la Sierra Madre Oriental*. México D.F. (MEX): CONANP and GIZConvention on Biological Diversity [CBD]. 2022. *Decision adopted by the Conference of the Parties to the Convention on Biological Diversity 15/4. Kunming-Montreal Global Biodiversity Framework*. Montreal (CAN): CBD Secretariat; December 2022. [Accessed October 4th, 2025]. https://www.cbd.int/doc/decisions/cop-15/cop-15-dec-04-es.pdf

Coro G, Sana L, and Bove P. 2024. An open science automatic workflow for multi-model species distribution estimation. *International Journal of Data Science and Analytics* 20:1131–1150. https://doi.org/10.1007/s41060-024-00517-w

Delso Á, Fajardo J, and Muñoz J. 2021. Protected area networks do not represent unseen biodiversity. *Scientific Reports* 11:12275. https://doi.org/10.1038/s41598-021-91651-z

Dinerstein E, Joshi AR, Hahn NR, Lee ATL, Vynne C, Burkart K, Asner GP *et al.* 2024. Conservation Imperatives: securing the last unprotected terrestrial sites harboring irreplaceable biodiversity. *Frontiers in Science* 2:1349350. https://doi.org/10.3389/fsci.2024.1349350

Formoso A. and Teta P. 2019. Richness, endemism and conservation of sigmodontine rodents in Argentina. *Mastozoología Neotropical* 26:99–116. https://doi.org/10.31687/saremMN.19.26.1.0.17

Garcia N, Campos JC, Alírio J, Duarte L., Arenas-Castro S, Pôças I *et al.* 2025. Assessing spatial and temporal trends over time in potential species richness using satellite time-series and ecological niche models. *Biodiversity and Conservation* 34:429–446. https://doi.org/10.1007/s10531-024-02979-7

Garza-Torres HA, Zamora-Tovar C, and Requena-Lara GN. 2024. Áreas naturales protegidas. In: *La biodiversidad en Tamaulipas. Estudio de Estado*. Vol. III. Ciudad de México (MEX): CONABIO; p. 29–35.

Godínez-Gómez O, Schank C, Mas J, and Mendoza E. 2020. An integrative analysis of threats affecting protected areas in a biodiversity stronghold in Southeast Mexico. *Global Ecology and Conservation* 24:e01297. https://doi.

org/10.1016/j.gecco.2020.e01297
Goyenechea Mayer-Goyenechea I, Montiel-Canales G, Márquez J, Hornung-Leoni CT, Castillo-Cerón JM, and Manríquez-Morán NL. 2025. Unraveling Biogeographic Boundaries Within the Sierra Madre Oriental, México: An Endemicity Analysis Using a Taxonomically Diverse Dataset. *Ecology and Evolution* 15:e70779. https://doi.org/10.1002/ece3.70779
Hanson JO, McCune JL, Alamenciak T, and Bennett JR. 2026. Increasing the credibility of conservation plans through citizen science. *Biological Conservation* 313:111552. https://doi.org/10.1016/j.biocon.2025.111552
Hijmans RJ. 2023. *terra: Spatial data analysis*. https://CRAN.R-project.org/package=terra
Hutchinson A, Zito AR, and McGowan PJK. 2025. Pathways for transforming biodiversity governance: An examination of the Global Biodiversity Framework's Considerations. *Ambio* (2025). https://doi.org/10.1007/s13280-025-02215-8
Hutchinson GE. 1957. Concluding remarks. Concluding remarks. *Cold Spring Harbor Symposia on Quantitative Biology* 22:415-427. https://doi.org/10.1101/SQB.1957.022.01.039
Instituto Nacional de Ecología y Cambio Climático [INECC]. 2021. *México ante el cambio climático*. México D.F. (MEX): INECC; march, 2026. [Accessed March 24th, 2026]. https://cambioclimatico.gob.mx/escenarios-de-cambio-climatico/
Instituto Nacional de Estadística, Geografía e Informática, Comisión Nacional para el Conocimiento and Uso de la Biodiversidad and Instituto Nacional de Ecología [INEGI, CONABIO and INE]. 2008. *Ecorregiones Terrestres de México. Escala 1:1,000,000*. México, D. F. (MEX): CONABIO.
Intergovernmental Science-Policy Platform on Biodiversity and Ecosystem Services [IPBES]. 2019. *Global assessment report on biodiversity and ecosystem services of the Intergovernmental Science-Policy Platform on Biodiversity and Ecosystem Services*. Bonn (DEU): IPBES Secretariat. https://doi.org/10.5281/ZENODO.6417333
León-Paniagua L, García Trejo E, Arroyo-Cabrales J, and Castañeda-Rico S. 2004. Patrones biogeográficos de la mastofauna. In: Luna I, Morrone JJ, and Espinosa D, editores. *Biodiversidad de la Sierra Madre Oriental*. México D.F. (MEX): Las Prensas de Ciencias; p. 469–479.
Lindsø LK, Rivrud IM, König EA, Herland A, and Mysterud A. 2025. Diel Niche of Sympatric Small Mammals Revealed by Year-Round Camera Trapping. *Ecology and Evolution* 15:e71590. https://doi.org/10.1002/ece3.71590
McGowan PJK, Hutchinson A., Brooks TM, Elliott W, Hoffmann M, Mair L *et al.* 2024. Understanding and achieving species elements in the Kunming–Montreal Global Biodiversity Framework, *BioScience* 74(9):614–623. https://doi.org/10.1093/biosci/biae065
McLeod AI. 2022. Kendall: Kendall rank correlation and Mann–Kendall trend test. *R package version*. 2.2.1. https://CRAN.R- project.org/package=Kendall
Moreno C, Reyes JA, and Wallace G. 2015. Corredor ecológico de la Sierra Madre Oriental (CESMO): Conectando voluntades para el desarrollo sustentable en un territorio de alta biodiversidad. *Territorios* 3:23–24.
Morrone JJ. 2020. *The Mexican Transition Zone. A Natural Biogeographic Laboratory to Study Biotic Assembly*. Cham (CH): Springer Cham. https://doi.org/10.1007/978-3-030-47917-6
Mouillot D, Velez L, Albouy C, Casajus N, Claudet J, Delbaret V *et al.* 2024. The socioeconomic and environmental niche of protected areas reveals global conservation gaps and opportunities. *Nature Communications* 15:9007. https://doi.org/10.1038/s41467-024-53241-1
Munguía M., Trejo I, González-Salazar C, and Pérez-Maqueo O. 2016. Human impact gradient on mammalian biodiversity. *Global Ecology and Conservation* 6:79-92. https://doi.org/10.1016/j.gecco.2016.01.004
Nori J, Loyola R, and Villalobos F. 2020. Priority areas for conservation of and research focused on terrestrial vertebrates. *Conservation Biology* 34:1281–1291. https://doi.org/10.1111/cobi.13476
Palfrey R, Oldekop JA, and Holmes G. 2022. Privately protected areas increase global protected area coverage and connectivity. *Nature Ecology & Evolution* 6:730–737. https://doi.org/10.1038/s41559-022-01715-0
Pebesma E and Bivand R. 2023. *Spatial Data Science: With Applications in R*. Chapman and Hall/CRC. https://doi.org/10.1201/9780429459016
Programa de las Naciones Unidas para el Desarrollo and Comisión Nacional de Áreas Naturales Protegidas [PNUD and CONANP]. 2019. *Proyecto Resiliencia*. Áreas Naturales Protegidas. Soluciones naturales a retos globales. México: PNUD and CONANP.
Pulido-Chadid K, Rahbek C, and Geldmann J. 2025. Evaluating protected areas' coverage of threats to terrestrial biodiversity. *Conservation Biology* e70086. https://doi.org/10.1111/cobi.70086
Ramírez-Pulido J and Castro-Campillo A. 1990. Regionalización mastofaunística (mamíferos). Mapa IV. 8. A. In: *Atlas Nacional de México*. Vol III. México: Instituto de Geografía-UNAM
Rahman DA, Sutopo S, Giri MS, Surya RA, Muttaqin M, and Condro AA. 2025. Linking climate vulnerability and future distribution for the threatened lesser-known species, Sumatran serow: A spatial conservation perspective. *Environmental and Sustainability Indicators* 28:100915. https://doi.org/10.1016/j.indic.2025.100915
R Core Team. 2021. *R: A language and environment for statistical computing*. R Foundation for Statistical Computing. V. 2.14.2. Vienna (Austria). https://www.R-project.org/
Revollo-Cadima SG and Salazar-Bravo J. 2024. Identifying areas of conservation importance based on spatial patterns of evolutionary diversity for non-volant small mammals in the Andean Puna. *Journal of Arid Environments* 224:105230. https://doi.org/10.1016/j.jaridenv.2024.105230.

Rey PL, Martin C, and Guisan A. 2024. Conservation importance of non-threatened species through their direct linkages with nature's contributions to people. *Biological Conservation* 297:110733. https://doi.org/10.1016/j.biocon.2024.110733

Rodríguez-Ruíz ER, Arriaga-Flores JC, Márquez-Ruíz MJ, Garza-Torres HA, and Monroy Ojeda A. 2025. Potential geographic distribution of the ornate hawk-eagle (*Spizaetus ornatus*) in Northeastern Mexico: an assessment of environmental suitability and conservation implications. *The Southwestern Naturalist* 69:1–11. https://doi.org/10.1894/0038-4909-69.4.3

Ruíz-Jiménez C, Alcántara O, and Luna I. 2004. Límites. In: Luna I, Morrone JJ, and Espinosa D, editores. *Biodiversidad de la Sierra Madre Oriental*. México D.F. (MEX): Las Prensas de Ciencias; p. 7–24.

Sarukhán J and Jiménez R. 2016. Generating intelligence for decision making and sustainable use of natural capital in Mexico. *Current Opinion in Environmental Sustainability* 19:153–159. https://doi.org/10.1016/j.cosust.2016.02.002

Secretaría del Medio Ambiente y Recursos Naturales [SEMARNAT]. 2010. Modificación del Anexo Normativo III, Lista de especies en riesgo de la Norma Oficial Mexicana NOM-059-SEMARNAT-2010, Protección ambiental-Especies nativas de México de flora y fauna silvestres-Categorías de riesgo y especificaciones para su inclusión, exclusión o cambio-Lista de especies en riesgo, publicada el 30 de diciembre de 2010. In: *Diario Oficial de la Federación, 14 de noviembre de 2019*. Ciudad de México (MEX): Gobierno de México; p 32–134.

Secretaría del Medio Ambiente y Recursos Naturales, Comisión Nacional de Áreas Naturales Protegidas, and World Wildlife Fund Mexico [SEMARNAT, CONANP, and WWF Mexico]. 2025. *Roadmap to meet or exceed Target 3 of the Global Biodiversity Framework in Mexico*. Ciudad de México (MEX): SEMARNAT, CONANP and WWF Mexico.

Sosa M and Ivanova A. 2025. Assessment of financing for biodiversity conservation in Mexico: links between biodiversity and climate change adaptation funds. *Diversity* 17:2–24. https://doi.org/10.3390/d17030185

Steigerwald E, Chen J, Oshiro J, Vredenburg VT, Catenazzi A, and Koo MS. 2024. Microreserves are an important tool for amphibian conservation. *Communications Biology* 7:1177. https://doi.org/10.1038/s42003-024-06510-0

Thompson KL, Chase JM., Remelgado R, Meyer C. 2025. The interacting effects of climate and land-cover change on bird communities in the United States. *Ecography* e07949. https://doi.org/10.1002/ecog.07949

Thuiller W, Guéguen M, Renaud J, Karger DN, and Zimmermann NE. 2019. Uncertainty in ensembles of global biodiversity scenarios. *Nature Communications* 10:1446. https://doi.org/10.1038/s41467-019-09519-w

Ureta C, Ramírez-Barrón M, Sánchez-García EA, Cuervo-Robayo AP, Munguía-Carrara M, Mendoza-Ponce A *et al.* 2022. Species, taxonomic, and functional group diversities of terrestrial mammals at risk under climate change and land-use/cover change scenarios in Mexico. *Global Change Biology* 28:6992–7008. https://doi.org/10.5281/zenodo.7027856

Urquiza-Haas T, Tobón W, Kolb M, Lira-Noriega A, Contreras V, Alarcón J, and Koleff P. 2019. Assessing best practice for selecting surrogates and target–setting methods in a megadiverse country. *Animal Biodiversity and Conservation* 42:187–202. https://doi.org/10.32800/abc.2019.42.0187

Verde-Arregoitia LD. 2016, Investigating extinction risk in mammals. *Mammal Review* 46:17–29. https://doi.org/10.1111/mam.12049

Wang F, Shao W, Yu H, Kan G, He X, Zhang D *et al*. 2020. Re-evaluation of the Power of the Mann-Kendall Test for Detecting Monotonic Trends in Hydrometeorological Time Series. *Frontiers in Earth Science* 8:14. https://doi.org/10.3389/feart.2020.00014

Zaragoza-Quintana EP, Cotera-Correa M, Scott-Morales LM, and Pando-Moreno M. 2012. Uso histórico del pastizal en las áreas naturales protegidas para el perrito llanero mexicano (*Cynomys mexicanus*) en Nuevo León, México. In: Cervantes F and Ballesteros-Barrera C, editores. *Estudio sobre la biología de roedores silvestres mexicanos*. México D.F. (MEX): Universidad Nacional Autónoma de México, Universidad Autónoma Metropolitana. p. 105–115.

Zaragoza-Quintana EP, Cotera-Correa M, Scott-Morales LM, Pando-Moreno M, Estrada-Castillón AE, and González-Rodríguez H. 2022. Salud del ecosistema de pastizal y biomasa en áreas naturales protegidas para el perrito llanero mexicano (*Cynomys mexicanus*) en Nuevo León, México. *Acta Universitaria* 32:1–19. https://doi.org/10.15174/au.2022.3495

Zúñiga AH, Rau JR, Jaksic FM, Vergara PM, Encina-Montoya F, and Fuentes-Ramírez A. 2021. Rodent assemblage composition as indicator of fire severity in a protected area of south-central Chile. *Austral Ecology* 46:249–260. https://doi.org/10.1111/aec.12975

Zurell D, Bocedi G, Velazco SJE, Gonzalez A, Purvis A, Wintle B *et al.* 2025. Predicting the way forward for the Global Biodiversity Framework. *Proceedings of the National Academy of Sciences* 122:e2501695122. https://doi.org/10.1073/pnas.2501695122

Associated editors: Giovani Hernández Canchola and Pablo Colunga Salas
Submitted: January 5, 2026; Reviewed: March 5, 2026
Accepted: May 8, 2026; Published online: May 29, 2026

THERYA, 2026, Vol. 17(2):327-342 DOI: 10.12933/therya.2026.6274 ISSN 2007-3364

Undervalued habitat or impoverished guild? Explaining the scarcity of living semiaquatic sigmodontine rodents (Cricetidae)

Erika Cuéllar Soto[1], Carola Cañón[2], and Ulyses F. J. Pardiñas[3*]

[1]Department of Biology, College of Science, Sultan Qaboos University, Muscat, Oman. E-mail: e.soto@squ.edu.com (ECS).
[2]Cape Horn International Center for Global Change Studies and Biocultural Conservation (CHIC), Puerto Williams; Pontificia Universidad Católica de Chile, Facultad de Ciencias Biológicas, Departamento de Ecología; and Instituto Milenio Centro de Regulación del Genoma (CRG), Santiago, Chile. E-mail: carolacanonv@gmail.com (CC).
[3]Instituto de Diversidad y Evolución Austral (IDEAus-CONICET), Puerto Madryn, Argentina; and Instituto Nacional de Biodiversidad (INABIO), Quito, Ecuador.
[*]Corresponding author: ulyses@cenpat-conicet.gob.ar

Sigmodontines (Rodentia: Cricetidae), the most diverse extant radiation of Neotropical rodents (91 genera, 507 species), include only a small fraction of taxa exhibiting morphological and ecological specializations associated with a semiaquatic mode of life. These specializations are unevenly distributed within the subfamily, being largely restricted to Ichthyomyini and to a limited number of mostly large-bodied species within Oryzomyini. Here, we examine the taxonomic, phylogenetic, and geographic distribution of semiaquatic sigmodontines within a historical framework. Phylogenetic analyses and ancestral-state reconstructions indicate that amphibious habits evolved convergently in these two lineages from a terrestrial ancestor. The resulting patterns reveal a marked phylogenetic clustering and a pronounced geographic asymmetry, with semiaquatic forms largely absent from extensive lowland and southern freshwater systems. These patterns are consistent with a scenario in which ecological constraints and historical processes jointly shaped the current distribution of semiaquatic taxa. In particular, predation pressure within continental freshwater environments may have limited successful colonization by small mammals, while occupation of predator-poor habitats may have facilitated localized diversification. In addition, paleontological and biogeographic evidence suggests that semiaquatic sigmodontines were more diverse and geographically widespread in the past, with subsequent reductions in diversity. In this context, the contemporary scarcity of semiaquatic sigmodontine rodents can be interpreted as consistent with a combination of ecological filtering associated with freshwater habitats and historical reductions in diversity through extinction. Comparison with murid rodents suggests that continental freshwater environments may represent a challenging ecological domain for small muroids more broadly.

Keywords: Ichthyomyini; Miocene; Oryzomyini; predation; South America.

Los sigmodontinos (Rodentia: Cricetidae), la radiación más diversa de roedores neotropicales contemporáneos (91 géneros, 507 especies), incluyen solo una pequeña fracción de taxones que exhiben especializaciones morfológicas y ecológicas asociadas a un modo de vida semiacuático. Estas especializaciones se distribuyen de manera desigual dentro de la subfamilia, estando restringidas principalmente a Ichthyomyini y a un número limitado de especies, en su mayoría de gran tamaño, dentro de Oryzomyini. En este estudio, examinamos la distribución taxonómica, filogenética y geográfica de los sigmodontinos semiacuáticos dentro de un marco histórico. Los análisis filogenéticos y las reconstrucciones de estados ancestrales indican que los hábitos anfibios evolucionaron convergentemente en estos dos linajes a partir de un ancestro terrestre. Los patrones resultantes revelan una marcada agrupación filogenética y una marcada asimetría geográfica, con formas semiacuáticas prácticamente ausentes en extensos sistemas de tierras bajas y de agua dulce del sur. Estos patrones son consistentes con un escenario en el que las limitaciones ecológicas y los procesos históricos moldearon conjuntamente la distribución actual de los taxones semiacuáticos. En particular, la presión de la depredación en los ambientes continentales de agua dulce pudo haber limitado la colonización exitosa por parte de pequeños mamíferos, mientras que la ocupación de hábitats con pocos depredadores pudo haber facilitado la diversificación localizada. Además, la evidencia paleontológica y biogeográfica sugiere que los sigmodontinos semiacuáticos fueron más diversos y geográficamente más extendidos en el pasado, con reducciones posteriores en la diversidad. En este contexto, la escasez actual de roedores sigmodontinos semiacuáticos puede interpretarse como consistente con una combinación de filtrado ecológico asociado a los hábitats de agua dulce y reducciones históricas en la diversidad por extinción. La comparación con los roedores múridos sugiere que los ambientes continentales de agua dulce pueden representar un dominio ecológico desafiante para los pequeños muroideos en general.

Palabras clave: América del Sur; depredación; Ichthyomyini; Mioceno; Oryzomyini.

Freshwater environments have repeatedly served as arenas for ecological innovation and lineage diversification among mammals, providing opportunities for dispersal, foraging, and niche expansion across evolutionary timescales (e.g., Hood 2020; He *et al.* 2021; Román-Palacios *et al.* 2022; Farina *et al.* 2023). In the Neotropics, this opportunity is particularly pronounced: the continent harbors some of the largest and most persistent river basins and wetland systems on Earth, forming an extensive freshwater network throughout much of the Cenozoic (e.g., Clapperton 1993). In principle, such conditions might be expected to promote repeated evolutionary responses to aquatic and semiaquatic habitats. However, the relationship between ecological opportunity and diversification is not necessarily direct, and the extent to which environmental availability translates into adaptive expansion varies among clades (e.g., Alhajeri *et al.* 2016; Maestri *et al.* 2017; 2022).

Within this context, sigmodontine rodents (Cricetidae:

Sigmodontinae), one of the most diverse mammalian radiations in South America, present an apparent paradox. Despite their extensive diversification across terrestrial environments, they exhibit a strikingly limited representation of semiaquatic forms (e.g., Hershkovitz 1969; Pine *et al.* 1981; Voss 1988; Pardiñas *et al.* 2017). This discrepancy between the widespread availability of freshwater habitats and the restricted occurrence of amphibious adaptations raises fundamental questions about the processes that structure ecological diversification in this group.

The Neotropics encompass four of the largest river basins on Earth—the Amazon, Orinoco, La Plata, and São Francisco—which together cover nearly two-thirds of the South American continent (Ayres and Clutton-Brock 1992). Among these, the Amazon River alone drains approximately 7,050,000 km^2—almost 40% of the continent—and includes more than 1,000 tributaries (Ramos *et al.* 2026). When extensive wetland systems such as the Pantanal and the Iberá–Ñeembucú complex are also considered (Junk 2013; Urcola *et al.* 2025), South America emerges as a region exceptionally rich in surface freshwater habitats (Hurlbert *et al.* 1981). These environments have persisted through major climatic and tectonic events, providing long-term ecological continuity and repeated opportunities for aquatic and amphibious life histories to evolve (Clapperton 1993).

Despite this environmental context, sigmodontine rodents, the most species-rich and geographically widespread mammalian radiation in the Neotropics, exhibit only a modest degree of specialization toward semiaquatic environments. Of the more than 500 living species currently recognized (Brito and Pardiñas 2025), only a small proportion display morphological and behavioral traits associated with amphibious habits (e.g., Massoia 1976; Voss 1988; Bianchini and Delupi 1993; Patton *et al.* 2015; Pardiñas *et al.* 2017). Moreover, these adaptations are phylogenetically clustered, being largely restricted to Ichthyomyini and to a limited subset of Oryzomyini, whereas the majority of sigmodontine lineages remain terrestrial, scansorial, or semifossorial (and more rarely, arboreal; see Brito *et al.* 2021). This pattern indicates that transitions into freshwater environments have been rare and unevenly distributed across the phylogeny.

Several non-exclusive explanations may account for this pattern. One possibility is that freshwater habitats have been effectively underutilized by sigmodontines, either due to intrinsic biological constraints or to persistent ecological pressures limiting successful colonization. Predation risk, particularly from aquatic and semiaquatic vertebrates, has been proposed as a potential factor reducing the fitness of small mammals in freshwater systems (Wolff and Guthrie 1985). Alternatively, the present-day scarcity of semiaquatic sigmodontines may reflect a process of guild impoverishment, in which amphibious forms were more diverse in the past but experienced differential extinction during the Neogene or Quaternary. Under this scenario, extant diversity would represent a residual subset of a historically broader ecological spectrum (Voss 1988).

Distinguishing among these alternatives requires a historical perspective that integrates phylogenetic, ecological, and paleontological evidence. In this study, we compile information on mode of life across sigmodontine rodents and analyze its distribution within a molecular phylogenetic framework. Using ecomorphological classification and ancestral-state reconstruction, we document the phylogenetic placement and evolutionary distribution of semiaquatic habits. These analyses are not designed to directly test causal mechanisms, but rather to characterize patterns of ecological diversification and to provide a basis for evaluating alternative explanatory scenarios.

Based on these patterns, we explore the extent to which the limited representation of semiaquatic sigmodontines is consistent with (1) ecological constraints associated with freshwater environments or (2) historical reductions in diversity through extinction. More broadly, this case provides an opportunity to examine how ecological opportunity, constraint, and historical contingency interact to shape functional diversity within a major continental mammal radiation.

Materials and methods

Taxonomic and ecological data. Three recent and comprehensive syntheses of sigmodontine diversity (Patton *et al.* 2005; Pardiñas *et al.* 2017; Brito and Pardiñas 2025) were used as the primary taxonomic sources (Supplementary Data SD1). The dataset includes 507 species distributed in 91 genera, representing all the recognized sigmodontine contemporary richness.

Each species was classified as semiaquatic or non-semiaquatic based on a combination of external morphological traits and published natural history information. This classification follows an integrative approach commonly used in comparative ecomorphological studies (e.g., Maestri *et al.* 2017; 2022), in which ecological categories are inferred from concordant morphological and behavioral evidence.

Semiaquatic forms were defined as species exhibiting at least two of the following morphological features: (1) bi-layered pelage composed of a dense woolly underfur and a superficial overfur; (2) a continuous comb of stiff hairs along the metatarsal margins and between the digits, fringing the sole of the pes; (3) midventral tail hairs conspicuously longer than those on the dorsal and lateral surfaces; (4) moderately developed webbing between digits II–IV of the manus; (5) highly developed and numerous mystacial vibrissae; (6) nostrils positioned high on the snout, anterolaterally placed and posteriorly expanded by a small diverticulum flanked by a developed *ala nasi ventralis*; (7) small but distinct interdigital and metacarpal pedal pads; (8) a prismatic basal cross-section of the tail; and (9) well-developed interdigital webbing between pedal digits II–IV. These characters have

been repeatedly identified as indicative of adaptation to aquatic environments in sigmodontines and other muroid rodents, reflecting behaviors such as swimming, diving, foraging, dispersal, nesting, and reproduction in freshwater systems (e.g., Sierra de Soriano 1965; 1969; Hershkovitz 1966; 1969; Starrett and Fisler 1970; Massoia 1976; Miller and Anderson 1977; Esher *et al.* 1978; Pine *et al.* 1981; Voss 1988; 2015a; 2015b; Kerbis Peterhans and Patterson 1995; Weksler 2006; Santori *et al.* 2008; Rowe *et al.* 2014).

Molecular data and phylogenetic analyses. To infer phylogenetic relationships, nucleotide sequences were retrieved from GenBank for four unlinked loci widely used in rodent systematics: the mitochondrial cytochrome *b* gene (cytb) and the nuclear genes interphotoreceptor retinoid-binding protein (IRBP), growth hormone receptor (GHR), and recombination activating gene 1 (RAG1). The dataset includes representatives of all sigmodontine genera for which molecular data are available, excluding *Casiomys* and *Gyldenstolpia*, and incorporates 19 outgroup taxa representing other cricetid subfamilies and more distantly related muroids (Supplementary Data SD2). To maximize phylogenetic coverage while minimizing redundancy, a single representative species per genus was included in the main analysis.

Sequences were aligned separately for each gene using MAFFT v7 under default parameters, implemented in ClustalX, and subsequently inspected and edited in AliView. Alignments were trimmed to preserve reading frame integrity, resulting in final lengths of 1,140 bp (cytb), 1,184 bp (IRBP), 796 bp (GHR), and 2,022 bp (RAG1). The concatenated dataset comprised 5,142 bp.

Phylogenetic inference was conducted under the Maximum Likelihood (ML; Stamatakis 2014) criterion using IQ-TREE v2.2. Each gene was treated as an independent partition to allow locus-specific substitution models, which were selected using ModelFinder. Node support was assessed using ultrafast bootstrap (UFBoot) and SH-aLRT tests, each with 10,000 replicates. The resulting ML topology was visualized and annotated in FigTree v1.4 and used as the framework for subsequent analyses.

Mode of life classification and ancestral-state reconstruction. A discrete matrix of seven ecomorphological categories—arboreal, cursorial, saltatorial, scansorial, semiaquatic, semifossorial, and wader—was compiled from published ecological and behavioral sources. When species-level information was unavailable, genera were coded based on the predominant morphology exhibited by their constituent species. Each taxon was assigned a single dominant ecomorphological state using a categorical coding scheme appropriate for discrete-state evolutionary models.

Ancestral-state reconstructions were performed in Mesquite v3.7 (Maddison and Maddison 2019) using Maximum Likelihood under the Mk1 model, which assumes equal transition rates among states. Although this model does not accommodate potential asymmetries in transition probabilities among ecological states, it provides a conservative framework for reconstructing general patterns of trait evolution across the phylogeny.

The ML phylogeny obtained in IQ-TREE was imported into Mesquite and linked to the ecomorphological dataset. Likelihoods of alternative character states were estimated for all internal nodes and visualized using proportional-symbol reconstructions.

Analyses were conducted using default optimization settings (20 million iterations, sampling every 1,000 steps). Reconstructions were inspected for consistency with tree topology. Final trees and character-state graphics were exported as vector files and edited in Inkscape for figure preparation.

Results

Diversity of semiaquatic sigmodontines. Analysis of extant sigmodontine diversity indicates that only a small fraction of species can be classified as semiaquatic (Supplementary Data SD1). These include (1) all currently recognized members of Ichthyomyini (22 species in seven genera) and (2) a limited subset of Oryzomyini, comprising 15 species distributed among *Amphinectomys* (1 species), *Holochilus* (7), *Lundomys* (1), and *Nectomys* (6). Together, these taxa represent approximately 7% of living sigmodontine species and 12% of genera (n = 507 species; n = 91 genera; Supplementary Data SD1).

Several additional genera—three oryzomyines (*Oryzomys*, *Pseudoryzomys*, *Sigmodontomys*) and two akodontines (*Gyldenstolpia*, *Scapteromys*)—have historically been associated with aquatic environments (e.g., Hershkovitz 1966; Ávila-Pires 1972; Massoia 1976; Esher *et al.* 1978; Voss and Myers 1991; Voss and Carleton 1993; Pardiñas *et al.* 2009). However, available morphological and natural history evidence does not support their inclusion among semiaquatic taxa. In *Scapteromys*, individuals inhabit terrestrial and river-margin habitats, construct burrows, nest on dry ground, and engage in climbing activities (Massoia and Fornes 1964; Hershkovitz 1966; Barlow 1969). *Oryzomys* tolerates flooded environments but lacks the morphological traits observed in semiaquatic sigmodontines (Esher *et al.* 1978; Weksler 2006). Following Kerbis Peterhans and Patterson (1995), these genera are here classified as waders. Under this classification, wader taxa represent approximately 3% of sigmodontine species and 5% of genera (Supplementary Data SD1).

Other genera occasionally proposed as semiaquatic, such as *Mindomys* and *Neotomys*, were excluded from both semiaquatic and wader categories based on currently available evidence (Pardiñas *et al.* 2015; Brito *et al.* 2021).

Phylogenetic analyses. The maximum-likelihood analysis of the concatenated dataset recovered a well-resolved phylogeny (Figure 1). Major sigmodontine tribes were recovered with strong statistical support and with relationships congruent with previous multilocus reconstructions (e.g., Leite *et al.* 2014; Gonçalves *et al.* 2020; Parada *et al.* 2021; Pardiñas *et al.* 2022; 2024; Bangs *et al.* 2025).

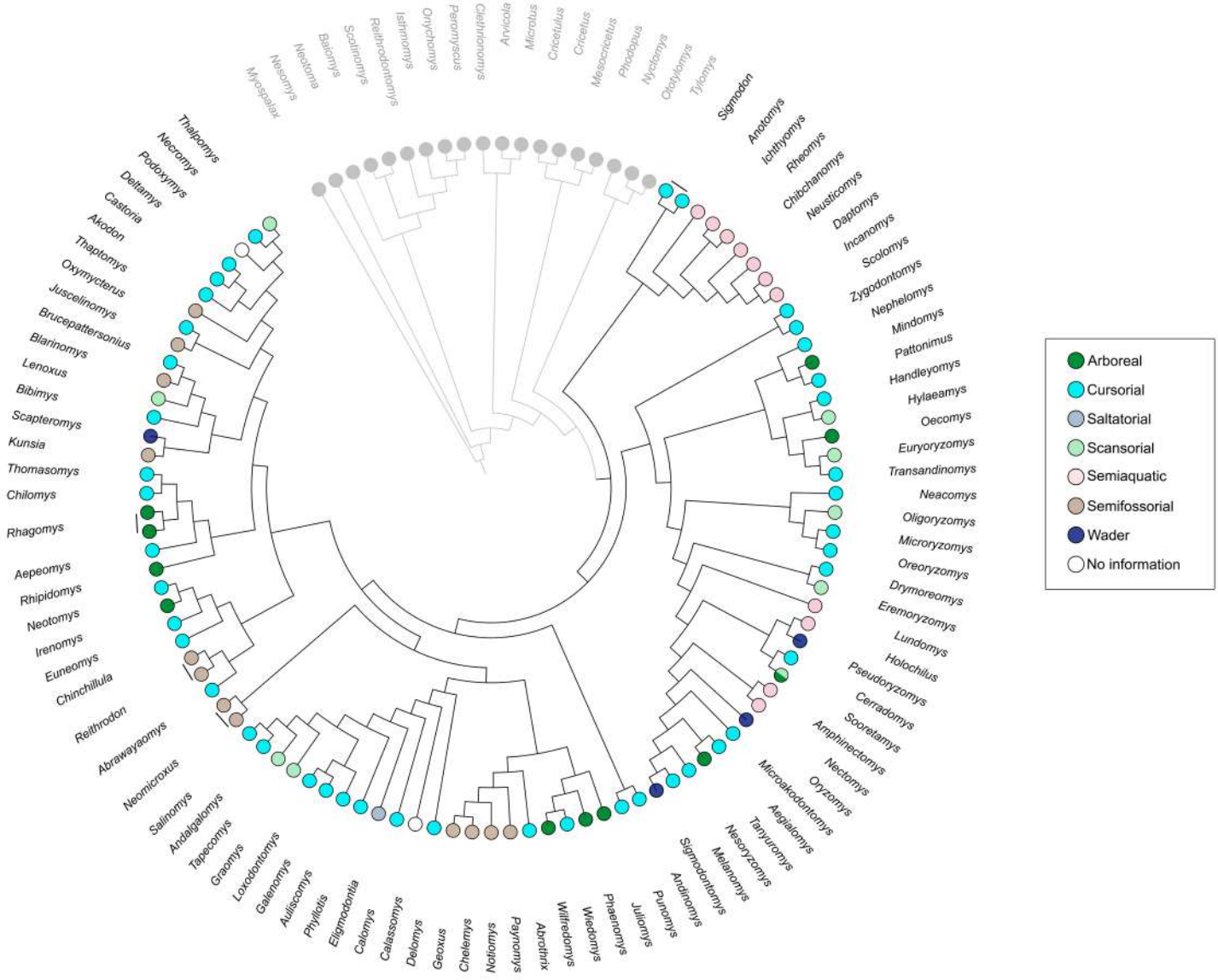

Figure 1. Phylogeny of Sigmodontinae showing the assignment of analyzed genera to ecomorphological categories.

Within Sigmodontinae, Oryzomyini, Phyllotini, Akodontini, Thomasomyini, and Abrotrichini were recovered as monophyletic (UFBoot > 95; SH-aLRT > 0.90). Oryzomyini constituted the earliest-diverging lineage within the sampled sigmodontines, followed by successive divergences involving the akodontine–phyllotine complex and the thomasomyine–abrotrichine assemblage. Outgroup taxa provided a stable root for the ingroup topology and recovered Sigmodontinae within Cricetidae.

The ancestral reconstruction of ecomorphological categories estimated a log-likelihood value of −132.83 and an overall transition rate of 1.18. The proportional-likelihood reconstruction recovered the ancestral sigmodontine condition as cursorial, with a markedly higher likelihood than alternative states (Figure 2).

Independent transitions toward arboreal and scansorial conditions were reconstructed in multiple oryzomyine and thomasomyine lineages. Semiaquatic ecomorphologies were reconstructed independently within Ichthyomyini and Oryzomyini. Semifossorial conditions were recovered primarily within the akodontine complex. Saltatorial morphologies occurred only in a limited number of terminal branches.

Semiaquatic sigmodontines exhibit a geographically heterogeneous distribution (Figure 3). Ichthyomyines are associated primarily with streams and rivers of Andean and montane regions in northwestern South America and Central America (Voss 1988, 2015a). In contrast, lowland wetlands and river systems of eastern tropical, subtropical, and temperate South America are occupied mainly by a small number of oryzomyine taxa, principally *Holochilus* and *Nectomys* (e.g., Hershkovitz 1955; Bonvicino and Weksler 2015; Chiquito 2015; Prado *et al.* 2021).

No semiaquatic sigmodontines were recorded from southern South America. The southernmost extant representatives correspond to *Holochilus brasiliensis* and *Holochilus lagigliai*, which reach the northern limit of Patagonia (Formoso *et al.* 2010; Pardiñas *et al.* 2013; Figure

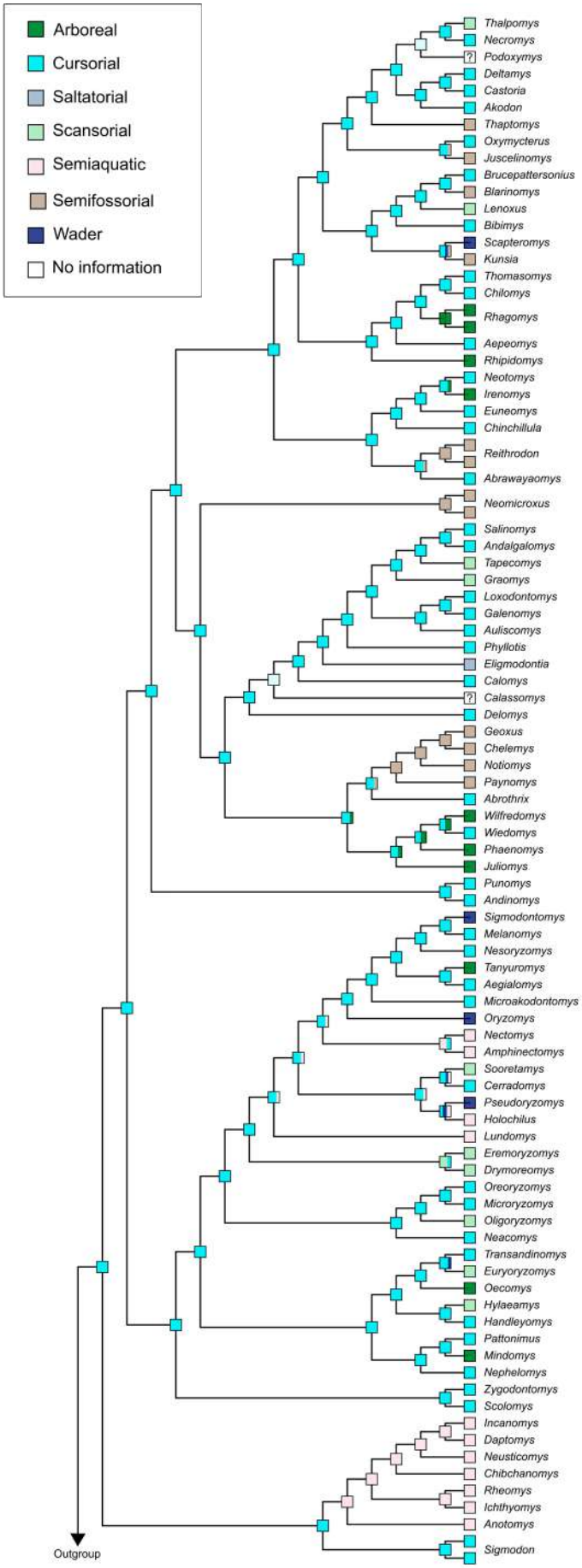

Figure 2. Ancestral-state reconstruction of ecomorphological categories within Sigmodontinae.

3). Fossil records indicate broader past distributions for some semiaquatic taxa (Figure 4).

Discussion

Evolutionary rarity of freshwater specialization. Our phylogenetic and ancestral-state reconstructions indicate that semiaquaticity evolved independently within Sigmodontinae but remained restricted to a limited number of lineages. This combination of repeated origin and limited diversification raises the question of why freshwater specialization remained uncommon despite its apparent evolutionary accessibility.

Our results indicate that semiaquatic sigmodontines constitute only a small fraction of the extant diversity of the subfamily, both taxonomically and phylogenetically. Only two major lineages—Ichthyomyini and a restricted subset of Oryzomyini—include species exhibiting the suite of traits associated with freshwater specialization. Most sigmodontine genera associated with humid or seasonally flooded habitats instead correspond to wader forms lacking the morphological specializations characteristic of sustained swimming and diving.

The ancestral-state reconstruction further suggests that the earliest sigmodontines were primarily cursorial (see also Rodríguez-Serrano *et al.* 2008). From this ancestral condition, multiple locomotor strategies evolved independently across the subfamily, including arboreal, scansorial, semifossorial, and semiaquatic forms (e.g., Hershkovitz 1969). The repeated emergence of semiaquaticity demonstrates that freshwater adaptation evolved convergently within Sigmodontinae and was therefore evolutionarily accessible. At the same time, its restricted representation indicates that relatively few lineages followed this trajectory.

This combination of evolutionary accessibility and low diversification is notable. In many mammalian radiations, ecological opportunities associated with freshwater systems have promoted repeated colonization and diversification (Fish 1992; Fish *et al.* 2002). In sigmodontines, however, semiaquaticity remained both geographically restricted and taxonomically limited despite the broad ecological diversification achieved by the subfamily throughout South America (Patton *et al.* 2015; Pardiñas *et al.* 2017).

Convergent evolution of semiaquatic adaptations. Adaptation to freshwater environments imposes multiple functional challenges for small mammals, including locomotion, thermoregulation, feeding, and predator avoidance (e.g., Voss 1988; Fish 1992; Fish *et al.* 2002). Several morphological specializations observed in semiaquatic sigmodontines appear associated with these challenges. Dense insulating fur likely reduces heat loss during immersion (Santori *et al.* 2008), whereas enlarged hindfeet, interdigital webbing, and laterally compressed tails probably enhance swimming efficiency (e.g., Starrett and Fisler 1970; Voss 1988).

Figure 3. Schematic geographic distributions of the two sigmodontine rodent groups that include semiaquatic forms, superimposed on a map of Middle and South America highlighting the main contemporary fluvial systems.

Ichthyomyines represent the most specialized expression of these adaptations within Sigmodontinae. Members of this tribe exhibit traits facilitating swimming, diving, and prey capture in shallow, fast-flowing streams (e.g., Starrett and Fisler 1970; Voss 1988; Salazar-Bravo *et al.* 2023). Nevertheless, semiaquatic specialization is not restricted to ichthyomyines. Oryzomyine taxa occupying freshwater environments independently evolved several comparable traits, including expanded interdigital webbing, enlarged pes, dorsoventrally flattened heads, reduced pinnae, nostril-closing folds, and dense underfur (Hershkovitz 1955; Sierra de Soriano 1965; 1969; Massoia 1976; Voss and Carleton 1993).

Thermal constraints may also contribute to the distribution of semiaquatic forms. Small mammals experience rapid heat loss in aquatic environments, generating energetic demands that frequently favor larger body sizes in semiaquatic taxa (Wolff and Guthrie 1985). Consistent with this expectation, *Holochilus* and *Lundomys* rank among the largest sigmodontines (Hershkovitz 1955; Weksler 2006).

Taken together, these patterns indicate that both major sigmodontine clades—Oryzomyalia and Sigmodontalia—independently evolved comparable functional solutions to freshwater challenges. The critical question, therefore, is not whether sigmodontines were capable of freshwater adaptation, but why so few lineages underwent this transition.

Geographic asymmetry and environmental constraints. The distribution of semiaquatic sigmodontines exhibits a pronounced geographic asymmetry. Ichthyomyines are concentrated primarily in Andean and montane systems of northwestern South America and Central America (Voss 1988; 2015a; Salazar-Bravo *et al.* 2023), whereas lowland wetlands and floodplains of eastern South America are occupied mainly by a few oryzomyine genera, especially

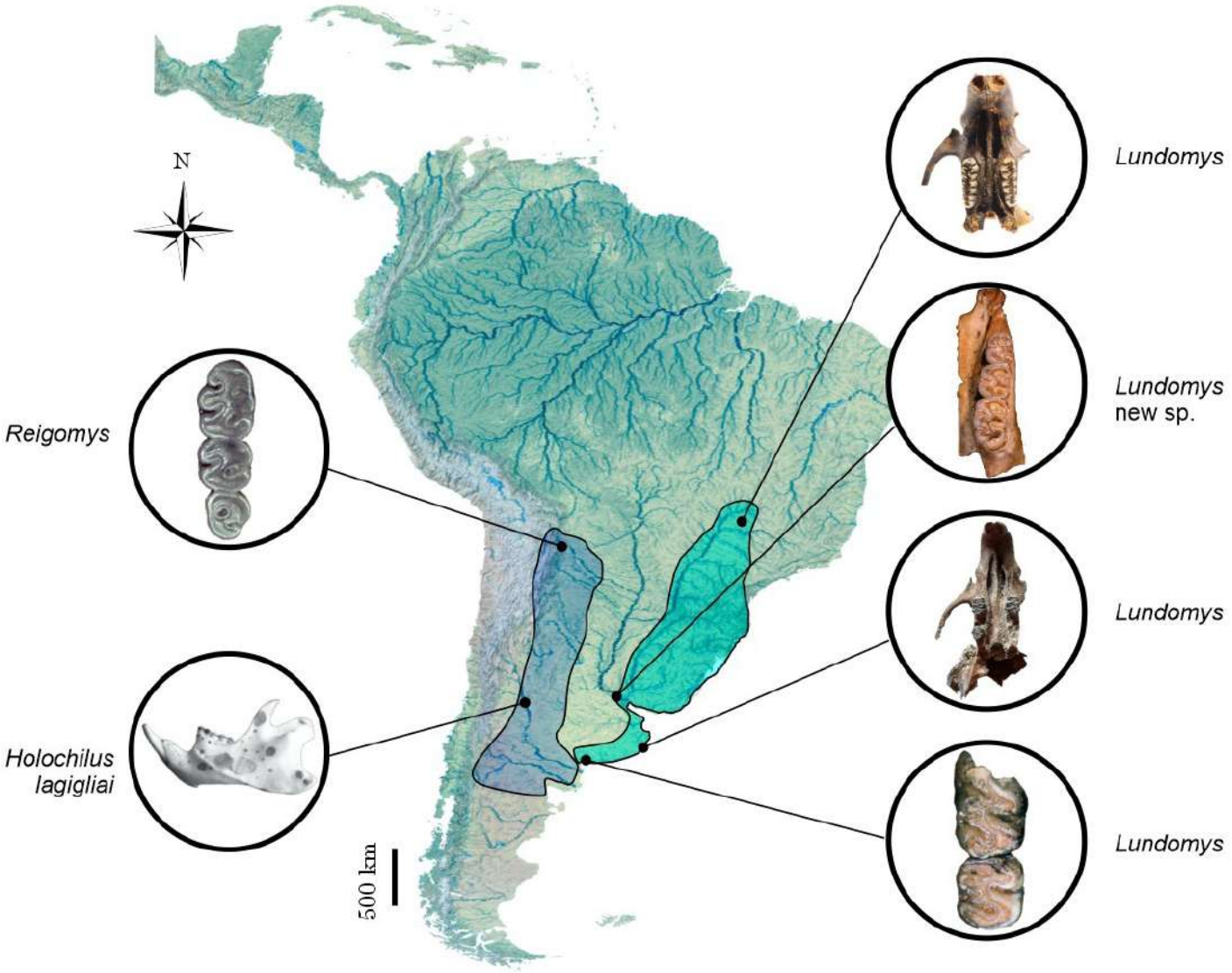

Figure 4. Selected fossil craniodental remains of sigmodontines hypothesized to represent extinct semiaquatic taxa, together with the maximum Pleistocene range of *Lundomys molitor* (colored area to the right) and the Holocene extension of the distribution of *Holochilus* (colored area to the left). Based on multiple sources.

Holochilus and *Nectomys* (e.g., Hershkovitz 1955; Bonvicino and Weksler 2015; Chiquito 2015; Prado *et al.* 2021). In contrast, southern South America lacks any extant semiaquatic sigmodontine fauna (Lessa *et al.* 2012; Chebez *et al.* 2014).

This pattern suggests that freshwater specialization was not only rare, but also spatially constrained. The absence of semiaquatic forms in southern regions may partially reflect present climatic conditions. Small-bodied aquatic and semiaquatic mammals experience substantial energetic constraints in cold environments because of their high surface-area-to-volume ratios and the high thermal conductivity of water, which greatly increase heat loss and thermoregulatory demands (Scholander *et al.* 1950; McNab 1978; Dawson and Fanning 1981). Additionally, paleoenvironmental evidence indicates substantial reduction and fragmentation of wetland systems during the Late Quaternary and Holocene, potentially reducing the availability of suitable freshwater habitats across southern South America (e.g., Roig 1991; Stoessel *et al.* 2008; Pardiñas and Teta 2011; Hadler *et al.* 2026).

The paleontological record supports this interpretation. Fossil occurrences of *Holochilus* and *Lundomys* indicate broader past distributions (e.g., Pardiñas and Lezcano 1995; Pardiñas 1999; Teta *et al.* 2005; Teta and Pardiñas 2006), including regions that currently lack extensive freshwater systems, such as Bolivian Chaco (e.g., Hoffstetter 1968; Pardiñas and Galliari 1998; Coltorti *et al.* 2012) and northern Patagonia (e.g., Fernández and Crivelli-Montero 2004; Fernández *et al.* 2011; Pardiñas and Teta 2011). These records suggest that semiaquatic taxa formerly occupied habitats that later disappeared or became substantially reduced.

Historical timing, ecological opportunity, and niche saturation. Sigmodontine diversification likely began in northern South America following colonization from Central and North America during the late Miocene (Prevosti *et al.* 2021; Ronez *et al.* 2021b; 2023; Candela *et al.* 2023; Romano *et al.* 2023). One possible explanation for the

low representation of semiaquatic forms is that freshwater niches were already occupied by other mammalian groups at the onset of sigmodontine radiation. This hypothesis of niche saturation (Northfield *et al.* 2010; Cassini 2020) directs attention to marsupials and caviomorph rodents.

Among marsupials, freshwater specialization is rare, with *Chironectes* representing the only extant semiaquatic form (Pine *et al.* 1981; Stein and Patton 2008). Caviomorph rodents include amphibious taxa such as *Hydrochoerus* and *Myocastor*, as well as species capable of diving, such as *Cuniculus* (Patton *et al.* 2015). In addition, the fossil record documents a Miocene–Pleistocene diversity of true or potentially semiaquatic caviomorphs (e.g., Vucetich *et al.* 2015; Kerber *et al.* 2016; Rasia 2026). However, given the marked body-size differences separating these rodents from sigmodontines, direct ecological competition may have been limited.

An alternative explanation involves evolutionary timing. Molecular estimates place the initial sigmodontine diversification at approximately 10-8 Ma (e.g., Parada *et al.* 2021; Bangs *et al.* 2025), whereas the earliest confident fossil records appear around 5.7 Ma (Prevosti *et al.* 2021; Candela *et al.* 2023; Romano *et al.* 2023). Although the fossil record remains incomplete, the existence of a specialized ichthyomyine radiation suggests that time alone is unlikely to explain the limited diversification of semiaquatic forms. Semiaquatic oryzomyines appear later within the tribe (Percequillo *et al.* 2021), potentially accounting for their more limited degree of specialization. Differences in evolutionary rates among ecological guilds may instead have contributed to the observed asymmetry (Maestri *et al.* 2017).

Predation as a macroecological filter. Predation risk may represent an additional factor constraining freshwater colonization by sigmodontines. Although direct observations remain scarce, predation by fishes on sigmodontine rodents has been documented in multiple regions (e.g., Mann 1978; Pardiñas *et al.* 2004; Vitule *et al.* 2015; Borges *et al.* 2025).

Neotropical freshwater ecosystems harbor exceptionally diverse predator assemblages. The Amazon basin alone contains more than 3,000 fish species (Junk 2007), including numerous large predators (Reis *et al.* 2016). Freshwater predation pressure further includes reptiles, birds, and mammals. Fossil assemblages from Late Miocene and Pliocene deposits indicate that this predator diversity has deep temporal roots (e.g., Sánchez-Villagra *et al.* 2010; Carrillo-Briceño *et al.* 2019; Cadena *et al.* 2020; Viñola López *et al.* 2025).

Under these conditions, freshwater systems may function as strong biotic filters (*sensu* Vermeij 1991), limiting the establishment and diversification of small mammalian lineages. Although this hypothesis remains difficult to test directly, the structure and diversity of Neotropical predator assemblages are broadly consistent with such an interpretation.

A synthetic scenario: habitat undervaluation and extinction. Integrating these observations, we propose a working hypothesis in which predation risk and extinction jointly shaped the current scarcity of semiaquatic sigmodontines. During the late Miocene, northern South America comprised a mosaic of freshwater and brackish systems (e.g., Lundberg *et al.* 1998; de Souza *et al.* 2021; McDermott 2021), partly representing the remnants of the Pebas system encountered by early sigmodontines during their colonization of the continent (Ronez *et al.* 2021b, 2023). Lowland lineages may have been constrained by intense predation pressure from aquatic vertebrates, whereas an early lineage colonizing Andean environments encountered clearer, shallower streams with fewer large predators, facilitating the radiation of Ichthyomyini. Concurrently, a small number of lowland oryzomyines colonized marshes and ponds with comparatively reduced predation pressure, evolving larger body sizes (e.g., *Holochilus* and *Nectomys*, with the largest species reaching approximately 250–300 g, and *Lundomys*, exceeding 300 g; Massoia 1976; Voss and Carleton 1993) and herbivorous tendencies as additional defensive strategies.

The present scarcity of semiaquatic sigmodontines may also partly reflect extinction. Several extinct taxa plausibly associated with freshwater environments are known from Pleistocene deposits, including †*Carletonomys*, †*Ichthyurodon*, †*Noronhomys*, and †*Reigomys* (Steppan 1996; Carleton and Olson 1999; Pardiñas 2008; Machado *et al.* 2014; Pardiñas and Barbière 2018; Barbière 2019). If these rodents occupied semiaquatic niches, their disappearance would substantially alter the apparent historical diversity of this ecological guild.

A similar pattern is suggested by the fossil distribution of extant semiaquatic genera. Fossil records indicate that *Holochilus* and *Lundomys* formerly occupied broader geographic areas than at present, including regions currently lacking extensive wetlands or permanent freshwater systems. These contractions are consistent with major paleoenvironmental changes during the Late Quaternary, particularly wetland reduction and increasing aridity in parts of southern South America (e.g., López and Chiavazza 2021).

Integrating these observations, the current distribution of semiaquatic sigmodontines may reflect the combined effects of ecological filtering and extinction. Freshwater colonization likely occurred repeatedly but remained limited by predation pressure and environmental constraints, whereas subsequent climatic and habitat changes may have further reduced the diversity and distribution of these lineages.

Freshwater specialization in a broader muroid context. Comparison with Murinae—the only muroid subfamily comparable to Sigmodontinae in diversity and geographic extent (e.g., Denys *et al.* 2017)—reinforces the broader significance of these patterns. Despite a longer evolutionary history and wider distribution (e.g., Aghová *et al.* 2018; López-Antoñanzas *et al.* 2024), murines also include

relatively few semiaquatic taxa (e.g., Musser and Heaney 1992; Helgen 2005; Rowe *et al.* 2014; Denys *et al.* 2017).

This convergence suggests that freshwater environments may represent a broadly challenging ecological domain for small muroid rodents rather than a constraint unique to sigmodontines. In this context, sigmodontines appear relatively successful rather than exceptionally limited, having independently evolved semiaquatic forms in at least two major lineages.

Notably, within Oryzomyalia, only Oryzomyini evolved fully semiaquatic representatives, paralleling the remarkable ecological flexibility already documented for this tribe (Ronez *et al.* 2021a; Bover *et al.* 2025). More generally, the uneven distribution of semiaquaticity across Sigmodontinae suggests that ecological opportunity and evolutionary potential were not uniformly distributed within the subfamily (e.g., Alhajeri *et al.* 2016; Missagia *et al.* 2023). These patterns provide a useful framework for future investigations into the ecological and macroevolutionary processes shaping functional diversification in continental mammal radiations.

Conclusions

The limited representation of semiaquatic sigmodontine rodents is unlikely to reflect an absence of evolutionary potential, nor solely a consequence of restricted time or ecological opportunity. Instead, the available phylogenetic and ecomorphological evidence indicates that semiaquatic adaptations evolved convergently within the subfamily—primarily in Ichthyomyini and in a small subset of Oryzomyini—demonstrating that freshwater colonization was feasible, but comparatively rare.

The patterns documented here are consistent with a scenario in which persistent ecological constraints and historical processes jointly shaped this outcome. In particular, predation risk within continental freshwater systems may have acted as an important selective filter, limiting the number of lineages able to exploit aquatic habitats and favoring either occupation of predator-poor montane environments or shifts toward traits such as larger body size in lowland systems. These constraints may have been further amplified by extinction, as suggested by the fossil record and by evidence of range contraction in semiaquatic taxa during the Quaternary.

Viewed in a broader muroid context, the sigmodontine case appears illustrative rather than exceptional. Freshwater environments may represent a challenging ecological domain for small mammals, despite their spatial extent and long-term persistence. In this framework, the present-day scarcity of semiaquatic sigmodontines can be interpreted as consistent with a combination of ecological filtering associated with freshwater habitats and historical reductions in diversity through extinction. More generally, this case highlights how ecological constraints and historical contingency interact to shape the distribution of functional traits within continental mammal radiations.

Acknowledgments

This contribution forms part of a volume honoring Livia León-Paniagua, whose career has made a lasting impact on the study of mammals. Through her rigorous work in taxonomy, systematics, and ecology, as well as her commitment to academic training and museum-based research, she has substantially advanced knowledge of the mammalian fauna of Mexico. This study benefited from discussions conducted over many years, including during fieldwork, with C. Galliari. S. Bogan generously assisted with bibliographic guidance and shared his extensive knowledge of extant and fossil fishes, and F. Carlini also contributed relevant literature. This manuscript was completed during a sabbatical period undertaken by the senior author at the Oman National Natural History Museum (Muscat, Oman), approved by CONICET (Argentina) and kindly authorized by A. Aljabri Al Khuwair. The revisions provided by two anonymous referees contribute substantially to the present version. We are grateful to all individuals and institutions mentioned above for their support. Finally, we acknowledge the use of ChatGPT for assistance in refining the linguistic clarity and grammatical style of the manuscript. This study was financially supported by Agencia Nacional de Promoción de la Investigación, el Desarrollo Tecnológico y la Innovación grant #2020-2068 (to UFJP).

Declaration of Artificial Intelligence use

Artificial intelligence was used exclusively to assist with language editing and stylistic refinement of the manuscript. Specifically, the authors used ChatGPT (OpenAI; model version GPT-5.2) to improve clarity, grammar, coherence, and consistency of academic

English. ChatGPT is accessible via: https://openai.com/chatgpt. AI tools were not used for data generation, data analysis, figure preparation, image manipulation, statistical analyses, or interpretation of results. All scientific content, analyses, conclusions, and final editorial decisions are entirely the responsibility of the authors.

Author contributions

The authors accepted responsibility for the entire content of this manuscript and approved its submission. Erika Cuéllar Soto and Ulyses F. J. Pardiñas: conceptualization, investigation, supervision, writing–original draft. Carola Cañón: laboratory analysis. All the authors: Writing–review and editing.

Data availability

The datasets generated and analyzed during the current study are included (Supplementary Data); the concatenated matrix, alignment partitions, and Mesquite project files are available upon request; fossils mentioned or discussed are available in the following public biological repositories: CNP: Colección de Mamíferos, Centro Nacional Patagónico, Puerto Madryn, Chubut, Argentina; FMNH: Field Museum,

Chicago, Illinois, United States; MLP: Museo de La Plata, La Plata, Argentina.

Supplementary data

SD1. A list of living genera and species of sigmodontine rodents indicating those considered semiaquatic and waders. Numbers updated to December 2025.
SD2. List of sequences downloaded from GenBank that were used to construct the phylogeny.

Literature cited

Aghová T, Kimura Y, Bryja J, Dobigny G, Granjon L, and Kergoat GJ. 2018. Fossils know it best: using a new set of fossil calibrations to improve the temporal phylogenetic framework of murid rodents (Rodentia: Muridae). *Molecular Phylogenetics and Evolution* 128:98–111. https://doi.org/10.1016/j.ympev.2018.07.017

Alhajeri BH, Schenk JJ, and Steppan SJ. 2016. Ecomorphological diversification following continental colonization in muroid rodents (Rodentia: Muroidea). *Biological Journal of the Linnean Society* 117:463–481. https://doi.org/10.1111/bij.12695

Ávila-Pires FD. 1972. A new subspecies of *Kunsia fronto* (Winge, 1888) from Brazil (Rodentia, Cricetidae). *Revista Brasileira de Biologia* 32:419–422.

Ayres JM, and Clutton-Brock TH. 1992. River boundaries and species range size in Amazonian primates. *American Naturalist* 140:531–537.

Bangs MR, Percequillo AR, Pacheco V, and Steppan SJ. 2025. Phylogenomics of sigmodontine rodents (Cricetidae: Sigmodontinae): cloud forests and Pliocene extinction explain the timing and spread of an iconic South American radiation. *PLoS One* 20:e0317165. https://doi.org/10.1371/journal.pone.0317165

Barbière F. 2019. Estudio de la diversidad de sigmodontinos (Mammalia, Rodentia) plio-pleistocénicos de Argentina, con énfasis en la tribu Phyllotini [PhD thesis]. [Tucumán (ARG)]: Universidad Nacional de Tucumán.

Barlow JC. 1969. Observations on the biology of rodents in Uruguay. *Life Science Contributions, Royal Ontario Museum* 75:1–59.

Bianchini JC, and Delupi H. 1993. Mammalia. In: Castellanos ZA de, editor. *Fauna de agua dulce de la República Argentina*. Vol. 44, Fasc. 2. La Plata (ARG): Museo de La Plata; p. 1–79.

Bonvicino CR, and Weksler M. 2015. Genus *Nectomys* Peters, 1861. In: Patton JL, Pardiñas UFJ, and D'Elía G, editors. *Mammals of South America*. Vol. 2, *Rodents*. Chicago (EEUU): University of Chicago Press; p. 369–377.

Borges MDC, Paes JASV, Santos FTR, Giongo P, Sampaio WMS, Sanches HCS, *et al.* 2025. Predation of *Bibimys labiosus* (Rodentia: Cricetidae) by *Hoplias intermedius* (Characiformes: Erythrinidae) in the Cerrado, with a review of Sigmodontinae predation by fishes. *Food Webs* 43:e00396. https://doi.org/10.1016/j.fooweb.2025.e00396

Bover P, Brito J, Castellanos FX, Cuellar Soto E, Hutterer R, Alfaro-Ibáñez MP, *et al*. 2025. Revisiting the taxonomy and biogeography of the largest sigmodontine rodent (Rodentia, Cricetidae) through ancient DNA. *Zoological Journal of the Linnean Society* 205:zlaf167. https://doi.org/10.1093/zoolinnean/zlaf167

Brito J, and Pardiñas UFJ. 2025. Sigmodontine rodent diversity: the Frankenstein paradox. *Mammalia Aequatorialis* 7:57–66. https://doi.org/10.59763/mam.aeq.v7i1.118

Brito J, Tinoco N, Curay J, and Pardiñas UFJ. 2021. New morphological data on the rare sigmodontine *Mindomys hammondi* (Rodentia, Cricetidae), an arboreal oryzomyine from north-western Andean montane forests. *Neotropical Biodiversity and Conservation* 16:397–410. https://doi.org/10.3897/neotropical.16.e65875

Cadena EA, Scheyer TM, Carrillo-Briceño JD, Sánchez R, Aguilera-Socorro OA, Vanegas A, *et al.* 2020. The anatomy, paleobiology, and evolutionary relationships of the largest extinct side-necked turtle. *Science Advances* 6:eaay4593. https://doi.org/10.1126/sciadv.aay4593

Candela AM, Abello MA, Reguero MA, García Esponda C, Pardiñas UFJ, Zurita AA, *et al.* 2023. The late Miocene mammals from the Humahuaca Basin (northwestern Argentina) provide new evidence on the initial stages of the Great American Biotic Interchange. *Papers in Palaeontology* 9:e1527. https://doi.org/10.1002/spp2.1527

Carleton MD, and Olson SL. 1999. Amerigo Vespucci and the rat of Fernando de Noronha: a new genus and species of Rodentia (Muridae: Sigmodontinae) from a volcanic island off Brazil's continental shelf. *American Museum Novitates* 3256:1–59.

Carrillo-Briceño JD, Reyes-Cespedes AE, Salas-Gismondi R, and Sánchez R. 2019. A new vertebrate continental assemblage from the Tortonian of Venezuela. *Swiss Journal of Palaeontology* 138:237–248. https://doi.org/10.1007/s13358-018-0180-y

Cassini MH. 2020. A review of the critics of invasion biology. *Biological Reviews* 95:1467–1478. https://doi.org/10.1111/brv.12624

Chebez JC, Pardiñas UFJ, and Teta P. 2014. *Mamíferos terrestres de la Patagonia: Sur de Argentina y Chile*. Buenos Aires (ARG): Vazquez Mazzini Editores.

Chiquito EA. 2015. Sistemática do gênero *Nectomys* Peters, 1861 (Cricetidae: Sigmodontinae) [PhD thesis]. [São Paulo (BRA)]: Universidade de São Paulo.

Clapperton C. 1993. *Quaternary geology and geomorphology of South America*. Amsterdam (NLD): Elsevier.

Coltorti M, Fazia JD, Paredes Ríos F, and Tito G. 2012. Ñuagapua (Chaco, Bolivia): evidence for the latest occurrence of megafauna in association with human remains in South America. *Journal of South American Earth Sciences* 33:56–67. https://doi.org/10.1016/j.jsames.2011.07.003

Dawson TJ, and Fanning FD. 1981. Thermal and energetic problems of semiaquatic mammals: A study of the Australian water rat, including comparisons with the platypus. *Physiological Zoology* 54:285–296. https://doi.org/10.1086/physzool.54.3.30159943

Denys C, Taylor PJ, and Aplin KP. 2017. Family Muridae (true mice and rats, gerbils and relatives). In: Wilson DE, Lacher TE, and Mittermeier RA, editors. *Handbook of the mammals of the world.* Vol. 7, *Rodents II*. Barcelona (SPA): Lynx Edicions; p. 536–597.

de Souza ÉMS, Freitas L, Ramos EKS, Selleghin-Veiga G, Rachid-Ribeiro MC, *et al.* 2021. The evolutionary history of manatees told by their mitogenomes. *Scientific Reports* 11:3564. https://doi.org/10.1038/s41598-021-82390-2

Esher RJ, Wolfe JL, and Layne JN. 1978. Swimming behavior of rice rats (*Oryzomys palustris*) and cotton rats (*Sigmodon hispidus*). *Journal of Mammalogy* 59:551–558. https://doi.org/10.2307/1380231

Farina BM, Berta A, and Slater GJ. 2023. Dollo meets Bergmann: morphological evolution in secondarily aquatic mammals. *Proceedings of the Royal Society B* 290:20231099. https://doi.org/10.1098/rspb.2023.1099

Fernández MM, and Crivelli-Montero EA. 2004. Excavaciones de rescate en Rincón Chico 2/87, provincia del Neuquén. In: Civalero T, Fernández P, and Guráieb AG, editors. *Contra viento y marea. Arqueología de Patagonia*. Buenos Aires (ARG): Instituto Nacional de Antropología y Pensamiento Latinoamericano y Sociedad Argentina de Antropología; p. 701–714.

Fernández FJ, Del Papa L, Moreira GJ, Prates L, and De Santis LJM. 2011. Small mammal remains recovered from two archaeological sites in the middle and lower Negro River valley (Late Holocene, Argentina): taphonomic issues and paleoenvironmental implications. *Quaternary International* 245:136–147. https://doi.org/10.1016/j.quaint.2010.12.027

Fish FE. 1992. Aquatic locomotion. In: Tomasi T, and Horton T, editors. *Mammalian energetics: interdisciplinary views of metabolism and reproduction*. Ithaca (EEUU): Cornell University Press; p. 34–63.

Fish FE, Smelstojs J, Baudinettes RV, and Reynolds PS. 2002. Fur does not fly, it floats: buoyancy of pelage in semi-aquatic mammals. *Aquatic Mammals* 28:103–112.

Formoso A, Udrizar-Sauthier D, and Pardiñas UFJ. 2010. *Holochilus brasiliensis* (Desmarest, 1819) (Mammalia, Rodentia, Sigmodontinae): distribution extension. *Check List* 6:195–197. https://doi.org/10.15560/6.2.195

Gonçalves PR, Christoff AU, Machado LF, Bonvicino CR, Peters FB, and Percequillo AR. 2020. Unraveling deep branches of the Sigmodontinae tree (Rodentia: Cricetidae) in eastern South America. *Journal of Mammalian Evolution* 27:139–160. https://doi.org/10.1007/s10914-018-9444-y

Hadler P, Fernández FJ, Tammone MN, and Pardiñas UFJ. 2026. Emergence of the recent mammal assemblage: A Holocene history. In Melletti M, Gallina Tessaro S, Ortega J, and Tirira DG, editors. *Mammals of Middle and South America: History, biogeography, conservation.* Springer. https://doi.org/10.1007/978-3-031-43163-0_37-1

He K, Eastman TG, Czolacz H, Li S, Shinohara A, Kawada S, *et al*. 2021. Myoglobin primary structure reveals multiple convergent transitions to semi-aquatic life in the world's smallest mammalian divers. *eLife* 10:e66797. https://doi.org/10.7554/eLife.66797

Helgen KM. 2005. The amphibious murines of New Guinea (Rodentia, Muridae): the generic status of *Baiyankamys* and description of a new species of *Hydromys*. *Zootaxa* 913:1–20. https://doi.org/10.11646/zootaxa.913.1.1

Hershkovitz P. 1955. South American marsh rats, genus *Holochilus*, with a summary of sigmodont rodents. *Fieldiana: Zoology* 37:639–673.

Hershkovitz P. 1966. South American swamp and fossorial rats of the scapteromyine group (Cricetinae, Muridae), with comments on the glans penis in murid taxonomy. *Zeitschrift für Säugetierkunde* 31:81–149.

Hershkovitz P. 1969. The recent mammals of the Neotropical Region: a zoogeographic and ecological review. *Quarterly Review of Biology* 44:1–70.

Hoffstetter, R. 1968. Ñuapua, un gisement de vertébrés pléistocénes dans le Chaco Bolivien. *Bulletin du Muséum National d'Histoire Naturelle, 2e série* 40:823–836.

Hood GA. 2020. *Semi-aquatic mammals: ecology and biology*. Baltimore (EEUU): Johns Hopkins University Press.

Hurlbert SH, Rodríguez G, and Santos ND, editors. 1981. *Aquatic biota of tropical South America. Part 2, Anarthropoda.* San Diego (EEUU): San Diego State University.

Junk WJ. 2007. Freshwater fishes of South America: their biodiversity, fisheries, and habitats—a synthesis. *Aquatic Ecosystem Health & Management* 10:228–242. https://doi.org/10.1080/14634980701356733

Junk WJ. 2013. Current state of knowledge regarding South America wetlands and their future under global climate change. *Aquatic Sciences* 75:113–131. https://doi.org/10.1007/s00027-012-0253-8

Kerber L, Negri FR, Ribeiro AM, Vucetich MG, and De Souza-Filho JP. 2016. Late Miocene potamarchine rodents from southwestern Amazonia, Brazil—with description of new taxa. *Acta Palaeontologica Polonica* 61:191–203. http://dx.doi.org/10.4202/app.00091.2014

Kerbis Peterhans JC, and Patterson BD. 1995. The Ethiopian water mouse *Nilopegamys* Osgood, with comments on semi-aquatic adaptations in African Muridae. *Zoological Journal of the Linnean Society* 113:329–349. https://doi.org/10.1006/zjls.1995.0012

Leite RN, Kolokotronis SO, Almeida FC, Werneck FN, Rogers DS, and Weksler M. 2014. In the wake of invasion: tracing the historical biogeography of the South American cricetid radiation (Rodentia: Sigmodontinae). *PLoS One* 9:e100687. https://doi.org/10.1371/journal.pone.0100687

Lessa EP, D'Elía G, and Pardiñas UFJ. 2012. Mammalian biogeography of Patagonia and Tierra del Fuego. In Patterson BD, and Costa LP, editors. *Bones, clones, and biomes: an 80-million year history of recent neotropical mammals*. Chicago (EEUU): University of Chicago Press; p. 379–398.

López JM, and Chiavazza H. 2021. Ancient wetlands in the arid environments of central western Argentina: a palaeoecological perspective based on archaeological small mammal remains. *Journal of South American Earth Sciences* 106:103023. https://doi.org/10.1016/j.jsames.2020.103023

López-Antoñanzas R, Simões TR, Condamine FL, Dirnberger M, and Peláez-Campomanes P. 2024. Bayesian tip-dated timeline for diversification and major biogeographic events in Muroidea (Rodentia), the largest mammalian radiation. *BMC Biology* 22:270. https://doi.org/10.1186/s12915-024-02053-2

Lundberg JG, Marshall LG, Guerrero J, Horton B, Malabarba MCSL, and Wesselingh F. 1998. The stage for Neotropical fish diversification: a history of tropical South American rivers. In: Malabarba MCSL, Reis RE, Vari RP, Lucena ZMS, and Lucena CAS, editors. *Phylogeny and classification of Neotropical fishes*. Porto Alegre (BRA): Edipucrs; p. 13–48.

Machado LF, Leite YLR, Christoff AU, and Giugliano LG. 2014. Phylogeny and biogeography of tetralophodont rodents of the tribe Oryzomyini (Cricetidae: Sigmodontinae). *Zoologica Scripta* 43:119–130. https://doi.org/10.1111/zsc.12041

Maddison WP, and Maddison DR. 2019. *Mesquite: a modular system for evolutionary analysis. Version 3.61*. https://www.mesquiteproject.org

Maestri R, Monteiro LR, Fornel R, Upham NS, Patterson BD, and de Freitas TRO. 2017. The ecology of a continental evolutionary radiation: is the radiation of sigmodontine rodents adaptive? *Evolution* 71:610–632. https://doi.org/10.1111/evo.13155

Maestri R, Luza AL, Hartz SM, de Freitas TRO, and Patterson BD. 2022. Bridging macroecology and macroevolution in the radiation of sigmodontine rodents. *Evolution* 76:1790–1805. https://doi.org/10.1111/evo.14561

Mann FG. 1978. Los pequeños mamíferos de Chile. Marsupiales, quirópteros, edentados y roedores. *Gayana Zoología* 40:1–342.

Massoia E. 1976. Mammalia. In: Ringuelet R, editor. *Fauna de agua dulce de la República Argentina*. Vol. 44. Buenos Aires (ARG): Fundación Editorial Ciencia y Cultura; p. 1–128.

Massoia E, and Fornes A. 1964. Notas sobre el género *Scapteromys* (Rodentia: Cricetidae). I. Sistemática, distribución geográfica y rasgos etoecológicos de *Scapteromys tumidus* (Waterhouse). *Physis, Sección C* 24:279–297.

McDermott A. 2021. A sea in the Amazon: did the Caribbean sweep into the western Amazon millions of years ago, shaping the region's rich biodiversity? *Proceedings of the National Academy of Sciences of the United States of America* 118:e2102396118. https://doi.org/10.1073/pnas.2102396118

McNab BK. 1978. The evolution of endothermy in the phylogeny of mammals. *American Naturalist* 112:1–21. https://doi.org/10.1086/283242

Miller LM, and Anderson S. 1977. Bodily proportions of Uruguayan myomorph rodents. *American Museum Novitates* 2615:1–10.

Missagia RV, Casali DM, Patterson BD, and Perini FA. 2023. Decoupled patterns of diversity and disparity characterize an ecologically specialized lineage of Neotropical cricetids. *Evolutionary Biology* 50:181–196. https://doi.org/10.1007/s11692-022-09596-8

Musser GG, and Heaney LR. 1992. Philippine rodents: definitions of *Tarsomys* and *Limnomys* plus a preliminary assessment of phylogenetic patterns among native Philippine murines (Murinae, Muridae). *Bulletin of the American Museum of Natural History* 211:1–138.

Northfield TD, Gretchen BS, Ives AR, and Snyder WE. 2010. Niche saturation reveals resource partitioning among consumers. *Ecology Letters* 13:338–348. https://doi.org/10.1111/j.1461-0248.2009.01428.x

Parada A, Hanson J, and D'Elía G. 2021. Ultraconserved elements improve the resolution of difficult nodes within the rapid radiation of Neotropical sigmodontine rodents (Cricetidae: Sigmodontinae). *Systematic Biology* 70:1090–1100. https://doi.org/10.1093/sysbio/syab023

Pardiñas UFJ. 1999. Fossil murids: Taxonomy, paleoecology, and paleoenvironments. *Quaternary of South America and Antarctic Peninsula* 12:225–254.

Pardiñas UFJ. 2008. A new genus of oryzomyine rodent (Cricetidae: Sigmodontinae) from the Pleistocene of Argentina. *Journal of Mammalogy* 89:1270–1278. https://doi.org/10.1644/07-MAMM-A-099.1

Pardiñas UFJ, and Barbière F. 2018. The Pleistocene record attributed to the cricetid genus *Nectomys* (Rodentia, Sigmodontinae): unexpected connections. *Mammalia* 82:201–206. https://doi.org/10.1515/mammalia-2017-0020

Pardiñas UFJ, and Galliari CA. 1998. Sigmodontinos (Rodentia, Muridae) del Holoceno inferior de Bolivia. *Revista Española de Paleontología* 13:17–25.

Pardiñas UFJ, and Lezcano MJ. 1995. Cricétidos (Mammalia, Rodentia) del Pleistoceno tardío del nordeste de la provincia de Buenos Aires (Argentina): aspectos sistemáticos y paleoambientales. *Ameghiniana* 32:249–265.

Pardiñas UFJ, and Teta P. 2011. Fossil history of the marsh rats of the genera *Holochilus* and *Lundomys* (Cricetidae, Sigmodontinae) in southern South America. *Estudios Geológicos* 67:111–129. https://doi.org/10.3989/egeol.40347.136

Pardiñas UFJ, Brito J, Soto EC, and Cañón C. 2024. Comparative morphology of the rhinarium and upper lip in sigmodontine rodents: refined nomenclature, intertribal variation in a phylogenetic framework, and

functional inferences. *Journal of Morphology* 285:e21760. https://doi.org/10.1002/jmor.21760

Pardiñas UFJ, Cirignoli S, Laborde J, and Richieri A. 2004. Nuevos datos sobre la distribución de *Irenomys tarsalis* (Philippi, 1900) (Rodentia: Sigmodontinae) en Argentina. *Mastozoología Neotropical* 11:99–104.

Pardiñas UFJ, D'Elía G, and Teta P. 2009. Una introducción a los mayores sigmodontinos vivientes: revisión de *Kunsia* Hershkovitz, 1966 y descripción de un nuevo género (Rodentia: Cricetidae). *Arquivos do Museu Nacional* 66:509–594.

Pardiñas UFJ, Myers P, León-Paniagua L, Ordoñez-Garza N, Cook JA, Krystufek B, *et al.* 2017. Family Cricetidae (true hamsters, voles, lemmings and New World rats and mice). In: Wilson DE, Lacher TE, and Mittermeier RA, editors. *Handbook of the mammals of the world*. Vol. 7, *Rodents II*. Barcelona (SPA): Lynx Edicions; p. 204–279.

Pardiñas UFJ, Teta P, and Salazar-Bravo J. 2015. A new tribe of Sigmodontinae rodents (Cricetidae). *Mastozoología Neotropical* 22:171–186.

Pardiñas UFJ, Teta P, Voglino D, and Fernández F. 2013. Enlarging rodent diversity in west-central Argentina: a new species of the genus *Holochilus* (Cricetidae, Sigmodontinae). *Journal of Mammalogy* 94:231–240. https://doi.org/10.1644/12-MAMM-A-216

Pardiñas UFJ, Tinoco N, Barbière F, Ronez C, Cañón C, Lessa G, *et al*. 2022. Morphological disparity in a hyperdiverse mammal clade: a new morphotype and tribe of Neotropical cricetids. *Zoological Journal of the Linnean Society* 196:1013–1038. https://doi.org/10.1093/zoolinnean/zlac016

Patton JL, Pardiñas UFJ, and D'Elía G, editors. 2015. *Mammals of South America*. Vol. 2, *Rodents*. Chicago (EEUU): University of Chicago Press.

Percequillo AR, Prado JR, Abreu EF, Dalapicolla J, Pavan AC, Chiquito EDA, *et al.* 2021. Tempo and mode of evolution of oryzomyine rodents (Rodentia, Cricetidae, Sigmodontinae): a phylogenomic approach. *Molecular Phylogenetics and Evolution* 159:107120. https://doi.org/10.1016/j.ympev.2021.107120

Pine RH, Pine NE, and Bruner SD. 1981. Mammalia. In: Hurlbert SH, Rodríguez G, and Santos ND, editors. *Aquatic biota of tropical South America*. Part 2, *Anarthropoda*. San Diego (EEUU): San Diego State University; p. 267–298.

Prado JR, Knowles LL, and Percequillo AR. 2021. New species boundaries and the diversification history of marsh rat taxa clarify historical connections among ecologically and geographically distinct wetlands of South America. *Molecular Phylogenetics and Evolution* 155:106992. https://doi.org/10.1016/j.ympev.2020.106992

Prevosti FJ, Romano CO, Forasiepi AM, Hemming S, Bonini R, Candela AM, *et al.* 2021. New radiometric 40Ar–39Ar dates and faunistic analyses refine evolutionary dynamics of Neogene vertebrate assemblages in southern South America. *Scientific Reports* 11:9830. https://doi.org/10.1038/s41598-021-89135-1

Ramos VA, Germani G, Knapp GW, Griffin EC, Gade DW, Minkel CW, *et al*. 2026. *South America. Encyclopedia Britannica*. Chicago (EEUU): The Britannica Group; May 5th, 2026. [Accessed May 8th, 2026]. https://www.britannica.com/place/South-America

Rasia LL. 2026. Reassessing the hyperdiverse dinomyid (Rodentia, Caviomorpha) assemblage from the Late Miocene Ituzaingó Formation (Entre Ríos Province, Argentina). *Ameghiniana* 63:33–56. http://dx.doi.org/10.5710/AMGH.07.12.2025.3663

Reis RE, Albert JS, Di Dario F, Mincarone MM, Petry P, and Rocha LA. 2016. Fish biodiversity and conservation in South America. *Journal of Fish Biology* 89:12–47. https://doi.orgf/10.1111/jfb.13016

Rodríguez-Serrano E, Palma RE, and Hernández CE. 2008. The evolution of ecomorphological traits within the Abrothrichini (Rodentia: Sigmodontinae): a Bayesian phylogenetics approach. *Molecular Phylogenetics and Evolution* 48:473–480. https://doi.org/10.1016/j.ympev.2008.05.012

Roig V. 1991. Desertification and distribution of mammals in the Southern Cone of South America. Part III Conservation policy and management. In Mares MA, and Schmidly DJ, editors. *Latin American mammalogy. History, biodiversity and conservation*. Oklahoma (EEUU): University of Oklahoma Press; p. 239–279.

Román-Palacios C, Wiens JJ, and Adams DC. 2022. The origins of global biodiversity on land, sea, and freshwater. *Ecology Letters* 25:2325–2338. https://doi.org/10.1111/ele.14090

Romano CO, Bonini R, Hemming S, Cenizo M, Pardiñas UFJ, and Prevosti FJ. 2023. Advances in the understanding of Neogene mammalian fauna in the Pampean region (Central Argentina) through revising "biozone" hypotheses based on new dates and biochronological analyses. *Ameghiniana* 60:465–491. https://doi.org/10.5710/AMGH.07.07.2023.3551

Ronez C, Brito J, Hutterer R, Martin RA, and Pardiñas UFJ. 2021a. Tribal allocation and biogeographical significance of one of the largest sigmodontine rodents, the extinct Galápagos *Megaoryzomys* (Cricetidae). *Historical Biology* 33:1920–1932. https://doi.org/10.1080/08912963.2020.1752202

Ronez C, Carrillo-Briceño JD, Hadler P, Sánchez-Villagra MR, and Pardiñas UFJ. 2023. Pliocene sigmodontine rodents (Mammalia: Cricetidae) in northernmost South America: test of biogeographic hypotheses and revised evolutionary scenarios. *Royal Society Open Science* 10:221417. https://doi.org/10.1098/rsos.221417

Ronez C, Martin RA, Kelly TS, Barbière F, and Pardiñas UFJ. 2021b. A brief critical review of sigmodontine rodent origins, with emphasis on paleontological data. *Mastozoología Neotropical* 28:e0495. https://doi.org/10.31687/saremMN.21.28.1.0.07

Rowe KC, Achmadi AS, and Esselstyn JA. 2014. Convergent evolution of aquatic foraging in a new genus and species

(Rodentia: Muridae) from Sulawesi Island, Indonesia. *Zootaxa* 3815:541–564. https://doi.org/10.11646/zootaxa.3815.4.5

Salazar-Bravo J, Tinoco N, Zeballos H, Brito J, Arenas-Viveros D, Marín-C D, *et al.* 2023. Systematics and diversification of the Ichthyomyini (Cricetidae, Sigmodontinae) revisited: evidence from molecular, morphological, and combined approaches. *PeerJ* 11:e14319. https://doi.org/10.7717/peerj.14319

Sánchez-Villagra MR, Aguilera OA, and Carlini AA, editors. 2010. *Urumaco and Venezuelan paleontology: the fossil record of the northern Neotropics*. Bloomington (EEUU): Indiana University Press.

Santori RT, Vieira MV, Rocha-Barbosa O, Magnan-Neto JA, and Gobbi N. 2008. Water absorption of the fur and swimming behavior of semiaquatic and terrestrial oryzomine rodents. *Journal of Mammalogy* 89:1152–1161. https://doi.org/10.1644/07-MAMM-A-339.1

Scholander PF, Hock R, Walters V, Johnson F, and Irving L. 1950. Heat regulation in some Arctic and tropical mammals and birds. *Biological Bulletin* 99:237–258. https://doi.org/10.2307/1538741

Sierra de Soriano B. 1965. Algunas estructuras externas relacionadas con la vida anfibia en dos especies del género *Holochilus* Brandt, 1835 (Muridae, Cricetinae). *Revista de la Facultad de Humanidades y Ciencias* 22:209–220.

Sierra de Soriano B. 1969. Algunos caracteres externos de cricetinos y su relación con el grado de adaptación a la vida acuática (Rodentia). *Physis* 28:471–486.

Stamatakis A. 2014. RAxML version 8: a tool for phylogenetic analysis and post-analysis of large phylogenies. *Bioinformatics* 30:1312–1313. https://doi.org/10.1093/bioinformatics/btu033

Starrett A, and Fisler GF. 1970. Aquatic adaptations of the water mouse, *Rheomys underwoodi*. *Contributions in Science, Los Angeles County Museum* 182:1–14.

Stein BR, and Patton JL. 2008. Genus *Chironectes* Illiger, 1811. In: Gardner AL, editor. *Mammals of South America*. Vol. 1, *Marsupials, xenarthrans, shrews, and bats*. Chicago (EEUU): University of Chicago Press; p. 14–17.

Steppan SJ. 1996. A new species of *Holochilus* (Rodentia: Sigmodontinae) from the middle Pleistocene of Bolivia and its phylogenetic significance. *Journal of Vertebrate Paleontology* 16:522–530. https://doi.org/10.1080/02724634.1996.10011337

Stoessel L, Bogan S, Martínez G, and Agnolin F. 2008. Implicaciones paleoambientales de la presencia del género *Ceratophrys* (Anura, Ceratophryinae) en contextos arqueológicos de la transición pampeano patagónica en el Holoceno tardío (curso inferior del Río Colorado, Argentina). *Magallania* 36:195–203. http://dx.doi.org/10.4067/S0718-22442008000200015

Teta P, and Pardiñas UFJ. 2006. Pleistocene record of the marsh rat of the genus *Lundomys* in southern South America: paleoclimatic significance. *Current Research in the Pleistocene* 23:202–204.

Teta P, Medina M, Pastor S, Rivero D, and Paradela H. 2005. *Holochilus brasiliensis* (Rodentia, Cricetidae) en conjuntos arqueofaunísticos del Holoceno tardío de la provincia de Córdoba (Argentina). *Mastozoología Neotropical* 12:271–275.

Urcola MR, Urcola JI, Michat MC, and Torres PLM. 2025. The Hydradephaga (Coleoptera, Dytiscidae, Gyrinidae, Haliplidae, Noteridae) of the Iberá wetlands, the second largest wetland area of South America. *ZooKeys* 1259:287–307. https://doi.org/10.3897/zookeys.1259.164084

Vermeij GJ. 1991. When biotas meet: understanding biotic interchange. *Science* 253:1099–1104. https://doi.org/10.1126/science.253.5024.1099

Viñola López LW, Vélez-Juarbe J, Münch P, Almonte Milan JN, Antoine P-O, Marivaux L, *et al.* 2025. A South American sebecid from the Miocene of Hispaniola documents the presence of apex predators in early West Indies ecosystems. *Proceedings of the Royal Society B* 292:20242891. https://doi.org/10.1098/rspb.2024.2891

Vitule JRS, Freitas MO, Ribeiro VM, and Bornatowski H. 2015. First records of Sigmodontinae (Mammalia) predation by *Oligosarcus hepsetus* (Cuvier, 1829) (Characiformes, Characidae) in Atlantic Rain Forest rivers of southern Brazil. *Pan-American Journal of Aquatic Sciences* 10:328–331.

Voss RS. 1988. Systematics and ecology of ichthyomyine rodents (Muroidea): patterns of morphological evolution in a small adaptive radiation. *Bulletin of the American Museum of Natural History* 188:258–493.

Voss RS. 2015a. Tribe Ichthyomyini Vorontsov, 1959. In: Patton JL, Pardiñas UFJ, and D'Elía G, editors. *Mammals of South America*. Vol. 2, *Rodents*. Chicago (EEUU): University of Chicago Press; p. 279–291.

Voss RS. 2015b. Genus *Lundomys* Voss and Carleton, 1993. In: Patton JL, Pardiñas UFJ, and D'Elía G, editors. *Mammals of South America*. Vol. 2, *Rodents*. Chicago (EEUU): University of Chicago Press; p. 346–348.

Voss RS, and Carleton MD. 1993. A new genus for *Hesperomys molitor* Winge and *Holochilus magnus* Hershkovitz, with comments on phylogenetic relationships and oryzomyine monophyly. *American Museum Novitates* 3085:1–39.

Voss RS, and Myers P. 1991. *Pseudoryzomys simplex* (Rodentia: Muridae) and the significance of Lund's collections from the caves of Lagoa Santa, Brazil. *Bulletin of the American Museum of Natural History* 206:414–432.

Vucetich MG, Arnal M, Deschamps CM, Pérez ME, and Vieytes EC. 2015. A brief history of caviomorph rodents as told by the fossil record. In: Vasallo AI, and Antenucci D, editors. *Biology of caviomorph rodents: diversity and evolution*. Mendoza (ARG): SAREM Series A, Mammalogical Research, Sociedad Argentina para el Estudio de los Mamíferos; p. 11–62.

Weksler M. 2006. Phylogenetic relationships of oryzomine rodents (Muroidea: Sigmodontinae): separate and

combined analyses of morphological and molecular data. *Bulletin of the American Museum of Natural History* 296:1–149. https://doi.org/10.1206/0003-0090(2006)296[0001:PROORM]2.0.CO;2

Wolff JO, and Guthrie RD. 1985. Why are aquatic small mammals so large? *Oikos* 45:365–373. https://doi.org/10.2307/3565572

Associated editors: Giovani Hernández Canchola and Pablo Colunga Salas
Submitted: January 13, 2026; Reviewed: March 21, 2026
Accepted: May 9, 2026; Published online: May 29, 2026